

EFFECTS OF DUAL-SPECIES BIOFILM INTERACTIONS ON ANTIMICROBIAL RESISTANCE: *CANDIDA ALBICANS* AND *PSEUDOMONAS AERUGINOSA*

by

Farhana Alam

A thesis submitted to the University of Birmingham for the degree of DOCTOR OF PHILOSOPHY

Institute of Microbiology and Infection
School of Biosciences
College of Life and Environmental Sciences
University of Birmingham
May 2021

UNIVERSITY OF
BIRMINGHAM

University of Birmingham Research Archive

e-theses repository

This unpublished thesis/dissertation is copyright of the author and/or third parties. The intellectual property rights of the author or third parties in respect of this work are as defined by The Copyright Designs and Patents Act 1988 or as modified by any successor legislation.

Any use made of information contained in this thesis/dissertation must be in accordance with that legislation and must be properly acknowledged. Further distribution or reproduction in any format is prohibited without the permission of the copyright holder.

ABSTRACT

The bacterium, *Pseudomonas aeruginosa*, and the fungus, *Candida albicans*, commonly co-infect the lungs of Cystic Fibrosis patients, and the surfaces of surgical and burn wounds. Both species form extensive, structured biofilms on the surfaces of mucosa and medical devices. The main objective of this research was to determine whether *P. aeruginosa–C. albicans* biofilm interactions impact antimicrobial tolerance. Antimicrobial susceptibilities of single- and dual-species biofilms were investigated using an *in vitro* biofilm assay, and biofilms were visualised using a range of microscopy techniques. Dual-species RNA sequencing of biofilm cells revealed transcriptional changes during *P. aeruginosa–C. albicans* biofilm interactions. The data show that *C. albicans* protects *P. aeruginosa* biofilm cells from the effects of meropenem. We propose that this protection is likely mediated by fungal extracellular matrix polysaccharides, specifically mannan and ß-glucan, and potentially also via adhesion of *P. aeruginosa* cells to *C. albicans* hyphae. Conversely, *P. aeruginosa* potentiates the activity of amphotericin B against *C. albicans* biofilm cells. With support from the dual-species transcriptomic data, we propose that this occurs as a result of *P. aeruginosa* secreted phenazines, which lead to oxidative stress in *C. albicans* cells. These findings have direct clinical implications for the treatment of co-infected patients.

ACKNOWLEDGEMENTS

Completing a PhD during an historically momentous time has made for an unparalleled experience. Personally, I bought my first house, got married, and stepped towards a new career path. In the wider context, Britain – my home nation – left the European Union, necessitating the stockpiling of laboratory supplies, which ran precariously low at times. The global COVID-19 pandemic, which continues as I write this, turned the experience into "PhD, interrupted" and made the lab group doubly thankful for proactive stockpiling. Finally, Bangladesh – my ancestral home – is celebrating its 50th year as an independent country.

I would like to thank my supervisors, Rebecca Hall and Jessica Blair, whose support continued seamlessly throughout – I wish you both happiness and (further) success for the future. Thank you to everybody involved in the Wellcome Trust Antimicrobials & Antimicrobial Resistance doctoral training programme, both at Birmingham and Nottingham – it has been an immense privilege. Thank you also to all members of the Host and Pathogen Interactions Lab, 2016–2021 – I could not have chosen a more welcoming and friendly group.

Thank you to my husband, Michael, for everything, but especially for reminding me that taking breaks is definitely allowed. Thank you to our cats, Jupiter and Juno, for making life infinitely more fun and immeasurably more picturesque.

STATEMENT OF COLLABORATIVE WORK

This is to state that parts of this thesis contain data that were obtained through collaborative work. Collaborators and their contributions are listed below, and are also stated in Chapter 2.

1. **Scanning electron microscopy of biofilms**

Sample preparation was performed by Paul Stanley and Theresa Morris (Centre for Electron Microscopy, University of Birmingham, UK).

2. **Confocal microscopy of biofilms**

Imaging of biofilm samples and quantification of biofilm thickness were performed by Dr Alessandro di Maio (Birmingham Advanced Light Microscopy facility, University of Birmingham, UK).

3. **Fluorescence microscopy of biofilm cells**

Imaging of biofilm samples was performed by Dr Joao Correia (School of Biosciences, University of Birmingham, UK).

4. **Dual-species RNA sequencing**

RNA extraction, library preparation, RNA sequencing, and bioinformatics analyses were carried out by GeneWiz® as a paid service. The deliverables from this service, which contributed to the data presented in this thesis, include: lists of differentially expressed genes, principle component analysis plots, and volcano plots of global transcriptional changes. Graphs provided directly by GeneWiz® are credited in the relevant Figure Legends.

DECLARATION OF AUTHORSHIP

This is to confirm that Farhana Alam was first author and major contributor to the publication '*Candida albicans* enhances meropenem tolerance of *Pseudomonas aeruginosa* in a dual-species biofilm.' This was published in *Journal of Antimicrobial Chemotherapy* in April 2020, with Dr Rebecca A. Hall as the corresponding author and Dr Jessica M. A. Blair as co-author with equal contribution to the corresponding author (Appendix I). Text from this publication has been included in the following thesis entitled "Effects of dual-species biofilm interactions on antimicrobial resistance: *Candida albicans* and *Pseudomonas aeruginosa*," submitted to the University of Birmingham in May 2021. Parts of this publication have been included in Chapters 2, 3, and 5, with further declarations included at the beginning of each chapter.

Signed:

		
Farhana Alam	Dr Rebecca A. Hall (corresponding author)	Dr Jessica M. A. Blair (co-author; contribution equal to corresponding author)

TABLE OF CONTENTS

List of Figures **XI**

List of Tables **XVI**

List of Abbreviations **XVII**

1 INTRODUCTION **1**

1.1 Antimicrobial resistance – a global challenge **1**

1.2 *Pseudomonas aeruginosa* **3**

1.2.1 Clinical importance 3

1.2.2 Pathogenesis and virulence mechanisms 4

1.2.2.1 Quorum sensing 4

1.2.2.2 Siderophores 6

1.2.2.3 Phenazines 6

1.2.2.4 Exotoxins and exoenzymes 7

1.2.2.5 Secretion systems 8

1.2.3 Antibiotic resistance 11

1.2.3.1 Meropenem 12

1.2.4 Biofilms 14

1.2.4.1 *Pseudomonas aeruginosa* biofilm composition 15

1.2.4.2 Bacterial biofilm-specific resistance mechanisms 18

1.3 *Candida* species **26**

1.3.1 *Candida albicans* – clinical importance 27

1.3.2 *Candida albicans* – pathogenesis and virulence mechanisms 27

1.3.2.1 Polymorphism 28

1.3.2.2 Adhesins 30

1.3.2.3 Invasins 30

1.3.2.4 Secreted hydrolases 31

1.3.2.5 Candidalysin toxin 32

1.3.3 *Candida albicans* biofilms 33

1.3.3.1 Fungal biofilm-specific resistance mechanisms 33

1.3.4 Biofilms of non-*albicans Candida* species 35

1.3.5 Antifungals and antifungal resistance 36

1.3.5.1 Amphotericin B 37
1.3.6 *C. albicans* interactions with bacteria 39
1.3.6.1 Interactions with Gram-positive bacteria 39
1.3.6.2 Interactions with Gram-negative bacteria 41
1.4 *P. aeruginosa* and *C. albicans* interactions 44
1.4.1 Clinical importance 44
1.4.2 Interactions via direct contact 45
1.4.3 Interactions via secreted metabolites 46
1.5 Aims of this research 49
2 MATERIALS AND METHODS 50
2.1 Strains and growth conditions 51
2.2 Formation of dual-species biofilms 53
2.2.1 Formation of dual-species biofilms with lower starting concentrations of *C. albicans* 53
2.2.2 Formation of *P. aeruginosa* biofilms in the presence of dead *C. albicans* 54
2.2.3 Formation of *P. aeruginosa* biofilms in the presence of fungal ECM components 54
2.2.4 Formation of *C. albicans* biofilms in the presence of dead *P. aeruginosa* 54
2.2.5 Formation of *C. albicans* biofilms in the presence of purified *P. aeruginosa* rhamnolipid 55
2.2.6 Formation of *C. albicans* biofilms in the presence of supernatant from mature biofilms 55
2.2.7 Formation of *C. albicans* biofilms in the presence of reactive oxygen species (ROS)-inducing agents 55
2.2.8 Formation of *C. albicans* biofilms in the presence of purified *P. aeruginosa* phenazines 56
2.3 Planktonic assay 56
2.4 Determination of *P. aeruginosa* susceptibility to meropenem 57
2.5 Scanning electron microscopy of biofilms 57
2.6 Confocal microscopy of biofilms 58
2.7 Quantification of ergosterol 58
2.7.1 Filipin staining and fluorescence microscopy of biofilm cells 58

2.7.2 Quantification of fluorescence 59
2.8 Dual-species RNA sequencing of biofilms 59
2.8.1 Biofilm formation 59
2.8.2 RNA extraction, library preparation and RNA sequencing 60
2.8.3 Bioinformatics analyses 61
2.8.4 Enrichment analyses 63
2.9 Statistical analysis 64
3 *CANDIDA ALBICANS* ENHANCES MEROPENEM TOLERANCE OF *PSEUDOMONAS AERUGINOSA* IN A DUAL-SPECIES BIOFILM 65
3.1 Introduction 66
3.2 Results 68
3.2.1 *C. albicans* increases the tolerance of *P. aeruginosa* to meropenem in dual-species biofilms 68
3.2.2 Meropenem tolerance is not maintained following subculture of *P. aeruginosa* biofilm cells 74
3.2.3 Increased tolerance of *P. aeruginosa* to meropenem is specific to dual-species biofilms 75
3.2.4 Increased *P. aeruginosa* tolerance to meropenem is dependent on fungal viability 76
3.2.5 *C. dubliniensis* also enhances *P. aeruginosa* meropenem tolerance in dual-species biofilms 77
3.2.6 Fungal cell wall polysaccharides enhance *P. aeruginosa* tolerance to meropenem 79
3.2.7 *C. albicans* cell wall glycosylation is important for protection against meropenem 81
3.2.8 Increased tolerance of *P. aeruginosa* to meropenem is strain-specific 85
3.2.9 *C. albicans* does not enhance *P. aeruginosa* tolerance to other antibiotics 88
3.2.10 *C. albicans* protects a *P. aeruginosa* Cystic Fibrosis isolate from meropenem 92
3.3 Discussion 93

4 DUAL-SPECIES RNA SEQUENCING 98

4.1 Introduction 98

4.2 Results 101

4.2.1 Scaling up the biofilm assay 101

4.2.2 Exploratory analysis of transcriptional data 104

4.2.3 *P. aeruginosa* biofilm transcriptional response to meropenem 109

4.2.4 Effect of *C. albicans* on *P. aeruginosa* response to meropenem 116

4.2.4.1 *C. albicans* has only a minor effect on the *P. aeruginosa* biofilm transcriptional response to meropenem 123

4.2.5 *C. albicans* biofilm transcriptional response to meropenem 126

4.2.5.1 Single-species *C. albicans* response to meropenem 126

4.2.5.2 Dual-species *C. albicans* response to meropenem 128

4.2.6 *P. aeruginosa* transcriptional response to *C. albicans* 131

4.2.6.1 *P. aeruginosa* response to *C. albicans* in untreated biofilms 131

4.2.6.2 *P. aeruginosa* response to *C. albicans* in meropenem-treated biofilms 138

4.2.7 *C. albicans* transcriptional response to *P. aeruginosa* 140

4.2.7.1 *C. albicans* response to *P. aeruginosa* in untreated biofilms 140

4.2.7.2 *C. albicans* response *P. aeruginosa* in meropenem-treated biofilms 147

4.3 Discussion 154

4.3.1 *P. aeruginosa* transcriptional responses 154

4.3.2 *C. albicans* transcriptional responses 161

4.3.3 Conclusions 165

5 *PSEUDOMONAS AERUGINOSA* POTENTIATES AMPHOTERICIN B ACTIVITY AGAINST *CANDIDA ALBICANS* IN A DUAL-SPECIES BIOFILM 167

5.1 Introduction 168

5.2 Results 172

5.2.1 *P. aeruginosa* significantly enhances *C. albicans* sensitivity to amphotericin B 172

5.2.2 The presence of *P. aeruginosa* enhances amphotericin B sensitivity to a greater extent than lower *C. albicans* starting concentrations 175

5.2.3 Purified *P. aeruginosa* rhamnolipids do not enhance *C. albicans* sensitivity to amphotericin B 176
5.2.4 Increased *C. albicans* sensitivity to amphotericin B occurs more quickly in the presence of *P. aeruginosa* PAO1 than other *P. aeruginosa* strains 179
5.2.5 Potentiation of amphotericin B against *C. albicans* is specific to dual-species biofilms 182
5.2.6 Potentiation of amphotericin B activity against *C. albicans* is dependent on *P. aeruginosa* viability 183
5.2.7 Supernatants from mature biofilms have no effect on amphotericin B efficacy against *C. albicans* biofilm cells 184
5.2.8 *C. albicans* sensitivity to amphotericin B is also enhanced by *E. coli* MG1655 in a dual-species biofilm 186
5.2.9 *P. aeruginosa* PAO1 also increases *C. dubliniensis* sensitivity to amphotericin B in a dual-species biofilm 187
5.2.10 *P. aeruginosa* does not induce an increase in *C. albicans* membrane ergosterol 189
5.2.11 *C. albicans* ergosterol biosynthesis is significantly downregulated in the presence of *P. aeruginosa* 194
4.2.12 There is significant downregulation of *C. albicans* superoxide dismutase genes in the presence of *P. aeruginosa* 196
5.2.13 The induction of reactive oxygen species potentiates amphotericin B activity against *C. albicans* biofilm cells 197
5.2.14 A *C. albicans sod2*Δ/Δ mutant strain has significantly enhanced susceptibility to amphotericin B 199
5.2.15 *P. aeruginosa* phenazines significantly potentiate amphotericin B activity against *C. albicans* biofilm cells 201
5.3 Discussion 205
6 DISCUSSION 216
6.1 Enhanced *P. aeruginosa* tolerance to meropenem in dual-species biofilms 217
6.1.1 Sequestration of meropenem by biofilm ECM molecules 217
6.1.2 Adherence of *P. aeruginosa* to fungal hyphae 219

6.1.3 Insights from transcriptomic data 221
6.1.3.1 Potential role of siderophores 221
6.1.3.2 Potential role of phenazines 222
6.1.3.3 Potential role of the OprD porin 222
6.2 Potentiation of amphotericin B activity against *C. albicans* in dual-species biofilms 223
6.2.1 Accumulation of intracellular ROS 223
6.2.1.1 Induction of ROS in *C. albicans* 223
6.2.1.2 Significant downregulation of *SOD2* in *C. albicans* 224
6.2.2 Inhibition of hyphal formation 226
6.2.3 Insights from transcriptomic data 227
6.2.3.1 Potential role of iron limitation 227
6.3 Clinical implications 228
6.4 Future perspectives 230
6.4.1 Enhancing *C. albicans* biofilm susceptibility to antifungals 230
6.4.2 A more clinically-relevant biofilm model 231
REFERENCES 233
APPENDIX I: PUBLICATIONS 263
APPENDIX II: DUAL-SPECIES RNA-SEQ SUPPLEMENTARY DATA 288
i. Sequence Quality & Mapping Statistics 288
ii. *P. aeruginosa* Significant DEGs: Comparison Between Single- and Dual-Species Responses to Meropenem 290
iii. *C. albicans* Significant DEGs: Response to *P. aeruginosa* in Untreated Biofilms 292
iv. *C. albicans* Significant DEGs: Response to *P. aeruginosa* in Meropenem-Treated Biofilms 311

LIST OF FIGURES

Figure 1.1	Virulence factors and antibiotic resistance mechanisms of *Pseudomonas aeruginosa*	10
Figure 1.2	Biofilm antimicrobial resistance mechanisms	18
Figure 1.3	Selected *C. albicans* pathogenesis and virulence mechanisms	29
Figure 1.4	Differences in biofilm architecture between different *Candida* species	36
Figure 1.5	Selected interactions between *P. aeruginosa* and *C. albicans*	48
Figure 2.1	GeneWiz® RNA sequencing library preparation workflow	61
Figure 3.1	*C. albicans* SC5314 increases the tolerance of *P. aeruginosa* PAO1 to meropenem in a dual-species biofilm	70
Figure 3.2	SEM analysis of biofilms of *P. aeruginosa* PAO1 and *C. albicans* SC5314	72
Figure 3.3	Three-dimensional reconstructions of biofilms from confocal z-stacks	73
Figure 3.4	Quantification of biofilm thickness from confocal microscopy images	74
Figure 3.5	Increased *P. aeruginosa* meropenem tolerance in the presence of *C. albicans* is biofilm-specific	76
Figure 3.6	Increased tolerance to meropenem is dependent on fungal viability	77
Figure 3.7	*C. dubliniensis* also enhances tolerance of *P. aeruginosa* to meropenem in dual-species biofilms	78
Figure 3.8	Mannan and glucan enhance *P. aeruginosa* biofilm tolerance to meropenem	80
Figure 3.9	*C. albicans* cell wall glycosylation is important for protection against meropenem	83
Figure 3.10	SEM analysis of biofilms of *P. aeruginosa* PAO1 and *C. albicans* cell wall glycosylation mutants	84
Figure 3.11	Increased tolerance of *P. aeruginosa* to meropenem is strain-specific and does not involve interactions with fungal chitin	87
Figure 3.12	*C. albicans* does not enhance *P. aeruginosa* tolerance to other antibiotics	91
Figure 3.13	*C. albicans* enhances meropenem tolerance of the *P. aeruginosa* CF (Midlands 1) isolate	93
Figure 4.1	Viable counts from the dual-species RNA-seq biofilm samples	103

Figure 4.2 Summary of transcriptional responses of *P. aeruginosa* biofilm cells to *C. albicans* and to meropenem treatment 106

Figure 4.3 Summary of transcriptional responses of *C. albicans* biofilm cells to *P. aeruginosa* and to meropenem treatment 107

Figure 4.4 Roadmap of results from RNA-seq analyses 108

Figure 4.5 Global transcriptional changes within single-species *P. aeruginosa* biofilm cells in response to meropenem treatment 111

Figure 4.6 Distribution of significantly differentially expressed *P. aeruginosa* genes in the Gene Ontology (GO) category Biological Process, in response to treatment of single-species biofilms with 5 µg/mL meropenem 112

Figure 4.7 Distribution of significantly differentially expressed *P. aeruginosa* genes in the Gene Ontology (GO) category Molecular Function, in response to treatment of single-species biofilms with 5 µg/mL meropenem 113

Figure 4.8 Distribution of significantly differentially expressed *P. aeruginosa* genes in the Gene Ontology (GO) category Cellular Component, in response to treatment of single-species biofilms with 5 µg/mL meropenem 114

Figure 4.9 KEGG pathways assigned to significantly differentially expressed *P. aeruginosa* genes, in response to treatment of single-species biofilms with 5 µg/mL meropenem 115

Figure 4.10 Global transcriptional changes within *P. aeruginosa* cells in response to meropenem treatment of dual-species *P. aeruginosa–C. albicans* biofilms 118

Figure 4.11 Distribution of significantly differentially expressed *P. aeruginosa* genes in the Gene Ontology (GO) category Biological Process, in response to meropenem treatment of dual-species *P. aeruginosa–C. albicans* biofilms 119

Figure 4.12 Distribution of significantly differentially expressed *P. aeruginosa* genes in the Gene Ontology (GO) category Molecular Function, in response to meropenem treatment of dual-species *P. aeruginosa–C. albicans* biofilms 120

Figure 4.13 Distribution of significantly differentially expressed *P. aeruginosa* genes in the Gene Ontology (GO) category Cellular Component, in response to meropenem treatment of dual-species *P. aeruginosa–C. albicans* biofilms 121

Figure 4.14 KEGG pathways assigned to significantly differentially expressed *P. aeruginosa* genes, in response to meropenem treatment of dual-species *P. aeruginosa–C. albicans* biofilms 122

Figure 4.15 *P. aeruginosa* genes that are significantly differentially expressed in response to meropenem treatment, between single- and dual-species biofilms 125

Figure 4.16 Global transcriptional changes within single-species *C. albicans* biofilm cells in response to meropenem treatment 127

Figure 4.17 Global transcriptional changes within *C. albicans* cells in response to meropenem treatment of dual-species *C. albicans*–*P. aeruginosa* biofilms 129

Figure 4.18 Global transcriptional changes within *P. aeruginosa* cells in response to the presence of *C. albicans* in untreated dual-species biofilms 133

Figure 4.19 Distribution of significantly differentially expressed *P. aeruginosa* genes in the Gene Ontology (GO) category Biological Process, in response to the presence of *C. albicans* in untreated dual-species biofilms 134

Figure 4.20 Distribution of significantly differentially expressed *P. aeruginosa* genes in the Gene Ontology (GO) category Molecular Function, in response to the presence of *C. albicans* in untreated dual-species biofilms 135

Figure 4.21 Distribution of significantly differentially expressed *P. aeruginosa* genes in the Gene Ontology (GO) category Cellular Component, in response to the presence of *C. albicans* in untreated dual-species biofilms 136

Figure 4.22 KEGG pathways assigned to significantly differentially expressed *P. aeruginosa* genes, in response to the presence of *C. albicans* in untreated dual-species biofilms 137

Figure 4.23 Global transcriptional changes within *P. aeruginosa* cells in response to the presence of *C. albicans* in meropenem-treated dual-species biofilms 139

Figure 4.24 Global transcriptional changes of *C. albicans* biofilm cells in response to the presence of *P. aeruginosa* in untreated dual-species biofilms 142

Figure 4.25 Distribution of significantly differentially expressed *C. albicans* genes in the Gene Ontology (GO) category Biological Process, in response to the presence of *P. aeruginosa* in untreated dual-species biofilms 143

Figure 4.26 Distribution of significantly upregulated and downregulated *C. albicans* genes in the Gene Ontology (GO) category Molecular Function, in response to the presence of *P. aeruginosa* in untreated dual-species biofilms 144

Figure 4.27 Distribution of significantly differentially expressed *C. albicans* genes in the Gene Ontology (GO) category Cellular Component, in response to the presence of *P. aeruginosa* in untreated dual-species biofilms 145

Figure 4.28 KEGG pathways assigned to significantly differentially expressed *C. albicans* genes, in response to the presence of *P. aeruginosa* in untreated dual-species biofilms 146

Figure 4.29 Global transcriptional changes of *C. albicans* biofilm cells in response to the presence of *P. aeruginosa* in meropenem-treated dual-species biofilms 149

Figure 4.30 Distribution of significantly differentially expressed *C. albicans* genes in the Gene Ontology (GO) category Biological Process, in response to the presence of *P. aeruginosa* in meropenem-treated dual-species biofilms 150

Figure 4.31 Distribution of significantly differentially expressed *C. albicans* genes in the Gene Ontology (GO) category Molecular Function, in response to the presence of *P. aeruginosa* in meropenem-treated dual-species biofilms 151

Figure 4.32 Distribution of significantly differentially expressed *C. albicans* genes in the Gene Ontology (GO) category Cellular Component, in response to the presence of *P. aeruginosa* in meropenem-treated dual-species biofilms 152

Figure 4.33 KEGG pathways assigned to significantly differentially expressed *C. albicans* genes, in response to the presence of *P. aeruginosa* in meropenem-treated dual-species biofilms 153

Figure 5.1 *P. aeruginosa* greatly enhances *C. albicans* sensitivity to amphotericin B, but has no effect on sensitivity to fluconazole 174

Figure 5.2 The presence of *P. aeruginosa* enhances amphotericin B sensitivity to a greater extent than lower *C. albicans* starting concentrations 176

Figure 5.3 Purified *P. aeruginosa* rhamnolipids do not enhance *C. albicans* sensitivity to amphotericin B 178

Figure 5.4 Increased *C. albicans* sensitivity to amphotericin B occurs more quickly in the presence of *P. aeruginosa* PAO1 than other *P. aeruginosa* strains 181

Figure 5.5 Potentiation of amphotericin B against *C. albicans* is specific to dual-species biofilms 182

Figure 5.6 Potentiation of amphotericin B activity against *C. albicans* is dependent on *P. aeruginosa* viability 183

Figure 5.7 Supernatants from mature biofilms have no effect on amphotericin B efficacy against *C. albicans* biofilm cells 185

Figure 5.8 *C. albicans* sensitivity to amphotericin B is also enhanced by *E. coli* MG1655 in a dual-species biofilm 187

Figure 5.9 *P. aeruginosa* PAO1 also increases *C. dubliniensis* sensitivity to amphotericin B in a dual-species biofilm 188

Figure 5.10 There is less potentiation of amphotericin B against *C. albicans upc2*Δ/Δ; a strain with lower membrane ergosterol levels 190

Figure 5.11 Fluorescence microscopy images of mono- and dual-species biofilms 192

Figure 5.12 Quantification of CTCF (Corrected Total Cell Fluorescence) from fluorescence microscopy images 193

Figure 5.13 Incubation with agents that increase intracellular ROS levels leads to potentiation of amphotericin B activity against *C. albicans* biofilm cells 199

Figure 5.14 Biofilms of a *C. albicans sod2*Δ/Δ knockout strain show significantly increased susceptible to amphotericin B 200

Figure 5.15 *P. aeruginosa* phenazines significantly potentiate amphotericin B activity against *C. albicans* biofilm cells 203

Figure 5.16 Potentiation of AmB activity is lost when *C. albicans* is co-incubated with *P. aeruginosa phz*Δ mutant strains 205

Figure 6.1 Proposed model for enhanced *P. aeruginosa* meropenem tolerance in a dual-species biofilm with *C. albicans* 220

Figure 6.2 Proposed model for potentiation of AmB activity against *C. albicans* cells in a dual-species biofilm with *P. aeruginosa* 226

LIST OF TABLES

Table 1.1	The WHO global priority pathogens list	2
Table 2.1	Bacterial species and strains used in this research	51
Table 2.2	Fungal species and strains used in this research	52
Table 4.1	Significantly differentially expressed *C. albicans* genes in response to meropenem treatment of dual-species *C. albicans*–*P. aeruginosa* biofilms	130
Table 5.1	Transcriptional changes to *C. albicans* ergosterol biosynthetic genes in response to the presence of *P. aeruginosa* in a dual-species biofilm	195
Table 5.2	Transcriptional changes to genes in the *C. albicans* 'removal of superoxide radicals' pathway, in response to the presence of *P. aeruginosa* in a dual-species biofilm	197

LIST OF ABBREVIATIONS

1-HP	1-hydroxyphenazine
3O-C_{12}-HSL	*N*-3-oxo-dodecanoyl-L-homoserine lactone (Las)
5MPCA	5-methyl phenazine-1-carboxylic acid betaine
ABC	adenosine triphosphate-binding cassette
AHL(s)	*N*-acyl-L-homoserine lactone(s)
AIDS	Acquired Immune Deficiency Syndrome
AmB	amphotericin B
AMR	antimicrobial resistance
ANOVA	analysis of variance
ATP	adenosine triphosphate
C_4-HSL	*N*-butyryl-L-homoserine lactone (Rhl)
Ca^{2+}	calcium ion
CDC	Centres for Disease Control
cDNA	complementary deoxyribonucleic acid
CF	Cystic Fibrosis
CFTR	Cystic Fibrosis Transmembrane conductance Regulator
CFU	colony-forming units
CGD	*Candida* Genome Database
Cu	copper
DEG(s)	differentially expressed gene(s)
DMEM	Dulbecco's Modified Eagle Medium
DNA	deoxyribonucleic acid

DNase	deoxyribonuclease
ECM	extracellular matrix
eDNA	extracellular deoxyribonucleic acid
EPS	extracellular polymeric substances
EV(s)	extracellular vesicle(s)
FDR	false discovery rate
Fe^{2+}	ferrous iron
Fe^{3+}	ferric iron
GC	guanine-cytosine
GO	gene ontology
H_2O_2	hydrogen peroxide
HIV	Human Immunodeficiency Virus
KEGG	Kyoto Encyclopaedia of Genes and Genomes
LB	lysogeny broth
LPS	lipopolysaccharide(s)
MDR	multi-drug resistant
MFS	major facilitator superfamily
Mg^{2+}	magnesium ion
MHB	Mueller Hinton broth
MIC(s)	minimum inhibitory concentration(s)
Mn	manganese
mRNA	messenger ribonucleic acid
MRSA	methicillin-resistant *Staphylococcus aureus*
N_2	nitrogen

NAC	non-*albicans Candida*
OD_{600}	optical density (absorbance at 600 nm wavelength)
OMV(s)	outer membrane vesicle(s)
ORF	open reading frame
Padj	adjusted P-value
PBP(s)	penicillin-binding protein(s)
PBS	phosphate-buffered saline
PCA	phenazine-1-carboxylic acid
PC	principal component
PCN	phenazine-1-carboxamide
PCR	polymerase chain reaction
Pel	pellicle formation
PFA	paraformaldehyde
PMS	phenazine methosulfate
PQS	*Pseudomonas* quinolone signal
Psl	polysaccharide synthesis locus
PYO	pyocyanin
QS	quorum sensing
RNA	ribonucleic acid
RNA-seq	ribonucleic acid sequencing
RND	resistance-nodulation division
RNS	reactive nitrogen species
ROS	reactive oxygen species
rpm	revolutions per minute

RPMI	Roswell Park Memorial Institute Medium
rRNA	ribosomal ribonucleic acid
RSCV(s)	rugose small colony variant(s)
SAP(s)	secreted aspartyl proteinase(s)
SEM	scanning electron microscopy
SEM	standard error of the mean
SOD(s)	superoxide dismutase(s)
TCA	tricarboxylic acid cycle
VAP	ventilator-associated pneumonia
VVC	vulvovaginal candidiasis
WHO	World Health Organisation
YPD	yeast extract peptone dextrose
Zn	zinc

1 INTRODUCTION

1.1 ANTIMICROBIAL RESISTANCE – A GLOBAL CHALLENGE

The incidence of antimicrobial resistance (AMR) in pathogens that are important to human health has seen an inexorable increase since the first antibiotic, penicillin, was launched in the 1940s (Hutchings *et al.*, 2019). No new classes of antibiotic have been discovered since the 1980s. In 2016, the O'Neill report on AMR was released, which estimates that 10 million deaths per year will be attributed to drug-resistant infections by the year 2050 (O'Neill, 2016), unless steps are taken to address the problem. However, this prediction has been criticised by some as unreliable and sensationalist, as it was modelled using uncertain estimates of the current global burden of AMR, and was based on the assumption that all infections will be drug-resistant by 2050, which is unlikely to be the case (de Kraker *et al.*, 2016). Some of the next steps suggested in the O'Neill report include: increasing public awareness of AMR; reducing unnecessary use of existing antimicrobials; improving global surveillance of drug resistance and antimicrobial consumption; and promoting the development of new rapid diagnostic technologies, and alternatives to antibiotics (O'Neill, 2016). Also in 2016, the World Health Organisation (WHO) released a global priority pathogens list, identifying the antibiotic-resistant bacteria against which research and development of new therapeutics is most urgently needed, excluding *Mycobacterium tuberculosis*, which is already considered a global priority (World Health Organisation, 2017). The list was split into three tiers of priority: critical, high and medium (Table 1.1). Although the report focused on bacteria, the fungus *Candida auris* recently became the first fungal pathogen to be considered a global health threat

(Mahmoudi *et al.*, 2019). Drug-resistant *C. auris* has now been added to the "urgent threats" list by the Centers for Disease Control and Prevention (CDC) in the USA, whilst drug-resistant *Candida* are considered a "serious threat" (Centers for Disease Control and Prevention, 2019).

Table 1.1. The WHO global priority pathogens list. The antibiotic-resistant bacteria for which the research & development of new and effective antibiotic treatments is a priority (World Health Organisation, 2017).

Priority Tier	Bacterial species	Antibiotic resistance profile
1. CRITICAL	*Acinetobacter baumannii*	Carbapenem-resistant
	Pseudomonas aeruginosa	Carbapenem-resistant
	Enterobacteriaceae	Carbapenem-resistant; 3rd generation cephalosporin-resistant
2. HIGH	*Enterococcus faecium*	Vancomycin-resistant
	Staphylococcus aureus	Methicillin-resistant; Vancomycin intermediate and resistant
	Helicobacter pylori	Clarithromycin-resistant
	Campylobacter	Fluoroquinolone-resistant
	Salmonella spp.	Fluoroquinolone-resistant
	Neisseria gonorrhoeae	Fluoroquinolone-resistant; 3rd generation cephalosporin-resistant
3. MEDIUM	*Streptococcus pneumoniae*	Penicillin-non-susceptible
	Haemophilus influenzae	Ampicillin-resistant
	Shigella spp.	Fluoroquinolone-resistant

1.2 *PSEUDOMONAS AERUGINOSA*

Pseudomonas aeruginosa is an opportunistic, Gram-negative, bacterial pathogen that infects a large range of hosts, including humans, mice, nematodes, insects, plants and amoebae (Feinbaum *et al.*, 2012). *P. aeruginosa* can also survive in abiotic environments, such as in water and soil, and on surfaces within hospitals (Feinbaum *et al.*, 2012). In humans, *P. aeruginosa* causes disease in cases of epithelial damage or immunocompromised patients, affecting a variety of sites within the body. Infection sites include surgical and burn wounds, skin and soft tissues, the cornea, the brain, the heart, the bloodstream and the respiratory tract (Dubern *et al.*, 2015). *P. aeruginosa* causes both acute and chronic infections, depending on the site of infection (Feinbaum *et al.*, 2012).

1.2.1 Clinical importance

Prior to the 1980s, *P. aeruginosa* was mainly associated with the infection of burn wounds, but it has now become a major nosocomial pathogen, accounting for around 10% of all hospital-acquired infections worldwide (Chatterjee *et al.*, 2016). *P. aeruginosa* is also a key pathogen of Cystic Fibrosis (CF) patients, many of whom are thought to become infected by *P. aeruginosa* within the first three years of life, with 70–80% becoming chronically infected by their teenage years (Lyczak *et al.*, 2002). CF is caused by a mutation affecting the function of the CFTR (Cystic Fibrosis Transmembrane conductance Regulator) protein, thus preventing the efficient movement of chloride ions out of epithelial cells, resulting in dehydration and thickening of the mucus layer lining these cells (La Rosa *et al.*, 2019). Thick mucus is not easily moved by the beating of cilia, so provides an ideal environment for microbes to cause

chronic infection. Consequently, CF patients receive long-term antibiotic treatment; however, this promotes the development of increased resistance to antibiotics amongst CF lung microbes (Davies and Davies, 2010).

1.2.2 Pathogenesis and virulence mechanisms

Whether *P. aeruginosa* infection is acute or chronic has a significant impact upon disease prognosis and treatment options. An acute infection, such as a burn wound infection, can quickly become systemic via the bloodstream and can cause death in a matter of days. However, chronic infections, such as in CF lungs, resist clearance efforts by both immune responses and antibiotic treatment, and can persist for years (Crousilles *et al.*, 2015). In cases where *P. aeruginosa* causes chronic infection, isolated strains exhibit greater resistance to antibiotics (e.g. tobramycin, meropenem and ciprofloxacin), relative to strains isolated from acute infection sites. This effect is also correlated with mode of growth; biofilm cells are more resistant to antibiotics than planktonic cells (Sherrard *et al.*, 2014). The versatility of *P. aeruginosa* is due, in large part, to its substantive arsenal of secreted virulence factors and the presence of at least six different types of secretion system (Crousilles *et al.*, 2015, Jurado-Martin *et al.*, 2021).

1.2.2.1 Quorum sensing

Many *P. aeruginosa* virulence factors are regulated by quorum sensing (QS), which refers to signalling pathways that govern microbial group behaviours via cell–cell communication. The *P. aeruginosa* QS signal molecules are of two types: *N*-acyl-L-homoserine lactones (AHLs) and alkyl quinolones (AQs) (Jakobsen *et al.*, 2013,

Chatterjee *et al.*, 2020). All *P. aeruginosa* cells secrete these signal molecules, also known as autoinducers (AIs), at a basal level; when the bacterial population size increases, the AI concentrations exceed a threshold level and activate specific transcriptional regulators, which in turn regulate the transcription of specific sets of genes (Chatterjee *et al.*, 2020, Thi *et al.*, 2020). In the early exponential phase of *P. aeruginosa* growth, QS signalling cascades are activated by two AHLs: Las (3O-C_{12}-HSL, *N*-3-oxo-dodecanoyl-L-homoserine lactone) and Rhl (C_4-HSL, *N*-butyryl-L-homoserine lactone). Las and Rhl bind and activate the transcriptional regulators, LasR and RhlR, respectively. LasR induces transcription of *lasI*, which encodes a synthase for further production of Las, whilst RhlR induces transcription of *rhlI*, which encodes the synthase for further production of Rhl. LasR is also able to induce transcription of the *rhlR* gene, connecting the two signalling cascades (Thi *et al.*, 2020, Chatterjee *et al.*, 2020). A third *P. aeruginosa* QS system is associated with the late exponential phase of growth and with iron limitation (Thi *et al.*, 2020); it involves the AQ autoinducer molecule, PQS (*Pseudomonas* quinolone signal, 2-heptyl-3-hydroxy-4-quinolone). PQS binds to the PqsR transcriptional regulator, which activates transcription of *pqsABCDEH* genes, increasing production of PQS. PqsR production is activated by LasR, but inhibited by RhlR; meanwhile, PqsR can activate production of RhlR, thus interconnecting all three *P. aeruginosa* QS systems (Thi *et al.*, 2020, Chatterjee *et al.*, 2020). A fourth QS system was recently proposed, called IQS (2-(2-hydroxyphenyl)-thiazole-4-carbaldehyde), but the candidate molecule was subsequently shown to be an aeruginaldehyde, which is a by-product in the biosynthetic pathway of the siderophore, pyochelin (Thi *et al.*, 2020, Chatterjee *et al.*, 2020).

The sets of genes that are regulated by the QS transcriptional regulators, Las, Rhl and PQS, include numerous virulence factors and, consequently, QS mutants exhibit vastly reduced levels of virulence *in vivo* (Crousilles *et al.*, 2015). Gene products regulated by QS include siderophores, phenazines, proteases, lipases, exotoxins, rhamnolipids, exoenzymes, exopolysaccharides, hydrogen cyanide and lectins (Thi *et al.*, 2020, Chatterjee *et al.*, 2020, Jakobsen *et al.*, 2013). In fact, it is thought that the expression of approximately 4–6% of all *P. aeruginosa* genes is regulated by QS (Jakobsen *et al.*, 2013).

1.2.2.2 Siderophores

Siderophores are small molecules that can chelate free iron from the environment (Figure 1.1). *P. aeruginosa* produces two siderophores: pyoverdine and pyochelin. Pyoverdine is the major siderophore, and is essential for *P. aeruginosa* colonisation of the CF lung (O'Brien and Fothergill, 2017). Pyochelin is structurally different to pyoverdine, and is thought to be the siderophore with the lowest molecular weight of all known bacterial or fungal siderophores (Chatterjee *et al.*, 2020). Pyochelin is thought to have high affinity for zinc, as well as iron, and potentially plays a role in inducing oxidative stress within host cells (Chatterjee *et al.*, 2020).

1.2.2.3 Phenazines

Phenazines are small cyclic molecules, which produce pigments and are redox-active. The *P. aeruginosa* phenazine biosynthetic genes are regulated by QS (Higgins *et al.*, 2018). *P. aeruginosa* produces four main phenazines: phenazine-1-carboxylic

acid (PCA), pyocyanin (PYO), phenazine-1-carboxamide (PCN) and 1-hydroxyphenazine (1-HP). A fifth, less stable phenazine molecule is also made as an intermediate product, called 5-methyl phenazine-1-carboxylic acid betaine (5MPCA) (Mavrodi *et al.*, 2001). PCA is the predominant phenazine produced by clinical isolates of *P. aeruginosa*, and the concentrations of PYO in CF sputum can be as high as 135 μM (Chatterjee *et al.*, 2020). Phenazine molecules can diffuse across cell membranes of host cells or competing microbes and disrupt intracellular electron flow; for example, in eukaryotic cells, phenazines disrupt oxidative phosphorylation at the mitochondrial inner membrane, leading to the generation of intracellular reactive oxygen species (ROS) and reactive nitrogen species (RNS), resulting in oxidative damage (Figure 1.1) (Chatterjee *et al.*, 2020).

1.2.2.4 Exotoxins and exoenzymes

Among the many secreted virulence factors produced by *P. aeruginosa* are exotoxins A, S, T, U and Y (Figure 1.1). Exotoxin A inhibits host cell protein synthesis, making it one of the most toxic of all the *P. aeruginosa* virulence factors (Chatterjee *et al.*, 2016, Michalska and Wolf, 2015). Exotoxin U is also highly potent, with phospholipase activity, which causes damage to host cell membranes, leading to cell death (Sato and Frank, 2004). Exotoxins S, T and Y affect the actin cytoskeleton of host cells, which can disrupt phagocytic activity and affect host invasion dynamics (Engel and Balachandran, 2009).

P. aeruginosa secretes several proteases (Figure 1.1), including alkaline protease (AprA), which inhibits host immune system functions, such as phagocytosis and the

activation of the complement pathway (Chatterjee *et al.*, 2016). Protease IV (PrpL) can cleave a number of immunologically important proteins, including immunoglobulins, complement proteins and fibrinogen (Engel *et al.*, 1998). LasA is a zinc metalloprotease and LasB is an elastase, which breaks down elastin and leads to host tissue damage (Chatterjee *et al.*, 2020). *P. aeruginosa* secretes three types of phospholipase C; one with haemolytic activity (PlcH) and two without (PlcN and PlcB) (Filloux, 2011). Inhibition of the haemolytic phospholipase C can protect lung function in a mouse model of lung infection (Wargo *et al.*, 2011), demonstrating its importance in *P. aeruginosa* infections of the lung.

1.2.2.5 Secretion systems

Six *P. aeruginosa* secretion systems are currently described, with roles in delivering virulence factors to extracellular spaces or directly into neighbouring cells (Chatterjee *et al.*, 2020). The type I secretion system (T1SS) secretes AprA and the heme acquisition protein, HasAp (Chatterjee *et al.*, 2020, Filloux, 2011). Among the proteins secreted by the type II secretion system (T2SS) are ExoA, LasA, LasB, PlcH, PlcN, PlcB, lipases (LipA and LipB) and chitin-binding protein (CbpD) (Chatterjee *et al.*, 2020, Filloux, 2011). The type III secretion system (T3SS) is responsible for secretion of Exotoxins S, T, U and Y (Filloux, 2011). Unlike the others, the type IV secretion system (T4SS) is not thought be involved in the secretion of virulence factors, but is associated with horizontal gene transfer (Chatterjee *et al.*, 2020). The type V secretion system (T5SS) secretes an esterase (EstA) that is involved in rhamnolipid production, as well as adhesins (Filloux, 2011), indicating important roles in biofilm formation and cell adhesion (Chatterjee *et al.*, 2020). The proteins that make up the

type VI secretion system (T6SS) machinery are encoded by three different gene clusters, called haemolysin co-regulated protein (Hcp) secretion islands I, II and III (H1-T6SS, H2-T6SS and H3-T6SS) (Filloux, 2011). The T6SS is associated with *P. aeruginosa* virulence and communication with neighbouring bacterial cells (Chatterjee *et al.*, 2020). The genes encoding T6SS proteins are more highly expressed in biofilm cells than planktonic cells (Chen *et al.*, 2020), suggesting a role for this secretion system in biofilm formation.

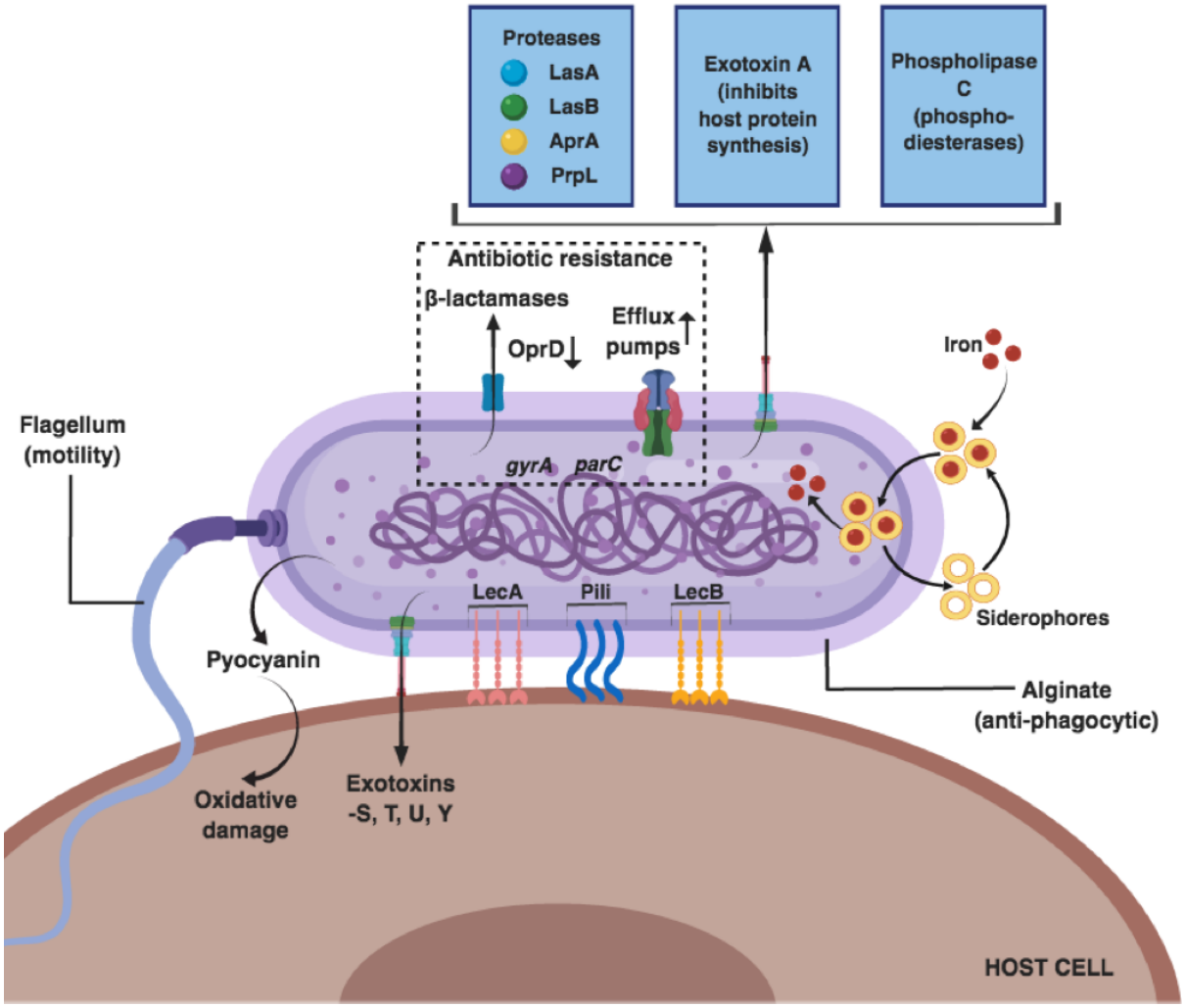


Figure 1.1. Virulence factors and antibiotic resistance mechanisms of *Pseudomonas aeruginosa*. Virulence factors produced by *P. aeruginosa* include proteases (LasA, LasB, AprA and PrpL), exotoxins (A, S, T, U and Y), phospholipase C, siderophores (pyoverdine and pyochelin), and phenazines (e.g. pyocyanin). Factors that promote cell–cell adhesion include pili and lectins (LecA and LecB), while the exopolysaccharide alginate aids in immune evasion. *P. aeruginosa* antibiotic resistance mechanisms include the secretion of ß-lactamase enzymes, reduced production of the OprD porin, upregulation of efflux pump genes, and mutations in the genes encoding DNA gyrase (*gyrA*) and topoisomerase IV (*parC*). Based on work by Chatterjee *et al.* (2016). Figure created with BioRender.com.

1.2.3 Antibiotic resistance

Many strains of *P. aeruginosa* have become resistant to most classes of antibiotic over the past few decades (Dubern *et al.*, 2015). The World Health Organisation lists carbapenem-resistant *P. aeruginosa* as a “critical priority pathogen” for which the research and development of antibiotics is urgently required (World Health Organisation, 2017). The antibiotic resistance mechanisms employed by *P. aeruginosa* are numerous and varied (Figure 1.1).

I. Beta-lactamase enzymes

Some *P. aeruginosa* strains produce their own ß-lactamase enzymes, including extended-spectrum ß-lactamases (ESBLs) and metallo-ß-lactamases, whilst other strains acquire genes encoding ß-lactamase enzymes via horizontal gene transfer. The ß-lactamase enzymes TEM, OXA and PSE can confer resistance to carbapenems and some cephalosporins, such as ceftazidime (Chatterjee *et al.*, 2016, Rodríguez-Martínez *et al.*, 2009).

II. Efflux pumps

Resistance to ß-lactam antibiotics is also provided by efflux pumps in *P. aeruginosa*, which act to remove the antibiotic molecules from within cells (Figure 1.1). Upregulation of genes encoding the MexAB-OprM pump increases resistance to aminoglycosides, carbapenems and cephalosporins (Fusté *et al.*, 2013), whilst increased production of MexEF-OprN and MexCD-OprJ pumps increases resistance to fluoroquinolones (Chatterjee *et al.*, 2016).

III. Reduced outer membrane permeability

The high levels of AMR in *P. aeruginosa* are often explained by reduced outer membrane permeability, as *P. aeruginosa* does not contain any general diffusion porins, unlike many other bacterial species (Fusté *et al.*, 2013). Membrane permeability is further reduced by downregulation of expression of the *oprD* porin gene, which can confer resistance to imipenem, or inactivation of the OprD porin protein, which reduces the effectiveness of meropenem. This is because the OprD porin acts as a route through which these carbapenem antibiotics enter *P. aeruginosa* cells (Figure 1.1) (Chatterjee *et al.*, 2016, Fusté *et al.*, 2013, Rodríguez-Martínez *et al.*, 2009).

IV. Resistance mutations

Finally, mutations in the *gyrA* gene, encoding DNA gyrase, and the *parC* gene, encoding topoisomerase IV, give rise to quinolone resistance (Figure 1.1) (Fusté *et al.*, 2013). Despite being a last-resort antibiotic, due to its toxicity, colistin is the only drug with which the most resistant strains of *P. aeruginosa* can be treated, when carbapenems fail (Chatterjee *et al.*, 2016). This is of clinical importance because around 45% of CF patients are colonised with multi-drug resistant (MDR) strains of *P. aeruginosa*, which are correlated with a greater decline in lung function when compared to patients infected by more susceptible strains (Sherrard *et al.*, 2014).

1.2.3.1 Meropenem

Of the various classes of ß-lactam antibiotics, carbapenems are the class with the highest potency and the broadest spectrum of activity. This is because

carbapenems have a high binding affinity for penicillin-binding proteins (PBPs) and are stable against the action of ß-lactamase enzymes (Papp-Wallace *et al.*, 2011). Carbapenems cannot easily diffuse through bacterial cell walls, but enter through outer-membrane porins, after which the drug traverses the periplasm, binding and inhibiting the peptidase domain of PBPs. This results in weakening of peptidoglycan structure, eventually leading to bacterial cell death via osmotic lysis (Papp-Wallace *et al.*, 2011). The carbapenem meropenem is the first-line antibiotic for the treatment of *P. aeruginosa* infections in the CF lung, for which it is often combined with tobramycin (Cystic Fibrosis Trust, 2009).

The main ways in which *P. aeruginosa* resistance to meropenem can arise are via loss of the OprD outer-membrane porin, upregulation of the MexAB-OprM efflux pump, or acquisition of carbapenemase-encoding genes through horizontal gene transfer (Botelho *et al.*, 2019, Fusté *et al.*, 2013). *P. aeruginosa* also has chromosomally-encoded ß-lactamase enzymes, which are overproduced when biofilm cells are treated with ß-lactam antibiotics (Høiby *et al.*, 2010). Loss of OprD results in a 4– to 32–fold increase in resistance to meropenem (Fowler and Hanson, 2014). As well as mutations, inactivation of the *oprD* porin gene can also be caused by the transposition of insertion sequence (IS) elements into the *oprD* gene or its promoter region (Fowler and Hanson, 2014). The MexAB-OprM efflux pump belongs to the resistance-nodulation-division (RND) superfamily of efflux pumps. In *P. aeruginosa*, upregulation of efflux is caused by mutations in genes encoding transcriptional regulatory proteins (Papp-Wallace *et al.*, 2011). An additional mechanism associated with increased resistance to meropenem is downregulation of PBP production, through mutations in

the genes encoding these proteins (Rodríguez-Martínez *et al.*, 2009, López-Causapé *et al.*, 2017). The mechanisms leading to meropenem resistance in *P. aeruginosa* are frequently multifactorial, involving a combination of these (Rodríguez-Martínez *et al.*, 2009).

The acquisition of carbapenem-resistant *P. aeruginosa* in hospitals is associated with admission to ICU (intensive care unit) or prior antibiotic use, specifically piperacillin-tazobactam, vancomycin or carbapenems (Raman *et al.*, 2018). In ICUs, the prevalence of carbapenem-resistance in *P. aeruginosa* isolates can be as high as 27.7% (Botelho *et al.*, 2019), presenting a major treatment challenge. Furthermore, ß-lactam-resistant strains of *P. aeruginosa* are frequently found in the CF lung (Høiby *et al.*, 2010).

1.2.4 Biofilms

Biofilms are structured communities of microbial cells, which are ensnared within a matrix of extracellular polymeric substances (EPS), including polysaccharides, proteins, extracellular DNA (eDNA) and lipids (Lindsay and Hogan, 2014). It is thought that 80% of all microbial infections in humans are biofilm-related (Lohse *et al.*, 2018, Van Acker *et al.*, 2014, Rodrigues *et al.*, 2019). Biofilms can be formed by both bacteria and fungi on the surfaces of infected tissue, including the oral cavity, the vulvovaginal region, the gastrointestinal tract, the lungs, on burn wounds, and on the surfaces of medical devices, such as catheters (Lohse *et al.*, 2018).

The process of biofilm formation is similar across kingdoms and can be viewed as cyclical. Cells first adhere to a substrate and initiate biofilm formation. The cells then proliferate to form a mature biofilm that is encased within secreted extracellular matrix (ECM) material. Some cells are then able to disperse from the biofilm and seed new infection sites (Lohse *et al.*, 2018). The initial attachment stage is reversible until ECM components (polysaccharides, proteins, eDNA) are produced, which provide structural support to form a firmer attachment to the substrate (Van Acker *et al.*, 2014).

1.2.4.1 *Pseudomonas aeruginosa* biofilm composition

P. aeruginosa biofilms have been studied extensively, due to their clinical impact; biofilm formation is the most important survival strategy of *P. aeruginosa* in the CF lung (Høiby *et al.*, 2010). The initial attachment of *P. aeruginosa* cells to a substrate is mediated by surface structures, such as pili and flagella, proteins, such as the lectins, LecA and LecB (Figure 1.1), and extracellular polysaccharides. Polysaccharides are the key components during the development and growth of *P. aeruginosa* biofilms, whilst extracellular DNA is important for providing structural stability to the mature biofilm matrix (Mann and Wozniak, 2012).

Alginate is an abundant polysaccharide in *P. aeruginosa* biofilms. It provides structural support to the biofilm matrix, due to the rigidity provided by numerous ß-1,3 and ß-1,4 bonds between the L-guluronic and D-mannuronic acid monomers. Overproduction of alginate, mediated by mutation of *mucA*, is frequently observed in *P. aeruginosa* biofilm cells isolated from CF lungs, giving these strains a mucoid phenotype (Mann and Wozniak, 2012). Alginate's ability to sequester reactive oxygen species enables

mucoid *P. aeruginosa* strains from resisting phagocytosis by host immune cells (Figure 1.1), promoting persistent infection (Høiby *et al.*, 2010). Therefore, overproduction of alginate provides a selective advantage to *P. aeruginosa* cells in a CF lung environment.

However, alginate is not essential for *P. aeruginosa* biofilm formation; in non-mucoid strains, the polysaccharides Psl (polysaccharide synthesis locus) and Pel (pellicle formation) play key roles in biofilm formation and matrix structural integrity (Jennings *et al.*, 2015). Both Psl and Pel can be cell-associated or secreted into the biofilm ECM. Psl is an uncharged polysaccharide, which comprises pentasaccharide monomers composed of D-mannose, L-rhamnose and D-glucose molecules in a 3:1:1 ratio (Mann and Wozniak, 2012, Passos da Silva *et al.*, 2019). The structure of Pel is currently undefined, but it is known to be cationic, and composed of *N*-acetylgalactosamine and *N*-acetylglucosamine, joined by 1,4-glycosidic bonds (Jennings *et al.*, 2015). *P. aeruginosa* PA14 strains are unable to produce Psl, so Pel is the most abundant polysaccharide. Conversely, in PAO1 strains, Psl is the main polysaccharide, though some Pel is produced too, and both promote cell–cell adhesion and structural stability of the ECM. There are also *P. aeruginosa* strains called rugose small colony variants (RSCVs), which overproduce both Psl and Pel, and show enhanced adherence and aggregation. RSCVs are frequently isolated from biofilms, both *in vitro* and *in vivo* (Mann and Wozniak, 2012, Jennings *et al.*, 2015).

Both Pel and Psl interact with other molecules to enhance the stability of the *P. aeruginosa* biofilm matrix. Extracellular DNA (eDNA) is released into the *P. aeruginosa*

biofilm matrix from cells that have undergone programmed cell death. Pel can cross-link eDNA, via ionic binding enabled by their opposing charges, forming a web-like structure that provides extra structural support, especially in *P. aeruginosa* strains that lack Psl (Jennings *et al.*, 2015). The *P. aeruginosa* lectin, LecB, binds to the mannose side-chains of Psl, coordinating the localisation of Psl, enhancing cell retention, and promoting the structural integrity of the biofilm matrix (Passos da Silva *et al.*, 2019).

Other *P. aeruginosa* biofilm matrix components include cyclic ß-glucans, lipopolysaccharides (LPS), outer membrane vesicles (OMVs), proteins, and rhamnolipids. Rhamnolipids are glycolipid biosurfactants (biological surface-active agents) composed of L-rhamnose and ß-hydroxydecanoic acid, which can induce a destabilising effect on the cell membranes of neighbouring cells (Mann and Wozniak, 2012, Chatterjee *et al.*, 2020). They are produced at a mature stage of *P. aeruginosa* biofilm development, under the control of QS signals, and can exist as mono-rhamnolipids and di-rhamnolipids (Thi *et al.*, 2020, Chatterjee *et al.*, 2020). Rhamnolipids are thought to play a role in the maintenance of fluid-filled channels within the biofilm architecture, through disruption of cell–cell and cell–surface interactions (Davey *et al.*, 2003), as well as facilitating the detachment of *P. aeruginosa* cells from mature biofilms (Chatterjee *et al.*, 2020). High concentrations of rhamnolipids are observed in sputum samples from CF patients with chronic *P. aeruginosa* infection, but the significance of rhamnolipid production on disease severity is unclear (Mann and Wozniak, 2012).

1.2.4.2 Bacterial biofilm-specific resistance mechanisms

Biofilm cells are generally less susceptible to antimicrobials than planktonic cells; MICs (minimum inhibitory concentrations) for biofilm cells can be 100 to 1,000× greater than for planktonic cells (Hill *et al.*, 2005, Mah, 2012). The decreased susceptibility of biofilms to antimicrobials is due to multifactorial resistance mechanisms (Figure 1.2), which vary depending on the antimicrobial drug, the microbial strain and species, the age or stage of the biofilm, and the growth conditions (Stewart, 2015, Van Acker *et al.*, 2014, Mah, 2012). The mechanisms discussed below are illustrated by examples from *P. aeruginosa* biofilms.

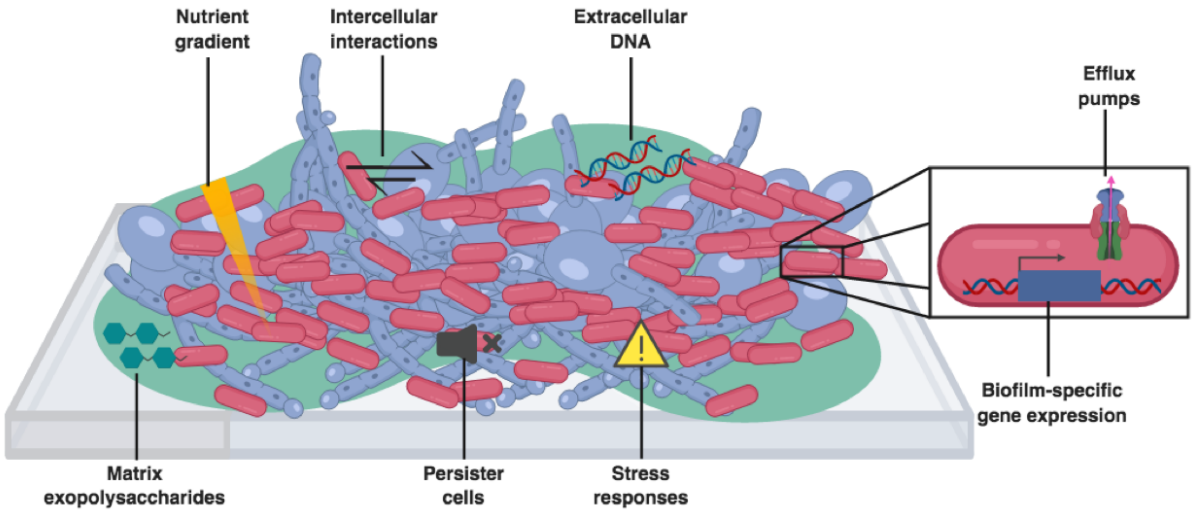


Figure 1.2. Biofilm antimicrobial resistance mechanisms. The range of antimicrobial resistance mechanisms employed by biofilm cells include persister cells, matrix exopolysaccharides, nutrient gradients, intercellular interactions, stress responses, efflux pumps, biofilm-specific gene expression and extracellular DNA. Based on work by Hall and Mah (2017). Figure created with BioRender.com.

I. Persister cells

The cells that remain after antimicrobial treatment are known as persister cells, which are dormant cells with little or no metabolic activity and which therefore have

inactive drug targets (Mah, 2012). Persister cells can be found in both planktonic and biofilm cultures for the majority of bacterial species (LaFleur *et al.*, 2006).

Another mechanism by which persister cells have decreased susceptibility to antimicrobials is by avoiding antimicrobial-induced production of reactive oxygen species (ROS). The actions of some antibiotics are enhanced by the induction of lethal levels of ROS (Dwyer *et al.*, 2015); this is a result of hyperactivation of the electron transport chain, which stimulates superoxide production, resulting in damage to iron-sulphur (Fe-S) clusters within proteins. This occurs by oxidation of Fe^{2+} to form Fe^{3+}, and the production of hydroxyl radicals (•OH), which can damage DNA and lead to cell death (Imlay, 2013, Dwyer *et al.*, 2009). In some bacterial species, persister cells can reduce the production of ROS and •OH, e.g. *Burkholderia cenocepacia* persister cells downregulate the TCA (tricarboxylic acid) cycle to achieve this (Hall and Mah, 2017, Van Acker *et al.*, 2013).

II. Matrix exopolysaccharides

The idea that antimicrobials generally show poor diffusion through biofilm layers has decreasing support, as culture conditions and biofilm thickness also both affect diffusion rate (Hall and Mah, 2017). Fluoroquinolones, such as ofloxacin and ciprofloxacin, are able to penetrate all layers of *P. aeruginosa* biofilms (Walters *et al.*, 2003). Where antibiotics do show poor movement through biofilms, it is actually due to sequestration rather than poor diffusion rates. In alginate-producing mucoid strains of *P. aeruginosa*, aminoglycoside antibiotics, such as gentamicin and tobramycin, penetrate the biofilm matrix more slowly than ß-lactam antibiotics, due to binding of

aminoglycosides to alginate in the outer layers of the biofilm (Van Acker *et al.*, 2014). Both alginate and Psl are overproduced by *P. aeruginosa* strains isolated from the CF lung (Rossi *et al.*, 2020). Although Psl is an uncharged molecule, it can provide resistance to cationic antimicrobial compounds, such as colistin and tobramycin (Jennings *et al.*, 2015, Beaudoin *et al.*, 2017).

III. Nutrient gradient

The rate of diffusion of antimicrobials through a biofilm is important because the cells are not mixing as they would in a planktonic culture, where the mixing action ensures uniform environmental conditions so that all cells are exposed to the full dose. Rather, cells deeper within the biofilm may initially get very low exposure to the antimicrobial, affording them time to mount a defence response (Hall and Mah, 2017, Jefferson *et al.*, 2005). Biofilm formation results in stratifications (Walters *et al.*, 2003), whereby different layers have differing levels of oxygen, nutrients, metabolic activity and growth, thus creating microenvironments (Hall and Mah, 2017, Mah, 2012). This heterogeneity means that the metabolically active, dividing cells at the upper surface are more sensitive to antibiotics, relative to cells located more deeply within the biofilm structure (Flemming and Wingender, 2010, Hill *et al.*, 2005, Walters *et al.*, 2003).

IV. Intercellular interactions

Both *lasR* and *rhlR* encode molecules that are essential to *P. aeruginosa* QS signalling pathways. When both are knocked out, biofilm cells show increased resistance to tobramycin (Bjarnsholt *et al.*, 2005). The process of quorum-quenching involves removal of QS molecules once a biofilm has already established. This is

necessary because QS mutants form scant biofilms, which are not comparable to wild-type biofilm structures. Quorum-quenching has demonstrated an increase in biofilm susceptibility to antibiotics (Hall and Mah, 2017), demonstrating the importance of QS in biofilm resistance.

Intercellular interactions within biofilms can be intra– or interspecies. As well as QS, these interactions can also involve transfer of plasmids via conjugation. This is likely to be more efficient in biofilms than it is in planktonic cultures, due to the cells being both sessile and in closer proximity during this mode of growth (Savage *et al.*, 2013). Interactions may also involve the mobilisation of integrons that contain antibiotic resistance genes, or simply the acquisition of eDNA from the environment (Hall and Mah, 2017).

V. Stress responses

The stringent response is a highly conserved signalling pathway that enables bacteria to survive in conditions of nutrient limitation (Hauryliuk *et al.*, 2015). The stringent response may be responsible for reducing antibiotic-induced oxidative stress in bacterial biofilm cells, by maintaining high catalase and superoxide dismutase (SOD) activity; this has been observed in *P. aeruginosa* in response to nutrient limitation (Khakimova *et al.*, 2013). This suggests that nutrient supplementation may increase the susceptibility of biofilm cells to antibiotics (Hall and Mah, 2017).

VI. Efflux pumps

There are over 12 operons encoding resistance-nodulation division (RND) pumps within the *P. aeruginosa* genome, which are implicated in the efflux of a wide range of antibiotic drugs (Fernandez and Hancock, 2012). Efflux pumps are known to play a role in planktonic cell resistance to antibiotics, but there is increasing evidence for a role in biofilm resistance too (Hall and Mah, 2017). Of particular interest is the heterogeneous expression of the genes encoding the MexAB-OprM and MexCD-OprJ pumps; they are more highly expressed in cells closer to the outer edges of biofilms (De Kievit *et al.*, 2001). The *P. aeruginosa* MexCD-OprJ pump may be a biofilm-specific defence mechanism against azithromycin; when planktonic and sessile cells are exposed to azithromycin, *mexC* is only expressed in the sessile cells, which do not express it in the absence of the drug (Gillis *et al.*, 2005).

VII. Biofilm-specific gene expression

There is differential expression of genes when cells switch from planktonic to biofilm growth (Mah, 2012). AmpC is a ß-lactamase enzyme that is encoded by the *P. aeruginosa* chromosome, and is secreted into the biofilm matrix, preventing antibiotics from reaching cells within the biofilm (Bagge *et al.*, 2000). Its expression is induced by the presence of ceftazidime and imipenem. Mature biofilms show increased resistance to ceftazidime and meropenem compared to younger ones, which may be due to the accumulation of ß-lactamase over time, in the biofilm matrix (Bowler *et al.*, 2012).

The *ndvB* gene in *P. aeruginosa* encodes the membrane-bound NdvB glucosyltransferase enzyme. This enzyme catalyses the production of cyclic ß-1,3-

glucans, which are released into the periplasm or secreted into the biofilm matrix (Sadovskaya *et al.*, 2010). These glucans contain a negative charge, which allows them to interact with cationic antibiotics, and they have been observed to bind and sequester kanamycin in the periplasm (Sadovskaya *et al.*, 2010). Expression of the *ndvB* transcript is 20x higher in biofilm cells than in planktonic cells; furthermore, when the gene is deleted, cells show decreased tolerance to several antibiotics (Beaudoin *et al.*, 2012). NdvB regulates the expression of over 24 other genes, including ethanol oxidation genes, which are implicated in tobramycin resistance. When *ndvB* is knocked out, these ethanol oxidation genes are downregulated (Beaudoin *et al.*, 2012). Like *ndvB*, the ethanol oxidation genes are much more highly expressed in biofilm cells than in planktonic cells, and their deletion makes biofilm cells 4x more susceptible to tobramycin, but has no effect on planktonic cells (Beaudoin *et al.*, 2012). However, the mechanism by which NdvB affects antibiotic tolerance is yet to be elucidated (Hall and Mah, 2017).

In *P. aeruginosa*, expression of the *brlR* (biofilm resistance locus regulator) gene, which encodes a MerR-like transcriptional regulator, leads to biofilm-specific transcriptional activation of the genes encoding the MexCD-OprJ and MexEF-OprN efflux pumps (Liao *et al.*, 2013, Liao and Sauer, 2012). Not only does this result in the increased efflux of antibiotic compounds, but also leads to the leakage of ß-lactamase enzymes into the periplasm and biofilm matrix, which are therefore able to hydrolyse ß-lactam antibiotics prior to cell entry, thus enhancing biofilm cell survival. The BrlR protein is present in the *P. aeruginosa* biofilm proteome, but not in the planktonic proteome, whilst its transcription levels are also greater in biofilm cells (Southey-Pillig

et al., 2005, Liao and Sauer, 2012). BrlR binds to cyclic-di-GMP to autoregulate its own expression. The high levels of cyclic-di-GMP in biofilms could explain why *brlR* transcription is much greater in biofilms than in planktonic cells (Chambers *et al.*, 2014). Deletion of *brlR* in *P. aeruginosa* PAO1 leads to a 4-fold decrease in biofilm tolerance to tobramycin, but has no effect in planktonic cells (Liao and Sauer, 2012), presumably through downregulation of efflux pumps in the deletion mutant. The mutant also shows a 4-fold increase in *ndvB* gene expression compared to the wild-type strain, suggesting interaction of these genes within a regulatory pathway (Beaudoin *et al.*, 2012, Van Acker *et al.*, 2014).

Alongside changes in gene expression when cells switch from a planktonic to a biofilm mode of growth, the switch may also result in an increased mutation rate. Strains of *P. aeruginosa* isolated from CF patients are frequently found to be hypermutable and possess defective DNA repair mechanisms (Mandsberg *et al.*, 2009). This increased mutation frequency may be a result of increased oxidative stress within biofilms (Boles and Singh, 2008).

VIII. Extracellular DNA

Extracellular DNA within a biofilm matrix may be endogenous or exogenous in origin. Endogenously, it can be released through QS cascades, via OMVs, or by lysis of some biofilm cells (Jakubovics *et al.*, 2013). Exogenous eDNA can be incorporated into the biofilm matrix from other species and is implicated in horizontal gene transfer within biofilms (Bae *et al.*, 2014, Chiang *et al.*, 2013). The negative charge of eDNA means that it can sequester positively-charged antibiotics, such as tobramycin,

impeding their ability to penetrate the biofilm matrix and reach cells (Chiang *et al.*, 2013). eDNA can also chelate positively-charged ions, such as Mg^{2+}, reducing their levels and availability for assimilation into biofilm cells (Mulcahy *et al.*, 2008). The eDNA in *P. aeruginosa* biofilms can bind to the phenazines, PYO and PCN, helping to retain these phenazine molecules within the biofilm so that they can act as extracellular electron shuttles that aid biofilm cell metabolism (Saunders *et al.*, 2020).

1.3 *CANDIDA* SPECIES

The most prevalent opportunistic fungi affecting human health are members of the *Candida* genus, with *Candida albicans* being the most frequently isolated species worldwide, with a 63.8% isolation frequency amongst *Candida* isolates (Papon *et al.*, 2013, Sharma *et al.*, 2019). Infections caused by *Candida* species predominantly affect hosts with impaired immunity (e.g. AIDS, organ transplants, chemotherapy, immunosuppressant therapy), and can be superficial (cutaneous or mucosal) or systemic (bloodstream infection) (Papon *et al.*, 2013, Nishimoto *et al.*, 2019). Alongside *C. albicans*, *Candida* species of clinical importance include *Candida glabrata* (11.3% isolation frequency), *Candida tropicalis* (7.2%), *Candida parapsilosis* (6.0%) and *Candida krusei* (2.4%), whilst species of lower prominence include *Candida guilliermondii* (0.7%), *Candida lusitaniae* (0.6%) and *Candida dubliniensis* (0.1%) (Papon *et al.*, 2013). More recently, *Candida auris* has been named an emerging pathogen, due to high-profile cases of multidrug-resistant strains being isolated (Sharma *et al.*, 2019).

Some *Candida* species are polymorphic, with the ability to switch between different morphologies, such as yeast and hyphae. The only species able to form true hyphae (in which segments share cytoplasmic content) are *C. albicans* and *C. dubliniensis*, whilst *C. tropicalis* can form hyphae only under specific growth conditions, but readily forms pseudohyphae (in which segments are truly septate) (Papon *et al.*, 2013, Whibley and Gaffen, 2015). Pseudohyphae can also be formed by *C. parapsilosis* and, under some conditions, *C. krusei* (Sharma *et al.*, 2019). The ability of these *Candida*

species to switch morphologies is linked to their virulence and can have an impact on their antifungal drug susceptibility (Sharma *et al.*, 2019).

1.3.1 *Candida albicans* – clinical importance

Candida albicans is a highly polymorphic, saccharomycete fungus, exhibiting up to nine different growth morphologies (Gow and Yadav, 2017, Noble *et al.*, 2017). *C. albicans* is a commensal of humans, existing asymptomatically in the gut, the female reproductive tract, the mouth or on the skin of healthy individuals (Lohse *et al.*, 2018). However, changes in the host environment, such as use of antibiotics or immunosuppressants, can result in a switch to pathogenicity. Localised infections are mainly dermal or mucosal, but dissemination of *C. albicans* can result in fatal bloodstream infections with a mortality rate exceeding 40%–60% (Lohse *et al.*, 2018, Nishimoto *et al.*, 2019). In the CF lung, *Candida* and *Aspergillus* are the most prevalent fungal genera, with *C. albicans*, *C. dubliniensis* and *C. parapsilosis* the most frequently isolated *Candida* species (Azzam *et al.*, 2019). In one study, the frequency with which *C. albicans* was isolated from the lungs of CF patients was 75.5% (Bakare *et al.*, 2003), making it the most frequently isolated fungal species from the CF lung. However, the detection and isolation of *Candida* species from the CF lung is not routinely performed (Haiko *et al.*, 2019), so the prevalence may be even greater.

1.3.2 *Candida albicans* – pathogenesis and virulence mechanisms

The most prevalent localised *C. albicans* infections are oral candidiasis and vulvovaginal candidiasis (VVC) (Mayer *et al.*, 2013). Oral candidiasis is most common in people with HIV, whilst VVC is thought to affect around 75% of all women at some

point during their lifetime (Mayer *et al.*, 2013). The success of *C. albicans* as an infectious agent is due to a host of virulence factors and the ability to adapt to different niches.

1.3.2.1 Polymorphism

C. albicans cells can exhibit numerous morphologies, including yeast cells, pseudohyphae, hyphae, white cells, opaque cells and chlamydospores (spore-like cells with thick cell walls) (Mayer *et al.*, 2013). The transition from one morphology to another is induced by environmental factors; for example, the induction of hyphal growth is associated with alkaline pH, nutrient starvation, increased CO_2 levels, temperatures above 37°C, and surface contact (Mayer *et al.*, 2013, Talapko *et al.*, 2021). The switch from white to opaque cells is associated with increased pathogenicity (Figure 1.3) (Mayer *et al.*, 2013, Talapko *et al.*, 2021). The *C. albicans* cell wall is composed of an inner layer of chitin and ß-glucans, and an outer layer of proteins that are heavily glycosylated with mannans (Gow *et al.*, 2012). The cell wall protects fungal cells from stressors, such as osmotic stress and temperature changes, as well as playing a crucial role in host immune responses (Talapko *et al.*, 2021). Different *C. albicans* morphologies have altered cell wall structures; for example, hyphal cells have much higher levels of chitin than yeast cells, but lower levels of exposed ß-glucan, resulting in altered immune responses within hosts (Talapko *et al.*, 2021, Bojang *et al.*, 2021). The yeast morphology is typically associated with the dissemination of *C. albicans* within a host, whilst the hyphal morphology is associated with invasion and penetration of host tissues, so both are important for *C. albicans* pathogenicity (Mayer *et al.*, 2013, Talapko *et al.*, 2021).

Alongside tissue invasion, the formation of hyphae is associated with the upregulation of expression of genes encoding hypha-associated virulence factors. These include hyphal wall protein (Hwp1), adhesins, invasins, secreted aspartyl proteases (SAPs), phospholipases and the candidalysin toxin (Mayer *et al.*, 2013, Talapko *et al.*, 2021, Bojang *et al.*, 2021).

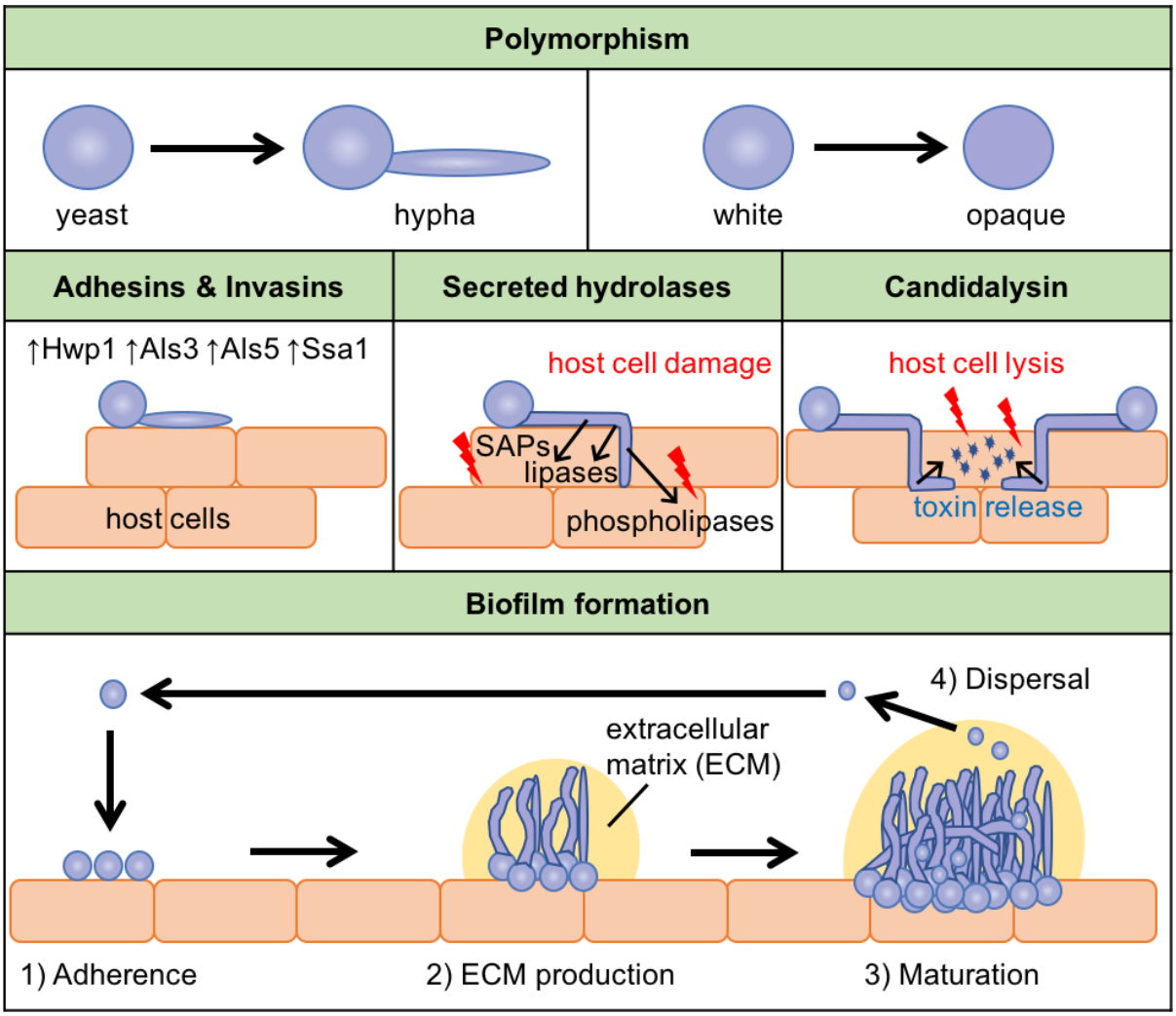


Figure 1.3. Selected *C. albicans* pathogenesis and virulence mechanisms. The *C. albicans* yeast-to-hypha transition and white-to-opaque switching are linked to pathogenicity and altered host immune responses. Upon contact with surfaces, *C. albicans* cells overproduce adhesins, such as Hwp1, Als3 and Als5. Invasins, such as Als3 and Ssa1, lead to induced endocytosis by host cells. Invading hyphae release secreted hydrolases, such as SAPs (secreted aspartyl proteinases), lipases and phospholipases, which result in host cell damage. Accumulation of the candidalysin toxin can lead to host cell lysis. Biofilm formation involves four stages: 1) adherence of yeast cells to a surface; 2) hyphal growth and ECM production; 3) maturation to form a complex biofilm structure; and 4) dispersal of yeast cells, which may go on to seed new infection sites.

1.3.2.2 Adhesins

Adhesins are proteins that enable adherence to host cells or other microbial cells, or to abiotic surfaces. Hwp1, Als3 and Als5 function as adhesins, enabling *C. albicans* cells to adhere to an infection surface (Figure 1.3) (Bojang *et al.*, 2021). Als3 and Als5 are members of a family of eight *C. albicans* agglutinin-like sequence (ALS) proteins (Als1–7 and Als9), all of which function as adhesins (Talapko *et al.*, 2021). The *ALS3* gene is of particular interest because its upregulation has been observed during infection of oral epithelial cells, and in VVC infections (Mayer *et al.*, 2013).

1.3.2.3 Invasins

The invasion of host tissues by *C. albicans* can be achieved actively, through hyphal growth and penetration, or passively, by induced endocytosis. Invasins are cell-surface proteins that bind to ligands on host cell surfaces, thereby inducing the process of endocytosis. In *C. albicans*, the two main invasins are Als3 and Ssa1 (Figure 1.3), the latter of which is a member of the heat shock protein 70 (Hsp70) family of proteins (Mayer *et al.*, 2013).

1.3.2.4 Secreted hydrolases

Once *C. albicans* cells have adhered to a host cell surface and initiated hyphal growth, the hyphae secrete hydrolases. There are three classes of *C. albicans* secreted hydrolases: **I.** secreted aspartyl proteinases (SAPs); **II.** lipases; and **III.** phospholipases (Figure 1.3) (Mayer *et al.*, 2013).

I. Secreted aspartyl proteinases

C. albicans produces a family of ten secreted aspartyl proteinases (SAPs), which are associated with adherence to host cells and tissues (Naglik *et al.*, 2003). Sap4, Sap5 and Sap6 are particularly associated with the yeast-to-hypha transition, while Sap2 is the most abundantly produced SAP out of the ten (Naglik *et al.*, 2003). SAPs contribute to *C. albicans* virulence by catabolism of a broad range of host proteins, including mucin and immunoglobulins, thus interfering with the host immune response (Naglik *et al.*, 2003).

II. Lipases

A family of ten lipases is produced by *C. albicans*, of which all except Lip7 are encoded by genes containing an N-terminal signal sequence for extracellular release of the gene product (Hube *et al.*, 2000). All ten *LIP* genes are expressed during the yeast-to-hypha transition, and these Lip enzymes degrade a broad range of lipid substrates. Crucially, *LIP* genes are expressed even when *C. albicans* is grown in media that lacks lipids; this suggests that the main role of these lipases is not cellular metabolism, but virulence and persistence in hosts, as lipids are major constituents of host cell membranes (Hube *et al.*, 2000).

III. Phospholipases

C. albicans produces four families of phospholipases (A–D), as well as a lysophospholipase and a lysophospholipase-transacylase (Niewerth and Korting, 2001). Phospholipases A–D digest phosphatidylcholines, which are a class of phospholipids found in the cell membranes of host cells, thus playing a major role in *C. albicans* virulence. Class B phospholipases are of particular note in pathogenesis because, unlike classes A, C and D, they are extracellularly localised (Niewerth and Korting, 2001).

1.3.2.5 Candidalysin toxin

Candidalysin is the first classical virulence toxin known to be produced by a fungal pathogen of human hosts (Moyes *et al.*, 2016). It is a cytolytic peptide, which permeabilises host cell membranes, resulting in epithelial damage and inducing an epithelial immune response (Moyes *et al.*, 2016). Candidalysin can also result in the lysis of red blood cells (Naglik *et al.*, 2019). Production of the candidalysin toxin is unique to invasive *C. albicans* hyphal cells, making it particularly important in systemic infections. The induced epithelial response is dose-dependent, being activated only when the number of hyphae exceeds a particular threshold (Figure 1.3) (Naglik *et al.*, 2019, Moyes *et al.*, 2016).

Another important *C. albicans* virulence factor is the ability to form biofilms on biotic surfaces, such as host epithelial cells or other microbial cells, and on abiotic surfaces, such as catheters, dentures and prostheses.

1.3.3 *Candida albicans* biofilms

C. albicans biofilm formation is initiated by the adherence of yeast cells to a surface. The yeast cells grow and multiply, forming layers. Hyphal cells proliferate in the upper layers of the biofilm, and the cells release extracellular matrix (ECM) material that encases the mature biofilm (Figure 1.3) (Lohse *et al.*, 2018, Mayer *et al.*, 2013). The *C. albicans* biofilm ECM is composed of glycoproteins (55%), carbohydrates (25%), lipids (15%) and nucleic acids (5%) (Zarnowski *et al.*, 2014, Lohse *et al.*, 2018). The most abundant types of carbohydrate in the ECM are mannans, which are often found in association with ß-1,6-glucans, while ß-1,3-glucans are present in lower concentrations (Ponde *et al.*, 2021, Lohse *et al.*, 2018). In a similar manner to bacterial biofilms, the eDNA found in *C. albicans* biofilms provides structural stability, but is not essential for the initial formation of the biofilm (Ponde *et al.*, 2021, Lohse *et al.*, 2018). Other ECM components are thought to originate from lysed cells, as enzymes found in the ECM of mature *C. albicans* biofilms often do not contain a signal peptide, suggesting they were not secreted (Pereira *et al.*, 2020, Lohse *et al.*, 2018). The final stage of the *C. albicans* biofilm cycle is the detachment and dispersion of yeast cells from the mature biofilm, which can go on to seed new infection sites (Figure 1.3) (Lohse *et al.*, 2018, Mayer *et al.*, 2013).

1.3.3.1 Fungal biofilm-specific resistance mechanisms

Fungal biofilms exhibit resistance to all classes of antifungal, with azoles being almost entirely ineffective against them. The high concentrations of antifungal drugs that are required to kill fungal biofilm cells result in side effects such as damage to the kidneys or liver (Lohse *et al.*, 2018).

In fungal biofilms, a wide range of antifungal drugs are known to be sequestered by ß-1,3-glucans in the biofilm extracellular matrix, meaning that very little of the drug actually reaches the cells (Van Acker *et al.*, 2014). Furthermore, *C. albicans* persister cells are not found in planktonic cultures, but are unique to biofilms (LaFleur *et al.*, 2006), thus further enhancing the antifungal resistance of *C. albicans* biofilms.

Similarly to antibiotic-treated bacterial biofilms, upregulation of *SOD* genes has been observed when *C. albicans* biofilm cells are treated with the antifungal drug miconazole, resulting in decreased ROS levels (Kobayashi *et al.*, 2002). Conversely, *sod4*Δ*/sod5*Δ double knockout mutants show increased ROS levels and a resultant decrease in the number of persister cells (Bink *et al.*, 2011). This indicates that *C. albicans* stress responses can influence biofilm antifungal resistance.

In fungi, there are two major classes of efflux pumps; the ATP-binding cassette (ABC) pumps and the major facilitator superfamily (MFS) transporters (Cannon *et al.*, 2009). The resistance of *C. albicans* biofilm cells to azoles is enabled by the upregulation of genes encoding two ABC pumps, *CDR1* and *CDR2*, and an MFS pump, *MDR1*, relative to their expression in planktonic cells (Ramage *et al.*, 2002). Mdr1 and Cdr1 are involved in conferring rapid tolerance to biofilm cells, upon attachment to a surface. This is supported by the observation that fluconazole tolerance is induced very early on in biofilm formation; the level of tolerance after 24 h remains the same as it was at 2 h, suggesting that attachment to a surface is the factor that induces *MDR1* and *CDR1* overexpression (Mateus *et al.*, 2004).

1.3.4 Biofilms of non-*albicans Candida* species

With the exception of *C. glabrata*, all of the most prevalent *Candida* species are able to form robust biofilms, which exhibit increased tolerance to antifungals, especially azoles, and are less easily cleared by host defences (Sharma *et al.*, 2019, Cavalheiro and Teixeira, 2018). Biofilms formed by *C. glabrata* consist entirely of yeast cells, which cluster tightly and form multiple layers; *C. parapsilosis* biofilms are also formed predominantly from clustered yeast cells (Cavalheiro and Teixeira, 2018). There is evidence to suggest that the ability to form hyphae or pseudohyphae results in more robust biofilms, potentially due to filamentous cells expressing a greater number of adhesion proteins, such as Als3 and Hwp1, which both anchor the biofilm to the substratum and enable yeast cells to adhere more effectively (Sharma *et al.*, 2019).

The composition of the biofilm extracellular matrix (ECM) varies between different *Candida* species (Figure 1.4). The most confluent and heterogeneous biofilms are formed by *C. albicans*, and this is the species for which clinical isolates are most able to form biofilms (Sardi *et al.*, 2013, Cavalheiro and Teixeira, 2018). Biofilms formed by *C. glabrata* are much thinner than those formed by *C. albicans*, but the *C. glabrata* ECM contains relatively large quantities of carbohydrates and proteins (431.3 ±179.6 and 226 ±58.6 mg/g average biofilm dry weight, respectively) (Silva *et al.*, 2009). Conversely, *C. tropicalis* biofilms have a low carbohydrate and protein content (24.6 ±15.9 and 43.4 ±12.7 mg/g average biofilm dry weight, respectively), with hexosamine as the main carbohydrate (27.4% of total carbohydrate) rather than ß-glucan (Silva *et al.*, 2009, Cavalheiro and Teixeira, 2018). Instead of ECM material, the majority of the biomass of *C. tropicalis* biofilms is attributed to the multiple layers of large yeast-

shaped cells and hyphae, which form a thick and heterogeneous biofilm structure (Silva *et al.*, 2009). *C. parapsilosis* produces very little ECM, which consists mainly of carbohydrate (611.2 ±206.5 mg/g average biofilm dry weight), with very little protein present (50.9 ±21.4 mg/g average biofilm dry weight) (Silva *et al.*, 2009, Cavalheiro and Teixeira, 2018). Additionally, the architecture of mature biofilms may differ depending on whether the biofilm has been grown *in vitro* or *in vivo* (Dominguez *et al.*, 2018).

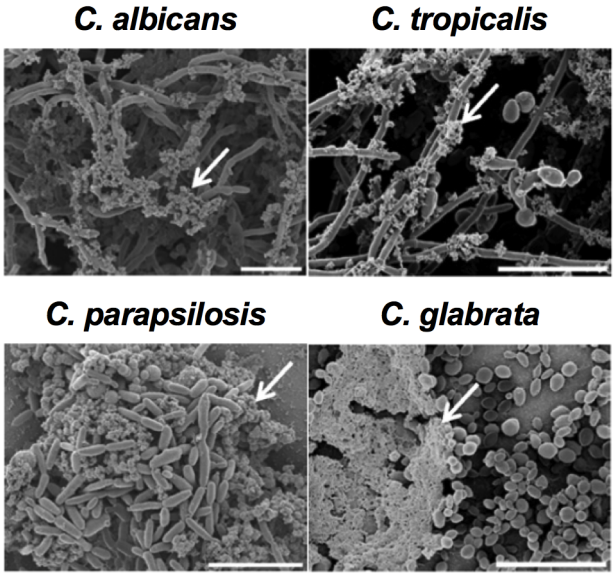


Figure 1.4. Differences in biofilm architecture between different *Candida* species. SEM images of fungal biofilms grown for 24 h on coverslips. Arrows indicate ECM material. Scale bar = 20 μm. SEM images reproduced from Dominguez *et al.* (2018).

1.3.5 Antifungals and antifungal resistance

There are three main classes of antifungal drug: azoles, echinocandins and polyenes. Azoles are most commonly used for the treatment of *Candida* infections, with fluconazole as the first-line treatment option. Azoles work by inhibiting the production of the 14α-lanosterol demethylase protein, which is encoded by the *ERG11* gene, and is required for ergosterol biosynthesis (Revie *et al.*, 2018, Nishimoto *et al.*,

2019). Ergosterol is important for *Candida* cell membrane integrity, as it regulates membrane fluidity and permeability (Rodrigues, 2018). In *C. albicans* cells, azole therapy results in ergosterol biosynthesis switching to an alternative pathway, causing the accumulation of the toxic compound, 14α-methylergosta-8,24(28)-dien-3ß,6α-diol, and impairment of cell growth (Nishimoto *et al.*, 2019, Revie *et al.*, 2018).

Rates of resistance to fluconazole are generally low in *C. albicans*, but high in *C. glabrata*. However, azole resistance is becoming more common, especially in strains isolated from patients on long-term azole therapy (Nishimoto *et al.*, 2019). Mechanisms of azole resistance include overexpression of the Cdr1, Cdr2 and Mdr1 efflux pumps, overexpression of the Upc2 transcription factor and resultant upregulation of *ERG11* (Revie *et al.*, 2018, Nishimoto *et al.*, 2019), mutations in the *ERG11* gene (Vasicek *et al.*, 2014), aneuploidy, and biofilm formation (Nishimoto *et al.*, 2019).

1.3.5.1 Amphotericin B

Amphotericin B (AmB) is a polyene antifungal drug that was first approved for use in treating invasive fungal infections in 1957 (Perlin *et al.*, 2017). AmB targets ergosterol in fungal cell membranes, leading to disintegration of the membrane. For decades, it has been the gold standard for treatment of systemic fungal infections (Anderson *et al.*, 2014, Grela *et al.*, 2019). However, AmB is nephrotoxic and hematotoxic with increasing dosage, with side effects resulting from non-selective interactions with cholesterol in host cell membranes (Kamiński, 2014). Lipid formulations (e.g. liposomal AmB) are less toxic, but more costly, so the use of AmB is not as widespread as that of azoles and echinocandins (Perlin *et al.*, 2017).

The mechanism of action of AmB is not entirely understood and there are several proposed models for the interaction between AmB and ergosterol. The most widely accepted mechanism of action is the ion-channel model, which proposes that AmB molecules form pores that traverse the phospholipid bilayer of fungal cell membranes. The pores are stabilised by AmB-ergosterol interactions and result in the leakage of K^+ ions and other molecules out of the cell, impairing cellular functions (Kamiński, 2014). A second model proposes that AmB induces the formation of reactive oxygen species (ROS), such as superoxide ($O_2^{\bullet-}$), hydrogen peroxide (H_2O_2), and hydroxyl radicals ($^{\bullet}OH$), leading to oxidative cell damage (Kamiński, 2014). The third model is the surface adsorption model, which proposes that AmB binds and sequesters ergosterol at the outer surface of the fungal cell membrane, with a perpendicular orientation relative to the phospholipid molecules. This results in membrane destabilisation (Kamiński, 2014). Finally, the fourth model is the extramembranous sterol sponge model, proposing that AmB forms large aggregates on the surfaces of fungal cell membranes and extracts ergosterol from the phospholipid bilayer (Kamiński, 2014, Anderson *et al.*, 2014, Perlin *et al.*, 2017). The resultant deficiency of ergosterol leads to fungal cell death, as certain ergosterol-dependent cellular processes cannot take place, such as endocytosis, cell division and cell signalling (Anderson *et al.*, 2014).

Acquired resistance to AmB is not very common (Anderson *et al.*, 2014, Perlin *et al.*, 2017, Revie *et al.*, 2018). Where it does occur, AmB resistance can arise through a reduction in the ratio of ergosterol to phospholipid in the fungal cell membrane

(Kamiński, 2014, Perlin *et al.*, 2017). Furthermore, prior treatment with an azole, which lowers ergosterol levels, may confer AmB resistance (Perlin *et al.*, 2017).

1.3.6 *C. albicans* interactions with bacteria

Within human hosts, there are numerous sites at which *C. albicans* is found to interact with bacteria, both Gram-positive and Gram-negative.

1.3.6.1 Interactions with Gram-positive bacteria

Amongst the Gram-positives, the species most commonly found to interact with *C. albicans* is *Staphylococcus aureus*; sites of interaction include the skin, medical devices, the oral cavity and neonatal bloodstream infections (Lohse *et al.*, 2018). Studies of dual-species biofilms of *C. albicans* and the *S. aureus* Newman strain show that the bacterial cells use the fungal hyphae as a scaffold for biofilm formation. The biofilm architecture is stabilised by eDNA and provides enhanced tolerance against the antifungal drug, miconazole (Kean *et al.*, 2017). Synergism between *C. albicans* and methicillin-resistant *S. aureus* (MRSA) has also been observed, resulting in protection of MRSA from vancomycin treatment, with fungal ß-1,3-glucan playing a role in this protection (Harriott and Noverr, 2009, Kong *et al.*, 2016). Furthermore, in a mouse peritonitis infection model, sub-lethal doses of *C. albicans* and *S. aureus* result in greater mortality after co-infection than when each infects alone (Peters and Noverr, 2013). Dual-species proteomic analysis of mono- and dual-species biofilms of *C. albicans* and *S. aureus* reveals that a total of 27 proteins were upregulated in both species when co-cultured. These included proteins involved in growth, metabolism, stress and enhanced virulence (Peters *et al.*, 2010).

On the skin and on medical devices, biofilm interactions are found between *C. albicans* and *Staphylococcus epidermidis* (Lohse *et al.*, 2018). *S. epidermidis* can adhere to both yeast and hyphal *C. albicans* cells in a dual-species catheter biofilm model (Adam *et al.*, 2002). The dual-species biofilm cells are more tolerant to both fluconazole and vancomycin, relative to mono-species. The enhanced fluconazole tolerance is attributed to protection conferred by the extracellular matrix material produced by *S. epidermidis* biofilm cells (Adam *et al.*, 2002, Peleg *et al.*, 2010).

Interactions between *C. albicans* and *Streptococcus* species, such as *S. mutans*, *S. oralis* or *S. gordonii* are found in the oral cavity, associated with dental caries and denture stomatitis (Jarosz *et al.*, 2009, Bamford *et al.*, 2009). *S. oralis* and *S. gordonii* interact with the fungal cell wall adhesins, Als1 and Als3, enabling the formation of mixed-species biofilms. In contrast, *S. mutans* secretes α-glucans, which interact with the *C. albicans* cell surface via mannoproteins, enabling the formation of mixed biofilms on surfaces that would not usually be colonised by *C. albicans*, such as tooth enamel (Hwang *et al.*, 2017, Ranjan and Dongari-Bagtzoglou, 2018). In an *in vitro* oral biofilm model, the presence of *Streptococcus sanguinis*, *Streptococcus gordonii*, *Actinomyces odontolyticus* and *Actinomyces viscosus* was linked to increased *C. albicans* hyphal formation and upregulation of virulence genes (Morse *et al.*, 2019). The virulence genes measured in this study were *ALS3*, *EPA1* (epithelial adhesion 1), *HWP1*, *PLD1* and *PLD4* (phospholipase D 1 and 4), and *SAP4* and *SAP6* (Morse *et al.*, 2019). However, the addition of a fifth bacterial species, *Porphyromonas gingivalis*, inhibited hyphal production and downregulated these *C. albicans* virulence genes (Morse *et al.*,

2019). This suggests that, in a mixed biofilm, one species is capable of overriding the modulatory effects of others.

In the gastrointestinal tract and on medical devices, *Enterococcus faecalis* interacts with *C. albicans*. *E. faecalis* releases the bacteriocin, EntV, which inhibits hyphal formation and can disrupt mature *C. albicans* biofilms, resulting in reduced virulence in a mouse model (Graham *et al.*, 2017, Nogueira *et al.*, 2019). *C. albicans* adheres to *E. faecalis* cells using the cell wall-associated Sap9, which is important for *C. albicans* biofilm formation (Dutton *et al.*, 2016a).

Interactions have also been found between *C. albicans* and the anaerobic *Clostridium perfringens*, which is found in the human gut (Lohse *et al.*, 2018). *C. albicans* biofilms provide hypoxic microniches, enabling *C. perfringens* to proliferate despite an external aerobic environment (Fox *et al.*, 2014).

1.3.6.2 Interactions with Gram-negative bacteria

The most common sites at which *C. albicans* interacts with Gram-negative bacteria include the respiratory tract, the gut, the urinary tract, on the tubing of mechanical ventilators, and on the surfaces of intravenous or urinary catheters (Lohse *et al.*, 2018). These bacteria include *Escherichia coli*, *Acinetobacter baumannii*, *Burkholderia cenocepacia* and *Pseudomonas aeruginosa*.

Interactions with *E. coli* are found in the gut, urinary tract, in the bloodstream and on medical devices. In the urinary tract, *C. albicans* is unable to attach to the bladder

endothelium alone, but is able to do so in the presence of *E. coli*, which binds to the mannose in the fungal cell wall, thus facilitating attachment of *C. albicans* (Levison and Pitsakis, 1987). Lipopolysaccharides (LPS) from *E. coli* can enhance biofilm growth of *C. albicans*, but this is not the case for other *Candida* species, such as *C. tropicalis*, *C. dubliniensis*, *C. krusei*, and *C. parapsilosis*, for which *E. coli* inhibits biofilm growth in the urinary tract (Bandara *et al.*, 2009). The fungal polysaccharide β-1,3-glucan has been implicated in protecting *E. coli* biofilm cells from antibiotic-mediated killing. The presence of *C. albicans* in a mixed *C. albicans–E. coli* biofilm resulted in increased tolerance to ofloxacin, whilst treatment with lyticase, which results in degradation of β-1,3-glucan, reduced this tolerance. An *E. coli* mutant that overexpressed the genes responsible for β-1,3-glucan synthesis showed even greater tolerance to ofloxacin (De Brucker *et al.*, 2015). Additionally, in a mouse peritonitis infection model, co-infection with *C. albicans* and *E. coli* results in higher lethality than when each species infects alone (Klaerner *et al.*, 1997).

Interactions between *C. albicans* and *A. baumannii* are found in cases of ventilator-associated pneumonia (VAP), bloodstream infections, and in catheters (Lohse *et al.*, 2018). The interaction is antagonistic, as *A. baumannii* can kill the filamentous form of *C. albicans* by attaching to the hyphae and triggering apoptosis (Gaddy *et al.*, 2009, Krüger *et al.*, 2019). The attachment of *A. baumannii* cells to *C. albicans* hyphae is mediated by the bacterial outer membrane protein A (OmpA), which is also implicated in the observed induction of apoptosis (Peleg *et al.*, 2010, Gaddy *et al.*, 2009). If *C. albicans* is able to proliferate first and form a mature biofilm, it can inhibit the growth of *A. baumannii* via secretion of farnesol, which disrupts bacterial membrane integrity

(Peleg *et al.*, 2008, Kostoulias *et al.*, 2016). This indicates that the outcome of co-infection by these two species is dependent on the specific environmental growth conditions.

Both *B. cenocepacia* and *P. aeruginosa* interact with *C. albicans* in the lung, especially in cases of Cystic Fibrosis (CF) (Lohse *et al.*, 2018). The *B. cenocepacia* diffusible signal factor (BDSF) is structurally similar to the *C. albicans* QS molecule, farnesol. BDSF can inhibit *C. albicans* filamentation (Boon *et al.*, 2008) and adherence of *C. albicans* cells to urinary catheters, in an *in vitro* model (Peleg *et al.*, 2010, Nogueira *et al.*, 2019). There is an abundance of studies focusing on direct and indirect interactions between *P. aeruginosa* and *C. albicans*.

1.4 *P. AERUGINOSA* AND *C. ALBICANS* INTERACTIONS

1.4.1 Clinical importance

P. aeruginosa and *C. albicans* are commonly co-isolated from the sputum of CF patients (Trejo-Hernández *et al.*, 2014). CF is characterised by a thickening of the mucus layer lining the endothelium of the respiratory tract, which provides an ideal environment for colonisation (Muthig *et al.*, 2010). CF patients are therefore treated with antibiotics from an early age and over a long period of time. Co-colonisation by *P. aeruginosa* and *C. albicans* can lead to worsening of disease progression. In an *in vivo* zebrafish model of mucosal lung infection, *C. albicans* and *P. aeruginosa* have been shown to synergistically enhance virulence and mortality (Bergeron *et al.*, 2017). This was achieved through increased *C. albicans* pathogenesis and host inflammation, when co-infected with *P. aeruginosa* (Bergeron *et al.*, 2017). Chronic *P. aeruginosa* colonisation in the lungs of CF patients has been correlated with increased likelihood of *C. albicans* colonisation, suggesting a synergistic interaction that leads to a greater decline in lung function (Dhamgaye *et al.*, 2016, Gileles-Hillel *et al.*, 2015). Similarly, persistent *C. albicans* infection increases the likelihood of *P. aeruginosa* colonisation in the CF lung (Chotirmall *et al.*, 2010, Krüger *et al.*, 2019). In a study of 130 patients with CF and 186 patients with other respiratory disorders, the co-existence of *P. aeruginosa* and *C. albicans* in the sputum of CF patients was more frequent (22.3% co-isolation frequency) than in the sputum of patients with other respiratory disorders (11.8%) (Haiko *et al.*, 2019).

P. aeruginosa and *C. albicans* can both be causative agents of ventilator-associated pneumonia (VAP), which is caused by microbial colonisation of endotracheal tubing

and has a mortality rate of 10–40% (Rodrigues *et al.*, 2017). Co-colonisation by *P. aeruginosa* and *C. albicans* occurs in 26% of VAP infections (Bandara *et al.*, 2020b, Azoulay *et al.*, 2006). Studies have shown that *C. albicans* colonisation results in greater susceptibility to pseudomonal VAP and that co-colonisation results in more severe clinical outcomes (Hamet *et al.*, 2012). This is supported by a clinical study on patients on mechanical ventilation, in which antifungal treatment reduced the likelihood of developing *P. aeruginosa* infections (Nseir *et al.*, 2007).

When *P. aeruginosa* colonises burns, surgical wounds, and implanted medical devices (Engel and Balachandran, 2009, Turner *et al.*, 2014), these patients are often prone to further infections, with *C. albicans* also capable of opportunistically colonising these surfaces (Dhamgaye *et al.*, 2016, Dixon and Hall, 2015, Peleg *et al.*, 2010).

1.4.2 Interactions via direct contact

P. aeruginosa can form biofilms on the surfaces of *C. albicans* hyphae, and was originally found to be unable to bind to the yeast form of the fungus (Hogan and Kolter, 2002, Brand *et al.*, 2008). However, later work indicates that *P. aeruginosa* is also able to bind to yeast cells (Bandara *et al.*, 2010). It is hypothesised that type IV pili on the surfaces of *P. aeruginosa* cells mediate this inter-kingdom interaction by sensing the fungal surface and then retracting to increase cell-cell proximity (Fourie and Pohl, 2019). On the *C. albicans* cell surface, *O*-mannan is implicated in protecting against killing of fungal cells by *P. aeruginosa* (Brand *et al.*, 2008). When a mixed-species biofilm containing *C. albicans*, *P. aeruginosa* and *S. aureus* is established on a wound model, and treated with antibiotics, or combination antibiotic-fluconazole therapy, the

biofilm composition alters, but the total cell number remains the same (Townsend *et al.*, 2017). This implies that the *C. albicans* hyphae and biofilm ECM provide a scaffold upon which bacteria, such as *P. aeruginosa*, can attach to form a polymicrobial biofilm and that these interspecies interactions increase AMR.

1.4.3 Interactions via secreted metabolites

Alongside physical interactions, *P. aeruginosa* and *C. albicans* also communicate via secreted metabolites. *P. aeruginosa* LPS molecules reduce the growth rate and metabolic activity of *C. albicans* biofilms, and inhibit hyphal morphogenesis (Figure 1.5) (Bandara *et al.*, 2013). Furthermore, both species produce quorum sensing molecules. *P. aeruginosa* can inhibit hyphal growth in *C. albicans* by the action of the secreted QS molecule, 3O-C_{12}-HSL (Hogan *et al.*, 2004, McAlester *et al.*, 2008). This *P. aeruginosa* QS molecule can also decrease *C. albicans* sensitivity to the antifungal, fluconazole, by inducing the upregulation of efflux pump genes and ergosterol biosynthesis genes (Figure 1.5) (Bandara *et al.*, 2020b). Conversely, the secretion of *C. albicans* QS molecule, farnesol, inhibits the *Pseudomonas* quinolone signal (PQS), which is responsible for regulating numerous virulence factors (Figure 1.5) (Fourie and Pohl, 2019).

Another group of molecules secreted by *P. aeruginosa* are phenazines, which are low molecular weight compounds that are involved in redox reactions, and which can influence biofilm morphology (Dietrich *et al.*, 2013). Phenazines are associated with inducing increased levels of toxic ROS in *C. albicans* (Figure 1.5) (Morales *et al.*, 2010). When *C. albicans* cells are exposed to *P. aeruginosa* phenazines, the fungal

cells increase production of ethanol (Morales *et al.*, 2013). The *P. aeruginosa* cells respond to the higher ethanol levels by increasing phenazine production and promoting biofilm formation (Figure 1.5). This positive feedback loop of *P. aeruginosa* phenazine production in response to *C. albicans*–derived ethanol levels has been observed on the surfaces of bronchial epithelial cells (Chen *et al.*, 2014). The implication of this is increased virulence within hosts when there is co-infection, and reduced clearance upon antimicrobial treatment.

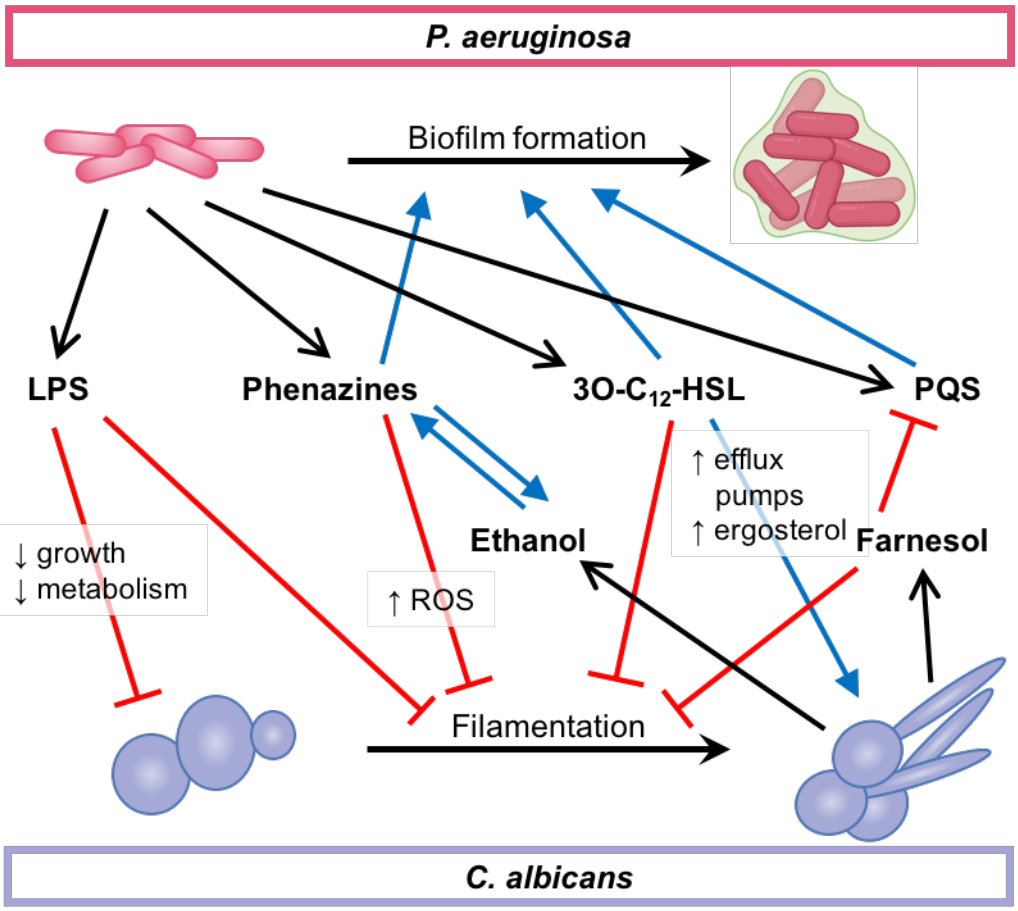


Figure 1.5. Selected interactions between *P. aeruginosa* and *C. albicans*. *P. aeruginosa* secretes LPS (lipopolysaccharides), which inhibit growth, metabolism and filamentation in *C. albicans*. *P. aeruginosa* phenazines induce ROS (reactive oxygen species) and inhibit filamentation in *C. albicans*. Exposure to *P. aeruginosa* phenazines induces ethanol production in *C. albicans* cells, which leads to increased phenazine production and promotion of *P. aeruginosa* biofilm production. The *P. aeruginosa* QS molecule, 3O-C_{12}-HSL, inhibits *C. albicans* filamentation, but induces upregulation of genes encoding efflux pumps and enzymes of the ergosterol biosynthesis pathway. The *C. albicans* QS molecule, farnesol, inhibits the *P. aeruginosa* QS molecule, PQS (*Pseudomonas* quinolone signal). Farnesol also inhibits *C. albicans* filamentation. Red lines: inhibition; blue arrows: induction.

1.5 AIMS OF THIS RESEARCH

While there is an abundance of studies into the physical and chemical interactions between *P. aeruginosa* and *C. albicans*, little is known about how their interactions in dual-species biofilms impact antimicrobial resistance. Therefore, the main focus of this study was to determine the impact of dual-species biofilm interactions on the antibiotic tolerance of *P. aeruginosa* and the antifungal tolerance of *C. albicans*.

The aims of this research were to:

1) Determine the impact of dual-species biofilms on the antibiotic tolerance of *P. aeruginosa*.

2) Identify the transcriptional changes that occur in *P. aeruginosa* and *C. albicans* cells, between mono- and dual-species biofilm growth.

3) Determine the impact of dual-species biofilms on the antifungal tolerance of *C. albicans*.

2 MATERIALS AND METHODS

Parts of this chapter have been previously published:

Alam, F., Catlow, D., Di Maio, A., Blair, J. M. A. and Hall, R. A. (2020) '*Candida albicans* enhances meropenem tolerance of *Pseudomonas aeruginosa* in a dual-species biofilm', *J Antimicrob Chemother*, 75(4), pp. 925–935.

2.1 STRAINS AND GROWTH CONDITIONS

Bacterial species and strains used in this research are listed in Table 2.1, while fungal species and strains are listed in Table 2.2. *P. aeruginosa*, *A. baumanni*, *B. cenocepacia*, *E. coli* and *S. aureus* strains were maintained on and cultured in Miller modified LB; *Candida* strains in yeast extract peptone dextrose (YPD) medium; and *E. faecalis*, *E. faecium* and *S. epidermidis* strains in brain-heart infusion (BHI) medium. All strains were grown at 37°C, with aeration at 200 rpm. Antimicrobials (from Sigma-Aldrich, UK) were used at the following concentrations (μg/mL): meropenem (0, 1, 2.5, 5, 10); ceftazidime (0, 2.5, 5); ofloxacin (0, 0.5); ciprofloxacin (0, 0.05); tobramycin (0, 2); amphotericin B (0, 0.5, 1, 2, 4, 8); fluconazole (0, 250, 500, 750, 1000).

Table 2.1. Bacterial species and strains used in this research.

Strain	Name in text	Genotype	Reference
***Pseudomonas aeruginosa* strains**			
ATCC15692	PAO1	Wild-type	ATCC15692
CF (Midlands 1)	CF (Midlands 1) isolate	Clinical isolate	(Scott and Pitt, 2004)
CF (Liverpool)	CF (Liverpool) isolate	Clinical isolate	(Cheng *et al.*, 1996)
Respiratory isolate	Respiratory isolate	Clinical isolate	N. Cumley, Queen Elizabeth Hospital, Birmingham, UK
PAO1	PAO1 WT	Wild-type	(Jacobs *et al.*, 2003)
-	PAO1 *cbpD*Δ	Transposon-insertion knockout of *CbpD*	(Jacobs *et al.*, 2003)
-	PAO1 *chiC*Δ	Transposon-insertion knockout of *ChiC*	(Jacobs *et al.*, 2003)
PA14	PA14(1) or PA14	Clinical isolate UCBPP-PA14, wild-type	(Rahme *et al.*, 1995)
PA14 *phz*Δ	*phz*Δ	Deletions of operons *phzA1–G1* and *phzA2–G2*	(Dietrich *et al.*, 2006)
PA14 *pvdA*Δ *pchE*Δ	*pvdA*Δ/*pchE*Δ	Deletions of *pvdA* and *pchE*	(Wang *et al.*, 2011)
PA14 *phz*Δ *pvdA*Δ *pchE*Δ	*phz*Δ/*pvdA*Δ/*pchE*Δ	Deletions of *pvdA*, *pchE*, and operons *phzA1–G1* and *phzA2–G2*	(Wang *et al.*, 2011)
PA14	PA14 WT or PA14(2)	Wild-type	(Liberati *et al.*, 2006)
-	PA14 *cbpD*Δ	Transposon-insertion knockout of *CbpD*	(Liberati *et al.*, 2006)
-	PA14 *chiC*Δ	Transposon-insertion knockout of *ChiC*	(Liberati *et al.*, 2006)
Other bacterial species and strains			
AYE	*Acinetobacter baumannii*	Clinical isolate	(Poirel *et al.*, 2003)
K56-2	*Burkholderia cenocepacia*	Clinical isolate – Cystic Fibrosis	(Sokol *et al.*, 1999)
DH5α	*Escherichia coli*	Cloning strain, non-virulent	(Hanahan *et al.*, 1991)
MG1655	*Escherichia coli*	Wild-type, derivative of strain K-12	(Bachmann, 1996)
V583	*Enterococcus faecalis*	Clinical isolate, Vn^r, TIGR sequence strain	(Sahm *et al.*, 1989)
Aus0004	*Enterococcus faecium*	Clinical isolate	(Lam *et al.*, 2012)
Newman	*Staphylococcus aureus*	Reference isolate, methicillin-resistant	ATCC13420
-	*Staphylococcus epidermidis*	Clinical isolate	Queen Elizabeth Hospital, Birmingham, UK

Vn^r (vancomycin-resistant); TIGR (The Institute for Genomic Research)

Table 2.2. Fungal species and strains used in this research.

Strain	Name in text	Genotype	Reference
***Candida albicans* strains**			
SC5314	SC5314	Type strain	(Sobel, 1997)
NGY152	NGY152	*ura3*Δ::*imm434/ura3*Δ::*imm434; RPS1/rps1*Δ::*URA3*	(Hobson *et al.*, 2004)
NGY355	*pmr1*Δ	u*ra3*Δ::*imm434/ura3*Δ::*imm434; pmr1*Δ::*hisG/pmr1*Δ::*hisG; RPS10/rps10*Δ::*URA3*	(Bates *et al.*, 2005)
NGY356	*pmr1*Δ + *PMR1*	*ura3*Δ::*imm434/ura3*Δ::*imm434; pmr1*Δ::*hisG/pmr1*Δ::*hisG; RPS1/rps1*Δ::Clp10-*PMR1*	(Bates *et al.*, 2005)
CDH15	*mnn4*Δ	*ura3*Δ::*imm434/ura3*Δ::*imm434; mnn4*Δ::*hisG/mnn4*Δ::*hisG; RPS10*::*URA3*	(Hobson *et al.*, 2004)
CDH13	*mnn4*Δ + *MNN4*	*ura3*Δ::*imm434/ura3*Δ::*imm434; mnn4*Δ::*hisG/mnn4*Δ::*hisG; RPS10*::[Clp10-*MNN4-URA3*]$_n$	(Hobson *et al.*, 2004)
NGY582	*mnn2*Δ	*ura3*Δ::*imm434/ura3*Δ::*imm434; mnn2*Δ::*dpi200/mnn2*Δ::*dpi200; RPS1/rps1*Δ::Clp10	(Hall *et al.*, 2013)
NGY583	*mnn2*Δ + *MNN2*	*ura3*Δ::*imm434/ura3*Δ::*imm434; mnn2*Δ*::dpl200/mnn2*Δ*::dpl200; RPS1/rps1*Δ*::*Clp10-*MNN2*	(Hall *et al.*, 2013)
NGY600	*mnn2–26*Δ	*ura3*Δ*::imm434/ura3*Δ*::imm434; mnn2*Δ*::dpl200/mnn2*Δ*::dpl200; mnn22*Δ*::dpl200/mnn2*Δ*::dpl200; mnn23*Δ*::dpl200/mnn23*Δ*::dpl200; mnn24*Δ*::dpl200/mnn24*Δ*::dpl200; mnn26*Δ*::dpl200/mnn26*Δ*::dpl200; mnn21*Δ*::dpl200/mnn21*Δ*::dpl200; RPS1/rps1*Δ*::*Clp10	(Hall *et al.*, 2013)
NGY337	*mnt1*Δ/*mnt2*Δ	*ura3*Δ*::imm434/ura3*Δ*::imm434; mnt1*Δ*::hisG/mnt1*Δ*::hisG; mnt2*Δ*::hisG/mnt2*Δ*::hisG; RPS10/rps10*Δ::Clp10	(Munro *et al.*, 2005)
NGY335	*mnt1*Δ/*mnt2*Δ + *MNT1*	*ura3*Δ*::imm434/ura3*Δ*::imm434; mnt1*Δ*::hisG/mnt1*Δ*::hisG; mnt2*Δ*::hisG/mnt2*Δ*::hisG; RPS10/rps10*Δ::Clp10-*MNT1*	(Munro *et al.*, 2005)
SN152	SN152	*his1*Δ/*his1*Δ; *leu2*Δ/*leu2*Δ; *arg4*Δ/*arg4*Δ; *URA3*/*ura3*Δ::*imm434*; *IRO1/iro1*Δ::*imm434*	(Noble and Johnson, 2005)
*upc2*Δ/Δ	*upc2*Δ/Δ	*his1*Δ/*his1*Δ; *leu2*Δ/*leu2*Δ; *arg4*Δ/*arg4*Δ; *URA3*/*ura3*Δ::*imm434*; *IRO1/iro1*Δ::*imm434; upc2*Δ::*C.dubliniensisHIS1/upc2*Δ::*C.maltosaLEU2*	(Noble *et al.*, 2010)
*sod1*Δ/Δ	*sod1*Δ/Δ	*his1*Δ/*his1*Δ; *leu2*Δ/*leu2*Δ; *arg4*Δ/*arg4*Δ; *URA3*/*ura3*Δ::*imm434*; *IRO1/iro1*Δ::*imm434; sod1*Δ::*C.dubliniensisHIS1/sod1*Δ::*C.maltosaLEU2*	(Noble *et al.*, 2010)
*sod2*Δ/Δ	*sod2*Δ/Δ	*his1*Δ/*his1*Δ; *leu2*Δ/*leu2*Δ; *arg4*Δ/*arg4*Δ; *URA3*/*ura3*Δ::*imm434*; *IRO1/iro1*Δ::*imm434; sod2*Δ::*C.dubliniensisHIS1/sod2*Δ::*C.maltosaLEU2*	(Noble *et al.*, 2010)
*sod3*Δ/Δ	*sod3*Δ/Δ	*his1*Δ/*his1*Δ; *leu2*Δ/*leu2*Δ; *arg4*Δ/*arg4*Δ; *URA3*/*ura3*Δ::*imm434*; *IRO1/iro1*Δ::*imm434; sod3*Δ::*C.dubliniensisHIS1/sod3*Δ::*C.maltosaLEU2*	(Noble *et al.*, 2010)
*sod4*Δ/Δ	*sod4*Δ/Δ	*his1*Δ/*his1*Δ; *leu2*Δ/*leu2*Δ; *arg4*Δ/*arg4*Δ; *URA3*/*ura3*Δ::*imm434*; *IRO1/iro1*Δ::*imm434; sod4*Δ::*C.dubliniensisHIS1/sod4*Δ::*C.maltosaLEU2*	(Noble *et al.*, 2010)
*sod5*Δ/Δ	*sod5*Δ/Δ	*his1*Δ/*his1*Δ; *leu2*Δ/*leu2*Δ; *arg4*Δ/*arg4*Δ; *URA3*/*ura3*Δ::*imm434*; *IRO1/iro1*Δ::*imm434; sod5*Δ::*C.dubliniensisHIS1/sod5*Δ::*C.maltosaLEU2*	(Noble *et al.*, 2010)
*sod4–5*Δ/Δ	*sod4–5*Δ/Δ	*his1*Δ/*his1*Δ; *leu2*Δ/*leu2*Δ; *arg4*Δ/*arg4*Δ; *URA3*/*ura3*Δ::*imm434*; *IRO1/iro1*Δ::*imm434; sod4*Δ::*C.dubliniensisHIS1/sod4*Δ::*C.maltosaLEU2; sod5*Δ::*C.dubliniensisHIS1/sod5*Δ::*C.maltosaLEU2*	(Noble *et al.*, 2010)
*sod4–6*Δ/Δ	*sod4–6*Δ/Δ	*his1*Δ/*his1*Δ; *leu2*Δ/*leu2*Δ; *arg4*Δ/*arg4*Δ; *URA3*/*ura3*Δ::*imm434*; *IRO1/iro1*Δ::*imm434; sod4*Δ::*C.dubliniensisHIS1/sod4*Δ::*C.maltosaLEU2; sod5*Δ::*C.dubliniensisHIS1/sod5*Δ::*C.maltosaLEU2; sod6*Δ::*C.dubliniensisHIS1/sod6*Δ::*C.maltosaLEU2*	(Noble *et al.*, 2010)
Non-*albicans Candida* strains			
WU284	*Candida dubliniensis*	Wild-type	(Morschhäuser *et al.*, 1999)
CAY676	*Candida tropicalis*	Type strain	ATCCMYA-3404
CLIB214	*Candida parapsilosis*	Type strain	(Zwolinska-Wcislo *et al.*, 1998)
AM16/0701	*Candida krusei*	Clinical isolate	D. MacCallum, University of Aberdeen, Scotland, UK
ATCC2001	*Candida glabrata*	Type strain	ATCC2001

2.2 FORMATION OF DUAL-SPECIES BIOFILMS

Biofilms were grown in 96-well plates as previously described (Merritt *et al.*, 2005). Briefly, cultures were washed twice in PBS and bacterial cultures diluted to OD_{600} of 0.2, and *Candida* strains diluted to 1×10^6 cells/mL in Mueller Hinton broth (MHB), or DMEM supplemented with 1% L-glutamine. Bacterial ($2.4x10^6$) and *Candida* (1×10^5) cells were incubated statically in flat-bottom 96-well plates for 2 h at 37°C to enable attachment, then non-adhered cells were removed and replaced with fresh MHB media. After 24 h, the media was replaced with fresh MHB media containing the appropriate amount of antimicrobial, or vehicle control, for an additional 2–18 h. To disrupt biofilms, media was replaced with 100 µl PBS containing 50 µg/mL DNase, and incubated at 37°C for 1 h. Biofilms were detached using a water bath sonicator and/or by scraping using sterile pipette tips. Biofilm cells were resuspended and serially diluted 1 in 10 in PBS, and plated onto cetrimide agar (to determine viable *P. aeruginosa* CFU) and YPD agar supplemented with 100 µg/mL tetracycline (to determine viable *Candida* CFU). Experiments were performed with three technical and at least three biological replicates.

2.2.1 Formation of dual-species biofilms with lower starting concentrations of *C. albicans*

Single- and dual-species biofilms ± 2 µg/mL amphotericin B were grown as above, but with varying starting numbers of *C. albicans* cells: 1×10^5, 1×10^4, 1×10^3, 1×10^2 or 1×10^1. Subsequently, biofilms were quantified as above. Experiments were performed with three technical and three biological replicates.

2.2.2 Formation of *P. aeruginosa* biofilms in the presence of dead *C. albicans*

To kill *C. albicans*, stationary-phase cultures were washed with PBS and cells either heat-killed at 100°C in PBS for 1 h, or fixed in 1 mL 4% paraformaldehyde (PFA) at room temperature for 1 h. Cells were then washed with PBS and diluted in MHB to 1×10^6 cells/mL. Subsequently, biofilms were established and quantified as above.

2.2.3 Formation of *P. aeruginosa* biofilms in the presence of fungal ECM components

Single-species *P. aeruginosa* biofilms were established and grown for 24 h in MHB supplemented, at either 0 or 24 h, with 0.25 mg/mL glucan (from *Saccharomyces cerevisiae*), laminarin (from *Laminaria digitata*), mannan (from *Saccharomyces cerevisiae*), or chitosan (all obtained from Sigma-Aldrich, UK). After 24 h, media was replaced with MHB containing the appropriate amount of antibiotic, and biofilms were subsequently incubated and quantified as above.

2.2.4 Formation of *C. albicans* biofilms in the presence of dead *P. aeruginosa*

To kill *P. aeruginosa*, stationary-phase cultures were washed with PBS and cells either heat-killed at 100°C in PBS for 1 h, or fixed in 1 mL 4% paraformaldehyde (PFA) at room temperature for 1 h. Cells were then washed with PBS and diluted in MHB to OD_{600} of 0.8 to mimic *P. aeruginosa* concentrations recovered from mature biofilms. Subsequently, biofilms were established and quantified as above.

2.2.5 Formation of *C. albicans* biofilms in the presence of purified *P. aeruginosa* rhamnolipid

Single-species *C. albicans* biofilms were established and grown for 24 h in MHB supplemented, at either 0 or 24 h, with 1000–2000 μg/mL rhamnolipid (90% pure, from *P. aeruginosa*, obtained from Sigma-Aldrich, UK). After 24 h, media was replaced with MHB containing the appropriate amount of antifungal, and biofilms were subsequently incubated and quantified as above.

2.2.6 Formation of *C. albicans* biofilms in the presence of supernatant from mature biofilms

Single- and dual-species biofilms were established as described above, but with 96 technical replicates. After 24 h, biofilm supernatants were removed, and technical replicates pooled and filter-sterilised (0.2 μm filters). Biofilm supernatants were then snap-frozen in liquid N_2 and stored at -20°C for up to 6 days, until required. Single-species *C. albicans* biofilms were established as described above, in media containing 50% MHB and 50% biofilm supernatant. After 24 h, media was replaced with 50:50 MHB:supernatant containing the appropriate amount of antifungal, and biofilms were subsequently incubated and quantified as above.

2.2.7 Formation of *C. albicans* biofilms in the presence of reactive oxygen species (ROS)-inducing agents

Biofilms were established as described above. After 3 h, media was removed and replaced with MHB containing 10 mM hydrogen peroxide, 0.2 mM menadione, or 0.1 mM hypoxanthine and 0.16 mU/mL xanthine oxidase (all from Sigma-Aldrich, UK). At

24 h, media was replaced with MHB containing the appropriate amount of antifungal, and biofilms were subsequently incubated and quantified as above.

2.2.8 Formation of *C. albicans* biofilms in the presence of purified *P. aeruginosa* phenazines

Biofilms were established as described above. After 3 h, media was removed and replaced with MHB containing 40 μM purified phenazine, including phenazine-1-carboxylic acid (Apollo Scientific), phenazine methosulfate (Sigma-Aldrich, UK), pyocyanin (Sigma-Aldrich, UK), 1-hydroxyphenazine (Tokyo Chemical Industry UK Ltd.), or a combination. Phenazine solutions were protected from light and 96-well plates were covered with foil. At 24 h, media was replaced with MHB containing the appropriate amount of antifungal, and biofilms were subsequently incubated and quantified as above.

2.3 PLANKTONIC ASSAY

P. aeruginosa ($2.4x10^7$) and/or *C. albicans* ($1x10^6$) cells were added to 14 mL vent-capped culture tubes in a final volume of 2 mL MHB. Cultures were incubated at 37°C with aeration at 200 rpm, for 3 h; the appropriate amount of antimicrobial was added and cultures incubated for an additional 2–18 h. Cultures were sonicated in a water bath sonicator, mixed further by pipetting up and down, and then serially diluted and plated for viable counts. Experiments were performed with three technical replicates and at least three biological replicates.

2.4 DETERMINATION OF *P. AERUGINOSA* SUSCEPTIBILITY TO MEROPENEM

The MICs of meropenem were determined for *P. aeruginosa* strains according to the standardised broth microdilution method, using Mueller Hinton broth (Andrews, 2001). Concentrations of meropenem used were 0, 1, 2, 4, 8, 16 and 32 µg/mL. MICs were determined for *P. aeruginosa* strains using cells grown on LB agar and cells recovered from biofilms. MICs were determined as the lowest concentration of meropenem that caused no visible growth.

2.5 SCANNING ELECTRON MICROSCOPY OF BIOFILMS

Biofilms were prepared for scanning electron microscopy (SEM) using a previously published protocol (Harriott and Noverr, 2009), with modifications. Single- and dual-species biofilms were grown on cell culture-treated plastic coverslips (Thermo Fisher Scientific) in 24-well plates for 24 h, after which the MHB media was replaced with fresh MHB containing 0 or 5 µg/mL meropenem. At 48 h, coverslips were washed twice with PBS and samples fixed in 2.5% glutaraldehyde in 0.1M phosphate buffer for 1 h, at 4°C. Samples were dehydrated using increasing ethanol concentrations (50%, 70%, 90%, 100%), twice for 15 min each. Ethanol was replaced with liquid CO_2 and heated up to the critical point, to dry the samples. Each coverslip was mounted on a stub and sputter-coated with platinum. SEM images were captured using a Philips XL30 ESEM-FEG (Environmental Scanning Electron Microscope with Field Emission Gun). Preparation of samples was performed by Paul Stanley and Theresa Morris (Centre for Electron Microscopy, University of Birmingham).

2.6 CONFOCAL MICROSCOPY OF BIOFILMS

Single- and dual-species biofilms ± 5 µg/mL meropenem were grown as described above, scaled up to a final volume of 6 mL, in 6-well plates. Media was replaced with PBS containing 5 µg/mL propidium iodide (stains dead cells), 1 µM Syto 9 (dyes DNA) and 3 µg/mL calcofluor white (stains fungal cell wall chitin), and incubated at 4ºC in the dark for 1 h. Biofilms were then fixed by adding 4% PFA, incubated at 4ºC in the dark for 1 h, and then washed twice with PBS. Confocal microscopy was performed using a Leica SP8 system equipped with Leica DM6 upright microscope, 40x/0.80 objective, and 402, 488 and 561 nm lasers. Biofilms were imaged directly in wells with a water dipping lens. Z-stack scans were taken at 2–3 different areas within each well and processed with Fiji and LASx software. Imaging and quantification of biofilm thickness were performed by Dr Alessandro di Maio (Birmingham Advanced Light Microscopy facility, University of Birmingham).

2.7 QUANTIFICATION OF ERGOSTEROL

2.7.1 Filipin staining and fluorescence microscopy of biofilm cells

Single- and dual-species biofilms were established as described above, with six replicate wells per biofilm. At 24 h, MHB media was removed, biofilms were washed once with PBS, and incubated with 4% PFA for 1 h, at room temperature. Biofilms were then disrupted and detached using sterile pipette tips. Cells from three replicate wells were combined into 1.5 mL Eppendorf tubes, so each biofilm was represented by two technical replicate samples. PFA was removed from samples by washing with PBS, after which samples were re-suspended in fresh PBS and stored at 4°C overnight. Subsequently, filipin staining was performed as previously described (Leventhal *et al.*,

2001). PBS was removed and replaced with 75 µL fresh PBS containing 0.05 mg/mL filipin (Sigma-Aldrich, UK). Samples were covered with foil, to prevent photo-bleaching of filipin, and incubated for 2 h, at room temperature. Samples were washed once with PBS, re-suspended in 75 µL fresh PBS, and mounted onto glass slides. Samples were imaged on a Zeiss AxioObserver at 63x magnification, with 30–33 images captured per sample. Images were obtained from three biological replicates. Imaging was performed by Dr Joao Correia (University of Birmingham).

2.7.2 Quantification of fluorescence

The fluorescence intensity of filipin corresponds to ergosterol levels in fungal cells (Sekiya and Nozawa, 1983). Images were analysed using FIJI (Fiji Is Just ImageJ) software (Schindelin *et al.*, 2012). Up to five cells per image were outlined, as well as five spherical areas containing no cells (background fluorescence readings). The mean corrected total cell fluorescence (CTCF) was calculated for each image, in which CTFC = integrated density ÷ (area of cell x mean fluorescence of background readings). Data were analysed using 1-way ANOVA and Holm-Sidak's multiple comparisons test.

2.8 Dual-species RNA sequencing of biofilms

2.8.1 Biofilm formation

Single- and dual-species biofilms were grown in triplicate, in 6-well plates, scaled up to a final volume of 6 mL. After 24 h, the MHB media was replaced with fresh MHB containing 0 or 5 µg/mL meropenem. At 4 h, the media was removed and replaced with 2 mL PBS containing 50 µg/mL DNase, which had been incubated at 37°C. Sterile cell scrapers were used to detach biofilm cells and technical replicates

were pooled and mixed in a cooled 15-mL Falcon tube, on ice. A 50 µL volume of biofilm cells was removed and serially diluted 1 in 10 in sterile PBS, and plated onto cetrimide agar (to determine *P. aeruginosa* CFU) and YPD agar supplemented with 100 µg/mL tetracycline (to determine *C. albicans* CFU). The biofilm cell samples were centrifuged at 3500 rpm, at 4°C, for 5 min, to form cell pellets. The supernatant was removed, and cell pellets were snap frozen in liquid nitrogen, before being stored at -70°C, until required. Four biological replicate samples were packaged on dry ice and shipped to GeneWiz®, UK, for RNA extraction, sequencing and bioinformatics analyses.

2.8.2 RNA extraction, library preparation and RNA sequencing

RNA extraction was performed using the QIAGEN RNeasy® Plus Mini Kit. Library preparation was done in the following stages: A) Ribosomal RNA depletion. For this stage, two different probes were used – one targeting *P. aeruginosa* rRNA and another targeting *C. albicans* rRNA; B) RNA fragmentation and random priming; C) First and second strand cDNA synthesis; D) End repair, 5' phosphorylation and dA-tailing; E) Adapter ligation, PCR enrichment and sequencing (Figure 2.1). Paired-end sequencing was performed using Illumina HiSeq 4000 (2x150bp configuration, single index, per lane). RNA extraction, library preparation and RNA sequencing were carried out by GeneWiz® as a paid service.

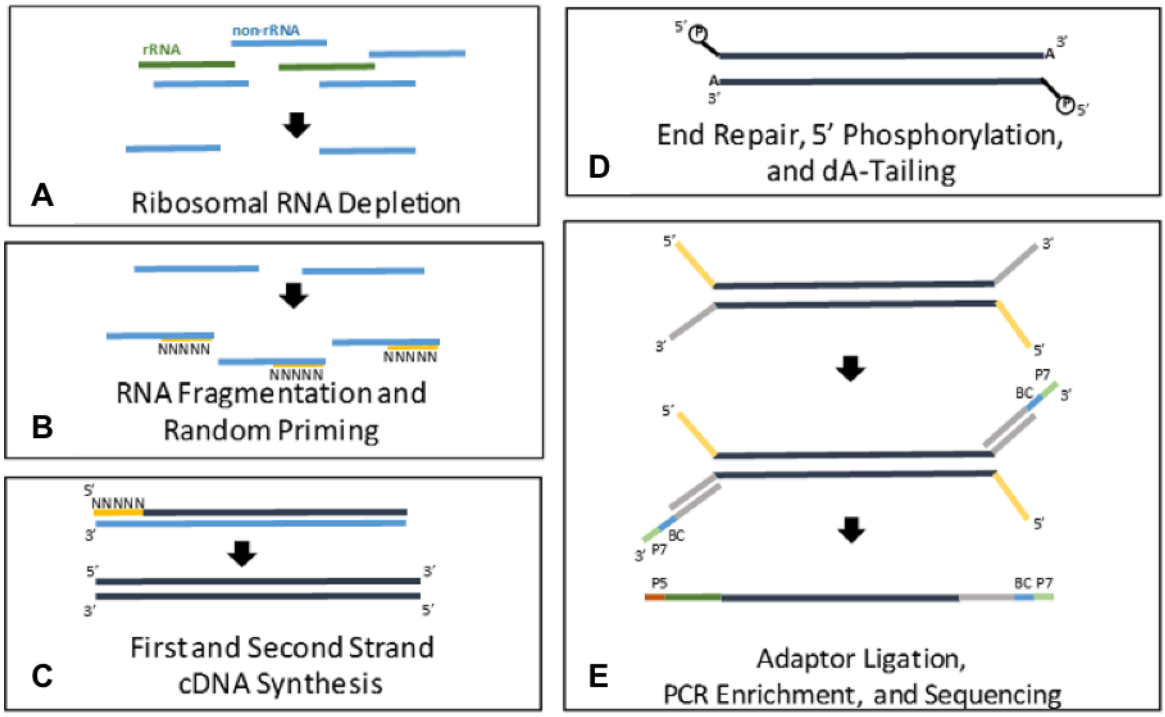


Figure 2.1. GeneWiz® RNA sequencing library preparation workflow. Stages include: **A**. Ribosomal RNA depletion, using separate probes for *C. albicans* rRNA and for *P. aeruginosa* rRNA; **B.** RNA fragmentation and random priming; **C.** First and second strand cDNA synthesis; **D.** End repair, 5' phosphorylation and dA-tailing; **E.** Adapter ligation, PCR enrichment and sequencing. Figure provided by GeneWiz®.

2.8.3 Bioinformatics analyses

Sequence quality of each sample was evaluated by determination of the number of reads, the yield (Mbases), the mean quality score, and the percentage of reads over 30 bases in length. FastQC software was used to determine per base sequence quality and per sequence GC content.

Sequence reads were trimmed to remove possible adapter sequences and nucleotides with poor quality, using Trimmomatic v.0.36. The trimmed reads were mapped to the following reference genomes, available on ENSEMBL, using the STAR aligner v.2.5.2b.

- C_albicans_SC5314 (http://www.candidagenome.org/download/sequence/C_albicans_SC5314/Assembly21/current/)
- P_aeruginosa_PAO1 (https://www.ncbi.nlm.nih.gov/nuccore/NC_002516.2)

The STAR aligner is a splice aligner that detects splice junctions and incorporates them to help align the entire read sequences. Reads obtained from dual-species biofilm samples were mapped to each reference genome separately. BAM files were generated as a result of this step.

Unique gene hit counts were calculated using featureCounts from the Subread package v.1.5.2. The hit counts were summarised and reported using the gene_id feature in the annotation file. Only unique reads that fell within exonic regions were counted. For each gene or open reading frame (ORF) per genome, output data tables included: name, region, expression value, transcripts per million (TPM), reads per kilobase per million (RPKM), gene length, unique gene reads, and total gene reads.

After extraction of gene hit counts, the data were used for downstream differential expression analysis. Using DESeq2, a comparison of gene expression between the relevant groups of samples was performed. The Wald test was used to generate p-values and $\log_2$ fold changes. Principal component analysis (PCA) was performed to reveal the similarities within and between groups, with PCA plots included in the output. Volcano plots were also included in the output, which show global transcriptional change across the groups compared.

Bioinformatics analyses were carried out by GeneWiz® as a paid service. Sequencing reads and gene hit count tables are available at the Gene Expression Omnibus (GEO) database (https://www.ncbi.nlm.nih.gov/geo/), under accession number GSE167137.

2.8.4 Enrichment analyses

For *P. aeruginosa* transcriptomic analysis, differential expression of genes between conditions was considered significant if the adjusted P-value (Padj) was ≤0.05. Gene ontology (GO) analysis was done using KOBAS 3.0 software (KEGG (Kyoto Encyclopaedia of Genes and Genomes) Orthology Based Annotation System) (Xie *et al.*, 2011). KOBAS 3.0 works by determining which GO terms are statistically significantly associated with the input gene list by performing the Fisher's exact test with the Benjamini and Hochberg method for false discovery rate (FDR) correction. The level of enrichment of GO terms is determined by its enrichment ratio, which is calculated by taking the number of genes annotated to a specific GO term from the input differentially expressed gene (DEG) list, and dividing it by the total number of genes assigned to that GO term in the KEGG orthology database for the selected species. KEGG pathway enrichment analysis was also done using KOBAS 3.0 software (Xie *et al.*, 2011), using the same statistical methods as described above.

For *C. albicans* transcriptomic analysis, differential expression of genes between conditions was considered significant if the adjusted P-value (Padj) was ≤0.05 and the $\log_2$ fold change was ≥1 (Dutton *et al.*, 2016b, Bruno *et al.*, 2015, Fourie *et al.*, 2021). Gene ontology (GO) analysis was done using the *Candida* Genome Database (CGD) Gene Ontology Slim Mapper (Skrzypek *et al.*, 2017, Arnaud *et al.*, 2009). This tool

maps the annotations from each gene list to GO Slim terms, which are broad, high-level GO terms that are specific to the selected *Candida* species; in this case, *C. albicans* (Skrzypek *et al.*, 2017). KEGG pathway enrichment analysis was done using KOBAS 3.0 software (Xie *et al.*, 2011), as described previously.

2.9 STATISTICAL ANALYSIS

Statistical analyses were done using GraphPad Prism 9.1.0 software. Viable counts data from *C. albicans* biofilm assays, and from the dual-species RNA-seq biofilm samples, were $\log_{10}$-transformed to enable statistical analyses of large, $\log_{10}$-scale changes in viable counts between experimental conditions. Unless otherwise stated, data were analysed using 2-way ANOVA and Holm-Sidak's multiple comparisons test.

3 *CANDIDA ALBICANS* ENHANCES MEROPENEM TOLERANCE OF *PSEUDOMONAS AERUGINOSA* IN A DUAL-SPECIES BIOFILM

Parts of this chapter have been previously published:

Alam, F., Catlow, D., Di Maio, A., Blair, J. M. A. and Hall, R. A. (2020) '*Candida albicans* enhances meropenem tolerance of *Pseudomonas aeruginosa* in a dual-species biofilm', *J Antimicrob Chemother*, 75(4), pp. 925–935.

3.1 INTRODUCTION

Research on the interactions between *Pseudomonas aeruginosa* and *Candida albicans* has focused predominantly on physical and molecular interactions, and their effects on growth, morphology and virulence (Lopez-Medina *et al.*, 2015, Trejo-Hernández *et al.*, 2014, Chen *et al.*, 2014, Bandara *et al.*, 2013, Cugini *et al.*, 2010, Hogan *et al.*, 2004). However, little is known of how their interactions affect antimicrobial drug efficacy. Studies on mono-species *C. albicans* and *P. aeruginosa* biofilms have linked biofilm extracellular matrix (ECM) material to antimicrobial drug inhibition. For example, the fungal polysaccharide ß-1,3-glucan sequesters the antifungal, fluconazole (Taff *et al.*, 2012), whilst the *P. aeruginosa* exopolysaccharides Pel and Psl are implicated in the inhibition of various antibiotics, including tobramycin (Hall and Mah, 2017).

Dual-species biofilm studies have shown that *C. albicans* can enhance the antibiotic tolerance of other bacterial species, including *Staphylococcus aureus* and *Escherichia coli* (Kong *et al.*, 2016, De Brucker *et al.*, 2015). Antibiotic protection was enhanced by *C. albicans* strains that secrete high levels of β-1,3-glucan, whilst inhibiting glucan synthesis with the antifungal, caspofungin, re-sensitised the bacteria to the antibiotic (Kong *et al.*, 2016). In mixed *C. albicans–S. aureus* biofilms, β-1,3-glucan was shown to coat the bacteria, impairing the ability of vancomycin to reach the bacterial cells (Kong *et al.*, 2016). Kong *et al.* (2016) demonstrated that increased tolerance of *S. aureus* to vancomycin is also observed in the presence of purified mannan or total *C. albicans* biofilm matrix material (Kong *et al.*, 2016). Kong *et al.* (2016) therefore proposed a barrier model as the mechanism of action, whereby secreted *C. albicans*

cell wall polysaccharides coat bacterial cells and act as a barrier to impede antibiotic access to the bacterial cells (Kong *et al.*, 2016). In a similar manner, β-1,3-glucan was shown to enhance ofloxacin tolerance of *E. coli* cells when grown in a mixed *C. albicans–E. coli* biofilm (De Brucker *et al.*, 2015). However, De Brucker *et al.* (2015) proposed an alternative model for the protective mechanism. De Brucker *et al.* (2015) suggested sequestration of ofloxacin by β-1,3-glucan, leading to a decreased rate of ofloxacin penetration into the biofilm. This would result in *E. coli* cells being exposed to a low initial concentration of ofloxacin, potentially giving the cells sufficient time to initiate a defensive response (De Brucker *et al.*, 2015).

The frequency of co-infection by *C. albicans* and *P. aeruginosa* highlights the clinical importance of gaining a greater understanding of the impact of this cross-kingdom interaction on antimicrobial tolerance. Meropenem is a first-line antibiotic for treating *Pseudomonas* infections in the CF lung (Cystic Fibrosis Trust, 2009). Meropenem is a carbapenem ß-lactam, which targets penicillin-binding proteins within Gram-negative bacteria, causing inhibition of cell wall peptidoglycan synthesis, ultimately leading to osmotic lysis of bacterial cells (Fernandez *et al.*, 2013, Papp-Wallace *et al.*, 2011). Meropenem is administered intravenously, as a 15–30-minute infusion at 1–2 g (adult dose), three times daily, for two weeks (Nicolau, 2008). When *P. aeruginosa* biofilms are treated with clinical doses of meropenem, only bacteria at the biofilm peripheries are killed, whilst cells closer to the base remain viable (Haagensen *et al.*, 2015). In patients, the meropenem concentration found in epithelial lining fluid one hour post-treatment is 5.3 μg/mL (Nicolau, 2008), with the clinical breakpoint of *Pseudomonas*

being >8 µg/mL (EuCAST, 2020a). Therefore, slight deviations in tolerance of *P. aeruginosa* to meropenem could impede clearance of the infection.

In this study, we observed that dual-species *P. aeruginosa–C. albicans* biofilms displayed enhanced tolerance to meropenem. This protection was provided through active secretion of fungal ECM components, specifically mannan and ß-glucan. Therefore, co-colonisation of *P. aeruginosa* and *C. albicans*, within the CF lung, may result in small reservoirs of protected *P. aeruginosa*, which could survive antimicrobial treatment and reseed the infection site.

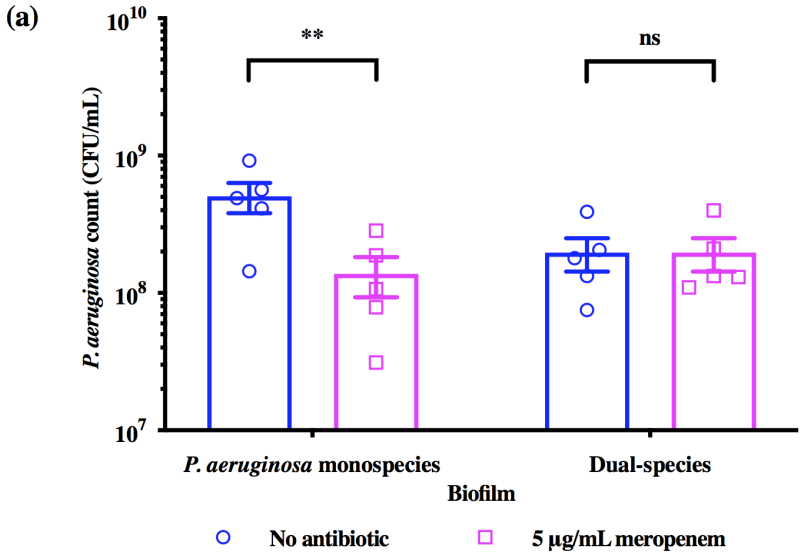
3.2 RESULTS

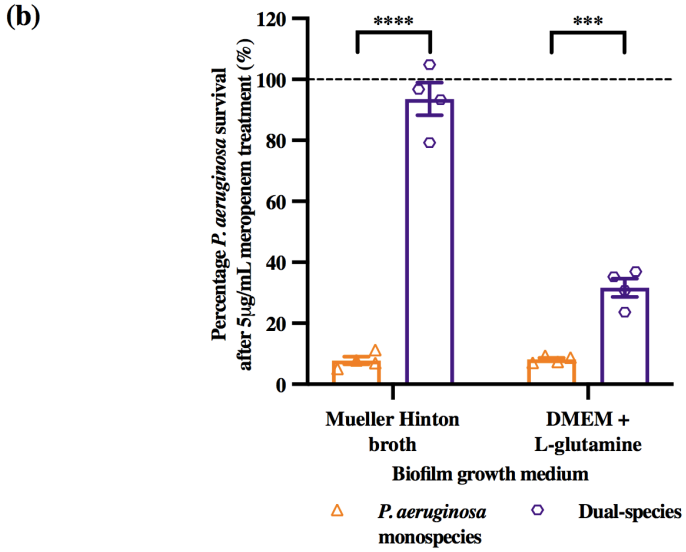
3.2.1 *C. albicans* increases the tolerance of *P. aeruginosa* to meropenem in dual-species biofilms

To determine whether the presence of *C. albicans* within a *P. aeruginosa* biofilm is able to enhance the tolerance of *P. aeruginosa* to meropenem, mono-species (*P. aeruginosa*) and dual-species (*P. aeruginosa–C. albicans*) biofilms were grown for 24 h and then treated with meropenem. *P. aeruginosa* survival was then quantified by viable counts. Given that the actual concentration of meropenem in the lung immediately after administration is between 5–6 µg/mL (Nicolau, 2008), this drug concentration was the focus of the study. The viability of *P. aeruginosa* mono-species biofilms was reduced to 25.35% when treated with 5 µg/mL meropenem, indicating *P. aeruginosa* biofilm cells are susceptible to meropenem (Figure 3.1a). Fewer *P. aeruginosa* cells were recovered from dual-species biofilms, which is likely due to nutrient competition. However, in the presence of *C. albicans*, meropenem was non-

effective against *P. aeruginosa* in both MHB (Figure 3.1a) and DMEM (Figure 3.1b), indicating that this inter–kingdom interaction negatively affects meropenem efficacy. Viable counts of *C. albicans* confirmed that meropenem has no effect on *C. albicans* (Figure 3.1c). Fewer *C. albicans* cells were recovered from dual-species biofilms, as shown by the ~2$\log_{10}$ drop in *C. albicans* CFU/mL (Figure 3.1c), suggesting nutrient competition and reduced *C. albicans* viability in the presence of *P. aeruginosa*.

To visualise the structure of the biofilms, samples were analysed by scanning electron microscopy and confocal microscopy. Mono-species *P. aeruginosa* biofilms were significantly reduced in the presence of meropenem, while in the meropenem-treated dual-species biofilms, significant levels of *P. aeruginosa* colonised the fungal hyphae, forming tight associations to the fungal surfaces (Figure 3.2), thus confirming the viable counts data. In agreement with this, the biofilm thickness was lower in meropenem-treated dual-species biofilms (Figure 3.3 and 3.4), indicating dense packing of bacterial cells against fungal hyphae, creating a more compact biofilm structure. Therefore, the presence of *C. albicans* enhances the tolerance of *P. aeruginosa* to meropenem.


(a)
**
ns
P. aeruginosa count (CFU/mL)
P. aeruginosa monospecies
Dual-species
Biofilm
No antibiotic
5 µg/mL meropenem


(b)
****
***
Percentage P. aeruginosa survival after 5µg/mL meropenem treatment (%)
Mueller Hinton broth
DMEM + L-glutamine
Biofilm growth medium
P. aeruginosa monospecies
Dual-species

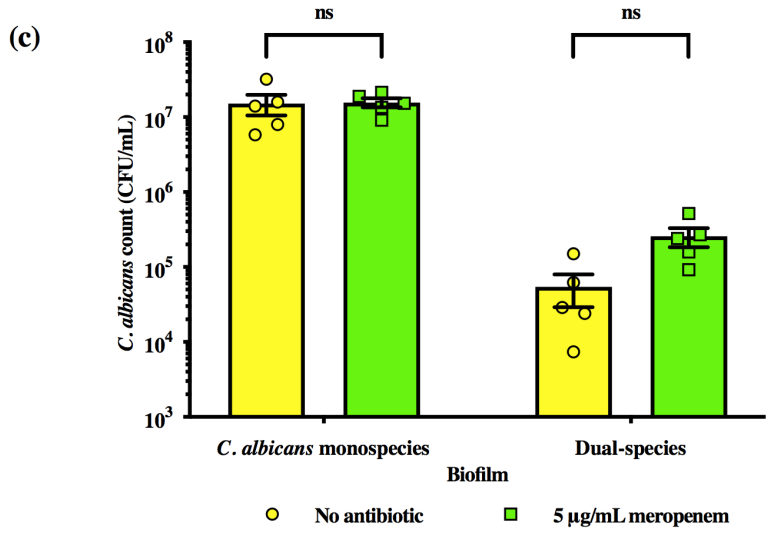

(c)
ns
ns
C. albicans count (CFU/mL)
C. albicans monospecies
Dual-species
Biofilm
No antibiotic
5 µg/mL meropenem

Figure 3.1. *C. albicans* SC5314 increases the tolerance of *P. aeruginosa* PAO1 to meropenem in a dual-species biofilm. (a) Preformed 24 h biofilms were incubated in Mueller Hinton broth containing no antibiotic or 5 µg/mL meropenem, for 18 h. Data are the mean ± the SEM from 5 biological replicates. **(b)** Preformed 24 h biofilms were incubated in Mueller Hinton broth or DMEM (supplemented with 1% L-glutamine) containing no antibiotic or 5 µg/mL meropenem, for 18 h. Data show the mean ± the SEM from 4 biological replicates. **(c)** Meropenem has no effect on *C. albicans* biofilm viability, whereas the dual-species interaction reduces *C. albicans* viability by ~2$\log_{10}$ change in CFU/mL. Preformed 24 h biofilms were incubated in Mueller Hinton broth containing no antibiotic or 5 µg/mL meropenem, for 18 h. Data are the mean ± the SEM from 5 biological replicates. Data were analysed using 2-way ANOVA and Holm-Sidak's multiple comparisons test (ns not significant; ** $P < 0.01$; *** $P < 0.001$; **** $P < 0.0001$).

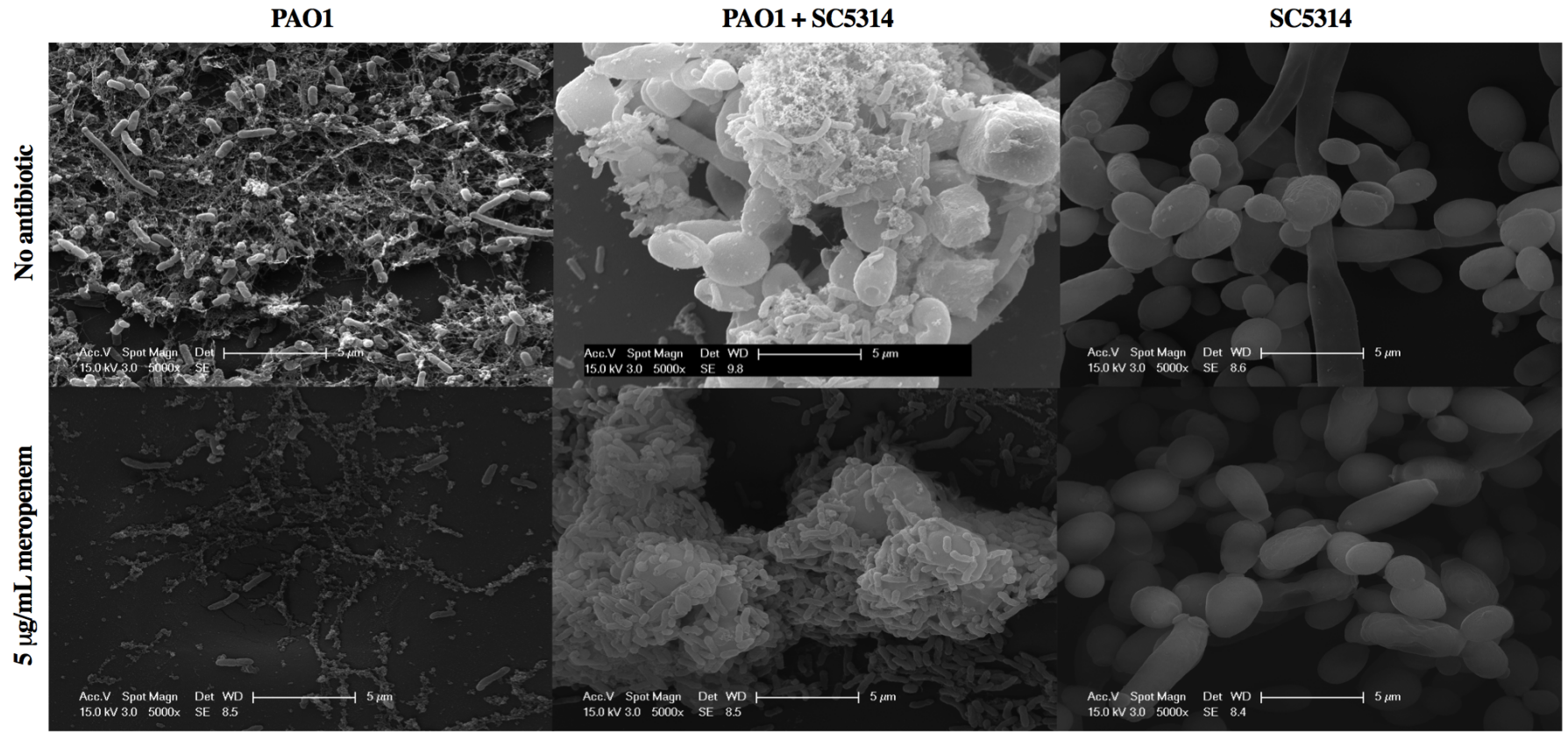


Figure 3.2. SEM analysis of biofilms of *P. aeruginosa* PAO1 and *C. albicans* SC5314. Meropenem treatment of mono-species *P. aeruginosa* biofilms results in reduced numbers of bacterial cells, whilst the presence of *C. albicans* in the dual-species biofilm enhances meropenem tolerance; the tight association of *P. aeruginosa* cells to fungal surfaces is visible. *C. albicans* alone is unaffected by meropenem.

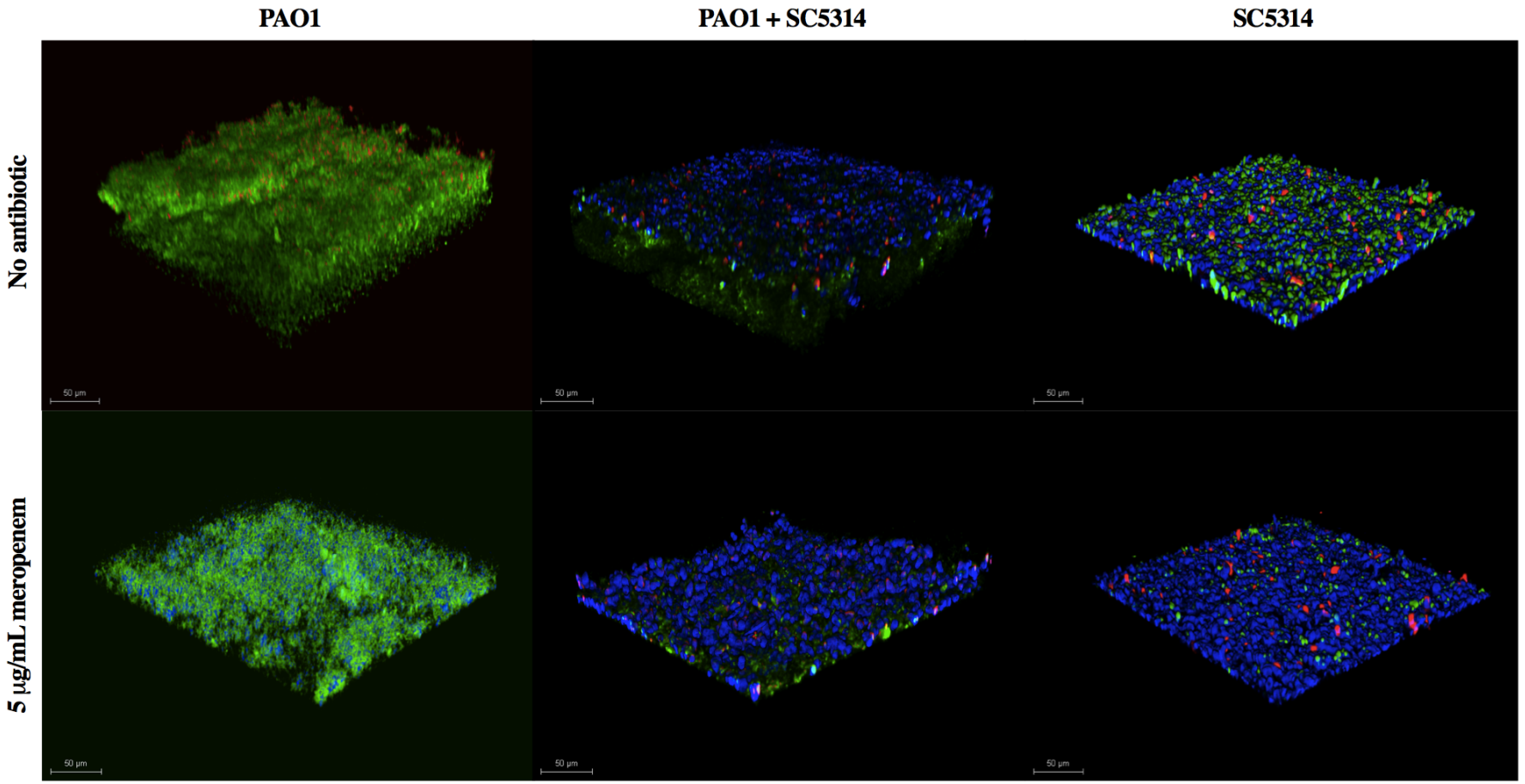


Figure 3.3. Three-dimensional reconstructions of biofilms from confocal z-stacks. Red indicates propidium iodide stain (dead cells), green indicates Syto 9 dye (DNA), and blue indicates calcofluor white stain (chitin).

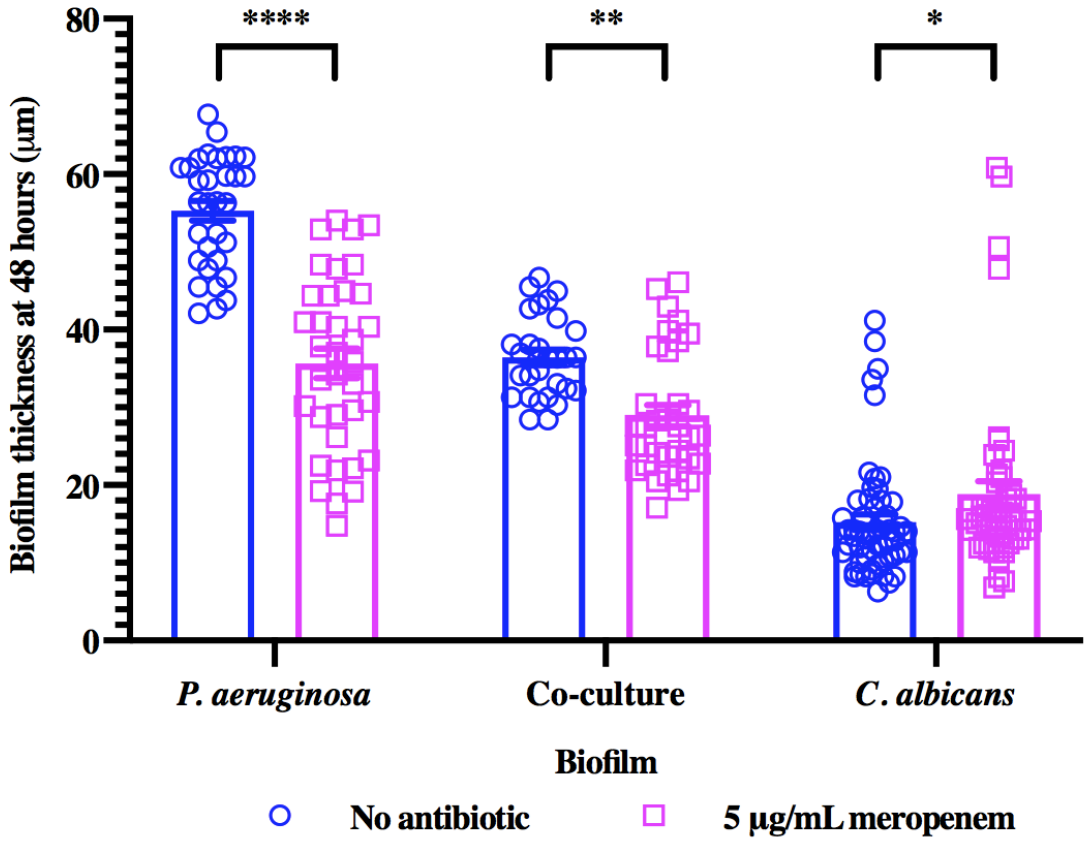


Figure 3.4. Quantification of biofilm thickness from confocal microscopy images. Preformed 24 h biofilms were incubated in Mueller Hinton broth containing 0 or 5 µg/mL meropenem, for 18 h. Biofilms were fixed, stained and washed, before confocal images were taken from 2–3 areas per biofilm. Data show the mean ± the SEM from 2 biological replicates. Data were analysed using 2-way ANOVA and Holm-Sidak's multiple comparisons test (ns not significant; * $P < 0.05$; ** $P < 0.01$; **** $P < 0.0001$).

3.2.2 Meropenem tolerance is not maintained following subculture of *P. aeruginosa* biofilm cells

The selective pressure from antibiotic use increases the likelihood of cells developing resistance. The sessile nature and close proximity of biofilm cells promotes cell-cell interactions (Savage *et al.*, 2013), increasing horizontal gene transfer and mutation frequencies relative to planktonic cells (Olsen, 2015). Furthermore, the presence of *C. albicans* increases *P. aeruginosa* mutation rates (Trejo-Hernández *et*

al., 2014). To determine whether the observed increase in meropenem tolerance of *P. aeruginosa* was due to selection for resistance mutations, the meropenem MICs of cells recovered from both *P. aeruginosa* mono- and dual-species biofilms that had been treated with 5 µg/mL meropenem, or untreated, were determined by standard broth microdilution MIC assay, and compared to the MIC of the starter culture. The MIC of *P. aeruginosa* PAO1 under all tested conditions was 4 µg/mL. These data suggest that *P. aeruginosa* cells recovered from treated biofilms were not resistant to meropenem and, therefore, the observed increased tolerance was unlikely due to selection for resistance mutations.

3.2.3 Increased tolerance of *P. aeruginosa* to meropenem is specific to dual-species biofilms

Enhanced survival of *P. aeruginosa* as a result of interactions with *C. albicans* has previously been observed in planktonic cultures, through inter-kingdom communication via secreted metabolites (Chen *et al.*, 2014). To determine whether the observed increase in meropenem tolerance of *P. aeruginosa* was specific to biofilms, the susceptibility of *P. aeruginosa* to meropenem in the presence of *C. albicans* was tested during planktonic growth. At all meropenem concentrations tested, there was no significant difference in *P. aeruginosa* survival whether in the presence or absence of *C. albicans* (Figure 3.5), suggesting that *C. albicans*-mediated protection is biofilm-specific.

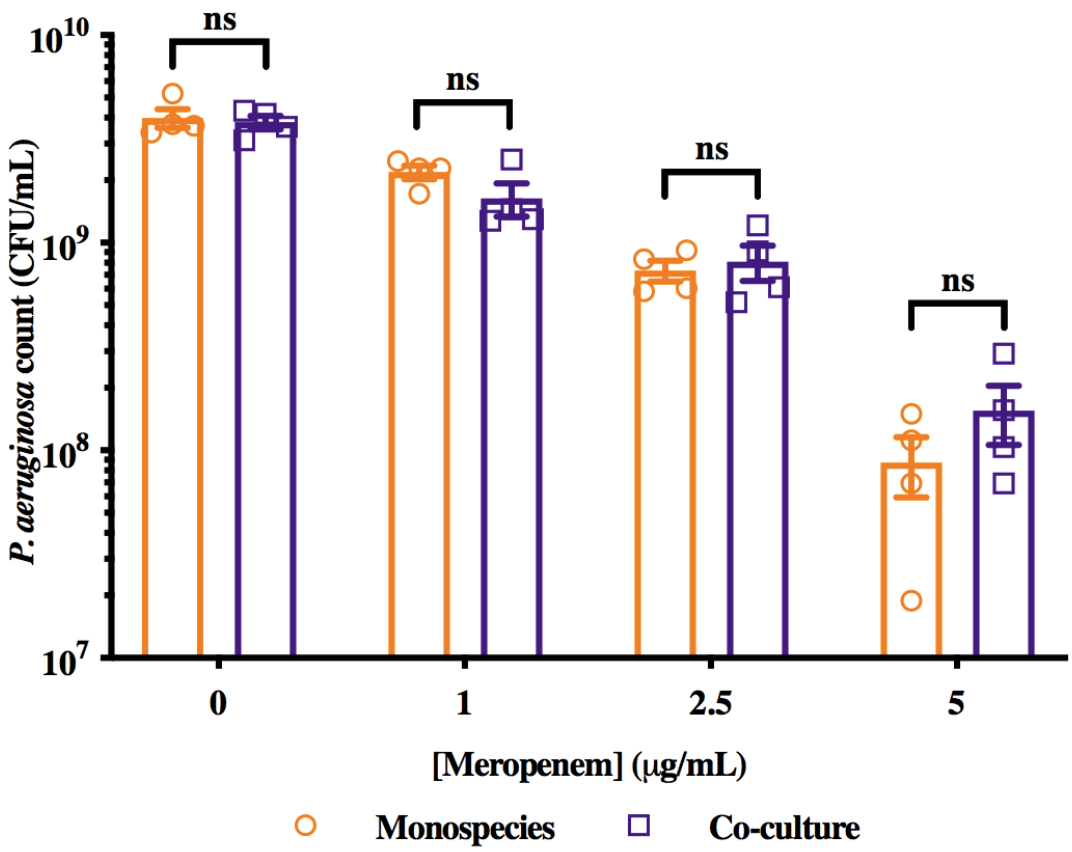


Figure 3.5. Increased *P. aeruginosa* meropenem tolerance in the presence of *C. albicans* is biofilm-specific. Planktonic cultures were grown for 3 h and subsequently incubated in Mueller Hinton broth containing 0, 1, 2.5 or 5 μg/mL meropenem, for 18 h. Data are the mean ± the SEM from 4 biological replicates. Data were analysed using 2-way ANOVA and Holm-Sidak's multiple comparisons test (ns not significant).

3.2.4 Increased *P. aeruginosa* tolerance to meropenem is dependent on fungal viability

Production of fungal biofilm ECM is an active process, involving secretion of glycoproteins, polysaccharides, lipids and nucleic acids (Lohse *et al.*, 2018). To determine whether the protective effect of *C. albicans* is mediated by an active or passive mechanism, *P. aeruginosa* biofilms were grown in the presence of either heat-killed *C. albicans* (disrupts the fungal cell wall, denatures proteins, and causes cell lysis), or by fixing the *C. albicans* cells in 4% PFA (maintains cell structure). However,

in the presence of heat-killed or PFA-fixed *C. albicans*, *P. aeruginosa* remained susceptible to meropenem (Figure 3.6), suggesting that *C. albicans* actively protects *P. aeruginosa* from meropenem.

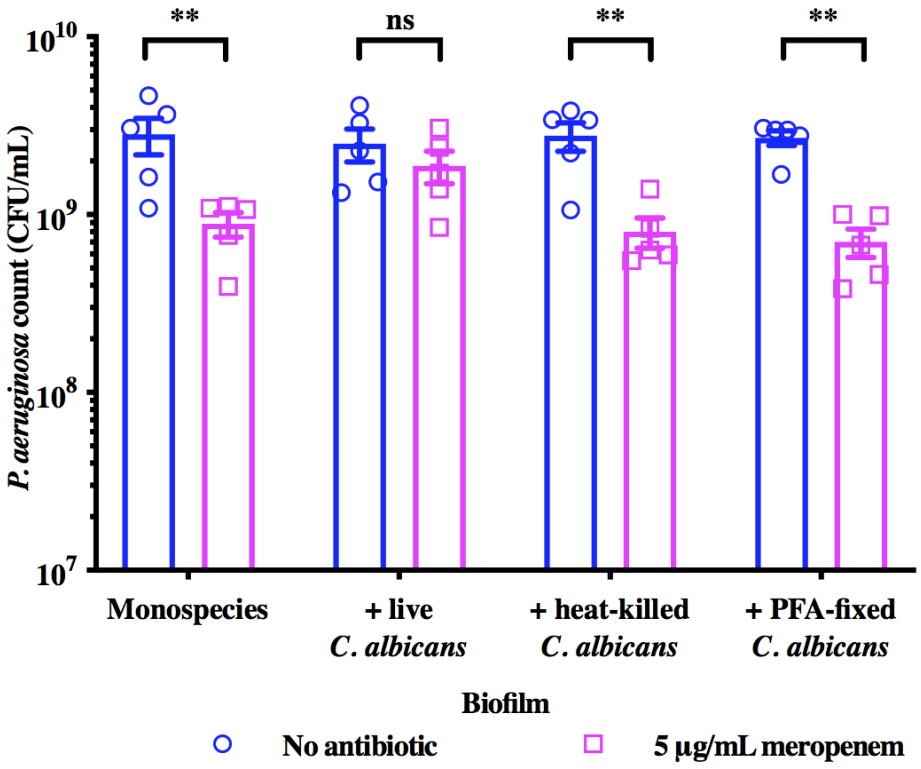


Figure 3.6. Increased tolerance to meropenem is dependent on fungal viability. Preformed 24 h biofilms were incubated in Mueller Hinton broth containing no antibiotic or 5 µg/mL meropenem, for 18 h. Data are the mean ± the SEM from 5 biological replicates. Data were analysed using 2-way ANOVA and Holm-Sidak's multiple comparisons test (ns not significant; ** $P < 0.01$).

3.2.5 *C. dubliniensis* also enhances *P. aeruginosa* meropenem tolerance in dual-species biofilms

Only a few species of the *Candida* genus are associated with disease in humans, including *C. albicans*, *C. dubliniensis*, *C. tropicalis*, *C. parapsilosis*, *C. krusei* and *C. glabrata* (Whibley and Gaffen, 2015). To determine whether other *Candida* species can also protect *P. aeruginosa* from meropenem, biofilms were grown in the

presence of these clinically-relevant non-*albicans Candida* (NAC) species. Of the NAC species tested, only *C. dubliniensis* increased the tolerance of *P. aeruginosa* to meropenem (Figure 3.7). *C. dubliniensis* is phylogenetically most closely related to *C. albicans* (Papon *et al.*, 2013), indicating that *C. albicans* and *C. dubliniensis* may enhance *P. aeruginosa* meropenem tolerance in a similar manner.

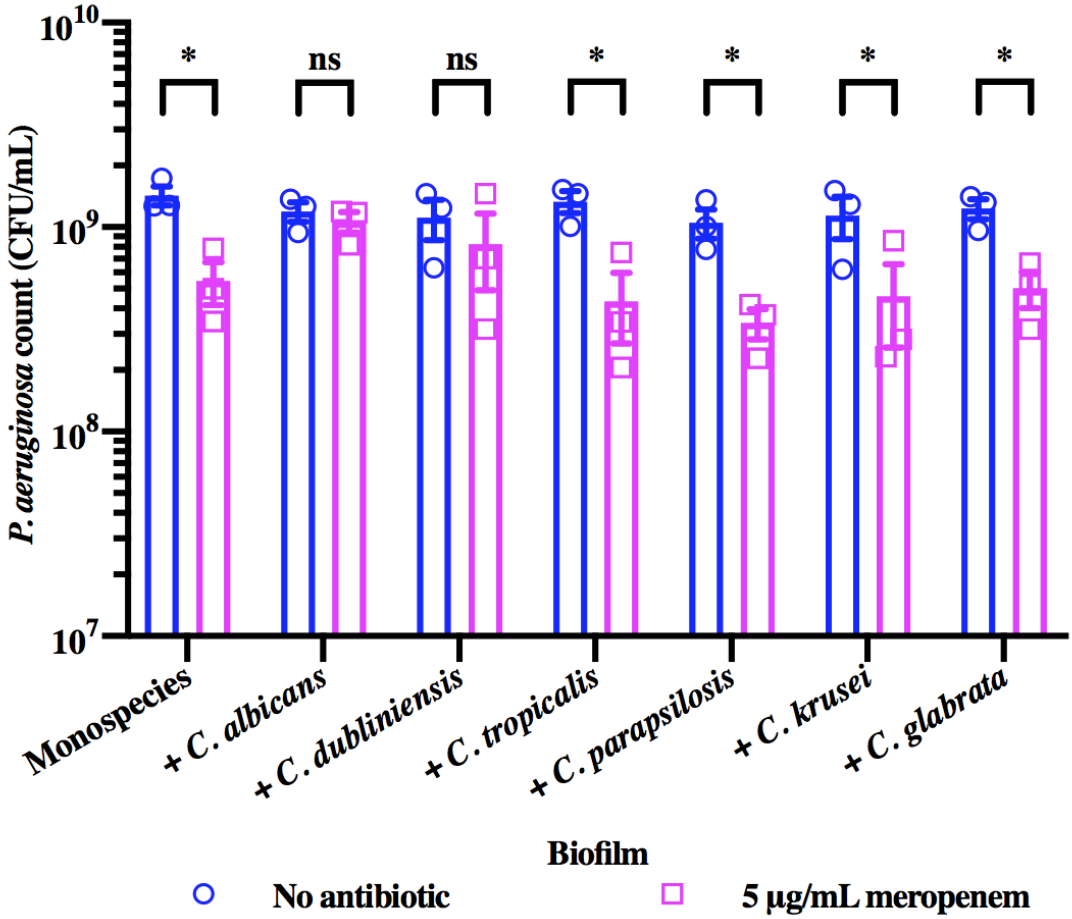


Figure 3.7. *C. dubliniensis* also enhances tolerance of *P. aeruginosa* to meropenem in dual-species biofilms. Preformed 24 h biofilms were incubated in Mueller Hinton broth containing no antibiotic or 5 µg/mL meropenem, for 18 h. Data are the mean ± the SEM from 3 biological replicates. Data were analysed using 2-way ANOVA and Holm-Sidak's multiple comparisons test (ns not significant; * $P < 0.05$).

3.2.6 Fungal cell wall polysaccharides enhance *P. aeruginosa* tolerance to meropenem

The secretion of ECM polymers, specifically polysaccharides, by *C. albicans* biofilm cells is linked to increased antifungal resistance of fungal biofilms (Taff *et al.*, 2013, Nett *et al.*, 2007). However, there is increasing evidence that fungal ECM polysaccharides also contribute to antibiotic resistance in dual-species biofilms (Harriott and Noverr, 2009, Kong *et al.*, 2016, De Brucker *et al.*, 2015). To determine whether secreted fungal cell wall polymers play a role in protecting *P. aeruginosa*, mono-species *P. aeruginosa* biofilms were grown in the presence of purified fungal cell wall polysaccharides, including glucan (a mix of ß-1,3-glucan and ß-1,6-glucan), laminarin (an isoform of ß-1,3-glucan), mannan, and chitosan (de-acetylated chitin). Both mannan and glucan enhanced the tolerance of *P. aeruginosa* to meropenem in biofilms (Figure 3.8a), but not in planktonic cultures (Figure 3.8b). To determine whether mannan and glucan have independent effects, *P. aeruginosa* biofilms were supplemented with glucan and mannan in combination. However, no additive effect was observed (Figure 3.8c). To gain some insight into whether mannan and glucan were binding and sequestering meropenem, or whether these polysaccharides were forming a 'protective coating' on the *P. aeruginosa* biofilm, the effect of changing the time point at which mannan and glucan were added was investigated. Mannan and glucan, either alone or in combination, were added to the meropenem-containing media, which was added to mature biofilms (24-h growth), alongside controls containing no meropenem. Results from these experiments showed that mannan and glucan also protected *P. aeruginosa* when added to mature biofilms at the same time as meropenem (Figure 3.8d), suggesting that the polysaccharides may sequester or

inhibit the activity of the drug. These data refute the ‘protective coating’ hypothesis, as the polysaccharides would not have had the opportunity to form a barrier over the biofilms when added at the same time as meropenem. Therefore, *C. albicans* actively secretes mannan and/or glucan into the biofilm ECM, which protects *P. aeruginosa* from meropenem, likely through binding and sequestration of the antibiotic drug molecules.

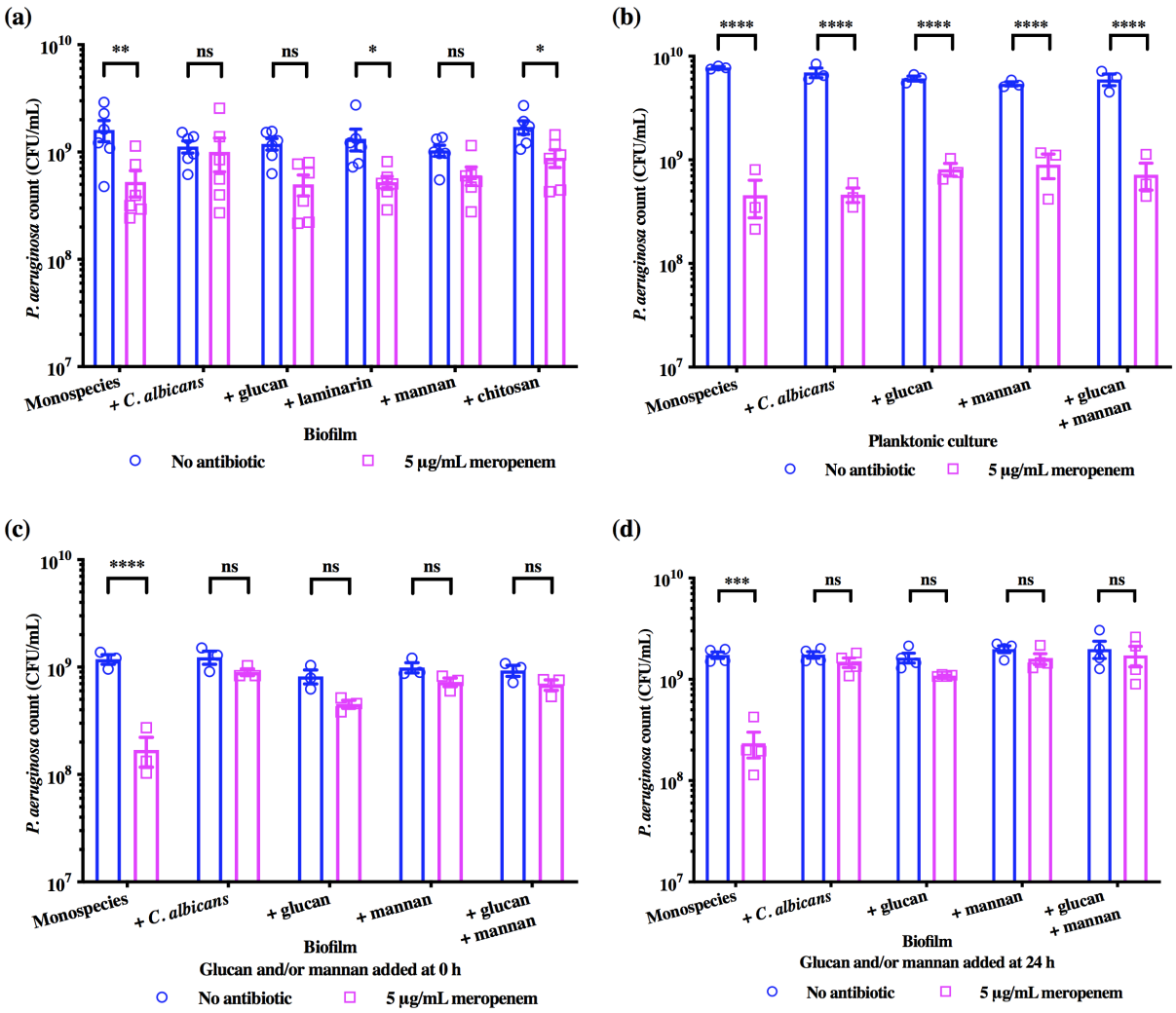


Figure 3.8. Mannan and glucan enhance *P. aeruginosa* biofilm tolerance to meropenem. Fungal polysaccharides were used at a final concentration of 0.25 mg/mL. **(a)** Mannan and glucan enhance *P. aeruginosa* biofilm tolerance to 5 µg/mL meropenem. Preformed 24 h biofilms were incubated in Mueller Hinton broth containing no antibiotic or 5 µg/mL meropenem, for 18 h. Data are the mean ± the SEM from 6 biological replicates. **(b)** Enhanced meropenem tolerance from mannan and glucan is biofilm-specific. Planktonic cultures supplemented with exogenous mannan and/or glucan were grown for 3 h and subsequently incubated in Mueller Hinton broth containing 5 µg/mL meropenem for 18 h. Data are the mean ± the SEM from 3 biological replicates. **(c)** The effects of mannan and glucan are not additive. Data are the mean ± the SEM from 3 biological replicates. **(d)** Mannan and glucan enhance *P. aeruginosa* biofilm tolerance to meropenem, even when added to pre-formed biofilms. Pre-formed 24 h biofilms were incubated for 18 h in Mueller Hinton broth containing no antibiotic, 5 µg/mL meropenem, 0.25 mg/mL mannan or glucan, or a combination of these. Data are the mean ± the SEM from 4 biological replicates. Data were analysed using 2-way ANOVA and Holm-Sidak's multiple comparisons test (ns not significant; * $P < 0.05$; ** $P < 0.01$; *** $P < 0.001$; **** $P < 0.0001$).

3.2.7 *C. albicans* cell wall glycosylation is important for protection against meropenem

To further investigate the role of fungal mannan in meropenem tolerance, the ability of *C. albicans* cell wall glycosylation mutants to protect *P. aeruginosa* was quantified. *C. albicans* has two major forms of mannan, the extensively branched *N*-linked mannan and the simple, linear *O*-linked mannan. Deletion of genes involved in key steps in glycosylation result in the incorporation of altered mannan epitopes in the cell wall (Figure 3.9a) and within the biofilm ECM (Sheth *et al.*, 2011, Murciano *et al.*, 2011, Hall *et al.*, 2013).

To determine the role of these glycosylation structures in protecting *P. aeruginosa* from the actions of meropenem, mutants defective in general protein glycosylation (*pmr1*Δ, ATPase required for transporting Ca^{2+} and Mn^{2+} ions into the Golgi), *N*-mannan phosphomannan incorporation *(mnn4*Δ), *N*-mannan side chain elaboration (*mnn2*Δ, *mnn2-26*Δ), and *O*-mannan biosynthesis (*mnt1*Δ*/mnt2*Δ) were tested for their ability to

protect *P. aeruginosa* from meropenem. The *pmr1*Δ mutant causes loss of a Golgi Ca^{2+}/Mn^{2+} ATPase, affecting numerous mannosyltransferases, so the extent of truncation of the α-1,6-mannose backbone is variable (Sheth *et al.*, 2011, Murciano *et al.*, 2011), whilst only the unsubstituted α-1,6-mannose backbone of *N*-mannan remains in the *mnn2-26*Δ sextuple mutant (Figure 3.9a).

Deletion of genes required for *N*-mannan biosynthesis (*mnn4*, *mnn2-26* and *pmr1*) reduced the ability of *C. albicans* to protect *P. aeruginosa* from meropenem (Figure 3.9b-c). SEM analysis showed very few bacterial cells surviving meropenem-treatment in dual-species biofilms with the *C. albicans* glycosylation mutants, most clearly seen with *mnn4*Δ and *mnt1*Δ/*mnt2*Δ (Figure 3.10), but bacteria that did survive were closely adhered to the fungal cell surface, suggesting that cell-cell adherence may play a role in meropenem tolerance. In agreement with this, deletion of genes involved in *O*-mannan biosynthesis (*mnt1*/*mnt2*), which have previously been shown to be involved in bacterial attachment to *C. albicans* (Brand *et al.*, 2008), had the greatest impact on *P. aeruginosa* protection (Figure 3.9d and Figure 3.10). This indicates that protection of *P. aeruginosa* requires full elaboration of fungal mannan.

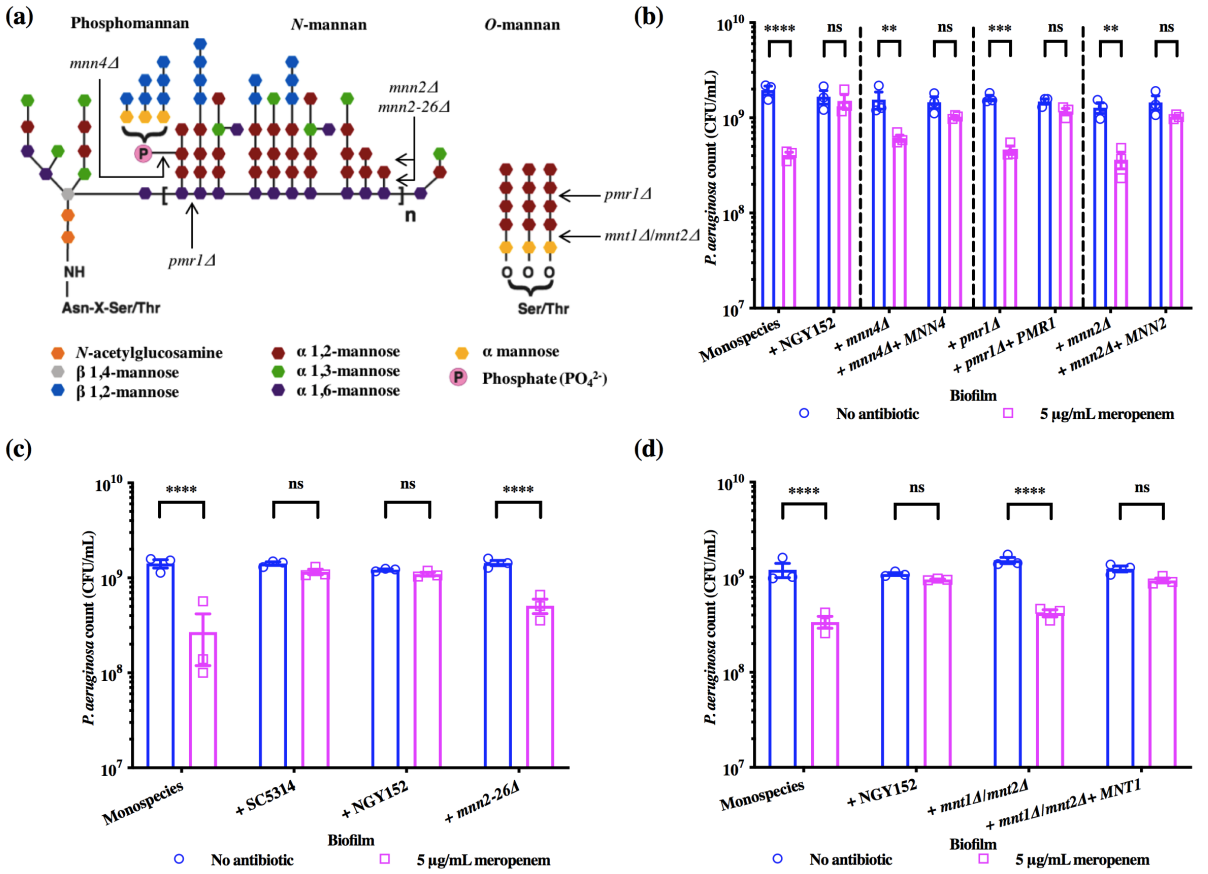


Figure 3.9. *C. albicans* cell wall glycosylation is important for protection against meropenem (a) Schematic diagram representing the structure of *N*-mannan (including phosphomannan) and *O*-linked mannan of *C. albicans* (Sheth *et al.*, 2011, Hall *et al.*, 2013). The points of truncation of the mutants used in this study are indicated by arrows. **(b)** *N*-mannan glycosylation is important for protection against meropenem. Preformed 24 h biofilms were incubated in Mueller Hinton broth containing no antibiotic or 5 µg/mL meropenem, for 18 h. The *N*-mannan glycosylation mutants, *mnn4*Δ, *pmr1*Δ, or *mnn2*Δ inhibit the ability of *C. albicans* to protect *P. aeruginosa*. Tolerance to meropenem is restored in reconstituted control strains. **(c)** The *mnn2-26*Δ sextuple mutant inhibits the ability of *C. albicans* to protect *P. aeruginosa*. **(d)** *O*-mannan glycosylation is important for protection against meropenem. The *mnt1*Δ/*mnt2*Δ double mutant inhibits the ability of *C. albicans* to protect *P. aeruginosa*. Meropenem tolerance is restored when *MNT1* is reconstituted. Data are the mean ± the SEM from 3 biological replicates. Data were analysed using 2-way ANOVA and Holm-Sidak's multiple comparisons test (ns not significant; ** P < 0.01; *** P < 0.001; **** P < 0.0001).

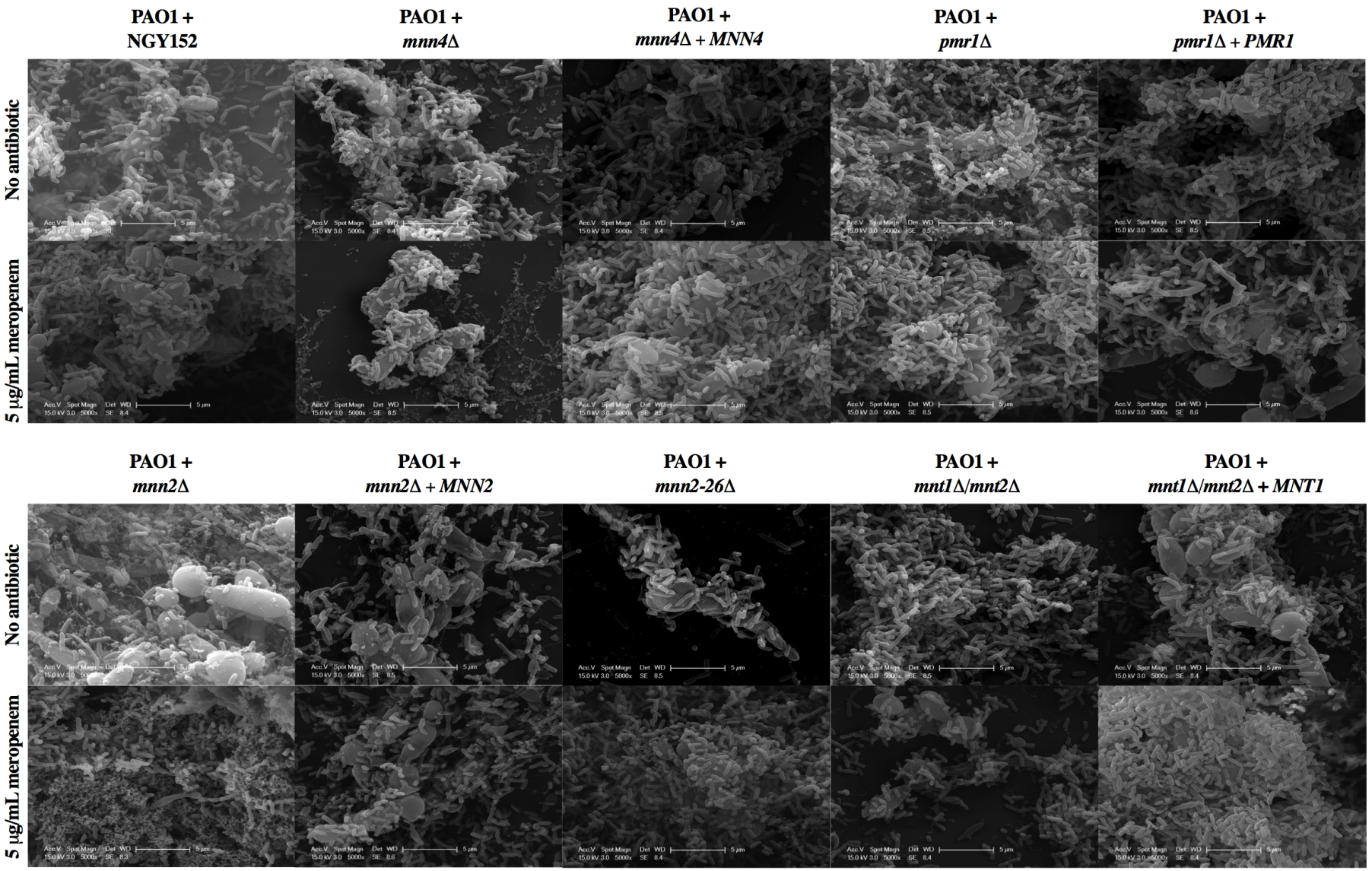

PAO1 + NGY152
PAO1 + mnn4Δ
PAO1 + mnn4Δ + MNN4
PAO1 + pmr1Δ
PAO1 + pmr1Δ + PMR1
No antibiotic
5 μg/mL meropenem
PAO1 + mnn2Δ
PAO1 + mnn2Δ + MNN2
PAO1 + mnn2-26Δ
PAO1 + mnt1Δ/mnt2Δ
PAO1 + mnt1Δ/mnt2Δ + MNT1
No antibiotic
5 μg/mL meropenem

Figure 3.10. SEM analysis of biofilms of *P. aeruginosa* PAO1 and *C. albicans* cell wall glycosylation mutants. Deletion of genes required for fungal *N*-mannan biosynthesis (*mnn4*, *pmr1*, *mnn2* or *mnn2-26*) or *O*-mannan biosynthesis (*mnt1*/*mnt2*) reduced the ability of *C. albicans* to protect *P. aeruginosa* from meropenem, as indicated by the reduction in the number of bacterial cells following meropenem treatment, most clearly visible with *mnn4*Δ; the majority of surviving bacteria are in close contact with fungal cells. When the genes (*MNN4*, *PMR1*, *MNN2* or *MNT1*) are reconstituted, the protective effect is restored, as evidenced by the abundance of *P. aeruginosa* cells coating the fungi in the meropenem-treated samples.

3.2.8 Increased tolerance of *P. aeruginosa* to meropenem is strain-specific

In addition to mannan, the *C. albicans* cell wall polysaccharide, chitin, is also involved in attachment to *P. aeruginosa* cells. Chitin is a linear polymer composed of *N*-acetylglucosamine residues linked together by 1,4-glycosidic bonds. Interactions with fungal chitin are mediated by *P. aeruginosa* chitin-binding protein D (CbpD), which is present on the surfaces of *P. aeruginosa* cells, but the protein is also released extracellularly via the type II secretion system (Ovchinnikova *et al.*, 2013, Frederiksen *et al.*, 2013). *P. aeruginosa* CbpD is involved in forming strong physical interactions with *C. albicans* hyphae. A *P. aeruginosa cbpD*Δ mutant strain shows reduced adhesion to *C. albicans* hyphae when compared to the PAO1 wild-type strain, whilst complementation with *CBPD* restores the strong adhesion forces (Ovchinnikova *et al.*, 2013).

To determine the role of fungal chitin in protecting *P. aeruginosa* from the actions of meropenem, *P. aeruginosa* mutants defective in CbpD biosynthesis (*cbpD*Δ) or chitinase synthesis (*chiC*Δ) were tested for their ability to protect *P. aeruginosa* from meropenem. The *P. aeruginosa chiC* gene encodes the extracellular enzyme, chitinase, which degrades chitin, but the mechanism by which the enzyme is secreted is unknown (Folders *et al.*, 2001). Expression of *chiC* is upregulated in *P. aeruginosa* clinical isolates from lung epithelial cells, relative to laboratory strains, indicating a role

for chitinase in infection or virulence (Frederiksen *et al.*, 2013). *P. aeruginosa cbpD*Δ and *chiC*Δ mutant strains were tested in both PAO1 WT and PA14 WT backgrounds, obtained from transposon mutant libraries (Jacobs *et al.*, 2003, Liberati *et al.*, 2006), with the relevant parental strains as controls.

C. albicans enhanced meropenem tolerance of the PAO1 laboratory strain (ATCC15692) that was used throughout this study (Figure 3.11a). However, *C. albicans* did not enhance meropenem tolerance of *P. aeruginosa* in either the *cbpD*Δ or *chiC*Δ mutant strains; furthermore, *C. albicans* did not enhance meropenem tolerance in either parental strain, PAO1 WT or PA14 WT (Figure 3.11b and 3.11c). This indicates that increased tolerance of *P. aeruginosa* to meropenem is strain-specific. The observation that these *P. aeruginosa* wild-type background strains did not show enhanced meropenem tolerance means that we cannot infer from these experiments whether or not fungal chitin plays a role.

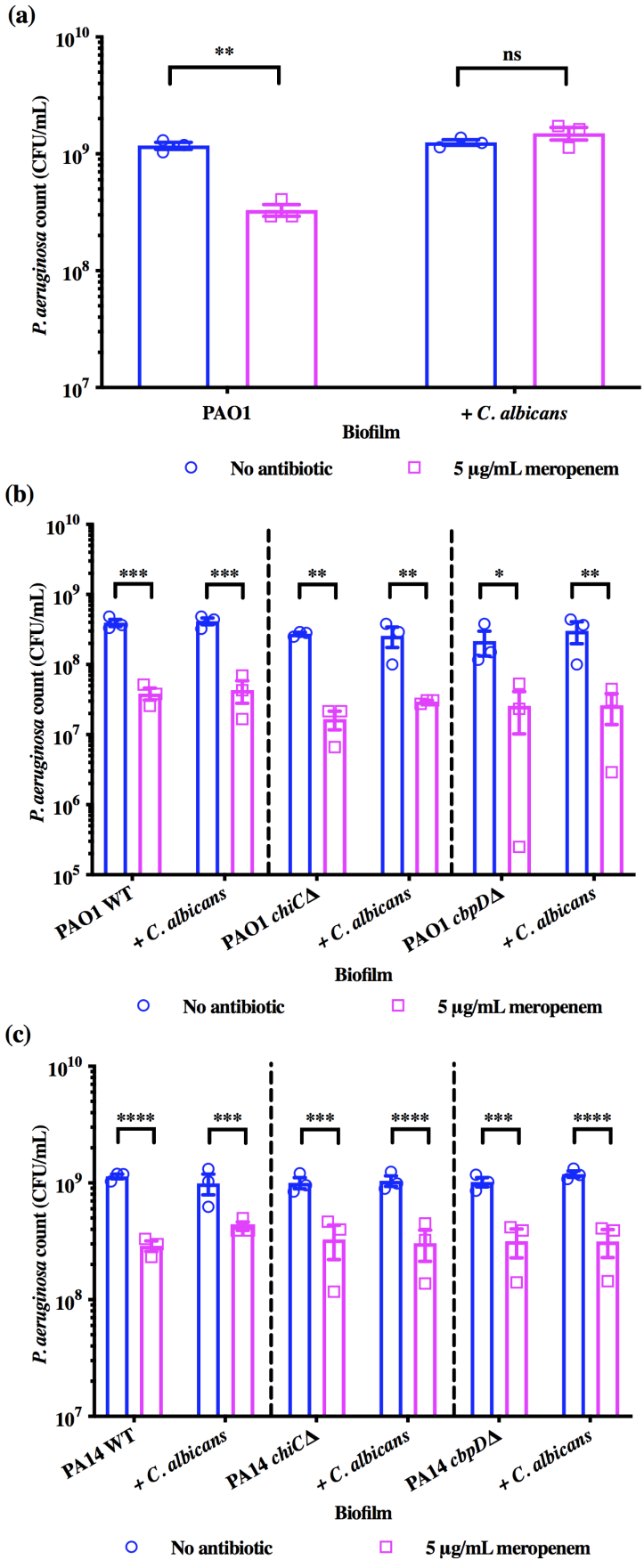

(a)
10^{10}
10^{9}
10^{8}
10^{7}
P. aeruginosa count (CFU/mL)
**
ns
PAO1
+ C. albicans
Biofilm
No antibiotic
5 µg/mL meropenem
(b)
10^{10}
10^{9}
10^{8}
10^{7}
10^{6}
10^{5}
P. aeruginosa count (CFU/mL)
***
***
**
**
*
**
PAO1 WT
+ C. albicans
PAO1 chiCΔ
+ C. albicans
PAO1 cbpDΔ
+ C. albicans
Biofilm
No antibiotic
5 µg/mL meropenem
(c)
10^{10}
10^{9}
10^{8}
10^{7}
P. aeruginosa count (CFU/mL)
****
***
***
****
***
****
PA14 WT
+ C. albicans
PA14 chiCΔ
+ C. albicans
PA14 cbpDΔ
+ C. albicans
Biofilm
No antibiotic
5 µg/mL meropenem

Figure 3.11. Increased tolerance of *P. aeruginosa* to meropenem is strain-specific and does not involve interactions with fungal chitin. Preformed 24 h biofilms were incubated in Mueller Hinton broth containing no antibiotic or 5 µg/mL meropenem, for 18 h. (a) *C. albicans* enhances meropenem tolerance of *P. aeruginosa* PAO1 (ATCC15692) in a dual species biofilm. (b) *C. albicans* does not enhance meropenem tolerance of *cbpD*∆ or *chiC*∆ mutant strains, or of the WT, in a PAO1 background (Jacobs *et al.*, 2003). (c) *C. albicans* does not enhance meropenem tolerance of *cbpD*∆ or *chiC*∆ mutant strains, or of the WT, in a PA14 background (Liberati *et al.*, 2006). Data are the mean ± the SEM from 3 biological replicates. Data were analysed using 2-way ANOVA and Holm-Sidak's multiple comparisons test (ns not significant; * P < 0.05; ** P < 0.01; *** P < 0.001; **** P < 0.0001).

3.2.9 *C. albicans* does not enhance *P. aeruginosa* tolerance to other antibiotics

To determine whether the protective effect conferred by *C. albicans* was confined to meropenem-treated *P. aeruginosa* biofilm cells, or if it applied to a broader range of antibiotic drugs, mono- and dual-species biofilms were treated with different classes of antibiotic. The aim of these experiments was to decipher whether the antibiotic mode of action was important for the protective mechanism. Alongside the carbapenem, meropenem, the other classes of antibiotic tested were a cephalosporin and two fluoroquinolone antibiotics. Carbapenems are broad-spectrum antibiotics that bind to penicillin-binding proteins (PBPs) and inhibit synthesis of bacterial cell walls (Fusté *et al.*, 2013). Cephalosporins also affect bacterial cell wall structure by targeting PBPs and inhibiting peptidoglycan synthesis (Hutchings *et al.*, 2019). Both carbapenems and cephalosporins are ß-lactam antibiotics, i.e. their chemical structure includes a ß-lactam ring (Fernandez *et al.*, 2013). However, fluoroquinolones work by inhibiting DNA gyrase and topoisomerase IV enzymes, thus affecting DNA replication and transcription (Hutchings *et al.*, 2019).

Meropenem is combined with tobramycin for the treatment of *P. aeruginosa* infections in the CF lung (Cystic Fibrosis Trust, 2009). Tobramycin is an aminoglycoside antibiotic, which targets the 16S rRNA of the bacterial 30S ribosomal subunit, thus

inhibiting protein synthesis (Hutchings *et al.*, 2019, Hall and Mah, 2017); the concentration of tobramycin found in the epithelial lining fluid 2 h after treatment is 1.67 µg/mL (Carcas *et al.*, 1999). The third-generation cephalosporin, ceftazidime, is a first-line therapy for the treatment of *P. aeruginosa* infections; the concentration of ceftazidime found in the epithelial lining fluid following a standard dose (20 mg per kg of body weight) is 6 µg/mL (Cousson *et al.*, 2015). The fluoroquinolone, ciprofloxacin, is used to treat chronic *P. aeruginosa* infections in the CF lung (Wagner *et al.*, 2016); the concentration of ciprofloxacin found in the epithelial lining fluid 24 h after a 500 mg dose is negligible (Gotfried *et al.*, 2001). Like ciprofloxacin, oxfloxacin is a second-generation fluoroquinolone antibiotic. Increased ofloxacin tolerance has been shown in *E. coli*, when grown as dual-species *E. coli–C. albicans* biofilms (De Brucker *et al.*, 2015); therefore, ofloxacin was tested to determine whether this effect is also observed with *P. aeruginosa*. Furthermore, combination treatment of meropenem with the antifungal drugs, fluconazole and amphotericin B, were also tested.

To determine whether the presence of *C. albicans* also affects tolerance of *P. aeruginosa* biofilm cells to these other clinically-relevant antibiotics, mono- and dual-species biofilms were treated with 5 and 10 µg/mL meropenem, 2.5 and 5 µg/mL ceftazidime, 0.5 µg/mL ofloxacin, 0.05 µg/mL ciprofloxacin, 2 µg/mL tobramycin, or a combination of 5 µg/mL meropenem with either 2 µg/mL tobramycin, 250 µg/mL fluconazole, or 1 µg/mL amphotericin B. However, the presence of *C. albicans* did not provide protection against these antimicrobial treatments (Figure 3.12), suggesting that the mechanism by which *C. albicans* confers enhanced tolerance is likely due to the chemical structure of meropenem. The observation that *C. albicans* did not provide protection against an increased concentration (10 µg/mL) of meropenem (Figure

3.12a) suggests that any protection conferred by the presence of *C. albicans* in these biofilms was counteracted by the greater reduction in *P. aeruginosa* cells, caused by the increased antibiotic concentration. Furthermore, sufficient numbers of *C. albicans* cells must be present in the biofilm in order to provide protection from meropenem, as neither combination meropenem–fluconazole nor meropenem–amphotericin B treatment maintained the protective effect (Figure 3.12b).

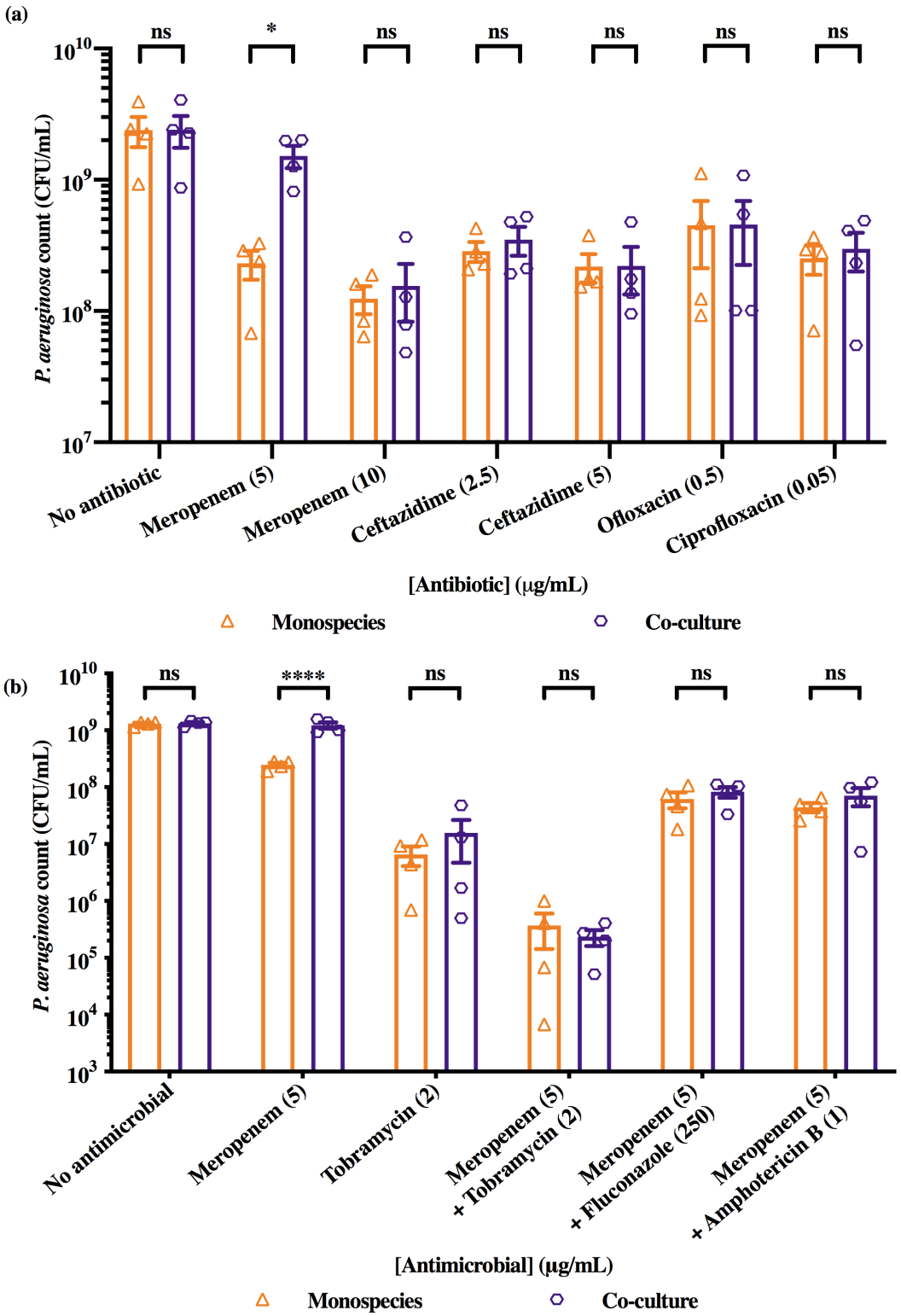

(a)
ns
*
ns
ns
ns
ns
ns
P. aeruginosa count (CFU/mL)
No antibiotic
Meropenem (5)
Meropenem (10)
Ceftazidime (2.5)
Ceftazidime (5)
Ofloxacin (0.5)
Ciprofloxacin (0.05)
[Antibiotic] (μg/mL)
Monospecies
Co-culture
(b)
ns
****
ns
ns
ns
ns
P. aeruginosa count (CFU/mL)
No antimicrobial
Meropenem (5)
Tobramycin (2)
Meropenem (5) + Tobramycin (2)
Meropenem (5) + Fluconazole (250)
Meropenem (5) + Amphotericin B (1)
[Antimicrobial] (μg/mL)
Monospecies
Co-culture

Figure 3.12. *C. albicans* does not enhance *P. aeruginosa* tolerance to other antibiotics. Preformed 24 h biofilms were incubated for 18 h in Mueller Hinton broth containing meropenem (5 or 10 µg/mL), ceftazidime (2.5 or 5 µg/mL), ofloxacin (0.5 µg/mL), ciprofloxacin (0.05 µg/mL), tobramycin (2 µg/mL), or combinations of 5 µg/mL meropenem + either 2 µg/mL tobramycin, 250 µg/mL fluconazole, or 1 µg/mL amphotericin B. **(a)** *C. albicans* does not enhance *P. aeruginosa* tolerance to 10 µg/mL meropenem, ceftazidime, ofloxacin, or ciprofloxacin. **(b)** *C. albicans* does not enhance *P. aeruginosa* tolerance to tobramycin or combination meropenem–tobramycin, meropenem–fluconazole or meropenem–amphotericin B treatment. Data are the mean ± the SEM from 4 biological replicates. Data were analysed using 2-way ANOVA and Holm-Sidak's multiple comparisons test (ns not significant; * $P < 0.05$; **** $P < 0.0001$).

3.2.10 *C. albicans* protects a *P. aeruginosa* Cystic Fibrosis isolate from meropenem

To explore the clinical relevance of the above findings, the ability of *C. albicans* to increase the tolerance of clinical *P. aeruginosa* isolates to meropenem was tested. Clinical isolates from a non-CF respiratory sample (from Queen Elizabeth Hospital, Birmingham) and two CF isolates – the Midlands 1 strain (Scott and Pitt, 2004) and the Liverpool strain (Cheng *et al.*, 1996) – were tested. First, to confirm that these clinical isolates were susceptible to meropenem, MICs were performed on mono-species biofilms. Similar to the PAO1 laboratory strain, the Midlands 1 CF isolate was sensitive to 5 µg/mL meropenem, while the Liverpool CF isolate and the non-CF respiratory isolate were insensitive to this concentration of meropenem, with a biofilm MIC of 16 µg/mL for both. When the meropenem-sensitive, *P. aeruginosa* (Midlands 1) CF isolate was grown in a dual-species biofilm with *C. albicans*, meropenem was less effective at killing the *P. aeruginosa* biofilm cells (Figure 3.13). This suggests that, in CF patients, co-colonisation with *C. albicans* may increase the tolerance of *P. aeruginosa* to meropenem.

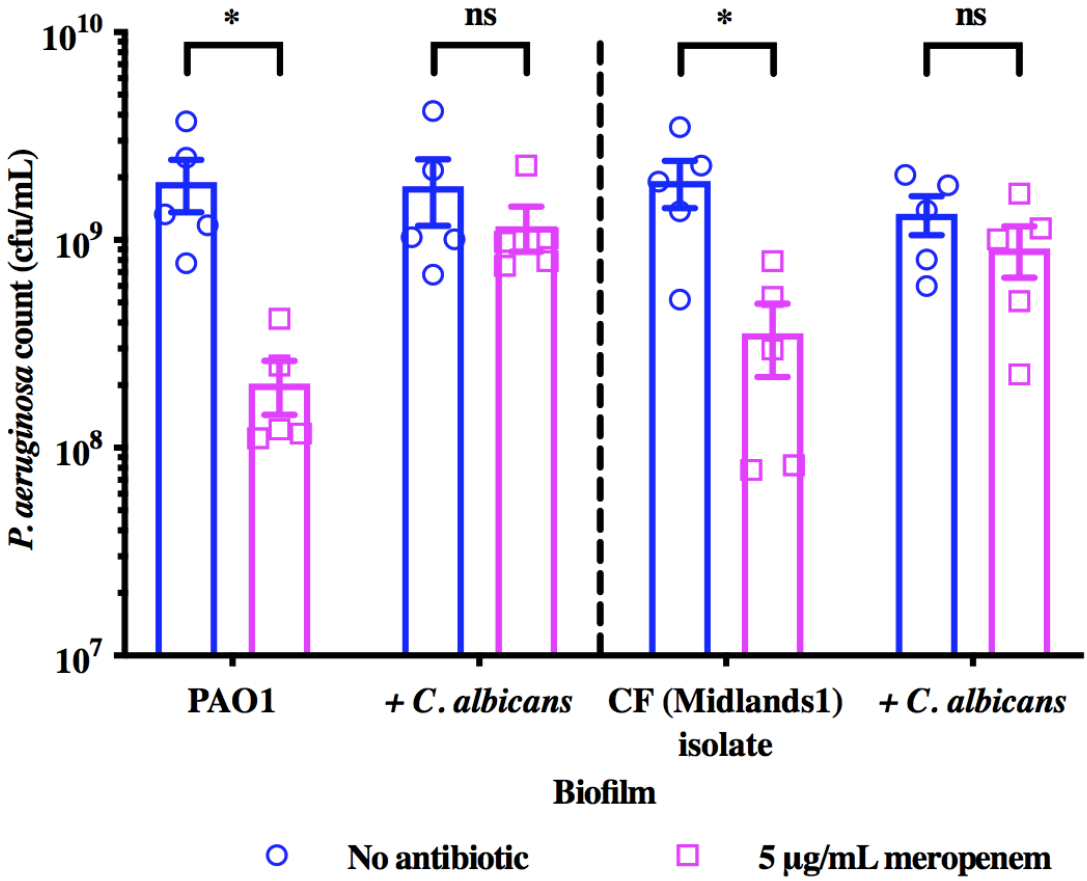


Figure 3.13. *C. albicans* enhances meropenem tolerance of the *P. aeruginosa* CF (Midlands 1) isolate. Preformed 24 h biofilms were incubated in Mueller Hinton broth containing no antibiotic or 5 µg/mL meropenem, for 18 h. Data are the mean ± the SEM from 5 biological replicates. Data were analysed using 2-way ANOVA and Holm-Sidak's multiple comparisons test (ns not significant; * $P < 0.05$).

3.3 Discussion

P. aeruginosa and *C. albicans* are commonly co-isolated from the sputum of CF patients (Trejo-Hernández *et al.*, 2014), where the thickened mucus layer lining the endothelium of the lower respiratory tract provides an ideal environment for biofilm formation (Muthig *et al.*, 2010, Williams *et al.*, 2016). Chronic *P. aeruginosa* colonisation in the CF lung is correlated with increased likelihood of *C. albicans* colonisation, indicating a synergistic interaction that leads to a greater decline in lung function (Dhamgaye *et al.*, 2016, Gileles-Hillel *et al.*, 2015). These data show that *C.*

albicans significantly enhanced *P. aeruginosa* biofilm tolerance to 5 μg/mL meropenem in both a laboratory strain and a CF isolate. Although the protective effect was relatively small (<1log_{10} change in *P. aeruginosa* CFU/mL), this may still have clinical relevance. For example, the clinical breakpoint of *P. aeruginosa* for meropenem is >8 μg/mL (EuCAST, 2020a); this increase in tolerance could push the required meropenem concentration over the clinical breakpoint, categorising the infection as meropenem-resistant. This has direct implications for the treatment of CF patients who present with co-infection in the clinic. Standard doses of meropenem may become insufficient for treating *P. aeruginosa* infection, with combination antibiotic–antifungal therapy being a potentially more effective therapeutic option.

The protective effect of *C. albicans* was biofilm-specific and dependent upon fungal ECM components. This is consistent with other reports where *C. albicans* ECM components have been shown to provide protection against ofloxacin and vancomycin in dual-species biofilms with *E. coli* and *S. aureus*, respectively (De Brucker *et al.*, 2015, Kong *et al.*, 2016). However, in contrast to these studies, where *C. albicans* ECM components provide protection to a range of antimicrobials, *C. albicans* ECM components only increased *P. aeruginosa* tolerance to 5 μg/mL meropenem. This suggests the mechanism by which *C. albicans* ECM components enhance meropenem tolerance may be different to those proposed for other antibiotics. When dual-species biofilms were treated with a higher meropenem concentration, of 10 μg/mL, the protective effect from *C. albicans* was lost. However, 10 μg/mL is greater than the clinical dose of meropenem (Haagensen *et al.*, 2015), and would result in more than just the peripheral biofilm bacterial cells being killed, leading to insufficient numbers for observable *C. albicans*-mediated tolerance. Considering the effect was

not seen for other ß-lactam antibiotics (i.e. ceftazidime), this suggests the protective mechanism may depend on chemical structure, or ability to bind mannan or ß-glucan, rather than the mode of action of the antibiotic.

Previously, mannan and ß-glucan have been shown to bind and sequester antimicrobials, limiting their diffusion through biofilms (De Brucker *et al.*, 2015). Therefore, it is possible that the actual concentration of meropenem within dual-species biofilms is significantly lower. The observation that increased *P. aeruginosa* tolerance to meropenem is maintained when mannan and/or glucan are added to mature biofilms, i.e. at the same time-point as meropenem-treatment, indicates that the drug is being sequestered by the fungal polysaccharides. Similar interactions have been observed in dual-species biofilms, in which *Streptococcus mutans* exopolysaccharides bind and sequester fluconazole, reducing its efficacy against *C. albicans* (Kim *et al.*, 2018). Alternatively, mannans or glucans may coat bacterial cells, providing a physical barrier that impedes drug permeation, supporting the proposed mechanism by which *S. aureus* is protected from vancomycin (Kong *et al.*, 2016).

The finding that the protective effect was observed for one *P. aeruginosa* PAO1 laboratory strain, but not another, indicates that the effect may be strain-specific and perhaps dependent upon the structure and composition of the biofilm formed by each individual strain. It is well known amongst microbiologists that PAO1 strains from different laboratories, both within and between research institutions, show phenotypic and genomic variations, resulting in problems of reproducibility between research groups (Diggle and Whiteley, 2020). Much of the phenotypic variation between different PAO1 strains manifests as alterations in levels of secreted molecules, such

as rhamnolipids, siderophores, phenazines, PQS, eDNA, and OMVs (Chandler *et al.*, 2018). Furthermore, the observed phenotypic variation does not appear to correlate with genetic changes, and is more likely a result of differential regulation of transcription and/or translation. Such phenotypic variation may even be observed in different PAO1 strains obtained from the same parental lineage, which have undergone continuous microevolution during multiple rounds of storage and culture (Chandler *et al.*, 2018). On the other hand, the PA14 laboratory strain historically originates from an environmental isolate, as a plant pathogen (Diggle and Whiteley, 2020), which may explain why it too did not behave similarly to the PAO1 laboratory strain used throughout this study.

Although *C. albicans* remains clinically the most commonly isolated *Candida* species, the prevalence of NAC species is increasing (Sardi *et al.*, 2013). *C. dubliniensis* was the only NAC species that protected *P. aeruginosa* from meropenem. This finding is of clinical relevance as, although less common than *C. albicans*, the prevalence of *C. dubliniensis* within CF patients ranges from 2.6–39.0%, and there are cases of *C. dubliniensis* being co-isolated with *P. aeruginosa* from the lower respiratory tracts of CF patients (Wahab *et al.*, 2014). *C. dubliniensis* is the most closely related NAC species to *C. albicans* and, as a result, their biofilms are structurally similar (Whibley and Gaffen, 2015, Papon *et al.*, 2013), with networks of yeast and hyphal cells embedded in a comparable ECM (Ramage *et al.*, 2001). Although the other NAC species produce biofilms, the compositions of their ECM are considerably different (Cavalheiro and Teixeira, 2018, Silva *et al.*, 2011), and their biofilms lack hyphae, which are important for bacterial attachment. SEM imaging confirmed that most bacteria in the treated dual-species biofilms were attached to fungal hyphae,

suggesting that this physical interaction is important for protection. This hypothesis is supported by the fact that removal of *O*-mannan, which is required for bacterial binding (Munro *et al.*, 2005, Brand *et al.*, 2008), reduced the ability of *C. albicans* to protect *P. aeruginosa*. However, given that purified carbohydrates were able to provide similar protection as *C. albicans*, it would suggest that ECM composition is the major contributing factor providing antimicrobial protection.

In conclusion, secreted *C. albicans* ECM polysaccharides protect *P. aeruginosa* by reducing the efficacy of meropenem. Clinically, this could result in persistent bacterial infection due to pockets of protected cells, which may then acquire true resistance as a result of continued exposure to sub-MIC concentrations of antibiotics. This highlights the importance of early diagnosis of dual-species biofilm infections, so that more efficacious therapeutic options, such as combination antibiotic–antifungal therapy, can be considered.

4 DUAL-SPECIES RNA SEQUENCING

4.1 INTRODUCTION

The transcriptome of a cell, or a population of cells, refers to the total RNA transcripts, and their individual quantities, present at a specific point in time and under specific growth conditions (Wang *et al.*, 2009). By comparing the transcriptomes of cells grown under different conditions, changes in gene expression can be quantified, analysed and used to generate testable hypotheses towards understanding phenotypic changes. In the last decade, RNA sequencing (RNA-seq) has become the dominant tool for transcriptomic analysis (Stark *et al.*, 2019), overtaking and replacing the hybridisation-based approach of microarrays (Wang *et al.*, 2009). The inexorable rise of RNA-seq is thanks to the many advantages of this sequence-based approach over microarray technology, including: 1) no previous knowledge of the genome sequence is required; 2) transcriptional sequences can be resolved to single-base resolution; 3) sequence variations can be detected, such as alternative splicing or single nucleotide polymorphisms (SNPs); 4) very low background signal, due to the high resolution of mapping; 5) large dynamic range, whereby transcripts can be detected at very high or very low levels; and 6) only small amounts of RNA are required per sample (Wang *et al.*, 2009).

For RNA-seq experiments in which the main aim is to quantify differentially expressed genes (DEGs), short-read complementary DNA (cDNA) sequencing is the most appropriate tool (Stark *et al.*, 2019). This generally involves the following steps: 1) RNA extraction from cell samples; 2) enrichment of mRNA by either rRNA depletion or poly(A) tail selection (Zhao *et al.*, 2018); 3) RNA fragmentation; 4) synthesis of

cDNA fragments of 150–200 base pairs in read length; 5) adaptor ligation; 6) PCR amplification of cDNA fragments; 7) sequencing, most often done using an Illumina platform (Stark *et al.*, 2019); and 8) analysis. The first stage of RNA-seq data analysis is quality control of raw read sequences, such as analysis of GC content and removal of adaptor sequences (Conesa *et al.*, 2016). For organisms with an available reference genome, such as is the case for both *C. albicans* and *P. aeruginosa*, reads are then mapped to the reference genome. At this stage an important quality control measure is the percentage of reads mapped to the reference genome; the expected percentage of mapped reads is in the region of 90%, but if the value falls below 70%, this is indicative of poor sequencing accuracy or the presence of DNA contamination (Conesa *et al.*, 2016). The next stage is quantification of transcripts by measurement of gene hit counts, after which differential gene expression analysis can be done between samples, to calculate fold changes in expression for each gene and to identify statistically significant DEGs (Conesa *et al.*, 2016). From output tables of fold changes and DEGs, further analyses can be performed, including clustering, e.g. principle component (PC) analysis, and enrichment analyses, e.g. gene ontology (GO) terms or pathway analyses (Wolf *et al.*, 2018).

The RNA-seq workflow requires some extra considerations when it is a dual-species RNA-seq experiment. When mapping reads from a dual-species sample to the genomes of the two relevant organisms, there are two possible approaches: 1) map reads to a concatenated genome, made up of both genomes in tandem, or 2) map reads to each genome separately (Wolf *et al.*, 2018). Although the first option is computationally easier, it can lead to the discarding of reads that map equally well to

both genomes (Wolf *et al.*, 2018), e.g. genes that may have high sequence similarity between organisms, so may result in the loss of potentially important data.

There are only a few examples in the literature of dual-species RNA-seq being used as a tool for understanding interactions between co-cultured microbial species. One example is the interaction between the oral microorganisms, *C. albicans* and *S. gordonii*; this dual-species interaction results in upregulation of *C. albicans* genes associated with filamentation and adhesion, whereas the transcriptional response of the *S. gordonii* cells is not as dramatic (Dutton *et al.*, 2016b). However, the transcriptional response of another oral microorganism, *S. mutans*, to the presence of *C. albicans* is more dramatic; there is significant upregulation of genes involved in carbohydrate transport and metabolism of pyruvate and galactose, but downregulation of genes involved in bacteriocin production (He *et al.*, 2017). Examples of dual-species RNA-seq to understand *C. albicans–P. aeruginosa* interactions include the following studies. An *in vivo* murine co-infection study shows downregulation of *P. aeruginosa* pyoverdine and pyochelin biosynthetic genes in the presence of *C. albicans*; this transcriptional response is replicated *in vitro* in the presence of *C. albicans* supernatant (Lopez-Medina *et al.*, 2015), and the authors propose a link between iron availability and *P. aeruginosa* virulence. Towards gaining a greater understanding of the *P. aeruginosa* response to *C. albicans*–produced ethanol (Chen *et al.*, 2014), dual-species RNA-seq reveals upregulation of *P. aeruginosa phoB*, which is involved in regulation of phosphatase activity; this upregulation is lost in the presence of the *C. albicans adh1*Δ/Δ mutant strain, which does not produce ethanol, but is rescued by exogenous ethanol (Doing *et al.*, 2020). PhoB is also involved in the production of 5-methyl-phenazine-1-carboxylic acid (5MPCA), a secreted *P. aeruginosa* phenazine

with antifungal activity, suggesting that the interplay between phenazines and *C. albicans*-produced ethanol is dependent upon phosphate levels (Doing *et al.*, 2020). However, at the time of the experiment reported here, there was no published research utilising dual-species RNA-seq to analyse bacterial–fungal interactions in a biofilm mode of growth.

This chapter presents the findings from dual-species RNA-seq analysis of *P. aeruginosa*–*C. albicans* biofilms. The aims of the analysis were 1) to determine the transcriptional responses of *P. aeruginosa* and *C. albicans* biofilm cells to one another, and 2) to determine the transcriptional responses of biofilm cells to treatment with 5 µg/mL meropenem.

4.2 Results

4.2.1 Scaling up the biofilm assay

In Chapter 3, it was observed that numbers of *C. albicans* cells recovered from dual-species biofilms were consistently lower than the numbers recovered from single-species biofilms, by approximately $2\log_{10}$ CFU/mL. Towards designing a robust dual-species RNA-seq experiment, it was necessary to ensure that sufficient numbers of biofilm cells, of both *P. aeruginosa* and *C. albicans*, could be recovered from biofilms for RNA extraction. Therefore, two major changes were made to the biofilm assay protocol: 1) the final volume of media per biofilm was scaled up from 200 µL (in 96-well microtitre plates) to 6 mL (in 6-well plates), and the numbers of cells were scaled up accordingly; 2) the duration of incubation of mature (24 h) biofilms with 0 or 5 µg/mL meropenem was reduced from 18 h to 4 h. The scaled-up volume would ensure there were sufficient numbers of cells of both species for RNA extraction. The reduced

meropenem incubation time would prevent a large reduction in numbers of *C. albicans* cells recovered from dual-species biofilms, relative to single-species, thus ensuring the observed *C. albicans* transcriptional changes would not be limited to cell death-associated processes.

There were four biological replicates of each biofilm sample, which were made up of three pooled technical replicates. The samples included single- and dual-species biofilm cells treated with 0 or 5 μg/mL meropenem, thus there were 24 samples in total. Prior to sample preparation for the dual-species RNA-seq experiment, 50 μL of biofilm cells were removed from each sample, for the quantification of biofilm cell numbers.

There was no significant difference in *P. aeruginosa* viability between untreated and meropenem-treated cells (Figure 4.1a), possibly as a result of the reduced meropenem incubation time. However, there was significantly ($P<0.05$) increased viability of meropenem-treated *P. aeruginosa* cells in dual-species than in single-species biofilms (Figure 4.1a), suggesting that the protective effect observed in Chapter 3 was also observed in the scaled-up biofilm.

The *C. albicans* data showed no significant difference in viability, either between single-species and dual-species, or between untreated and meropenem-treated biofilms (Figure 4.1b). Additionally, there was no cross-contamination of single-species biofilm samples, as shown by the zero recovery of *P. aeruginosa* cells from *C. albicans* single-species biofilms (Figure 4.1a), or *C. albicans* cells from *P. aeruginosa* single-species biofilms (Figure 4.1b).

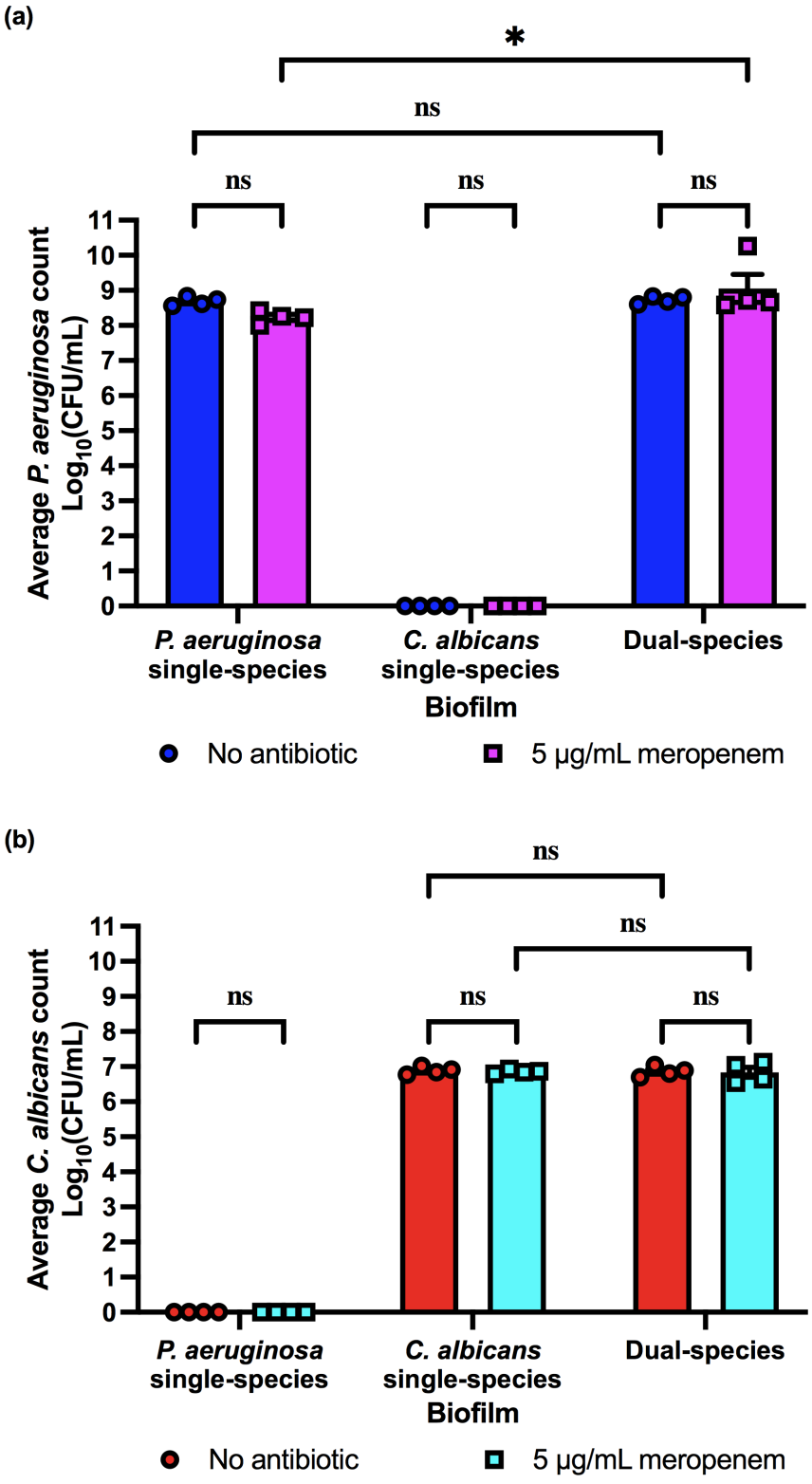


Figure 4.1. Viable counts from the dual-species RNA-seq biofilm samples. Preformed 24 h biofilms were incubated in Mueller Hinton broth containing 0 or 5 µg/mL meropenem, for 4 h. **(a)** *P. aeruginosa* viable counts; **(b)** *C. albicans* viable counts. Data are the mean ± the SEM from 4 biological replicates. Data were analysed using 2-way ANOVA and Holm-Sidak's multiple comparisons test (ns not significant; * $P < 0.05$).

Biofilm cell pellets were snap-frozen and stored at -70°C, before being sent to Genewiz® for RNA extraction, RNA-seq and bioinformatic analysis. The data from one biological replicate of *C. albicans* single-species biofilms were removed from the analyses, due to a low percentage of mapped reads; however, all other samples passed quality control (Appendix II.i.). Sequencing reads and gene hit count tables from this experiment are available at the Gene Expression Omnibus (GEO) database (https://www.ncbi.nlm.nih.gov/geo/), under accession number GSE167137.

4.2.2 Exploratory analysis of transcriptional data

Consistent with published RNA-seq analyses, *C. albicans* transcripts were considered to be significantly differentially expressed if the adjusted P (Padj) value was ≤0.05 and the $\log_2$ fold change was ≥1 (Dutton *et al.*, 2016b, Bruno *et al.*, 2015, Fourie *et al.*, 2021). However, when using these parameters to analyse the *P. aeruginosa* data, only two *P. aeruginosa* transcripts were considered significantly differentially expressed in response to *C. albicans* in untreated biofilms, and only one transcript in meropenem-treated biofilms, making it difficult to draw any biologically meaningful conclusions. Therefore, the stringency of parameters for *P. aeruginosa* DEGs was relaxed so that genes would be considered significantly differentially expressed if the Padj was ≤0.05.

Figure 4.2 summarises the numbers of significantly upregulated and downregulated (Padj ≤ 0.05) transcripts in the *P. aeruginosa* genome, in response to 1) *C. albicans* in untreated biofilms, 2) *C. albicans* in meropenem-treated biofilms, 3) meropenem treatment of single-species biofilms, and 4) meropenem treatment of dual-species biofilms.

Figure 4.3 summarises the numbers of significantly upregulated and downregulated (Padj ≤ 0.05 and $\log_2$ fold change ≥1) transcripts in the *C. albicans* genome, in response to 1) *P. aeruginosa* in untreated biofilms, 2) *P. aeruginosa* in meropenem-treated biofilms, 3) meropenem treatment of single-species biofilms, and 4) meropenem treatment of dual-species biofilms.

Figure 4.4 provides a roadmap to illustrate the order in which the results from the RNA-seq analyses are presented and discussed in this chapter.

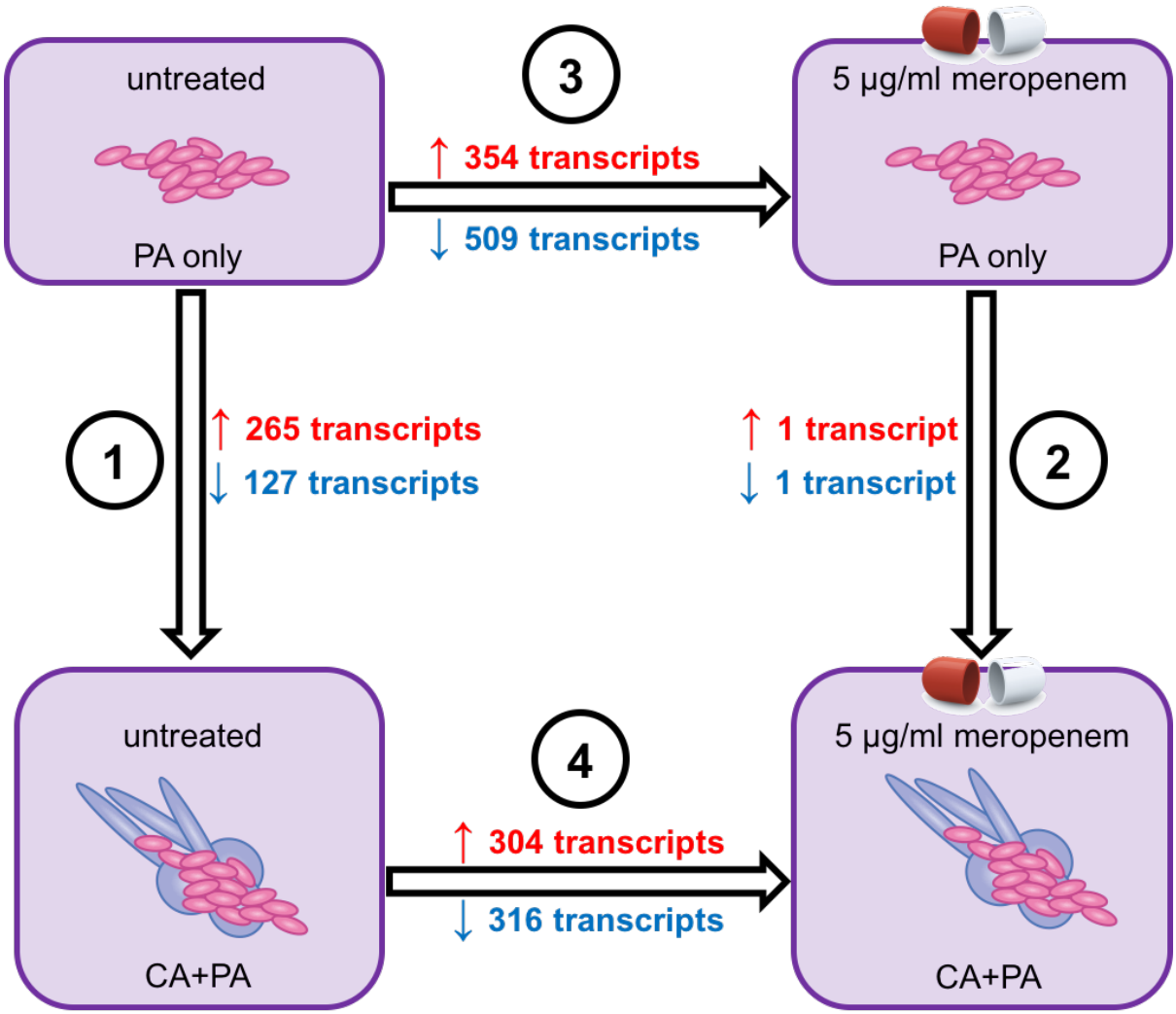


Figure 4.2. Summary of transcriptional responses of *P. aeruginosa* biofilm cells to *C. albicans* and to meropenem treatment. Numbers of significantly differentially expressed transcripts (Padj ≤ 0.05) in *P. aeruginosa* biofim cells were analysed in response to: **1)** *C. albicans* in untreated biofilms; **2)** *C. albicans* in biofilms treated with 5 µg/mL meropenem; **3)** treatment of single-species biofilms with 5 µg/mL meropenem; and **4)** treatment of dual-species biofilms with 5 µg/mL meropenem.
PA: *P. aeruginosa*; CA: *C. albicans*.
Red: numbers of significantly upregulated transcripts; Blue: numbers of significantly downregulated transcripts.

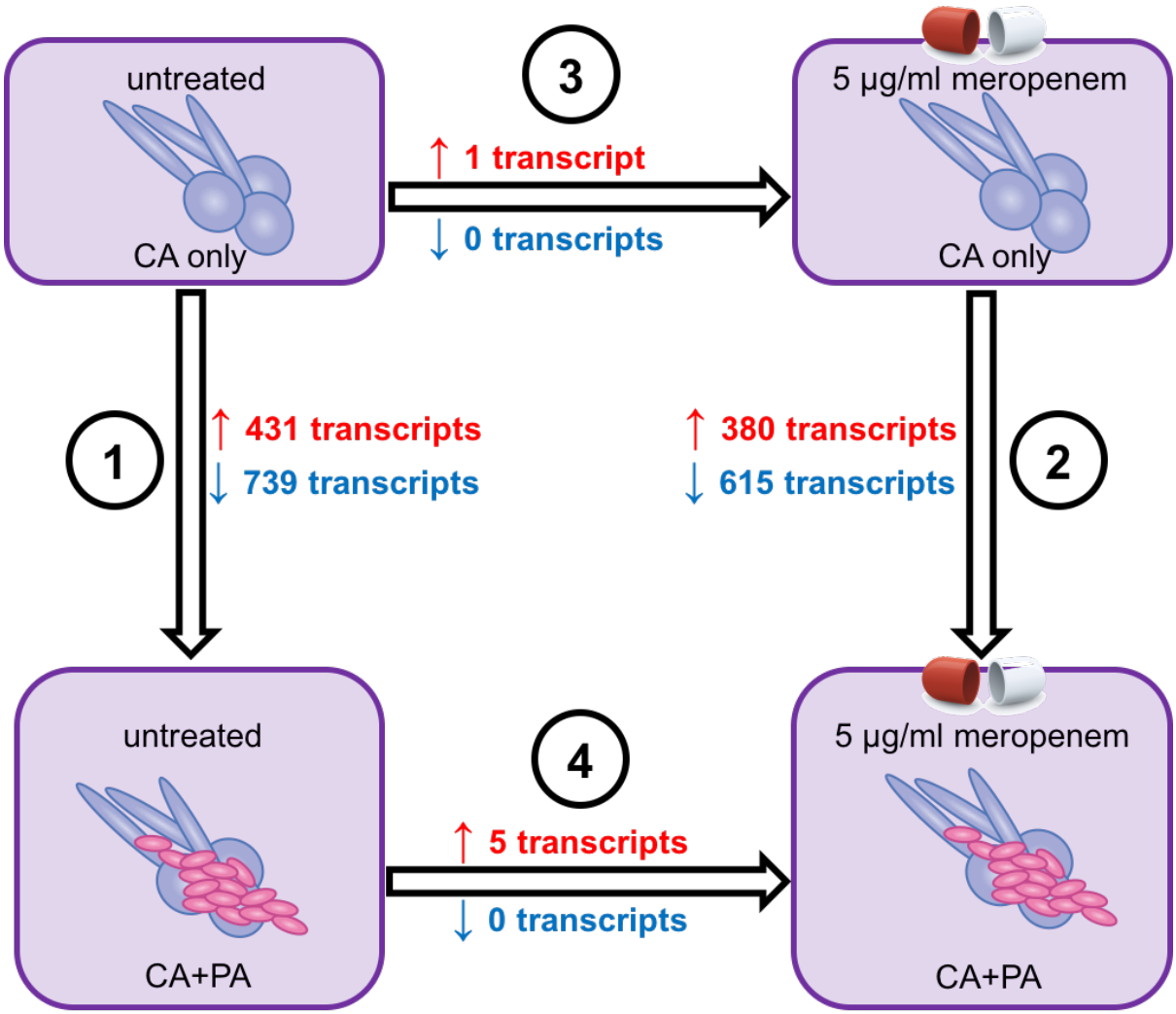


Figure 4.3. Summary of transcriptional responses of *C. albicans* biofilm cells to *P. aeruginosa* and to meropenem treatment. Numbers of significantly differentially expressed transcripts (Padj ≤ 0.05 and $\log_2$ fold change ≥ 1) in *C. albicans* biofim cells were analysed in response to: **1)** *P. aeruginosa* in untreated biofilms; **2)** *P. aeruginosa* in biofilms treated with 5 µg/mL meropenem; **3)** treatment of single-species biofilms with 5 µg/mL meropenem; and **4)** treatment of dual-species biofilms with 5 µg/mL meropenem.
CA: *C. albicans*; PA: *P. aeruginosa*.
Red: numbers of significantly upregulated transcripts; Blue: numbers of significantly downregulated transcripts.

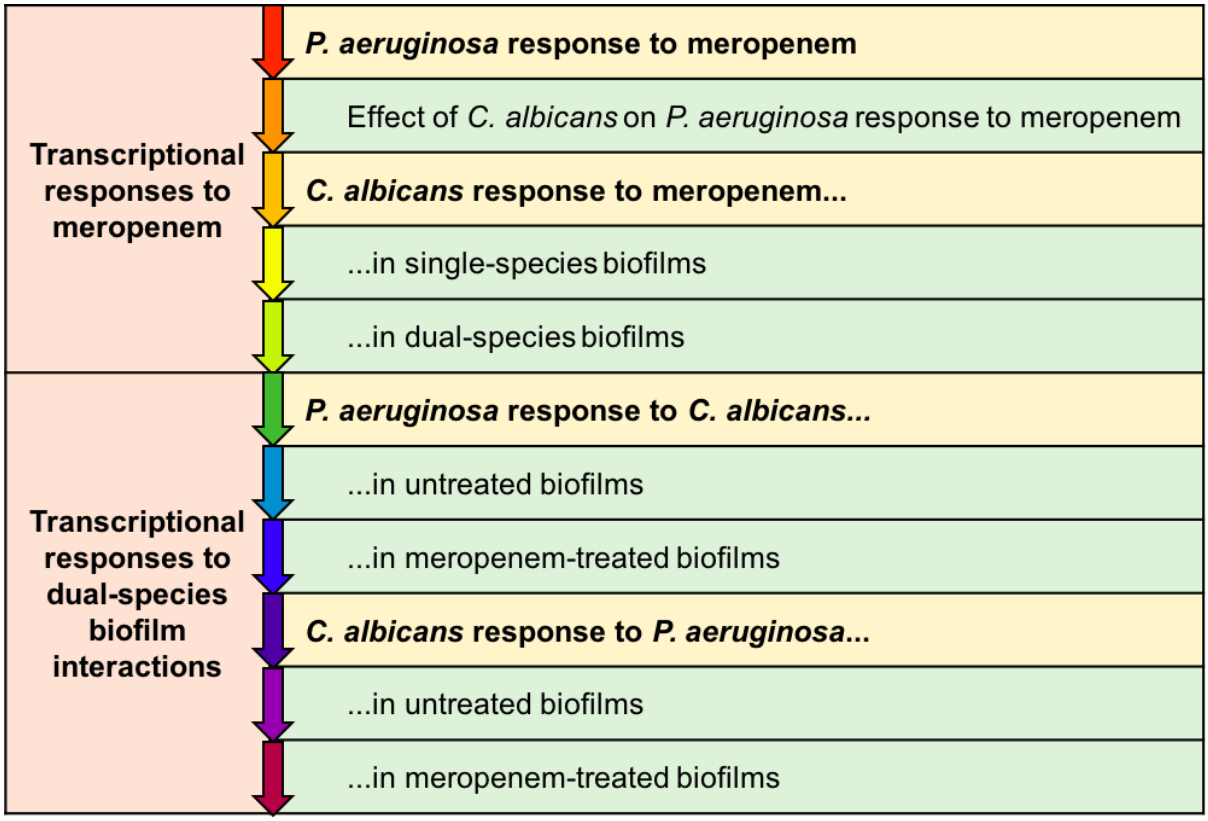


Figure 4.4. Roadmap of results from RNA-seq analyses. The transcriptional responses of *P. aeruginosa* and *C. albicans* biofilm cells to meropenem treatment are presented first. Transcriptional responses of *P. aeruginosa* and *C. albicans* to dual-species biofilm interactions are presented after this.

4.2.3 *P. aeruginosa* biofilm transcriptional response to meropenem

Principle component analysis revealed that untreated single-species *P. aeruginosa* biofilm cells formed a separate, distinct population to meropenem-treated cells (Figure 4.5a). This indicates that much of the variation in transcriptional profiles between the two conditions can be attributed to the meropenem treatment. In the meropenem-treated *P. aeruginosa* biofilm cells, 354 genes were significantly upregulated (Padj ≤0.05) and 509 genes were significantly downregulated relative to untreated cells (Figure 4.5b). The single most significantly upregulated gene in response to meropenem treatment of single-species *P. aeruginosa* biofilm cells was *ampC*, which encodes a ß-lactamase precursor (log_2 fold change = +7.75; Padj = $1.95x10^{-42}$).

Gene ontology (GO) terms provide a universal language for the annotation of genes or gene products, and are grouped into three categories: biological process, molecular function, and cellular component (Ashburner *et al.*, 2000). Enrichment analysis of significant DEGs provides a global overview of over- or under-represented GO terms using the annotations for the DEG list (Wolf *et al.*, 2018). GO terms analyses of *P. aeruginosa* significant DEGs were carried out for all GO terms categories; biological process (Figure 4.6), molecular function (Figure 4.7), and cellular component (Figure 4.8).

KEGG pathways are a collection of organism-specific maps of molecular pathways (Kanehisa *et al.*, 2017). KEGG pathway enrichment analysis of a list of significant DEGs reveals which pathways are over-/under-represented, thus giving an indication

of cellular activity. Results from KEGG pathway enrichment analyses of *P. aeruginosa* significant DEGs are shown in Figure 4.9.

In summary, treatment of single-species *P. aeruginosa* biofilms with 5 µg/mL meropenem resulted in significant upregulation of genes involved in maintenance of bacterial cell membrane and cell wall integrity, biofilm formation and extracellular polysaccharide biosynthesis, ribosomal structure and translation, siderophore biosynthesis (specifically pyochelin), type IV pilus formation, and the type VI secretion system. There was upregulation of genes involved in the twin-arginine translocation (Tat) secretion pathway, but downregulation of genes involved in the general secretory (Sec) pathway (Figure 4.9). However, the gene encoding the OprD porin, downregulation of which is associated with meropenem resistance (Khaledi *et al.*, 2016), was not significantly differentially expressed (log_2 fold change = +0.14; Padj = $6.57x10^{-1}$).

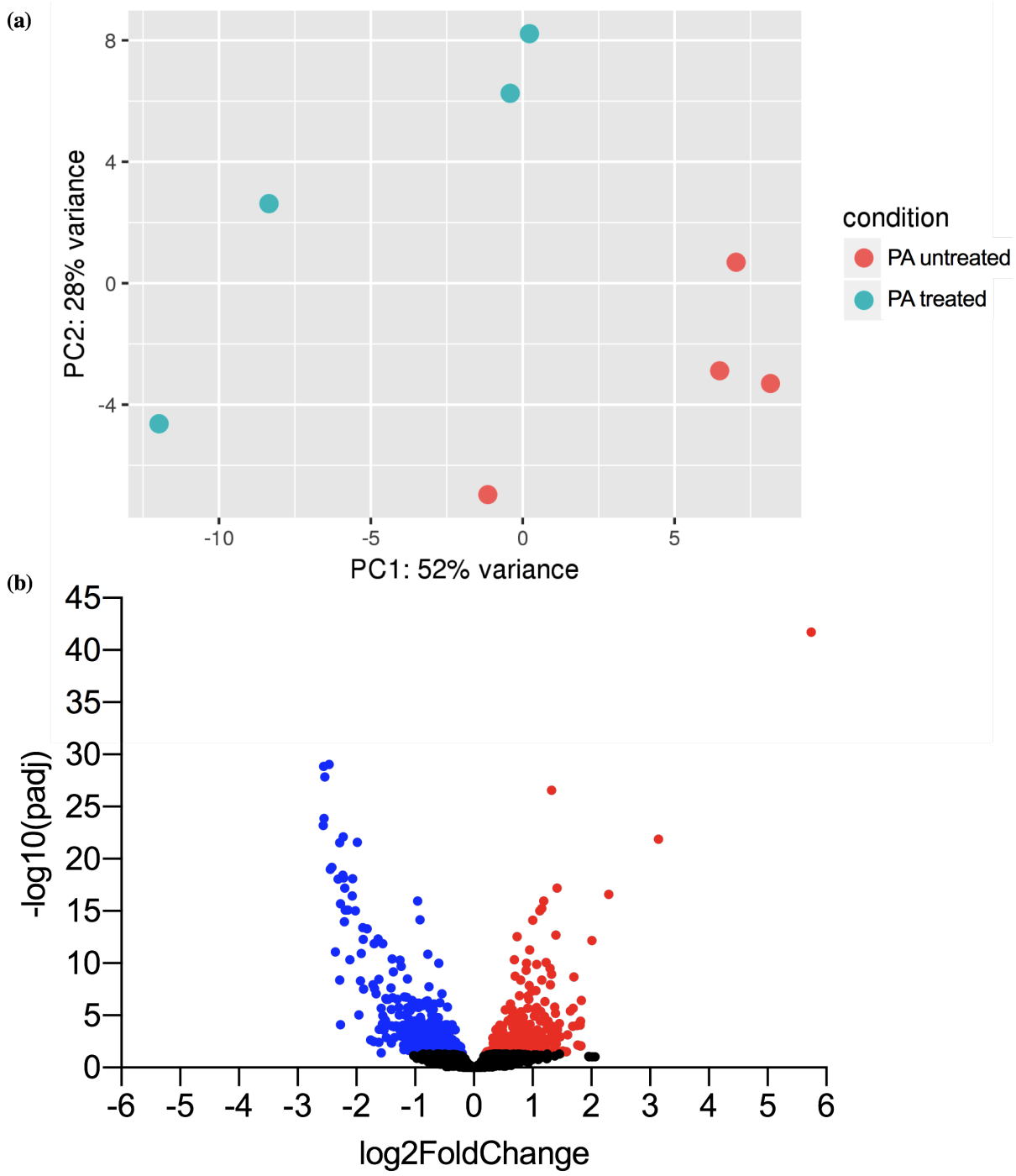


Figure 4.5. Global transcriptional changes within single-species *P. aeruginosa* biofilm cells in response to meropenem treatment. RNA was extracted from mature (24 h) biofilm cells that had been treated with 0 or 5 µg/mL meropenem for a further 4h, prior to RNA-seq. **(a)** Principle Component (PC) analysis of variance between biological replicates (PA *P. aeruginosa*). Figure provided by Genewiz®. **(b)** Volcano plot of global transcriptional changes. Each dot represents one gene in the *P. aeruginosa* genome. Red = significantly upregulated genes (Padj ≤ 0.05); Blue = significantly downregulated genes.

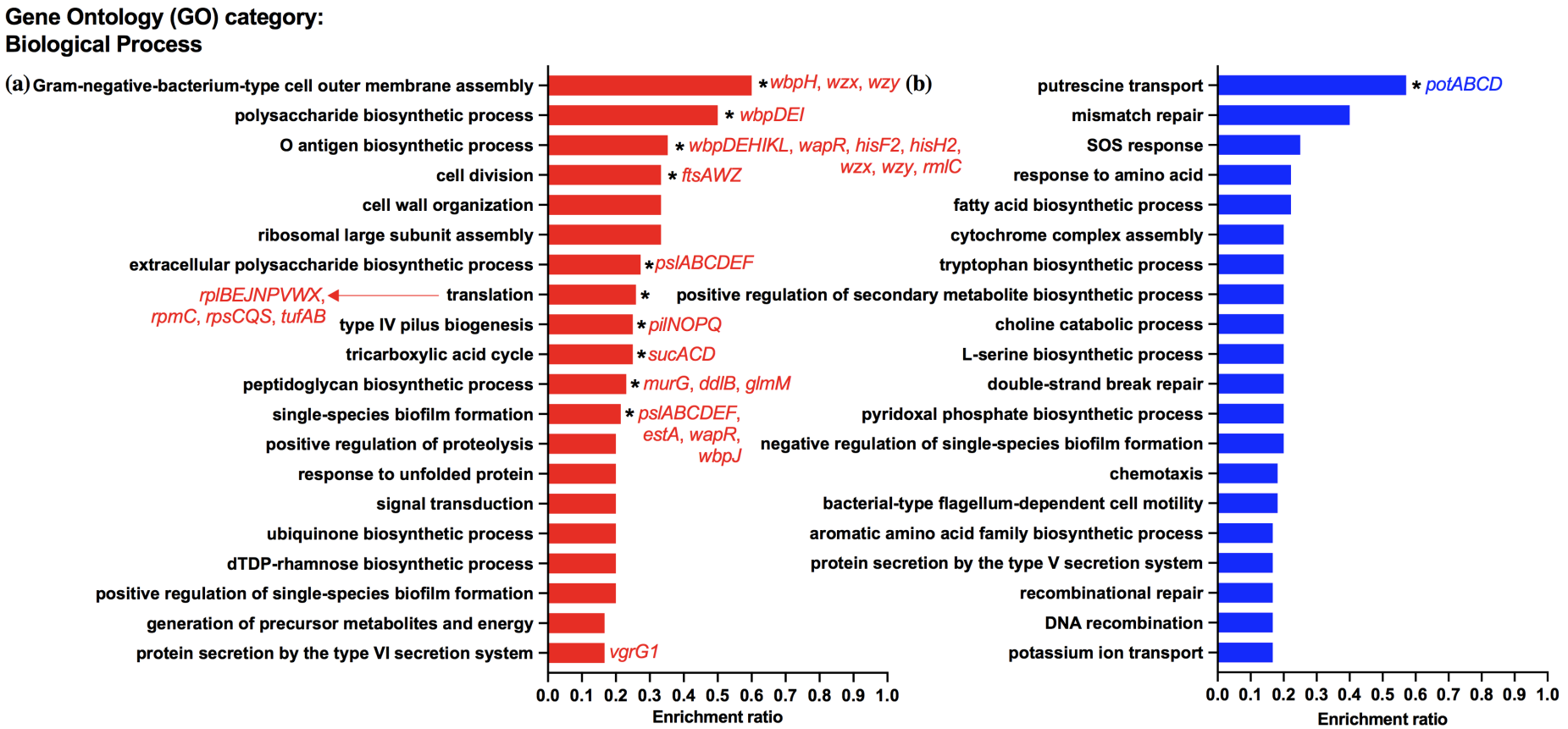


Figure 4.6. Distribution of significantly differentially expressed *P. aeruginosa* genes in the Gene Ontology (GO) category Biological Process, in response to treatment of single-species biofilms with 5 µg/mL meropenem. There were 354 significantly upregulated and 509 downregulated genes, which were assigned to GO terms under the Biological Process category. **(a)** Upregulated terms. **(b)** Downregulated terms. Data were analysed using Fisher's exact test and Benjamini and Hochberg method for FDR correction (* FDR ≤ 0.05).

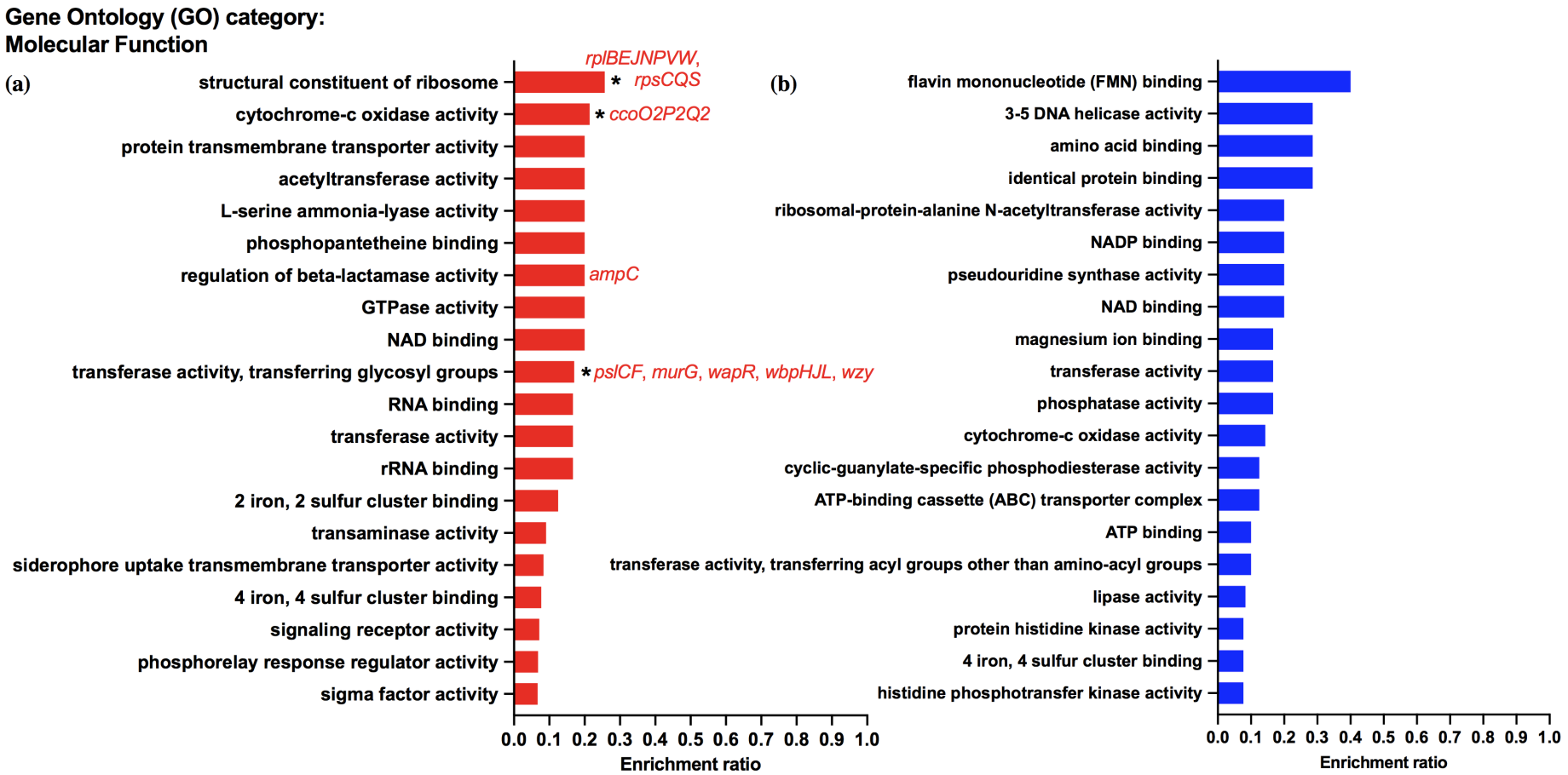


Figure 4.7. Distribution of significantly differentially expressed *P. aeruginosa* genes in the Gene Ontology (GO) category Molecular Function, in response to treatment of single-species biofilms with 5 µg/mL meropenem. There were 354 significantly upregulated and 509 downregulated genes, which were assigned to GO terms under the Molecular Function category. **(a)** Upregulated terms. **(b)** Downregulated terms. Data were analysed using Fisher's exact test and Benjamini and Hochberg method for FDR correction (* FDR ≤ 0.05).

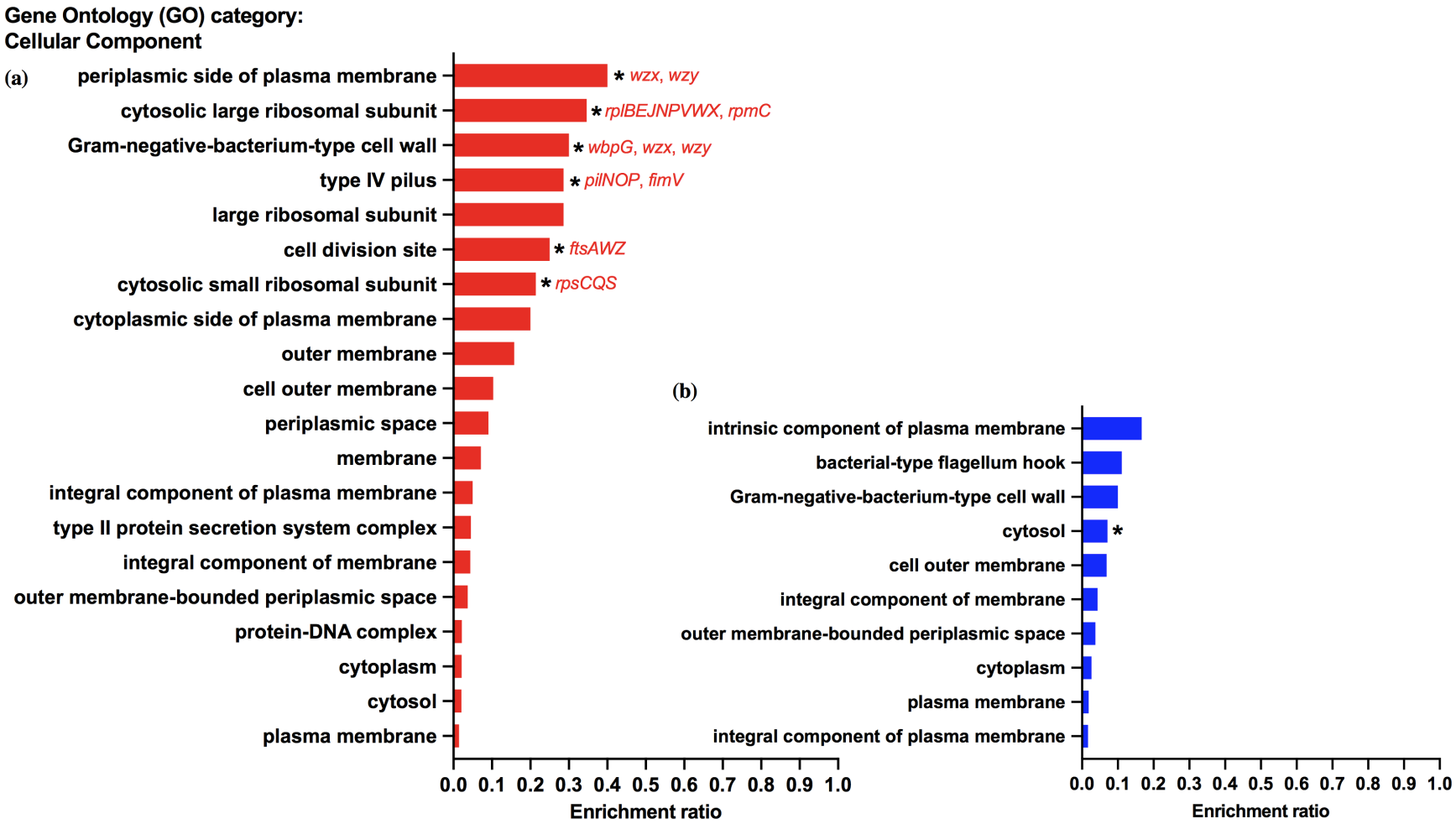


Figure 4.8. Distribution of significantly differentially expressed *P. aeruginosa* genes in the Gene Ontology (GO) category Cellular Component, in response to treatment of single-species biofilms with 5 µg/mL meropenem. There were 354 significantly upregulated and 509 downregulated genes, which were assigned to GO terms under the Cellular Component category. **(a)** Upregulated terms. **(b)** Downregulated terms. Data were analysed using Fisher's exact test and Benjamini and Hochberg method for FDR correction (* FDR ≤ 0.05).

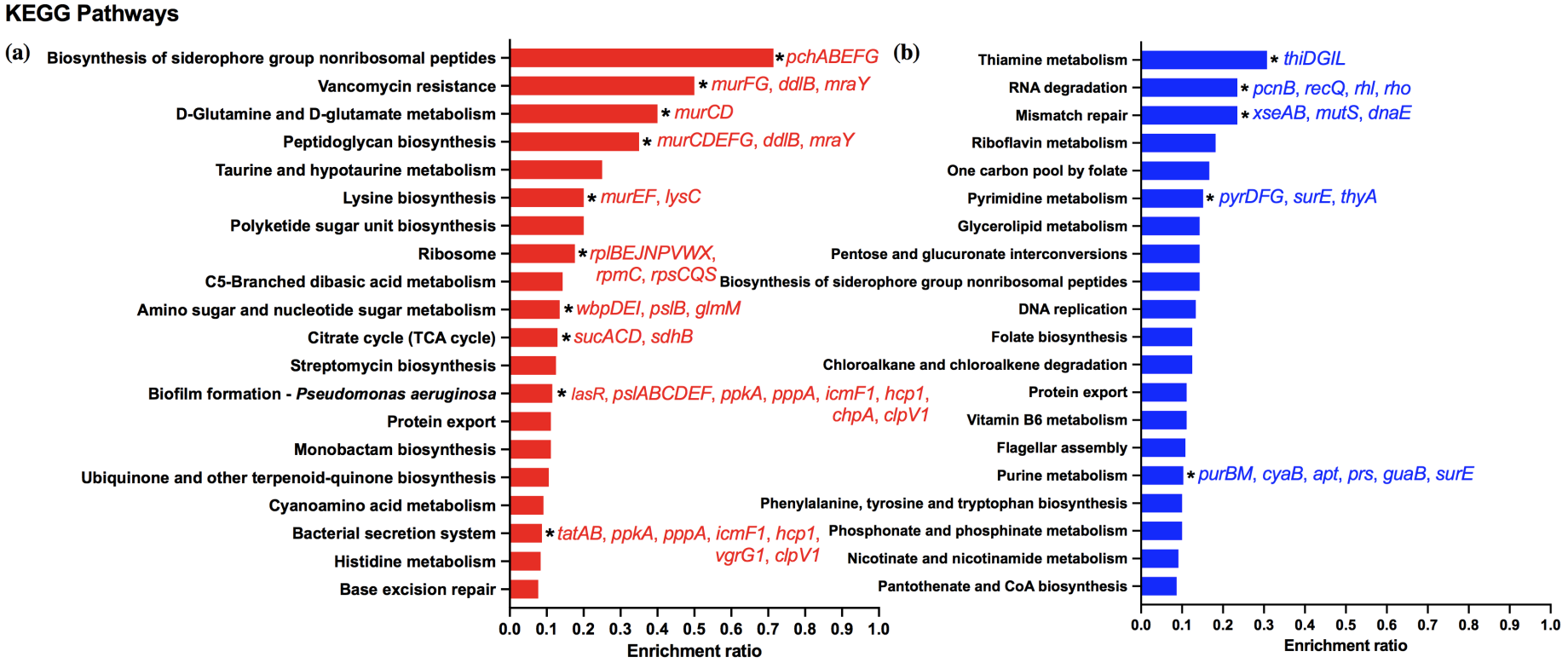


Figure 4.9. KEGG pathways assigned to significantly differentially expressed *P. aeruginosa* genes, in response to treatment of single-species biofilms with 5 µg/mL meropenem. Annotations from the 354 significantly upregulated **(a)** and 509 downregulated genes **(b)** were analysed for KEGG pathway enrichment. Data were analysed using Fisher's exact test and Benjamini gand Hochberg method for FDR correction (* FDR ≤ 0.05).

4.2.4 Effect of *C. albicans* on *P. aeruginosa* response to meropenem

To investigate the effect of *C. albicans* on the response of *P. aeruginosa* to meropenem, the *P. aeruginosa* transcriptional response to meropenem treatment was analysed in dual-species biofilm cells. Principle component analysis revealed that *P. aeruginosa* cells from untreated dual-species biofilms formed a separate, distinct population to those from meropenem-treated dual-species biofilms (Figure 4.10a). Furthermore, there was greater variation between transcriptional profiles of treated cells than untreated cells. Therefore, much of the variation in transcriptional profiles between the two conditions can be attributed to the meropenem treatment. In the meropenem-treated dual-species *P. aeruginosa* biofilm cells, 304 genes were significantly upregulated (Padj ≤0.05) and 316 genes were significantly downregulated relative to untreated dual-species biofilm cells (Figure 4.10b). As was the case with meropenem treatment of single-species biofilms, the single most significantly upregulated gene in response to meropenem treatment of dual-species *P. aeruginosa* biofilm cells was also *ampC* (log_2 fold change = +5.52; Padj = $1.95x10^{-47}$).

GO terms analyses of significant DEGs were carried out for all categories; biological process (Figure 4.11), molecular function (Figure 4.12), and cellular component (Figure 4.13). Results from KEGG pathway enrichment analyses are shown in Figure 4.14. In summary, treatment of dual-species *P. aeruginosa–C. albicans* biofilms with 5 µg/mL meropenem resulted in significant upregulation of *P. aeruginosa* genes involved in cell division, peptidoglycan biosynthesis, biofilm formation and extracellular polysaccharide biosynthesis, type VI secretion, and siderophore biosynthesis (specifically pyochelin). These transcriptional responses to meropenem were shared in common between single-species and dual-species *P. aeruginosa* biofilm cells. Also

in common was the non-significant differential expression of *oprD* (log_2 fold change = -0.03; Padj = $9.63x10^{-1}$).

In contrast to the single-species *P. aeruginosa* response to meropenem, dual-species biofilm cells do not show upregulation of genes involved in ribosome structure and translation; instead, there is significant downregulation of genes involved in amino acid binding (Figure 4.12b). Therefore, it is possible that the presence of *C. albicans* may have an inhibitory effect on translation in *P. aeruginosa* biofilm cells.

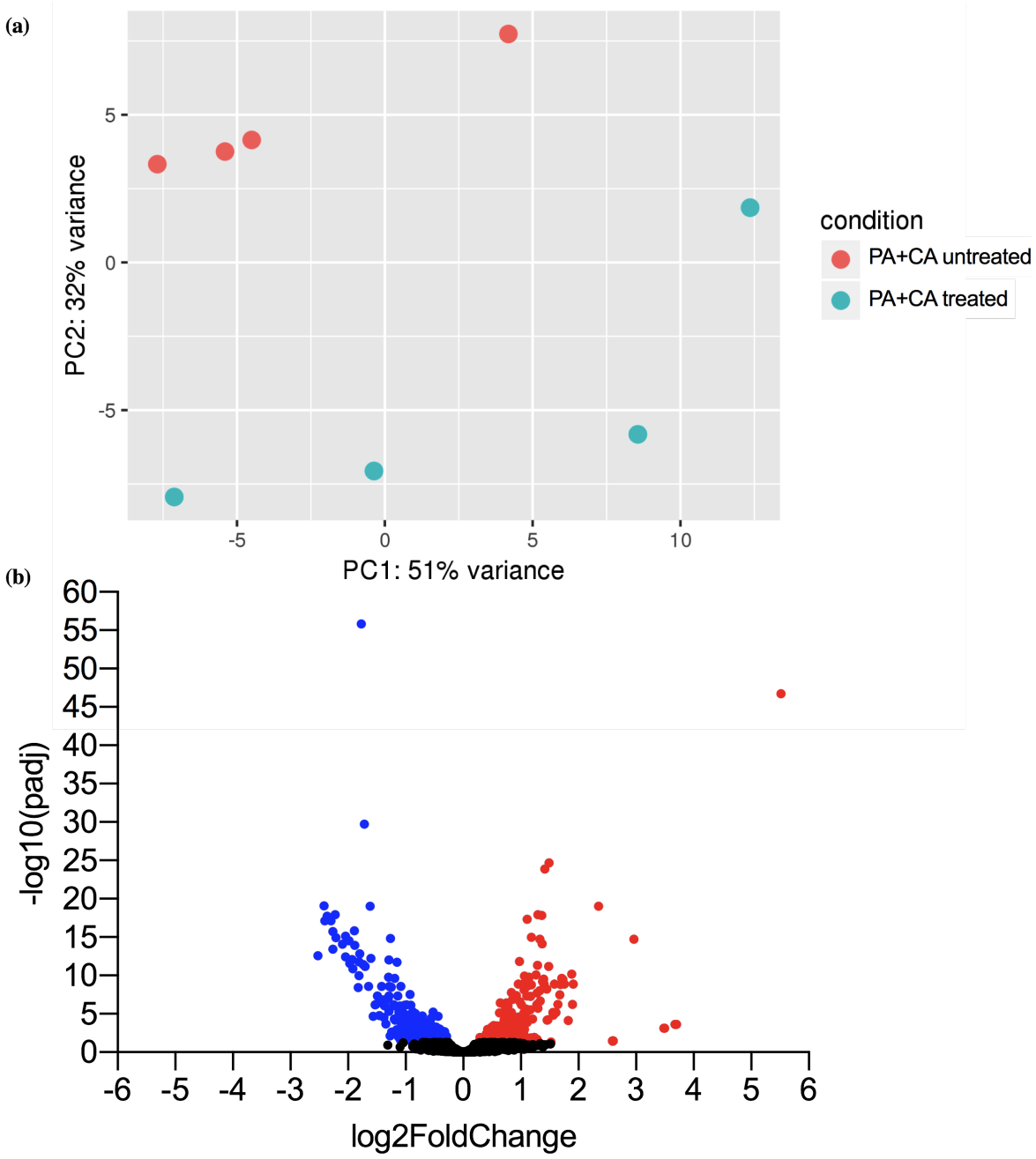


Figure 4.10. Global transcriptional changes within *P. aeruginosa* cells in response to meropenem treatment of dual-species *P. aeruginosa–C. albicans* biofilms. RNA was extracted from mature (24 h) biofilm cells that had been treated with 0 or 5 µg/mL meropenem for a further 4h, prior to RNA-seq. **(a)** Principle Component (PC) analysis of variance between biological replicates (PA *P. aeruginosa*; CA *C. albicans*). Figure provided by Genewiz®. **(b)** Volcano plot of global transcriptional changes. Each dot represents one gene in the *P. aeruginosa* genome. Red = significantly upregulated genes (Padj ≤ 0.05); Blue = significantly downregulated genes.

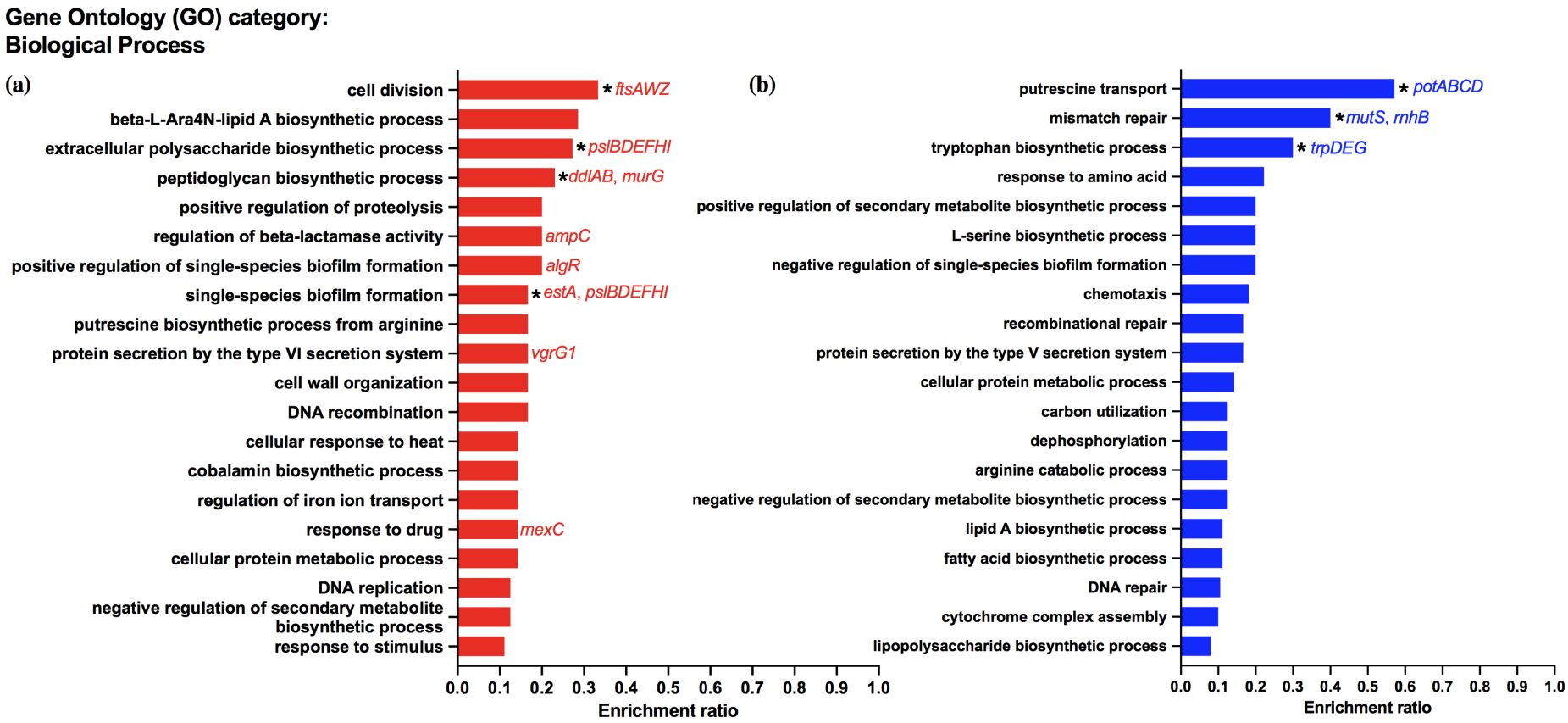


Figure 4.11. Distribution of significantly differentially expressed *P. aeruginosa* genes in the Gene Ontology (GO) category Biological Process, in response to meropenem treatment of dual-species *P. aeruginosa–C. albicans* biofilms. There were 304 significantly upregulated and 316 downregulated genes, which were assigned to GO terms under the Biological Process category. **(a)** Upregulated terms. **(b)** Downregulated terms. Data were analysed using Fisher's exact test and Benjamini and Hochberg method for FDR correction (* FDR ≤ 0.05).

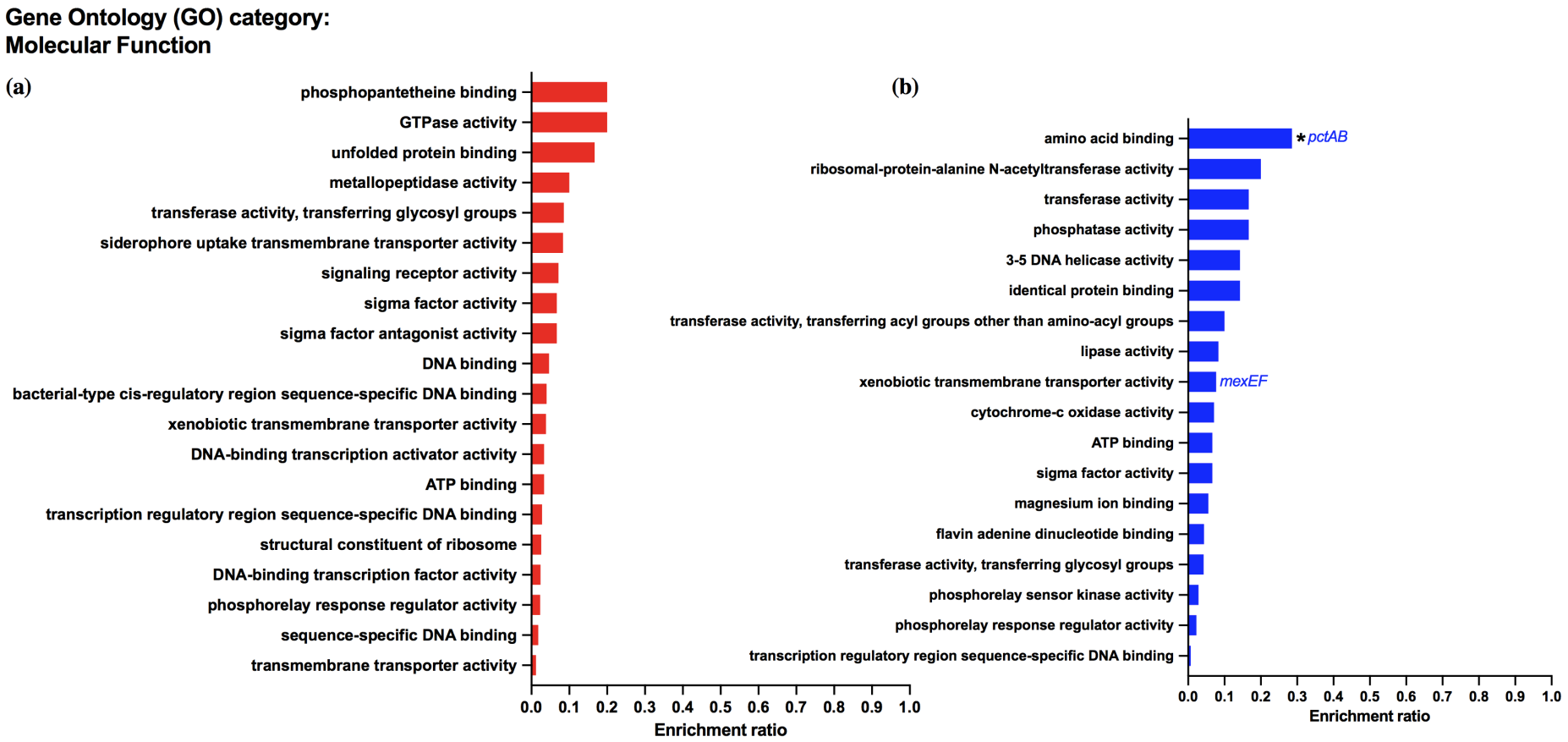


Figure 4.12. Distribution of significantly differentially expressed *P. aeruginosa* genes in the Gene Ontology (GO) category Molecular Function, in response to meropenem treatment of dual-species *P. aeruginosa*–*C. albicans* biofilms. There were 304 significantly upregulated and 316 downregulated genes, which were assigned to GO terms under the Molecular Function category. **(a)** Upregulated terms. **(b)** Downregulated terms. Data were analysed using Fisher's exact test and Benjamini and Hochberg method for FDR correction (* FDR ≤ 0.05).

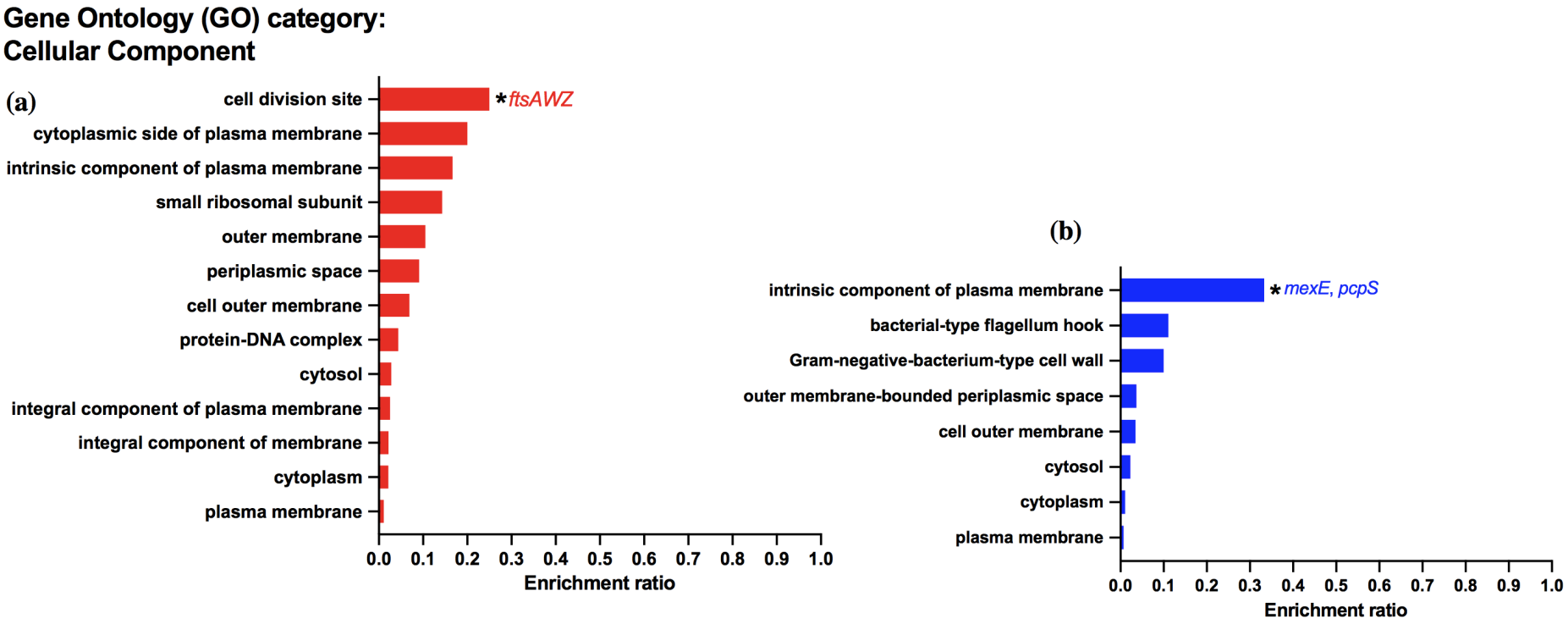


Figure 4.13. Distribution of significantly differentially expressed *P. aeruginosa* genes in the Gene Ontology (GO) category Cellular Component, in response to meropenem treatment of dual-species *P. aeruginosa–C. albicans* biofilms. There were 304 significantly upregulated and 316 downregulated genes, which were assigned to GO terms under the Cellular Component category. **(a)** Upregulated terms. **(b)** Downregulated terms. Data were analysed using Fisher's exact test and Benjamini and Hochberg method for FDR correction (* FDR ≤ 0.05).

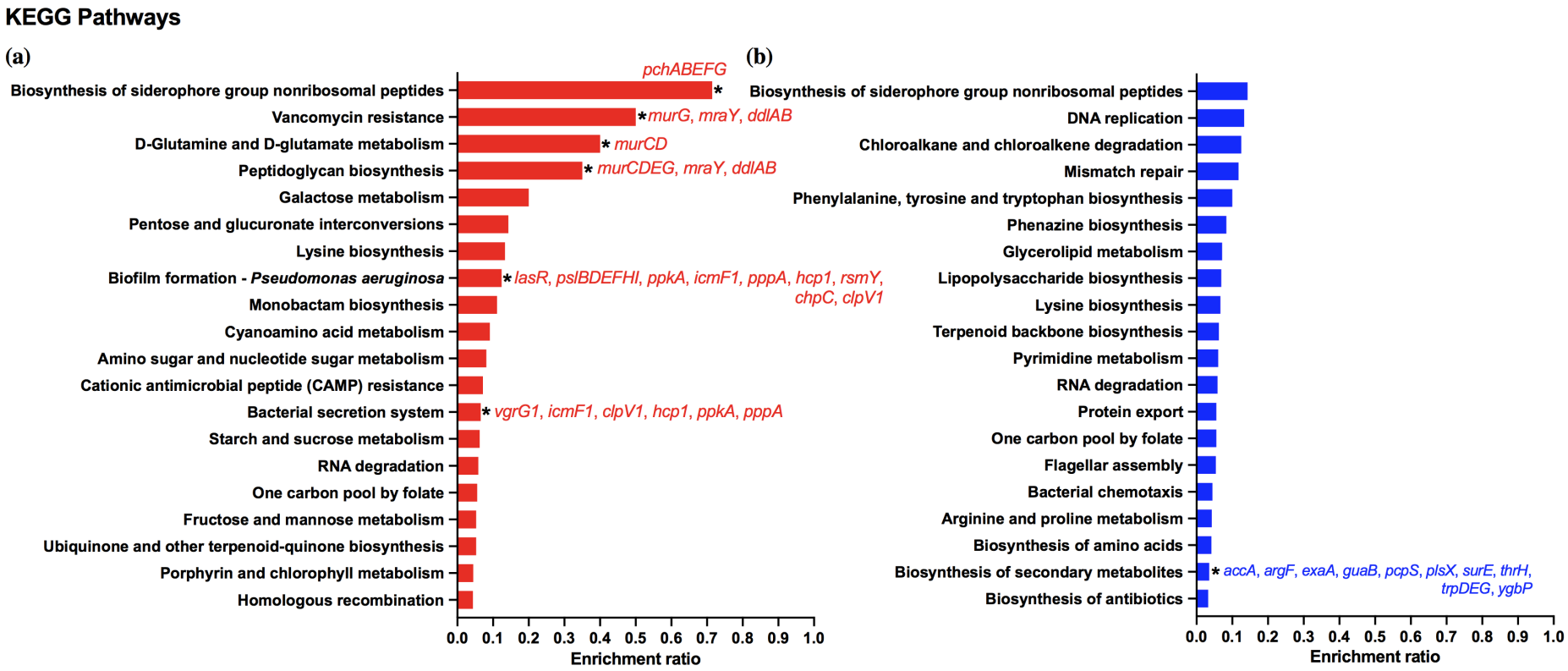


Figure 4.14. KEGG pathways assigned to significantly differentially expressed *P. aeruginosa* genes, in response to meropenem treatment of dual-species *P. aeruginosa–C. albicans* biofilms. Annotations from the 304 significantly upregulated **(a)** and 316 downregulated genes **(b)** were analysed for KEGG pathway enrichment. Data were analysed using Fisher's exact test and Benjamini gand Hochberg method for FDR correction (* FDR ≤ 0.05).

4.2.4.1 *C. albicans* has only a minor effect on the *P. aeruginosa* biofilm transcriptional response to meropenem

To further investigate the differences in the transcriptional responses to meropenem treatment between single- and dual-species *P. aeruginosa* biofilm cells, the significantly (Padj ≤ 0.05) upregulated and downregulated genes were compared using Venn diagrams. Of the genes that were significantly upregulated in response to treatment with 5 µg/mL meropenem, 181 (37.9%) genes were shared in common between single- and dual-species *P. aeruginosa* biofilm cells, 173 (36.3%) were unique to single-species cells, and 123 (25.8%) were unique to dual-species cells (Figure 4.15a). Among the upregulated genes that were unique to the dual-species meropenem response, there were 3 linked to outer membrane vesicles (*pagL*, *galU* and PA5441) (Choi *et al.*, 2011), 1 involved in cell wall synthesis (*ddlA*), 3 involved in biofilm formation (*pslH*, *pslI* and *algR*), and 3 involved in efflux (PA1809, *mexC* and PA3314). This suggests that the presence of *C. albicans* may increase the ability of *P. aeruginosa* biofilm cells to form robust biofilms, to secrete molecules via outer membrane vesicles (OMVs), and to expel molecules via the MexCD-OprJ efflux pump.

Of the genes that were significantly downregulated in response to meropenem treatment, 282 (51.9%) genes were shared in common between single- and dual-species *P. aeruginosa* biofilm cells, 227 (41.8%) were unique to single-species cells, while only 34 (6.3%) were unique to dual-species cells (Figure 4.19b). Among the few downregulated genes that were unique to the dual-species meropenem response, there were 6 involved in efflux or membrane transport (PA0603, PA0604, *mexE*, *mexF*, PA0860 and PA1051). This suggests that the presence of *C. albicans* may result in reduced production of the MexEF-OprN efflux pump in *P. aeruginosa* biofilm cells.

In summary, the presence of *C. albicans* has only a minor effect on the *P. aeruginosa* biofilm transcriptional response to meropenem. This is particularly the case for genes that are significantly downregulated in response to treatment with 5 µg/mL meropenem.

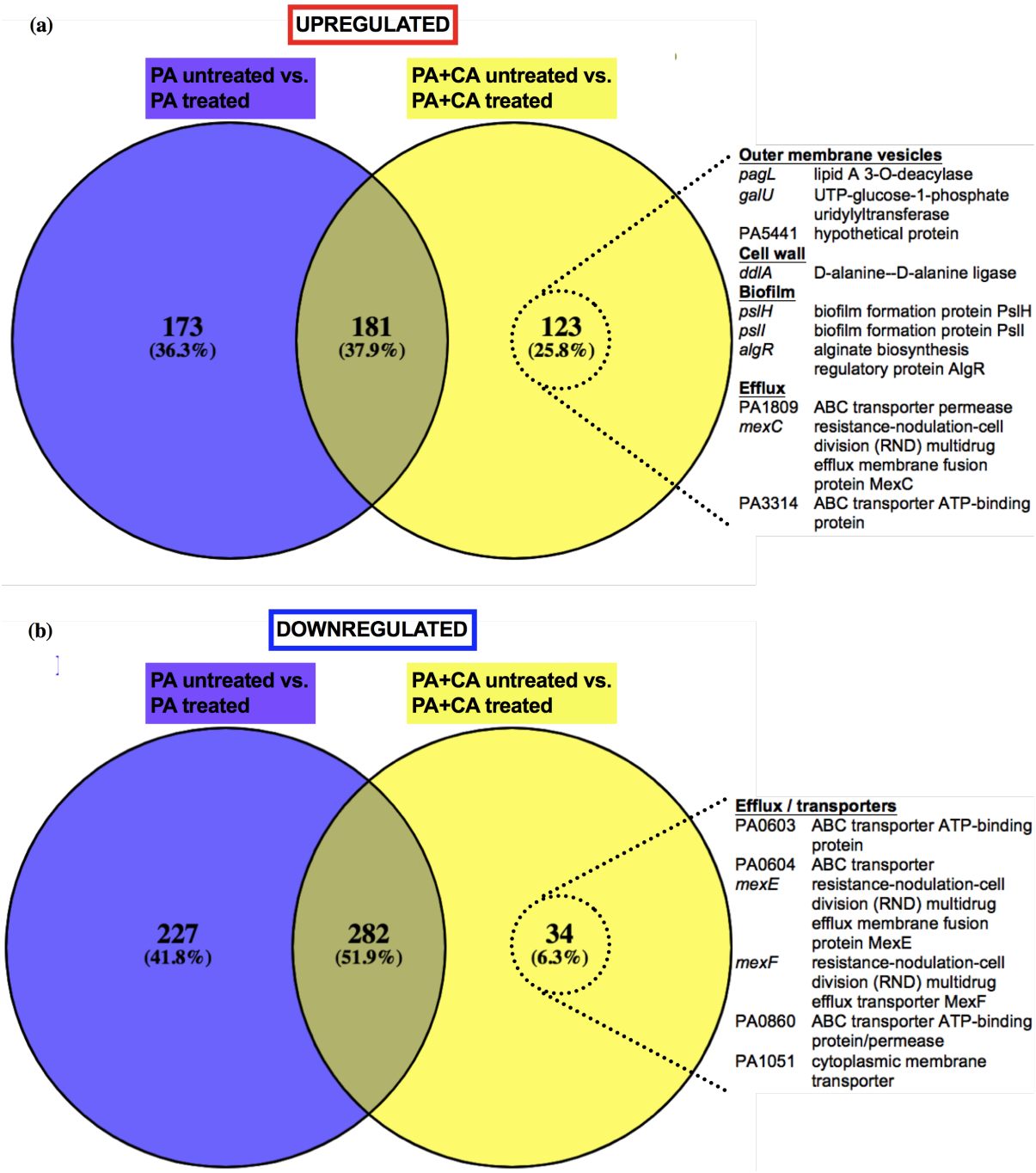


Figure 4.15. *P. aeruginosa* genes that are significantly differentially expressed in response to meropenem treatment, between single- and dual-species biofilms. Numbers of significantly upregulated **(a)** and significantly downregulated **(b)** genes (Padj ≤ 0.05), in response to treatment with 5 µg/mL meropenem, are compared between single- and dual-species biofilms (PA *P. aeruginosa*; CA *C. albicans*). Genes of interest, unique to the dual-species condition, are listed on the right hand side (see Appendix II.ii. for full gene lists).
Venn diagrams generated using Venny 2.1 (https://bioinfogp.cnb.csic.es/tools/venny/index.html)

4.2.5 *C. albicans* biofilm transcriptional response to meropenem

4.2.5.1 Single-species *C. albicans* response to meropenem

To confirm that meropenem has little or no effect on *C. albicans*, the transcriptional response of single-species biofilm cells to meropenem treatment was investigated. Principle component analysis revealed that variation in transcriptional profiles between the samples overlapped between the two conditions, and did not separate the samples into two distinct populations (Figure 4.16a). This indicates little or no transcriptional response to meropenem treatment in single-species *C. albicans* biofilm cells. In the meropenem-treated biofilm cells, only one *C. albicans* gene was significantly upregulated (Padj ≤0.05) by at least a $\log_2$ fold change of one and there were no significantly downregulate genes, relative to untreated cells (Figure 4.16b). The significantly upregulated gene was *PET18*, which encodes a protein with a predicted heme oxygenase domain ($\log_2$ fold change +1.46; Padj = 1.26×10^{-4}). These data confirm that single-species *C. albicans* biofilm cells show a negligible transcriptional response to treatment with 5 µg/mL meropenem.

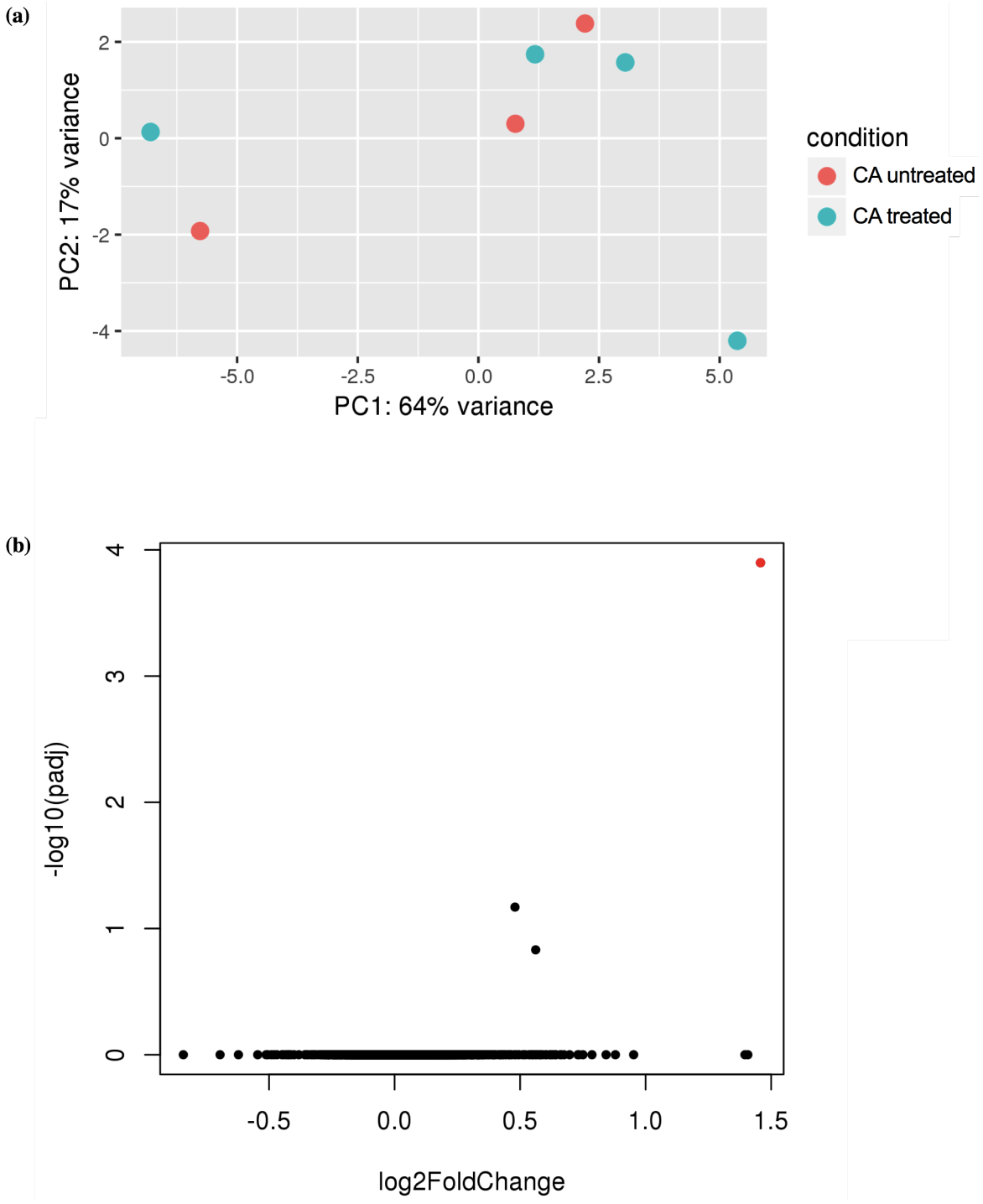


Figure 4.16. Global transcriptional changes within single-species *C. albicans* biofilm cells in response to meropenem treatment. RNA was extracted from mature (24 h) biofilm cells that had been treated with 0 or 5 µg/mL meropenem for a further 4h, prior to RNA-seq. **(a)** Principle Component (PC) analysis of variance between biological replicates (CA *C. albicans*). **(b)** Volcano plot of global transcriptional changes. Each dot represents one gene in the *C. albicans* genome. Red = significantly upregulated gene (Padj ≤ 0.05; $\log_2$ fold change ≥ 1). Figures provided by Genewiz®.

4.2.5.2 Dual-species *C. albicans* response to meropenem

To determine whether the *C. albicans* transcriptional response to meropenem treatment is similar or different between single-species and dual-species biofilm cells, *C. albicans* gene expression was analysed between untreated and treated *C. albicans–P. aeruginosa* biofilms. As was the case for the single-species comparison, principle component analysis revealed that variation in transcriptional profiles between the dual-species samples overlapped between the two conditions, and did not separate the samples into two distinct populations (Figure 4.17a). Again, this indicates little or no transcriptional response to meropenem treatment in dual-species *C. albicans* biofilm cells. Although a greater number of *C. albicans* genes were differentially expressed in response to meropenem treatment of dual-species biofilms, compared to mono-species, only five were significantly upregulated (Padj ≤ 0.05) by at least a $\log_2$ fold change of one and none were significantly downregulated (Figure 4.17b and Table 4.1).

All five of the *C. albicans* genes that were significantly upregulated in response to meropenem treatment of dual-species biofilms (*ATP9*, *NAD3*, *NAD6*, *COX1*, and CaalfMp08.4) encode proteins that are involved in oxidative phosphorylation at the mitochondrial membrane (Table 4.1). This suggests that *C. albicans* cells in dual-species biofilms may respond to meropenem by increasing the rate of aerobic respiration.

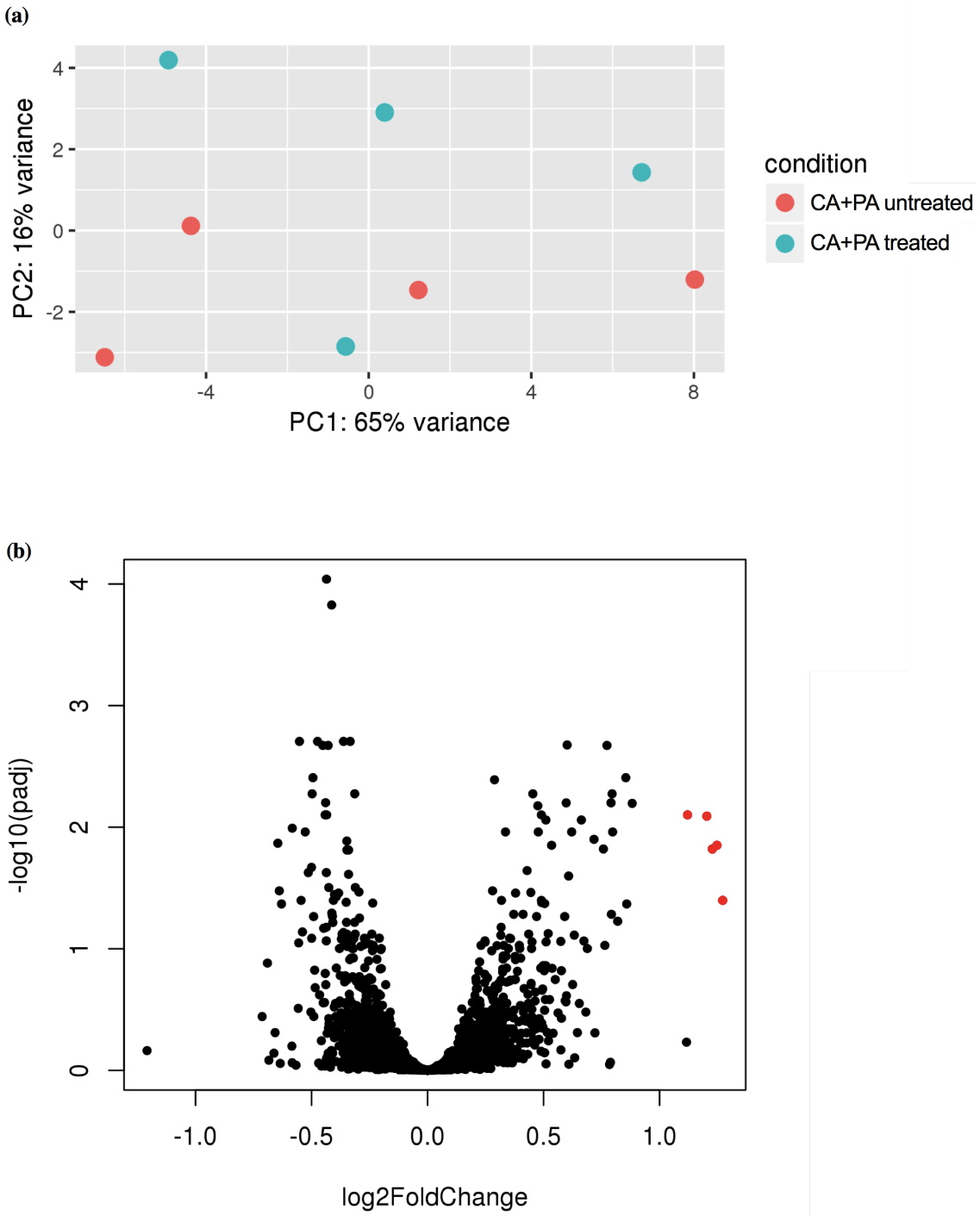


Figure 4.17. Global transcriptional changes within *C. albicans* cells in response to meropenem treatment of dual-species *C. albicans–P. aeruginosa* biofilms. RNA was extracted from mature (24 h) biofilm cells that had been treated with 0 or 5 µg/mL meropenem for a further 4h, prior to RNA-seq. **(a)** Principle Component (PC) analysis of variance between biological replicates (CA *C. albicans*; PA *P. aeruginosa*). **(b)** Volcano plot of global transcriptional changes. Each dot represents one gene in the *C. albicans* genome. Red = significantly upregulated genes (Padj ≤ 0.05; $\log_2$ fold change ≥ 1). Figures provided by Genewiz®.

Table 4.1. Significantly differentially expressed *C. albicans* genes in response to meropenem treatment of dual-species *C. albicans–P. aeruginosa* biofilms. Genes with an adjusted P-value ≤ 0.05 and a $\log_2$ fold change ≥ 1 were considered significantly differentially expressed.

Gene ID	Gene name	Gene product[x]	Fold change ($\log_2$)*	Adjusted P-value^
CaalfMp08.4	N/A	Putative endonuclease encoded by the first four exons and part of the fourth intron of the mitochondrial *COX1* gene	+1.27	4.00×10^{-02}
CaalfMp08	*COX1*	Subunit I of cytochrome c oxidase, which is the terminal member of the mitochondrial (mt) inner membrane electron transport chain	+1.25	1.41×10^{-02}
CaalfMp10	*NAD3*	Subunit 3 of NADH:ubiquinone oxidoreductase (NADH:ubiquinone dehydrogenase), a multisubunit enzyme complex (complex I) of the mitochondrial inner membrane that catalyzes the first step in mitochondrial respiration	+1.23	1.51×10^{-02}
CaalfMp05	*ATP9*	Subunit 9 of the F0 sector of mitochondrial F1F0 ATP synthase	+1.20	8.11×10^{-03}
CaalfMp02	*NAD6*	Subunit 6 of NADH:ubiquinone oxidoreductase (NADH:ubiquinone dehydrogenase), a multisubunit enzyme complex (complex I) of the mitochondrial inner membrane that catalyzes the first step in mitochondrial respiration	+1.12	7.92×10^{-03}

[x] Gene product details from FungiDB (fungidb.org)

* + upregulated; - downregulated; $\log_2 \geq 1.00$ is equivalent to ≥ 2-fold linear change

^ Adjusted P-values ≤ 0.05 were considered to be significant

4.2.6 *P. aeruginosa* transcriptional response to *C. albicans*

4.2.6.1 *P. aeruginosa* response to *C. albicans* in untreated biofilms

To investigate the impact of dual-species biofilm interactions on bacterial cells, the transcriptional changes in *P. aeruginosa* cells between untreated single-species biofilms and untreated *P. aeruginosa–C. albicans* dual-species biofilms were analysed. Principle component analysis revealed that variation in transcriptional profiles between the samples overlapped between the two conditions, and did not separate the samples into two distinct populations (Figure 4.18a). This suggests a weak transcriptional response to the presence of *C. albicans*. In the dual-species biofilm cells, 265 *P. aeruginosa* genes were significantly upregulated (Padj ≤0.05) and 127 genes were significantly downregulated relative to single-species biofilm cells (Figure 4.18b).

GO terms analyses of significant DEGs were carried out for all categories; biological process (Figure 4.19), molecular function (Figure 4.20), and cellular component (Figure 4.21). Results from KEGG pathway enrichment analyses are shown in Figure 4.22. In summary, the transcriptional response of *P. aeruginosa* cells to the presence of *C. albicans*, in untreated dual-species biofilms, includes a >2-fold greater number of genes being significantly upregulated than the number downregulated. Phenazine biosynthesis was the most highly enriched GO term and KEGG pathway to which significantly upregulated genes were assigned (Figures 4.18a and 4.21a), suggesting that there is a large increase in *P. aeruginosa* phenazine production in response to the presence of *C. albicans* cells in dual-species biofilms. There is also significant upregulation of genes involved in the PQS (*Pseudomonas* quinolone signal) quorum sensing pathway (Figure 4.22a) and biosynthesis of the siderophore, pyoverdine

(Figure 4.19a). Genes that are significantly downregulated in response to the presence of *C. albicans* include those involved in type IV pilus biogenesis, the general secretory (Sec) pathway, and amino acid biosynthesis (Figures 4.18b and 4.21b).

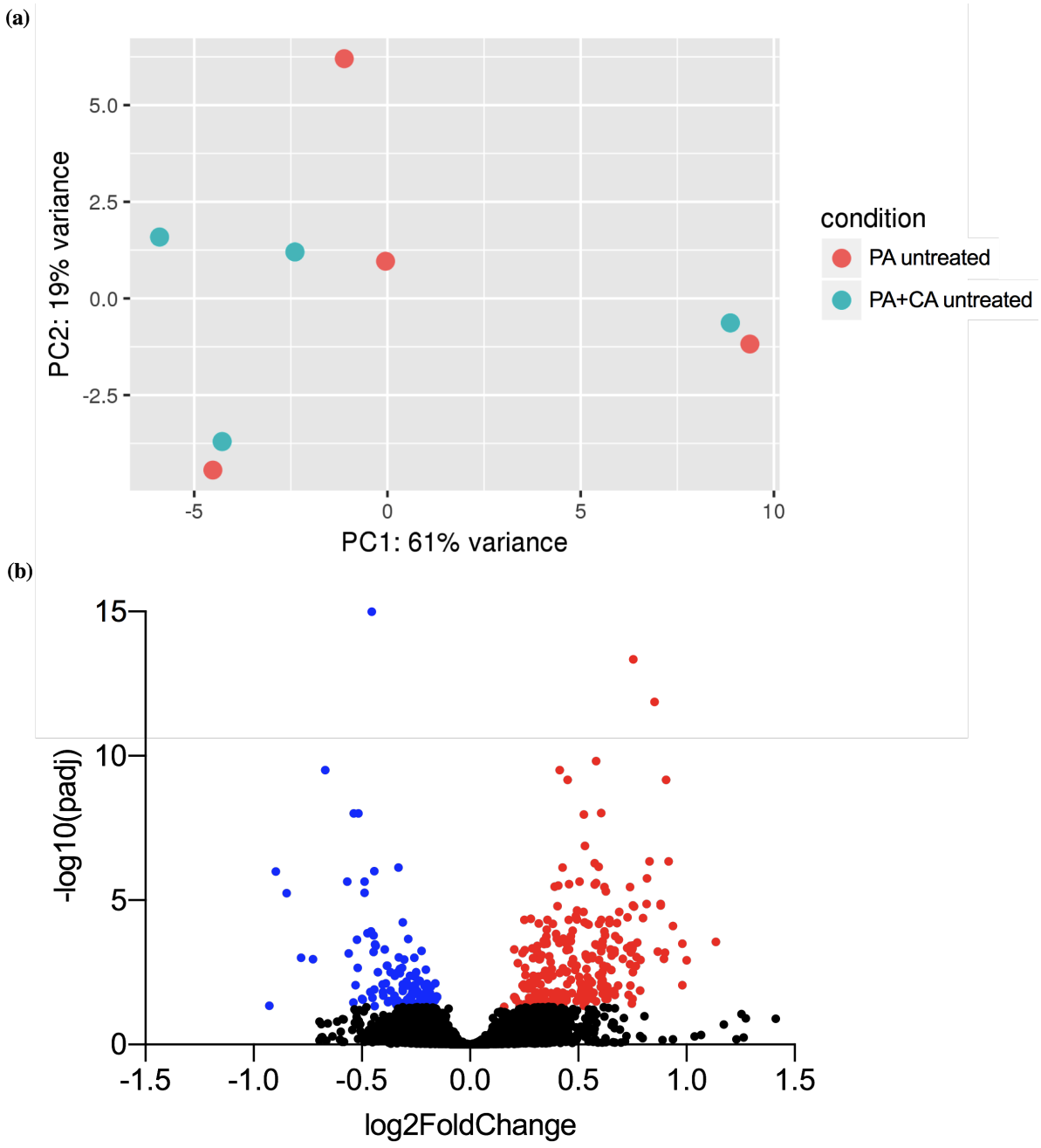


Figure 4.18. Global transcriptional changes within *P. aeruginosa* cells in response to the presence of *C. albicans* in untreated dual-species biofilms. RNA was extracted from mature (28 h) biofilm cells prior to RNA-seq. **(a)** Principle Component (PC) analysis of variance between biological replicates (PA *P. aeruginosa*; CA *C. albicans*). Figure provided by Genewiz®. **(b)** Volcano plot of global transcriptional changes. Each dot represents one gene in the *P. aeruginosa* genome. Red = significantly upregulated genes (Padj ≤ 0.05); Blue = significantly downregulated genes.

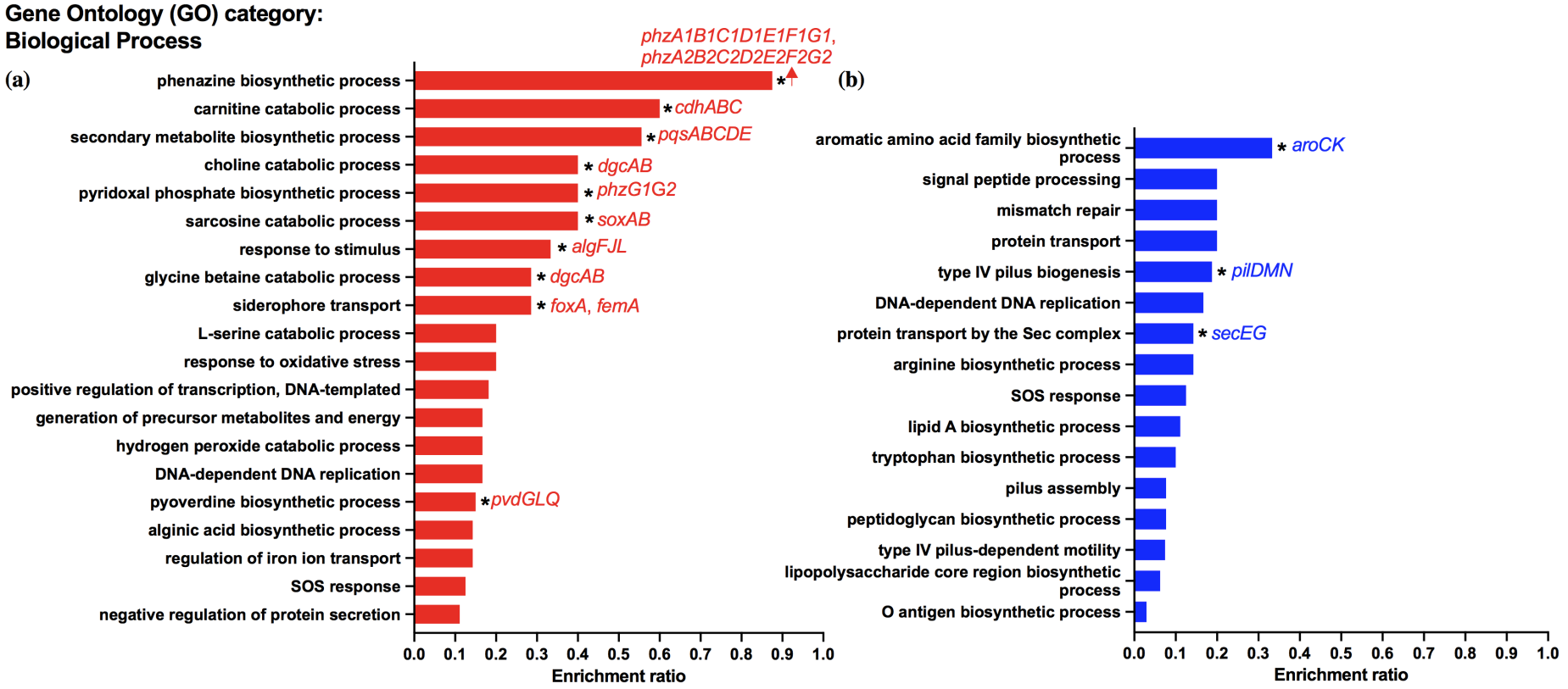


Figure 4.19. Distribution of significantly differentially expressed *P. aeruginosa* genes in the Gene Ontology (GO) category Biological Process, in response to the presence of *C. albicans* in untreated dual-species biofilms. There were 265 significantly upregulated and 127 downregulated genes, which were assigned to GO terms under the Biological Process category. **(a)** Upregulated terms. **(b)** Downregulated terms. Data were analysed using Fisher's exact test and Benjamini and Hochberg method for FDR correction (* FDR ≤ 0.05).

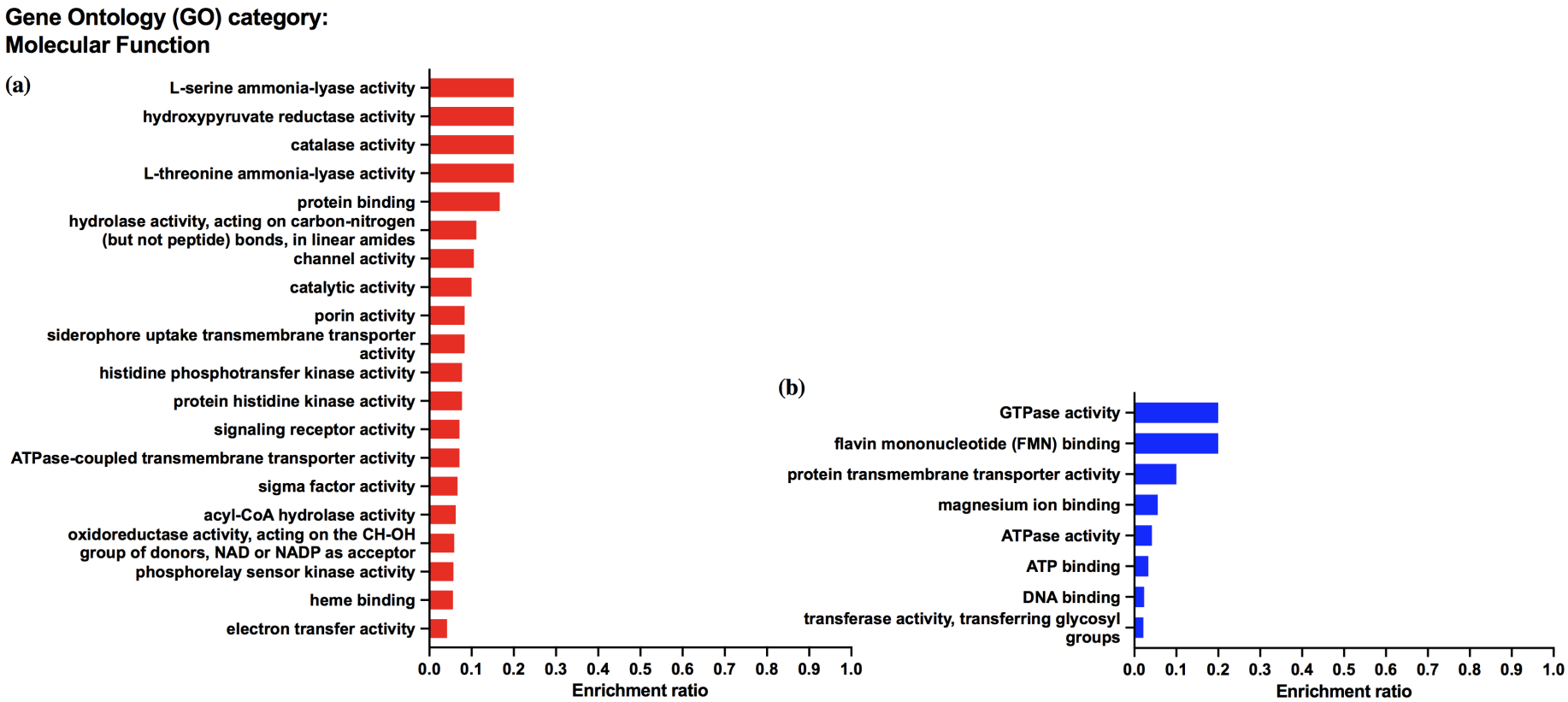


Figure 4.20. Distribution of significantly differentially expressed *P. aeruginosa* genes in the Gene Ontology (GO) category Molecular Function, in response to the presence of *C. albicans* in untreated dual-species biofilms. There were 265 significantly upregulated and 127 downregulated genes, which were assigned to GO terms under the Molecular Function category. **(a)** Upregulated terms. **(b)** Downregulated terms. Data were analysed using Fisher's exact test and Benjamini and Hochberg method for FDR correction.

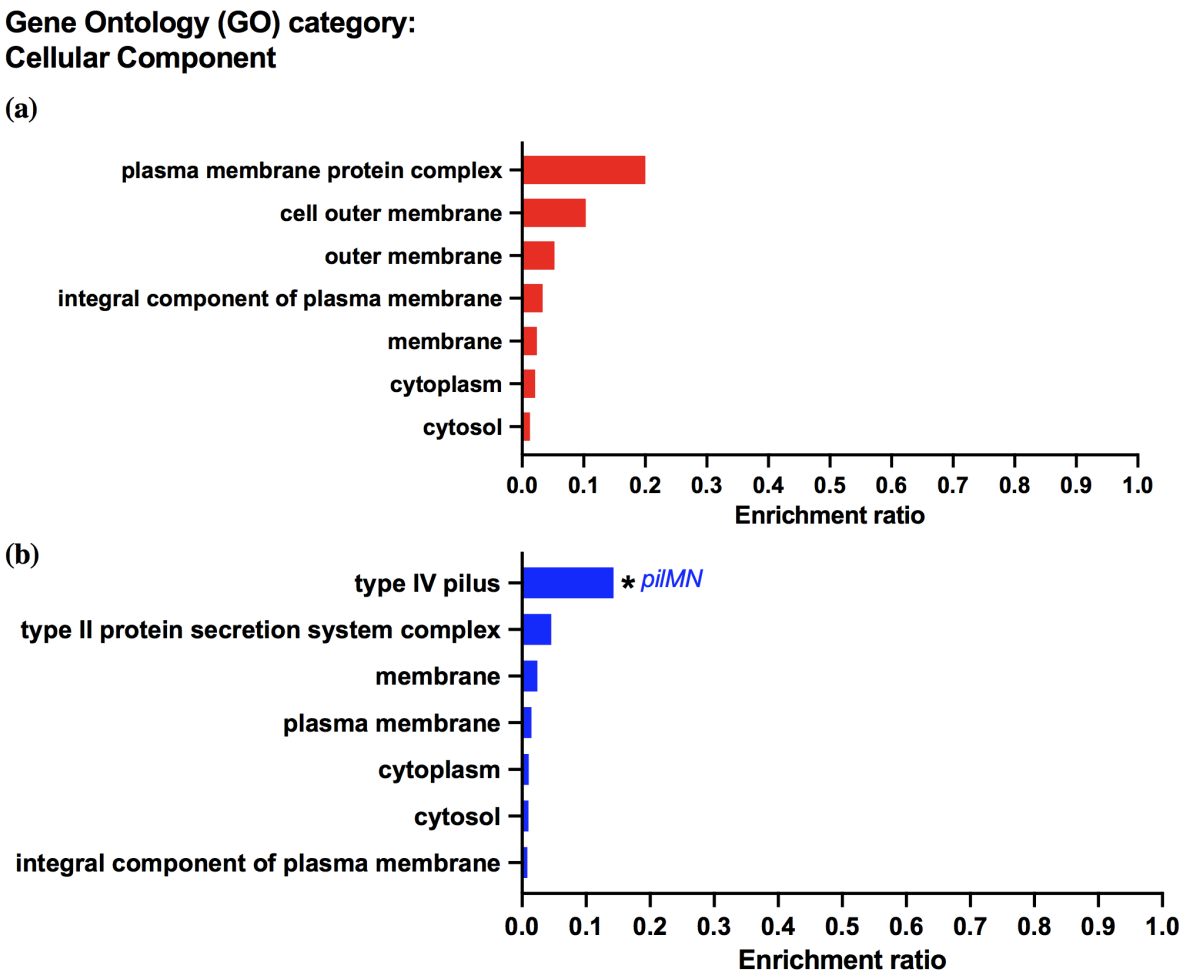


Figure 4.21. Distribution of significantly differentially expressed *P. aeruginosa* genes in the Gene Ontology (GO) category Cellular Component, in response to the presence of *C. albicans* in untreated dual-species biofilms. There were 265 significantly upregulated and 127 downregulated genes, which were assigned to GO terms under the Cellular Component category. **(a)** Upregulated terms. **(b)** Downregulated terms. Data were analysed using Fisher's exact test and Benjamini and Hochberg method for FDR correction (* FDR ≤ 0.05).

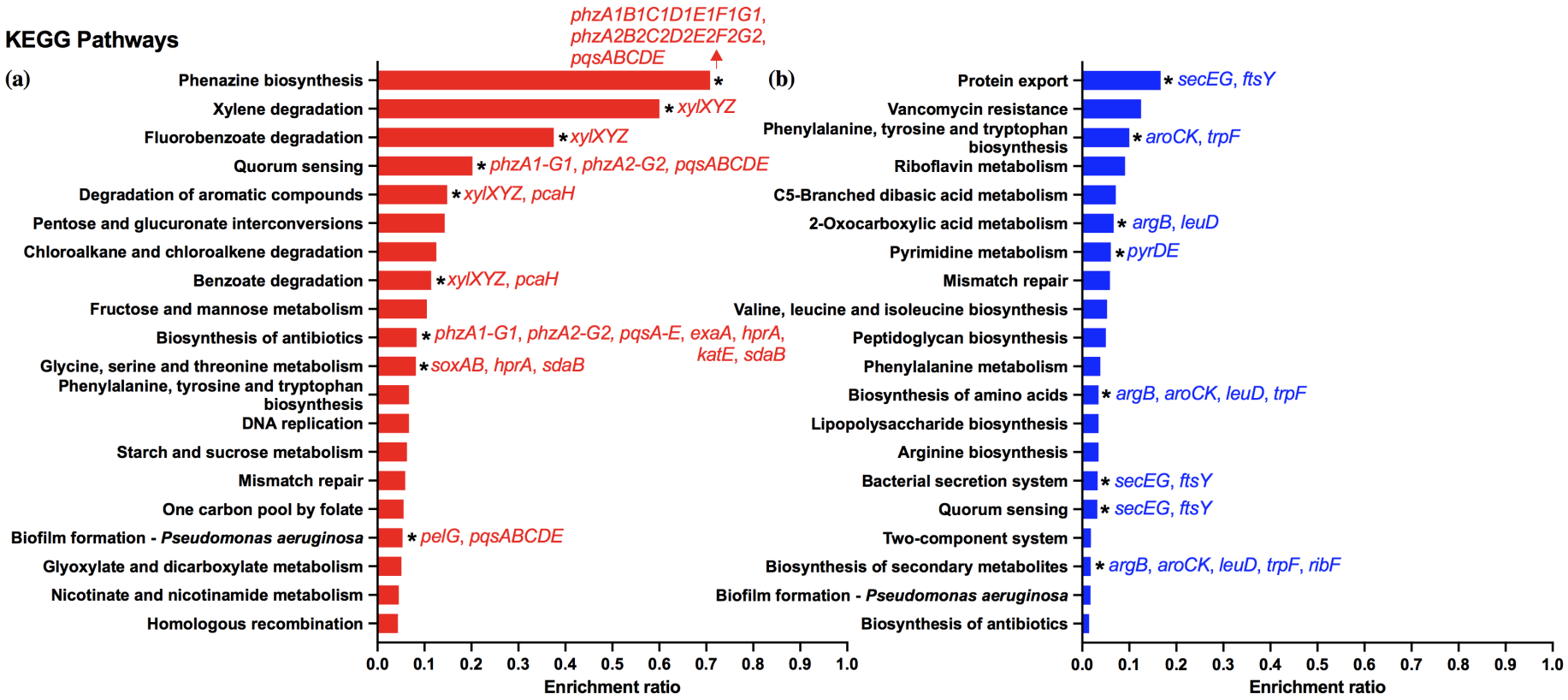


Figure 4.22. KEGG pathways assigned to significantly differentially expressed *P. aeruginosa* genes, in response to the presence of *C. albicans* in untreated dual-species biofilms. Annotations from the 265 significantly upregulated **(a)** and 127 downregulated genes **(b)** were analysed for KEGG pathway enrichment. Data were analysed using Fisher's exact test and Benjamini gand Hochberg method for FDR correction (* FDR ≤ 0.05).

4.2.6.2 *P. aeruginosa* response to *C. albicans* in meropenem-treated biofilms

To investigate whether the presence of meropenem affects the *P. aeruginosa* biofilm response to *C. albicans*, transcriptional changes in *P. aeruginosa* cells were analysed between meropenem-treated single-species biofilms and meropenem-treated *P. aeruginosa*–*C. albicans* dual-species biofilms. As with the untreated samples discussed above, principle component analysis revealed that variation in transcriptional profiles between the meropenem-treated samples overlapped between the two conditions; again, samples did not separate into two distinct populations (Figure 4.23a), indicating that the presence of *C. albicans* results in a weak transcriptional response within *P. aeruginosa* biofilm cells. In the dual-species biofilm cells, only one *P. aeruginosa* gene was significantly upregulated (Padj ≤0.05) and only one gene was significantly downregulated, relative to single-species biofilm cells (Figure 4.23b). The significantly upregulated gene was PA2664 (*fhp*), which encodes flavohemoprotein ($\log_2$ fold change +1.29; Padj 2.97×10^{-2}), while the significantly downregulated gene was PA3995, which encodes a putative transcriptional regulator ($\log_2$ fold change -0.51; Padj 3.57×10^{-6}).

The negligible transcriptional response of *P. aeruginosa* cells to the presence of *C. albicans*, in meropenem-treated biofilms, is in contrast to the response that was seen in untreated biofilms. This suggests that meropenem treatment may have a greater influence on *P. aeruginosa* gene expression than does the presence of *C. albicans* in the biofilm.

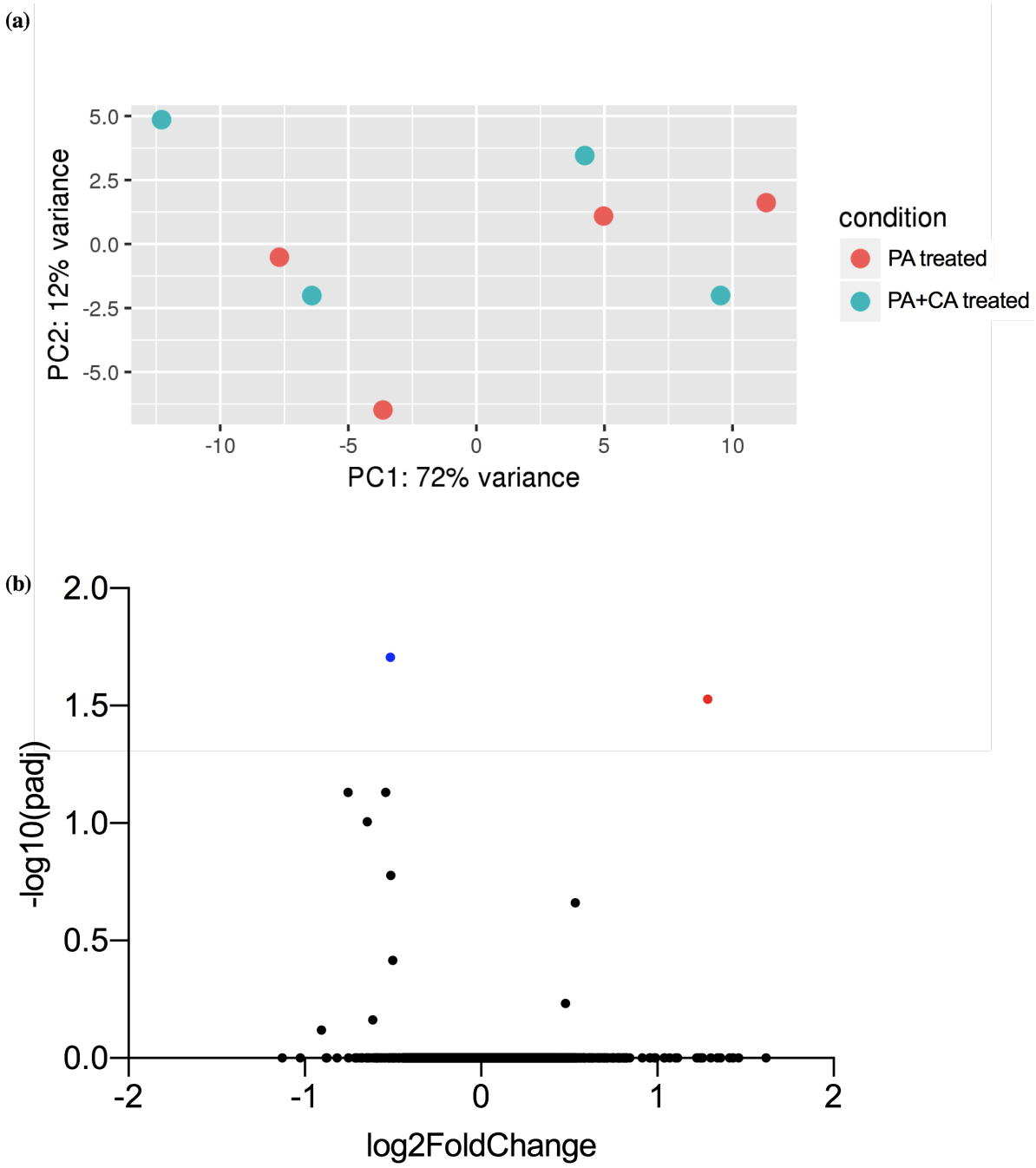


Figure 4.23. Global transcriptional changes within *P. aeruginosa* cells in response to the presence of *C. albicans* in meropenem-treated dual-species biofilms. RNA was extracted from mature (24 h) biofilm cells that had been treated with 5 µg/mL meropenem for a further 4h, prior to RNA-seq. **(a)** Principle Component (PC) analysis of variance between biological replicates (PA *P. aeruginosa*; CA *C. albicans*). Figure provided by Genewiz®. **(b)** Volcano plot of global transcriptional changes. Each dot represents one gene in the *P. aeruginosa* genome. Red = significantly upregulated gene (Padj ≤ 0.05); Blue = significantly downregulated gene.

4.2.7 *C. albicans* transcriptional response to *P. aeruginosa*

4.2.7.1 *C. albicans* response to *P. aeruginosa* in untreated biofilms

To investigate the impact of dual-species biofilm interactions on fungal cells, the transcriptional changes in *C. albicans* cells between untreated single-species biofilms and untreated *C. albicans–P. aeruginosa* dual-species biofilms were analysed. Principle component analysis revealed that single-species *C. albicans* biofilm samples formed a separate, distinct population to those from dual-species biofilms (Figure 4.24a). Furthermore, there was greater variation between transcriptional profiles of dual-species cells than single-species cells. Therefore, much of the variation in transcriptional profiles between the two conditions can be attributed to interactions with *P. aeruginosa*. In the dual-species condition, 431 *C. albicans* genes were significantly upregulated (Padj ≤ 0.05) and 739 genes were significantly downregulated by at least a $\log_2$ fold change of one (Figure 4.24b). The single most significantly upregulated *C. albicans* gene in response to the presence of *P. aeruginosa* was *INO1*, which encodes inositol-1-phosphate synthase ($\log_2$ fold change = +5.02; Padj = 1.51×10^{-294}). This enzyme is required for the production of *myo*-inositol, which is involved in several *C. albicans* cellular processes, including the production of membrane structures, such as glycosylphosphatidylinositol (GPI)-anchored proteins (Chen *et al.*, 2008).

GO terms analyses of significant DEGs were carried out for all categories; biological process (Figure 4.25), molecular function (Figure 4.26), and cellular component (Figure 4.27). Results from KEGG pathway enrichment analyses are shown in Figure 4.28. In summary, the global transcriptional changes of *C. albicans* biofilm cells in response to the presence of *P. aeruginosa* reveal many more downregulated genes

than upregulated genes. Of particular note are the downregulation of the ‘ribosome’ KEGG pathway (Figure 4.28b), alongside the high percentage abundances of the downregulated GO terms, ‘ribosome biogenesis’, ‘translation’, ‘ribosome’ and ‘RNA binding’ (Figures 4.24–4.26). These suggest an overall downregulation of protein synthesis in *C. albicans* biofilm cells, in response to the presence of *P. aeruginosa*.

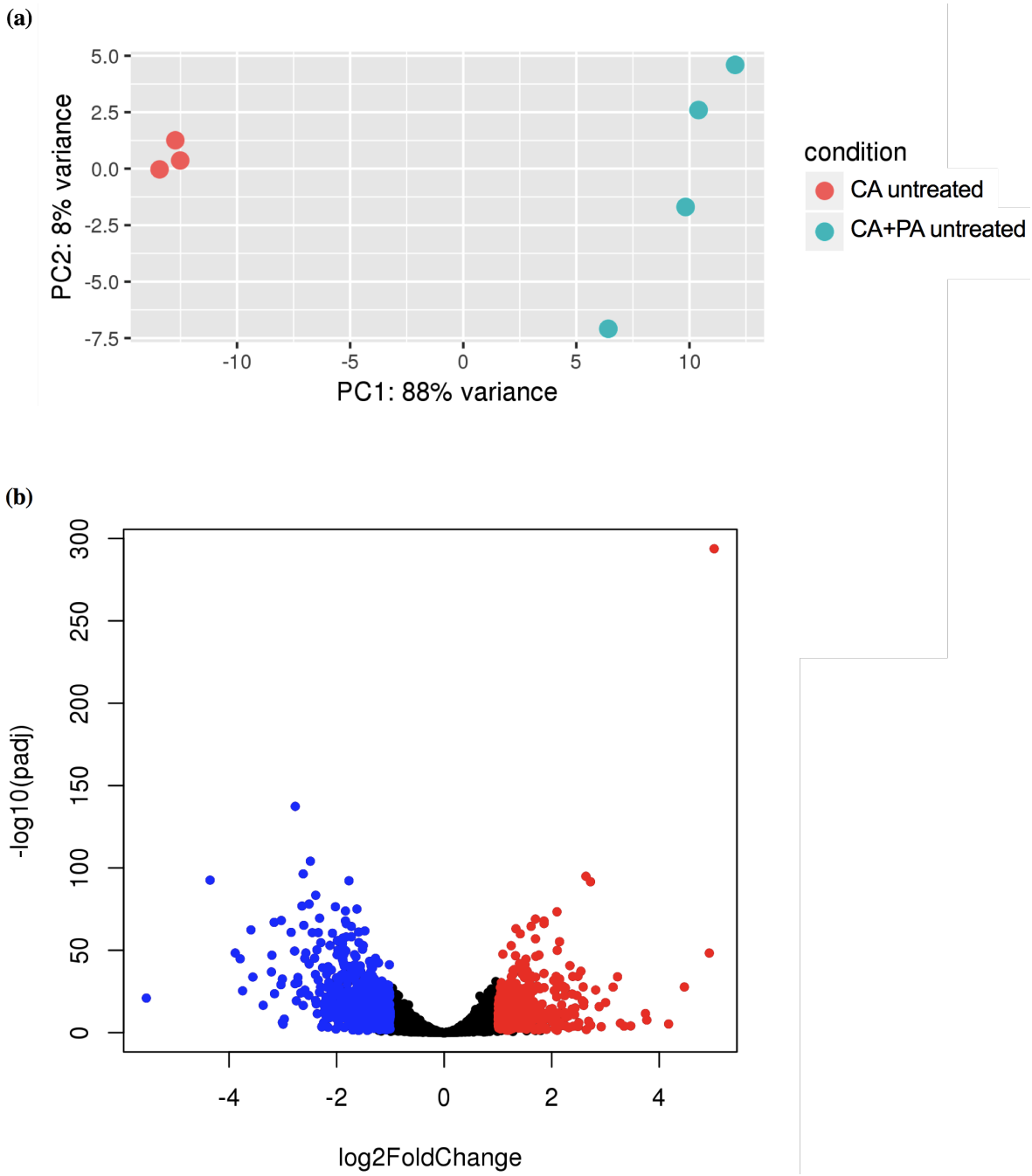


Figure 4.24. Global transcriptional changes of *C. albicans* biofilm cells in response to the presence of *P. aeruginosa* in untreated dual-species biofilms. RNA was extracted from mature (28 h) biofilm cells prior to RNA-seq. **(a)** Principle Component (PC) analysis of variance between biological replicates (CA *C. albicans*; PA *P. aeruginosa*). **(b)** Volcano plot of global transcriptional changes. Each dot represents one gene in the *C. albicans* genome. Red = significantly upregulated genes (Padj ≤ 0.05; $\log_2$ fold change ≥ 1); Blue = significantly downregulated genes. Figures provided by Genewiz®.

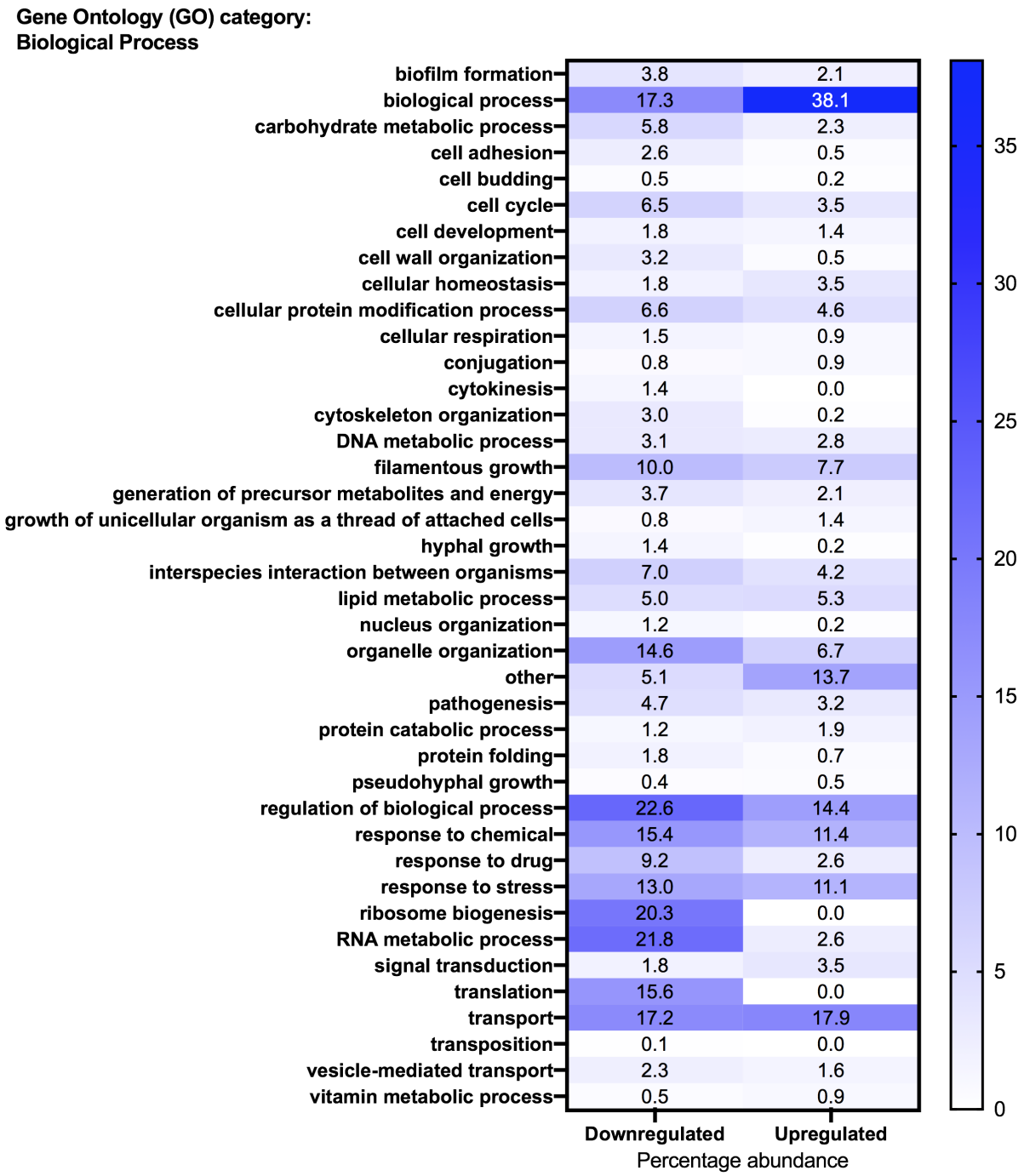


Figure 4.25. Distribution of significantly differentially expressed *C. albicans* genes in the Gene Ontology (GO) category Biological Process, in response to the presence of *P. aeruginosa* in untreated dual-species biofilms. There were 431 significantly upregulated and 739 downregulated genes (Padj ≤ 0.05 and $\log_2$ fold change ≥ 1), which were assigned as percentages to 40 GO Slim terms under the Biological Process category on the *Candida* Genome Database (CGD). See Tables S6 and S7 in Appendix II.iii. for full gene lists.

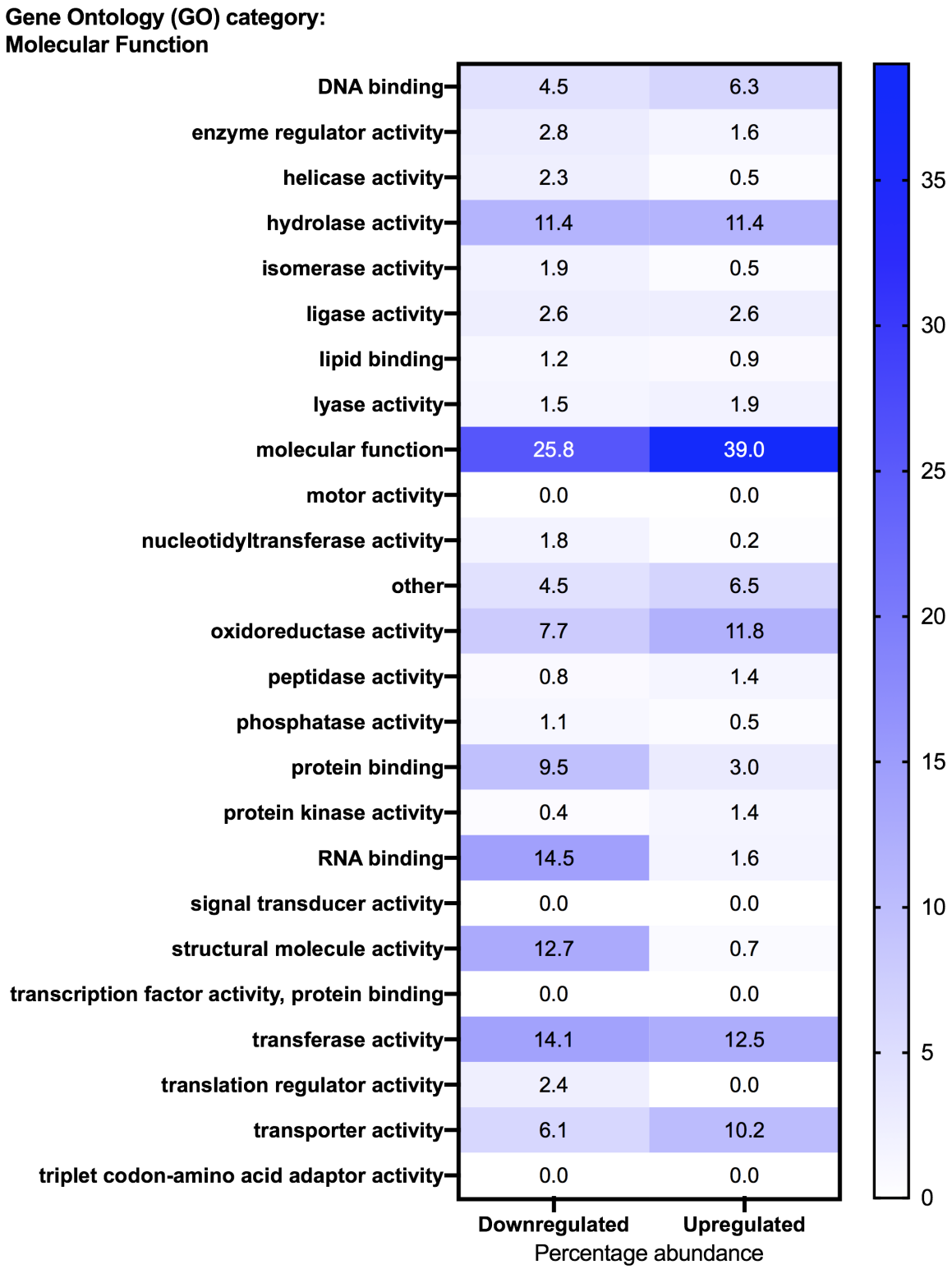


Figure 4.26. Distribution of significantly upregulated and downregulated *C. albicans* genes in the Gene Ontology (GO) category Molecular Function, in response to the presence of *P. aeruginosa* in untreated dual-species biofilms. There were 431 significantly upregulated and 739 downregulated genes (Padj ≤ 0.05 and $\log_2$ fold change ≥ 1), which were assigned as percentages to 25 GO Slim terms under the Molecular Function category on the *Candida* Genome Database (CGD). See Tables S8 and S9 in Appendix II.iii. for full gene lists.

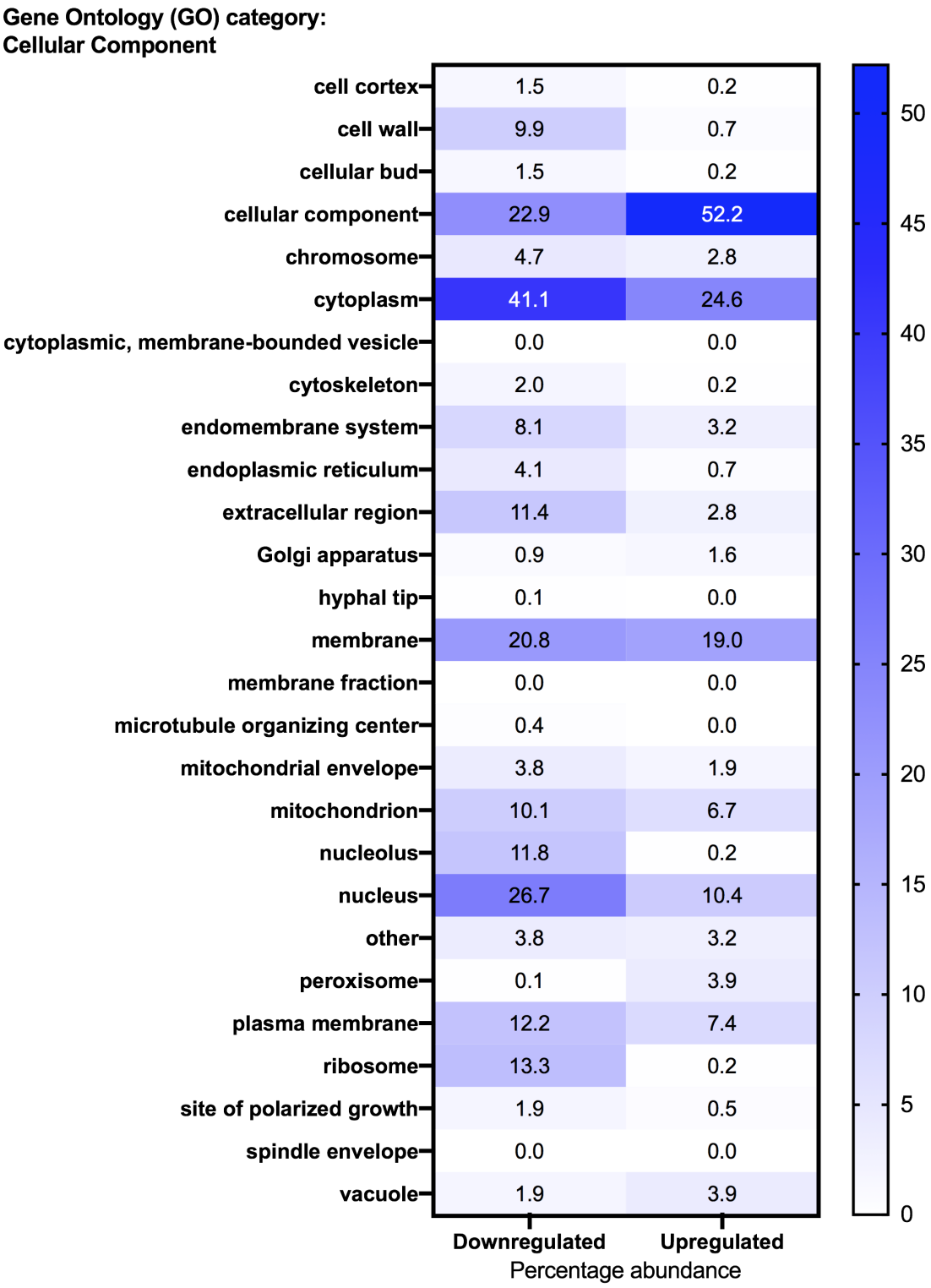


Figure 4.27. Distribution of significantly differentially expressed *C. albicans* genes in the Gene Ontology (GO) category Cellular Component, in response to the presence of *P. aeruginosa* in untreated dual-species biofilms. There were 431 significantly upregulated and 739 downregulated genes (Padj ≤ 0.05 and $\log_2$ fold change ≥ 1), which were assigned as percentages to 27 GO Slim terms under the Cellular Component category on the *Candida* Genome Database (CGD). See Tables S10 and S11 in Appendix II.iii. for full gene lists.

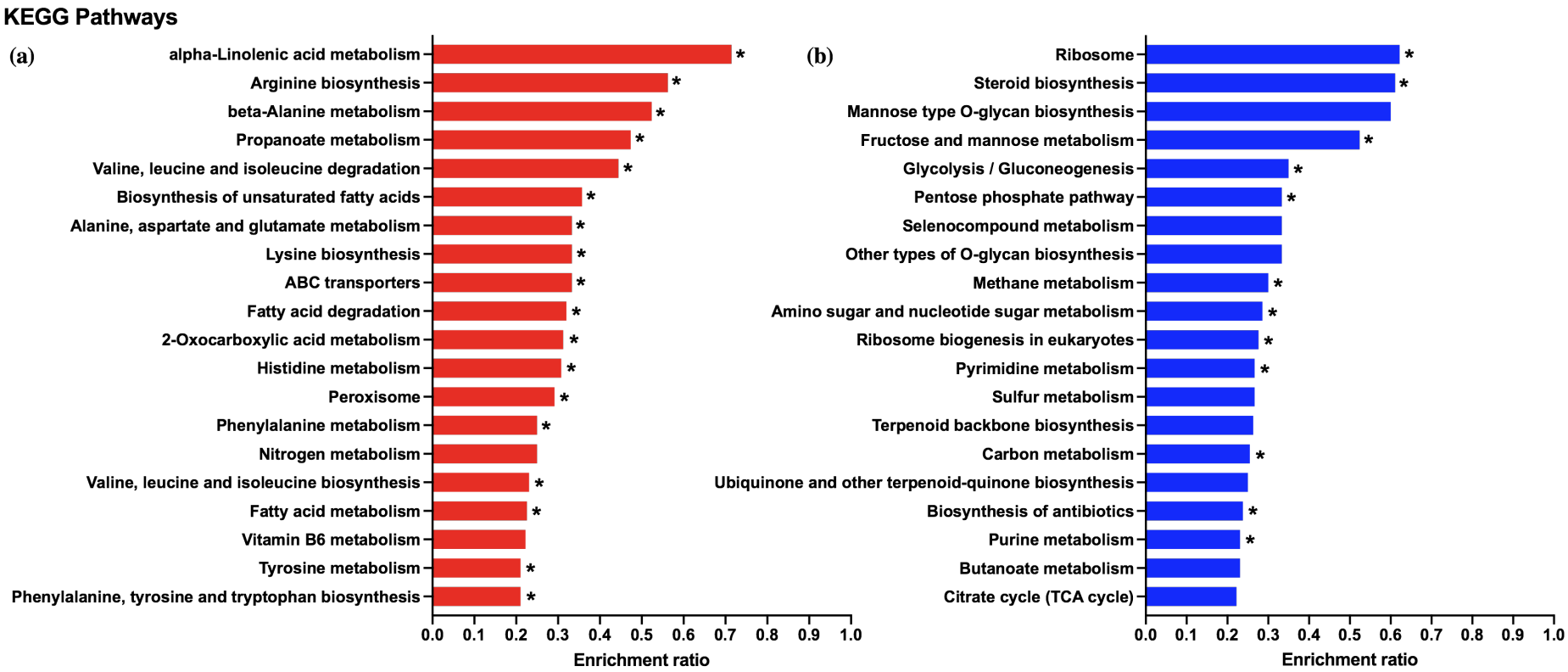


Figure 4.28. KEGG pathways assigned to significantly differentially expressed *C. albicans* genes, in response to the presence of *P. aeruginosa* in untreated dual-species biofilms. Annotations from the 431 significantly upregulated **(a)** and 739 downregulated genes **(b)** were analysed for KEGG pathway enrichment. Data were analysed using Fisher's exact test and Benjamini gand Hochberg method for FDR correction (* FDR ≤ 0.05). See Tables S12 and S13 in Appendix II.iii. for full gene lists.

4.2.7.2 *C. albicans* response *P. aeruginosa* in meropenem-treated biofilms

To determine whether treatment with 5 μg/mL meropenem had an effect on the *C. albicans* biofilm transcriptional response to *P. aeruginosa*, *C. albicans* gene expression profiles of meropenem-treated single- and dual-species biofilms were compared. Principle component analysis revealed that *C. albicans* cells from single-species biofilms formed a separate, distinct population to those from dual-species biofilms (Figure 4.29a). In comparison to the untreated single-species samples (Figure 4.24a), the transcriptional profiles of meropenem-treated single-species samples showed greater variance (Figure 4.29a); this may reflect the significant changes in expression of a small number of *C. albicans* genes in response to meropenem, which was previously observed (see section 4.2.5, above). In the meropenem-treated dual-species *C. albicans* biofilm cells, 380 genes were significantly upregulated (Padj ≤0.05) and 615 genes were significantly downregulated by at least a $\log_2$ fold change of one, relative to single-species (Figure 4.29b). As was the case with untreated biofilms, the most significantly upregulated *C. albicans* gene in response to the presence of *P. aeruginosa* in meropenem-treated biofilms was *INO1* ($\log_2$ fold change = +5.18; Padj = 1.32×10^{-249}).

GO terms analyses of significant DEGs were carried out for all categories; biological process (Figure 4.30), molecular function (Figure 4.31), and cellular component (Figure 4.32). Results from KEGG pathway enrichment analyses are shown in Figure 4.33. In summary, the global transcriptional changes of *C. albicans* cells, in response to the presence of *P. aeruginosa* in meropenem-treated biofilms, are very similar to those observed in untreated biofilms. As a result, the enriched GO terms and KEGG pathways are similar between the two comparisons. This is consistent with the

previous observation that meropenem treatment has very little transcriptional effect on *C. albicans* biofilm cells.

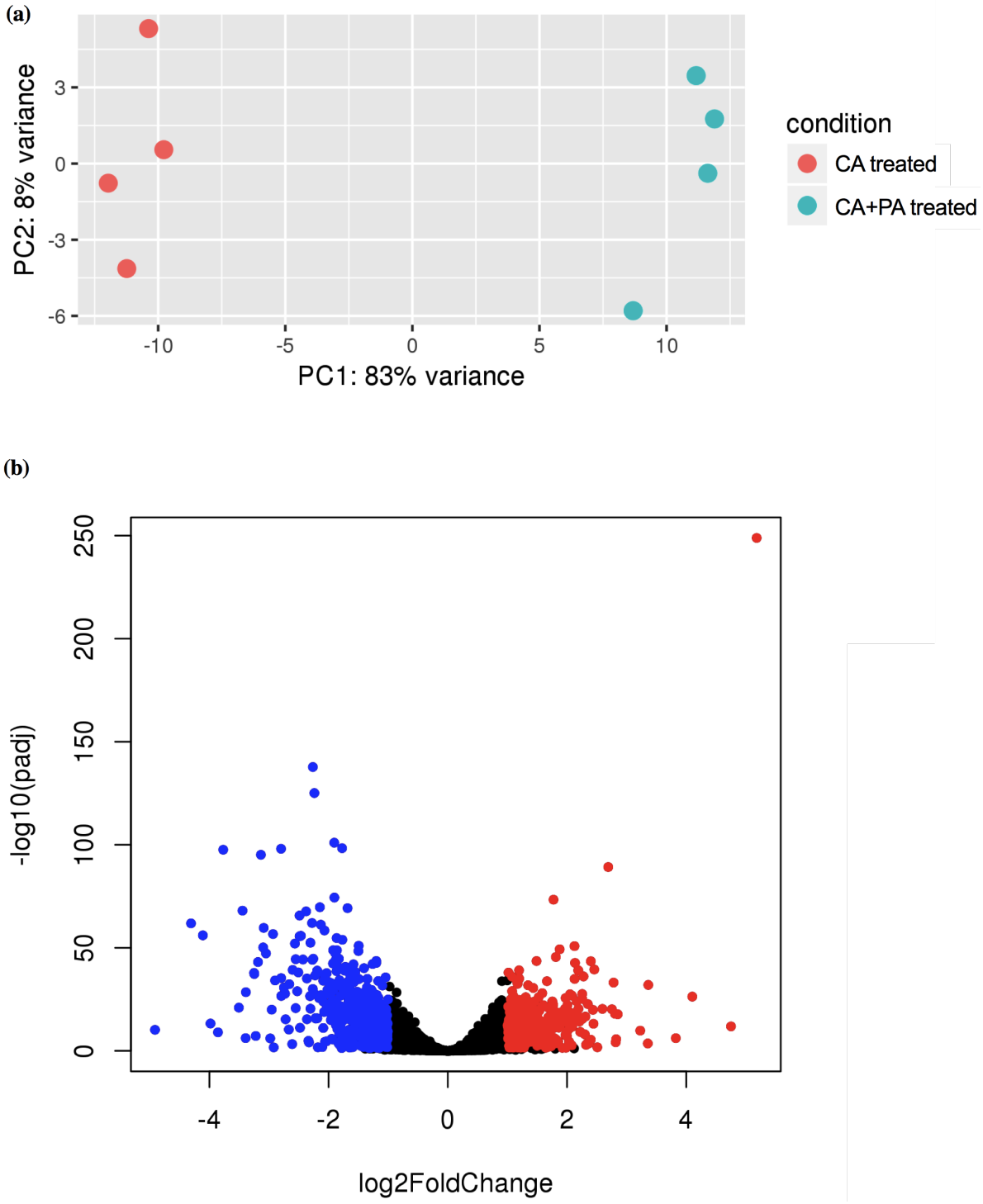


Figure 4.29. Global transcriptional changes of *C. albicans* biofilm cells in response to the presence of *P. aeruginosa* in meropenem-treated dual-species biofilms. RNA was extracted from mature (24 h) biofilm cells that had been treated with 5 µg/mL meropenem for a further 4h, prior to RNA-seq. **(a)** Principle Component (PC) analysis of variance between biological replicates (CA *C. albicans*; PA *P. aeruginosa*). **(b)** Volcano plot of global transcriptional changes. Each dot represents one gene in the *C. albicans* genome. Red = significantly upregulated genes (Padj ≤ 0.05; $\log_2$ fold change ≥ 1); Blue = significantly downregulated genes. Figures provided by Genewiz®.

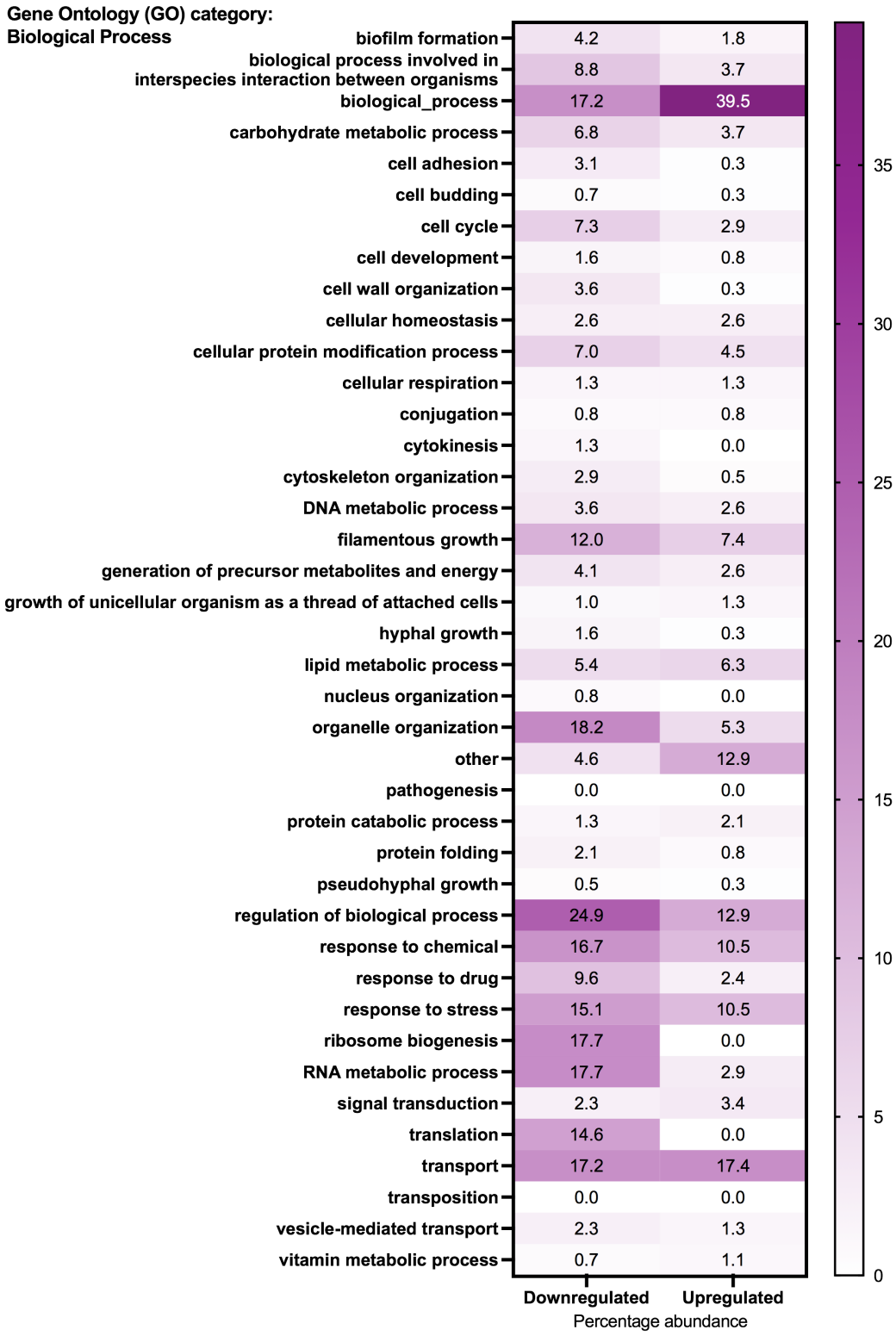


Figure 4.30. Distribution of significantly differentially expressed *C. albicans* genes in the Gene Ontology (GO) category Biological Process, in response to the presence of *P. aeruginosa* in meropenem-treated dual-species biofilms. There were 380 significantly upregulated and 615 downregulated genes (Padj ≤ 0.05 and $\log_2$ fold change ≥ 1), which were assigned as percentages to 40 GO Slim terms under the Biological Process category on the *Candida* Genome Database (CGD). See Tables S14 and S15 in Appendix II.iv. for full gene lists.

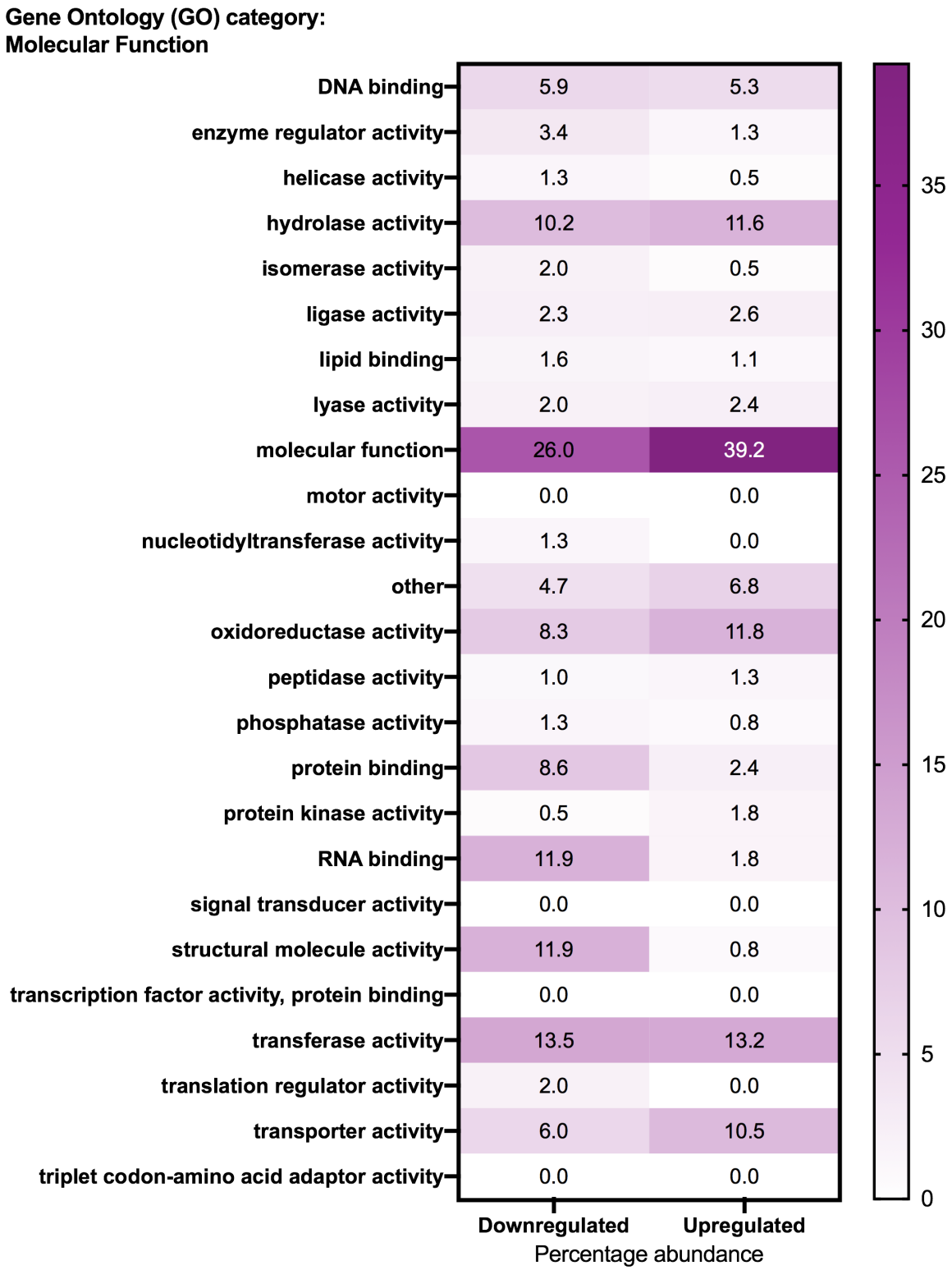


Figure 4.31. Distribution of significantly differentially expressed *C. albicans* genes in the Gene Ontology (GO) category Molecular Function, in response to the presence of *P. aeruginosa* in meropenem-treated dual-species biofilms. There were 380 significantly upregulated and 615 downregulated genes (Padj ≤ 0.05 and $\log_2$ fold change ≥ 1), which were assigned as percentages to 25 GO Slim terms under the Molecular Function category on the *Candida* Genome Database (CGD). See Tables S16 and S17 in Appendix II.iv. for full gene lists.

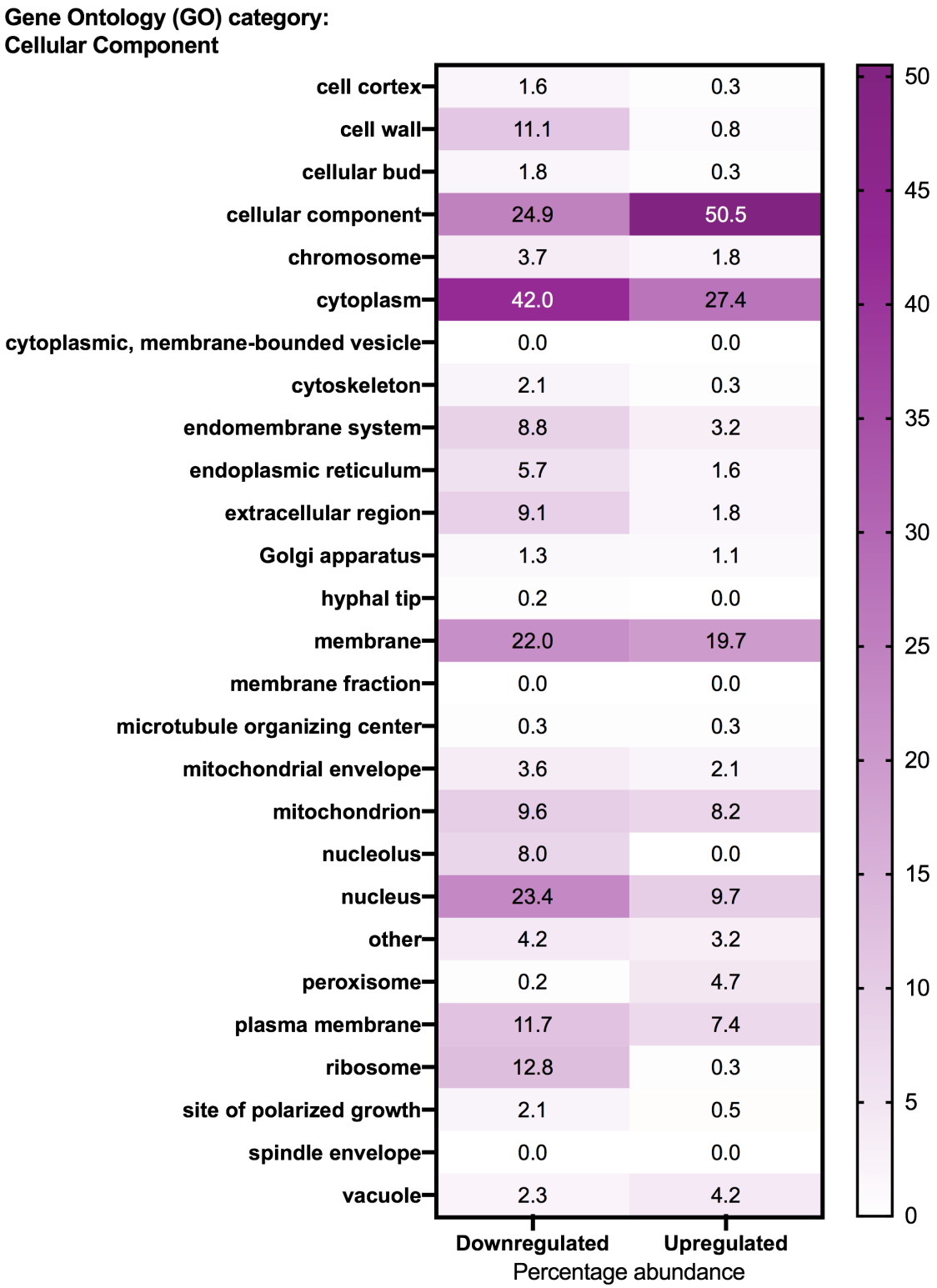


Figure 4.32. Distribution of significantly differentially expressed *C. albicans* genes in the Gene Ontology (GO) category Cellular Component, in response to the presence of *P. aeruginosa* in meropenem-treated dual-species biofilms. There were 380 significantly upregulated and 615 downregulated genes (Padj ≤ 0.05 and $\log_2$ fold change ≥ 1), which were assigned as percentages to 27 GO Slim terms under the Cellular Component category on the *Candida* Genome Database (CGD). See Tables S18 and S19 in Appendix II.iv. for full gene lists.

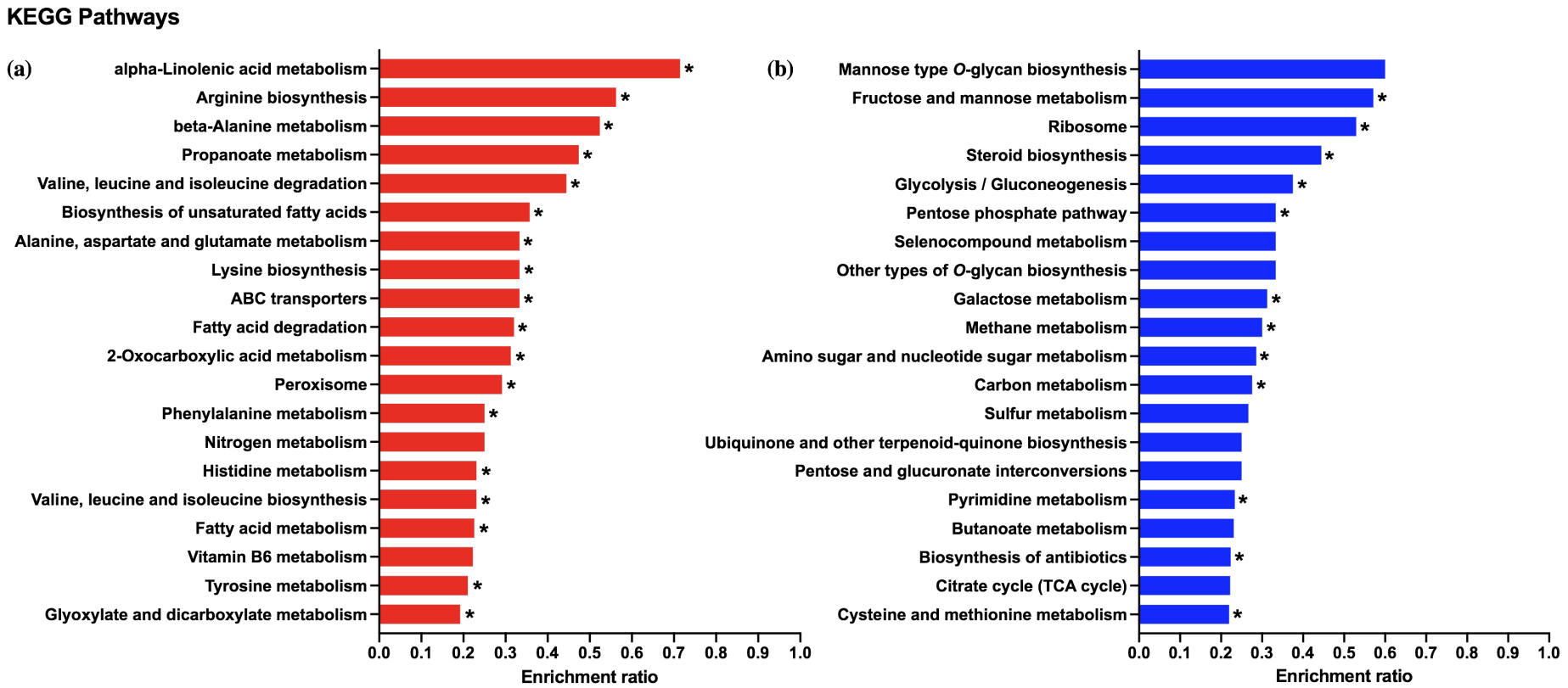


Figure 4.33. KEGG pathways assigned to significantly differentially expressed *C. albicans* genes, in response to the presence of *P. aeruginosa* in meropenem-treated dual-species biofilms. Annotations from the 380 significantly upregulated **(a)** and 615 downregulated genes **(b)** were analysed for KEGG pathway enrichment. Data were analysed using Fisher's exact test and Benjamini gand Hochberg method for FDR correction (* FDR ≤ 0.05). See Tables S20 and S21 in Appendix II.iv. for full gene lists.

4.3 DISCUSSION

4.3.1 *P. aeruginosa* transcriptional responses

When grown as dual-species biofilms with *C. albicans*, the most significantly upregulated pathway in *P. aeruginosa* biofilm cells was phenazine biosynthesis. This supports previous research showing *C. albicans*–mediated induction of phenazine production in *P. aeruginosa* (Doing *et al.*, 2020, Cugini *et al.*, 2010). Phenazine biosynthesis is controlled by enzymes encoded by two phenazine operons, *phzA1B1C1D1E1F1G1* (*phz1*) and *phzA2B2C2D2E2F2G2* (*phz2*), which have 98% sequence similarity, but are located on different parts of the *P. aeruginosa* PAO1 chromosome and have different promoter regions (Mavrodi *et al.*, 2001, Higgins *et al.*, 2018). All genes from both phenazine operons were significantly upregulated in dual-species biofilms. Phenazines are redox-active molecules that affect the redox balance of cells, the uptake of metabolites, gene expression, and have also been shown to enhance *P. aeruginosa* tolerance to the antibiotic, ciprofloxacin (Schiessl *et al.*, 2019). Therefore, the presence of *C. albicans* may promote antibiotic tolerance in *P. aeruginosa* biofilm cells, via upregulation of phenazine biosynthetic genes, which has clinical implications for the treatment of co-infected patients.

There was also significant upregulation of the *P. aeruginosa* quorum sensing pathway in response to *C. albicans*; specifically, all genes of the *pqsABCDE* operon were significantly upregulated. The *pqs* operon encodes several enzymes required for production of the *Pseudomonas* quinolone signal (PQS) (Higgins *et al.*, 2018). Furthermore, abundance of the PqsE enzyme results in increased promoter activity of both the *phz1* and *phz2* operons, thus controlling phenazine biosynthesis (Cugini *et al.*, 2010, Higgins *et al.*, 2018). Previous research shows that farnesol, secreted by *C.*

albicans, is responsible for inhibition of *P. aeruginosa* PQS production in planktonic interactions (Méar *et al.*, 2013). However, in biofilm interactions, the presence of *C. albicans* leads to high levels of PQS (Cugini *et al.*, 2010), which corroborates the observed upregulation of the *pqs* operon in the present study. PQS is known to be activated under conditions of iron limitation, leading to the production of phenazines and siderophores (Thi *et al.*, 2020), the latter of which scavenge iron from the environment (Diggle and Whiteley, 2020). Within *P. aeruginosa* biofilms, phenazines are thought to mop up molecular oxygen from oxic regions of the extracellular matrix, and release the oxygen to cells in anoxic regions of the biofilm (Saunders *et al.*, 2020). Furthermore, the siderophore biosynthetic genes, *pvdG*, *pvdL* and *pvdQ*, which encode proteins involved in the synthesis of pyoverdine, were also significantly upregulated in response to *C. albicans*. Therefore, the significant upregulation of *P. aeruginosa* genes required for the biosynthesis of PQS, phenazines and pyoverdine may be due to reduced availability of oxygen and iron, caused by nutrient competition between *P. aeruginosa* and *C. albicans* cells within the dual-species biofilm.

In contrast to untreated biofilms, there was a negligible transcriptional response to the presence of *C. albicans* in *P. aeruginosa* biofilms cells that had been treated with 5 µg/mL meropenem. This suggests that, upon antibiotic treatment, the *P. aeruginosa* transcriptional response to meropenem overrides the response to *C. albicans*. This is supported by the observation that the majority of significant changes in gene expression, in response to meropenem treatment, are shared between single-species and dual-species *P. aeruginosa* biofilm cells. In both cases, the gene with the greatest $\log_2$ fold increase in expression was *ampC*, which encodes a ß-lactamase precursor. This supports a previous study of the *P. aeruginosa* biofilm transcriptional response to

treatment with a carbapenem antibiotic, which also found *ampC* to be the gene with the greatest positive fold change in expression, by a large margin relative to all other genes in the genome (Bagge *et al.*, 2004). Upregulation of *ampC* is associated with increased resistance to ß-lactam antibiotics (Khaledi *et al.*, 2016). Another gene associated with meropenem resistance is *oprD*, which encodes the outer membrane porin (OprD) that is known to facilitate entry of carbapenem antibiotics into bacterial cells; *oprD* is therefore frequently found to be downregulated in meropenem-resistant strains, with the caveat that there is often a poor correlation between mRNA levels and protein levels (Khaledi *et al.*, 2016). Nevertheless, in the present study, *oprD* was not significantly differentially expressed in response to meropenem treatment, neither in single-species nor dual-species *P. aeruginosa* biofilm cells.

There were many transcriptional changes in common between single- and dual-species *P. aeruginosa* biofilm cell responses to meropenem. There was upregulation of peptidoglycan biosynthetic genes *murC*, *murD*, *murE*, *murG*, *ddlB* and *mraY*, and D-glutamine and D-glutamate metabolism genes *murC* and *murD*; this has previously been observed with imipenem treatment (Bagge *et al.*, 2004). Meropenem treatment also resulted in upregulation of genes encoding cell division proteins (*ftsA*, *ftsW* and *ftsZ*), which was also previously observed in response to imipenem (Bagge *et al.*, 2004). Increased peptidoglycan production and cell division, as a response to treatment with a ß-lactam antibiotic, may be a mechanism of counteracting the inhibitory effect of the antibiotic on cell wall biosynthesis.

Single-species and dual-species *P.* aeruginosa biofilm cells responded to meropenem treatment by upregulating extracellular polysaccharide biosynthetic genes, including

pslB, *pslD*, *pslE* and *pslF*. The polysaccharide Psl is known to enhance intercellular and cell–substrate interactions within biofilms, and protects the structure of the biofilm (Passos da Silva *et al.*, 2019). The *pslD* gene in particular appears to play an important role in biofilm formation, as it is commonly found in biofilm-forming clinical isolates of *P. aeruginosa* (Kamali *et al.*, 2020). Furthermore, Psl is thought to enhance *P. aeruginosa* biofilm tolerance to antibiotics, such as colistin, tobramycin, and ciprofloxacin, by sequestration of antibiotic molecules (Hall and Mah, 2017). Another significantly upregulated gene involved in biofilm formation was *lasR*, which encodes a transcriptional activator of elastase expression (Cugini *et al.*, 2010) and plays a major role in quorum sensing; the Las system sits at the head of the hierarchical *P. aeruginosa* QS cascade (Thi *et al.*, 2020). Therefore, meropenem treatment results in enhanced *P. aeruginosa* biofilm formation and extracellular matrix structural integrity. This may have the consequence of impeding diffusion of meropenem towards cells within the biofilm.

Another set of genes that were upregulated in both single- and dual-species biofilm cells were those encoding components of the type VI secretion system (T6SS): *ppkA* and *pppA*, which encode regulatory threonine kinase/phosphatase proteins; *clpV1*, which encodes an ATPase; *icmF1*, which encodes an inner membrane protein; and *vgrG1* and *hcp1*, which encode secreted effector proteins of the T6SS (Chen *et al.*, 2020). Although there has been no previous research linking antibiotic treatment to upregulation of T6SS activity in *P. aeruginosa*, this has been observed in both *A. baumannii* and *K. pneumoniae* (Wang *et al.*, 2018, Liu *et al.*, 2017). An *A. baumannii* Δ*vgrG* knockout strain showed enhanced resistance to ampicillin/sulbactam (Wang *et al.*, 2018), while sub-inhibitory concentrations of meropenem or ceftazidime induced

expression and secretion of the T6SS ATPase, ClpV, and the effector protein, Hcp (hemolysin-coregulated protein) (Liu *et al.*, 2017). The structure of the T6SS bears similarities to the cell-puncturing needle of bacteriophage viruses; the roles of the T6SS in *P. aeruginosa* include virulence within hosts, delivery of toxins to neighbouring microbes that are competing for resources, and biofilm formation (Chen *et al.*, 2015, Chen *et al.*, 2020). Therefore, upregulation of T6SS genes in response to meropenem treatment may be another mechanism, alongside upregulation of genes encoding Psl, by which *P. aeruginosa* cells enhance biofilm formation, as a mechanism for enhancing antibiotic tolerance.

The most enriched KEGG pathway to which significantly upregulated genes were assigned was biosynthesis of siderophore group non-ribosomal peptides. The specific *P. aeruginosa* genes that were upregulated in both single- and dual-species responses to meropenem were *pchA*, *pchB*, *pchE*, *pchF* and *pchG*, which encode proteins involved in the synthesis of pyochelin. Pyochelin is one of two siderophores, along with pyoverdine, that is produced by *P. aeruginosa* for scavenging iron from iron-limited environments (Diggle and Whiteley, 2020). The significant upregulation of pyochelin biosynthetic genes in response to meropenem treatment suggests that iron acquisition may be important in the bacterial response to meropenem. This is supported by research showing that iron supplementation of anaerobically grown *P. aeruginosa* biofilms confers resistance to meropenem by inducing a 4-fold increase in the MIC (Reid *et al.*, 2009). Therefore, upregulation of pyochelin biosynthetic genes, for enhanced iron uptake, may be an antibiotic resistance mechanism employed by cells located in anaerobic regions of *P. aeruginosa* biofilms. This indicates that

combination treatment of *P. aeruginosa* biofilm infections, with meropenem and an iron chelator, may be more effective than meropenem alone.

Some differences between the single- and dual-species *P. aeruginosa* responses to meropenem were the upregulation of genes encoding proteins involved in translation of mRNA to protein (*rplB*, *rplE*, *rplJ*, *rplN*, *rplP*, *rplV*, *rplW*, *rplX*, *rpmC*, *rpsC*, *rpsQ*, *rpsS*, *tufA* and *tufB*), and proteins involved in the tricarboxylic acid cycle (*sucA*, *sucC*, *sucD* and *sdhB*) and cytochrome-c oxidase activity (*ccoO2*, *ccoP2* and *ccoQ2*); these genes were significantly upregulated in single-species *P. aeruginosa* biofilm cells, but not in dual-species. This indicates that single-species *P. aeruginosa* biofilm cells upregulate both aerobic respiration and protein production in response to treatment with 5 μg/mL meropenem, but this does not occur when *C. albicans* is present in the biofilm.

To further understand the differences between single- and dual-species *P. aeruginosa* biofilm responses to meropenem, genes that were uniquely differentially regulated in the dual-species biofilms were focused upon. In Chapter 3, it was observed that the presence of *C. albicans* enhanced meropenem tolerance of *P. aeruginosa* in dual-species biofilms. Among the genes uniquely upregulated in meropenem-treated, dual-species *P. aeruginosa* biofilm cells, were three genes associated with biofilm formation: *pslH*, *pslI* and *algR*. The ability of Psl to enhance *P. aeruginosa* biofilm tolerance to antibiotics (Hall and Mah, 2017) was discussed earlier. Upregulation of *algR* indicates increased alginate production, which is the *P. aeruginosa* exopolysaccharide that is responsible for a mucoid phenotype and is associated with the increased antibiotic resistance of strains isolated from CF patients (Lee and Yoon,

2017). Enhanced *P. aeruginosa* biofilm production, via upregulation of alginate biosynthesis, has been observed in a previous study (Phuengmaung *et al.*, 2020). Therefore, further investigation into the role of alginate in enhancing meropenem tolerance of dual-species biofilm cells is warranted.

There were three *P. aeruginosa* genes associated with outer membrane vesicles (OMVs), which were uniquely upregulated in meropenem-treated, dual-species *P. aeruginosa* biofilm cells. This suggests a potential increase in OMV production in the presence of *C. albicans*. *P. aeruginosa* OMVs play various roles in biofilms, including secretion of the PQS molecule, as well as other signal molecules, and the release of extracellular DNA into the biofilm matrix (Thi *et al.*, 2020). Furthermore, it has been shown that *P. aeruginosa* OMVs can package and secrete the chromosomally-encoded ß-lactamase enzyme (Ciofu *et al.*, 2000). Although the OMV study was done with planktonic cultures, it is feasible to hypothesise that a similar phenomenon may occur in *P. aeruginosa* biofilms, so further investigation into the role of OMVs in antibiotic tolerance of biofilm cells would be an interesting avenue to explore.

Another set of genes that were uniquely differentially regulated within dual-species *P. aeruginosa* cells, in response to meropenem treatment, were genes encoding efflux pump proteins. Of particular note were the significant upregulation of *mexC* and the significant downregulation of *mexE* and *mexF*. This indicates that, in the presence of *C. albicans*, *P. aeruginosa* biofilm cells may respond to meropenem by increasing production of the MexCD-OprJ efflux pump, but decreasing production of MexEF-OprN. There are six RND family efflux pumps in *P. aeruginosa*: MexAB-OprM, MexCD-OprJ, MexEF-OprN, MexJK-OprM, MexXY-OprM and MexGHI-OpmD (Hulen *et al.*,

2020). Of these, MexAB-OprM and MexXY-OprM are most frequently associated with resistance to carbapenem antibiotics (Fusté *et al.*, 2013), but MexCD-OprJ is also thought to be linked with meropenem resistance (Hassuna *et al.*, 2020). Although upregulation of the *mexC* gene does not necessarily equate to increased production of the entire MexCD-OprJ efflux pump complex, it can be hypothesised that efflux of meropenem may be increased in the presence of *C. albicans*. RNA-seq analysis also revealed significant upregulation of two genes, and significant downregulation of three genes, associated with ABC transporters in meropenem-treated, dual-species *P. aeruginosa* biofilm cells. Very little is known about the role of ABC transporters in *P. aeruginosa* drug tolerance (Hulen *et al.*, 2020). Therefore, it would be interesting to carry out proteomic analyses of single- and dual-species biofilms to quantify levels of the various *P. aeruginosa* efflux proteins, and to measure efflux activity in *P. aeruginosa–C. albicans* biofilm interactions.

4.3.2 *C. albicans* transcriptional responses

Meropenem is an antibiotic that specifically targets PBPs in bacterial cell walls (Papp-Wallace *et al.*, 2011). The absence of this drug target in fungal cells means that meropenem should not affect *C albicans*. This is confirmed by the lack of transcriptional response to treatment with 5 μg/mL meropenem, in either single- or dual-species *C. albicans* biofilm cells. Furthermore, viable counts showed no significant difference in numbers of *C. albicans* cells recovered between untreated and meropenem-treated biofilms, either from single-species or dual-species biofilms. The overall transcriptional changes within *C. albicans* biofilm cells, in response to the presence of *P. aeruginosa*, were very similar between untreated and meropenem-treated biofilms. This was confirmed by the similarity of outcomes in GO term and

KEGG pathway enrichment analyses, and by the large proportion of significantly differentially regulated genes that were shared between the two comparisons. This provides further confirmation that treatment of single- or dual-species biofilms with 5 µg/mL meropenem has little to no effect on *C. albicans*.

Among the *C. albicans* responses to the presence of *P. aeruginosa* was the downregulation of genes assigned to the 'filamentous growth' GO term. This supports the observation that *P. aeruginosa* inhibits hyphal formation in *C. albicans* biofilm cells (Morales *et al.*, 2013, Hogan *et al.*, 2004, Grainha *et al.*, 2020). One of the most enriched pathways among the downregulated genes was the ribosome pathway, accompanied by enrichment of the 'translation' GO term. This inhibition of translation in *C. albicans* biofilm cells, in response to *P. aeruginosa* interactions, is in agreement with previous research (Fourie *et al.*, 2021).

Downregulation of *C. albicans* carbon metabolism and glycolysis/gluconeogenesis pathways was also observed in response to *P. aeruginosa*, indicating reduced respiratory rates in fungal cells. This is supported by published data showing that *P. aeruginosa* inhibits respiration in *C. albicans* (Trejo-Hernández *et al.*, 2014) and that this is associated with *P. aeruginosa* phenazine production (Morales *et al.*, 2013). Another *C. albicans* pathway that is significantly downregulated, in response to *P. aeruginosa* interactions, is the ergosterol biosynthesis pathway (represented by the 'steroid biosynthesis' KEGG pathway). This observation is in contrast with previous research showing that the *P. aeruginosa* quorum sensing molecule, 3O-C_{12}-HSL (*N*-3-oxo-dodecanoyl-L-homoserine lactone), upregulates expression of ergosterol biosynthetic genes (Bandara *et al.*, 2020b). The difference in *C. albicans*

transcriptional responses between these datasets may be attributed to differences in the growth conditions, as the methods employed by Bandara *et al.* (2020b) involved supplementation of single-species *C. albicans* biofilms with purified 3O-C_{12}-HSL, rather than growth of dual-species biofilms. This highlights the importance of studying microbes and not just their purified products.

The most significantly upregulated *C. albicans* gene, in response to dual-species biofilm growth with *P. aeruginosa*, in both untreated and meropenem-treated biofilms, was *INO1*, suggesting upregulation of the *myo*-inositol pathway. *Myo*-inositol is an essential component for the formation of GPI-anchors (Chen *et al.*, 2008). In *C. albicans* cells, GPI-anchored proteins include chitinases, aspartyl proteinases, superoxide dismutases, hyphal cell wall protein, *N*-linked mannoproteins and ß-glucan–associated cell wall proteins (Plaine *et al.*, 2008). Therefore, the upregulation of *INO1* may indicate increased cell wall remodelling of *C. albicans* in response to interactions with *P. aeruginosa*.

One of the most enriched fungal pathways to which upregulated genes were assigned, in response to *P. aeruginosa* biofilm interactions, was α-linolenic acid metabolism, which is part of the *C. albicans* fatty acid oxidation pathway that occurs within peroxisomes (Piekarska *et al.*, 2006). This was accompanied by enrichment of the peroxisome cellular component in GO term analysis. As well as fatty acid oxidation, another role of fungal peroxisomes is in detoxifying hydrogen peroxide (Chen *et al.*, 2016). The upregulation of genes associated with peroxisomes suggests that the presence of *P. aeruginosa* is linked to oxidative stress in *C. albicans* biofilm cells. This supports published research showing that *P. aeruginosa* phenazines induce the

production of reactive oxygen species (ROS) in fungal cells (Morales *et al.*, 2010, Morales *et al.*, 2013, Briard *et al.*, 2015). Furthermore, upregulation of *C. albicans* arginine biosynthetic genes has previously been observed as a response to increased levels of ROS (Jiménez-López *et al.*, 2013), which supports the observed upregulation of arginine biosynthesis pathway genes in the present study, in response to biofilm interactions with *P. aeruginosa*. The upregulation of genes associated with oxidative stress responses have been observed in previous research into the *C. albicans* transcriptional response to *P. aeruginosa* (Fourie *et al.*, 2021, Grainha *et al.*, 2020, Doing *et al.*, 2020).

A study reporting the transcriptional response of *C. albicans* to *P. aeruginosa* in a dual-species biofilm was published online very recently (Fourie *et al.*, 2021). However, at the time of writing, Fourie *et al.* (2021) had not yet made their transcriptomic data or supplementary tables publicly available, which unfortunately prevented the detailed comparing and contrasting of their findings to those of the present study. In brief, the study reported data from single-species RNA-seq of *C. albicans* transcripts taken from early static mono- and dual-species biofilms. The biofilms were grown in RPMI, in 9 cm Petri dishes covered in Parafilm, for 6 h at 37°C (Fourie *et al.*, 2021). Under these conditions, 653 *C. albicans* ORFs were significantly upregulated and 264 significantly downregulated at a $\log_2$ fold change threshold of ≥1, in response to the presence of *P. aeruginosa* (Fourie *et al.*, 2021). In contrast to the present study, the experimental set-up did not include a distinct adhesion phase and also promoted anaerobic growth. This may explain why the transcriptional changes observed in the study were dominated by responses to hypoxia and stress (Fourie *et al.*, 2021). Despite the

differences in experimental set-up, a more detailed comparison of the data against the findings of the present study may be insightful.

4.3.3 Conclusions

In dual-species *P. aeruginosa–C. albicans* biofilms, *P. aeruginosa* cells respond by upregulating genes associated with quorum sensing, including biosynthesis of PQS, phenazines and pyoverdine. This indicates that the bacterial cells are responding to limited oxygen and iron availability. Meanwhile, *C. albicans* cells respond by downregulating genes associated with ribosomes and translation, whilst upregulating genes associated with peroxisomal activity and arginine biosynthesis. This suggests that fungal cells are responding to oxidative stress. Hyphal formation is inhibited in dual-species *C. albicans* biofilm cells, as is ergosterol biosynthesis, thus indicating a major impact on fungal morphology and membrane integrity.

Treatment of biofilms with 5 μg/mL meropenem has no effect on *C. albicans* cells. Meanwhile, *P. aeruginosa* biofilm cells respond to the antibiotic by upregulating transcription of the chromosomally-encoded ß-lactamase gene, as well as genes associated with cell division and pyochelin biosynthesis. This suggests a link between iron availability and meropenem activity. Furthermore, there is upregulation of genes associated with biofilm production, including Las, Psl and T6SS genes, indicating enhanced biofilm extracellular matrix production as a tolerance mechanism against meropenem treatment. When dual-species biofilms are treated with meropenem, *P. aeruginosa* responds by upregulating even more genes encoding extracellular matrix components, including Psl and alginate.

In summary, the transcriptional responses observed in dual-species biofilms suggest that interaction with *C. albicans* may augment the *P. aeruginosa* response to meropenem treatment, by upregulating transcription of additional biofilm exopolysaccharide genes.

5 *PSEUDOMONAS AERUGINOSA* POTENTIATES AMPHOTERICIN B ACTIVITY AGAINST *CANDIDA ALBICANS* IN A DUAL-SPECIES BIOFILM

Parts of this chapter have been previously published:

Alam, F., Catlow, D., Di Maio, A., Blair, J. M. A. and Hall, R. A. (2020) '*Candida albicans* enhances meropenem tolerance of *Pseudomonas aeruginosa* in a dual-species biofilm', *J Antimicrob Chemother*, 75(4), pp. 925–935.

5.1 INTRODUCTION

The ability of *Candida* species to form biofilms has severe clinical implications. In a study of candidaemia patients at a hospital in Hungary, *Candida* isolates that were intermediate- or high-level biofilm producers, based on biomass and metabolic activity, were associated with a 61% increase in mortality (Vitális *et al.*, 2020). Among *Candida* isolates originating from fatal infections, 85% of *C. albicans* isolates were intermediate- or high-level biofilm producers, while all *C. tropicalis*, *C. parapsilosis* and *C. glabrata* isolates showed this phenotype (Vitális *et al.*, 2020). The entry of *Candida* cells into the bloodstream is frequently due to implanted medical devices, on which biofilms readily form; in fact, 70–80% of cases of candidemia are associated with central venous catheters (Rodrigues *et al.*, 2019). The ineffectiveness of azoles against *Candida* biofilms means that, if biofilm formation is suspected on a medical device, removal of the medical device is a more viable option than antifungal treatment, despite the invasiveness of the procedure (Lohse *et al.*, 2018).

The mechanisms by which *C. albicans* biofilm cells exhibit increased resistance to antifungal drugs, relative to planktonic cells, is an active field of research. Resistance mechanisms in *C. albicans* biofilms include upregulation of efflux pump genes, drug sequestration by matrix polymers, and development of persister cells (Lohse *et al.*, 2018). More recently, it has been shown that extracellular vesicles (EVs) produced by *C. albicans* biofilm cells are different to those produced by planktonic cells, and are involved in transporting biofilm extracellular matrix material and enhancing fluconazole resistance of *C. albicans* biofilms (Zarnowski *et al.*, 2018). Furthermore, *C. albicans* cellular morphogenesis is linked with antifungal susceptibility; enhanced hyphal

formation, which is seen in the biofilm mode of growth, is associated with increased tolerance to antifungal treatment (Sharma *et al.*, 2019).

It is already known that single-species *C. albicans* biofilms are highly resistant to fluconazole, which is the most commonly used antifungal drug for treating *Candida* infections (Lohse *et al.*, 2018). In a study aiming to establish biofilm inhibitory concentrations of antifungals, *C. albicans* biofilms were completely resistant to the highest fluconazole concentration tested (1,024 μg/mL) (Uppuluri *et al.*, 2011). This is considerably greater than the fluconazole MIC for planktonic *C. albicans* cells (4 μg/mL) (EuCAST, 2020b). *C. albicans* biofilm resistance to azoles is mainly attributed to the overexpression of efflux pumps (Pereira *et al.*, 2020), but can also be due to drug interactions with matrix polysaccharides, or the upregulation of genes in the ergosterol biosynthesis pathway (Silva *et al.*, 2017).

The increase in inhibitory concentrations of amphotericin B (AmB) between planktonic and biofilm *C. albicans* cells is not as dramatic as for fluconazole. The AmB MIC for planktonic *C. albicans* cells is 1 μg/mL (EuCAST, 2020b), increasing to 4 μg/mL for >50% inhibition of biofilm cells, and 16 μg/mL for >80% biofilm inhibition (Uppuluri *et al.*, 2011). The standard treatment for systemic mycoses originally involved a daily dose of 50 mg AmB, administered as 0.6–1.0 mg/kg given intravenously over 4–6 hours, resulting in a maximum serum concentration of 2.01 μg/mL (Fields Jr. *et al.*, 1970). The method of AmB administration has changed over recent years, due to infusion-related adverse events, such as deterioration of renal function (Bellmann and Smuszkiewicz, 2017). For the AmB deoxycholate formulation, a 1 mg test dose is first given to identify intolerant patients, in whom the severity of infusion-related adverse

events is too great. For AmB-tolerant patients, 0.25–0.3 mg/kg is administered once daily, later increasing to the maintenance dose of 0.6–1.0 mg/kg (or up to 1.5 mg/kg per day for highly resistant fungi) (Bellmann and Smuszkiewicz, 2017). Following these standard doses of AmB, the peak serum concentration is 1.7–2.8 μg/mL (Bellmann and Smuszkiewicz, 2017). In patients treated for invasive pulmonary mycoses, the concentration of AmB found in the lung epithelial lining fluid is 1.29 ±0.71 μg/mL for the AmB lipid complex formulation, and 1.60 ±0.58 μg/mL for liposomal AmB (Weiler *et al.*, 2009). Although resistance to amphotericin B treatment remains a rare occurrence in clinical settings, its relatively high cost and potential nephrotoxicity mean that it remains a second-line treatment for fungal infections (Pereira *et al.*, 2020).

A complicating factor for the treatment of *C. albicans* biofilm infections is that biofilms are often made up of multiple infecting species, the interactions between which can impact the effectiveness of antimicrobial treatment (Ponde *et al.*, 2021). Altered antifungal tolerance has been observed in dual-species biofilms of *C. albicans* and *Cutibacterium acnes*, which both contribute to infections on the surfaces of prosthetic joints (Bernard *et al.*, 2018). *C. acnes* adheres to both yeast and hyphal forms of *C. albicans*, but does not affect fungal viability (Bernard *et al.*, 2018). Single-species *C. albicans* biofilms show 70–90% fungal mortality when treated with micafungin, whereas the presence of *C. acnes* in a dual-species biofilm protects *C. albicans* cells from the action of micafungin, reducing fungal mortality to 35–40% (Bernard *et al.*, 2018). Another biofilm interaction commonly found on medical devices is between *C. albicans* and *Staphylococcus epidermidis*, particularly in catheter-associated infections (Adam *et al.*, 2002). In an *in vitro* catheter disk model of dual-species biofilm infection, extracellular polymers, produced by the *S. epidermidis* RP62A strain, inhibit

penetration of fluconazole through the biofilm matrix, enhancing fluconazole tolerance of the *C. albicans* biofilm cells (Adam *et al.*, 2002).

In the oral cavity, *C. albicans* interacts with *Streptococcus mutans*, forming biofilms that can lead to tooth decay in children (Kim *et al.*, 2018). *S. mutans* secretes an exoenzyme, GtfB, which binds to mannans on the *C. albicans* cell surface and catalyses the production of bacterial α-glucans, which reinforce the structure of the dual-species biofilm extracellular matrix (Hwang *et al.*, 2017). These *S. mutans* α-glucans have been shown to impede the diffusion of fluconazole, thus enhancing the fluconazole tolerance of *C. albicans* cells within the dual-species biofilm (Kim *et al.*, 2018). Another Gram-positive bacterial species that interacts with *C. albicans* is *Staphylococcus aureus*, causing co-infections of burn wounds, indwelling medical devices, and the CF lung (Kean *et al.*, 2017). *S. aureus* cells tightly attach to the hyphae of *C. albicans* biofilm cells, aided by extracellular DNA within the biofilm matrix; this enhances the biofilm-forming ability of the *S. aureus* cells, whilst also enhancing the tolerance of *C. albicans* to miconazole (Kean *et al.*, 2017).

As discussed in previous chapters, the physical and chemical interactions between *C. albicans* and *P. aeruginosa* are widely researched. This includes some research on the impact of this dual-species interaction on antifungal susceptibility. In dual-species planktonic interactions, 8-fold higher concentrations of amphotericin B (AmB) are required to kill *C. albicans* cells, relative to single-species (Rodrigues *et al.*, 2017). However, in dual-species biofilms, AmB (1 mg/L) has no effect on fungal viability when used as a monotherapy. Conversely, combination treatment of AmB + polymyxin B (PolyB) has a synergistic effect against dual-species biofilm cells, but only when AmB

is combined with a very high concentration of PolyB (256 mg/L), which exceeds concentrations that are safe for clinical use (Rodrigues *et al.*, 2017). Therefore, effective eradication of dual-species biofilms using AmB–PolyB combination therapy is complicated by the toxic effects of the high drug concentrations that would be required.

Other research has focused on the effect of *P. aeruginosa* secreted molecules on the antifungal susceptibility of *C. albicans* cells. The *P. aeruginosa* quorum sensing molecule, *N*-3-oxo-dodecanoyl-L-homoserine (3O-C_{12}-HSL), enhances *C. albicans* tolerance to fluconazole by inducing upregulation of genes associated with efflux, oxidative stress and fungal cell membrane integrity, and inhibiting the upregulation of sterol biosynthesis (Bandara *et al.*, 2020b). This has led to the proposal of a fluconazole + 3O-C_{12}-HSL combination therapy, with a liposomal delivery system, as a method for enhancing the susceptibility of *C. albicans* biofilm infections to fluconazole treatment (Bandara *et al.*, 2020a).

The aim of the research presented in this chapter is to determine the effect of *P. aeruginosa* on the antifungal susceptibility of *C. albicans* biofilm cells.

5.2 RESULTS

5.2.1 *P. aeruginosa* significantly enhances *C. albicans* sensitivity to amphotericin B

To identify whether biofilm interactions between *C. albicans* and *P. aeruginosa* have any impact on antifungal resistance, mature (24 h) biofilms were treated for 18 h with fluconazole, which targets ergosterol biosynthesis (Sharma *et al.*, 2019), or with

amphotericin B (AmB), which targets ergosterol in the fungal cell membrane (Kamiński, 2014). *C. albicans* cells in dual-species biofilms showed similar levels of sensitivity to fluconazole as single-species biofilms at 250, 750 and 1,000 μg/mL, and a small increase in sensitivity to 500 μg/mL fluconazole (Figure 5.1a). These fluconazole concentrations far exceed those that would be used in a clinical setting, as *C. albicans* biofilms cells can be as much as 4,000 times more resistant to fluconazole than planktonic cells (Ramage *et al.*, 2002). Therefore, *P. aeruginosa* does not increase the antifungal activity of fluconazole under the tested conditions. However, *C. albicans* cells in dual-species biofilms showed significantly enhanced sensitivity to AmB at all concentrations tested (0.5–8 μg/mL), with zero recovery of *C. albicans* cells from dual-species biofilms treated with ≥2 μg/mL AmB (Figure 5.1b). Therefore, *P. aeruginosa* enhances *C. albicans* sensitivity to AmB in a dual-species biofilm.

The lowest AmB concentration at which no *C. albicans* cells were recovered from dual-species biofilms was 2 μg/mL, which is within the range of concentrations found in pulmonary epithelial cells, and in serum, following clinical AmB doses (Fields Jr. *et al.*, 1970, Bellmann and Smuszkiewicz, 2017, Weiler *et al.*, 2009). Therefore, this AmB concentration was the focus of the remainder of this study.

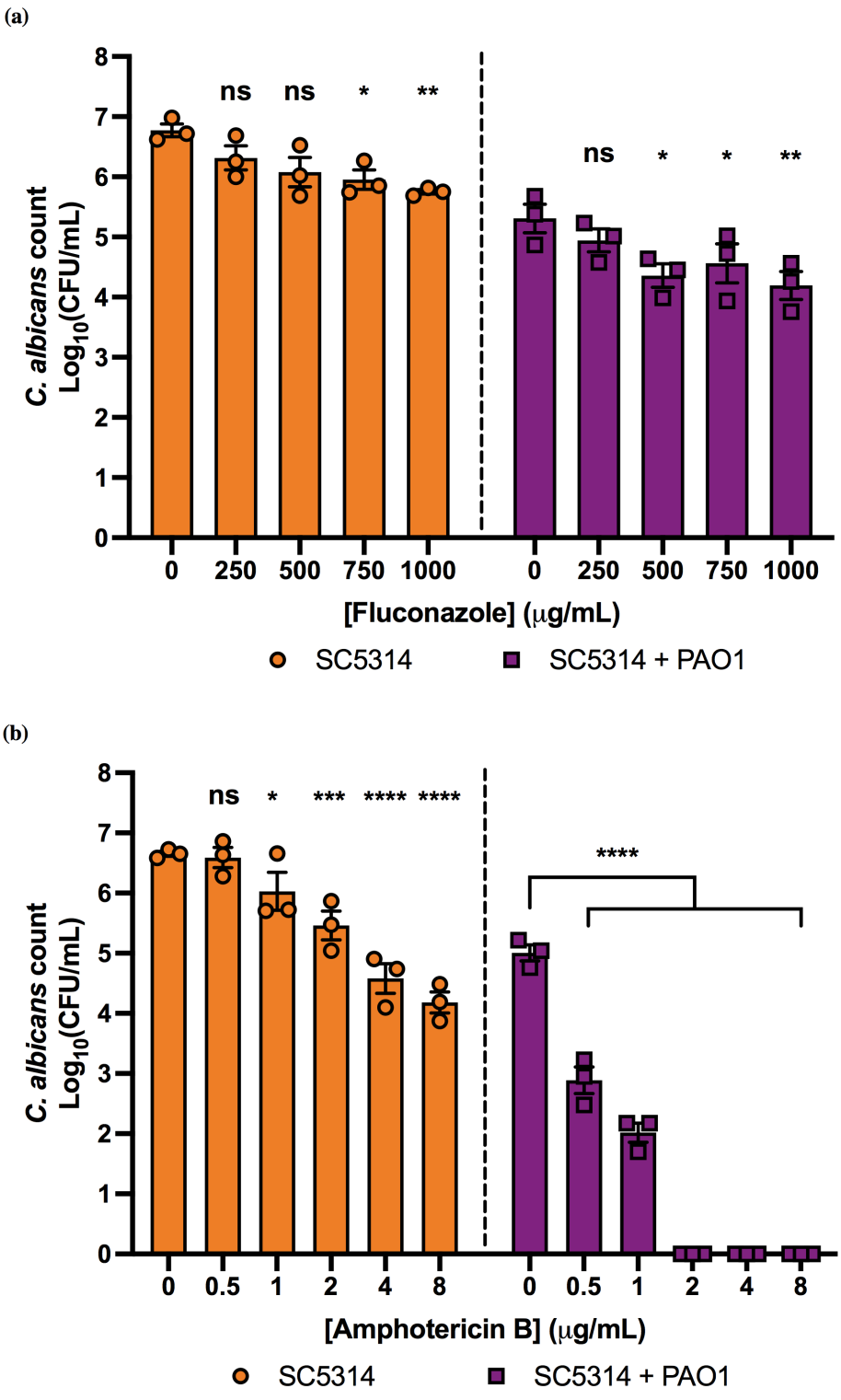


Figure 5.1. *P. aeruginosa* greatly enhances *C. albicans* sensitivity to amphotericin B, but has no effect on sensitivity to fluconazole. Preformed 24 h biofilms were incubated in Mueller Hinton broth containing **(a)** 0, 250, 500, 750 or 1000 μg/mL fluconazole, or **(b)** 0, 0.5, 1, 2, 4 or 8 μg/mL amphotericin B, for 18 h. Data are the $\log_{10}$(mean) ± the SEM from 3 biological replicates. Data were analysed using 2-way ANOVA and Holm-Sidak's multiple comparisons test (ns not significant; * $P < 0.05$; ** $P < 0.01$; *** $P < 0.001$; **** $P < 0.0001$).

5.2.2 The presence of *P. aeruginosa* enhances amphotericin B sensitivity to a greater extent than lower *C. albicans* starting concentrations

The numbers of *C. albicans* cells recovered from dual-species biofilms, in the absence of AmB treatment, were consistently lower than from single-species biofilms, by approximately 1.5 $\log_{10}$ CFU/mL (Figure 5.1). Therefore, it was important to determine whether AmB treatment is sufficient to eliminate *C. albicans* biofilm cells in a single-species biofilm, or whether this is only observed in dual-species biofilms. To test this, single-species *C. albicans* biofilms were grown from a range of starting concentrations (10^6, 10^5, 10^4, 10^3 and 10^2 cells/mL), alongside a standard dual-species biofilm for comparison. The mature (24 h) biofilms were treated with 2 µg/mL AmB for 18 h, and *C. albicans* survival was quantified by viable counts. As observed before, untreated dual-species biofilms showed a ~1.5 $\log_{10}$ drop in *C. albicans* recovery compared to single-species biofilms (Figure 5.2). Furthermore, there was zero recovery of *C. albicans* cells from dual-species biofilms treated with 2 µg/mL AmB, confirming the previously observed phenotype (Figure 5.2). Similar numbers of *C. albicans* cells (~7 $\log_{10}$ CFU/mL) were recovered from untreated single-species biofilms, regardless of the starting cell concentration (Figure 5.2). This indicates that the limiting factor for maximal growth of single-species *C. albicans* biofilms was either media nutrient levels or physical space. However, even with the lowest *C. albicans* starting concentration tested (10^2 cells/mL), treatment with 2 µg/mL AmB for 18 h was insufficient to eliminate *C. albicans* biofilm cells in single-species biofilms (Figure 5.2). This confirms that the enhanced AmB sensitivity of *C. albicans* cells within dual-species biofilms is dependent upon interactions with *P. aeruginosa*.

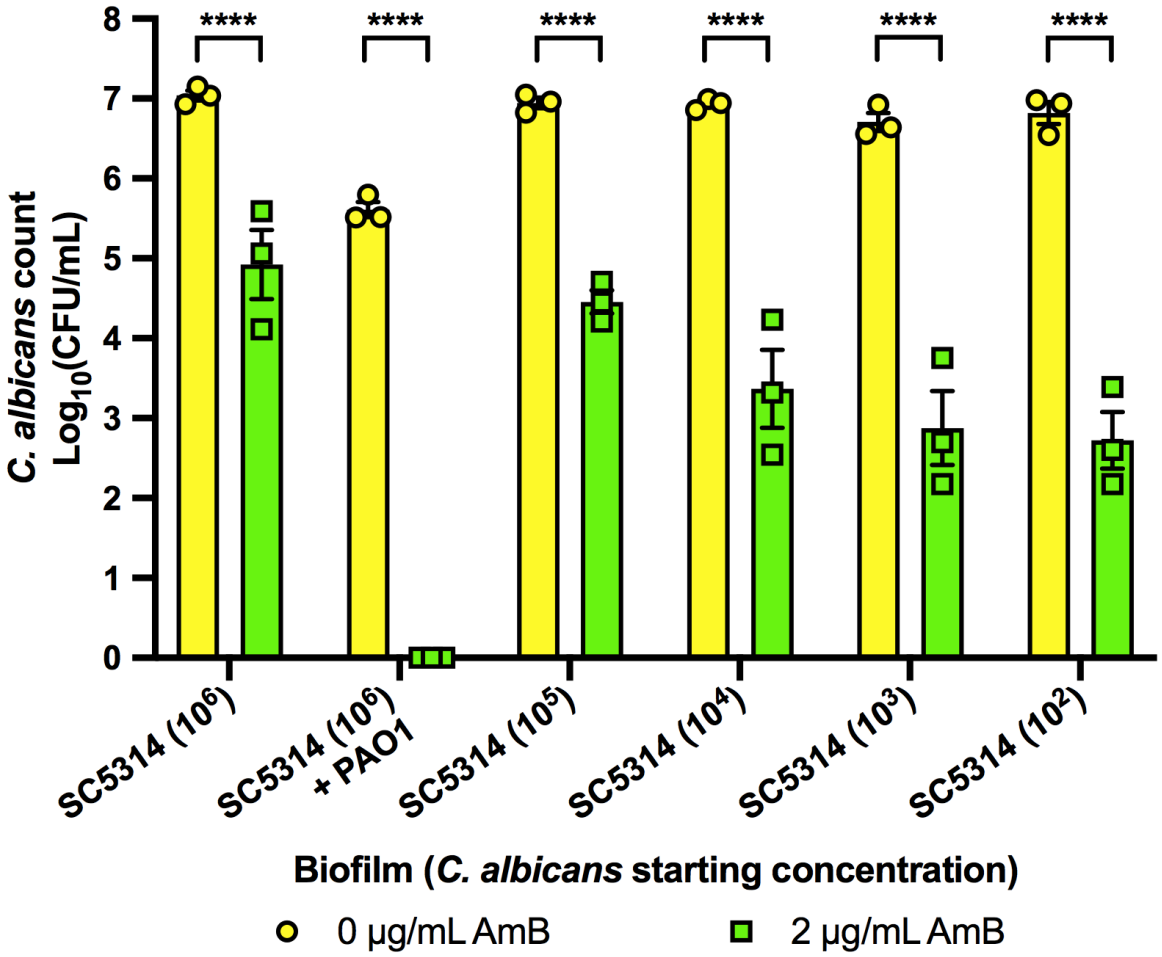


Figure 5.2. The presence of *P. aeruginosa* enhances amphotericin B sensitivity to a greater extent than lower *C. albicans* starting concentrations. Mono-species *C. albicans* biofilms were grown from starting concentrations of 10^6, 10^5, 10^4, 10^3 and 10^2 cells/mL and dual-species biofilms from a starting *C. albicans* concentration of 10^6 cells/mL. At 24 h, biofilms were incubated in Mueller Hinton broth containing 0 or 2 µg/mL amphotericin B (AmB), for 18 h. Data are the $\log_{10}$(mean) ± the SEM from 3 biological replicates. Data were analysed using 2-way ANOVA and Holm-Sidak's multiple comparisons test (**** $P < 0.0001$).

5.2.3 Purified *P. aeruginosa* rhamnolipids do not enhance *C. albicans* sensitivity to amphotericin B

Towards investigating the mechanism by which *P. aeruginosa* enhances AmB efficacy against *C. albicans*, the initial focus was on molecules that are upregulated in *P. aeruginosa* biofilms, and which have known anti-biofilm properties, namely rhamnolipids (Davey *et al.*, 2003). *P. aeruginosa* rhamnolipids can disrupt the cell

membrane of *S. aureus* cells in dual-species biofilms, resulting in increased efficacy of tobramycin against *S. aureus* (Radlinski *et al.*, 2017). Addition of purified *P. aeruginosa* single- and di-rhamnolipids resulted in an 8-fold decrease in the MIC of tobramycin against *S. aureus* biofilm cells (Radlinski *et al.*, 2017). In another study, *P. aeruginosa*-derived rhamnolipids were shown to disrupt mature bacterial biofilms; following incubation with 120–2000 μg/mL rhamnolipid, *S. aureus* biofilms were reduced by 68–89% and *S. epidermidis* biofilms were reduced by 44–96% (Ceresa *et al.*, 2019). As well as bacterial biofilms, *P. aeruginosa* rhamnolipids can also disrupt *C. albicans* biofilms (Singh *et al.*, 2013). In a study of *C. albicans* biofilms grown on polystyrene surfaces, 160 μg/mL of *P. aeruginosa* di-rhamnolipid removed 50% of *C. albicans* cells following 2 h of treatment (Singh *et al.*, 2013). Increasing the concentration of di-rhamnolipid to 5,000 μg/mL resulted in the removal of up to 90% of *C. albicans* biofilm cells (Singh *et al.*, 2013).

To test whether *P. aeruginosa* rhamnolipids play a role in the observed increase in *C. albicans* sensitivity to AmB, purified *P. aeruginosa* rhamnolipids were added to single-species *C. albicans* biofilms. The rhamnolipid mixture used was 90% pure and consisted of rhamnolipid molecules with varying fatty acid tail lengths. The rhamnolipid concentrations used were 1000 and 2000 μg/mL. These concentrations mimic rhamnolipid levels found in *P. aeruginosa* biofilms that have been exposed to neutrophils as part of the human innate immune response, such as in the CF lung (Alhede *et al.*, 2009). The mature (24 h) biofilms were treated with 2 μg/mL AmB for 18 h, and *C. albicans* survival was quantified by viable counts. The presence of purified *P. aeruginosa* rhamnolipids did not enhance *C. albicans* sensitivity to AmB, neither when added during biofilm formation (0 h) nor when added to mature biofilms (24 h)

(Figure 5.3). This suggests that rhamnolipids are unlikely to be involved in the mechanism by which *P. aeruginosa* enhances *C. albicans* sensitivity to AmB.

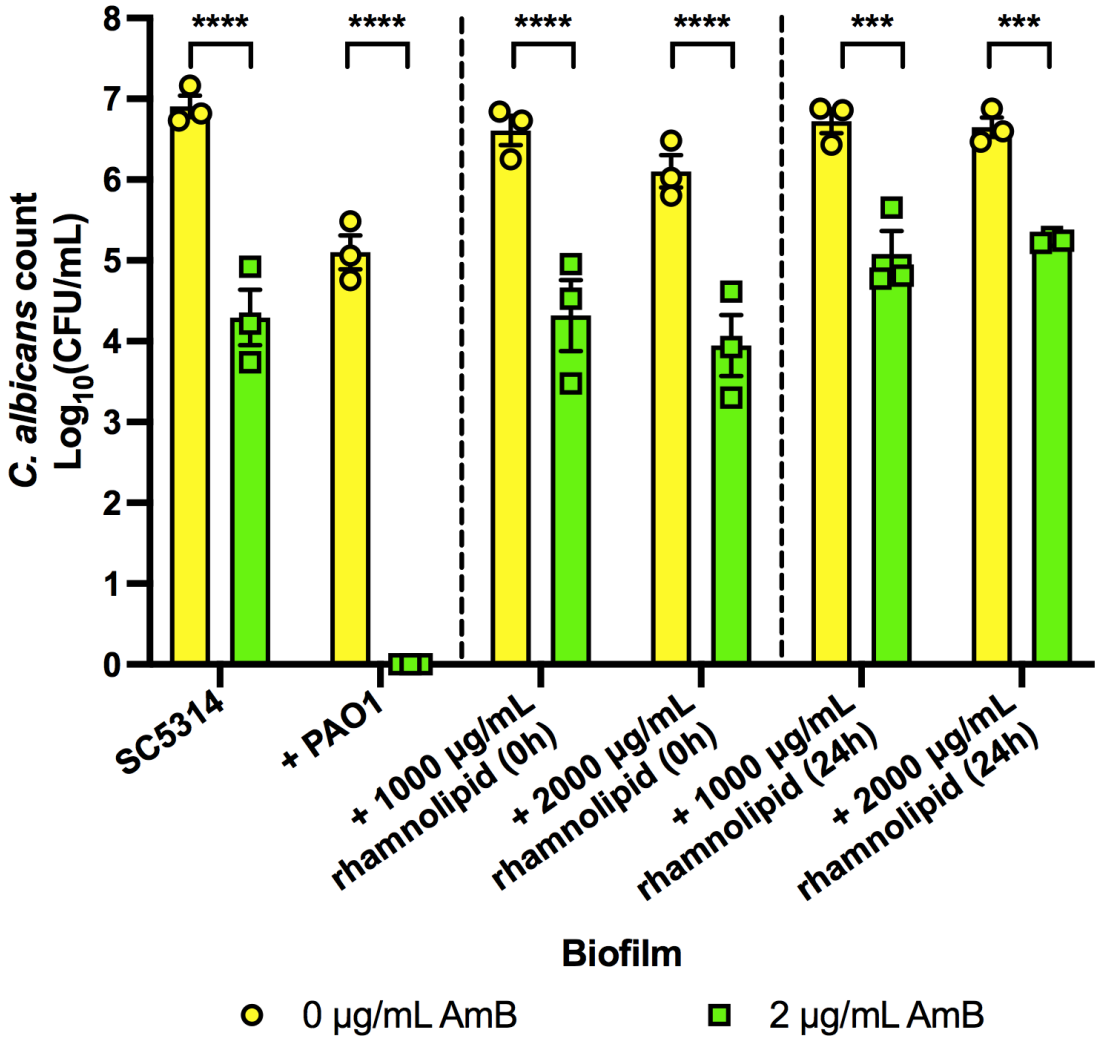


Figure 5.3. Purified *P. aeruginosa* rhamnolipids do not enhance *C. albicans* sensitivity to amphotericin B. Mono-species *C. albicans* biofilms were supplemented with 0, 1000 or 2000 µg/mL rhamnolipid, either during biofilm formation (0 h) or following biofilm maturation (24 h). At 24 h, mono- and dual-species biofilms were incubated in Mueller Hinton broth containing 0 or 2 µg/mL amphotericin B (AmB), for 18 h. Data are the $\log_{10}$(mean) ± the SEM from 3 biological replicates. Data were analysed using 2-way ANOVA and Holm-Sidak's multiple comparisons test (*** $P < 0.001$; **** $P < 0.0001$).

5.2.4 Increased *C. albicans* sensitivity to amphotericin B occurs more quickly in the presence of *P. aeruginosa* PAO1 than other *P. aeruginosa* strains

To determine whether other *P. aeruginosa* strains were able to enhance *C. albicans* sensitivity to AmB, dual-species *C. albicans* biofilms were grown in the presence of other *P. aeruginosa* laboratory strains and clinical isolates. The laboratory strains tested were two PA14 strains: PA14(1) (Rahme *et al.*, 1995) and PA14(2) (Liberati *et al.*, 2006). The clinical strains tested were two CF strains: the Midlands 1 strain (Scott and Pitt, 2004) and the Liverpool strain (Cheng *et al.*, 1996). In the absence of AmB treatment, recovery of *C. albicans* biofilm cells from dual-species biofilms was similar across all biofilms tested: ~5 $\log_{10}$ CFU/mL recovery (Figure 5.4a and b). When mature (24 h) biofilms were treated with 2 μg/mL AmB for 18 h, *C. albicans* cells in dual-species biofilms showed significantly enhanced sensitivity to AmB, in the presence of all *P. aeruginosa* strains tested; in all cases, there was zero recovery of *C. albicans* cells (Figure 5.4a).

Previous research has shown that AmB binds to fungal cells in a matter of minutes, and changes to cell ultrastructure can be observed after just 30 minutes' exposure to AmB (Grela *et al.*, 2019). This suggested that the biofilm assay could be shortened in duration, with the additional advantage of increasing the quantity of data that could be obtained within a fixed period of time. Therefore, the biofilm assay with the different *P. aeruginosa* strains was repeated, but the mature (24 h) biofilms were treated with 2 μg/mL AmB for a reduced incubation time of 2 h. After this, *C. albicans* survival was quantified by viable counts. Following 2 h AmB treatment, zero *C. albicans* cells were recovered from dual-species biofilms with *P. aeruginosa* PAO1 (Figure 5.4b). However, in the presence of all other *P. aeruginosa* strains tested, the reduction in

numbers of *C. albicans* biofilm cells recovered was similar to that observed for single-species biofilms: a reduction of 1.1–1.7 $\log_{10}$ CFU/mL (Figure 5.4b). This temporal difference suggests that the mechanism by which *P. aeruginosa* potentiates AmB activity against *C. albicans* may differ between *P. aeruginosa* strains. This may be due to differences in *P. aeruginosa* secreted metabolites that affect the dual-species interaction, as indicated by the varying hues of overnight cultures from these strains (Figure 5.4c).

Following the observation that a reduced AmB incubation time was sufficient to produce the phenotype of interest, the biofilm assay protocol was shortened so that biofilms were incubated with AmB for 2 h (rather than 18 h) in all subsequent experiments.

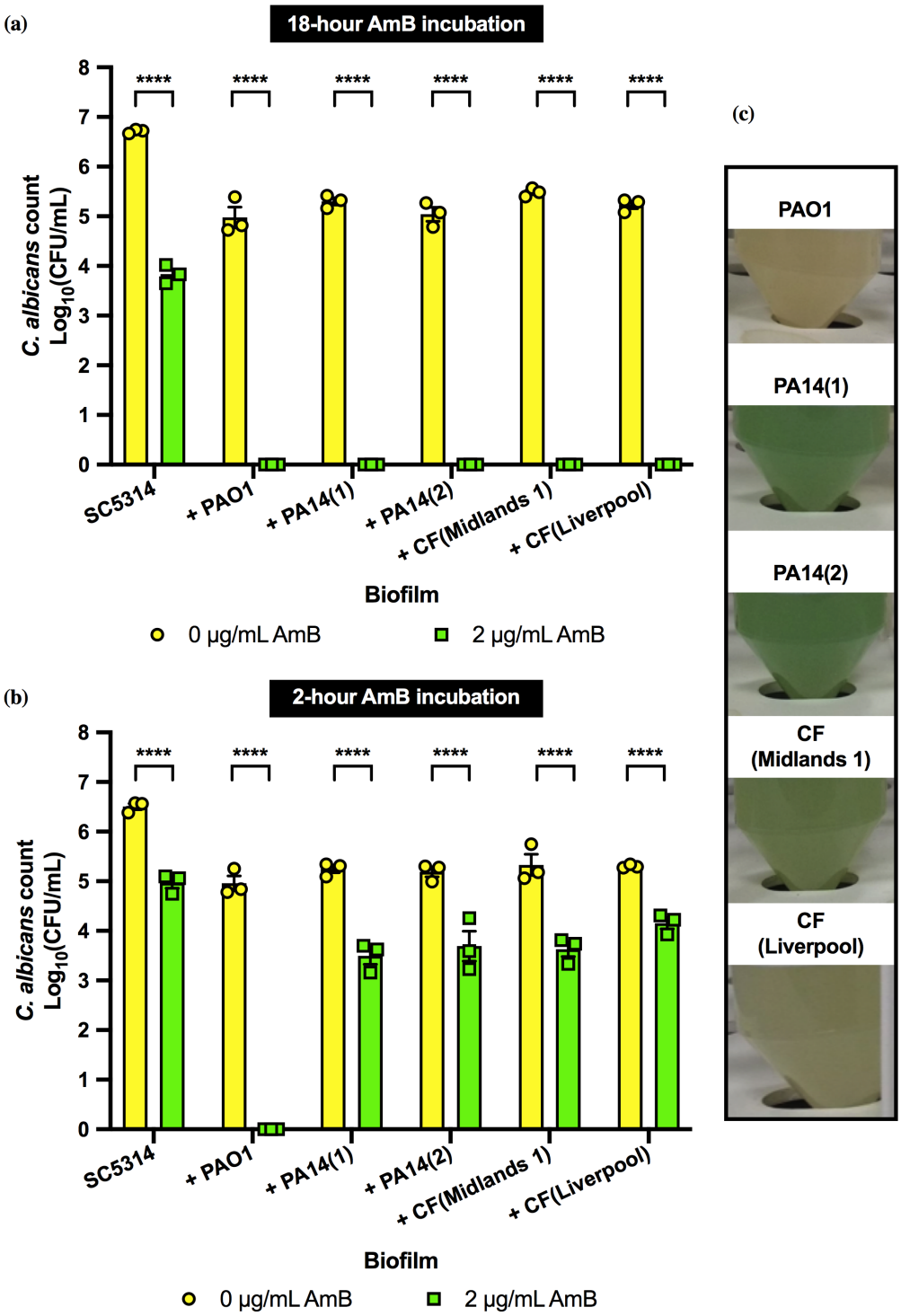


Figure 5.4. Increased *C. albicans* sensitivity to amphotericin B occurs more quickly in the presence of *P. aeruginosa* PAO1 than other *P. aeruginosa* strains. Preformed 24 h biofilms were incubated in Mueller Hinton broth containing 0 or 2 µg/mL amphotericin B (AmB) for **(a)** 18 hours, or **(b)** 2 hours. Data are the $\log_{10}$(mean) ± the SEM from 3 biological replicates. Data were analysed using 2-way ANOVA and Holm-Sidak's multiple comparisons test (**** $P < 0.0001$). **(c)** Overnight cultures of the *P. aeruginosa* strains used; differences in colour indicate differences in secreted metabolites between strains.

5.2.5 Potentiation of amphotericin B against *C. albicans* is specific to dual-species biofilms

To determine whether the observed potentiation of AmB activity against *C. albicans* was specific to biofilms, the susceptibility of *C. albicans* to AmB in the presence of *P. aeruginosa* was tested during planktonic growth. When single-species *C. albicans* planktonic cultures were treated with 2 µg/mL AmB, there was a ~3 $\log_{10}$ reduction in viability ($P < 0.0001$), whilst dual-species planktonic cultures showed a ~2 $\log_{10}$ reduction in *C. albicans* viability ($P < 0.001$) compared to untreated cultures (Figure 5.5). This suggests that there is no potentiation of AmB in dual-species planktonic cultures; the phenotype is biofilm-specific.

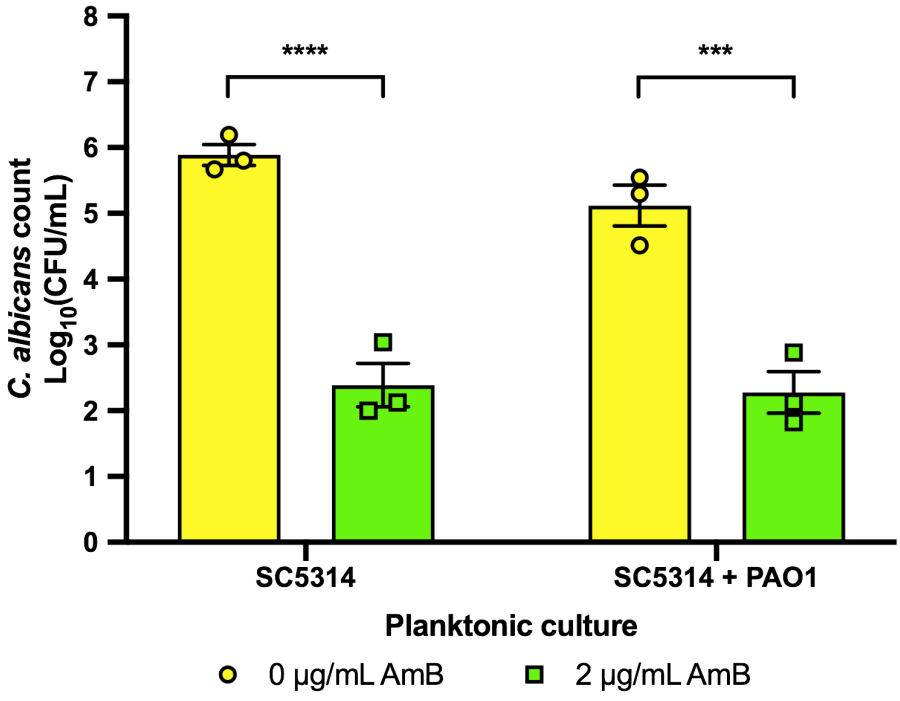


Figure 5.5. Potentiation of amphotericin B against *C. albicans* is specific to dual-species biofilms. Planktonic cultures were grown for 3 h and subsequently incubated in Mueller Hinton broth containing 0 or 2 µg/mL amphotericin B (AmB), for 2 h. Data are the $\log_{10}$(mean) ± the SEM from 3 biological replicates. Data were analysed using 2-way ANOVA and Holm-Sidak's multiple comparisons test (*** $P < 0.001$; **** $P < 0.0001$).

5.2.6 Potentiation of amphotericin B activity against *C. albicans* is dependent on *P. aeruginosa* viability

The molecules secreted by *P. aeruginosa* biofilm cells differ to those secreted by planktonic cells; for example, the polysaccharides alginate, Pel and Psl play major roles in providing structural stability to biofilms (Mann and Wozniak, 2012, Jennings *et al.*, 2015), but are not important for planktonic cells. To determine whether potentiation of AmB by *P. aeruginosa* is mediated by an active or passive mechanism, *C. albicans* biofilms were grown in the presence of either heat-killed *P. aeruginosa* (disrupts the bacterial cell wall, denatures proteins and causes cell lysis), or by fixing *P. aeruginosa* cells in 4% PFA (maintains cell structure). However, in the presence of heat-killed or PFA-fixed *P. aeruginosa*, there was no potentiation of AmB activity against *C. albicans* biofilm cells (Figure 5.6), suggesting that *P. aeruginosa* cells must be metabolically active to produce the effect.

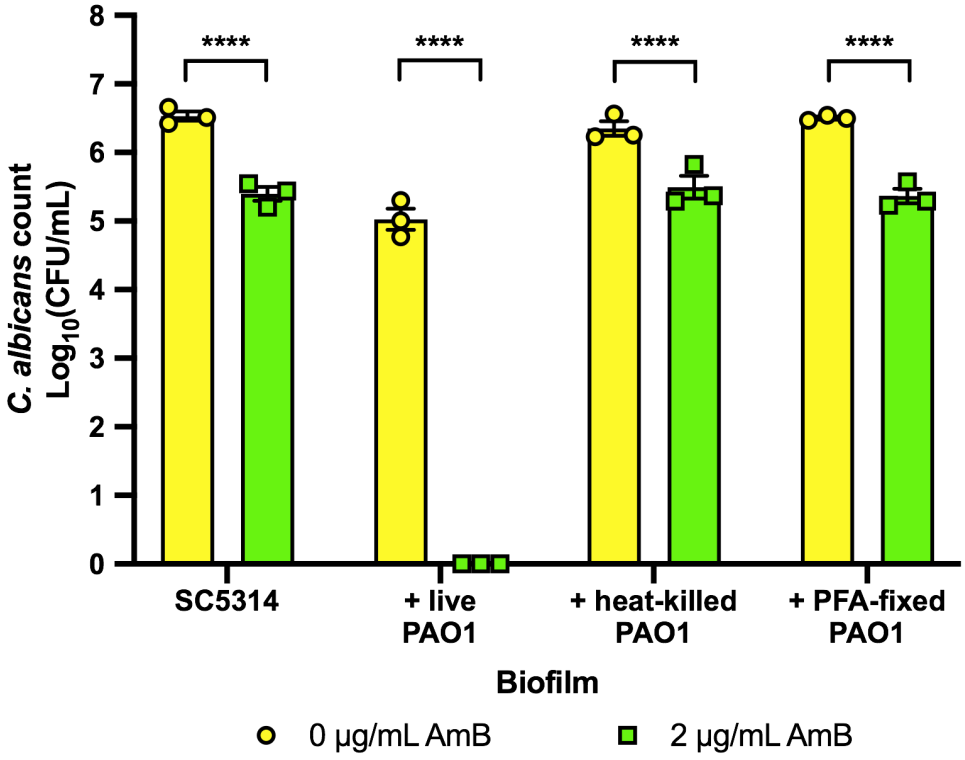


Figure 5.6. Potentiation of amphotericin B activity against *C. albicans* is dependent on *P. aeruginosa* viability. Preformed 24 h biofilms were incubated in Mueller Hinton broth containing 0 or 2 μg/mL amphotericin B (AmB), for 2 h. Data are the $\log_{10}$(mean) ± the SEM from 3 biological replicates. Data were analysed using 2-way ANOVA and Holm-Sidak's multiple comparisons test (**** $P < 0.0001$).

5.2.7 Supernatants from mature biofilms have no effect on amphotericin B efficacy against *C. albicans* biofilm cells

Having established that potentiation of AmB requires viable *P. aeruginosa* cells to be present in a dual-species biofilm with *C. albicans*, the next question was whether direct cell–cell contact was a prerequisite, or whether secreted metabolites from *P. aeruginosa* would be sufficient. To test this, supernatants were collected from mature (24 h) single- and dual-species biofilms, filter-sterilised and snap-frozen for storage prior to use. Single-species *C. albicans* biofilms were grown in media composed of a 50:50 ratio of Mueller Hinton broth and supernatant. However, none of the supernatants resulted in potentiation of AmB activity (Figure 5.7), suggesting that *P. aeruginosa* cells must be physically present in the biofilm.

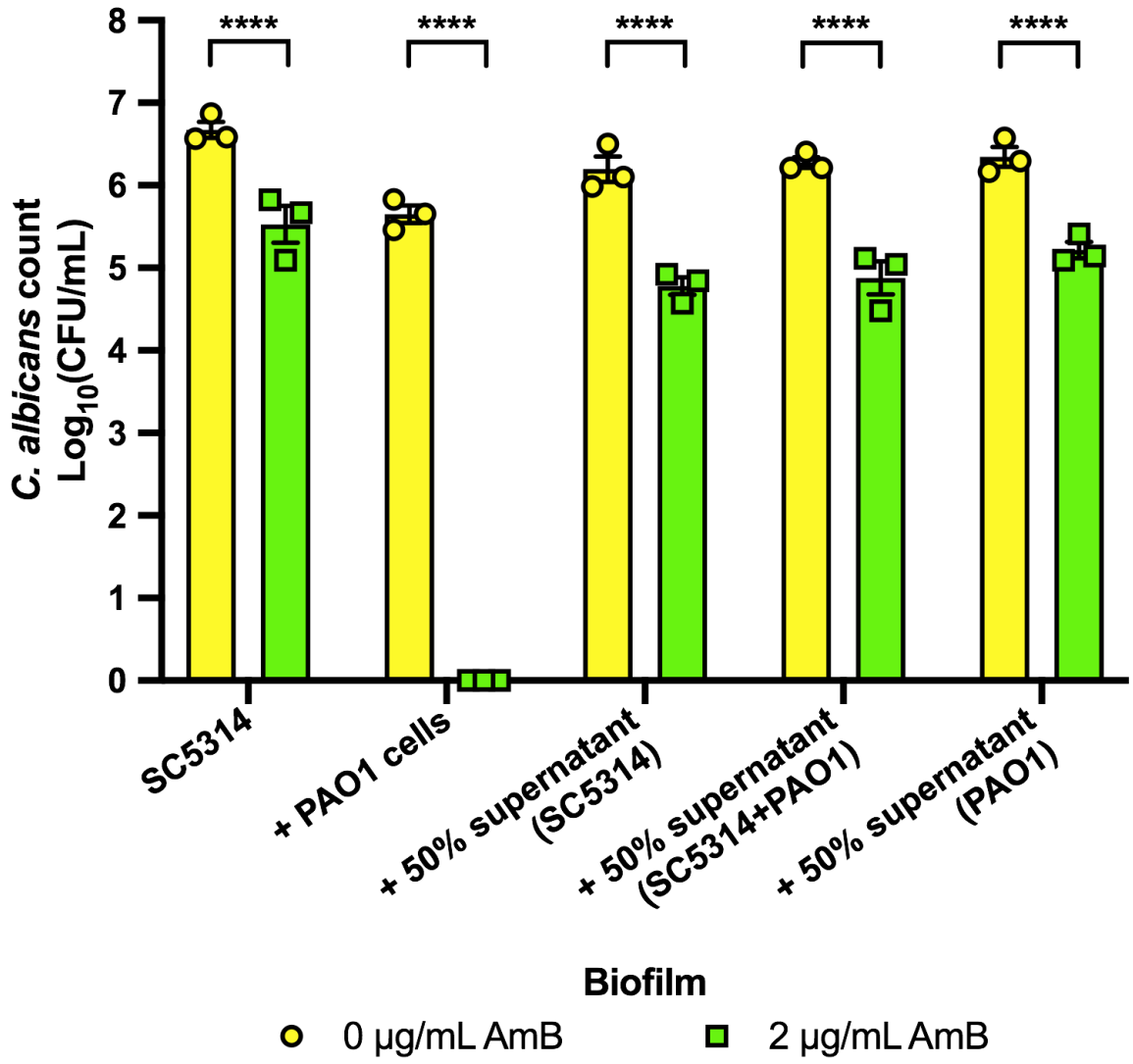


Figure 5.7. Supernatants from mature biofilms have no effect on amphotericin B efficacy against *C. albicans* biofilm cells. Supernatants were collected from 24 h biofilms and filter-sterilised. Mono- and dual-species control biofilms were incubated in Mueller Hinton broth. Mono-species biofilms were grown in 50:50 Mueller Hinton broth:supernatant for 24 h, after which media and supernatants were replenished and supplemented with 0 or 2 µg/mL amphotericin B (AmB), for 2 h. Data are the $\log_{10}$(mean) ± the SEM from 3 biological replicates. Data were analysed using 2-way ANOVA and Holm-Sidak's multiple comparisons test (**** $P < 0.0001$).

5.2.8 *C. albicans* sensitivity to amphotericin B is also enhanced by *E. coli* MG1655 in a dual-species biofilm

In the human host, *C. albicans* interacts with a range of bacterial species. These include: *E. coli* in the urinary tract and the gut, *A. baumannii* in ventilator-associated pneumonia, *B. cenocepacia* in the CF lung, *S. aureus* and *S. epidermidis* on skin (Lohse *et al.*, 2018), and *E. faecalis* and *E. faecium* in the gastrointestinal tract (Graham *et al.*, 2017). To investigate whether other clinically relevant bacteria affect *C. albicans* biofilm sensitivity to AmB, dual-species biofilms were grown with *E. coli*, *A. baumannii*, *B. cenocepacia*, *S. epidermidis*, *S. aureus*, *E. faecalis* and *E. faecium*. Mature (24 h) biofilms were treated with 2 μg/mL AmB for 2 h, and *C. albicans* survival was quantified by viable counts. Of the species tested, *E. coli* MG1655 enhanced *C. albicans* AmB sensitivity to a similar extent as *P. aeruginosa* PAO1 (Figure 5.8), with averages of 0, 50 and 250 *C. albicans* cells recovered from the three biological replicates of AmB-treated *C. albicans–E. coli* biofilms. This effect was not observed with the avirulent cloning strain *E. coli* DH5α, which had no effect on *C. albicans* AmB sensitivity (Figure 5.8). An increase in *C. albicans* sensitivity to AmB was also observed in the presence of *E. faecalis*, but *C. albicans* recovery never dropped as low as zero in these biofilms (Figure 5.8).

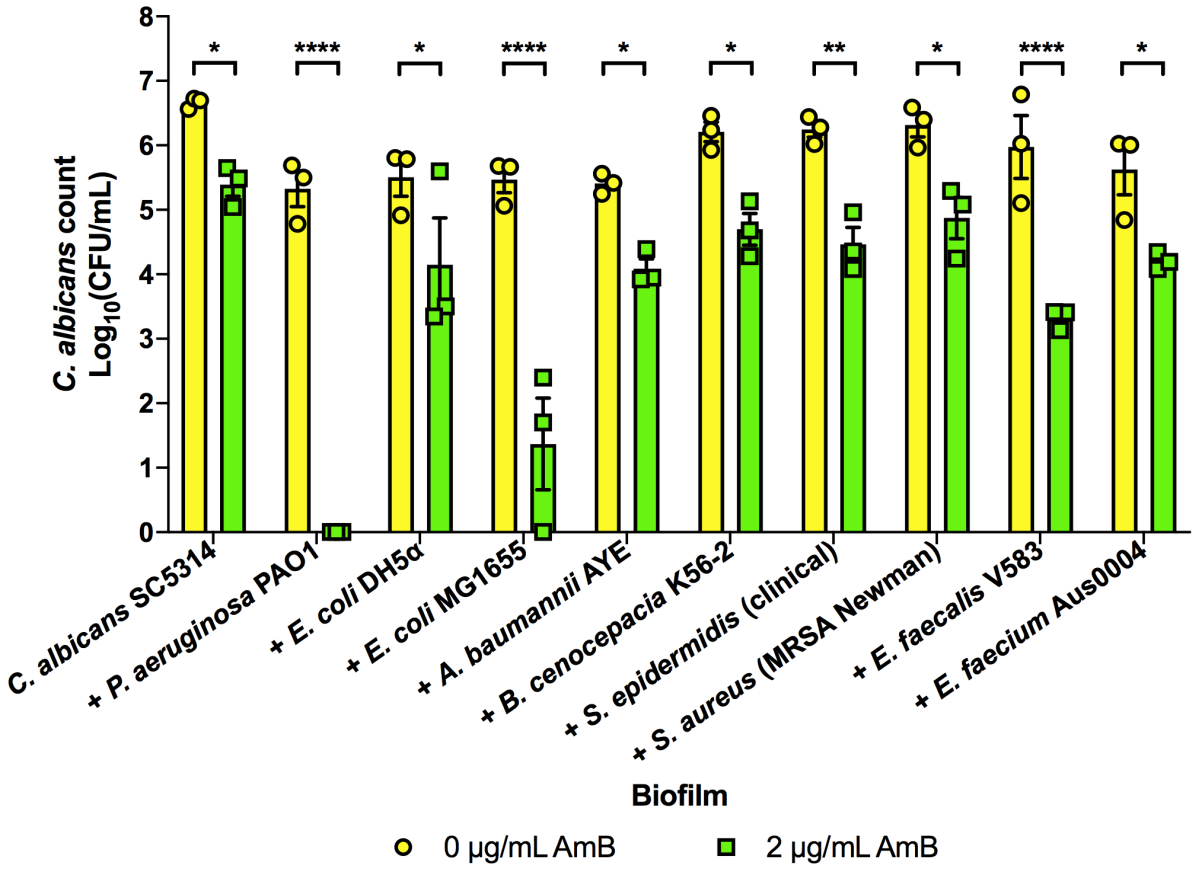


Figure 5.8. *C. albicans* sensitivity to amphotericin B is also enhanced by *E. coli* MG1655 in a dual-species biofilm. Preformed 24 h biofilms were incubated in Mueller Hinton broth containing 0 or 2 µg/mL amphotericin B (AmB) for 2 h. Data are the $\log_{10}$(mean) ± the SEM from 3 biological replicates. Data were analysed using 2-way ANOVA and Holm-Sidak's multiple comparisons test (* $P < 0.05$; ** $P < 0.01$; **** $P < 0.0001$).

5.2.9 *P. aeruginosa* PAO1 also increases *C. dubliniensis* sensitivity to amphotericin B in a dual-species biofilm

As discussed in Chapter 3, non-*albicans Candida* species of clinical relevance include *C. dubliniensis*, *C. tropicalis*, *C. parapsilosis*, *C. krusei* and *C. glabrata* (Whibley and Gaffen, 2015). To determine whether the presence of *P. aeruginosa* PAO1 can enhance the AmB sensitivity of other *Candida* species, single- and dual-species biofilms were grown and treated with 2 µg/mL AmB for 2 h. Like *C. albicans*, *C. dubliniensis* sensitivity to AmB was enhanced to such an extent that zero fungal cells were recovered from dual-species biofilms following 2 h of AmB treatment (Figure

5.9). The presence of *P. aeruginosa* resulted in no change in AmB sensitivity for *C. tropicalis*, *C. parapsilosis* or *C. krusei* (Figure 5.9), though *C. krusei* biofilms appeared resistant to 2 µg/mL AmB. In the case of *C. glabrata*, the presence of *P. aeruginosa* had the opposite effect, with a decrease in sensitivity to AmB (Figure 5.9). The differences in phenotype observed between these *Candida* species may be explained by differences in the structure and composition of their biofilms (Sharma *et al.*, 2019, Cavalheiro and Teixeira, 2018, Sardi *et al.*, 2013, Silva *et al.*, 2009).

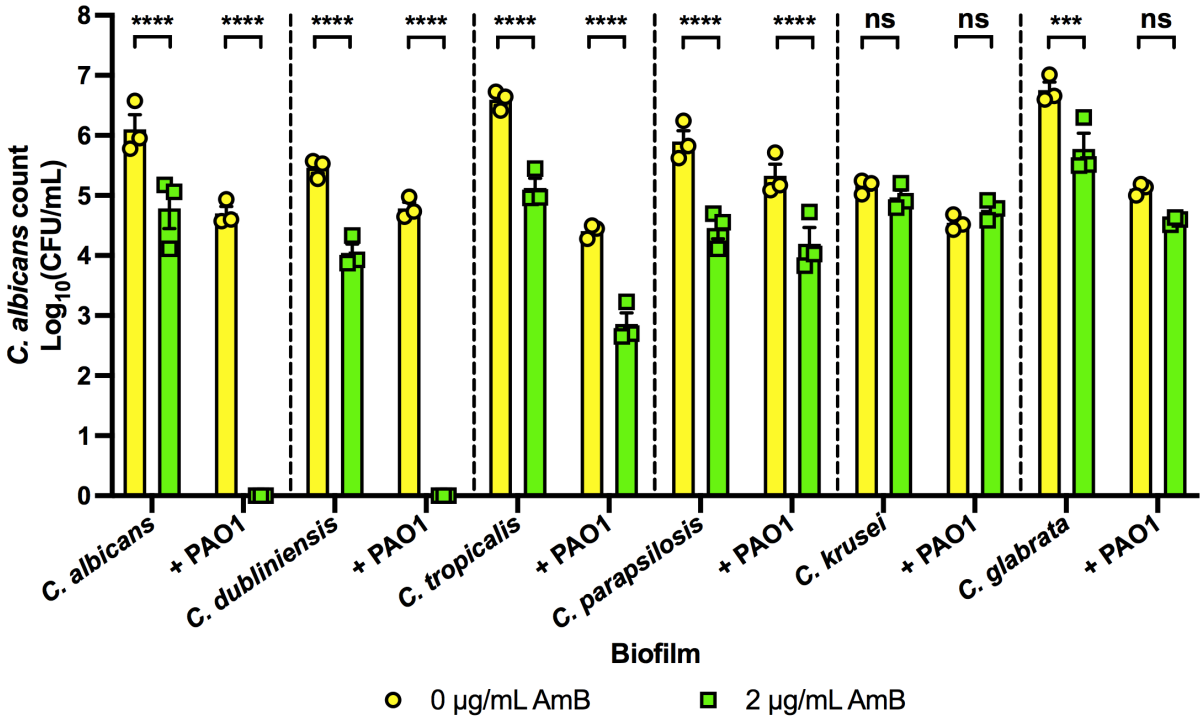


Figure 5.9. *P. aeruginosa* PAO1 also increases *C. dubliniensis* sensitivity to amphotericin B in a dual-species biofilm. Preformed 24 h biofilms were incubated in Mueller Hinton broth containing 0 or 2 µg/mL amphotericin B (AmB) for 2 h. Data are the $\log_{10}$(mean) ± the SEM from 3 biological replicates. Data were analysed using 2-way ANOVA and Holm-Sidak's multiple comparisons test (ns not significant; *** $P < 0.001$; **** $P < 0.0001$).

5.2.10 *P. aeruginosa* does not induce an increase in *C. albicans* membrane ergosterol

To understand the mechanism by which AmB activity is potentiated in dual-species biofilms, a logical focus for investigation was the AmB drug target, ergosterol. The hypothesis was that the presence of *P. aeruginosa* in the dual-species biofilm causes an increase in *C. albicans* membrane ergosterol levels, and this increase in levels of the drug target leads to increased AmB susceptibility. To test this hypothesis, dual-species biofilms were grown using a *C. albicans* strain with lower membrane ergosterol levels, to observe if the potentiation of AmB would be lost. Ergosterol is necessary for the structural integrity of fungal cell membranes (Rodrigues, 2018), so ergosterol-deficient cells would not be viable. Therefore, the strain used was a *upc2*Δ/Δ mutant in a *C. albicans* SN152 background. Upc2 is a transcription factor that binds to the promoter of *ERG2*, upregulating its expression (Silver *et al.*, 2004, MacPherson *et al.*, 2005); Erg2 is a key enzyme in the ergosterol biosynthesis pathway. Consequently, the *upc2*Δ/Δ strain produces lower levels of ergosterol in its cell membranes (Silver *et al.*, 2004). As with *C. albicans* SC5314, the *C. albicans* SN152 parental wild-type strain was much more sensitive to AmB in a dual-species biofilm, with zero recovery of fungal cells after 2 h of treatment with 2 μg/mL AmB (Figure 5.10). However, potentiation of AmB in dual-species biofilms was lost with the *upc2*Δ/Δ strain (Figure 5.10), suggesting that membrane ergosterol levels may be important in the mechanism.

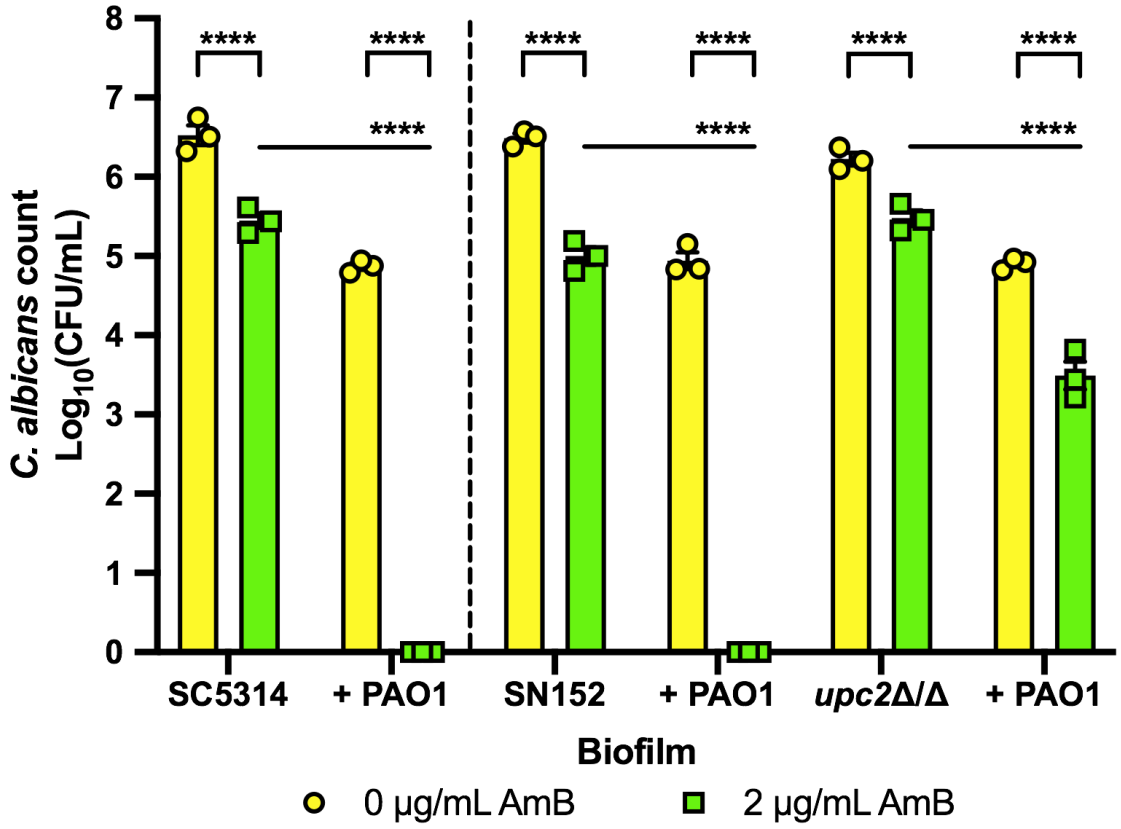


Figure 5.10. There is less potentiation of amphotericin B against *C. albicans upc2*Δ/Δ; a strain with lower membrane ergosterol levels. Preformed 24 h biofilms were incubated in Mueller Hinton broth containing 0 or 2 µg/mL amphotericin B (AmB) for 2 h. Data are the $\log_{10}$(mean) ± the SEM from 3 biological replicates. Data were analysed using 2-way ANOVA and Holm-Sidak's multiple comparisons test (**** $P < 0.0001$).

To visualise the biofilm cells, untreated samples from 24 h biofilms were stained with filipin, which binds to ergosterol, and analysed using fluorescence microscopy. *C. albicans* cells recovered from dual-species biofilms showed greatly reduced hyphal formation compared to single-species (Figure 5.11). However, quantification of filipin staining suggested that there was no significant difference in ergosterol levels between single- and dual-species biofilm cells (Figure 5.12). These data indicate that *P. aeruginosa* does not induce an increase in *C. albicans* membrane ergosterol levels in a dual-species biofilm. However, quantification of filipin staining suggested that the levels of ergosterol are similar between the parental control strain and the *upc2*Δ/Δ

mutant strain (Figure 5.12). This may indicate non-specific binding of filipin to lipids other than ergosterol; for example, sphingolipids are known to form complexes with ergosterol for lipid raft formation (Marek *et al.*, 2019), which may affect the binding specificity of filipin. Furthermore, filipin is known to bind to phospholipids and to derivatives of sterols (Smejkal *et al.*, 1996, Arthur *et al.*, 2011). Therefore, filipin staining may not directly correlate with ergosterol levels.

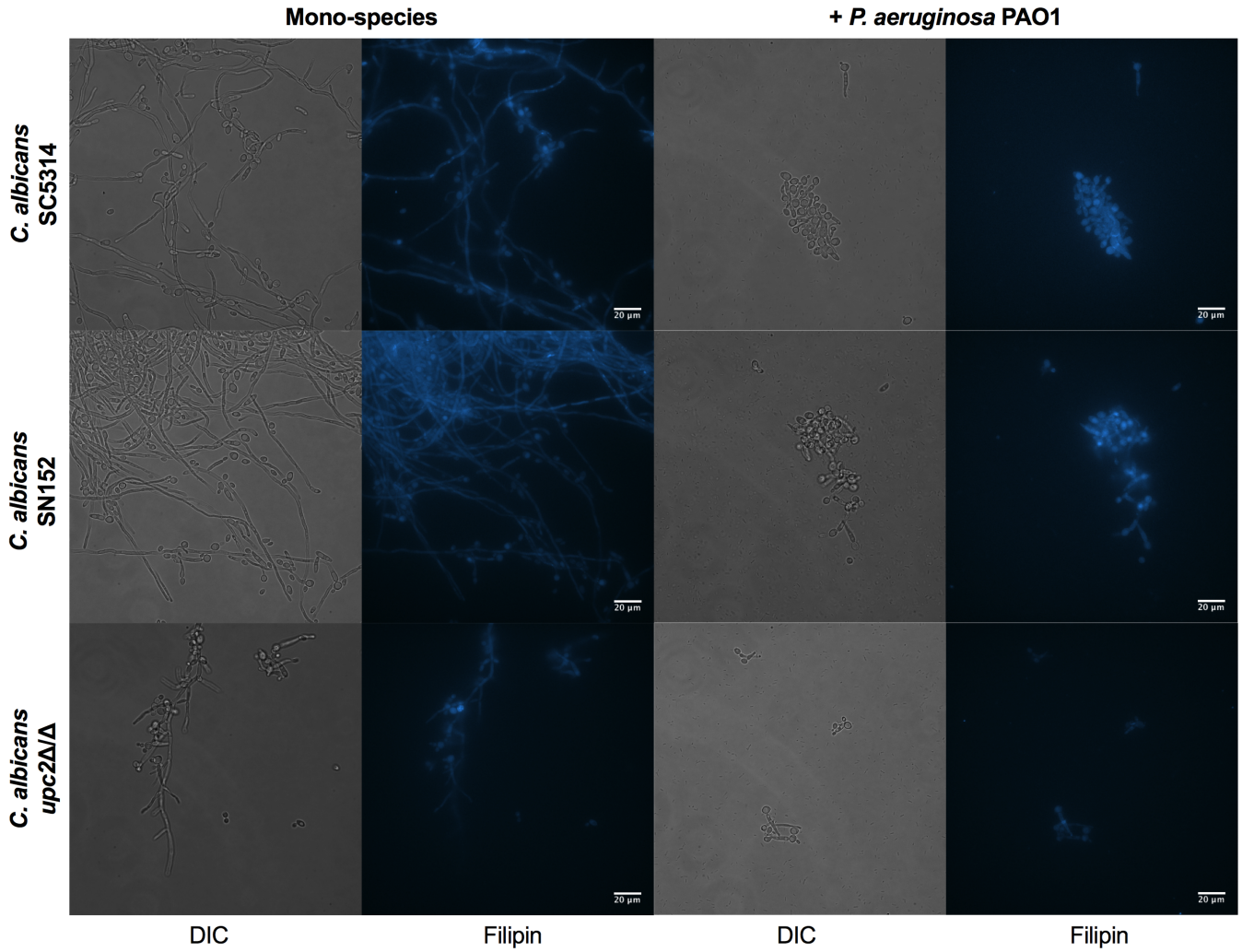


Figure 5.11. Fluorescence microscopy images of mono- and dual-species biofilms. Blue indicates filipin stain (ergosterol). Inhibition of *C. albicans* hyphae can clearly be seen in the presence of *P. aeruginosa* PAO1. Images are representative of data obtained from 3 biological replicates, with ~30 technical replicates each.

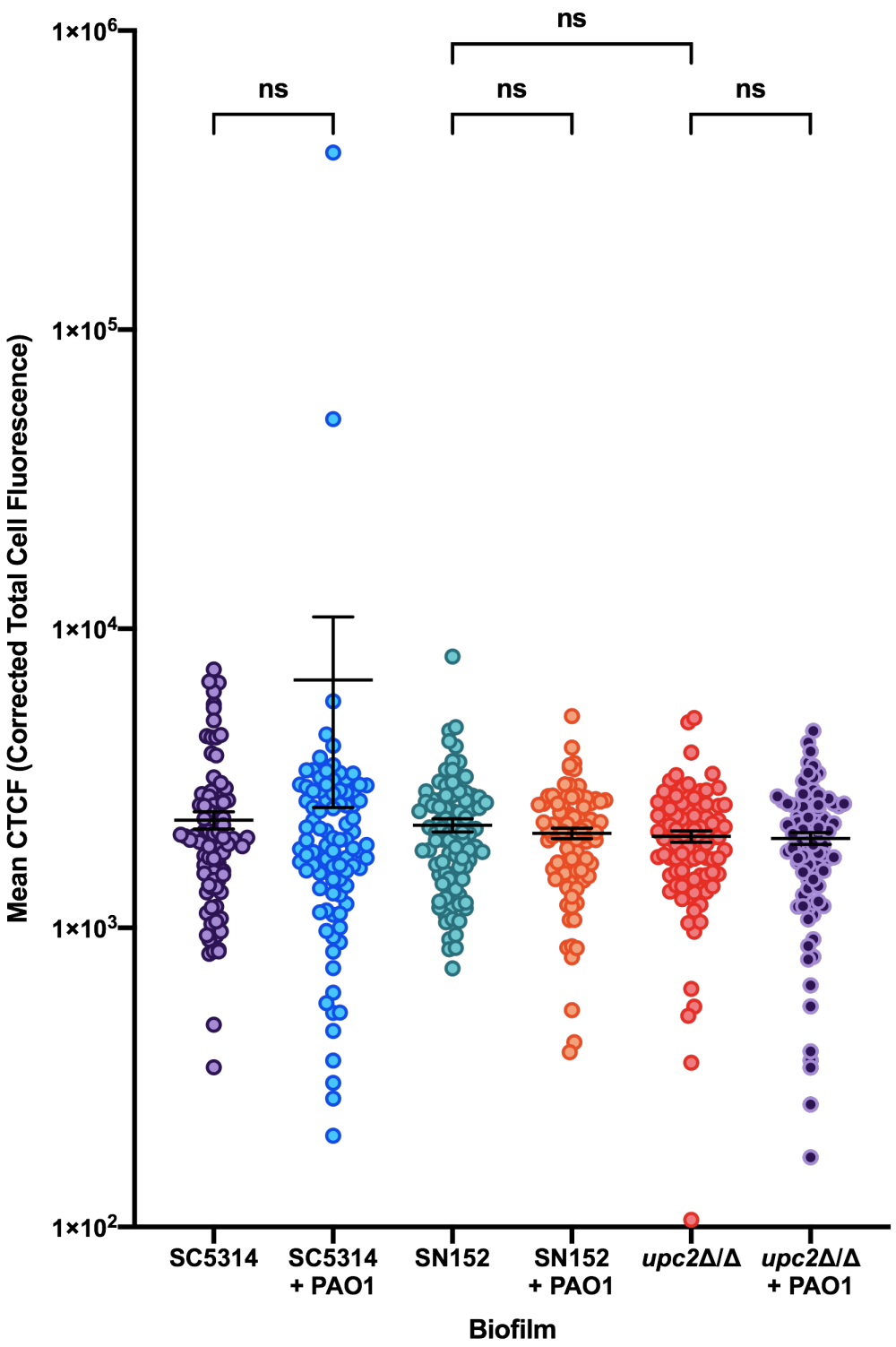


Figure 5.12. Quantification of CTCF (Corrected Total Cell Fluorescence) from fluorescence microscopy images. Biofilms were grown in Mueller Hinton broth for 24 h. Biofilms cells were fixed, detached and stained, before ~30 fluorescence images were taken per biofilm. Data show the mean ± the SEM from 3 biological replicates. Data were analysed using 1-way ANOVA and Holm-Sidak's multiple comparisons test (ns not significant).

5.2.11 *C. albicans* ergosterol biosynthesis is significantly downregulated in the presence of *P. aeruginosa*

To confirm whether there are transcriptional changes to *C. albicans* ergosterol biosynthetic genes in response to the presence of *P. aeruginosa*, the RNA-seq data presented in Chapter 4 was consulted. Of the 21 genes that are known to be involved in the ergosterol biosynthetic pathway, 20 were downregulated, of which 15 were significantly downregulated ($\log_2$ fold change ≥ 1.00 and adjusted P ≤ 0.05) (Table 5.1). Furthermore, the steroid biosynthesis KEGG pathway, to which ergosterol biosynthesis genes are annotated, was the second most enriched KEGG pathway amongst the 739 significantly downregulated genes, with an enrichment ratio of 0.61. The transcriptional data therefore refute the hypothesis that the presence of *P. aeruginosa* results in overproduction of fungal ergosterol; rather, ergosterol biosynthesis is significantly downregulated.

Table 5.1. Transcriptional changes to *C. albicans* ergosterol biosynthetic genes in response to the presence of *P. aeruginosa* in a dual-species biofilm. Genes with a $\log_2$ fold change ≥ 1.00 and an adjusted P-value ≤ 0.05 are shown in bold.

ORF	Gene name	Gene product[x]	Fold change ($\log_2$)*	Adjusted P-value^
ORF19.6026	***ERG2***	C-8 sterol isomerase	**-2.78**	**2.96×10^{-50}**
ORF19.7312	***ERG13***	3-hydroxy-3-methylglutaryl CoA synthase	**-2.49**	**7.56×10^{-105}**
ORF19.6105	***MVD***	Mevalonate diphosphate decarboxylase	**-2.41**	**6.10×10^{-46}**
ORF19.5178	***ERG5***	C-22 sterol desaturase	**-2.18**	**3.06×10^{-36}**
ORF19.1631	***ERG6***	Delta(24)-sterol C-methyltransferase	**-1.99**	**1.64×10^{-56}**
ORF19.5379	***ERG4***	C-24 sterol reductase	**-1.96**	**1.26×10^{-31}**
ORF19.1598	***ERG24***	C-14 sterol reductase	**-1.91**	**1.02×10^{-35}**
ORF19.1031	***HMG1***	Hydroxymethylglutaryl-CoA reductase	**-1.89**	**3.84×10^{-58}**
ORF19.767	***ERG3***	C-5 sterol desaturase	**-1.83**	**1.25×10^{-16}**
ORF19.3616	***ERG9***	Farnesyl-diphosphate farnesyl transferase	**-1.64**	**4.54×10^{-27}**
ORF19.3732	***ERG25***	C-4 methyl sterol oxidase	**-1.28**	**3.32×10^{-08}**
ORF19.1591	***ERG10***	Acetyl-CoA acetyltransferase	**-1.23**	**6.73×10^{-09}**
ORF19.4809	***ERG12***	Mevalonate kinase	**-1.04**	**5.04×10^{-12}**
ORF19.922	***ERG11***	Lanosterol 14-alpha-demethylase	**-1.03**	**2.41×10^{-06}**
ORF19.406	***ERG1***	Squalene epoxidase	**-1.02**	**1.89×10^{-12}**
ORF19.2909	*ERG26*	C-3 sterol dehydrogenase	-0.74	3.24×10^{-12}
ORF19.4491	*ERG20*	Farnesyl pyrophosphate synthetase	-0.58	1.71×10^{-09}
ORF19.2775	*IDI1*	Isopentenyl-diphosphate delta-isomerase	-0.50	9.16×10^{-04}
ORF19.4606	*ERG8*	Phosphomevalonate kinase	-0.39	3.36×10^{-05}
ORF19.1570	*ERG7*	2,3-epoxysqualene-lanosterol cyclase	-0.20	3.17×10^{-01}
ORF19.3240	*ERG27*	3-keto sterol reductase	+0.02	9.19×10^{-01}

[x] Gene product details from FungiDB (fungidb.org)

* + upregulated; - downregulated; $\log_2 \geq 1.00$ is equivalent to ≥ 2-fold linear change

^ Adjusted P-values ≤ 0.05 were considered to be significant

4.2.12 There is significant downregulation of *C. albicans* superoxide dismutase genes in the presence of *P. aeruginosa*

Having observed that ergosterol levels do not appear to play a role in enhancing *C. albicans* AmB susceptibility, a new hypothesis was required. As discussed in Chapter 1, one model for the mechanism of action of AmB is the induction of reactive oxygen species (ROS), such as superoxide ($O_2^{\bullet-}$), resulting in oxidative damage to fungal cells (Kamiński, 2014). Cells are protected from the destructive effects of ROS by antioxidant enzymes. Superoxide radicals are converted to hydrogen peroxide (H_2O_2) by superoxide dismutase (SOD) enzymes. Subsequently, H_2O_2 is broken down into water and oxygen by catalase (Martchenko *et al.*, 2004). *C. albicans* has six SOD enzymes, which have differing metal cofactors and cellular localisations: Sod1 is a Cu/Zn-SOD that is found in the cytosol and the intermembrane space of mitochondria; Sod2 is a Mn-SOD that is found in the mitochondrial matrix; Sod3 is an Mn-SOD that is found in the cytosol; finally, Sod4, Sod5 and Sod6 are Cu-SODs, which are unique to fungi, and are extracellularly attached to fungal cell membranes via GPI-anchors (Schatzman *et al.*, 2020, Broxton and Culotta, 2016, Martchenko *et al.*, 2004).

Transcriptomic analysis showed downregulation of genes annotated to the Biological Process GO term, 'response to stress' (Chapter 4, Figure 4.22). To determine whether *C. albicans SOD* genes are specifically downregulated in response to *P. aeruginosa*, the transcriptional responses of genes in the *C. albicans* 'removal of superoxide radicals' pathway were examined more closely. There was significant downregulation of *SOD5*, *SOD2* and *SOD1*, but significant upregulation of *SOD6* (log_2fold change ≥ 1.00 and adjusted $P \leq 0.05$) (Table 5.2). Furthermore, *SOD3* and *SOD4* were

downregulated, and *CAT1* was upregulated (Table 5.2). The significant downregulation of three out of six *C. albicans SOD* genes suggests that accumulation of superoxide radicals may play a role in enhancing AmB activity in the presence of *P. aeruginosa*.

Table 5.2. Transcriptional changes to genes in the *C. albicans* 'removal of superoxide radicals' pathway, in response to the presence of *P. aeruginosa* in a dual-species biofilm. Genes with a $\log_2$ fold change ≥ 1.00 and an adjusted P-value ≤ 0.05 are shown in bold.

ORF	Gene name	Gene product[x]	Fold change ($\log_2$)*	Adjusted P-value^
ORF19.2060	***SOD5***	Cu-containing superoxide dismutase	**-2.97**	**5.63×10^{-09}**
ORF19.3340	***SOD2***	Mitochondrial Mn-containing superoxide dismutase	**-1.85**	**5.29×10^{-17}**
ORF19.2770.1	***SOD1***	Cytosolic Cu- and Zn-containing superoxide dismutase	**-1.36**	**1.11×10^{-05}**
ORF19.2062	*SOD4*	Cu-containing superoxide dismutase	-0.59	3.04×10^{-03}
ORF19.7111.1	*SOD3*	Cytosolic Mn-containing superoxide dismutase	-0.54	4.10×10^{-01}
ORF19.6229	*CAT1*	Catalase	+0.43	1.54×10^{-01}
ORF19.2108	***SOD6***	Cu-containing superoxide dismutase	**+2.01**	**2.20×10^{-15}**

[x] Gene product details from FungiDB (fungidb.org)
* + upregulated; - downregulated; $\log_2$ ≥ 1.00 is equivalent to ≥ 2-fold linear change
^ Adjusted P-values ≤ 0.05 were considered to be significant

5.2.13 The induction of reactive oxygen species potentiates amphotericin B activity against *C. albicans* biofilm cells

To test the hypothesis that accumulation of ROS, such as superoxide radicals, leads to potentiation of AmB activity against *C. albicans* biofilm cells, single-species biofilms were incubated with ROS-inducing agents prior to treatment with 2 μg/mL AmB. Three ROS-inducing agents were used: 1) 10 mM H_2O_2, which results in general

oxidative stress within cells (Sokol-Anderson *et al.*, 1988); 2) 0.2 mM menadione, which generates intracellular superoxide radicals (Hwang *et al.*, 2002, Martchenko *et al.*, 2004); and 3) 0.1 mM hypoxanthine + 0.16 mU/mL xanthine oxidase, with which the enzymatic activity of xanthine oxidase first converts hypoxanthine to xanthine, and then to uric acid, releasing a superoxide radical at each stage; the xanthine oxidase-generated superoxide radicals are unable to diffuse across cell membranes, so remain extracellular (Robinett *et al.*, 2019, Youseff *et al.*, 2012).

Incubation of *C. albicans* single-species biofilms with either H_2O_2 or menadione, prior to AmB treatment, resulted in recovery of zero fungal cells; the same phenotype as AmB-treated *C. albicans–P. aeruginosa* biofilms (Figure 5.13). However, incubation with hypoxanthine + xanthine oxidase did not enhance AmB activity, but showed similar viability to single-species *C. albicans* biofilms (Figure 5.13). This suggests that increased ROS or intracellular superoxide levels potentiate AmB activity against *C. albicans* biofilm cells, but increased extracellular superoxide levels do not. The implication is that the dual-species interaction may lead to increased intracellular superoxide levels within *C. albicans* biofilm cells.

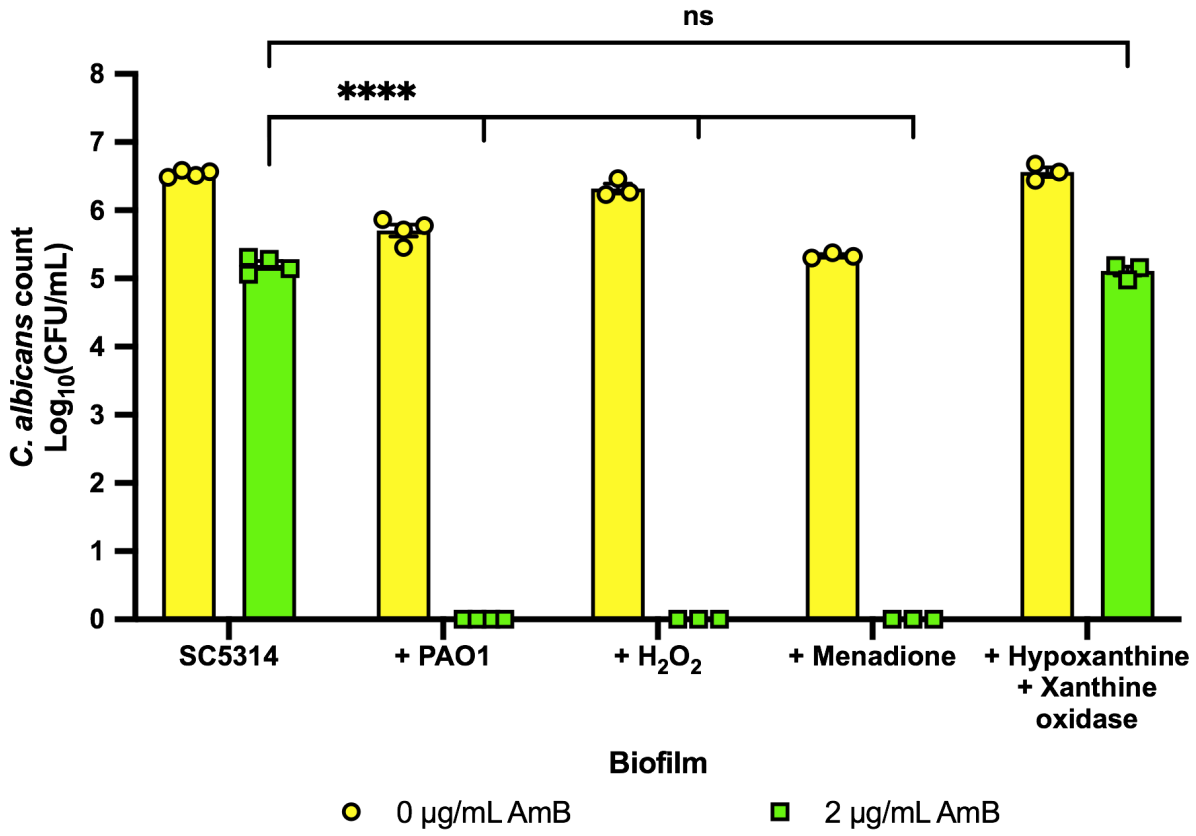


Figure 5.13. Incubation with agents that increase intracellular ROS levels leads to potentiation of amphotericin B activity against *C. albicans* biofilm cells. ROS-inducing agents (10 mM H_2O_2; 0.2 mM menadione; 0.1 mM hypoxanthine + 0.16 mU/mL xanthine oxidase) were added to *C. albicans* SC5314 biofilms after 3 h growth in Mueller Hinton broth. At 24 h, all biofilms were incubated with 0 or 2 µg/mL amphotericin B (AmB) for a further 2 h. Data are the $\log_{10}$(mean) ± the SEM from 3–4 biological replicates. Data were analysed using 2-way ANOVA and Holm-Sidak's multiple comparisons test (ns not significant; **** P < 0.0001).

5.2.14 A *C. albicans sod2*Δ/Δ mutant strain has significantly enhanced susceptibility to amphotericin B

Accumulation of superoxide within *C. albicans* biofilm cells may either be caused by increased production of superoxide radicals, or by downregulation of *SOD* genes, resulting in reduced removal of superoxide radicals from the cells. Having observed significant downregulation of *SOD1*, *SOD2* and *SOD5* in response to *P. aeruginosa* (Table 5.2), the effect of knocking out *SOD* genes on *C. albicans* AmB

susceptibility was investigated. Of the strains tested, only biofilms of the *sod2*Δ/Δ knockout strain showed significantly greater susceptibility to AmB (Figure 5.14). However, *C. albicans sod2*Δ/Δ viability never fell to zero, suggesting that loss or reduction of *SOD2* activity may only be a part of the mechanism by which *P. aeruginosa* mediates potentiation of AmB activity against *C. albicans* biofilm cells. Therefore, the focus was turned to transcriptional changes in *P. aeruginosa* cells when grown as dual-species biofilms with *C. albicans*.

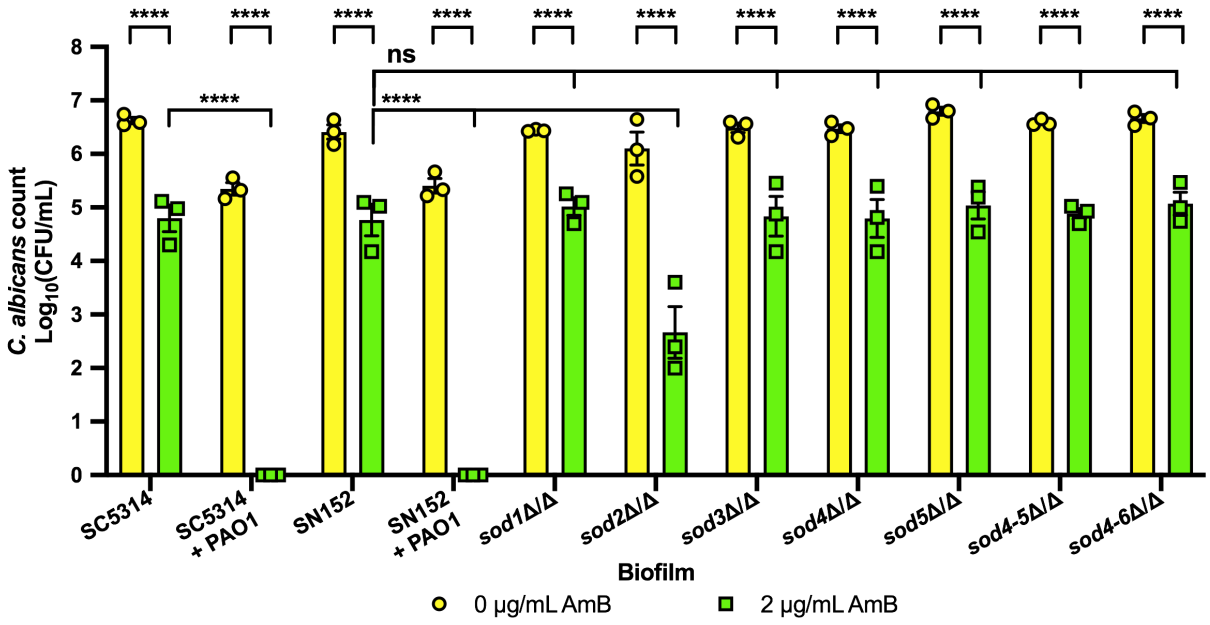


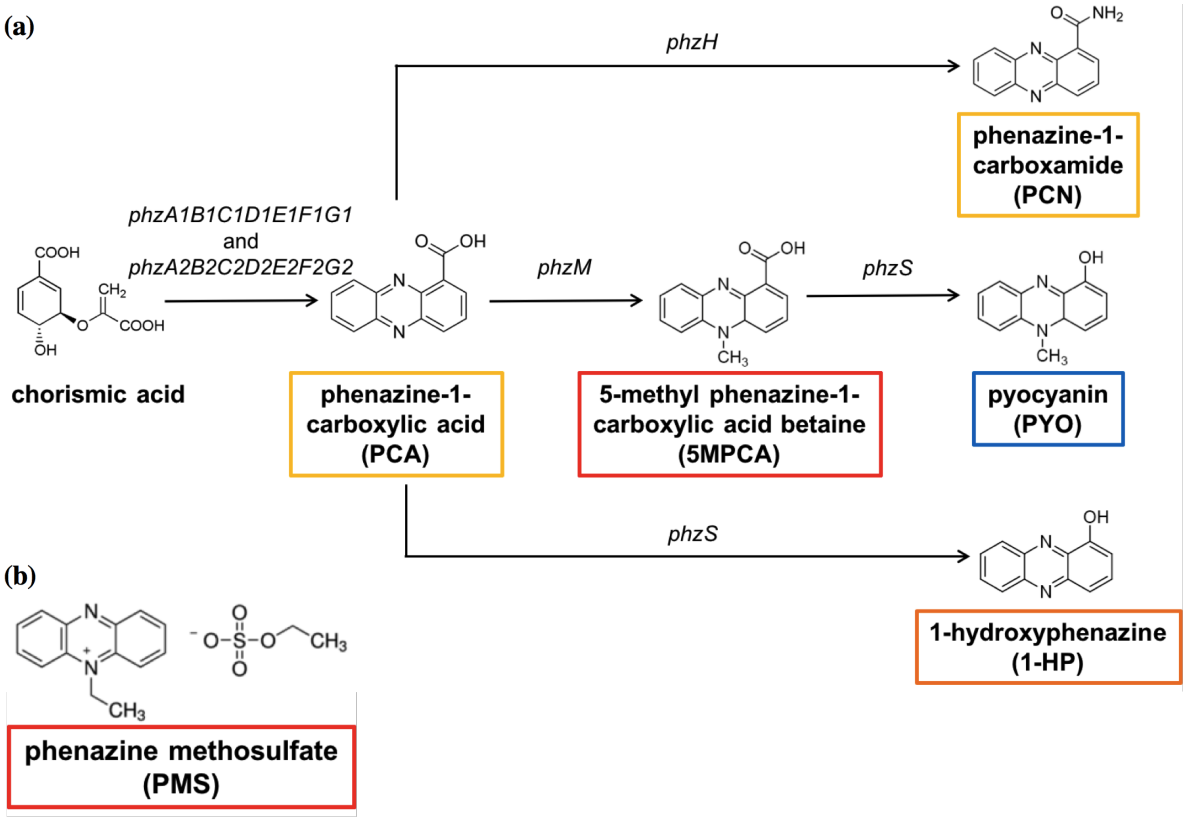
Figure 5.14. Biofilms of a *C. albicans sod2*Δ/Δ knockout strain show significantly increased susceptible to amphotericin B. Preformed 24 h biofilms were incubated in Mueller Hinton broth containing 0 or 2 µg/mL amphotericin B (AmB) for 2 h. Data are the $\log_{10}$(mean) ± the SEM from 3 biological replicates. Data were analysed using 2-way ANOVA and Holm-Sidak's multiple comparisons test (ns not significant; **** P < 0.0001).

5.2.15 *P. aeruginosa* phenazines significantly potentiate amphotericin B activity against *C. albicans* biofilm cells

The transcriptional data presented in Chapter 4 revealed significant upregulation of *P. aeruginosa* genes involved in phenazine biosynthesis, including all genes of both the *phz1* and *phz2* operons, in response to the presence of *C. albicans*. Phenazines are redox-active molecules that are naturally pigmented (Briard *et al.*, 2015). The *phz1* and *phz2* operons encode several enzymes that catalyse the conversion of chorismic acid to phenazine-1-carboxylic acid (PCA), which is yellow in colour (Figure 5.15a) and is one of five phenazine molecules produced by *Pseudomonas* species (Mavrodi *et al.*, 2001, Briard *et al.*, 2015). Three further phenazine biosynthetic enzymes (encoded by *phzH*, *phzM* and *phzS*) catalyse the formation of the other four phenazines from PCA (Mavrodi *et al.*, 2001). These are: 5-methyl phenazine-1-carboxylic acid betaine (5MPCA), which is red; phenazine-1-carboxamide (PCN), which is yellow; pyocyanin (PYO), which is blue; and 1-hydroxyphenazine (1-HP), which is orange (Figure 5.15a) (Mavrodi *et al.*, 2001, Briard *et al.*, 2015, Morales *et al.*, 2010). Phenazine methosulfate (PMS) is a commercially-available synthetic analogue of 5MPCA (Figure 5.15b), the latter of which is unstable in physiologically-relevant environments, so PMS is a useful substitute for research purposes (Morales *et al.*, 2010).

To investigate the effect of purified *P. aeruginosa* phenazines on the AmB susceptibility of *C. albicans* biofilm cells, single-species biofilms were incubated with purified PCA, PMS, PYO, 1-HP, or combinations of these, prior to treatment with 0 or 2 μg/mL AmB. Within the CF lung, the concentrations of phenazines are in the range

of 1–100 μM, but concentrations above 50 μM can result in depletion of Fe^{2+} ions from the environment, which can affect biofilm formation (Briard *et al.*, 2015). Therefore, the concentration of phenazines used in this assay was 40 μM. (PCN was not included in the experiment due to severe delays to the shipping of laboratory supplies caused by the consequences of Britain's exit from the European Union, and exacerbated by the COVID-19 global pandemic.) PYO and 1-HP had no effect on *C. albicans* AmB susceptibility, either alone or in combination (Figure 5.15c). PMS, either alone or in combination with 1-HP, significantly ($P < 0.0001$) enhanced *C. albicans* biofilm susceptibility to AmB; there was a smaller, but significant ($P < 0.05$) effect with PCA (Figure 5.15c). However, unlike co-incubation with *P. aeruginosa*, recovery of *C. albicans* cells from single-species biofilms did not fall to zero as a result of incubation with purified PMS or PCA (Figure 5.15c). Therefore, potentiation of AmB activity by PMS and PCA may be part of a more complex mechanism.


(a)
phzH
phenazine-1-carboxamide (PCN)
phzA1B1C1D1E1F1G1
and
phzA2B2C2D2E2F2G2
phzM
phzS
chorismic acid
phenazine-1-carboxylic acid (PCA)
5-methyl phenazine-1-carboxylic acid betaine (5MPCA)
pyocyanin (PYO)
phzS
1-hydroxyphenazine (1-HP)
(b)
phenazine methosulfate (PMS)

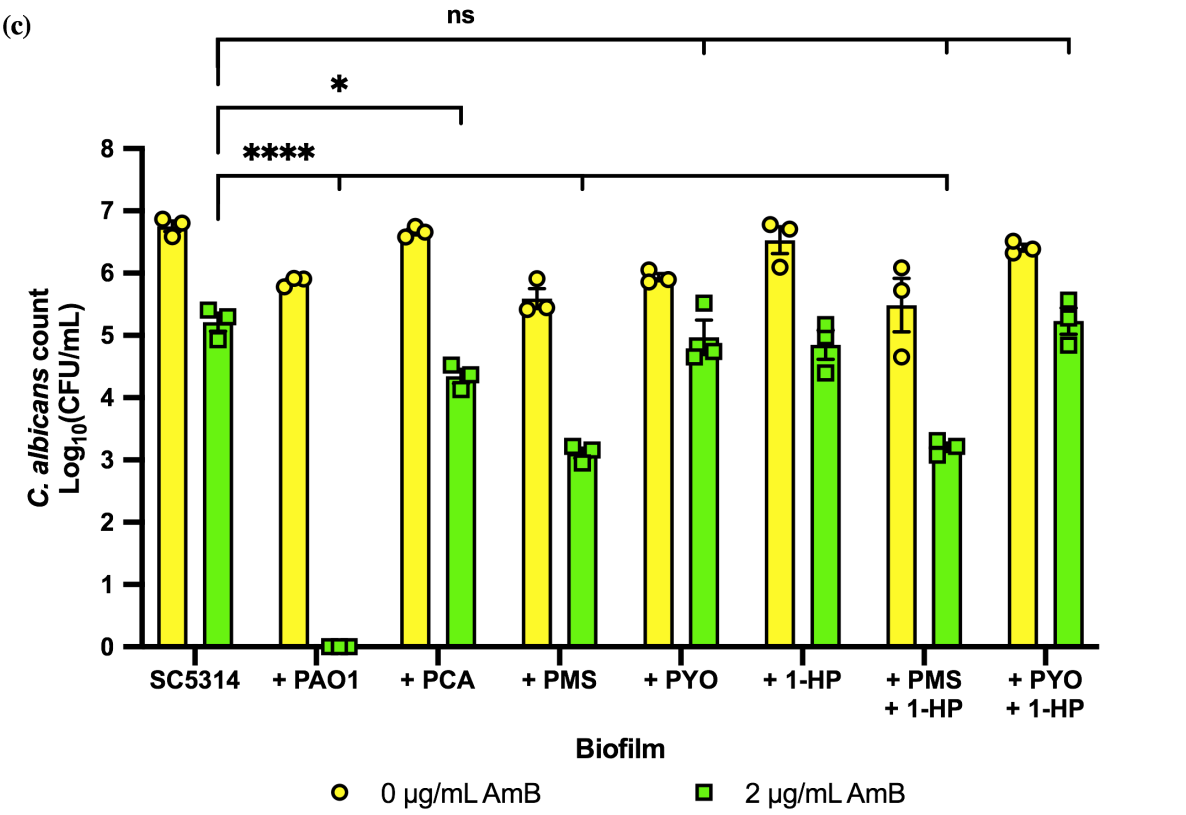

(c)
ns
*
****
C. albicans count Log10(CFU/mL)
0
1
2
3
4
5
6
7
8
SC5314
+ PAO1
+ PCA
+ PMS
+ PYO
+ 1-HP
+ PMS + 1-HP
+ PYO + 1-HP
Biofilm
0 µg/mL AmB
2 µg/mL AmB

Figure 5.15. *P. aeruginosa* phenazines significantly potentiate amphotericin B activity against *C. albicans* biofilm cells. (a) *P. aeruginosa* phenazine biosynthetic pathway. Figure adapted from Mavrodi *et al.* (2001). **(b)** Chemical structure of PMS, which is a synthetic analogue of 5MPCA. **(c)** Purified phenazines were added to *C. albicans* SC5314 biofilms after 3 h growth in Mueller Hinton broth. At 24 h, all biofilms were incubated with 0 or 2 µg/mL amphotericin B (AmB) for a further 2 h. Data are the $\log_{10}$(mean) ± the SEM from 3 biological replicates. Data were analysed using 2-way ANOVA and Holm-Sidak's multiple comparisons test (ns not significant; * $P < 0.05$; **** $P < 0.0001$).

To further investigate the effect of phenazines on *C. albicans* biofilm susceptibility to AmB, dual-species biofilms were grown with *P. aeruginosa* strains lacking the *phz1* and *phz2* operons. The *phz*Δ mutant was in a *P. aeruginosa* PA14 background, so PA14 was included as a wild-type dual-species control biofilm. Furthermore, a triple *phz*Δ/*pvdA*Δ/*pchE*Δ mutant and a double *pvdA*Δ/*pchE*Δ mutant were also available, enabling some insight into the effect of siderophores on *C. albicans* biofilm susceptibility to AmB. The *pvdA* gene encodes L-ornithine N5-oxygenase, which is involved in pyoverdine biosynthesis, whilst the *pchE* gene encodes dihydroaeruginoic acid synthetase, which is involved in pyochelin biosynthesis. In the dual-species control biofilms, the presence of *P. aeruginosa* PA14 did not potentiate AmB activity to the same extent as PAO1 (Figure 5.16). *P. aeruginosa* PA14 strains produce PYO as the dominant phenazine (Das and Manefield, 2012), but purified PYO was observed to have no effect on *C. albicans* AmB susceptibility (Figure 5.15c); this may explain why the potentiation effect is smaller in the presence of PA14 than with PAO1. Nevertheless, using the PA14 dual-species biofilm as the wild-type control revealed that co-incubation with either the *phz*Δ or the *phz*Δ/*pvdA*Δ/*pchE*Δ strain significantly rescued *C. albicans* viability (Figure 5.16). This implies a role for phenazines in potentiating AmB activity against *C. albicans* biofilm cells. Co-incubation with the

*pvdA*Δ/*pchE*Δ strain had no effect (Figure 5.16), suggesting that siderophore production does not influence *C. albicans* biofilm susceptibility to AmB.

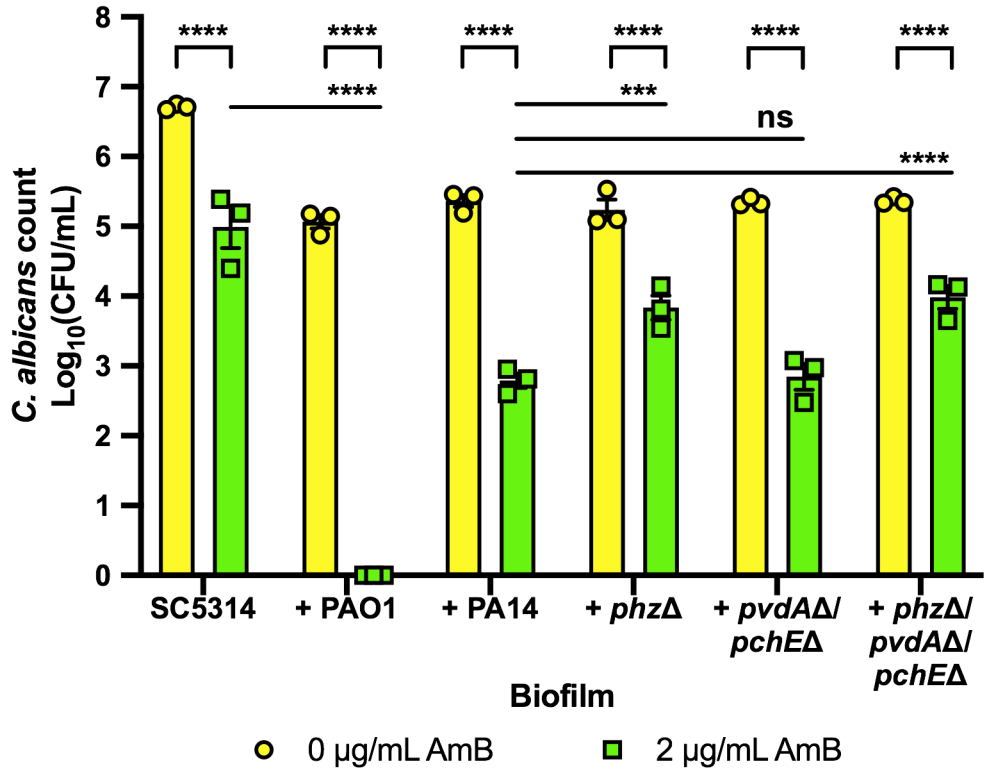


Figure 5.16. Potentiation of AmB activity is lost when *C. albicans* is co-incubated with *P. aeruginosa phz*Δ mutant strains. Preformed 24 h biofilms were incubated in Mueller Hinton broth containing 0 or 2 µg/mL amphotericin B (AmB) for 2 h. Data are the $\log_{10}$(mean) ± the SEM from 3 biological replicates. Data were analysed using 2-way ANOVA and Holm-Sidak's multiple comparisons test (ns not significant; *** $P < 0.001$; **** $P < 0.0001$).

5.3 Discussion

The data presented here show that *P. aeruginosa* significantly potentiates amphotericin B activity against *C. albicans* biofilm cells, resulting in zero recovery of fungal cells from dual-species biofilms that have been treated with the biologically-relevant concentration of 2 µg/mL AmB. This has direct implications for the treatment of co-infected patients. Amphotericin B can be nephrotoxic and hematotoxic at

increasing dosages (Kamiński, 2014), whilst less toxic formulations, such as liposomal AmB, can be costly (Perlin *et al.*, 2017). For co-infected patients, lowered doses of amphotericin B, as part of a combination therapy with an antibiotic, may be a promising therapeutic strategy, reducing both adverse reactions and treatment costs.

The numbers of fungal cells recovered from dual-species *C. albicans–P. aeruginosa* biofilms was consistently lower than the numbers recovered from single-species *C. albicans* biofilms, by approximately 1–2 $\log_{10}$ CFU/mL, even in the absence of antifungal treatment. This supports data presented in Chapter 3 and previous data showing that *P. aeruginosa* has an inhibitory effect on *in vitro C. albicans* biofilm development. The proposed mechanisms by which this inhibition occurs varies, including inhibition of hyphal development and impedance of biofilm formation by *P. aeruginosa* lipopolysaccharides (LPS) (Bandara *et al.*, 2010, Bandara *et al.*, 2013), inhibition of filamentation by *P. aeruginosa* phenazines (Morales *et al.*, 2013), and disruption of *C. albicans* biofilms by *P. aeruginosa* rhamnolipids (Singh *et al.*, 2013). This reduction in *C. albicans* viable counts in dual-species biofilms may potentially result in an increased AmB concentration per fungal cell, thus enhancing the effect of the drug. This could be corrected by the addition of more *C. albicans* cells to the biofilm following the initial co-incubation with *P. aeruginosa*; however, this may have a disruptive effect on the mature biofilm structure, thus introducing further confounding variables.

The potentiation of AmB in dual-species cultures was biofilm-specific and dependent upon the presence of viable, metabolically active *P. aeruginosa* cells. The lack of

change in *C. albicans* susceptibility to AmB between single- and dual-species planktonic cultures is in contrast with the findings of Rodrigues *et al.* (2017), who found an 8-fold increase in the AmB MIC for dual-species, planktonic *C. albicans*. However, this is likely due to differences in methodology between studies. Rodrigues *et al.* (2017) used trypic soy agar/broth for maintenance and growth of *P. aeruginosa*, and Sabouraud dextrose agar/broth for *C. albicans* (Rodrigues *et al.*, 2017), whereas the present study used LB for maintenance and growth of *P. aeruginosa*, and YPD for *C. albicans*. Furthermore, Rodrigues *et al.* (2017) measured specific MIC values of planktonic-grown cells in a broth microdilution method that used RPMI 1640 broth (Rodrigues *et al.*, 2017), whereas the present study measured *C. albicans* viability following planktonic growth in Mueller Hinton broth, and did not measure specific MIC values for *C. albicans*.

When *C. albicans* cells were grown in the presence of supernatants from mature biofilms, the AmB potentiation effect was lost, seeming to suggest that the phenotype did not depend on a secreted factor from *P. aeruginosa* biofilm cells. However, the set-up of the supernatant experiment has several limitations that prevent this conclusion from being drawn with confidence. First, the biofilm supernatants were collected without disrupting the biofilms, meaning that any secreted molecules deep within the biofilms, which had not diffused out into the media, were not present in the supernatant. Second, supernatants were snap-frozen and stored at -20°C for up to 6 days, before being thawed for use in the assay. However, this means that any unstable or short-lived molecules would be ineffective. Third, *C. albicans* growth in a 50:50 ratio of Mueller Hinton broth and supernatant may have introduced nutrient limitation, due

to a reduced volume of growth medium. Finally, the 50:50 ratio also meant that any secreted molecules within the supernatant were diluted to half of their usual concentration, which would mask any effect that is concentration-dependent.

Despite the limitations of the supernatant experiment, one group of secreted *P. aeruginosa* molecules that can be ruled out of the mechanism with greater confidence is rhamnolipids. In dual-species *C. albicans–P. aeruginosa* biofilms, production of *P. aeruginosa* rhamnolipids is increased as part of the induction of virulence factor production (Trejo-Hernández *et al.*, 2014). Previous research shows that *P. aeruginosa*-derived rhamnolipids can disperse biofilms formed by both bacterial and fungal species, including *Desulfovibrio vulgaris*, *E. coli*, *S. aureus* (Wood *et al.*, 2018, Ceresa *et al.*, 2019), *S. epidermidis* (Ceresa *et al.*, 2019), *C. tropicalis* (Borah *et al.*, 2019) and *C. albicans* (Singh *et al.*, 2013). However, many of these studies quantified the biofilm mass remaining after exposure to rhamnolipids, but did not measure the viability of the biofilm cells. Where cell viability was measured, a shift from biofilm to planktonic mode of growth was observed, rather than any killing effect (Ceresa *et al.*, 2019). Indeed, the mode of action of rhamnolipid-mediated *C. albicans* biofilm dispersal is through disruption of the fungal ECM (Singh *et al.*, 2013). In the present study, there was no reduction in viability of AmB-treated *C. albicans* biofilm cells, following exposure to rhamnolipids, compared to the control. Considering that the experimental set-up of the biofilm assay retains the biofilm cells within a closed system, these data are consistent with the literature, i.e. *P. aeruginosa* rhamnolipids do not affect viability of *C. albicans* biofilm cells, but may affect their cell–cell and cell–substratum adhesion.

To investigate whether the potentiation of AmB activity was unique to *P. aeruginosa* PAO1, or whether it was a common phenotype across other *C. albicans*–bacterial dual-species biofilms, the biofilm assay was repeated using different *P. aeruginosa* strains, as well as different bacterial species that frequently co-infect with *C. albicans*. The *P. aeruginosa* strains tested included two PA14 strains and two CF isolates, and all of these potentiated AmB activity more slowly (after 18 h AmB incubation) than the PAO1 strain (after 2 h AmB incubation). This may be explained by differences in secreted molecules between the strains. *P. aeruginosa* biofilm cells secrete the polysaccharides Psl and Pel into the ECM, which both play roles in biofilm structural stability. However, PAO1 strains produce much more Psl than Pel, whilst PA14 strains are unable to produce any Psl (Mann and Wozniak, 2012, Jennings *et al.*, 2015). Furthermore, there are differences in the phenazines secreted by PAO1 and PA14 strains, with pyocyanin being the dominant phenazine that is produced at much higher levels in PA14 strains compared to PAO1 strains (Das and Manefield, 2012). Pyocyanin is blue in colour (Briard *et al.*, 2015), so its presence turns LB broth bright green; this was clearly visible in the overnight cultures of both PA14 strains and the Midlands 1 CF isolate, whilst the overnight cultures of PAO1 remained yellow. Furthermore, *P. aeruginosa* strains isolated from CF patients are generally more slow-growing than PAO1, and often overproduce alginate, which aids their persistence in infected lungs (Høiby *et al.*, 2010, Rossi *et al.*, 2020). The differences observed between different *P. aeruginosa* strains indicate that the factor(s) mediating the rapid potentiation of AmB activity may be more common in PAO1 strains, or unique to the specific PAO1 strain used in the present study. In future, the effect of differences in

levels of secreted molecules could be further investigated by quantifying the production of Pel, Psl, alginate, and phenazines by different *P. aeruginosa* strains, using high-performance liquid chromatography (HPLC) (Schiessl *et al.*, 2019).

Of the other bacterial species tested, *E. coli* MG1655 also significantly potentiated the activity of AmB against *C. albicans* in a dual-species biofilm, whilst a smaller significant effect was seen with *E. faecalis* V583. A recent study on planktonic cultures showed that *E. coli* MG1655 can kill *C. albicans* SC5314 cells by secreting a molecule that is dependent upon depletion of Mg^{2+} ion availability, which the authors propose is likely to be a bacteriocin (Cabral *et al.*, 2018). Depletion of Mg^{2+} is likely to occur within biofilms because negatively charged extracellular DNA, which is a common biofilm ECM component, is known to chelate cations (Mulcahy *et al.*, 2008). Therefore, the dramatic reduction in *C. albicans* viability in AmB-treated *C. albicans–E. coli* biofilms may be due to a combinatorial effect of a bacteriocin and the antifungal drug. The *E. faecalis* V583 bacteriocin, EntV, has be shown to reduce *C. albicans* virulence and biofilm formation in dual-species biofilms, via inhibition of filamentation, but with no effect on fungal viability (Graham *et al.*, 2017). This may explain why the potentiation of AmB activity in the presence of *E. faecalis* was never great enough to result in complete loss of *C. albicans* viability. Inhibition of hyphal formation is a common effect of both *E. faecalis* and *P. aeruginosa* on *C. albicans* cells, but their differing effects on *C. albicans* viability may be a pivotal factor in the magnitude of AmB potentiation arising from the dual-species biofilm interaction.

P. aeruginosa-mediated potentiation of AmB activity was not specific to *C. albicans*, but was also seen with *C. dubliniensis*. As discussed in earlier chapters, *C. dubliniensis* is the most closely related *Candida* species to *C. albicans* and the only one also capable of forming true hyphae (Papon *et al.*, 2013). Furthermore, the composition and architecture of their biofilms are comparable (Ramage *et al.*, 2001, Whibley and Gaffen, 2015). This suggests that physical interaction of *P. aeruginosa* cells with fungal hyphae may be important in the mechanism by which AmB activity is enhanced.

Having established that *P. aeruginosa* rhamnolipids are unlikely to be involved in potentiation of AmB activity, but that attachment to hyphae may play a role, the focus of attention was turned to *C. albicans* cellular features. The most logical feature with which to start was ergosterol; the drug target of AmB. Dual-species biofilms of *C. albicans upc2*Δ/Δ, which has reduced membrane ergosterol levels (Silver *et al.*, 2004), rescued *C. albicans* viability when treated with AmB, compared to the wild-type. This suggested that *P. aeruginosa* may potentiate AmB activity by inducing overproduction of ergosterol in *C. albicans* biofilm cells. However, when ergosterol levels were quantified by filipin staining, there was no observable difference in fluorescence between single- and dual-species. This suggested that *C. albicans* ergosterol levels are not increased in the presence of *P. aeruginosa*, which was confirmed by transcriptomic data showing significant downregulation of ergosterol biosynthesis in dual-species *C. albicans* cells. Surprisingly, there was no significant difference in fluorescence between *C. albicans upc2*Δ/Δ and its parental control *C. albicans* SN152, suggesting that ergosterol levels were similar in both strains. This may have been

caused by non-specific binding of filipin to other lipids, such as phospholipids or derivatives of ergosterol (Smejkal *et al.*, 1996, Arthur *et al.*, 2011). Formation of lipid rafts, which contain high concentrations of ergosterol and sphingolipids, are essential for biofilm formation (Alim *et al.*, 2018). *C. albicans* biofilm cells contain much higher concentrations of sphingolipids, and numbers of lipid rafts, than planktonic cells (Alim *et al.*, 2018). Therefore, the presence of more complex lipid–lipid interactions in biofilm cells, compared to planktonic cells, indicates that a more sensitive method may be required for quantifying ergosterol levels in fungal biofilm cells. This could include solid-phase extraction (SPE) of total ergosterol from samples, followed by HPLC analysis (Gilbert *et al.*, 2002, Tong *et al.*, 2014), gas chromatography–mass spectrometry (GC-MS) (Lau *et al.*, 2006), or UV spectroscopy (Vella and Laratta, 2017). However, a major drawback shared by these quantification methods is that they require samples to be destroyed for analysis. Previous research in which ergosterol levels were quantified in *C. albicans upc2*Δ/Δ, or in *Saccharomyces cerevisiae upc2*Δ, utilised ergosterol extraction followed by spectrophotometric analysis (Silver *et al.*, 2004, Yang *et al.*, 2015), rather than staining with filipin, indicating that this may have been a more appropriate method.

Transcriptomic analysis revealed significant downregulation of superoxide dismutase genes (*SOD1*, *SOD2* and *SOD5*) in dual-species *C. albicans* cells. This raised the possibility that increased ROS levels may be contributing to the enhanced AmB susceptibility of *C. albicans* biofilm cells in co-culture. This is further supported by the significant upregulation of the arginine biosynthesis pathway in dual-species fungal cells, which was observed in Chapter 4, as arginine biosynthetic genes are known to

be upregulated in response to ROS (Jiménez-López *et al.*, 2013). The first evidence of oxidative damage being a mode of AmB action was observed as early as 1986; *C. albicans* protoplasts were protected from AmB activity when supplemented with exogenous catalase or SODs (Sokol-Anderson *et al.*, 1986). Furthermore, induction of superoxide production using paraquat, a superoxide generator, enhanced AmB activity against *C. albicans*, with a 10-fold reduction in the AmB MIC (Okamoto *et al.*, 2004). This was supported by the observation that the ROS-inducing agent, H_2O_2, or the intracellular superoxide generator, menadione, abolished *C. albicans* biofilm viability in a similar manner to co-culturing with *P. aeruginosa*. However, incubation with hypoxanthine and xanthine oxidase, which generate extracellular superoxide, had no effect; this is in agreement with the significant upregulation of *SOD6* in dual-species *C. albicans* cells, as Sod6 is localised to the extracellular surface of fungal cells (Broxton and Culotta, 2016). This suggests that increased ROS levels, particularly intracellularly, results in potentiation of AmB activity against *C. albicans* biofilm cells. However, a limitation of this conclusion is that superoxide levels were not quantified in the experiment. In future, the effects of the ROS-inducing agents could be confirmed using a commercially-available superoxide detection kit, which would quantify superoxide production and monitor its localisation by fluorescence microscopy.

Previous research shows that inhibition of Cu-SODs potentiates AmB activity against *C. albicans* biofilm cells (De Brucker *et al.*, 2013). Cells treated with AmB in combination with diethyl dithio carbamate (DDC), which chelates copper and thereby inhibits the Cu-containing SODs 1, 4, 5 and 6, showed a 10,000-fold reduction in viability compared to AmB treatment alone (De Brucker *et al.*, 2013). In the present

study, a *C. albicans sod2*Δ/Δ strain formed biofilms that were significantly more susceptible to AmB than the wild-type, but no effect was seen with other *sod* knockouts. In agreement with this, Sod2 is essential in the *Aspergillus fumigatus* protective response against ROS and reactive nitrogen species, which are induced by *P. aeruginosa* phenazines (Briard *et al.*, 2015). The induction of ROS by *P. aeruginosa* phenazines has also been shown in *C. albicans* (Morales *et al.*, 2010). The increased effectiveness of AmB under ROS-inducing conditions (Okamoto *et al.*, 2004) may explain the observed potentiation of AmB activity when *C. albicans* biofilms were incubated with phenazine methosulfate (PMS) or phenazine-1-carboxylic acid (PCA). Furthermore, co-incubation of *C. albicans* with *P. aeruginosa phz*Δ, which lacks the two *phz* operons and therefore does not produce phenazines, rescued *C. albicans* biofilm tolerance to AmB, compared to the wild-type. However, these experiments could be improved by the quantification of ROS, which would confirm the link between the presence of phenazines and the induction of ROS in the *C. albicans* biofilm cells.

In conclusion, *P. aeruginosa* may potentiate AmB activity against *C. albicans* biofilm cells in a two-pronged attack. First, significant upregulation of *P. aeruginosa* phenazine biosynthesis induces ROS production in *C. albicans*. Second, the dual-species interaction results in significant downregulation of *C. albicans SOD2*, reducing the ability of fungal cells to remove intracellular ROS. The resultant high levels of ROS enhance the effectiveness of AmB against *C. albicans* cells in a dual-species biofilm. The clinical implication of this is that lower AmB dosages could be required, for the clearance of *C. albicans* biofilm infections, if AmB is administered in combination with

a phenazine derivative or a ROS-inducing agent that can be targeted specifically to the intracellular compartments of fungal cells.

6 DISCUSSION

Approximately 80% of infections in humans are biofilm-related (Rodrigues *et al.*, 2019, Lohse *et al.*, 2018, Van Acker *et al.*, 2014) and biofilm cells can be up to 100–1,000 times more resistant to antimicrobial treatment than planktonic cells (Mah, 2012, Hill *et al.*, 2005). Therefore, in a background of increasing global incidence of AMR and a lag in progress of antimicrobial drug development (Hutchings *et al.*, 2019), advancing our understanding of biofilm infections is of paramount importance.

P. aeruginosa is the most frequently isolated microorganism from the CF lung, and co-infection with *C. albicans* accelerates the decline in lung function (Gileles-Hillel *et al.*, 2015). Co-infection with *P. aeruginosa* and *C. albicans* also occurs in ventilator-associated pneumonia, burns, surgical wounds, and implanted medical devices (Trejo-Hernández *et al.*, 2014, Bandara *et al.*, 2020b, Dhamgaye *et al.*, 2016, Dixon and Hall, 2015, Peleg *et al.*, 2010). Although there is a wealth of research into *P. aeruginosa–C. albicans* interactions, our understanding of their interactions within dual-species biofilms is in its infancy. Furthermore, very little is known about how these interactions affect antimicrobial susceptibility, and the clinical implications of these effects.

This research aimed to determine the impact of *P. aeruginosa–C. albicans* biofilms on antimicrobial tolerance using a combination approach of *in vitro* biofilm assays, imaging, and dual-species RNA-seq. The data revealed that *C. albicans* protects *P. aeruginosa* biofilm cells from the effects of meropenem; this protection is likely

mediated by fungal ECM polysaccharides, specifically mannan and ß-glucan, and by cell–cell adhesion. Conversely, *P. aeruginosa* potentiates the activity of amphotericin B against *C. albicans* cells; this is hypothesised to occur as a result of *P. aeruginosa* secreted phenazines, which inhibit filamentation, and which may lead to the accumulation of ROS in *C. albicans* cells.

6.1 Enhanced *P. aeruginosa* tolerance to meropenem in dual-species biofilms

6.1.1 Sequestration of meropenem by biofilm ECM molecules

In this study, we showed that mannans and ß-glucans, secreted by *C. albicans* into the biofilm ECM, play a role in enhancing *P. aeruginosa* tolerance to meropenem. This is achieved either through the binding and sequestering of meropenem molecules, in a similar mechanism to that proposed for enhanced *C. albicans*–mediated *E. coli* biofilm tolerance to ofloxacin (De Brucker *et al.*, 2015), or through the coating of bacterial cells, as has been proposed for enhanced *S. aureus* biofilm tolerance to vancomycin in the presence of *C. albicans* (Kong *et al.*, 2016). Support for the drug sequestration hypothesis comes from the observation that the protective effect of *C. albicans* was not seen with other antibiotic molecules, and pre-incubation of meropenem with purified mannans and/or ß-glucans maintained the protective effect. The observation that *P. aeruginosa* ofloxacin tolerance was not increased in this study may be explained by differences in *E. coli–C. albicans* versus *P. aeruginosa–C. albicans* biofilm interactions. In the study by De Brucker *et al.* (2015), *E. coli–C. albicans* biofilm interactions did not affect the viability of either bacterial or

fungal cells (De Brucker *et al.*, 2015), whereas the present study showed reduced *C. albicans* viability in the presence of *P. aeruginosa*. Therefore, it is possible that sequestration of meropenem by *C. albicans* ECM polysaccharides may be part of a more complex, or multifactorial, protective mechanism than that proposed for enhanced *E. coli* ofloxacin tolerance.

Dual-species RNA-seq data revealed that the most highly upregulated *C. albicans* gene, in response to the presence of *P. aeruginosa*, was *INO1*, which is essential for the production of GPI anchors (Chen *et al.*, 2008). In *C. albicans*, both *N*-linked mannoproteins and ß-glucan–associated cell wall proteins are attached to the fungal cell wall via GPI-anchors (Chen *et al.*, 2008). This raises the possibility that interactions with *P. aeruginosa* may lead to an increased rate of incorporation of fungal cell wall components into the *C. albicans* cell wall, to support the secretion of mannans and ß-glucans into the biofilm ECM. In the *C. albicans* biofilm ECM, mannans and ß-glucans are known to exist in a mannan–glucan complex (MGCx), which is assembled extracellularly following individual secretion of each molecule (Mitchell *et al.*, 2015). These MGCx structures contribute to the high levels of fluconazole resistance observed in *C. albicans* biofilms, through sequestration of the drug (Mitchell *et al.*, 2015). If future research is able to link upregulation of *INO1* with enhanced production of MGCx structures, this could lend further support to the hypothesis that *C. albicans* protects *P. aeruginosa* biofilm cells from meropenem via sequestration of the drug by ECM polysaccharides.

Biofilm ECM components secreted by *P. aeruginosa* may also play a role in the enhanced meropenem tolerance of dual-species biofilms. Significant upregulation of *P. aeruginosa* genes encoding the Psl polysaccharide was observed in dual-species biofilms. Overproduction of Psl has previously been shown to enhance *P. aeruginosa* tolerance to colistin, tobramycin and ciprofloxacin, through sequestration of antibiotic molecules (Hall and Mah, 2017). However, this hypothesised role for Psl in sequestering meropenem needs to be confirmed through use of Psl inhibitors or *P. aeruginosa* strains lacking Psl biosynthetic genes, as well as supplementation of *P. aeruginosa* biofilms with exogenous Psl. In addition, overproduction of Psl is linked to enhanced adherence and aggregation of *P. aeruginosa* biofilm cells (Jennings *et al.*, 2015).

6.1.2 Adherence of *P. aeruginosa* to fungal hyphae

Imaging of biofilms by both SEM and confocal microscopy showed that, upon meropenem treatment of dual-species biofilms, *P. aeruginosa* cells were tightly clustered and adhered to *C. albicans* cells, which is consistent with the observed upregulation of *P. aeruginosa* genes encoding Psl in dual-species, and suggests that adhesion may play a role in the protective effect. This hypothesis is further supported by the observation that removal of *C. albicans* cell wall *O*-mannan, which is involved in bacterial binding (Munro *et al.*, 2005, Brand *et al.*, 2008), resulted in loss of the protective effect. One hypothesis for how adherence may enhance meropenem tolerance could be that aggregation of *P. aeruginosa* cells upon *C. albicans* cell surfaces results in physical shielding of bacterial cells that are deep within the biofilm structure. However, this needs to be confirmed by further research.

Formation of hyphae is important for *C. albicans* adherence, as there is greater production of adhesion proteins in hyphal cells relative to yeast cells (Sharma *et al.*, 2019). The observation that the protective effect was limited to *C. albicans* and *C. dubliniensis*, which are the only true hyphae-forming *Candida* species (Papon *et al.*, 2013), provides further support for the role of hyphal adherence in enhancing *P. aeruginosa* meropenem tolerance. Of all *Candida* species, *C. dubliniensis* biofilms are structurally and compositionally most similar to *C. albicans* biofilms (Ramage *et al.*, 2001), so this observation also lends support to the hypothesis that biofilm ECM polysaccharides play a role in the protective effect. Therefore, it is possible that both proposed mechanisms may play a role (Figure 6.1).

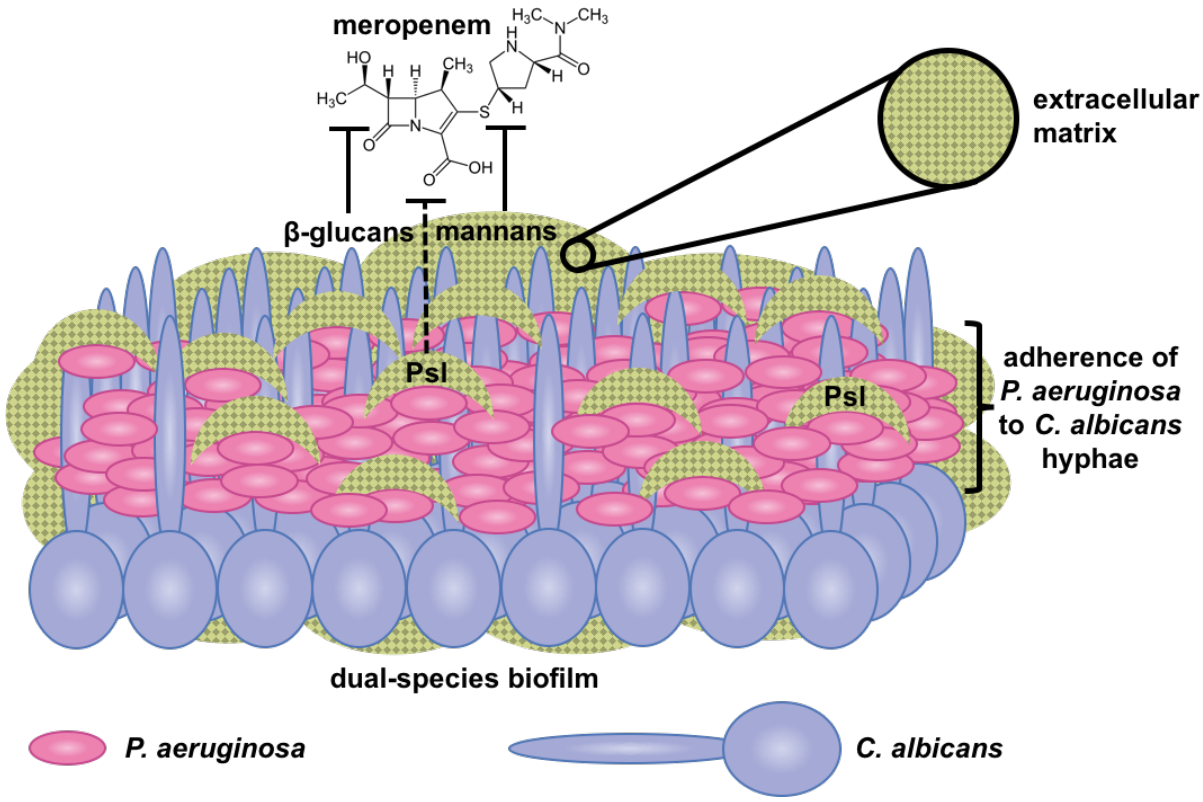


Figure 6.1. Proposed model for enhanced *P. aeruginosa* meropenem tolerance in a dual-species biofilm with *C. albicans*. *C. albicans* cells secrete ß-glucans and mannans into the biofilm extracellular matrix (ECM). These polysaccharides bind and sequester meropenem, thus reducing the concentration of meropenem reaching *P. aeruginosa* cells within the biofilm. Meanwhile, *P. aeruginosa* cells increase production of the biofilm ECM polysaccharide, Psl, which enhances *P. aeruginosa* cell aggregation and adherence to *C. albicans* hyphae. Psl may also sequester meropenem, further impeding its access to *P. aeruginosa* cells.

6.1.3 Insights from transcriptomic data

6.1.3.1 Potential role of siderophores

The *P. aeruginosa* response to meropenem, both in single- and dual-species biofilm cells, included significant upregulation of genes encoding the siderophore, pyochelin. However, the presence of *C. albicans* in untreated biofilms resulted in significant upregulation of genes involved in biosynthesis of the other *P. aeruginosa* siderophore, pyoverdine. Crucially, pyoverdine has higher affinity for extracellular Fe^{3+} than does pyochelin (Banin *et al.*, 2005). In the presence of *C. albicans*, increased *P. aeruginosa* iron acquisition may also contribute to the protective mechanism, as previous research links iron acquisition to enhanced meropenem tolerance (Reid *et al.*, 2009). Supplementation of *P. aeruginosa* biofilms with exogenous iron leads to a significant increase in the meropenem MIC, with the authors proposing that iron availability supports both *P. aeruginosa* replication and biofilm formation, while chelation of iron disrupts biofilm structure (Reid *et al.*, 2009). This hypothesis could be tested by reducing the ability of *P. aeruginosa* to acquire iron, using strains lacking siderophore biosynthetic genes, and observing whether the protective effect of *C. albicans* is lost. Furthermore, single-species *P. aeruginosa* biofilms could be supplemented with exogenous Fe^{3+} to confirm the findings of Reid *et al.* (2009) using the strains and growth conditions of the present study.

6.1.3.2 Potential role of phenazines

As well as pyoverdine biosynthetic genes, co-incubation with *C. albicans* resulted in significant upregulation of *P. aeruginosa* phenazine biosynthetic genes. Previous research links phenazine production, specifically PCA and PCN, to enhanced *P. aeruginosa* biofilm tolerance to ciprofloxacin, tobramycin and carbenicillin (Schiessl *et al.*, 2019). The authors propose that phenazines act as reducing agents in oxygen-depleted regions of the biofilm, thus aiding cellular metabolism (Schiessl *et al.*, 2019). This is supported by research showing that PCN and PYO play a role in shuttling oxygen from cells in oxic regions of biofilms to cells in anoxic regions (Saunders *et al.*, 2020). The mechanism by which phenazines promote tobramycin tolerance is thought to involve reduction of the proton motive force, as a result of altered respiration rates, but the mechanisms resulting in ciprofloxacin or carbenicillin tolerance are unclear (Schiessl *et al.*, 2019). The contribution of phenazines to meropenem tolerance could be tested using *P. aeruginosa* strains lacking phenazine biosynthetic genes, to observe whether the protective effect of *C. albicans* is lost. Supplementation of single-species *P. aeruginosa* biofilms with exogenous phenazines may reveal whether increased phenazine levels alone can enhance meropenem tolerance.

6.1.3.3 Potential role of the OprD porin

The outer membrane porin, OprD, facilitates entry of carbapenem antibiotics into *P. aeruginosa* cells, so *oprD* is often downregulated in meropenem-resistant strains (Khaledi *et al.*, 2016). Despite this, no significant change in *oprD* expression was observed in response to meropenem treatment of either single- or dual-species

biofilm cells. However, dual-species *P. aeruginosa* cells showed significant downregulation of genes involved in ribosome structure and protein translation, which was not observed in single-species, suggesting that the presence of *C. albicans* may inhibit protein translation in *P. aeruginosa.* Furthermore, previous research shows that there is often a poor correlation between *oprD* mRNA levels and OprD protein levels (Khaledi *et al.*, 2016). This raises the possibility that, despite a lack of significant change in *oprD* transcript abundance, there may be fewer OprD proteins being synthesised in dual-species *P. aeruginosa* cells, which could contribute to the observed enhancement of meropenem tolerance. To confirm this hypothesis, proteomic analysis of biofilm cells would need to be done.

6.2 Potentiation of amphotericin B activity against *C. albicans* in dual-species biofilms

6.2.1 Accumulation of intracellular ROS

6.2.1.1 Induction of ROS in *C. albicans*

This study showed significant upregulation of *P. aeruginosa* phenazine biosynthetic genes in response to *C. albicans* in a dual-species biofilm. *P. aeruginosa* phenazines have previously been shown to induce ROS production in *C. albicans* cells (Morales *et al.*, 2010), leading to the hypothesis that ROS induction could be a possible mechanism for the potentiation of AmB activity. This hypothesis is supported by the observation that dual-species biofilm formation with a *P. aeruginosa* strain lacking phenazine biosynthetic genes rescued *C. albicans* viability, relative to wild-

type. However, this evidence is limited by the lack of a definitive link between phenazine exposure and increased ROS levels.

Transcriptomic data showed that, in response to *P. aeruginosa*, the two most enriched KEGG pathways among significantly upregulated *C. albicans* genes were α-linolenic acid metabolism and arginine biosynthesis, both of which are associated with oxidative stress in *C. albicans* (Chen *et al.*, 2016, Jiménez-López *et al.*, 2013). Upregulation of α-linolenic acid metabolism genes is associated with increased peroxisomal activity, which includes the detoxification of ROS-derived H_2O_2 (Chen *et al.*, 2016); indeed, the *C. albicans* peroxisome KEGG pathway was also significantly enriched among significantly upregulated genes, in response to *P. aeruginosa*. Upregulation of arginine biosynthetic genes has previously been shown in *C. albicans* interactions with macrophages, in response to the phagocyte oxidative burst (Jiménez-López *et al.*, 2013). In addition, upregulation of *C. albicans* oxidative stress-associated genes, in response to *P. aeruginosa*, is supported by published transcriptomic studies (Fourie *et al.*, 2021, Grainha *et al.*, 2020, Doing *et al.*, 2020). Furthermore, supplementation of *C. albicans* biofilms with ROS-inducing agents enhanced AmB efficacy, which corroborates research showing that incubation with a superoxide generator significantly reduces the AmB MIC for *C. albicans* (Okamoto *et al.*, 2004).

6.2.1.2 Significant downregulation of *SOD2* in *C. albicans*

The *C. albicans* SOD enzymes, Sod1–6, are required for protection against oxidative damage (Martchenko *et al.*, 2004). ROS production is a mechanism of action of AmB (Mesa-Arango *et al.*, 2014) and, consequently, significant upregulation of

SOD2 is usually observed in AmB-treated *C. albicans* cells (Liu *et al.*, 2005). This was supported by the observation that removal of *SOD2* potentiated AmB activity against single-species *C. albicans* biofilm cells. Therefore, it would be reasonable to expect *C. albicans SOD* genes to be upregulated in response to *P. aeruginosa* cells that are overproducing ROS-inducing phenazine molecules (Morales *et al.*, 2010). However, significant downregulation of *C. albicans SOD* genes, including *SOD2*, was observed in dual-species biofilms. Therefore, it is possible that downregulation of *SOD2* may have led to increased *C. albicans* AmB susceptibility in the dual-species biofilm. This is in support of previous research showing that Sod2 is essential for protecting *A. fumigatus* cells from *P. aeruginosa* phenazine-induced ROS (Briard *et al.*, 2015).

These data suggest that increased *P. aeruginosa* phenazine production may induce oxidative stress in *C. albicans* biofilm cells by both increasing intracellular ROS levels and decreasing the removal of superoxide via downregulation of *SOD2*. The resultant accumulation of ROS is hypothesised to potentiate the activity of AmB against *C. albicans* biofilm cells (Figure 6.2). However, further research is needed to determine the exact mechanism linking ROS accumulation with enhanced AmB efficacy.

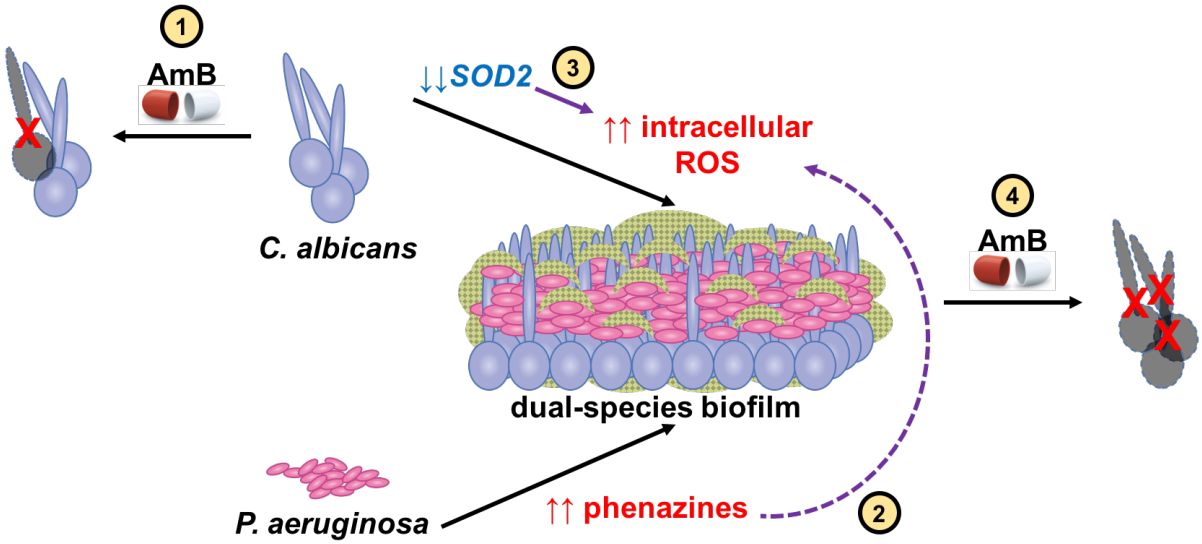


Figure 6.2. Proposed model for potentiation of AmB activity against *C. albicans* cells in a dual-species biofilm with *P. aeruginosa*. (1) Treatment of a single-species *C. albicans* biofilm with 2 μg/mL AmB kills some, but not all, cells. **(2)** In a dual-species biofilm, *P. aeruginosa* phenazine production is increased, which may induce an increase in *C. albicans* ROS levels. **(3)** The dual-species interaction also induces significant downregulation of *C. albicans SOD2*, inhibiting the removal of intracellular superoxide, and leading to a further increase in ROS levels. **(4)** The accumulation of intracellular ROS may result in potentiation of AmB activity, so treatment of dual-species biofilms with 2 μg/mL AmB is able to kill all *C. albicans* biofilm cells.
AmB, amphotericin B; ROS, reactive oxygen species.

6.2.2 Inhibition of hyphal formation

It is well established in the literature that *P. aeruginosa* inhibits hyphal formation in *C. albicans* biofilm cells via the actions of phenazines and QS molecules (Morales *et al.*, 2013, Hogan *et al.*, 2004, Grainha *et al.*, 2020). It was therefore unsurprising to observe significant downregulation of *C. albicans* genes involved in filamentous growth, such as *HWP1* and *HWP2*, alongside significant upregulation of *P. aeruginosa* QS and phenazine biosynthetic genes in dual-species biofilm cells. Furthermore, *P. aeruginosa* is known to bind to *C. albicans* hyphae and cause hyphal cell death via secretion of phenazines and phospholipase C (Dhamgaye *et al.*, 2016). As discussed previously, imaging of biofilms showed tight adherence of *P. aeruginosa* cells to *C.*

albicans hyphae. Therefore, the presence of *P. aeruginosa* may both inhibit hyphal formation and kill existing hyphal cells. The ability to form hyphae is associated with increased tolerance to antifungal treatment (Sharma *et al.*, 2019), so the reduction in numbers of hyphae may contribute to the potentiation of AmB activity against *C. albicans*. This is supported by the observation that the effect was only seen in true hyphae-forming *Candida* species, i.e. *C. albicans* and *C. dubliniensis*. A role for hyphal adherence is also supported by the observation that dual-species planktonic cultures did not show enhanced AmB activity. In planktonic cultures, *C. albicans* cells were predominantly in the yeast morphology, and the continual mixing of planktonic cells reduced the ability of *P. aeruginosa* to adhere to any hyphae present in the culture. This hypothesis could be investigated further by comparing the biofilm AmB susceptibility of wild-type strains against yeast-locked strains of *C. albicans* and *C. dubliniensis*.

6.2.3 Insights from transcriptomic data

6.2.3.1 Potential role of iron limitation

As discussed previously, *P. aeruginosa* pyoverdine biosynthetic genes were significantly upregulated in the presence of *C. albicans*. This may give *P. aeruginosa* cells an advantage in the inter-species competition for iron. Iron limitation is possibly a contributing factor in the reduction of *C. albicans* viability that was consistently observed in dual-species biofilms (by ~1–2 $\log_{10}$ *C. albicans* CFU/mL). This is supported by research showing that the sequestration of iron by *P. aeruginosa* siderophores can inhibit *C. albicans* growth (Trejo-Hernández *et al.*, 2014, Fourie *et al.*, 2018). Furthermore, there is evidence to suggest that the phenazine molecule 1-

HP, when present at high concentrations, may be able to chelate iron (Briard *et al.*, 2015, Fourie *et al.*, 2018). Therefore, enhanced *P. aeruginosa* iron acquisition, resulting from upregulation of siderophore (and potentially phenazine) biosynthetic genes, may contribute to reduced *C. albicans* viability in dual-species biofilms. In addition, it could be hypothesised that iron limitation may contribute to the increased susceptibility of *C. albicans* biofilm cells to AmB. This hypothesis is supported by research showing that, when grown under iron-limited conditions, *C. albicans* biofilm daughter cells (i.e. cells that have dispersed from the biofilm) show significantly increased susceptibility to AmB treatment (Baillie and Douglas, 1998).

6.3 Clinical implications

The enhanced meropenem tolerance of *P. aeruginosa*, in a dual-species biofilm with *C. albicans*, has direct implications for the treatment of co-infected patients. Following standard meropenem treatment, protected *P. aeruginosa* cells may disperse from the biofilm and seed new infections sites. Here, the cells may acquire true resistance, as a result of selection pressure from continued exposure to antibiotic treatment. In addition, the increased tolerance of dual-species *P.* aeruginosa biofilm cells may push the required meropenem concentration above the clinical breakpoint of >8 μg/mL (EuCAST, 2020a), resulting in the infection being classified as meropenem-resistant. This highlights the importance of early diagnosis of co-infection, in which combination antibiotic–antifungal therapy would be a more appropriate first-line therapy.

However, the data presented here also suggest that co-infection may enhance the effectiveness of AmB against *C. albicans*. Therefore, the order in which antimicrobial drugs are administered, as part of a combination therapy, is of vital importance. There is a lack of clinical data on the effects of *P. aeruginosa–C. albicans* co-infection on antifungal susceptibility, partly because there are no established treatment guidelines for cases of co-infection, so clinical practices are highly variable (Fourie and Pohl, 2019). These data indicate that it would be beneficial for AmB treatment to be administered prior to meropenem treatment. The potentiation effect of *P. aeruginosa* would possibly eradicate *C. albicans* cells from the biofilm co-infection. After this, *P. aeruginosa* cells could be treated with meropenem and, in the absence of any live *C. albicans*, there would be no protective effect and thus no enhanced tolerance. This stepwise combination therapy may therefore enhance the clearance of both species in a biofilm co-infection.

The potentiation of AmB by *P. aeruginosa* phenazines also has clinical implications for the treatment of single-species *C. albicans* biofilm infections, as it suggests the potential for improving the clinical efficacy of AmB therapy. Considering the toxicity of AmB at high doses (Kamiński, 2014), and the high cost per dose (Perlin *et al.*, 2017), a combination therapy that enables an AmB dose reduction could be beneficial in terms of both reduced side effects and costs. However, phenazines are toxic to mammalian cells (Vilaplana and Marco, 2020), which prohibits their use in combination with AmB. Furthermore, combining AmB with a ROS-inducing agent would also harm host cells through oxidative stress. The observed potentiation of AmB in a *C. albicans sod2*Δ/Δ strain raises the possibility of combining AmB treatment with an agent that

inhibits Sod2 activity. Considering Sod2 is an Mn-SOD, examining the effect of combining AmB with a manganese chelator may be a research direction worth pursuing. However, combining AmB with an Mn^{2+}-chelator would harm host cells because Mn^{2+} is essential for the normal functioning of Golgi in mammalian cells (Foulquier and Legrand, 2020). Therefore, the development of a drug combination that will work against fungal cells, without harming mammalian cells, is needed. This could potentially be in the form of a pro-drug that is inactive until metabolised through a fungal-specific pathway, such as is the case for the antifungal drug 5-fluorocytosine (5-FC). Once inside fungal cells, 5-FC is first deaminated to 5-fluorouracil (5-FU), which is fungistatic. 5-FU is eventually converted to 5-fluorouridine triphosphate, which disrupts RNA transcripts and inhibits the synthesis of essential proteins (Vermes *et al.*, 2000, Yu *et al.*, 2020). Therefore, further work is needed to develop a pro-drug for use in combination with AmB, which can specifically induce intracellular ROS or reduce Sod2 activity within fungal cells. Alternatively, packaging a ROS-inducing agent or a Sod2-inhibiting agent into AmBisome, which are commercially-available liposomal vesicles containing AmB (Walker *et al.*, 2018), may enable the targeted delivery of combination therapy to *C. albicans* cells.

6.4 FUTURE PERSPECTIVES

6.4.1 Enhancing *C. albicans* biofilm susceptibility to antifungals

The data presented here indicate a link between *P. aeruginosa* phenazines, *C. albicans SOD2*, ROS levels, and potentiation of AmB activity against *C. albicans* biofilm cells. However, the mechanisms by which these are linked is unclear. Sod2 is an Mn-SOD that is located in *C. albicans* mitochondria (Broxton and Culotta, 2016).

There are several studies that propose the induction of oxidative stress as a mechanism of action of AmB (Sokol-Anderson *et al.*, 1986, Okamoto *et al.*, 2004), including research showing that AmB induces ROS production specifically in the mitochondria of *A. fumigatus* (Shekhova *et al.*, 2017). Furthermore, inhibition of SODs is associated with enhanced AmB activity (De Brucker *et al.*, 2013, Briard *et al.*, 2015). Deletion of *SOD2*, in particular, is associated with increased *C. albicans* susceptibility to redox-cycling agents (Hwang *et al.*, 2003), and to *P. aeruginosa* phenazine-induced ROS (Briard *et al.*, 2015).

A greater understanding of the mechanisms governing these interactions may lead to the development of combination therapies that enhance the activity of AmB, and perhaps other antifungals, against *C. albicans* biofilms. Therefore, further research into how these factors interact to affect *C. albicans* antifungal susceptibility would be of great clinical interest.

6.4.2 A more clinically-relevant biofilm model

The work presented here proposes models for the mechanisms by which *C. albicans* enhances *P. aeruginosa* meropenem tolerance, and *P. aeruginosa* potentiates AmB activity against *C. albicans*, in a dual-species biofilm. However, these conclusions are based on *in vitro* assays, which somewhat limits the extent to which findings can be generalised.

The variability in phenotypic outcomes when using different *P. aeruginosa* strains in dual-species biofilm assays was discussed in Chapter 5. Such variability is also

observed in host-pathogen interaction studies; research into pathogenesis mechanisms of *P. aeruginosa* in alveolar and bronchial cells, using two reference strains (PAO1 and PA14) and three clinical isolates, showed that invasion rates and intracellular persistence differed greatly depending on the infecting *P. aeruginosa* strain (Del Mar Cendra and Torrents, 2020). This highlights the importance of choosing the most suitable *P. aeruginosa* strain, based on research objectives. In the present study, *C. albicans*-mediated enhancement of meropenem tolerance was confirmed in a *P. aeruginosa* CF strain. Furthermore, testing of clinical isolates confirmed that potentiation of AmB activity against *C. albicans* was observed in response to two different *P. aeruginosa* CF strains. Therefore, the data presented here provide a robust foundation for further enhancing the clinical impact of this research. In future, it would be interesting to replicate these findings using *P. aeruginosa* and *C. albicans* clinical strains co-isolated from the same patient.

The clinical implications of this research could be further supported by replicating the findings in a biofilm model that is more representative of the *in vivo* infection environment. For example, a recently optimised *ex vivo* porcine model of CF lung infection was shown to support the growth of complex biofilm structures that closely mimic those seen in explanted CF lung tissue, and which are absent from *in vitro* biofilm models (Harrington *et al.*, 2020). Therefore, an *ex vivo* porcine model would be a suitable biofilm model in which the findings of the present study could be confirmed in future.

REFERENCES

Adam, B., Baillie, G. S. and Douglas, L. J. (2002) 'Mixed species biofilms of *Candida albicans* and *Staphylococcus epidermidis*', *J Med Microbiol,* 51(4), pp. 344-349, doi: 10.1099/0022-1317-51-4-344.

Alhede, M., Bjarnsholt, T., Jensen, P. O., Phipps, R. K., Moser, C., Christophersen, L., Christensen, L. D., van Gennip, M., Parsek, M., Hoiby, N., Rasmussen, T. B. and Givskov, M. (2009) '*Pseudomonas aeruginosa* recognizes and responds aggressively to the presence of polymorphonuclear leukocytes', *Microbiology,* 155(Pt 11), pp. 3500-3508, doi: 10.1099/mic.0.031443-0.

Alim, D., Sircaik, S. and Panwar, S. L. (2018) 'The significance of lipids to biofilm formation in *Candida albicans*: an emerging perspective', *J Fungi (Basel),* 4(4), doi: 10.3390/jof4040140.

Anderson, T. M., Clay, M. C., Cioffi, A. G., Diaz, K. A., Hisao, G. S., Tuttle, M. D., Nieuwkoop, A. J., Comellas, G., Maryum, N., Wang, S., Uno, B. E., Wildeman, E. L., Gonen, T., Rienstra, C. M. and Burke, M. D. (2014) 'Amphotericin forms an extramembranous and fungicidal sterol sponge', *Nat Chem Biol,* 10(5), pp. 400-406.

Andrews, J. M. (2001) 'Determination of minimum inhibitory concentrations', *J Antimicrob Chemother,* 48(Suppl. S1), pp. 5–16.

Arnaud, M. B., Costanzo, M. C., Shah, P., Skrzypek, M. S. and Sherlock, G. (2009) 'Gene Ontology and the annotation of pathogen genomes: the case of *Candida albicans*', *Trends Microbiol,* 17(7), pp. 295-303, doi: 10.1016/j.tim.2009.04.007.

Arthur, J. R., Heinecke, K. A. and Seyfried, T. N. (2011) 'Filipin recognizes both GM1 and cholesterol in GM1 gangliosidosis mouse brain', *J Lipid Res,* 52(7), pp. 1345-1351, doi: 10.1194/jlr.M012633.

Ashburner, M., Ball, C. A., Blake, J. A., Botstein, D., Butler, H., Cherry, J. M., Davis, A. P., Dolinski, K., Dwight, S. S., Eppig, J. T., Harris, M. A., Hill, D. P., Issel-Tarver, L., Kasarkis, A., Lewis, S., Matese, J. C., Richardson, J. E., Ringwald, M., Rubin, G. M. and Sherlock, G. (2000) 'Gene Ontology: tool for the unification of biology', *Nat Genet,* 25, pp. 25-29.

Azoulay, E., Timsit, J.-F., Tafflet, M., de Lassence, A., Darmon, M., Zahar, J.-R., Adrie, C., Garrouste-Orgeas, M., Cohen, Y., Mourvillier, B. and Schlemmer, B. (2006) '*Candida* colonization of the respiratory tract and subsequent *Pseudomonas* ventilator-associated pneumonia', *Chest,* 129(1), pp. 110-117.

Azzam, S. Z., Cayme, G. J. and Martinez, L. R. (2019) 'Polymicrobial interactions involving fungi and their importance for the environment and in human disease', *Microb Pathog,* 140, pp. 103942, doi: 10.1016/j.micpath.2019.103942.

Bachmann, B. J. (1996) 'Derivations and genotypes of some mutant derivatives of *Escherichia coli* K-12', *In,* F. C. Neidhart *et al*. (ed.), *Escherichia coli* and *Salmonella*: cellular and molecular biology, 2nd ed., vol. 2. ASM Press, Washington, D.C.

Bae, J., Oh, E. and Jeon, B. (2014) 'Enhanced transmission of antibiotic resistance in *Campylobacter jejuni* biofilms by natural transformation', *Antimicrob Agents Chemother,* 58(12), pp. 7573-7575, doi: 10.1128/AAC.04066-14.

Bagge, N., Ciofu, O., Skovgaard, L. T. and Høiby, N. (2000) 'Rapid development *in vitro* and *in vivo* of resistance to ceftazidime in biofilm–growing *Pseudomonas aeruginosa* due to chromosomal ß-lactamase', *APMIS,* 108(9), pp. 589-600.

Bagge, N., Schuster, M., Hentzer, M., Ciofu, O., Givskov, M., Greenberg, E. P. and Hoiby, N. (2004) '*Pseudomonas aeruginosa* biofilms exposed to imipenem exhibit changes in global gene expression and beta-lactamase and alginate production', *Antimicrob Agents Chemother,* 48(4), pp. 1175-1187, doi: 10.1128/aac.48.4.1175-1187.2004.

Baillie, G. S. and Douglas, L. J. (1998) 'Iron-limited biofilms of *Candida albicans* and their susceptibility to amphotericin B', *Antimicrob Agents Chemother,* 42(8), pp. 2146-2149, doi: 10.1128/AAC.42.8.2146.

Bakare, N., Rickerts, V., Bargon, J. and Just-Nübling (2003) 'Prevalence of *Aspergillus fumigatus* and other fungal species in the sputum of adult patients with cystic fibrosis', *Mycoses,* 46(1-2), pp. 19-23.

Bamford, C. V., d'Mello, A., Nobbs, A. H., Dutton, L. C., Vickerman, M. M. and Jenkinson, H. F. (2009) '*Streptococcus gordonii* modulates *Candida albicans* biofilm formation through intergeneric communication', *Infect Immun,* 77(9), pp. 3696-3704, doi: 10.1128/IAI.00438-09.

Bandara, H., Hewavitharana, A. K., Shaw, P. N., Smyth, H. D. C. and Samaranayake, L. P. (2020a) 'A novel, quorum sensor-infused liposomal drug delivery system suppresses *Candida albicans* biofilms', *Int J Pharm,* 578, pp. 119096, doi: 10.1016/j.ijpharm.2020.119096.

Bandara, H. M., BP, K. C., Watt, R. M., Jin, L. J. and Samaranayake, L. P. (2013) '*Pseudomonas aeruginosa* lipopolysaccharide inhibits *Candida albicans* hyphae formation and alters gene expression during biofilm development', *Mol Oral Microbiol,* 28(1), pp. 54-69, doi: 10.1111/omi.12006.

Bandara, H. M., Yau, J. Y., Watt, R. M., Jin, L. J. and Samaranayake, L. P. (2009) '*Escherichia coli* and its lipopolysaccharide modulate *in vitro Candida* biofilm formation', *J Med Microbiol,* 58(Pt 12), pp. 1623-1631, doi: 10.1099/jmm.0.012989-0.

Bandara, H. M., Yau, J. Y., Watt, R. M., Jin, L. J. and Samaranayake, L. P. (2010) '*Pseudomonas aeruginosa* inhibits *in-vitro Candida* biofilm development', *BMC Microbiol,* 10, pp. 125, doi: 10.1186/1471-2180-10-125.

Bandara, H. M. H. N., Wood, D. L. A., Vanwonterghem, I., Hugenholtz, P., Cheung, B. P. K. and Samaranayake, L. P. (2020b) 'Fluconazole resistance in *Candida albicans* is induced by *Pseudomonas aeruginosa* quorum sensing', *Sci Rep,* 10(1), pp. 7769, doi: 10.1038/s41598-020-64761-3.

Banin, E., Vasil, M. L. and Greenberg, E. P. (2005) 'Iron and *Pseudomonas aeruginosa* biofilm formation', *Proc Natl Acad Sci U S A,* 102(31), pp. 11076-11081, doi: 10.1073/pnas.0504266102.

Bates, S., MacCallum, D. M., Bertram, G., Munro, C. A., Hughes, H. B., Buurman, E. T., Brown, A. J., Odds, F. C. and Gow, N. A. (2005) '*Candida albicans* Pmr1p, a secretory pathway P-type Ca2+/Mn2+-ATPase, is required for glycosylation and virulence', *J Biol Chem,* 280(24), pp. 23408-23415, doi: 10.1074/jbc.M502162200.

Beaudoin, T., Yau, Y. C. W., Stapleton, P. J., Gong, Y., Wang, P. W., Guttman, D. S. and Waters, V. (2017) '*Staphylococcus aureus* interaction with *Pseudomonas aeruginosa* biofilm enhances tobramycin resistance', *NPJ Biofilms Microbiomes,* 3, pp. 25, doi: 10.1038/s41522-017-0035-0.

Beaudoin, T., Zhang, L., Hinz, A. J., Parr, C. J. and Mah, T. F. (2012) 'The biofilm-specific antibiotic resistance gene *ndvB* is important for expression of ethanol oxidation genes in *Pseudomonas aeruginosa* biofilms', *J Bacteriol,* 194(12), pp. 3128-3136, doi: 10.1128/JB.06178-11.

Bellmann, R. and Smuszkiewicz, P. (2017) 'Pharmacokinetics of antifungal drugs: practical implications for optimized treatment of patients', *Infection,* 45(6), pp. 737-779, doi: 10.1007/s15010-017-1042-z.

Bergeron, A. C., Seman, B. G., Hammond, J. H., Archambault, L. S., Hogan, D. A. and Wheeler, R. T. (2017) '*Candida* and *Pseudomonas* interact to enhance virulence of mucosal infection in transparent zebrafish', *Infect Immun*, doi: 10.1128/IAI.00475-17.

Bernard, C., Renaudeau, N., Mollichella, M. L., Quellard, N., Girardot, M. and Imbert, C. (2018) '*Cutibacterium acnes* protects *Candida albicans* from the effect of micafungin in biofilms', *Int J Antimicrob Agents,* 52(6), pp. 942-946, doi: 10.1016/j.ijantimicag.2018.08.009.

Bink, A., Vandenbosch, D., Coenye, T., Nelis, H., Cammue, B. P. and Thevissen, K. (2011) 'Superoxide dismutases are involved in *Candida albicans* biofilm persistence against miconazole', *Antimicrob Agents Chemother,* 55(9), pp. 4033-4037, doi: 10.1128/AAC.00280-11.

Bjarnsholt, T., Jensen, P. Ø., Burmolle, M., Hentzer, M., Haagensen, J. A., Hougen, H. P., Calum, H., Madsen, K. G., Moser, C., Molin, S., Høiby, N. and Givskov, M. (2005) '*Pseudomonas aeruginosa* tolerance to tobramycin, hydrogen peroxide and polymorphonuclear leukocytes is quorum-sensing dependent', *Microbiology,* 151(Pt 2), pp. 373-383, doi: 10.1099/mic.0.27463-0.

Bojang, E., Ghuman, H., Kumwenda, P. and Hall, R. A. (2021) 'Immune sensing of *Candida albicans*', *Journal of Fungi,* 7(2), doi: 10.3390/jof7020119.

Boles, B. R. and Singh, P. K. (2008) 'Endogenous oxidative stress produces diversity and adaptability in biofilm communities', *Proc Natl Acad Sci U S A,* 105(34), pp. 12503-12508.

Boon, C., Deng, Y., Wang, L. H., He, Y., Xu, J. L., Fan, Y., Pan, S. Q. and Zhang, L. H. (2008) 'A novel DSF-like signal from *Burkholderia cenocepacia* interferes with *Candida albicans* morphological transition', *ISME J,* 2(1), pp. 27-36, doi: 10.1038/ismej.2007.76.

Borah, S. N., Sen, S., Goswami, L., Bora, A., Pakshirajan, K. and Deka, S. (2019) 'Rice based distillers dried grains with solubles as a low cost substrate for the production of a novel rhamnolipid biosurfactant having anti-biofilm activity against *Candida tropicalis*', *Colloids Surf B Biointerfaces,* 182, pp. 110358, doi: 10.1016/j.colsurfb.2019.110358.

Botelho, J., Grosso, F. and Peixe, L. (2019) 'Antibiotic resistance in *Pseudomonas aeruginosa* - Mechanisms, epidemiology and evolution', *Drug Resist Updat,* 44, pp. 100640, doi: 10.1016/j.drup.2019.07.002.

Bowler, L. L., Zhanel, G. G., Ball, T. B. and Saward, L. L. (2012) 'Mature *Pseudomonas aeruginosa* biofilms prevail compared to young biofilms in the presence of ceftazidime', *Antimicrob Agents Chemother,* 56(9), pp. 4976-4979, doi: 10.1128/AAC.00650-12.

Brand, A., Barnes, J. D., Mackenzie, K. S., Odds, F. C. and Gow, N. A. (2008) 'Cell wall glycans and soluble factors determine the interactions between the hyphae of *Candida albicans* and *Pseudomonas aeruginosa*', *FEMS Microbiol Lett,* 287(1), pp. 48-55, doi: 10.1111/j.1574-6968.2008.01301.x.

Briard, B., Bomme, P., Lechner, B. E., Mislin, G. L., Lair, V., Prevost, M. C., Latge, J. P., Haas, H. and Beauvais, A. (2015) '*Pseudomonas aeruginosa* manipulates redox and iron homeostasis of its microbiota partner *Aspergillus fumigatus* via phenazines', *Sci Rep,* 5, pp. 8220, doi: 10.1038/srep08220.

Broxton, C. N. and Culotta, V. C. (2016) 'SOD enzymes and microbial pathogens: surviving the oxidative storm of infection', *PLoS Pathog,* 12(1), pp. e1005295, doi: 10.1371/journal.ppat.1005295.

Bruno, V. M., Shetty, A. C., Yano, J., Fidel, P. L., Jr., Noverr, M. C. and Peters, B. M. (2015) 'Transcriptomic analysis of vulvovaginal candidiasis identifies a role for the NLRP3 inflammasome', *mBio,* 6(2), doi: 10.1128/mBio.00182-15.

Cabral, D. J., Penumutchu, S., Norris, C., Morones-Ramirez, J. R. and Belenky, P. (2018) 'Microbial competition between *Escherichia coli* and *Candida albicans* reveals a soluble fungicidal factor', *Microb Cell,* 5(5), pp. 249-255, doi: 10.15698/mic2018.05.631.

Cannon, R. D., Lamping, E., Holmes, A. R., Niimi, K., Baret, P. V., Keniya, M. V., Tanabe, K., Niimi, M., Goffeau, A. and Monk, B. C. (2009) 'Efflux-mediated antifungal drug resistance', *Clin Microbiol Rev,* 22(2), pp. 291-321, doi: 10.1128/CMR.00051-08.

Carcas, A. J., García-Satué, J. L., Zapater, P. and Frías-Iniesta, J. (1999) 'Tobramycin penetration into epithelial lining fluid of patients with pneumonia', *Clin Pharmacol Ther,* 65(3), pp. 245-250.

Cavalheiro, M. and Teixeira, M. C. (2018) '*Candida* biofilms: threats, challenges, and promising strategies', *Front Med (Lausanne),* 5, pp. 28, doi: 10.3389/fmed.2018.00028.

Centers for Disease Control and Prevention (2019) 'Antibiotic resistance threats in the United States', *U.S. Department of Health and Human Services,* Atlanta, GA.

Ceresa, C., Tessarolo, F., Maniglio, D., Tambone, E., Carmagnola, I., Fedeli, E., Caola, I., Nollo, G., Chiono, V., Allegrone, G., Rinaldi, M. and Fracchia, L. (2019) 'Medical-grade silicone coated with rhamnolipid R89 Is effective against *Staphylococcus* spp. biofilms', *Molecules,* 24(21), doi: 10.3390/molecules24213843.

Chambers, J. R., Liao, J., Schurr, M. J. and Sauer, K. (2014) 'BrlR from *Pseudomonas aeruginosa* is a c-di-GMP-responsive transcription factor', *Mol Microbiol,* 92(3), pp. 471-487, doi: 10.1111/mmi.12562.

Chandler, C. E., Horspool, A. M., Hill, P. J., Wozniak, D. J., Schertzer, J. W., Rasko, D. A. and Ernst, R. K. (2018) 'Genomic and phenotypic diversity among ten laboratory isolates of *Pseudomonas aeruginosa* PAO1', *J Bacteriol*, doi: 10.1128/JB.00595-18.

Chatterjee, M., Anju, C. P., Biswas, L., Anil Kumar, V., Gopi Mohan, C. and Biswas, R. (2016) 'Antibiotic resistance in *Pseudomonas aeruginosa* and alternative therapeutic options', *Int J Med Microbiol,* 306(1), pp. 48-58, doi: 10.1016/j.ijmm.2015.11.004.

Chatterjee, P., Sass, G., Swietnicki, W. and Stevens, D. A. (2020) 'Review of potential *Pseudomonas* weaponry, relevant to the *Pseudomonas-Aspergillus* interplay, for the mycology community', *J Fungi (Basel),* 6(2), doi: 10.3390/jof6020081.

Chen, A. I., Dolben, E. F., Okegbe, C., Harty, C. E., Golub, Y., Thao, S., Ha, D. G., Willger, S. D., O'Toole, G. A., Harwood, C. S., Dietrich, L. E. and Hogan, D. A. (2014)

'*Candida albicans* ethanol stimulates *Pseudomonas aeruginosa* WspR-controlled biofilm formation as part of a cyclic relationship involving phenazines', *PLoS Pathog,* 10(10), pp. e1004480, doi: 10.1371/journal.ppat.1004480.

Chen, L., Zou, Y., Kronfl, A. A. and Wu, Y. (2020) 'Type VI secretion system of *Pseudomonas aeruginosa* is associated with biofilm formation but not environmental adaptation', *Microbiologyopen,* 9(3), pp. e991, doi: 10.1002/mbo3.991.

Chen, L., Zou, Y., She, P. and Wu, Y. (2015) 'Composition, function, and regulation of T6SS in *Pseudomonas aeruginosa*', *Microbiol Res,* 172, pp. 19-25, doi: 10.1016/j.micres.2015.01.004.

Chen, Y., Yu, Q., Wang, H., Dong, Y., Jia, C., Zhang, B., Xiao, C., Zhang, B., Xing, L. and Li, M. (2016) 'The malfunction of peroxisome has an impact on the oxidative stress sensitivity in *Candida albicans*', *Fungal Genet Biol,* 95, pp. 1-12, doi: 10.1016/j.fgb.2016.07.010.

Chen, Y. L., Kauffman, S. and Reynolds, T. B. (2008) '*Candida albicans* uses multiple mechanisms to acquire the essential metabolite inositol during infection', *Infect Immun,* 76(6), pp. 2793-2801, doi: 10.1128/IAI.01514-07.

Cheng, K., Smyth, R. L., Govan, J. R. W., Doherty, C., Winstanley, C., Denning, N., Heaf, D. P., van Saene, H. and Hart, C. A. (1996) 'Spread of β-lactam-resistant *Pseudomonas aeruginosa* in a cystic fibrosis clinic', *The Lancet,* 348(9028), pp. 639-642, doi: 10.1016/s0140-6736(96)05169-0.

Chiang, W. C., Nilsson, M., Jensen, P. Ø., Høiby, N., Nielsen, T. E., Givskov, M. and Tolker-Nielsen, T. (2013) 'Extracellular DNA shields against aminoglycosides in *Pseudomonas aeruginosa* biofilms', *Antimicrob Agents Chemother,* 57(5), pp. 2352-2361, doi: 10.1128/AAC.00001-13.

Choi, D. S., Kim, D. K., Choi, S. J., Lee, J., Choi, J. P., Rho, S., Park, S. H., Kim, Y. K., Hwang, D. and Gho, Y. S. (2011) 'Proteomic analysis of outer membrane vesicles derived from *Pseudomonas aeruginosa*', *Proteomics,* 11(16), pp. 3424-3429, doi: 10.1002/pmic.201000212.

Chotirmall, S. H., Greene, C. M. and McElvaney, N. G. (2010) '*Candida* species in cystic fibrosis: a road less travelled', *Medical Mycology,* 48(O1), pp. S114-S124, doi: 10.3109/13693786.2010.503320.

Ciofu, O., Beveridge, T. J., Kadurugamuwa, J., Walther-Rasmussen, J. and Høiby, N. (2000) 'Chromosomal β-lactamase is packaged into membrane vesicles and secreted from *Pseudomonas aeruginosa*', *J Antimicrob Chemother,* 45(1), pp. 9-13, doi: 10.1093/jac/45.1.9.

Conesa, A., Madrigal, P., Tarazona, S., Gomez-Cabrero, D., Cervera, A., McPherson, A., Szczesniak, M. W., Gaffney, D. J., Elo, L. L., Zhang, X. and Mortazavi, A. (2016)

'A survey of best practices for RNA-seq data analysis', *Genome Biol,* 17, pp. 13, doi: 10.1186/s13059-016-0881-8.

Cousson, J., Floch, T., Guillard, T., Vernet, V., Raclot, P., Wolak-Thierry, A. and Jolly, D. (2015) 'Lung concentrations of ceftazidime administered by continuous versus intermittent infusion in patients with ventilator-associated pneumonia', *Antimicrob Agents Chemother,* 59(4), pp. 1905-1909, doi: 10.1128/AAC.04232-14.

Crousilles, A., Maunders, E., Bartlett, S., Fan, C., Ukor, E.-F., Abdelhamid, Y., Baker, Y., Floto, A., Spring, D. R. and Welch, M. (2015) 'Which microbial factors really are important in *Pseudomonas aeruginosa* infections?', *Future Microbiol,* 10(11), pp. 1825-1836.

Cugini, C., Morales, D. K. and Hogan, D. A. (2010) '*Candida albicans*-produced farnesol stimulates *Pseudomonas* quinolone signal production in LasR-defective *Pseudomonas aeruginosa* strains', *Microbiology,* 156(Pt 10), pp. 3096-3107, doi: 10.1099/mic.0.037911-0.

Cystic Fibrosis Trust (2009) 'Antibiotic treatment for cystic fibrosis: report of the UK Cystic Fibrosis Trust antibiotic working group. 3rd Ed.', https://www.cysticfibrosis.org.uk/~/media/documents/life-with-cf/care-and-treatment/cd_antibiotic_treatment_for_cf_may_09.ashx?la=en.

Das, T. and Manefield, M. (2012) 'Pyocyanin promotes extracellular DNA release in *Pseudomonas aeruginosa*', *PLoS One,* 7(10), pp. e46718, doi: 10.1371/journal.pone.0046718.t001.

Davey, M. E., Caiazza, N. C. and O'Toole, G. A. (2003) 'Rhamnolipid surfactant production affects biofilm architecture in *Pseudomonas aeruginosa* PAO1', *J Bacteriol,* 185(3), pp. 1027-1036, doi: 10.1128/jb.185.3.1027-1036.2003.

Davies, J. and Davies, D. (2010) 'Origins and evolution of antibiotic resistance', *Microbiol Mol Biol Rev,* 74(3), pp. 417-433, doi: 10.1128/MMBR.00016-10.

De Brucker, K., Bink, A., Meert, E., Cammue, B. P. and Thevissen, K. (2013) 'Potentiation of antibiofilm activity of amphotericin B by superoxide dismutase inhibition', *Oxid Med Cell Longev,* 2013, pp. 704654, doi: 10.1155/2013/704654.

De Brucker, K., Tan, Y., Vints, K., De Cremer, K., Braem, A., Verstraeten, N., Michiels, J., Vleugels, J., Cammue, B. P. and Thevissen, K. (2015) 'Fungal ß-1,3-glucan increases ofloxacin tolerance of *Escherichia coli* in a polymicrobial *E. coli*/*Candida albicans* biofilm', *Antimicrob Agents Chemother,* 59(6), pp. 3052-3058, doi: 10.1128/AAC.04650-14.

De Kievit, T. R., Parkins, M. D., Gillis, R. J., Srikumar, R., Ceri, H., Poole, K., Iglewski, B. H. and Storey, D. G. (2001) 'Multidrug efflux pumps: expression patterns and contribution to antibiotic resistance in *Pseudomonas aeruginosa* biofilms', *Antimicrob Agents Chemother,* 45(6), pp. 1761-1770, doi: 10.1128/AAC.45.6.1761-1770.2001.

de Kraker, M. E., Stewardson, A. J. and Harbarth, S. (2016) 'Will 10 million people die a year due to antimicrobial resistance by 2050?', *PLoS Med,* 13(11), pp. e1002184, doi: 10.1371/journal.pmed.1002184.

Del Mar Cendra, M. and Torrents, E. (2020) 'Differential adaptability between reference strains and clinical isolates of *Pseudomonas aeruginosa* into the lung epithelium intracellular lifestyle', *Virulence,* 11(1), pp. 862-876, doi: 10.1080/21505594.2020.1787034.

Dhamgaye, S., Qu, Y. and Peleg, A. Y. (2016) 'Polymicrobial infections involving clinically relevant Gram-negative bacteria and fungi', *Cell Microbiol,* 18(12), pp. 1716-1722, doi: 10.1111/cmi.12674.

Dietrich, L. E., Okegbe, C., Price-Whelan, A., Sakhtah, H., Hunter, R. C. and Newman, D. K. (2013) 'Bacterial community morphogenesis is intimately linked to the intracellular redox state', *J Bacteriol,* 195(7), pp. 1371-1380, doi: 10.1128/JB.02273-12.

Dietrich, L. E., Price-Whelan, A., Petersen, A., Whiteley, M. and Newman, D. K. (2006) 'The phenazine pyocyanin is a terminal signalling factor in the quorum sensing network of *Pseudomonas aeruginosa*', *Mol Microbiol,* 61(5), pp. 1308-1321, doi: 10.1111/j.1365-2958.2006.05306.x.

Diggle, S. P. and Whiteley, M. (2020) 'Microbe Profile: *Pseudomonas aeruginosa*: opportunistic pathogen and lab rat', *Microbiology,* 166(1), pp. 30-33, doi: 10.1099/mic.0.000860.

Dixon, E. F. and Hall, R. A. (2015) 'Noisy neighbourhoods: quorum sensing in fungal-polymicrobial infections', *Cell Microbiol,* 17(10), pp. 1431-1441, doi: 10.1111/cmi.12490.

Doing, G., Koeppen, K., Occipinti, P., Harty, C. E. and Hogan, D. A. (2020) 'Conditional antagonism in co-cultures of *Pseudomonas aeruginosa* and *Candida albicans*: an intersection of ethanol and phosphate signaling distilled from dual-seq transcriptomics', *PLoS Genet,* 16(8), pp. e1008783, doi: 10.1371/journal.pgen.1008783.

Dominguez, E., Zarnowski, R., Sanchez, H., Covelli, A. S., Westler, W. M., Azadi, P., Nett, J., Mitchell, A. P. and Andes, D. R. (2018) 'Conservation and divergence in the *Candida* species biofilm matrix mannan-glucan complex structure, function, and genetic control', *mBio,* 9(2), doi: 10.1128/mBio.00451-18.

Dubern, J. F., Cigana, C., De Simone, M., Lazenby, J., Juhas, M., Schwager, S., Bianconi, I., Doring, G., Eberl, L., Williams, P., Bragonzi, A. and Camara, M. (2015) 'Integrated whole-genome screening for *Pseudomonas aeruginosa* virulence genes using multiple disease models reveals that pathogenicity is host specific', *Environ Microbiol,* 17(11), pp. 4379-4393, doi: 10.1111/1462-2920.12863.

Dutton, L. C., Jenkinson, H. F., Lamont, R. J. and Nobbs, A. H. (2016a) 'Role of *Candida albicans* secreted aspartyl protease Sap9 in interkingdom biofilm formation', *Pathog Dis,* 74(3), doi: 10.1093/femspd/ftw005.

Dutton, L. C., Paszkiewicz, K. H., Silverman, R. J., Splatt, P. R., Shaw, S., Nobbs, A. H., Lamont, R. J., Jenkinson, H. F. and Ramsdale, M. (2016b) 'Transcriptional landscape of trans-kingdom communication between *Candida albicans* and *Streptococcus gordonii*', *Mol Oral Microbiol,* 31(2), pp. 136-161, doi: 10.1111/omi.12111.

Dwyer, D. J., Collins, J. J. and Walker, G. C. (2015) 'Unraveling the physiological complexities of antibiotic lethality', *Annu Rev Pharmacol Toxicol,* 55, pp. 313-332, doi: 10.1146/annurev-pharmtox-010814-124712.

Dwyer, D. J., Kohanski, M. A. and Collins, J. J. (2009) 'Role of reactive oxygen species in antibiotic action and resistance', *Curr Opin Microbiol,* 12(5), pp. 482-489, doi: 10.1016/j.mib.2009.06.018.

Engel, J. and Balachandran, P. (2009) 'Role of *Pseudomonas aeruginosa* type III effectors in disease', *Curr Opin Microbiol,* 12(1), pp. 61-66, doi: 10.1016/j.mib.2008.12.007.

Engel, L. S., Hill, J. M., Caballero, A. R., Green, L. C. and O'Callaghan, R. J. (1998) 'Protease IV, a unique extracellular protease and virulence factor from *Pseudomonas aeruginosa*', *Journal of Biological Chemistry,* 273(27), pp. 16792-16797, doi: 10.1074/jbc.273.27.16792.

EuCAST (2020a) 'Breakpoint tables for interpretation of MICs and zone diameters. Version 10.0', *European Committee on Antimicrobial Susceptibility Testing,* http://www.eucast.org/.

EuCAST (2020b) 'Breakpoint tables for interpretation of MICs for antifungal agents, version 10.0', *European Committee on Antimicrobial Susceptibility Testing,* http://www.eucast.org/astoffungi/clinicalbreakpointsforantifungals/.

Feinbaum, R. L., Urbach, J. M., Liberati, N. T., Djonovic, S., Adonizio, A., Carvunis, A. R. and Ausubel, F. M. (2012) 'Genome-wide identification of *Pseudomonas aeruginosa* virulence-related genes using a *Caenorhabditis elegans* infection model', *PLoS Pathog,* 8(7), pp. e1002813, doi: 10.1371/journal.ppat.1002813.

Fernandez, L. and Hancock, R. E. (2012) 'Adaptive and mutational resistance: role of porins and efflux pumps in drug resistance', *Clin Microbiol Rev,* 25(4), pp. 661-681, doi: 10.1128/CMR.00043-12.

Fernandez, R., Amador, P. and Prudêncio, C. (2013) 'β-lactams: chemical structure, mode of action and mechanisms of resistance', *Rev Med Microbiol,* 24(1), pp. 7-17.

Fields Jr., B. T., Bates, J. H. and Abernathy, R. S. (1970) 'Amphotericin B serum concentrations during therapy', *J Appl Microbiol,* 19(6), pp. 955-959.

Filloux, A. (2011) 'Protein secretion systems in *Pseudomonas aeruginosa*: an essay on diversity, evolution, and function', *Front Microbiol,* 2, pp. 155, doi: 10.3389/fmicb.2011.00155.

Flemming, H. C. and Wingender, J. (2010) 'The biofilm matrix', *Nat Rev Microbiol,* 8(9), pp. 623-633, doi: 10.1038/nrmicro2415.

Folders, J., Algra, J., Roelofs, M. S., van Loon, L. C., Tommassen, J. and Bitter, W. (2001) 'Characterization of *Pseudomonas aeruginosa* chitinase, a gradually secreted protein', *J Bacteriol,* 183(24), pp. 7044-7052, doi: 10.1128/JB.183.24.7044-7052.2001.

Foulquier, F. and Legrand, D. (2020) 'Biometals and glycosylation in humans: congenital disorders of glycosylation shed lights into the crucial role of Golgi manganese homeostasis', *Biochim Biophys Acta Gen Subj,* 1864(10), pp. 129674, doi: 10.1016/j.bbagen.2020.129674.

Fourie, R., Cason, E. D., Albertyn, J. and Pohl, C. H. (2021) 'Transcriptional response of *Candida albicans* to *Pseudomonas aeruginosa* in a polymicrobial biofilm', *G3 (Bethesda)*, doi: 10.1093/g3journal/jkab042.

Fourie, R., Kuloyo, O. O., Mochochoko, B. M., Albertyn, J. and Pohl, C. H. (2018) 'Iron at the centre of *Candida albicans* interactions', *Front Cell Infect Microbiol,* 8, pp. 185, doi: 10.3389/fcimb.2018.00185.

Fourie, R. and Pohl, C. H. (2019) 'Beyond antagonism: the interaction between *Candida* species and *Pseudomonas aeruginosa*', *J Fungi (Basel),* 5(2), doi: 10.3390/jof5020034.

Fowler, R. C. and Hanson, N. D. (2014) 'Emergence of carbapenem resistance due to the novel insertion sequence IS*Pa*8 in *Pseudomonas aeruginosa*', *PLoS One,* 9(3), pp. e91299, doi: 10.1371/journal.pone.0091299.

Fox, E. P., Cowley, E. S., Nobile, C. J., Hartooni, N., Newman, D. K. and Johnson, A. D. (2014) 'Anaerobic bacteria grow within *Candida albicans* biofilms and induce biofilm formation in suspension cultures', *Curr Biol,* 24(20), pp. 2411-2416, doi: 10.1016/j.cub.2014.08.057.

Frederiksen, R. F., Paspaliari, D. K., Larsen, T., Storgaard, B. G., Larsen, M. H., Ingmer, H., Palcic, M. M. and Leisner, J. J. (2013) 'Bacterial chitinases and chitin-binding proteins as virulence factors', *Microbiology,* 159(Pt 5), pp. 833-847, doi: 10.1099/mic.0.051839-0.

Fusté, E., López-Jiménez, L., Segura, C., Gainza, E., Vinuesa, T. and Viñas, M. (2013) 'Carbapenem-resistance mechanisms of multidrug-resistant *Pseudomonas aeruginosa*', *J Med Microbiol,* 62(Pt 9), pp. 1317-1325, doi: 10.1099/jmm.0.058354-0.

Gaddy, J. A., Tomaras, A. P. and Actis, L. A. (2009) 'The *Acinetobacter baumannii* 19606 OmpA protein plays a role in biofilm formation on abiotic surfaces and in the interaction of this pathogen with eukaryotic cells', *Infect Immun,* 77(8), pp. 3150-3160, doi: 10.1128/IAI.00096-09.

Gilbert, J., Abramson, D., McCallum, B. and Clear, R. (2002) 'Comparison of Canadian *Fusarium graminearum* isolates for aggressiveness, vegetative compatibility, and production of ergosterol and mycotoxins', *Mycopathologia,* 153, pp. 209-215.

Gileles-Hillel, A., Shoseyov, D., Polacheck, I., Korem, M., Kerem, E. and Cohen-Cymberknoh, M. (2015) 'Association of chronic *Candida albicans* respiratory infection with a more severe lung disease in patients with cystic fibrosis', *Pediatr Pulmonol,* 50(11), pp. 1082-1089, doi: 10.1002/ppul.23302.

Gillis, R. J., White, K. G., Choi, K. H., Wagner, V. E., Schweizer, H. P. and Iglewski, B. H. (2005) 'Molecular basis of azithromycin-resistant *Pseudomonas aeruginosa* biofilms', *Antimicrob Agents Chemother,* 49(9), pp. 3858-3867, doi: 10.1128/AAC.49.9.3858-3867.2005.

Gotfried, M. H., Danziger, L. H. and Rodvold, K. A. (2001) 'Steady-state plasma and intrapulmonary concentrations of levofloxacin and ciprofloxacin in healthy adult subjects', *Chest,* 119(4), pp. 1114-1122, doi: 10.1378/chest.119.4.1114.

Gow, N. A., van de Veerdonk, F. L., Brown, A. J. and Netea, M. G. (2012) '*Candida albicans* morphogenesis and host defence: discriminating invasion from colonization', *Nat Rev Microbiol,* 10(2), pp. 112-122, doi: 10.1038/nrmicro2711.

Gow, N. A. R. and Yadav, B. (2017) 'Microbe Profile: *Candida albicans*: a shape-changing, opportunistic pathogenic fungus of humans', *Microbiology,* 163(8), pp. 1145-1147, doi: 10.1099/mic.0.000499.

Graham, C. E., Cruz, M. R., Garsin, D. A. and Lorenz, M. C. (2017) '*Enterococcus faecalis* bacteriocin EntV inhibits hyphal morphogenesis, biofilm formation, and virulence of *Candida albicans*', *Proc Natl Acad Sci U S A,* 114(17), pp. 4507-4512, doi: 10.1073/pnas.1620432114.

Grainha, T., Jorge, P., Alves, D., Lopes, S. P. and Pereira, M. O. (2020) 'Unraveling *Pseudomonas aeruginosa* and *Candida albicans* communication in coinfection scenarios: insights through network analysis', *Frontiers in Cellular and Infection Microbiology,* 10, , doi: 10.3389/fcimb.2020.550505.

Grela, E., Zdybicka-Barabas, A., Pawlikowska-Pawlega, B., Cytrynska, M., Wlodarczyk, M., Grudzinski, W., Luchowski, R. and Gruszecki, W. I. (2019) 'Modes of

the antibiotic activity of amphotericin B against *Candida albicans*', *Scientific Reports,* 9(1), doi: 10.1038/s41598-019-53517-3.

Haagensen, J. A., Verotta, D., Huang, L., Spormann, A. and Yang, K. (2015) 'New *in vitro* model to study the effect of human simulated antibiotic concentrations on bacterial biofilms', *Antimicrob Agents Chemother,* 59(7), pp. 4074-4081, doi: 10.1128/AAC.05037-14.

Haiko, J., Saeedi, B., Bagger, G., Karpati, F. and Özenci, V. (2019) 'Coexistence of *Candida* species and bacteria in patients with cystic fibrosis', *Eur J Clin Microbiol Infect Dis*, doi: 10.1007/s10096-019-03493-3.

Hall, C. W. and Mah, T. F. (2017) 'Molecular mechanisms of biofilm-based antibiotic resistance and tolerance in pathogenic bacteria', *FEMS Microbiol Rev,* 41(3), pp. 276-301, doi: 10.1093/femsre/fux010.

Hall, R. A., Bates, S., Lenardon, M. D., Maccallum, D. M., Wagener, J., Lowman, D. W., Kruppa, M. D., Williams, D. L., Odds, F. C., Brown, A. J. and Gow, N. A. (2013) 'The Mnn2 mannosyltransferase family modulates mannoprotein fibril length, immune recognition and virulence of *Candida albicans*', *PLoS Pathog,* 9(4), pp. e1003276, doi: 10.1371/journal.ppat.1003276.

Hamet, M., Pavon, A., Dalle, F., Pechinot, A., Prin, S., Quenot, J.-P. and Charles, P.-E. (2012) '*Candida* spp. airway colonization could promote antibiotic-resistant bacteria selection in patients with suspected ventilator-associated pneumonia', *Intensive Care Med,* 38(8), pp. 1272-1279, doi: 10.1007/s00134-012-2587-z.

Hanahan, D., Jessee, J. and Bloom, F. R. (1991) 'Plasmid transformation of *Escherichia coli* and other bacteria', *Method Enzymol,* 204, pp. 63-113.

Harrington, N. E., Sweeney, E. and Harrison, F. (2020) 'Building a better biofilm - formation of *in vivo*-like biofilm structures by *Pseudomonas aeruginosa* in a porcine model of cystic fibrosis lung infection', *Biofilm,* 2, pp. 100024, doi: 10.1016/j.bioflm.2020.100024.

Harriott, M. M. and Noverr, M. C. (2009) '*Candida albicans* and *Staphylococcus aureus* form polymicrobial biofilms: effects on antimicrobial resistance', *Antimicrob Agents Chemother,* 53(9), pp. 3914-3922, doi: 10.1128/AAC.00657-09.

Hassuna, N. A., Darwish, M. K., Sayed, M. and Ibrahem, R. A. (2020) 'Molecular epidemiology and mechanisms of high-level resistance to meropenem and imipenem in *Pseudomonas aeruginosa*', *Infect Drug Resist,* 13, pp. 285-293, doi: 10.2147/IDR.S233808.

Hauryliuk, V., Atkinson, G. C., Murakami, K. S., Tenson, T. and Gerdes, K. (2015) 'Recent functional insights into the role of (p)ppGpp in bacterial physiology', *Nat Rev Microbiol,* 13(5), pp. 298-309, doi: 10.1038/nrmicro3448.

He, J., Kim, D., Zhou, X., Ahn, S. J., Burne, R. A., Richards, V. P. and Koo, H. (2017) 'RNA-seq reveals enhanced sugar metabolism in *Streptococcus mutans* co-cultured with *Candida albicans* within mixed-species biofilms', *Front Microbiol,* 8, pp. 1036, doi: 10.3389/fmicb.2017.01036.

Higgins, S., Heeb, S., Rampioni, G., Fletcher, M. P., Williams, P. and Camara, M. (2018) 'Differential regulation of the phenazine biosynthetic operons by quorum sensing in *Pseudomonas aeruginosa* PAO1-N', *Front Cell Infect Microbiol,* 8, pp. 252, doi: 10.3389/fcimb.2018.00252.

Hill, D., Rose, B., Pajkos, A., Robinson, M., Bye, P., Bell, S., Elkins, M., Thompson, B., Macleod, C., Aaron, S. D. and Harbour, C. (2005) 'Antibiotic susceptibilities of *Pseudomonas aeruginosa* isolates derived from patients with cystic fibrosis under aerobic, anaerobic, and biofilm conditions', *J Clin Microbiol,* 43(10), pp. 5085-5090, doi: 10.1128/JCM.43.10.5085-5090.2005.

Hobson, R. P., Munro, C. A., Bates, S., MacCallum, D. M., Cutler, J. E., Heinsbroek, S. E., Brown, G. D., Odds, F. C. and Gow, N. A. (2004) 'Loss of cell wall mannosylphosphate in *Candida albicans* does not influence macrophage recognition', *J Biol Chem,* 279(38), pp. 39628-39635, doi: 10.1074/jbc.M405003200.

Hogan, D. A. and Kolter, R. (2002) '*Pseudomonas-Candida* interactions: an ecological role for virulence factors', *Science,* 296(5576), pp. 2229-2232, doi: 10.1126/science.1070784.

Hogan, D. A., Vik, A. and Kolter, R. (2004) 'A *Pseudomonas aeruginosa* quorum-sensing molecule influences *Candida albicans* morphology', *Mol Microbiol,* 54(5), pp. 1212-1223, doi: 10.1111/j.1365-2958.2004.04349.x.

Høiby, N., Ciofu, O. and Bjarnsholt, T. (2010) '*Pseudomonas aeruginosa* biofilms in cystic fibrosis', *Future Microbiol,* 5(11), pp. 1663-1674.

Hube, B., Stehr, F., Bossenz, M., Mazur, A., Kretschmar, M. and Shäfer, W. (2000) 'Secreted lipases of *Candida albicans*: cloning, characterisation and expression analysis of a new gene family with at least ten members', *Arch Microbiol,* 174, pp. 362-374, doi: 10.1007/.

Hulen, C., Racine, P. J., Chevalier, S., Feuilloley, M. and Lomri, N. E. (2020) 'Identification of the PA1113 gene product as an ABC transporter involved in the uptake of carbenicillin in *Pseudomonas aeruginosa* PAO1', *Antibiotics (Basel),* 9(9), doi: 10.3390/antibiotics9090596.

Hutchings, M., Truman, A. and Wilkinson, B. (2019) 'Antibiotics: past, present and future', *Curr Opin Microbiol,* 51, pp. 72-80, doi: 10.1016/j.mib.2019.10.008.

Hwang, C.-S., Rhie, G.-E., Oh, J.-H., Huh, W.-K., Yim, H.-S. and Kang, S.-O. (2002) 'Copper- and zinc-containing superoxide dismutase (Cu/ZnSOD) is required for the protection of *Candida albicans* against oxidative stresses and the expression of its full

virulence', *Microbiology,* 148(11), pp. 3705-3713, doi: 10.1099/00221287-148-11-3705.

Hwang, C. S., Baek, Y. U., Yim, H. S. and Kang, S. O. (2003) 'Protective roles of mitochondrial manganese-containing superoxide dismutase against various stresses in *Candida albicans*', *Yeast,* 20(11), pp. 929-941, doi: 10.1002/yea.1004.

Hwang, G., Liu, Y., Kim, D., Li, Y., Krysan, D. J. and Koo, H. (2017) '*Candida albicans* mannans mediate *Streptococcus mutans* exoenzyme GtfB binding to modulate cross-kingdom biofilm development *in vivo*', *PLoS Pathog,* 13(6), pp. e1006407, doi: 10.1371/journal.ppat.1006407.

Imlay, J. A. (2013) 'The molecular mechanisms and physiological consequences of oxidative stress: lessons from a model bacterium', *Nat Rev Microbiol,* 11(7), pp. 443-454, doi: 10.1038/nrmicro3032.

Jacobs, M. A., Alwood, A., Thaipisuttikul, I., Spencer, D., Haugen, E., Ernst, S., Will, O., Kaul, R., Raymond, C., Levy, R., Chun-Rong, L., Guenthner, D., Bovee, D., Olson, M. V. and Manoil, C. (2003) 'Comprehensive transposon mutant library of *Pseudomonas aeruginosa*', *Proc Natl Acad Sci U S A,* 100(24), pp. 14339-14344, doi: 10.1073/pnas.2036282100.

Jakobsen, T. H., Bjarnsholt, T., Jensen, P. Ø., Givskov, M. and Høiby, N. (2013) 'Targeting quorum sensing in *Pseudomonas aeruginosa* biofilms: current and emerging inhibitors', *Future Microbiol,* 8(7), pp. 901-921.

Jakubovics, N. S., Shields, R. C., Rajarajan, N. and Burgess, J. G. (2013) 'Life after death: the critical role of extracellular DNA in microbial biofilms', *Lett Appl Microbiol,* 57(6), pp. 467-475, doi: 10.1111/lam.12134.

Jarosz, L. M., Deng, D. M., van der Mei, H. C., Crielaard, W. and Krom, B. P. (2009) '*Streptococcus mutans* competence-stimulating peptide inhibits *Candida albicans* hypha formation', *Eukaryot Cell,* 8(11), pp. 1658-1664, doi: 10.1128/EC.00070-09.

Jefferson, K. K., Goldmann, D. A. and Pier, G. B. (2005) 'Use of confocal microscopy to analyze the rate of vancomycin penetration through *Staphylococcus aureus* biofilms', *Antimicrob Agents Chemother,* 49(6), pp. 2467-2473, doi: 10.1128/AAC.49.6.2467-2473.2005.

Jennings, L. K., Storek, K. M., Ledvina, H. E., Coulon, C., Marmont, L. S., Sadovskaya, I., Secor, P. R., Tseng, B. S., Scian, M., Filloux, A., Wozniak, D. J., Howell, P. L. and Parsek, M. R. (2015) 'Pel is a cationic exopolysaccharide that cross-links extracellular DNA in the *Pseudomonas aeruginosa* biofilm matrix', *Proc Natl Acad Sci U S A,* 112(36), pp. 11353-11358, doi: 10.1073/pnas.1503058112.

Jiménez-López, C., Collette, J. R., Brothers, K. M., Shepardson, K. M., Cramer, R. A., Wheeler, R. T. and Lorenz, M. C. (2013) '*Candida albicans* induces arginine

biosynthetic genes in response to host-derived reactive oxygen species', *Eukaryot Cell,* 12(1), pp. 91-100, doi: 10.1128/EC.00290-12.

Jurado-Martin, I., Sainz-Mejias, M. and McClean, S. (2021) '*Pseudomonas aeruginosa*: an audacious pathogen with an adaptable arsenal of virulence factors', *Int J Mol Sci,* 22(6), doi: 10.3390/ijms22063128.

Kamali, E., Jamali, A., Ardebili, A., Ezadi, F. and Mohebbi, A. (2020) 'Evaluation of antimicrobial resistance, biofilm forming potential, and the presence of biofilm-related genes among clinical isolates of *Pseudomonas aeruginosa*', *BMC Res Notes,* 13(1), pp. 27, doi: 10.1186/s13104-020-4890-z.

Kamiński, D. M. (2014) 'Recent progress in the study of the interactions of amphotericin B with cholesterol and ergosterol in lipid environments', *Eur Biophys J,* 43(10-11), pp. 453-467, doi: 10.1007/s00249-014-0983-8.

Kanehisa, M., Furumichi, M., Tanabe, M., Sato, Y. and Morishima, K. (2017) 'KEGG: new perspectives on genomes, pathways, diseases and drugs', *Nucleic Acids Res,* 45(D1), pp. D353-D361, doi: 10.1093/nar/gkw1092.

Kean, R., Rajendran, R., Haggarty, J., Townsend, E. M., Short, B., Burgess, K. E., Lang, S., Millington, O., Mackay, W. G., Williams, C. and Ramage, G. (2017) '*Candida albicans* mycofilms support *Staphylococcus aureus* colonization and enhances miconazole resistance in dual-species interactions', *Front Microbiol,* 8, pp. 258, doi: 10.3389/fmicb.2017.00258.

Khakimova, M., Ahlgren, H. G., Harrison, J. J., English, A. M. and Nguyen, D. (2013) 'The stringent response controls catalases in *Pseudomonas aeruginosa* and is required for hydrogen peroxide and antibiotic tolerance', *J Bacteriol,* 195(9), pp. 2011-2020, doi: 10.1128/JB.02061-12.

Khaledi, A., Schniederjans, M., Pohl, S., Rainer, R., Bodenhofer, U., Xia, B., Klawonn, F., Bruchmann, S., Preusse, M., Eckweiler, D., Dotsch, A. and Haussler, S. (2016) 'Transcriptome profiling of antimicrobial resistance in *Pseudomonas aeruginosa*', *Antimicrob Agents Chemother,* 60(8), pp. 4722-4733, doi: 10.1128/AAC.00075-16.

Kim, D., Liu, Y., Benhamou, R. I., Sanchez, H., Simon-Soro, A., Li, Y., Hwang, G., Fridman, M., Andes, D. R. and Koo, H. (2018) 'Bacterial-derived exopolysaccharides enhance antifungal drug tolerance in a cross-kingdom oral biofilm', *ISME J,* 12(6), pp. 1427-1442, doi: 10.1038/s41396-018-0113-1.

Klaerner, H. G., Uknis, M. E., Acton, R. D., Dahlberg, P. S., Carlone-Jambor, C. and Dunn, D. L. (1997) '*Candida albicans* and *Escherichia coli* are synergistic pathogens during experimental microbial peritonitis', *Journal of Surgical Research,* 70, pp. 161-165.

Kobayashi, D., Kondo, K., Uehara, N., Otokozawa, S., Tsuji, N., Yagihashi, A. and Watanabe, N. (2002) 'Endogenous reactive oxygen species is an important mediator

of miconazole antifungal effect', *Antimicrob Agents Chemother,* 46(10), pp. 3113-3117, doi: 10.1128/aac.46.10.3113-3117.2002.

Kong, E. F., Tsui, C., Kucharikova, S., Andes, D., Van Dijck, P. and Jabra-Rizk, M. A. (2016) 'Commensal protection of *Staphylococcus aureus* against antimicrobials by *Candida albicans* biofilm matrix', *MBio,* 7(5), pp. 12, doi: 10.1128/mBio.01365-16.

Kostoulias, X., Murray, G. L., Cerqueira, G. M., Kong, J. B., Bantun, F., Mylonakis, E., Khoo, C. A. and Peleg, A. Y. (2016) 'Impact of a cross-kingdom signaling molecule of *Candida albicans* on *Acinetobacter baumannii* physiology', *Antimicrob Agents Chemother,* 60(1), pp. 161-167, doi: 10.1128/AAC.01540-15.

Krüger, W., Vielreicher, S., Kapitan, M., Jacobsen, I. D. and Niemiec, M. J. (2019) 'Fungal-bacterial interactions in health and disease', *Pathogens,* 8(2), doi: 10.3390/pathogens8020070.

La Rosa, R., Johansen, H. K. and Molin, S. (2019) 'Adapting to the airways: metabolic requirements of *Pseudomonas aeruginosa* during the infection of cystic fibrosis patients', *Metabolites,* 9(10), doi: 10.3390/metabo9100234.

LaFleur, M. D., Kumamoto, C. A. and Lewis, K. (2006) '*Candida albicans* biofilms produce antifungal-tolerant persister cells', *Antimicrob Agents Chemother,* 50(11), pp. 3839-3846, doi: 10.1128/AAC.00684-06.

Lam, M. M., Seemann, T., Bulach, D. M., Gladman, S. L., Chen, H., Haring, V., Moore, R. J., Ballard, S., Grayson, M. L., Johnson, P. D., Howden, B. P. and Stinear, T. P. (2012) 'Comparative analysis of the first complete *Enterococcus faecium* genome', *J Bacteriol,* 194(9), pp. 2334-2341, doi: 10.1128/JB.00259-12.

Lau, A. P. S., Lee, A. K. Y., Chan, C. K. and Fang, M. (2006) 'Ergosterol as a biomarker for the quantification of the fungal biomass in atmospheric aerosols', *Atmospheric Environment,* 40(2), pp. 249-259, doi: 10.1016/j.atmosenv.2005.09.048.

Lee, K. and Yoon, S. S. (2017) '*Pseudomonas aeruginosa* biofilm, a programmed bacterial life for fitness', *J Microbiol Biotechnol,* 27(6), pp. 1053-1064, doi: 10.4014/jmb.1611.11056.

Leventhal, A. R., Chen, W., Tall, A. R. and Tabas, I. (2001) 'Acid sphingomyelinase-deficient macrophages have defective cholesterol trafficking and efflux', *J Biol Chem,* 276(48), pp. 44976-44983, doi: 10.1074/jbc.M106455200.

Levison, M. E. and Pitsakis, P. G. (1987) 'Susceptibility to experimental *Candida albicans* urinary tract infection in the rat', *The Journal of Infectious Diseases,* 155(5), pp. 841–846.

Liao, J. and Sauer, K. (2012) 'The MerR-like transcriptional regulator BrlR contributes to *Pseudomonas aeruginosa* biofilm tolerance', *J Bacteriol,* 194(18), pp. 4823-4836, doi: 10.1128/JB.00765-12.

Liao, J., Schurr, M. J. and Sauer, K. (2013) 'The MerR-like regulator BrlR confers biofilm tolerance by activating multidrug efflux pumps in *Pseudomonas aeruginosa* biofilms', *J Bacteriol,* 195(15), pp. 3352-3363, doi: 10.1128/JB.00318-13.

Liberati, N. T., Urbach, J. M., Miyata, S., Lee, D. G., Drenkard, E., Wu, G., Villanueva, J., Wei, T. and Ausubel, F. M. (2006) 'An ordered, nonredundant library of *Pseudomonas aeruginosa* strain PA14 transposon insertion mutants', *Proc Natl Acad Sci U S A,* 103(8), pp. 2833-2838, doi: 10.1073/pnas.0511100103.

Lindsay, A. K. and Hogan, D. A. (2014) '*Candida albicans*: molecular interactions with *Pseudomonas aeruginosa* and *Staphylococcus aureus*', *Fungal Biol Rev,* 28(4), pp. 85-96, doi: 10.1016/j.fbr.2014.10.002.

Liu, L., Ye, M., Li, X., Li, J., Deng, Z., Yao, Y. F. and Ou, H. Y. (2017) 'Identification and characterization of an antibacterial type VI secretion system in the carbapenem-resistant strain *Klebsiella pneumoniae* HS11286', *Front Cell Infect Microbiol,* 7, pp. 442, doi: 10.3389/fcimb.2017.00442.

Liu, T. T., Lee, R. E., Barker, K. S., Lee, R. E., Wei, L., Homayouni, R. and Rogers, P. D. (2005) 'Genome-wide expression profiling of the response to azole, polyene, echinocandin, and pyrimidine antifungal agents in *Candida albicans*', *Antimicrob Agents Chemother,* 49(6), pp. 2226-2236, doi: 10.1128/AAC.49.6.2226-2236.2005.

Lohse, M. B., Gulati, M., Johnson, A. D. and Nobile, C. J. (2018) 'Development and regulation of single- and multi-species *Candida albicans* biofilms', *Nat Rev Microbiol,* 16(1), pp. 19-31, doi: 10.1038/nrmicro.2017.107.

López-Causapé, C., Sommer, L. M., Cabot, G., Rubio, R., Ocampo-Sosa, A. A., Johansen, H. K., Figuerola, J., Cantón, R., Kidd, T. J., Molin, S. and Oliver, A. (2017) 'Evolution of the *Pseudomonas aeruginosa* mutational resistome in an international Cystic Fibrosis clone', *Sci Rep,* 7(1), pp. 5555, doi: 10.1038/s41598-017-05621-5.

Lopez-Medina, E., Fan, D., Coughlin, L. A., Ho, E. X., Lamont, I. L., Reimmann, C., Hooper, L. V. and Koh, A. Y. (2015) '*Candida albicans* inhibits *Pseudomonas aeruginosa* virulence through suppression of pyochelin and pyoverdine biosynthesis', *PLoS Pathog,* 11(8), pp. e1005129, doi: 10.1371/journal.ppat.1005129.

Lyczak, J. B., Cannon, C. L. and Pier, G. B. (2002) 'Lung infections associated with cystic fibrosis', *Clin Microbiol Rev,* 15(2), pp. 194-222, doi: 10.1128/cmr.15.2.194-222.2002.

MacPherson, S., Akache, B., Weber, S., De Deken, X., Raymond, M. and Turcotte, B. (2005) '*Candida albicans* zinc cluster protein Upc2p confers resistance to antifungal drugs and is an activator of ergosterol biosynthetic genes', *Antimicrob Agents Chemother,* 49(5), pp. 1745-1752, doi: 10.1128/AAC.49.5.1745-1752.2005.

Mah, T. F. (2012) 'Biofilm-specific antibiotic resistance', *Future Microbiol,* 7(9), pp. 1061-1072, doi: 10.2217/fmb.12.76.

Mahmoudi, S., Agha Kuchak Afshari, S., Aghaei Gharehbolagh, S., Mirhendi, H. and Makimura, K. (2019) 'Methods for identification of *Candida auris*, the yeast of global public health concern: A review', *J Mycol Med,* 29(2), pp. 174-179, doi: 10.1016/j.mycmed.2019.04.004.

Mandsberg, L. F., Ciofu, O., Kirkby, N., Christiansen, L. E., Poulsen, H. E. and Høiby, N. (2009) 'Antibiotic resistance in *Pseudomonas aeruginosa* strains with increased mutation frequency due to inactivation of the DNA oxidative repair system', *Antimicrob Agents Chemother,* 53(6), pp. 2483-2491, doi: 10.1128/AAC.00428-08.

Mann, E. E. and Wozniak, D. J. (2012) '*Pseudomonas* biofilm matrix composition and niche biology', *FEMS Microbiol Rev,* 36(4), pp. 893-916, doi: 10.1111/j.1574-6976.2011.00322.x.

Marek, M., Vincenzetti, V. and Martin, S. G. (2019) 'Sterol flow between the plasma membrane and the endosome is regulated by the LAM family protein Ltc1', *bioRxiv*, doi: 10.1101/720383.

Martchenko, M., Alarco, A.-M., Harcus, D. and Whiteway, M. (2004) 'Superoxide dismutases in *Candida albicans*: transcriptional regulation and functional characterization of the hyphal-induced *SOD5* gene', *Mol Biol Cell,* 15(2), pp. 456-467, doi: 10.1091/mbc.e03-03-0179.

Mateus, C., Crow Jr., S. A. and Ahearn, D. G. (2004) 'Adherence of *Candida albicans* to silicone induces immediate enhanced tolerance to fluconazole', *Antimicrob Agents Chemother,* 48(9), pp. 3358–3366.

Mavrodi, D. V., Bonsall, R. F., Delaney, S. M., Soule, M. J., Phillips, G. and Thomashow, L. S. (2001) 'Functional analysis of genes for biosynthesis of pyocyanin and phenazine-1-carboxamide from *Pseudomonas aeruginosa* PAO1', *J Bacteriol,* 183(21), pp. 6454-6465, doi: 10.1128/JB.183.21.6454-6465.2001.

Mayer, F. L., Wilson, D. and Hube, B. (2013) '*Candida albicans* pathogenicity mechanisms', *Virulence,* 4(2), pp. 119-128, doi: 10.4161/viru.22913.

McAlester, G., O'Gara, F. and Morrissey, J. P. (2008) 'Signal-mediated interactions between *Pseudomonas aeruginosa* and *Candida albicans*', *J Med Microbiol,* 57(Pt 5), pp. 563-569, doi: 10.1099/jmm.0.47705-0.

Méar, J. B., Kipnis, E., Faure, E., Dessein, R., Schurtz, G., Faure, K. and Guery, B. (2013) '*Candida albicans* and *Pseudomonas aeruginosa* interactions: more than an opportunistic criminal association?', *Med Mal Infect,* 43(4), pp. 146-151, doi: 10.1016/j.medmal.2013.02.005.

Merritt, J. H., Kadouri, D. E. and O'Toole, G. A. (2005) 'Growing and analyzing static biofilms', *Curr Protoc Microbiol,* Chapter 1, pp. Unit 1B 1, doi: 10.1002/9780471729259.mc01b01s00.

Mesa-Arango, A. C., Trevijano-Contador, N., Roman, E., Sanchez-Fresneda, R., Casas, C., Herrero, E., Arguelles, J. C., Pla, J., Cuenca-Estrella, M. and Zaragoza, O. (2014) 'The production of reactive oxygen species is a universal action mechanism of amphotericin B against pathogenic yeasts and contributes to the fungicidal effect of this drug', *Antimicrob Agents Chemother,* 58(11), pp. 6627-6638, doi: 10.1128/AAC.03570-14.

Michalska, M. and Wolf, P. (2015) '*Pseudomonas* exotoxin A: optimized by evolution for effective killing', *Front Microbiol,* 6, pp. 963, doi: 10.3389/fmicb.2015.00963.

Mitchell, K. F., Zarnowski, R., Sanchez, H., Edward, J. A., Reinicke, E. L., Nett, J. E., Mitchell, A. P. and Andes, D. R. (2015) 'Community participation in biofilm matrix assembly and function', *Proc Natl Acad Sci U S A,* 112(13), pp. 4092-4097, doi: 10.1073/pnas.1421437112.

Morales, D. K., Grahl, N., Okegbe, C., Dietrich, L. E., Jacobs, N. J. and Hogan, D. A. (2013) 'Control of *Candida albicans* metabolism and biofilm formation by *Pseudomonas aeruginosa* phenazines', *MBio,* 4(1), pp. e00526-00512, doi: 10.1128/mBio.00526-12.

Morales, D. K., Jacobs, N. J., Rajamani, S., Krishnamurthy, M., Cubillos-Ruiz, J. R. and Hogan, D. A. (2010) 'Antifungal mechanisms by which a novel *Pseudomonas aeruginosa* phenazine toxin kills *Candida albicans* in biofilms', *Mol Microbiol,* 78(6), pp. 1379-1392, doi: 10.1111/j.1365-2958.2010.07414.x.

Morschhäuser, J., Ruhnke, M., Michel, S. and Hacker, J. (1999) 'Identification of CARE-2-negative *Candida albicans* isolates as *Candida dubliniensis*', *Mycoses,* 42, pp. 29-32.

Morse, D. J., Wilson, M. J., Wei, X., Bradshaw, D. J., Lewis, M. A. O. and Williams, D. W. (2019) 'Modulation of *Candida albicans* virulence in *in vitro* biofilms by oral bacteria', *Lett Appl Microbiol*, doi: 10.1111/lam.13145.

Moyes, D. L., Wilson, D., Richardson, J. P., Mogavero, S., Tang, S. X., Wernecke, J., Hofs, S., Gratacap, R. L., Robbins, J., Runglall, M., Murciano, C., Blagojevic, M., Thavaraj, S., Forster, T. M., Hebecker, B., Kasper, L., Vizcay, G., Iancu, S. I., Kichik, N., Hader, A., Kurzai, O., Luo, T., Kruger, T., Kniemeyer, O., Cota, E., Bader, O., Wheeler, R. T., Gutsmann, T., Hube, B. and Naglik, J. R. (2016) 'Candidalysin is a fungal peptide toxin critical for mucosal infection', *Nature,* 532(7597), pp. 64-68, doi: 10.1038/nature17625.

Mulcahy, H., Charron-Mazenod, L. and Lewenza, S. (2008) 'Extracellular DNA chelates cations and induces antibiotic resistance in *Pseudomonas aeruginosa* biofilms', *PLoS Pathog,* 4(11), pp. e1000213, doi: 10.1371/journal.ppat.1000213.

Munro, C. A., Bates, S., Buurman, E. T., Hughes, H. B., Maccallum, D. M., Bertram, G., Atrih, A., Ferguson, M. A., Bain, J. M., Brand, A., Hamilton, S., Westwater, C., Thomson, L. M., Brown, A. J., Odds, F. C. and Gow, N. A. (2005) 'Mnt1p and Mnt2p of *Candida albicans* are partially redundant α-1,2-mannosyltransferases that participate in *O*-linked mannosylation and are required for adhesion and virulence', *J Biol Chem,* 280(2), pp. 1051-1060, doi: 10.1074/jbc.M411413200.

Murciano, C., Moyes, D. L., Runglall, M., Islam, A., Mille, C., Fradin, C., Poulain, D., Gow, N. A. and Naglik, J. R. (2011) '*Candida albicans* cell wall glycosylation may be indirectly required for activation of epithelial cell proinflammatory responses', *Infect Immun,* 79(12), pp. 4902-4911, doi: 10.1128/IAI.05591-11.

Muthig, M., Hebestreit, A., Ziegler, U., Seidler, M. and Muller, F. M. (2010) 'Persistence of *Candida* species in the respiratory tract of cystic fibrosis patients', *Med Mycol,* 48(1), pp. 56-63, doi: 10.3109/13693780802716532.

Naglik, J. R., Challacombe, S. J. and Hube, B. (2003) '*Candida albicans* secreted aspartyl proteinases in virulence and pathogenesis', *Microbiol Mol Biol Rev,* 67(3), pp. 400-428, table of contents, doi: 10.1128/mmbr.67.3.400-428.2003.

Naglik, J. R., Gaffen, S. L. and Hube, B. (2019) 'Candidalysin: discovery and function in *Candida albicans* infections', *Curr Opin Microbiol,* 52, pp. 100-109, doi: 10.1016/j.mib.2019.06.002.

Nett, J., Lincoln, L., Marchillo, K., Massey, R., Holoyda, K., Hoff, B., VanHandel, M. and Andes, D. (2007) 'Putative role of ß-1,3 glucans in *Candida albicans* biofilm resistance', *Antimicrob Agents Chemother,* 51(2), pp. 510-520, doi: 10.1128/AAC.01056-06.

Nicolau, D. P. (2008) 'Pharmacokinetic and pharmacodynamic properties of meropenem', *Clin Infect Dis,* 47 Suppl 1, pp. S32-40, doi: 10.1086/590064.

Niewerth, M. and Korting, H. C. (2001) 'Phospholipases of *Candida albicans*', *Mycoses,* 44, pp. 361-367.

Nishimoto, A. T., Sharma, C. and Rogers, P. D. (2019) 'Molecular and genetic basis of azole antifungal resistance in the opportunistic pathogenic fungus *Candida albicans*', *J Antimicrob Chemother,* 75(2), pp. 257-270, doi: 10.1093/jac/dkz400.

Noble, S. M., French, S., Kohn, L. A., Chen, V. and Johnson, A. D. (2010) 'Systematic screens of a *Candida albicans* homozygous deletion library decouple morphogenetic switching and pathogenicity', *Nat Genet,* 42(7), pp. 590-598, doi: 10.1038/ng.605.

Noble, S. M., Gianetti, B. A. and Witchley, J. N. (2017) '*Candida albicans* cell-type switching and functional plasticity in the mammalian host', *Nat Rev Microbiol,* 15(2), pp. 96-108, doi: 10.1038/nrmicro.2016.157.

Noble, S. M. and Johnson, A. D. (2005) 'Strains and strategies for large-scale gene deletion studies of the diploid human fungal pathogen *Candida albicans*', *Eukaryot Cell,* 4(2), pp. 298-309, doi: 10.1128/EC.4.2.298-309.2005.

Nogueira, F., Sharghi, S., Kuchler, K. and Lion, T. (2019) 'Pathogenetic impact of bacterial-fungal interactions', *Microorganisms,* 7(10), doi: 10.3390/microorganisms7100459.

Nseir, S., Jozefowicz, E., Cavestri, B., Sendid, B., Di Pompeo, C., Dewavrin, F., Favory, R., Roussel-Delvallez, M. and Durocher, A. (2007) 'Impact of antifungal treatment on *Candida-Pseudomonas* interaction: a preliminary retrospective case-control study', *Intensive Care Med,* 33(1), pp. 137-142, doi: 10.1007/s00134-006-0422-0.

O'Brien, S. and Fothergill, J. L. (2017) 'The role of multispecies social interactions in shaping *Pseudomonas aeruginosa* pathogenicity in the cystic fibrosis lung', *FEMS Microbiol Lett,* 364(15), doi: 10.1093/femsle/fnx128.

O'Neill, J. (2016) 'The review on antimicrobial resistance. Tackling drug-resistant infections globally: final report and recommendations.', *Rev Antimicrob Resist,* https://amr-review.org/sites/default/files/160525_Final paper_with cover.pdf.

Okamoto, Y., Aoki, S. and Mataga, I. (2004) 'Enhancement of amphotericin B activity against *Candida albicans* by superoxide radical', *Mycopathologia,* 158, pp. 9-15, doi: 10.1023/B:MYCO.0000038430.20669.80.

Olsen, I. (2015) 'Biofilm-specific antibiotic tolerance and resistance', *Eur J Clin Microbiol Infect Dis,* 34(5), pp. 877-886, doi: 10.1007/s10096-015-2323-z.

Ovchinnikova, E. S., Krom, B. P., Harapanahalli, A. K., Busscher, H. J. and van der Mei, H. C. (2013) 'Surface thermodynamic and adhesion force evaluation of the role of chitin-binding protein in the physical interaction between *Pseudomonas aeruginosa* and *Candida albicans*', *Langmuir,* 29(15), pp. 4823-4829, doi: 10.1021/la400554g.

Papon, N., Courdavault, V., Clastre, M. and Bennett, R. J. (2013) 'Emerging and emerged pathogenic *Candida* species: beyond the *Candida albicans* paradigm', *PLoS Pathog,* 9(9), pp. e1003550, doi: 10.1371/journal.ppat.1003550.

Papp-Wallace, K. M., Endimiani, A., Taracila, M. A. and Bonomo, R. A. (2011) 'Carbapenems: past, present, and future', *Antimicrob Agents Chemother,* 55(11), pp. 4943-4960, doi: 10.1128/AAC.00296-11.

Passos da Silva, D., Matwichuk, M. L., Townsend, D. O., Reichhardt, C., Lamba, D., Wozniak, D. J. and Parsek, M. R. (2019) 'The *Pseudomonas aeruginosa* lectin LecB binds to the exopolysaccharide Psl and stabilizes the biofilm matrix', *Nat Commun,* 10(1), pp. 2183, doi: 10.1038/s41467-019-10201-4.

Peleg, A. Y., Hogan, D. A. and Mylonakis, E. (2010) 'Medically important bacterial-fungal interactions', *Nat Rev Microbiol,* 8(5), pp. 340-349, doi: 10.1038/nrmicro2313.

Peleg, A. Y., Tampakakis, E., Fuchs, B. B., Eliopoulos, G. M., Moellering, R. C. and Mylonakis, E. (2008) 'Prokaryote-eukaryote interactions identified by using *Caenorhabditis elegans*', *Proc Natl Acad Sci U S A,* 105(38), pp. 14585-14590, doi: 10.1073/pnas.0805048105.

Pereira, R., Dos Santos Fontenelle, R. O., de Brito, E. H. S. and de Morais, S. M. (2020) 'Biofilm of *Candida albicans*: formation, regulation and resistance', *J Appl Microbiol*, doi: 10.1111/jam.14949.

Perlin, D. S., Rautemaa-Richardson, R. and Alastruey-Izquierdo, A. (2017) 'The global problem of antifungal resistance: prevalence, mechanisms, and management', *Lancet Infect Dis,* 17(12), pp. e383-e392, doi: 10.1016/S1473-3099(17)30316-X.

Peters, B. M., Jabra-Rizk, M. A., Scheper, M. A., Leid, J. G., Costerton, J. W. and Shirtliff, M. E. (2010) 'Microbial interactions and differential protein expression in *Staphylococcus aureus-Candida albicans* dual-species biofilms', *FEMS Immunol Med Microbiol,* 59(3), pp. 493-503, doi: 10.1111/j.1574-695X.2010.00710.x.

Peters, B. M. and Noverr, M. C. (2013) '*Candida albicans-Staphylococcus aureus* polymicrobial peritonitis modulates host innate immunity', *Infect Immun,* 81(6), pp. 2178-2189, doi: 10.1128/IAI.00265-13.

Phuengmaung, P., Somparn, P., Panpetch, W., Singkham-In, U., Wannigama, D. L., Chatsuwan, T. and Leelahavanichkul, A. (2020) 'Coexistence of *Pseudomonas aeruginosa* with *Candida albicans* enhances biofilm thickness through alginate-related extracellular matrix but Is attenuated by N-acetyl-L-cysteine', *Front Cell Infect Microbiol,* 10, pp. 594336, doi: 10.3389/fcimb.2020.594336.

Piekarska, K., Mol, E., van den Berg, M., Hardy, G., van den Burg, J., van Roermund, C., MacCallum, D., Odds, F. and Distel, B. (2006) 'Peroxisomal fatty acid beta-oxidation is not essential for virulence of *Candida albicans*', *Eukaryot Cell,* 5(11), pp. 1847-1856, doi: 10.1128/EC.00093-06.

Plaine, A., Walker, L., Da Costa, G., Mora-Montes, H. M., McKinnon, A., Gow, N. A., Gaillardin, C., Munro, C. A. and Richard, M. L. (2008) 'Functional analysis of *Candida albicans* GPI-anchored proteins: roles in cell wall integrity and caspofungin sensitivity', *Fungal Genet Biol,* 45(10), pp. 1404-1414, doi: 10.1016/j.fgb.2008.08.003.

Poirel, L., Menuteau, O., Agoli, N., Cattoen, C. and Nordmann, P. (2003) 'Outbreak of extended-spectrum beta-lactamase VEB-1-producing isolates of *Acinetobacter baumannii* in a French hospital', *J Clin Microbiol,* 41(8), pp. 3542-3547, doi: 10.1128/jcm.41.8.3542-3547.2003.

Ponde, N. O., Lortal, L., Ramage, G., Naglik, J. R. and Richardson, J. P. (2021) '*Candida albicans* biofilms and polymicrobial interactions', *Crit Rev Microbiol*, pp. 1-21, doi: 10.1080/1040841X.2020.1843400.

Radlinski, L., Rowe, S. E., Kartchner, L. B., Maile, R., Cairns, B. A., Vitko, N. P., Gode, C. J., Lachiewicz, A. M., Wolfgang, M. C. and Conlon, B. P. (2017) '*Pseudomonas aeruginosa* exoproducts determine antibiotic efficacy against *Staphylococcus aureus*', *PLoS Biol,* 15(11), pp. e2003981, doi: 10.1371/journal.pbio.2003981.

Rahme, L. G., Stevens, E. J., Wolfort, S. F., Shao, J., Tompkins, R. G. and Ausubel, F. M. (1995) 'Common virulence factors for bacterial pathogenicity in plants and animals', *Science,* 268(5219), pp. 1899-1902.

Ramage, G., Bachmann, S., Patterson, T. F. and Wickes, B. L. p.-R., J. L. (2002) 'Investigation of multidrug efflux pumps in relation to fluconazole resistance in *Candida albicans* biofilms', *J Antimicrob Chemother,* 49, pp. 973-980.

Ramage, G., Vande Walle, K., Wickes, B. L. and Lopez-Ribot, J. L. (2001) 'Biofilm formation by *Candida dubliniensis*', *J Clin Microbiol,* 39(9), pp. 3234-3240, doi: 10.1128/jcm.39.9.3234-3240.2001.

Raman, G., Avendano, E. E., Chan, J., Merchant, S. and Puzniak, L. (2018) 'Risk factors for hospitalized patients with resistant or multidrug-resistant *Pseudomonas aeruginosa* infections: a systematic review and meta-analysis', *Antimicrob Resist Infect Control,* 7, pp. 79, doi: 10.1186/s13756-018-0370-9.

Ranjan, A. and Dongari-Bagtzoglou, A. (2018) 'Tipping the balance: *C. albicans* adaptation in polymicrobial environments', *J Fungi (Basel),* 4(3), doi: 10.3390/jof4030112.

Reid, D. W., O'May, C., Kirov, S. M., Roddam, L., Lamont, I. L. and Sanderson, K. (2009) 'Iron chelation directed against biofilms as an adjunct to conventional antibiotics', *Am J Physiol Lung Cell Mol Physiol,* 296(5), pp. L857-858, doi: 10.1152/ajplung.00058.2009.

Revie, N. M., Iyer, K. R., Robbins, N. and Cowen, L. E. (2018) 'Antifungal drug resistance: evolution, mechanisms and impact', *Curr Opin Microbiol,* 45, pp. 70-76, doi: 10.1016/j.mib.2018.02.005.

Robinett, N. G., Culbertson, E. M., Peterson, R. L., Sanchez, H., Andes, D. R., Nett, J. E. and Culotta, V. C. (2019) 'Exploiting the vulnerable active site of a copper-only superoxide dismutase to disrupt fungal pathogenesis', *J Biol Chem,* 294(8), pp. 2700-2713, doi: 10.1074/jbc.RA118.007095.

Rodrigues, M. E., Gomes, F. and Rodrigues, C. F. (2019) '*Candida* spp./bacteria mixed biofilms', *J Fungi (Basel),* 6(1), doi: 10.3390/jof6010005.

Rodrigues, M. E., Lopes, S. P., Pereira, C. R., Azevedo, N. F., Lourenco, A., Henriques, M. and Pereira, M. O. (2017) 'Polymicrobial ventilator-associated pneumonia: fighting *in vitro Candida albicans-Pseudomonas aeruginosa* biofilms with antifungal-antibacterial combination therapy', *PLoS One,* 12(1), pp. e0170433, doi: 10.1371/journal.pone.0170433.

Rodrigues, M. L. (2018) 'The multifunctional fungal ergosterol', *mBio,* 9(5), doi: 10.1128/mBio.01755-18.

Rodríguez-Martínez, J. M., Poirel, L. and Nordmann, P. (2009) 'Molecular epidemiology and mechanisms of carbapenem resistance in *Pseudomonas aeruginosa*', *Antimicrob Agents Chemother,* 53(11), pp. 4783-4788, doi: 10.1128/AAC.00574-09.

Rossi, E., La Rosa, R., Bartell, J. A., Marvig, R. L., Haagensen, J. A. J., Sommer, L. M., Molin, S. and Johansen, H. K. (2020) '*Pseudomonas aeruginosa* adaptation and evolution in patients with cystic fibrosis', *Nat Rev Microbiol*, doi: 10.1038/s41579-020-00477-5.

Sadovskaya, I., Vinogradov, E., Li, J., Hachani, A., Kowalska, K. and Filloux, A. (2010) 'High-level antibiotic resistance in *Pseudomonas aeruginosa* biofilm: the *ndvB* gene is involved in the production of highly glycerol-phosphorylated ß-(1->3)-glucans, which bind aminoglycosides', *Glycobiology,* 20(7), pp. 895-904, doi: 10.1093/glycob/cwq047.

Sahm, D. F., Kissinger, J., Gilmore, M. S., Murray, P. R., Mulder, R., Solliday, J. and Clarke, B. (1989) '*In vitro* susceptibility studies of vancomycin-resistant *Enterococcus faecalis*', *Antimicrob Agents Chemother,* 33(9), pp. 1588-1591.

Sardi, J. C., Scorzoni, L., Bernardi, T., Fusco-Almeida, A. M. and Mendes Giannini, M. J. (2013) '*Candida* species: current epidemiology, pathogenicity, biofilm formation, natural antifungal products and new therapeutic options', *J Med Microbiol,* 62(Pt 1), pp. 10-24, doi: 10.1099/jmm.0.045054-0.

Sato, H. and Frank, D. W. (2004) 'ExoU is a potent intracellular phospholipase', *Mol Microbiol,* 53(5), pp. 1279-1290, doi: 10.1111/j.1365-2958.2004.04194.x.

Saunders, S. H., Tse, E. C. M., Yates, M. D., Otero, F. J., Trammell, S. A., Stemp, E. D. A., Barton, J. K., Tender, L. M. and Newman, D. K. (2020) 'Extracellular DNA promotes efficient extracellular electron transfer by pyocyanin in *Pseudomonas aeruginosa* biofilms', *Cell*, doi: 10.1016/j.cell.2020.07.006.

Savage, V. J., Chopra, I. and O'Neill, A. J. (2013) '*Staphylococcus aureus* biofilms promote horizontal transfer of antibiotic resistance', *Antimicrob Agents Chemother,* 57(4), pp. 1968-1970, doi: 10.1128/AAC.02008-12.

Schatzman, S. S., Peterson, R. L., Teka, M., He, B., Cabelli, D. E., Cormack, B. P. and Culotta, V. C. (2020) 'Copper-only superoxide dismutase enzymes and iron

starvation stress in *Candida* fungal pathogens', *J Biol Chem,* 295(2), pp. 570-583, doi: 10.1074/jbc.RA119.011084.

Schiessl, K. T., Hu, F., Jo, J., Nazia, S. Z., Wang, B., Price-Whelan, A., Min, W. and Dietrich, L. E. P. (2019) 'Phenazine production promotes antibiotic tolerance and metabolic heterogeneity in *Pseudomonas aeruginosa* biofilms', *Nat Commun,* 10(1), pp. 762, doi: 10.1038/s41467-019-08733-w.

Schindelin, J., Arganda-Carreras, I., Frise, E., Kaynig, V., Longair, M., Pietzsch, T., Preibisch, S., Rueden, C., Saalfeld, S., Schmid, B., Tinevez, J. Y., White, D. J., Hartenstein, V., Eliceiri, K., Tomancak, P. and Cardona, A. (2012) 'Fiji: an open-source platform for biological-image analysis', *Nat Methods,* 9(7), pp. 676-682, doi: 10.1038/nmeth.2019.

Scott, F. W. and Pitt, T. L. (2004) 'Identification and characterization of transmissible *Pseudomonas aeruginosa* strains in cystic fibrosis patients in England and Wales', *J Med Microbiol,* 53(Pt 7), pp. 609-615, doi: 10.1099/jmm.0.45620-0.

Sekiya, T. and Nozawa, Y. (1983) 'Reorganization of membrane ergosterol during cell fission events of *Candida albicans*: A freeze-fracture study of distribution of filipin—ergosterol complexes', *J Ultrastruct Res,* 83, pp. 48-57.

Sharma, J., Rosiana, S., Razzaq, I. and Shapiro, R. S. (2019) 'Linking cellular morphogenesis with antifungal treatment and susceptibility in *Candida* pathogens', *J Fungi (Basel),* 5(1), doi: 10.3390/jof5010017.

Shekhova, E., Kniemeyer, O. and Brakhage, A. A. (2017) 'Induction of mitochondrial reactive oxygen species production by itraconazole, terbinafine, and amphotericin B as a mode of action against *Aspergillus fumigatus*', *Antimicrob Agents Chemother,* 61(11), doi: 10.1128/AAC.00978-17.

Sherrard, L. J., Tunney, M. M. and Elborn, J. S. (2014) 'Antimicrobial resistance in the respiratory microbiota of people with cystic fibrosis', *Lancet,* 384(9944), pp. 703-713, doi: 10.1016/S0140-6736(14)61137-5.

Sheth, C. C., Hall, R., Lewis, L., Brown, A. J., Odds, F. C., Erwig, L. P. and Gow, N. A. (2011) 'Glycosylation status of the *C. albicans* cell wall affects the efficiency of neutrophil phagocytosis and killing but not cytokine signaling', *Med Mycol,* 49(5), pp. 513-524, doi: 10.3109/13693786.2010.551425.

Silva, S., Henriques, M., Martins, A., Oliveira, R., Williams, D. and Azeredo, J. (2009) 'Biofilms of non-*Candida albicans Candida* species: quantification, structure and matrix composition', *Med Mycol,* 47(7), pp. 681-689, doi: 10.3109/13693780802549594.

Silva, S., Negri, M., Henriques, M., Oliveira, R., Williams, D. W. and Azeredo, J. (2011) 'Adherence and biofilm formation of non-*Candida albicans Candida* species', *Trends Microbiol,* 19(5), pp. 241-247, doi: 10.1016/j.tim.2011.02.003.

Silva, S., Rodrigues, C. F., Araujo, D., Rodrigues, M. E. and Henriques, M. (2017) '*Candida* species biofilms' antifungal resistance', *J Fungi (Basel),* 3(1), doi: 10.3390/jof3010008.

Silver, P. M., Oliver, B. G. and White, T. C. (2004) 'Role of *Candida albicans* transcription factor Upc2p in drug resistance and sterol metabolism', *Eukaryot Cell,* 3(6), pp. 1391-1397, doi: 10.1128/EC.3.6.1391-1397.2004.

Singh, N., Pemmaraju, S. C., Pruthi, P. A., Cameotra, S. S. and Pruthi, V. (2013) '*Candida* biofilm disrupting ability of di-rhamnolipid (RL-2) produced from *Pseudomonas aeruginosa* DSVP20', *Appl Biochem Biotechnol,* 169(8), pp. 2374-2391, doi: 10.1007/s12010-013-0149-7.

Skrzypek, M. S., Binkley, J., Binkley, G., Miyasato, S. R., Simison, M. and Sherlock, G. (2017) 'The *Candida* Genome Database (CGD): incorporation of Assembly 22, systematic identifiers and visualization of high throughput sequencing data', *Nucleic Acids Res,* 45(D1), pp. D592-D596, doi: 10.1093/nar/gkw924.

Smejkal, G. B., Hoppe, G. and Hoff, H. F. (1996) 'Filipin as a fluorescent probe of lipoprotein-derived sterols on thin-layer chromatograms', *Anal Biochem,* 239, pp. 115-117.

Sobel, J. D. (1997) 'Vaginitis', *N Engl J Med,* 337, pp. 1896-1903.

Sokol, P. A., Darling, P., Woods, D. E., Mahenthiralingam, E. and Kooi, C. (1999) 'Role of ornibactin biosynthesis in the virulence of *Burkholderia cepacia*: characterization of *pvdA*, the gene encoding L-ornithine N5-oxygenase', *Infect Immun,* 67(9), pp. 4443-4455.

Sokol-Anderson, M., Sligh Jr., J. E., Elberg, S., Brajtburg, J., Kobayashi, G. S. and Medoff, G. (1988) 'Role of cell defense against oxidative damage in the resistance of *Candida albicans* to the killing effect of amphotericin B', *Antimicrob Agents Chemother,* 32(5), pp. 702-705, doi: 0.1128/AAC.32.5.702.

Sokol-Anderson, M. L., Brajtburg, J. and Medoff, G. (1986) 'Amphotericin B-induced oxidative damage and killing of *Candida albicans*', *J Infect Dis,* 154(1), pp. 76-83, doi: 10.1093/infdis/154.1.76.

Southey-Pillig, C. J., Davies, D. G. and Sauer, K. (2005) 'Characterization of temporal protein production in *Pseudomonas aeruginosa* biofilms', *J Bacteriol,* 187(23), pp. 8114-8126, doi: 10.1128/JB.187.23.8114-8126.2005.

Stark, R., Grzelak, M. and Hadfield, J. (2019) 'RNA sequencing: the teenage years', *Nature Reviews Genetics*, doi: 10.1038/s41576-019-0150-2.

Stewart, P. S. (2015) 'Antimicrobial tolerance in biofilms', *Microbiol Spectr,* 3(3), pp. MB-0010-2014, doi: 10.1128/microbiolspec.MB-0010-2014.

Taff, H. T., Mitchell, K. F., Edward, J. A. and Andes, D. R. (2013) 'Mechanisms of *Candida* biofilm drug resistance', *Future Microbiol,* 8(10), pp. 1325-1337, doi: 10.2217/fmb.13.101.

Taff, H. T., Nett, J. E., Zarnowski, R., Ross, K. M., Sanchez, H., Cain, M. T., Hamaker, J., Mitchell, A. P. and Andes, D. R. (2012) 'A *Candida* biofilm-induced pathway for matrix glucan delivery: implications for drug resistance', *PLoS Pathog,* 8(8), pp. e1002848, doi: 10.1371/journal.ppat.1002848.

Talapko, J., Juzbasic, M., Matijevic, T., Pustijanac, E., Bekic, S., Kotris, I. and Skrlec, I. (2021) '*Candida albicans* - the virulence factors and clinical manifestations of infection', *J Fungi (Basel),* 7(2), doi: 10.3390/jof7020079.

Thi, M. T. T., Wibowo, D. and Rehm, B. H. A. (2020) '*Pseudomonas aeruginosa* biofilms', *Int J Mol Sci,* 21(22), doi: 10.3390/ijms21228671.

Tong, S., Zhong, H., Yi, C., Cao, X., Firempong, C. K., Zheng, Q., Feng, Y., Yu, J. and Xu, X. (2014) 'Simultaneous HPLC determination of ergosterol and 22,23-dihydroergosterol in *Flammulina velutipes* sterol-loaded microemulsion', *Biomed Chromatogr,* 28(2), pp. 247-254, doi: 10.1002/bmc.3012.

Townsend, E. M., Sherry, L., Kean, R., Hansom, D., Mackay, W. G., Williams, C., Butcher, J. and Ramage, G. (2017) 'Implications of antimicrobial combinations in complex wound biofilms containing fungi', *Antimicrob Agents Chemother,* 61(9), pp. e00672-00617.

Trejo-Hernández, A., Andrade-Domínguez, A., Hernandez, M. and Encarnación, S. (2014) 'Interspecies competition triggers virulence and mutability in *Candida albicans-Pseudomonas aeruginosa* mixed biofilms', *ISME J,* 8(10), pp. 1974-1988, doi: 10.1038/ismej.2014.53.

Turner, K. H., Everett, J., Trivedi, U., Rumbaugh, K. P. and Whiteley, M. (2014) 'Requirements for *Pseudomonas aeruginosa* acute burn and chronic surgical wound infection', *PLoS Genet,* 10(7), pp. e1004518, doi: 10.1371/journal.pgen.1004518.

Uppuluri, P., Srinivasan, A., Ramasubramanian, A. and Lopez-Ribot, J. L. (2011) 'Effects of fluconazole, amphotericin B, and caspofungin on *Candida albicans* biofilms under conditions of flow and on biofilm dispersion', *Antimicrob Agents Chemother,* 55(7), pp. 3591-3593, doi: 10.1128/AAC.01701-10.

Van Acker, H., Sass, A., Bazzini, S., De Roy, K., Udine, C., Messiaen, T., Riccardi, G., Boon, N., Nelis, H. J., Mahenthiralingam, E. and Coenye, T. (2013) 'Biofilm-grown *Burkholderia cepacia* complex cells survive antibiotic treatment by avoiding production of reactive oxygen species', *PLoS One,* 8(3), pp. e58943, doi: 10.1371/journal.pone.0058943.

Van Acker, H., Van Dijck, P. and Coenye, T. (2014) 'Molecular mechanisms of antimicrobial tolerance and resistance in bacterial and fungal biofilms', *Trends Microbiol,* 22(6), pp. 326-333, doi: 10.1016/j.tim.2014.02.001.

Vasicek, E. M., Berkow, E. L., Flowers, S. A., Barker, K. S. and Rogers, P. D. (2014) '*UPC2* is universally essential for azole antifungal resistance in *Candida albicans*', *Eukaryot Cell,* 13(7), pp. 933-946, doi: 10.1128/EC.00221-13.

Vella, F. M. and Laratta, B. (2017) 'UV-based evaluation of ergosterol for monitoring the fungal exposure in Italian buffalo farms', *FEMS Microbiol Lett,* 364(22), doi: 10.1093/femsle/fnx224.

Vermes, A., Guchelaar, H.-J. and Dankert, J. (2000) 'Flucytosine: a review of its pharmacology, clinical indications, pharmacokinetics, toxicity and drug interactions', *J Antimicrob Chemother,* 46, pp. 171-179.

Vilaplana, L. and Marco, M. P. (2020) 'Phenazines as potential biomarkers of *Pseudomonas aeruginosa* infections: synthesis regulation, pathogenesis and analytical methods for their detection', *Anal Bioanal Chem,* 412(24), pp. 5897-5912, doi: 10.1007/s00216-020-02696-4.

Vitális, E., Nagy, F., Tóth, Z., Forgács, L., Bozó, A., Kardos, G., Majoros, L. and Kovács, R. (2020) '*Candida* biofilm production is associated with higher mortality in patients with candidaemia', *Mycoses*, doi: 10.1111/myc.13049.

Wagner, S., Sommer, R., Hinsberger, S., Lu, C., Hartmann, R. W., Empting, M. and Titz, A. (2016) 'Novel strategies for the treatment of *Pseudomonas aeruginosa* infections', *J Med Chem,* 59(13), pp. 5929-5969, doi: 10.1021/acs.jmedchem.5b01698.

Wahab, A. A., Taj-Aldeen, S. J., Kolecka, A., ElGindi, M., Finkel, J. S. and Boekhout, T. (2014) 'High prevalence of *Candida dubliniensis* in lower respiratory tract secretions from cystic fibrosis patients may be related to increased adherence properties', *Int J Infect Dis,* 24, pp. 14-19, doi: 10.1016/j.ijid.2014.03.1380.

Walker, L., Sood, P., Lenardon, M. D., Milne, G., Olson, J., Jensen, G., Wolf, J., Casadevall, A., Adler-Moore, J. and Gow, N. A. R. (2018) 'The viscoelastic properties of the fungal cell wall allow traffic of AmBisome as intact liposome vesicles', *MBio,* 9(1), pp. e02383-02317, doi: 10.1128/mBio.

Walters, M. C., 3rd, Roe, F., Bugnicourt, A., Franklin, M. J. and Stewart, P. S. (2003) 'Contributions of antibiotic penetration, oxygen limitation, and low metabolic activity to tolerance of *Pseudomonas aeruginosa* biofilms to ciprofloxacin and tobramycin', *Antimicrob Agents Chemother,* 47(1), pp. 317-323, doi: 10.1128/aac.47.1.317-323.2003.

Wang, J., Zhou, Z., He, F., Ruan, Z., Jiang, Y., Hua, X. and Yu, Y. (2018) 'The role of the type VI secretion system *vgrG* gene in the virulence and antimicrobial resistance

of *Acinetobacter baumannii* ATCC 19606', *PLoS One,* 13(2), pp. e0192288, doi: 10.1371/journal.pone.0192288.

Wang, Y., Wilks, J. C., Danhorn, T., Ramos, I., Croal, L. and Newman, D. K. (2011) 'Phenazine-1-carboxylic acid promotes bacterial biofilm development via ferrous iron acquisition', *J Bacteriol,* 193(14), pp. 3606-3617, doi: 10.1128/JB.00396-11.

Wang, Z., Gerstein, M. and Snyder, M. (2009) 'RNA-seq: a revolutionary tool for transcriptomics', *Nat Rev Genet,* 10(1), pp. 57-63, doi: 10.1038/nrg2484.

Wargo, M. J., Gross, M. J., Rajamani, S., Allard, J. L., Lundblad, L. K., Allen, G. B., Vasil, M. L., Leclair, L. W. and Hogan, D. A. (2011) 'Hemolytic phospholipase C inhibition protects lung function during *Pseudomonas aeruginosa* infection', *Am J Respir Crit Care Med,* 184(3), pp. 345-354, doi: 10.1164/rccm.201103-0374OC.

Weiler, S., Falkensammer, G., Hammerer-Lercher, A., Anliker, M., Vogelsinger, H., Joannidis, M., Dunzendorfer, S., Stein, M. and Bellmann, R. (2009) 'Pulmonary epithelial lining fluid concentrations after use of systemic amphotericin B lipid formulations', *Antimicrob Agents Chemother,* 53(11), pp. 4934-4937, doi: 10.1128/AAC.00796-09.

Whibley, N. and Gaffen, S. L. (2015) 'Beyond *Candida albicans*: mechanisms of immunity to non-*albicans Candida* species', *Cytokine,* 76(1), pp. 42-52, doi: 10.1016/j.cyto.2015.07.025.

Williams, C., Ranjendran, R. and Ramage, G. (2016) 'Pathogenesis of fungal infections in cystic fibrosis', *Curr Fungal Infect Rep,* 10(4), pp. 163-169, doi: 10.1007/s12281-016-0268-z.

Wolf, T., Kammer, P., Brunke, S. and Linde, J. (2018) 'Two's company: studying interspecies relationships with dual RNA-seq', *Curr Opin Microbiol,* 42, pp. 7-12, doi: 10.1016/j.mib.2017.09.001.

Wood, T. L., Gong, T., Zhu, L., Miller, J., Miller, D. S., Yin, B. and Wood, T. K. (2018) 'Rhamnolipids from *Pseudomonas aeruginosa* disperse the biofilms of sulfate-reducing bacteria', *NPJ Biofilms Microbiomes,* 4, pp. 22, doi: 10.1038/s41522-018-0066-1.

World Health Organisation (2017) 'Global priority list of antibiotic-resistant bacteria to guide research, discovery, and development of new antibiotics', http://www.who.int/medicines/publications/global-priority-list-antibiotic-resistant-bacteria/en/.

Xie, C., Mao, X., Huang, J., Ding, Y., Wu, J., Dong, S., Kong, L., Gao, G., Li, C. Y. and Wei, L. (2011) 'KOBAS 2.0: a web server for annotation and identification of enriched pathways and diseases', *Nucleic Acids Res,* 39, pp. W316-322, doi: 10.1093/nar/gkr483.

Yang, H., Tong, J., Lee, C. W., Ha, S., Eom, S. H. and Im, Y. J. (2015) 'Structural mechanism of ergosterol regulation by fungal sterol transcription factor Upc2', *Nat Commun,* 6, pp. 6129, doi: 10.1038/ncomms7129.

Youseff, B. H., Holbrook, E. D., Smolnycki, K. A. and Rappleye, C. A. (2012) 'Extracellular superoxide dismutase protects *Histoplasma* yeast cells from host-derived oxidative stress', *PLoS Pathog,* 8(5), pp. e1002713, doi: 10.1371/journal.ppat.1002713.

Yu, Y., Albrecht, K., Groll, J. and Beilhack, A. (2020) 'Innovative therapies for invasive fungal infections in preclinical and clinical development', *Expert Opin Investig Drugs,* 29(9), pp. 961-971, doi: 10.1080/13543784.2020.1791819.

Zarnowski, R., Sanchez, H., Covelli, A. S., Dominguez, E., Jaromin, A., Bernhardt, J., Mitchell, K. F., Heiss, C., Azadi, P., Mitchell, A. and Andes, D. R. (2018) '*Candida albicans* biofilm-induced vesicles confer drug resistance through matrix biogenesis', *PLoS Biol,* 16(10), pp. e2006872, doi: 10.1371/journal.pbio.2006872.

Zarnowski, R., Westler, W. M., Lacmbouh, G. A., Marita, J. M., Bothe, J. R., Bernhardt, J., Lounes-Hadj Sahraoui, A., Fontaine, J., Sanchez, H., Hatfield, R. D., Ntambi, J. M., Nett, J. E., Mitchell, A. P. and Andes, D. R. (2014) 'Novel entries in a fungal biofilm matrix encyclopedia', *MBio,* 5(4), pp. e01333-01314, doi: 10.1128/mBio.01333-14.

Zhao, S., Zhang, Y., Gamini, R., Zhang, B. and von Schack, D. (2018) 'Evaluation of two main RNA-seq approaches for gene quantification in clinical RNA sequencing: polyA+ selection versus rRNA depletion', *Sci Rep,* 8(1), pp. 4781, doi: 10.1038/s41598-018-23226-4.

Zwolinska-Wcislo, M., Budak, A., Trojanowska, D., Bogdal, J. and Stachura, J. (1998) 'Fungal colonization of the stomach and its clinical relevance', *Mycoses,* 41(7-8), pp. 327-334.

APPENDIX I: PUBLICATIONS

This appendix contains publications to which I have contributed during my PhD, in chronological order. All previously published work presented in this thesis was explicitly disclosed and appropriately referenced.

i. Kousser, C., Alam, F. and Hall, R. A. (May 2019) 'Fungal interactions in health and disease', *Microbiol Today*, 46(2), pp. 95–97.

ii. Alam, F., Catlow, D., Di Maio, A., Blair, J. M. A. and Hall, R. A. (2020) '*Candida albicans* enhances meropenem tolerance of *Pseudomonas aeruginosa* in a dual-species biofilm', *J Antimicrob Chemother*, 75(4), pp. 925–935.

iii. Alam, F. (Sep 2020) '*Candida albicans*: a shape-shifting fungus', *Biological Sciences Review*, 33(1), pp. 38–41.

Comment

Fungal interactions in health and disease

Courtney Kousser, Farhana Alam and Rebecca Hall

Fungi are important eukaryotic organisms, comprised of more than just mushrooms and moulds, and span beyond environmental saprophytes. Although not all are harmful, from the 100,000 fungal species identified to date, 300 are known to impact human health. These effects can be positive or negative, and this is largely mediated by their interactions with host cells and other resident microbes.

Microbiota: microbiome + mycobiome

The microbiome is a complex community of micro-organisms living on and within humans. The mycobiome represents the fungi present within the microbiota that play important roles in human health. Each anatomical site has a unique microbial fingerprint that can vary with health. For example, the intestinal mycobiome differs between obese and non-obese individuals, as does the oral mycobiome of HIV-positive patients and healthy individuals.

Candida spp. are the most prevalent fungi identified in the mycobiome and, through competition, can act as a protective barrier against invading pathogens. For instance, adapted *Candida albicans* can protect mice against *Aspergillus fumigatus*, *Pseudomonas aeruginosa*, and *Staphylococcus aureus*. On the other hand, fungi can also have negative effects. For example, colonisation by *Candida* and *Saccharomycetes* is associated with hepatitis B, and the presence of *Candida* can exacerbate disease severity and delay healing of lesions in ulcerative colitis and Crohn's disease patients. Furthermore, *Candida* colonisation is correlated with more severe instances of acute graft-versus-host disease following stem cell transplantation.

A polymicrobial world

Polymicrobial interactions dominate the world around us. Just as humans are social beings, microbes constantly form relationships with other organisms. These can be competitive, where microbes fight for resources and space; or co-operative, where they work together to survive inside the host. These interactions take place in the microbial flora of healthy individuals, and in the context of disease. Many infectious diseases are increasingly recognised as polymicrobial, presenting with aggressive pathologies and increased antimicrobial resistance, leading to poorer patient prognosis.

Most polymicrobial interactions occur within mixed biofilms, i.e. communities of cells ensnared within an extracellular matrix of secreted polymers. For example, the oral cavity hosts a cornucopia of fungal-bacterial interactions, thanks to its moist, nutrient-rich environment. The composition of oral biofilms is relatively similar among healthy individuals, due to the presence of a core microbiome; however, the microbial make-up can vary greatly from one individual to another in cases of disease. It is estimated that around 80% of all microbial infections are in the form of biofilms. Common infection

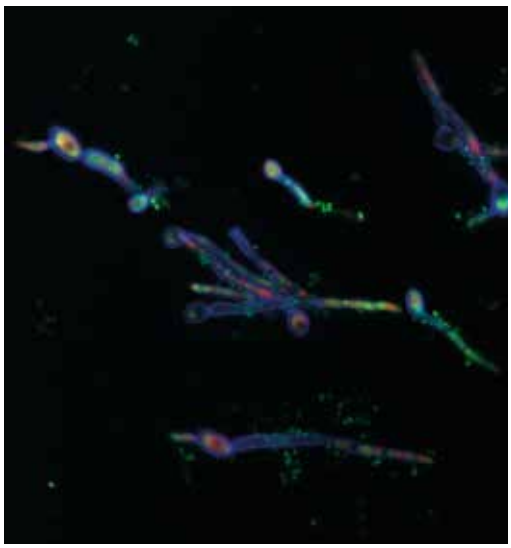


Fig. 1. Microscopic image of *Pseudomonas aeruginosa* attaching to *Candida albicans* hyphae. Dead fungi/bacteria are stained red, fungal chitin is stained purple, and nucleic acids are stained green. Emily Dixon

sites include implanted medical devices, burns, surgical wounds and mucosal surfaces, such as the lung epithelium in cystic fibrosis patients. The prolonged physical proximity of cells within biofilms encourages both intra- and inter-species communication.

The interactions between fungi and bacteria can be physical, chemical or metabolic. Fungal hyphae can provide a scaffold-like structure encouraging formation of fungal–bacterial biofilms or provide a means of transport to enable bacterial dissemination into host tissues. Both types of organism undergo quorum sensing (QS), which is the cell-density-dependent release of signalling molecules that regulate gene expression. The most well-studied cross-kingdom QS interactions are those between *C. albicans* and *P. aeruginosa*, some of which can directly affect virulence.

Antimicrobial resistance

Fungi feature prominently in the fight against antimicrobial resistance. There are currently three main classes of antifungals: azoles, polyenes and echinocandins. The most recent antifungals, anidulafungin and posaconazole, were developed in 2006. The classification, in 2018, of *Candida auris* as the first multi-drug-resistant fungal 'global outbreak pathogen' highlights the urgent need for novel antifungal therapies. As most infections are polymicrobial in nature, this has further implications for antimicrobial drug efficacy. For example, *Streptococcus mutans* has been shown to protect *C. albicans* biofilm cells from the effects of the antifungal fluconazole, via secretion of polymers that sequester the drug. Conversely, *C. albicans* can enhance the tolerance of *Escherichia coli* and *S. aureus* biofilm cells to the antibiotics ofloxacin and vancomycin, respectively. These co-operative interactions suggest that antibiotic–antifungal combination treatments would be clinically more efficacious in many cases.

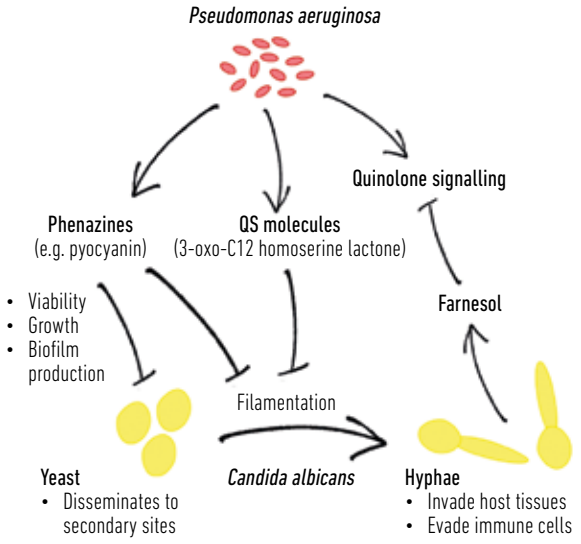


Fig. 3. **Schematic showing the complex ways in which fungi and bacteria can interact, using *Candida albicans* and *Pseudomonas aeruginosa* as an example.** Courtney Kousser and Emily Dixon

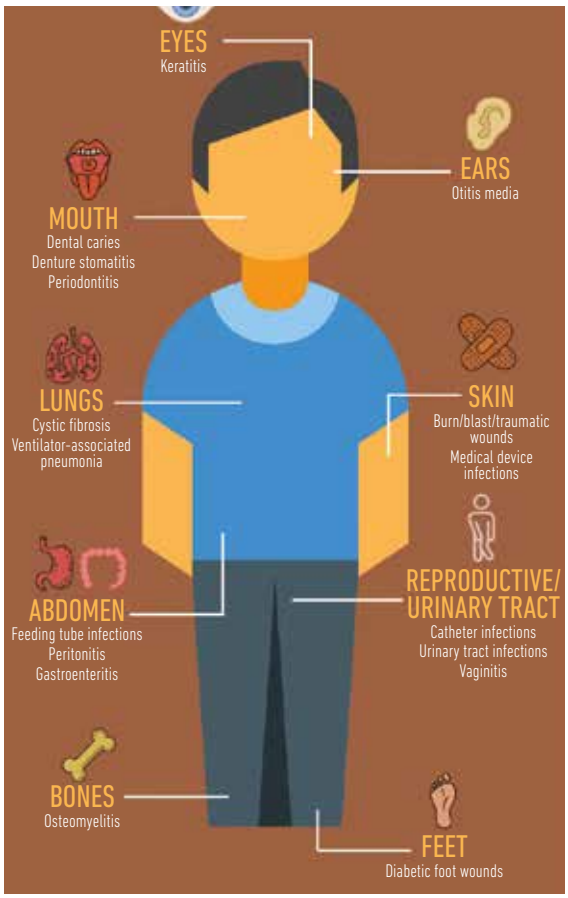


Fig. 2. **Sites of polymicrobial infections and interactions involving fungi.** Courtney Kousser

Training the immune system

Not all polymicrobial interactions involve direct microbe–microbe communication. Relationships between micro-organisms can also be facilitated by host cells. Fungal interactions with the immune system can influence how the host responds to future microbial invasions. For instance, previous sublethal infections with *C. albicans* can prime the immune system; an interaction mediated by the fungal cell wall component, β-glucan, and the phagocyte surface receptor, Dectin-1. This 'training' leads to enhanced leukocyte recruitment, cytokine production and infection clearance when exposed to secondary pathogens, such as *P. aeruginosa*, or repeated inoculation with *C. albicans*.

Future perspectives

Much is yet to be discovered about the myriad effects of fungi on human health and disease. For example, there is evidence that the fungal QS molecule farnesol can affect human fertility, by modulating sperm motility. The impact of other microbial communication molecules on human

health and disease are yet to be investigated, and who knows what implications these will hold for human health.

Further reading

Dhamgaye S, Qu Y, Peleg AY. Polymicrobial infections involving clinically relevant Gram-negative bacteria and fungi. *Cell Microbiol* 2016;18:1716–1722.

Ghannoum M, The Scientist. The Mycobiome;2016. https://www.the-scientist.com/features/the-mycobiome-34129 [accessed 26 February 2019].

Hall RA, Noverr MC. Fungal interactions with the human host: exploring the spectrum of symbiosis. *Curr Opin Microbiol* 2017;40:58–64.

Quinton, J. Fungal mediated innate immune memory, what have we learned? *Semin Cell Dev Biol,* in press.



Courtney Kousser

Institute of Microbiology and Infection, School of Biosciences, University of Birmingham, Edgbaston, Birmingham B15 2TT, UK

e **cak500@bham.ac.uk**

@cakousser

Courtney Kousser is a fourth year PhD student in Dr Rebecca A Hall's lab. Courtney's research focuses on the interaction between the deadly fungus, *Rhizopus microsporus,* and the opportunistic bacterium *Pseudomonas aeruginosa* within the host. She has been a member of the Microbiology Society since 2016 and won the 2018 Sir Howard Dalton Young Microbiologist of the Year Prize.



Farhana Alam

Institute of Microbiology and Infection, School of Biosciences, University of Birmingham, Edgbaston, Birmingham B15 2TT, UK

e **fxa576@student.bham.ac.uk**

@_farhana_alam

Farhana Alam is a second year PhD student working in Dr Rebecca Hall's lab. Her research, in collaboration with Dr Jessica Blair, focuses on fungal–bacterial polymicrobial biofilms and their effects on antimicrobial resistance.



Rebecca Hall

Institute of Microbiology and Infection, School of Biosciences, University of Birmingham, Edgbaston, Birmingham B15 2TT, UK

e **r.a.hall@bham.ac.uk**

@BECKS_182

hall-fungal-research.co.uk

Rebecca Hall is a current MRC-funded Career Development Award Fellow and Lecturer in Microbial Adaptation at the University of Birmingham. Rebecca is interested in how microbes adapt to the environment of the host and the consequences this adaptation has on disease progression. She has been a member of the Microbiology Society since 2014, and is a member of the Eukaryotic Division.

Why does microbiology matter?

Farhana: Microbes include a hugely versatile range of organisms. They are integral to the functioning of most ecosystems, yet we are still in our infancy in understanding their impact.

Courtney: Micro-organisms coat every surface around us, on us, and in our bodies. By understanding how microbes function and how they can impact us, we can better learn how to work with them or fight them.

Rebecca: Studying all aspects of microbiology is important to enhance our understanding and to make new discoveries. Microbiology has been at the heart of identifying the basic principles of life for decades. Even small pieces of the puzzle provide clarity to the larger picture, and open new avenues of exploration. At heart, everyone is a microbiologist, they might just not know it.

What advice would you give to someone starting out in this field?

Farhana: Read widely and don't limit yourself to your specific research area. There is much to be gained from inter-disciplinary learning; like any other form of life, microbiology does not occur in isolation!

Courtney: Attend conferences, speak to the intimidating Principal Investigator, and step outside of your comfort zone. You'll gain confidence and become an active, well-rounded member of the community.

Rebecca: One of the best ways to get to know people, and the field, is to go to a conference, to hear lots of excellent science, ask questions and share ideas. Also, the fungal community may be small, but we are mighty, collaborative and enjoy a good dance!

J Antimicrob Chemother
doi:10.1093/jac/dkz514

Journal of Antimicrobial Chemotherapy

Candida albicans enhances meropenem tolerance of *Pseudomonas aeruginosa* in a dual-species biofilm

Farhana Alam[1], Dominic Catlow[2], Alessandro Di Maio[3], Jessica M. A. Blair[2]† and Rebecca A. Hall [1,4]*†

[1]*Institute of Microbiology and Infection, School of Biosciences, University of Birmingham, Edgbaston, Birmingham B15 2TT, UK;* [2]*Institute of Microbiology and Infection, College of Medical and Dental Sciences, University of Birmingham, Edgbaston, Birmingham B15 2TT, UK;* [3]*Birmingham Advanced Light Microscopy, School of Biosciences, University of Birmingham, Edgbaston, Birmingham B15 2TT, UK;* [4]*Kent Fungal Group, School of Biosciences, University of Kent, Canterbury, CT2 7NZ, UK*

*Corresponding author. E-mail: R.A.Hall@bham.ac.uk
†These authors contributed equally to the article.

Received 24 June 2019; returned 30 July 2019; revised 18 October 2019; accepted 12 November 2019

Background: *Pseudomonas aeruginosa* is an opportunistic bacterium that infects the airways of cystic fibrosis patients, surfaces of surgical and burn wounds, and indwelling medical devices. Patients are prone to secondary fungal infections, with *Candida albicans* being commonly co-isolated with *P. aeruginosa*. Both *P. aeruginosa* and *C. albicans* are able to form extensive biofilms on the surfaces of mucosa and medical devices.

Objectives: To determine whether the presence of *C. albicans* enhances antibiotic tolerance of *P. aeruginosa* in a dual-species biofilm.

Methods: Single- and dual-species biofilms were established in microtitre plates and the survival of each species was measured following treatment with clinically relevant antibiotics. Scanning electron microscopy and confocal microscopy were used to visualize biofilm structure.

Results: *C. albicans* enhances *P. aeruginosa* biofilm tolerance to meropenem at the clinically relevant concentration of 5 mg/L. This effect is specific to biofilm cultures and is dependent upon *C. albicans* extracellular matrix polysaccharides, mannan and glucan, with *C. albicans* cells deficient in glycosylation structures not enhancing *P. aeruginosa* tolerance to meropenem.

Conclusions: We propose that fungal mannan and glucan secreted into the extracellular matrix of *P. aeruginosa*/*C. albicans* dual-species biofilms play a central role in enhancing *P. aeruginosa* tolerance to meropenem, which has direct implications for the treatment of coinfected patients.

Introduction

The majority of infections in humans are polymicrobial in nature, with common diseases no longer considered to be caused by a single aetiological agent.[1] The most prevalent polymicrobial infections include periodontitis, gastroenteritis, diabetic foot wounds, burn wounds and biofilm-associated infections.[1,2]

The genetic disease, cystic fibrosis (CF), is characterized by thickening of the mucus layer lining the endothelium of the respiratory tract, which provides an ideal environment for microbial colonization.[3] Reduced mucociliary clearance enables these microorganisms to persist and form polymicrobial biofilms on the mucosa of the lower respiratory tract.[1] The CF lung is a major site of interaction between *Pseudomonas aeruginosa* and *Candida albicans*.[4,5] Around 70% of CF patients become chronically infected with *P. aeruginosa* by the age of 30,[6] with *C. albicans* isolated from up to 75% of CF patients,[7] although sputum samples are often contaminated with microbes from the upper respiratory tract and oral cavity.[8] However, simultaneous colonization has been linked to severer clinical outcomes,[9,10] due to accelerated decline in lung function and worsening of disease progression.[10,11]

Biofilms are structured communities of microbial cells ensnared within a matrix of extracellular polymeric substances.[12,13] Biofilms are formed by bacterial and fungal species and an estimated 65%–80% of all microbial infections in humans are biofilm related.[2,14] This has important clinical implications as the MICs of antimicrobials for biofilm cells can be 100–1000 times greater than for planktonic cells.[15,16] Antimicrobial resistance in microorganisms poses an increasing challenge to public health worldwide,[17,18] making biofilms a particularly relevant topic of research.

© The Author(s) 2019. Published by Oxford University Press on behalf of the British Society for Antimicrobial Chemotherapy.
This is an Open Access article distributed under the terms of the Creative Commons Attribution License (http://creativecommons.org/licenses/by/4.0/), which permits unrestricted reuse, distribution, and reproduction in any medium, provided the original work is properly cited.

Previous work on interactions between *P. aeruginosa* and *C. albicans* has focused predominantly on physical and molecular interactions and their effects on growth, morphology and virulence.[19–24] However, little is known of how their interactions affect antimicrobial drug efficacy. Studies on mono-species *C. albicans* and *P. aeruginosa* biofilms have linked biofilm extracellular matrix (ECM) material to antimicrobial drug inhibition. For example, the fungal polysaccharide β-1,3-glucan sequesters the antifungal fluconazole,[25] whilst the *P. aeruginosa* exopolysaccharides Pel and Psl are implicated in the inhibition of various antibiotics, including tobramycin.[26] Therefore, a greater understanding of the impact of this cross-kingdom interaction on antimicrobial tolerance is of great clinical importance.

Meropenem is a first-line antibiotic for treating *Pseudomonas* infections in the CF lung.[27] Meropenem is a carbapenem β-lactam that targets PBPs within Gram-negative bacteria, causing inhibition of cell wall peptidoglycan synthesis, ultimately leading to osmotic lysis of bacterial cells.[28,29] Meropenem is administered intravenously as a 15–30 min infusion of 1–2 g (adult dose), thrice daily for 2 weeks.[30] When *P. aeruginosa* biofilms are treated with clinical doses of meropenem, only bacteria at the biofilm peripheries are killed, whilst cells closer to the base remain viable.[31] In patients, the meropenem concentration found in epithelial lining fluid 1 h post-treatment is 5.3 mg/L,[30] with the clinical breakpoint of *Pseudomonas* being >8 mg/L.[32] Therefore, slight deviations in tolerance of *P. aeruginosa* to meropenem could impede clearance of the infection. Here, we observed that *P. aeruginosa*/*C. albicans* dual-species biofilms displayed enhanced tolerance to meropenem. This protection was provided through active secretion of fungal ECM components, specifically mannan and β-glucan. Therefore, co-colonization of *P. aeruginosa* and *C. albicans* within the CF lung may result in small reservoirs of protected *P. aeruginosa*, which could survive antimicrobial treatment and reseed the infection site.

Materials and methods

Strains and growth conditions

Strains of *P. aeruginosa* and *Candida* species used in this study are listed in Table 1. *P. aeruginosa* strains were maintained on, and cultured in, Miller-modified LB and *C. albicans* strains in yeast extract peptone dextrose (YPD) medium. Both were grown at 37°C, with aeration at 200 rpm. Antimicrobials (from Sigma–Aldrich, UK) were used at the following concentrations (mg/L): meropenem, 0, 1, 2.5, 5 and 10; ceftazidime, 0 and 5; ciprofloxacin, 0 and 0.05; tobramycin, 0 and 2; and fluconazole, 0, 250, 500, 750 and 1000.

Formation of dual-species biofilms

Biofilms were grown in 96-well plates as previously described.[33] Briefly, cultures were washed twice in PBS and *P. aeruginosa* cultures diluted to OD_{600} of 0.2 and *Candida* strains diluted to 1×10^6 cells/mL in Mueller–Hinton broth (MHB) or DMEM supplemented with 1% L-glutamine. *P. aeruginosa* (2.4×10^6) and *Candida* (1×10^5) cells were incubated statically in flat-bottom 96-well plates for 2 h at 37°C to enable attachment, then non-adhered cells were removed and replaced with fresh medium. After 24h, the medium was replaced with fresh medium containing the appropriate amount of antimicrobial, or vehicle control, for an additional 18 h. To disrupt biofilms, medium was replaced with 100 μL of PBS containing 50 mg/L DNase and incubated at 37°C for 1 h. Biofilms were detached using a water bath sonicator, serially diluted 1 in 10 in PBS and plated onto cetrimide agar (to determine viable *P. aeruginosa* cfu) and YPD agar supplemented with 100 mg/L tetracycline (to determine viable *Candida* cfu). Experiments were performed with three technical and at least three biological replicates.

Formation of *P. aeruginosa* biofilms in the presence of dead *C. albicans* or ECM components

To inactivate *C. albicans*, stationary-phase cultures were washed with PBS and cells either heat-killed at 100°C in PBS for 1 h or fixed in 1 mL of 4% paraformaldehyde (PFA) at room temperature for 1 h. Cells were then washed with PBS and diluted in MHB to 1×10^6 cells/mL. Subsequently, biofilms were established and quantified as above.

Mono-species *P. aeruginosa* biofilms were established and grown for 24 h in MHB supplemented, at either 0 or 24 h, with 0.25 mg/mL glucan (from *Saccharomyces cerevisiae*), laminarin (from *Laminaria digitata*), mannan (from *S. cerevisiae*) or chitosan. All polysaccharides were obtained from Sigma–Aldrich, UK. After 24 h, medium was replaced with MHB containing the appropriate amount of antibiotic and biofilms were subsequently incubated and quantified as above.

Scanning electron microscopy of biofilms

Biofilms were prepared for scanning electron microscopy using a previously published protocol[34] with modifications. Single- and dual-species biofilms were grown on cell culture-treated plastic coverslips (Thermo Fisher Scientific) in 24-well plates for 24 h, after which the MHB medium was replaced with MHB with or without 5 mg/L meropenem. At 48 h, coverslips were washed twice with PBS and samples fixed in 2.5% glutaraldehyde in 0.1 M phosphate buffer for 1 h, at 4°C. Samples were dehydrated using increasing ethanol concentrations (50%, 70%, 90% and 100%) twice for 15 min each. Ethanol was replaced with liquid CO_2 and heated up to the critical point to dry the samples. Each coverslip was mounted on a stub and sputter-coated with platinum. Scanning electron microscopy images were captured using a Philips XL30 ESEM-FEG environmental scanning electron microscope.

Confocal microscopy of biofilms

Single- and dual-species biofilms with or without 5 mg/L meropenem were grown as above, scaled up to a final volume of 6 mL, in 6-well plates. Medium was replaced with PBS containing 5 mg/L propidium iodide (stains dead cells), 1 μM Syto 9 (dyes DNA) and 3 mg/L calcofluor white (stains fungal cell wall chitin) and incubated at 4°C in the dark for 1 h. Biofilms were then fixed by adding 4% PFA, incubated at 4°C in the dark for 1 h and then washed twice with PBS. Confocal microscopy was performed using a Leica SP8 system equipped with a Leica DM6 upright microscope, a ×40/0.80 objective and 402, 488 and 561 nm lasers. Biofilms were imaged directly in wells with a water-dipping lens. Z-stack scans were taken at two or three different areas within each well and processed with Fiji and LASx software.

Planktonic assay

P. aeruginosa (2.4×10^7) and *C. albicans* (1×10^6) cells were added to 14 mL vent-capped culture tubes in a final volume of 2 mL MHB. Cultures were incubated for 3 h at 37°C with aeration at 200 rpm; the appropriate amount of antibiotic was added and cultures incubated for an additional 18 h. Cultures were sonicated in a water bath sonicator and serially diluted and plated for viable counts. Experiments were performed with three technical and four biological replicates.

Table 1. Bacterial and fungal strains used in this study

Strain	Common name	Genotype	Reference/source
P. aeruginosa strains			
ATCC 15692	PAO1	WT	ATCC
Midlands 1	Midlands 1	clinical isolate	[48]
C. albicans strains			
SC5314	SC5314	type strain	[56]
NGY152	NGY152	*ura3Δ::imm34/ura3Δ::imm434; RPS1/rps1Δ::URA3*	[57]
NGY355	*pmr1Δ*	*ura3Δ::imm434/ura3Δ::imm434; pmr1Δ::hisG/pmr1Δ::hisG; RPS10/rps10Δ::URA3*	[58]
NGY356	*pmr1Δ + PMR1*	*ura3Δ::imm434/ura3Δ::imm434; pmr1Δ::hisG/pmr1Δ::hisG; RPS1/rps1Δ::*CIp10-*PMR1*	[58]
CDH15	*mnn4Δ*	*ura3Δ::imm434/ura3Δ::imm434; mnn4Δ::hisG/mnn4Δ::hisG; RPS10::URA3*	[57]
CDH13	*mnn4Δ + MNN4*	*ura3Δ::imm434/ura3Δ::imm434; mnn4Δ::hisG/mnn4Δ::hisG; RPS10::*[CIp10-*MNN4-URA3*]$_n$	[57]
NGY582	*mnn2Δ*	*ura3Δ::imm434/ura3Δ::imm434; mnn2Δ::dpi200/mnn2Δ::dpi200; RPS1/rps1Δ::*CIp10	[46]
NGY583	*mnn2Δ + MNN2*	*ura3Δ::imm434/ura3Δ::imm434; mnn2Δ::dpl200/mnn2Δ::dpl200; RPS1/rps1Δ::*CIp10-*MNN2*	[46]
NGY600	*Δmnn2-26*	*ura3Δ::imm434/ura3Δ::imm434; mnn2Δ::dpl200/mnn2Δ::dpl200; mnn22Δ::dpl200/mnn2Δ::dpl200; mnn23Δ::dpl200/mnn23Δ::dpl200; mnn24Δ::dpl200/mnn24Δ::dpl200; mnn26Δ::dpl200/mnn26Δ::dpl200; mnn21Δ::dpl200/mnn21Δ::dpl200; RPS1/rps1Δ::*CIp10	[46]
NGY337	*mnt1Δ/mnt2Δ*	*ura3Δ::imm434/ura3Δ::imm434; mnt1Δ::hisG/mnt1Δ::hisG; mnt2Δ::hisG/mnt2Δ::hisG; RPS10/rps10Δ::*CIp10	[55]
NGY335	*mnt1Δ/mnt2Δ + MNT1*	*ura3Δ::imm434/ura3Δ::imm434; mnt1Δ::hisG/mnt1Δ::hisG; mnt2Δ::hisG/mnt2Δ::hisG; RPS10/rps10Δ::*CIp10-*MNT1*	[55]
Non-*albicans Candida* strains			
WU284	*C. dubliniensis*	WT	[59]
CAY676	*C. tropicalis*	type strain	ATCC
CLIB214	*C. parapsilosis*	type strain	[60]
AM16/0701	*C. krusei*	clinical isolate	D. MacCallum, University of Aberdeen, Scotland, UK
ATCC 2001	*C. glabrata*	type strain	ATCC

Determination of P. aeruginosa susceptibility to meropenem

MICs of meropenem were determined for *P. aeruginosa* strains according to the standardized broth microdilution method using MHB.[35] Concentrations of meropenem used were 0, 1, 2, 4, 8, 16 and 32 mg/L. MICs were determined for *P. aeruginosa* strains using cells grown on LB agar and cells recovered from biofilms. MICs were the lowest concentrations of meropenem that caused no visible growth.

Statistical analysis

Statistical analyses were done using GraphPad Prism 8.0.0 software. Data were analysed using two-way ANOVA and Holm–Sidak's multiple comparisons test.

Results

C. albicans increases the tolerance of P. aeruginosa to meropenem in dual-species biofilms

To determine whether the presence of *C. albicans* within a *P. aeruginosa* biofilm can enhance tolerance of *P. aeruginosa* to meropenem, preformed mono-species (*P. aeruginosa*) and dual-species (*P. aeruginosa*/*C. albicans*) biofilms were treated with meropenem and *P. aeruginosa* survival quantified by viable counts. Given that the concentration of meropenem in the lung immediately after administration is between 5 and 6 mg/L,[30] this drug concentration was the focus of the study. The viability of *P. aeruginosa* mono-species biofilms was reduced to 25.35% when treated with 5 mg/L meropenem, indicating *P. aeruginosa* biofilm cells are susceptible to meropenem. Fewer *P. aeruginosa* cells were recovered from dual-species biofilms, which is likely due to nutrient competition. However, in the presence of *C. albicans*, meropenem was non-effective against *P. aeruginosa* in both MHB (Figure 1a) and DMEM (Figure S1, available as Supplementary data at *JAC* Online), indicating that this inter-kingdom interaction negatively affects meropenem efficacy.

To visualize the structure of the biofilms, samples were analysed by scanning electron microscopy and confocal microscopy. Mono-species *P. aeruginosa* biofilms were significantly reduced in the presence of meropenem, while in the meropenem-treated dual-species biofilms, significant levels of *P. aeruginosa* colonized

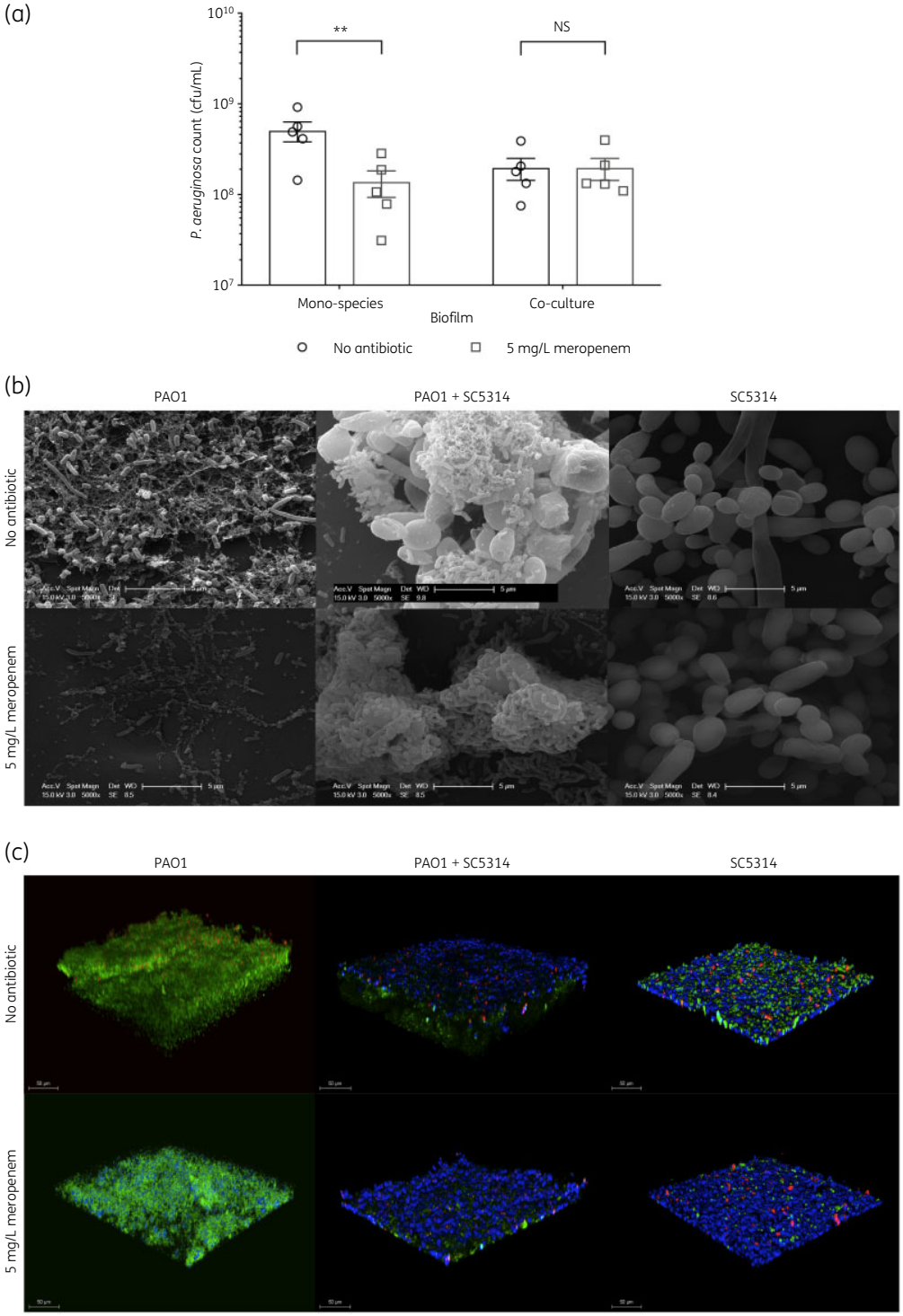


Figure 1. *C. albicans* increases the tolerance of *P. aeruginosa* to meropenem in a dual-species biofilm. (a) Preformed 24 h biofilms were incubated for 18 h in MHB containing no antibiotic or 5 mg/L meropenem. Data are the mean ± SEM from five biological replicates. Data were analysed using two-way ANOVA and Holm–Sidak's multiple comparisons test (**$P < 0.01$). NS, not significant. (b) Scanning electron microscopy analysis of biofilms. Meropenem treatment of mono-species *P. aeruginosa* biofilms results in death of bacterial cells, whilst the presence of *C. albicans* in the dual-species biofilm enhances meropenem tolerance; the tight association of *P. aeruginosa* cells to fungal surfaces is visible. *C. albicans* alone is unaffected by meropenem. (c) 3D reconstructions of biofilms from confocal z-stacks. Red indicates propidium iodide stain (dead cells), green indicates Syto 9 dye (DNA) and blue indicates calcofluor white stain (chitin).

the fungal hyphae (Figure 1b), confirming the cfu data. In agreement with this, the biofilm thickness was lower in meropenem-treated dual-species biofilms (Figure 1c and Figure S2), indicating dense packing of bacterial cells against fungal hyphae, creating a more compact biofilm structure. Therefore, the presence of *C. albicans* enhances the tolerance of *P. aeruginosa* to meropenem.

To identify whether this dual-species interaction had any impact on antifungal resistance, biofilms were treated with fluconazole. *C. albicans* cells in dual-species biofilms showed similar susceptibility levels to fluconazole as untreated controls at all tested concentrations. Therefore, the presence of *P. aeruginosa* does not affect the antifungal activity of fluconazole under the tested conditions (Figure S3).

Meropenem tolerance is not maintained following subculture of P. aeruginosa biofilm cells

The selective pressure from antibiotic use increases the likelihood of cells developing resistance. The sessile nature and close proximity of biofilm cells promotes cell–cell interactions,[36] increasing horizontal gene transfer and mutation frequencies relative to planktonic cells.[37] Furthermore, the presence of *C. albicans* increases *P. aeruginosa* mutation rates.[20] To determine whether the observed increase in meropenem tolerance of *P. aeruginosa* was due to selection for resistance mutations, the meropenem MICs for cells recovered from both *P. aeruginosa* mono- and dual-species biofilms that had been treated with 5 mg/L meropenem, or untreated, were determined by standard broth microdilution MIC assay and compared with the MIC for the starter culture. The MIC for *P. aeruginosa* under all tested conditions was 4 mg/L, suggesting that *P. aeruginosa* cells recovered from treated biofilms were not resistant to meropenem and, therefore, the observed increased tolerance was unlikely due to selection for resistance mutations.

Increased tolerance of P. aeruginosa to meropenem is specific to dual-species biofilms

Enhanced survival of *P. aeruginosa* as a result of interactions with *C. albicans* has previously been observed in planktonic cultures, through inter–kingdom communication via secreted metabolites.[21] To determine whether the observed increase in meropenem tolerance of *P. aeruginosa* was specific to biofilms, *P. aeruginosa* susceptibility to meropenem in the presence of *C. albicans* was tested during planktonic growth. At all meropenem concentrations tested, there was no significant difference in *P. aeruginosa* survival whether in the presence or absence of *C. albicans* (Table 2), suggesting that *C. albicans*-mediated protection is biofilm specific.

Increased P. aeruginosa tolerance to meropenem is dependent on fungal viability

Production of biofilm ECM is an active process, involving secretion of glycoproteins, polysaccharides, lipids and nucleic acids.[2] To determine whether the protective effect of *C. albicans* is mediated by an active or passive mechanism, *P. aeruginosa* biofilms were grown in the presence of either heat-killed *C. albicans* (disrupts the fungal cell wall, denatures proteins and causes cell lysis) or by fixing the *C. albicans* cells in 4% PFA (maintains cell structure). However, in the presence of heat-killed or PFA-fixed *C. albicans*, *P. aeruginosa* remained susceptible to meropenem (Figure 2), suggesting that *C. albicans* actively protects *P. aeruginosa* from meropenem.

Table 2. Increased *P. aeruginosa* meropenem tolerance in the presence of *C. albicans* is biofilm specific

Meropenem (mg/L)	Planktonic culture	*P. aeruginosa* count (cfu/mL), mean ± SEM	*P*
0	mono-species	$4.00\times10^{9}\pm4.14\times10^{8}$	0.9040
	co-culture	$3.81\times10^{9}\pm2.78\times10^{8}$	
1	mono-species	$2.19\times10^{9}\pm1.63\times10^{8}$	0.3218
	co-culture	$1.64\times10^{9}\pm2.97\times10^{8}$	
2.5	mono-species	$7.36\times10^{8}\pm8.39\times10^{7}$	0.9650
	co-culture	$8.12\times10^{8}\pm1.57\times10^{8}$	
5	mono-species	$8.75\times10^{7}\pm2.82\times10^{7}$	0.9650
	co-culture	$1.56\times10^{8}\pm4.92\times10^{7}$	

Planktonic cultures were grown for 3 h and subsequently incubated for 18 h in MHB containing 0, 1, 2.5 or 5 mg/L meropenem. Data are the mean ± SEM from four biological replicates. Data were analysed using two-way ANOVA and Holm–Sidak's multiple comparisons test.

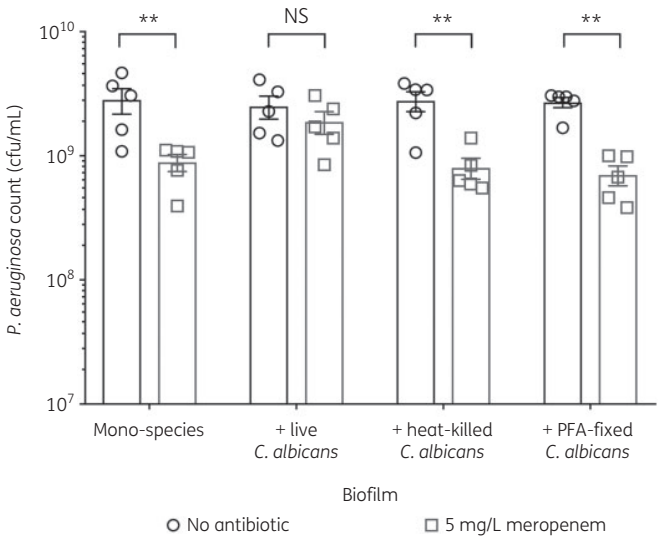


Figure 2. Increased tolerance to meropenem is dependent on fungal viability. Preformed 24 h biofilms were incubated for 18 h in MHB containing no antibiotic or 5 mg/L meropenem. Data are the mean ± SEM from five biological replicates. Data were analysed using two-way ANOVA and Holm–Sidak's multiple comparisons test (**$P<0.01$). NS, not significant.

Candida dubliniensis also enhances P. aeruginosa meropenem tolerance in dual-species biofilms

Only a few species of the *Candida* genus are associated with disease in humans, including *C. albicans*, *C. dubliniensis*, *Candida tropicalis*, *Candida parapsilosis*, *Candida krusei* and *Candida glabrata*.[38]

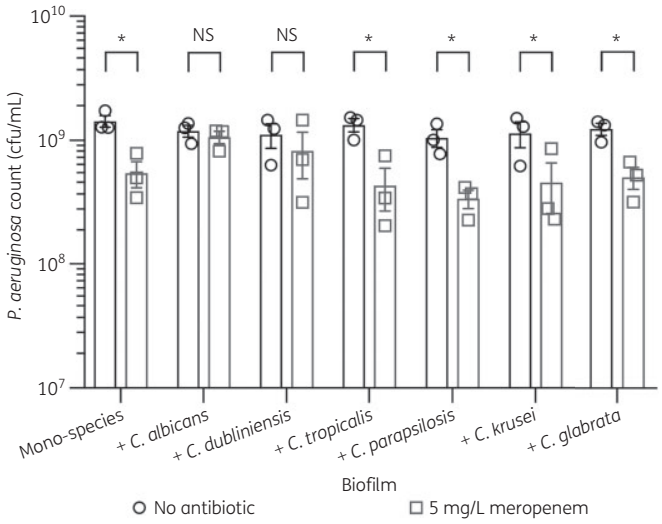


Figure 3. *C. dubliniensis* also enhances tolerance of *P. aeruginosa* to meropenem in dual-species biofilms. Preformed 24 h biofilms were incubated for 18 h in MHB containing no antibiotic or 5 mg/L meropenem. Data are the mean ± SEM from three biological replicates. Data were analysed using two-way ANOVA and Holm–Sidak's multiple comparisons test (*$P < 0.05$). NS, not significant.

To determine whether other *Candida* species can also protect *P. aeruginosa* from meropenem, biofilms were grown in the presence of these clinically relevant non-*albicans Candida* (NAC) species. Of the NAC species tested, only *C. dubliniensis* increased the tolerance of *P. aeruginosa* to meropenem (Figure 3). *C. dubliniensis* is phylogenetically most closely related to *C. albicans*,[39] indicating that *C. albicans* and *C. dubliniensis* may enhance *P. aeruginosa* meropenem tolerance in a similar manner.

Fungal cell wall polysaccharides enhance P. aeruginosa tolerance to meropenem

The secretion of ECM polymers, specifically polysaccharides, by *C. albicans* biofilm cells is linked to increased antifungal resistance of fungal biofilms.[40,41] However, there is increasing evidence that fungal ECM polysaccharides also contribute to antibiotic resistance in dual-species fungal/bacterial biofilms.[34,42,43] To determine whether secreted fungal cell wall polymers play a role in protecting *P. aeruginosa*, mono-species *P. aeruginosa* biofilms were grown in the presence of purified fungal cell wall polysaccharides, including glucan (a mix of β-1,3-glucan and β-1,6-glucan), laminarin (an isoform of β-1,3-glucan), mannan and chitosan (deacetylated chitin). Both mannan and glucan enhanced tolerance of *P. aeruginosa* to meropenem in biofilms (Figure 4a), but not in planktonic cultures (Figure 4c). To determine whether mannan and glucan have independent effects, *P. aeruginosa* biofilms were supplemented with glucan and mannan in combination. However, no additive effect was observed (Figure 4b). Mannan and glucan protected *P. aeruginosa* when added to mature biofilms at the same time as meropenem (Figure S4), suggesting that the polysaccharides may sequester or inhibit the activity of the drug. Therefore, *C. albicans* actively secretes mannan and/or glucan into the biofilm ECM, which protects *P. aeruginosa* from meropenem.

C. albicans cell wall glycosylation is important for protection against meropenem

To further investigate the role of fungal mannan in meropenem tolerance, the ability of *C. albicans* cell wall glycosylation mutants to protect *P. aeruginosa* was quantified. *C. albicans* has two major forms of mannan, the extensively branched N-linked mannan and the simple, linear O-linked mannan. Deletion of genes involved in key glycosylation steps results in the incorporation of altered mannan epitopes in the cell wall (Figure 5a) and within the ECM.[44–46] To elucidate the role of these glycosylation structures in protecting *P. aeruginosa* from meropenem, mutants defective in general protein glycosylation (*pmr1*Δ, ATPase required for transporting Ca^{2+} and Mn^{2+} ions into the Golgi), *N*-mannan phosphomannan incorporation (*mnn4*Δ), *N*-mannan side chain elaboration (*mnn2*Δ, *mnn2–26*Δ) and *O*-mannan biosynthesis (*mnt1*Δ/*mnt2*Δ) were tested for their ability to protect *P. aeruginosa* from meropenem. Deletion of genes required for *N*-mannan biosynthesis (*mnn4*, *mnn2–26* and *pmr1*) reduced the ability of *C. albicans* to protect *P. aeruginosa* from meropenem (Figure 5b and c). Scanning electron microscopy analysis showed very few bacterial cells surviving meropenem treatment in dual-species biofilms with *C. albicans* glycosylation mutants (Figure 5e) but bacteria that did survive were closely adhered to the fungal cell surface, suggesting cell–cell adherence may play a role in meropenem tolerance. In agreement with this, deletion of genes involved in *O*-mannan biosynthesis (*mnt1*/*mnt2*), which have previously been shown to be involved in bacterial attachment to *C. albicans*,[47] had the greatest impact on *P. aeruginosa* protection (Figure 5d and e). This indicates that protection of *P. aeruginosa* requires full elaboration of fungal mannan.

C. albicans does not enhance P. aeruginosa tolerance to other antibiotics

To determine whether the presence of *C. albicans* also affects tolerance of *P. aeruginosa* biofilm cells to other clinically relevant antibiotics, mono- and dual-species biofilms were treated with 5 mg/L ceftazidime, 0.05 mg/L ciprofloxacin, 2 mg/L tobramycin or a combination of 5 mg/L meropenem and 2 mg/L tobramycin. However, the presence of *C. albicans* did not provide protection against these antimicrobial treatments (Figure S5a and b), suggesting that the mechanism by which *C. albicans* confers enhanced tolerance is likely due to the chemical structure of meropenem.

C. albicans protects P. aeruginosa CF isolates from meropenem

To explore the clinical relevance of the above findings, the ability of *C. albicans* to increase meropenem tolerance of clinical CF isolates was tested. Mono-species biofilms of the Midlands 1 CF isolate[48] were susceptible to meropenem. However, *P. aeruginosa* survival was unaffected during growth in a dual-species biofilm with *C. albicans* (Figure 6), suggesting that in CF patients, co-colonization with *C. albicans* may increase *P. aeruginosa* tolerance to meropenem.

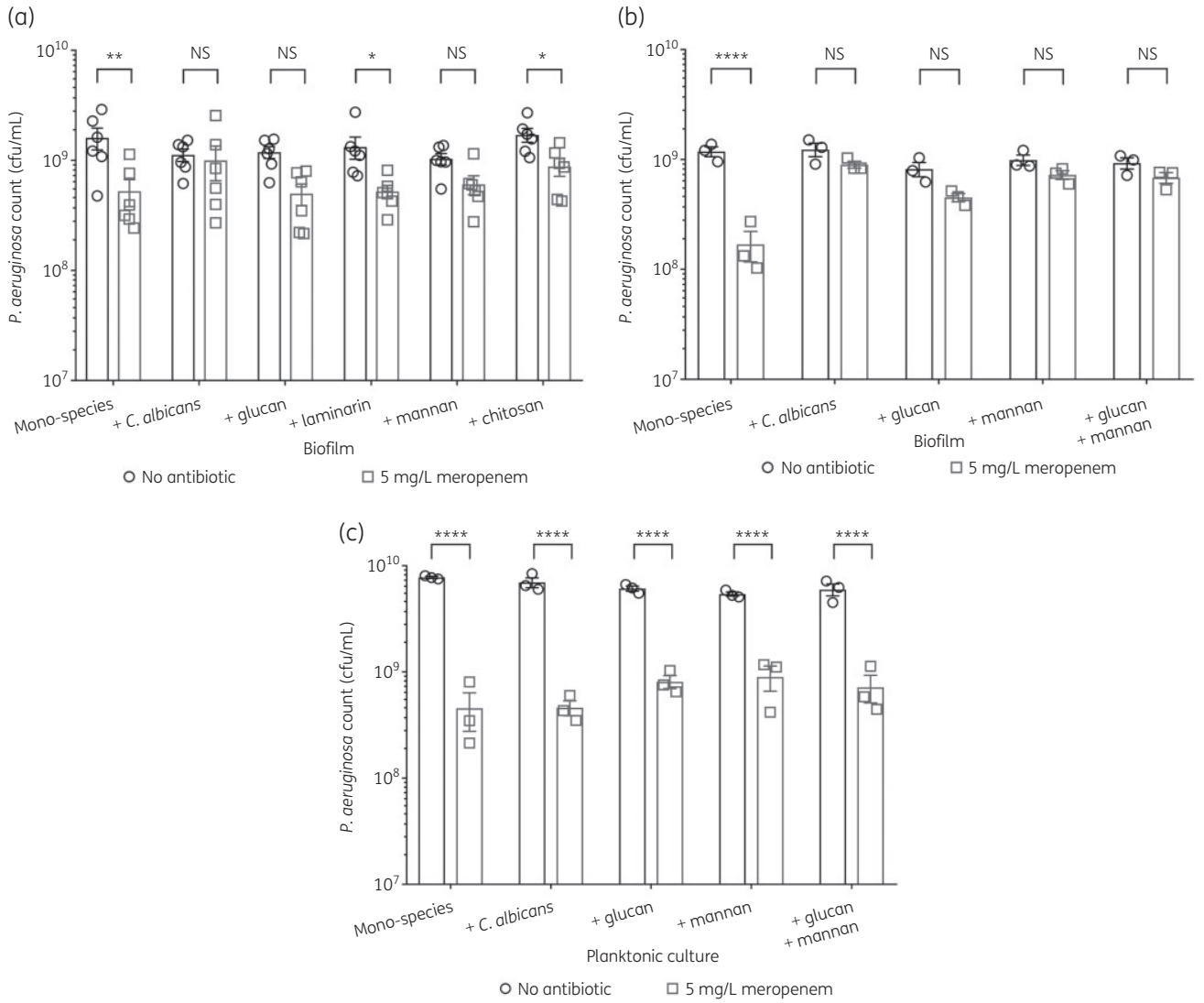


Figure 4. Mannan and glucan enhance *P. aeruginosa* biofilm tolerance to meropenem. Fungal polysaccharides were used at a final concentration of 0.25 mg/mL. (a) Mannan and glucan enhance *P. aeruginosa* biofilm tolerance to 5 mg/L meropenem. Preformed 24 h biofilms were incubated for 18 h in MHB containing no antibiotic or 5 mg/L meropenem. Data are the mean ± SEM from six biological replicates. (b) The effects of mannan and glucan are not additive. (c) Enhanced meropenem tolerance from mannan and glucan is biofilm specific. Planktonic cultures supplemented with exogenous mannan and/or glucan were grown for 3 h and subsequently incubated for 18 h in MHB containing 5 mg/L meropenem. Data are the mean ± SEM from three biological replicates. Data were analysed using two-way ANOVA and Holm–Sidak's multiple comparisons test (*$P < 0.05$, **$P < 0.01$ and ****$P < 0.0001$). NS, not significant.

Discussion

P. aeruginosa and *C. albicans* are commonly co-isolated from the sputum of CF patients,[20] where the thickened mucus layer lining the endothelium of the lower respiratory tract provides an ideal environment for biofilm formation.[3,7] Chronic *P. aeruginosa* colonization in the CF lung is correlated with increased likelihood of *C. albicans* colonization, indicating a synergistic interaction that leads to a greater decline in lung function.[10,11] Here, we show that *C. albicans* significantly enhanced *P. aeruginosa* biofilm tolerance to 5 mg/L meropenem in both a laboratory strain and a CF isolate. Although the protective effect was relatively small (<1 $\log_{10}$ change in *P. aeruginosa* cfu/mL), this may still have clinical relevance. For example, the clinical breakpoint of *P. aeruginosa* for meropenem is >8 mg/L;[32] this increased tolerance could push the required meropenem concentration over the clinical breakpoint, categorizing the infection as meropenem resistant. This has direct implications for treatment of CF patients who present with coinfection. Standard doses of meropenem may become insufficient for treating *P. aeruginosa* infection, with combination antibiotic/antifungal therapy being a potentially more effective therapeutic option.

The protective effect of *C. albicans* was biofilm specific and dependent upon fungal ECM components. This is consistent with

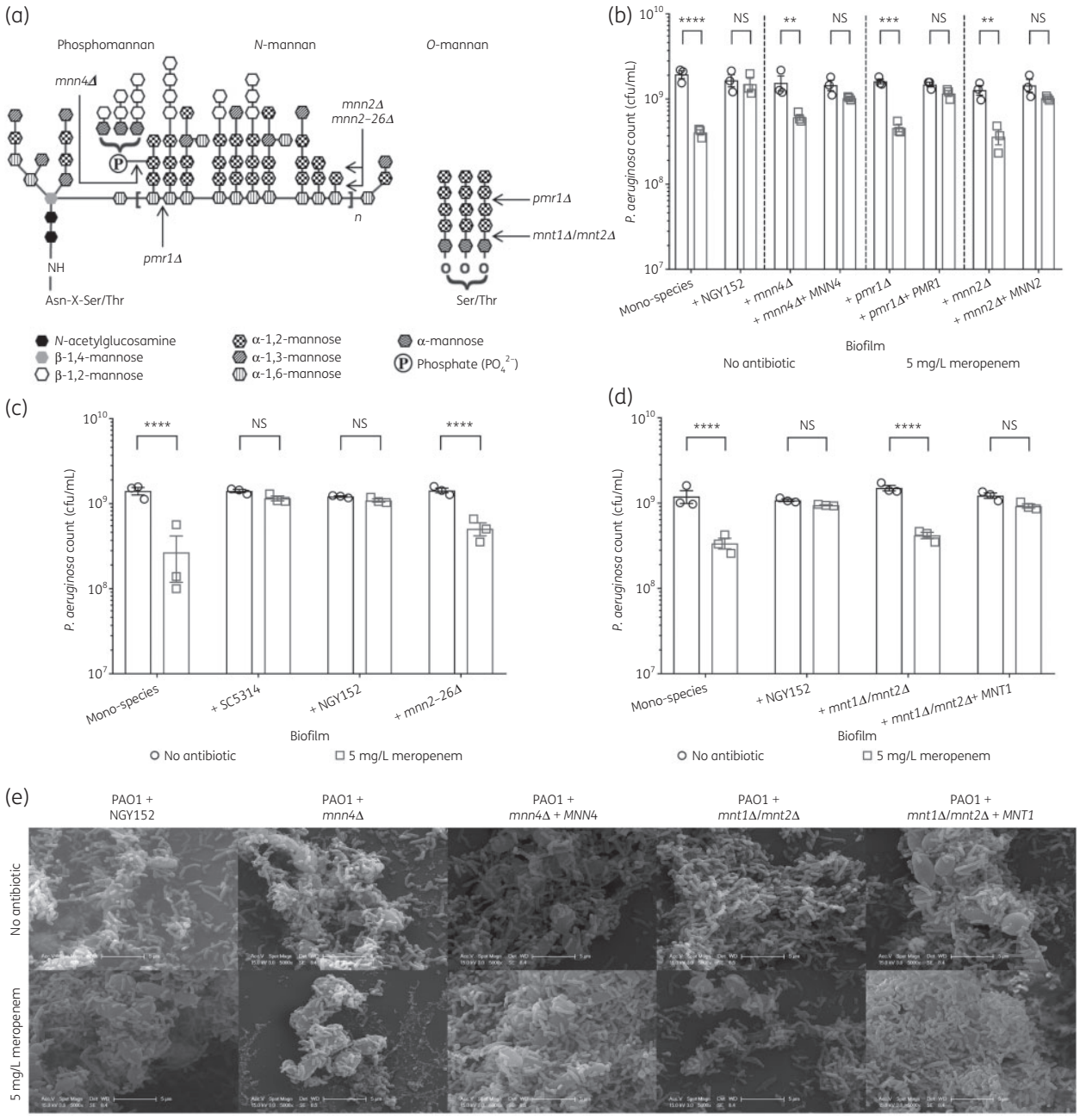


Figure 5. *C. albicans* cell wall glycosylation is important for protection against meropenem. (a) Schematic diagram representing the structure of *N*-mannan (including phosphomannan) and *O*-mannan of *C. albicans*.[44,46] The points of truncation of the mutants used in this study are indicated by arrows. The *pmr1*Δ mutant causes loss of a Golgi Ca^{2+}/Mn^{2+}-ATPase, affecting numerous mannosyltransferases, so the extent of truncation of the α-1,6-mannose backbone is variable.[44,45] (b) *N*-mannan glycosylation is important for protection against meropenem. Preformed 24 h biofilms were incubated for 18 h in MHB containing no antibiotic or 5 mg/L meropenem. The *N*-mannan glycosylation mutants (*mnn4*Δ, *pmr1*Δ or *mnn2*Δ) inhibit the ability of *C. albicans* to protect *P. aeruginosa*. Tolerance to meropenem is restored in reconstituted control strains. (c) The *mnn2–26*Δ sextuple mutant, in which only the unsubstituted α-1,6-mannose backbone of *N*-mannan remains, inhibits the ability of *C. albicans* to protect *P. aeruginosa*. (d) *O*-mannan glycosylation is important for protection against meropenem. The *mnt1*Δ/*mnt2*Δ double mutant inhibits the ability of *C. albicans* to protect *P. aeruginosa*. Meropenem tolerance is restored when *MNT1* is reconstituted. Data are the mean ± SEM from three biological replicates. Data were analysed using two-way ANOVA and Holm–Sidak's multiple comparisons test (**$P < 0.01$, ***$P < 0.001$ and ****$P < 0.0001$ in panels b, c and d). NS, not significant. (e) Scanning electron microscopy analysis of biofilms. Deletion of genes required for fungal *N*-mannan biosynthesis (*mnn4*) or *O*-mannan biosynthesis (*mnt1*/*mnt2*) reduced the ability of *C. albicans* to protect *P. aeruginosa* from meropenem, as indicated by the reduction in the number of bacterial cells following meropenem treatment; the majority of surviving bacteria are in close contact with fungal cells. When the genes (*MNN4* or *MNT1*) are reconstituted, the protective effect is restored, as evidenced by the abundance of *P. aeruginosa* cells coating the fungi in the meropenem-treated samples.

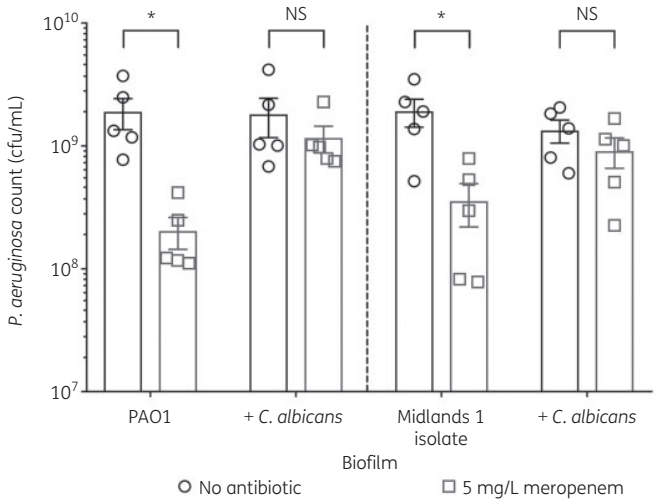


Figure 6. *C. albicans* enhances meropenem tolerance of a *P. aeruginosa* CF isolate. Preformed 24 h biofilms were incubated for 18 h in MHB containing no antibiotic or 5 mg/L meropenem. Data are the mean ± SEM from five biological replicates. Data were analysed using two-way ANOVA and Holm–Sidak's multiple comparisons test (*$P < 0.05$). NS, not significant.

other reports where *C. albicans* ECM components have been shown to provide protection against ofloxacin and vancomycin in dual-species biofilms with *Escherichia coli* and *Staphylococcus aureus*, respectively.[42,43] However, in contrast to these studies, where *C. albicans* ECM components provide protection against a range of antimicrobials, *C. albicans* ECM components only increased *P. aeruginosa* tolerance to meropenem. This suggests that the mechanism by which *C. albicans* ECM components enhance meropenem tolerance may be different to those proposed for other antibiotics. Considering the effect was not seen for other β-lactams (i.e. ceftazidime) this suggests the protective mechanism may depend on chemical structure or ability to bind mannan or β-glucan, rather than the mode of action.

Previously, mannan and β-glucan have been shown to bind and sequester antimicrobials, limiting their diffusion through biofilms.[43] Therefore, it is possible that the actual concentration of meropenem within dual-species biofilms is significantly lower. Similar interactions have been observed in dual-species biofilms where *Streptococcus mutans* exopolysaccharides bind and sequester fluconazole, reducing its efficacy against *C. albicans*.[49] Alternatively, mannans or glucans may coat bacterial cells, providing a physical barrier that impedes drug permeation, supporting the proposed mechanism by which *S. aureus* is protected from vancomycin.[42]

Although *C. albicans* remains clinically the most commonly isolated *Candida* species, the prevalence of NAC species is increasing.[50] *C. dubliniensis* was the only NAC species that protected *P. aeruginosa* from meropenem. This finding is of clinical relevance as, although less common than *C. albicans*, the prevalence of *C. dubliniensis* within CF patients ranges from 2.6% to 39.0% and there are cases of *C. dubliniensis* being co-isolated with *P. aeruginosa* from the lower respiratory tracts of CF patients.[51] *C. dubliniensis* is the most closely related NAC species to *C. albicans* and, as a result, their biofilms are structurally similar,[38,39] with networks of yeast and hyphal cells embedded in a comparable ECM.[52] Although the other NAC species produce biofilms, the composition of their ECM is considerably different[53,54] and their biofilms lack hyphae, which are important for bacterial attachment. Scanning electron microscopy confirmed that most bacteria in the treated dual-species biofilms were attached to fungal hyphae, suggesting that this interaction is important for protection. This hypothesis is supported by the fact that removal of *O*-mannan, which is required for bacterial binding,[47,55] reduced the ability of *C. albicans* to protect *P. aeruginosa*. However, given that purified carbohydrates were able to provide similar protection to *C. albicans*, it would suggest that ECM composition is the major contributing factor providing antimicrobial protection.

In conclusion, secreted *C. albicans* ECM polysaccharides protect *P. aeruginosa* by reducing the efficacy of meropenem. Clinically, this could result in persistent bacterial infection due to pockets of protected cells, which may then acquire true resistance as a result of continued exposure to subMIC concentrations of antibiotics. This highlights the importance of early diagnosis of dual-species biofilm infections, so that more efficacious therapeutic options, such as combination antibiotic/antifungal therapy, can be considered.

Acknowledgements

We would like to thank Paul Stanley and Theresa Morris, at the University of Birmingham's Centre for Electron Microscopy, for assistance with scanning electron microscopy sample preparation and imaging. We thank Neil Gow, for providing the *C. albicans* mannan glycosylation mutant strains, and Donna MacCallum, for providing the *C. krusei* strain.

Funding

F.A. is supported by the Wellcome Trust Antimicrobials and Antimicrobial Resistance (AAMR) doctoral training programme (108876/Z/15/Z). Work in the laboratory of J.M.A.B. is supported by a David Phillips Fellowship to J.M.A.B. (BB/M02623X/1). Work in the laboratory of R.A.H. is supported by an MRC Career Development Award (MR/L00903X/1) and the BBSRC (BB/R00966X/1).

Transparency declarations

None to declare.

Supplementary data

Figures S1 to S5 are available as Supplementary data at *JAC* Online.

References

1 Peters BM, Jabra-Rizk MA, O'May GA *et al*. Polymicrobial interactions: impact on pathogenesis and human disease. *Clin Microbiol Rev* 2012; **25**: 193–213.

2 Lohse MB, Gulati M, Johnson AD *et al*. Development and regulation of single- and multi-species *Candida albicans* biofilms. *Nat Rev Microbiol* 2018; **16**: 19–31.

3 Muthig M, Hebestreit A, Ziegler U *et al*. Persistence of *Candida* species in the respiratory tract of cystic fibrosis patients. *Med Mycol* 2010; **48**: 56–63.

4 Dixon EF, Hall RA. Noisy neighbourhoods: quorum sensing in fungal-polymicrobial infections. *Cell Microbiol* 2015; **17**: 1431–41.

5 O'Brien S, Fothergill JL. The role of multispecies social interactions in shaping *Pseudomonas aeruginosa* pathogenicity in the cystic fibrosis lung. *FEMS Microbiol Lett* 2017; **364**: fnx128.

6 Sherrard LJ, Tunney MM, Elborn JS. Antimicrobial resistance in the respiratory microbiota of people with cystic fibrosis. *Lancet* 2014; **384**: 703–13.

7 Williams C, Ranjendran R, Ramage G. Pathogenesis of fungal infections in cystic fibrosis. *Curr Fungal Infect Rep* 2016; **10**: 163–9.

8 Rana A, Sharma A, Pandey G. Diagnostic value of sputum Gram's stain and sputum culture in lower respiratory tract infections in a tertiary care hospital. *Int J Curr Microbiol App Sci* 2017; **6**: 4310–4.

9 Hamet M, Pavon A, Dalle F *et al*. *Candida* spp. airway colonization could promote antibiotic-resistant bacteria selection in patients with suspected ventilator-associated pneumonia. *Intensive Care Med* 2012; **38**: 1272–9.

10 Dhamgaye S, Qu Y, Peleg AY. Polymicrobial infections involving clinically relevant Gram-negative bacteria and fungi. *Cell Microbiol* 2016; **18**: 1716–22.

11 Gileles-Hillel A, Shoseyov D, Polacheck I *et al*. Association of chronic *Candida albicans* respiratory infection with a more severe lung disease in patients with cystic fibrosis. *Pediatr Pulmonol* 2015; **50**: 1082–9.

12 Lindsay AK, Hogan DA. *Candida albicans*: molecular interactions with *Pseudomonas aeruginosa* and *Staphylococcus aureus*. *Fungal Biol Rev* 2014; **28**: 85–96.

13 Flemming HC, Wingender J. The biofilm matrix. *Nat Rev Microbiol* 2010; **8**: 623–33.

14 Van Acker H, Van Dijck P, Coenye T. Molecular mechanisms of antimicrobial tolerance and resistance in bacterial and fungal biofilms. *Trends Microbiol* 2014; **22**: 326–33.

15 Mah TF. Biofilm-specific antibiotic resistance. *Future Microbiol* 2012; **7**: 1061–72.

16 Hill D, Rose B, Pajkos A *et al*. Antibiotic susceptibilities of *Pseudomonas aeruginosa* isolates derived from patients with cystic fibrosis under aerobic, anaerobic, and biofilm conditions. *J Clin Microbiol* 2005; **43**: 5085–90.

17 WHO. Global Priority List of Antibiotic-Resistant Bacteria to Guide Research, Discovery, and Development of New Antibiotics. 2017. http://www.who.int/medicines/publications/global-priority-list-antibiotic-resistant-bacteria/en/.

18 Holmes AH, Moore LSP, Sundsfjord A *et al*. Understanding the mechanisms and drivers of antimicrobial resistance. *Lancet* 2016; **387**: 176–87.

19 Lopez-Medina E, Fan D, Coughlin LA *et al*. *Candida albicans* inhibits *Pseudomonas aeruginosa* virulence through suppression of pyochelin and pyoverdine biosynthesis. *PLoS Pathog* 2015; **11**: e1005129.

20 Trejo-Hernández A, Andrade-Domínguez A, Hernandez M *et al*. Interspecies competition triggers virulence and mutability in *Candida albicans-Pseudomonas aeruginosa* mixed biofilms. *ISME J* 2014; **8**: 1974–88.

21 Chen AI, Dolben EF, Okegbe C *et al*. *Candida albicans* ethanol stimulates *Pseudomonas aeruginosa* WspR-controlled biofilm formation as part of a cyclic relationship involving phenazines. *PLoS Pathog* 2014; **10**: e1004480.

22 Bandara HM, Cheung BPK, Watt, RM *et al*. *Pseudomonas aeruginosa* lipopolysaccharide inhibits *Candida albicans* hyphae formation and alters gene expression during biofilm development. *Mol Oral Microbiol* 2013; **28**: 54–69.

23 Cugini C, Morales DK, Hogan DA. *Candida albicans*-produced farnesol stimulates *Pseudomonas* quinolone signal production in LasR-defective *Pseudomonas aeruginosa* strains. *Microbiology* 2010; **156**: 3096–107.

24 Hogan DA, Vik A, Kolter R. A *Pseudomonas aeruginosa* quorum-sensing molecule influences *Candida albicans* morphology. *Mol Microbiol* 2004; **54**: 1212–23.

25 Taff HT, Nett JE, Zarnowski R *et al*. A *Candida* biofilm-induced pathway for matrix glucan delivery: implications for drug resistance. *PLoS Pathog* 2012; **8**: e1002848.

26 Hall CW, Mah TF. Molecular mechanisms of biofilm-based antibiotic resistance and tolerance in pathogenic bacteria. *FEMS Microbiol Rev* 2017; **41**: 276–301.

27 Cystic Fibrosis Trust. Antibiotic Treatment for Cystic Fibrosis: Report of the UK Cystic Fibrosis Trust Antibiotic Working Group, 3rd Edition. 2009. https://www.cysticfibrosis.org.uk/~/media/documents/the-work-we-do/care/consensus-docs-with-new-address/anitbiotic-treatment.ashx?la=en.

28 Fernandez R, Amador P, Prudêncio C. β-Lactams: chemical structure, mode of action and mechanisms of resistance. *Rev Med Microbiol* 2013; **24**: 7–17.

29 Papp-Wallace KM, Endimiani A, Taracila MA *et al*. Carbapenems: past, present, and future. *Antimicrob Agents Chemother* 2011; **55**: 4943–60.

30 Nicolau DP. Pharmacokinetic and pharmacodynamic properties of meropenem. *Clin Infect Dis* 2008; **47** Suppl 1: S32–40.

31 Haagensen JA, Verotta D, Huang L *et al*. New *in vitro* model to study the effect of human simulated antibiotic concentrations on bacterial biofilms. *Antimicrob Agents Chemother* 2015; **59**: 4074–81.

32 EUCAST. Breakpoint Tables for Interpretation of MICs and Zone Diameters, Version 8.1. 2018. http://www.eucast.org/.

33 Merritt JH, Kadouri DE, O'Toole GA. Growing and analyzing static biofilms. *Curr Protoc Microbiol* 2005; Chapter 1.

34 Harriott MM, Noverr MC. *Candida albicans* and *Staphylococcus aureus* form polymicrobial biofilms: effects on antimicrobial resistance. *Antimicrob Agents Chemother* 2009; **53**: 3914–22.

35 Andrews JM. Determination of minimum inhibitory concentrations. *J Antimicrob Chemother* 2001; **48**: 5–16.

36 Savage VJ, Chopra I, O'Neill AJ. *Staphylococcus aureus* biofilms promote horizontal transfer of antibiotic resistance. *Antimicrob Agents Chemother* 2013; **57**: 1968–70.

37 Olsen I. Biofilm-specific antibiotic tolerance and resistance. *Eur J Clin Microbiol Infect Dis* 2015; **34**: 877–86.

38 Whibley N, Gaffen SL. Beyond *Candida albicans*: mechanisms of immunity to non-*albicans Candida* species. *Cytokine* 2015; **76**: 42–52.

39 Papon N, Courdavault V, Clastre M *et al*. Emerging and emerged pathogenic *Candida* species: beyond the *Candida albicans* paradigm. *PLoS Pathog* 2013; **9**: e1003550.

40 Taff HT, Mitchell KF, Edward JA *et al*. Mechanisms of *Candida* biofilm drug resistance. *Future Microbiol* 2013; **8**: 1325–37.

41 Nett J, Lincoln L, Marchillo K *et al*. Putative role of β-1,3 glucans in *Candida albicans* biofilm resistance. *Antimicrob Agents Chemother* 2007; **51**: 510–20.

42 Kong EF, Tsui C, Kucharikova S *et al*. Commensal protection of *Staphylococcus aureus* against antimicrobials by *Candida albicans* biofilm matrix. *MBio* 2016; **7**: e01365-16.

43 De Brucker K, Tan Y, Vints K *et al*. Fungal β-1,3-glucan increases ofloxacin tolerance of *Escherichia coli* in a polymicrobial *E. coli/Candida albicans* biofilm. *Antimicrob Agents Chemother* 2015; **59**: 3052–8.

44 Sheth CC, Hall R, Lewis L *et al*. Glycosylation status of the *C. albicans* cell wall affects the efficiency of neutrophil phagocytosis and killing but not cytokine signaling. *Med Mycol* 2011; **49**: 513–24.

45 Murciano C, Moyes DL, Runglall M *et al*. *Candida albicans* cell wall glycosylation may be indirectly required for activation of epithelial cell proinflammatory responses. *Infect Immun* 2011; **79**: 4902–11.

46 Hall RA, Bates S, Lenardon MD *et al*. The Mnn2 mannosyltransferase family modulates mannoprotein fibril length, immune recognition and virulence of *Candida albicans*. *PLoS Pathog* 2013; **9**: e1003276.

47 Brand A, Barnes JD, Mackenzie KS *et al*. Cell wall glycans and soluble factors determine the interactions between the hyphae of *Candida*

albicans and *Pseudomonas aeruginosa*. *FEMS Microbiol Lett* 2008; **287**: 48–55.

48 Scott FW, Pitt TL. Identification and characterization of transmissible *Pseudomonas aeruginosa* strains in cystic fibrosis patients in England and Wales. *J Med Microbiol* 2004; **53**: 609–15.

49 Kim D, Liu Y, Benhamou RI *et al*. Bacterial-derived exopolysaccharides enhance antifungal drug tolerance in a cross-kingdom oral biofilm. *ISME J* 2018; **12**: 1427–42.

50 Sardi JC, Scorzoni L, Bernardi T *et al*. *Candida* species: current epidemiology, pathogenicity, biofilm formation, natural antifungal products and new therapeutic options. *J Med Microbiol* 2013; **62**: 10–24.

51 Wahab AA, Taj-Aldeen SJ, Kolecka A *et al*. High prevalence of *Candida dubliniensis* in lower respiratory tract secretions from cystic fibrosis patients may be related to increased adherence properties. *Int J Infect Dis* 2014; **24**: 14–9.

52 Ramage G, Vande Walle K, Wickes BL *et al*. Biofilm formation by *Candida dubliniensis*. *J Clin Microbiol* 2001; **39**: 3234–40.

53 Cavalheiro M, Teixeira MC. *Candida* biofilms: threats, challenges, and promising strategies. *Front Med (Lausanne)* 2018; **5**: 28.

54 Silva S, Negri M, Henriques M *et al*. Adherence and biofilm formation of non-*Candida albicans Candida* species. *Trends Microbiol* 2011; **19**: 241–7.

55 Munro CA, Bates S, Buurman ET *et al*. Mnt1p and Mnt2p of *Candida albicans* are partially redundant α-1,2-mannosyltransferases that participate in *O*-linked mannosylation and are required for adhesion and virulence. *J Biol Chem* 2005; **280**: 1051–60.

56 Sobel JD. Vaginitis. *N Engl J Med* 1997; **337**: 1896–903.

57 Hobson RP, Munro CA, Bates S *et al*. Loss of cell wall mannosylphosphate in *Candida albicans* does not influence macrophage recognition. *J Biol Chem* 2004; **279**: 39628–35.

58 Bates S, MacCallum DM, Bertram G *et al*. *Candida albicans* Pmr1p, a secretory pathway P-type Ca^{2+}/Mn^{2+}-ATPase, is required for glycosylation and virulence. *J Biol Chem* 2005; **280**: 23408–15.

59 Morschhäuser J, Ruhnke M, Michel S *et al*. Identification of CARE-2-negative *Candida albicans* isolates as *Candida dubliniensis*. *Mycoses* 1999; **42**: 29–32.

60 Zwolinska-Wcislo M, Budak A, Trojanowska D *et al*. Fungal colonization of the stomach and its clinical relevance. *Mycoses* 1998; **41**: 327–34.

Supplementary data

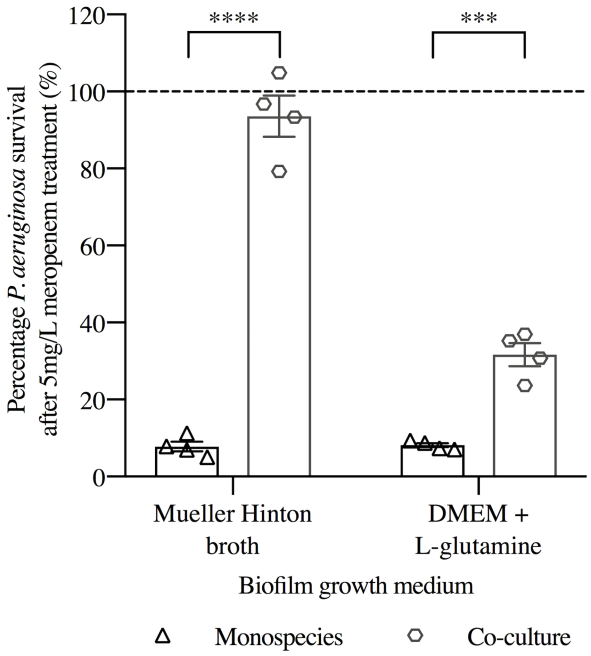


Figure S1. *C. albicans* increases the tolerance of *P. aeruginosa* to meropenem in both Mueller Hinton broth and DMEM. Preformed 24 h biofilms were incubated in DMEM (supplemented with 1% L-glutamine) or Mueller Hinton broth containing no antibiotic or 5 mg/L meropenem, for 18 h. Data show the mean ± the SEM from 4 biological replicates. Data were analysed using 2-way ANOVA and Holm-Sidak's multiple comparisons test (*** $P < 0.001$; **** $P < 0.0001$).

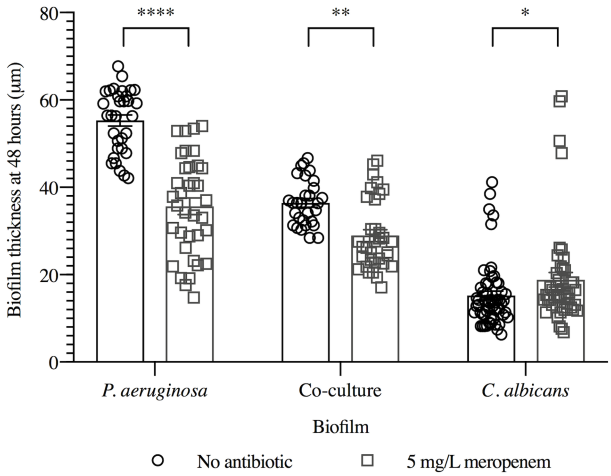


Figure S2. Quantification of biofilm thickness from confocal microscopy images. Preformed 24 h biofilms were incubated in Mueller Hinton broth containing 0 or 5 mg/L meropenem, for 18 h. Biofilms were fixed, stained and washed, before confocal images were taken from 2–3 areas per biofilm. Data show the mean ± the SEM from 2 biological replicates. Data were analysed using 2-way ANOVA and Holm-Sidak's multiple comparisons test (* $P < 0.05$; ** $P < 0.01$; **** $P < 0.0001$).

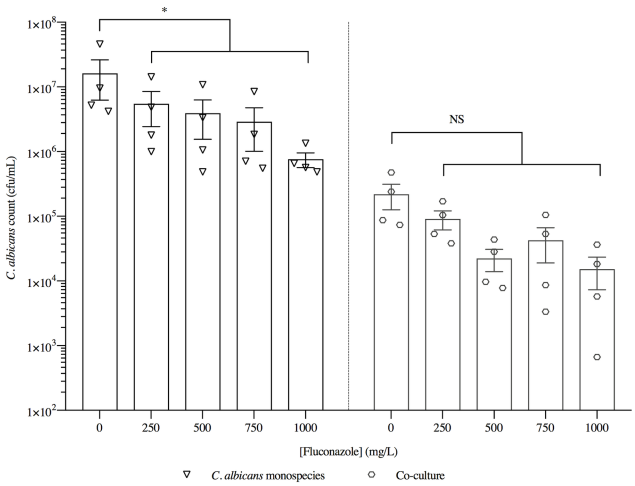


Figure S3. *P. aeruginosa* does not increase *C. albicans* sensitivity to fluconazole. Preformed 24 h biofilms were incubated in Mueller Hinton broth containing 0, 250, 500, 750 or 1000 mg/L fluconazole for 18 h. Data are the mean ± the SEM from 4 biological replicates. Data were analysed using 2-way ANOVA and Holm-Sidak's multiple comparisons test (* $P < 0.05$).

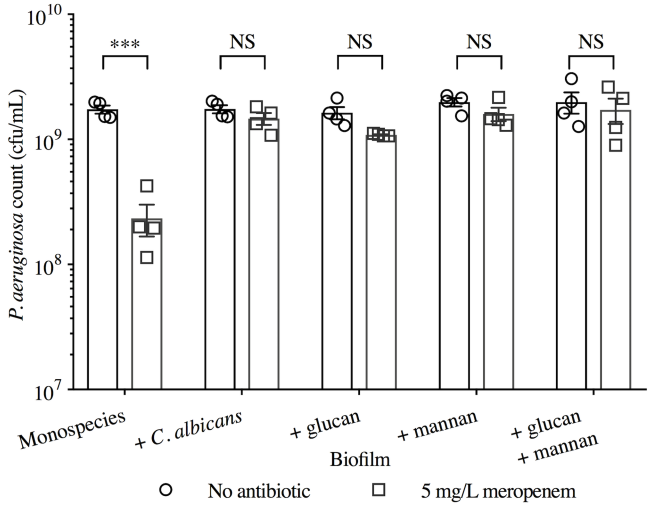


Figure S4. Mannan and glucan enhance *P. aeruginosa* biofilm tolerance to meropenem, even when added to pre-formed biofilms. Pre-formed 24 h biofilms were incubated for 18 h in Mueller Hinton broth containing no antibiotic, 5 mg/L meropenem, 0.25 mg/mL mannan or glucan, or a combination of these. Data are the mean ± the SEM from 4 biological replicates. Data were analysed using 2-way ANOVA and Holm-Sidak's multiple comparisons test (*** $P < 0.001$).

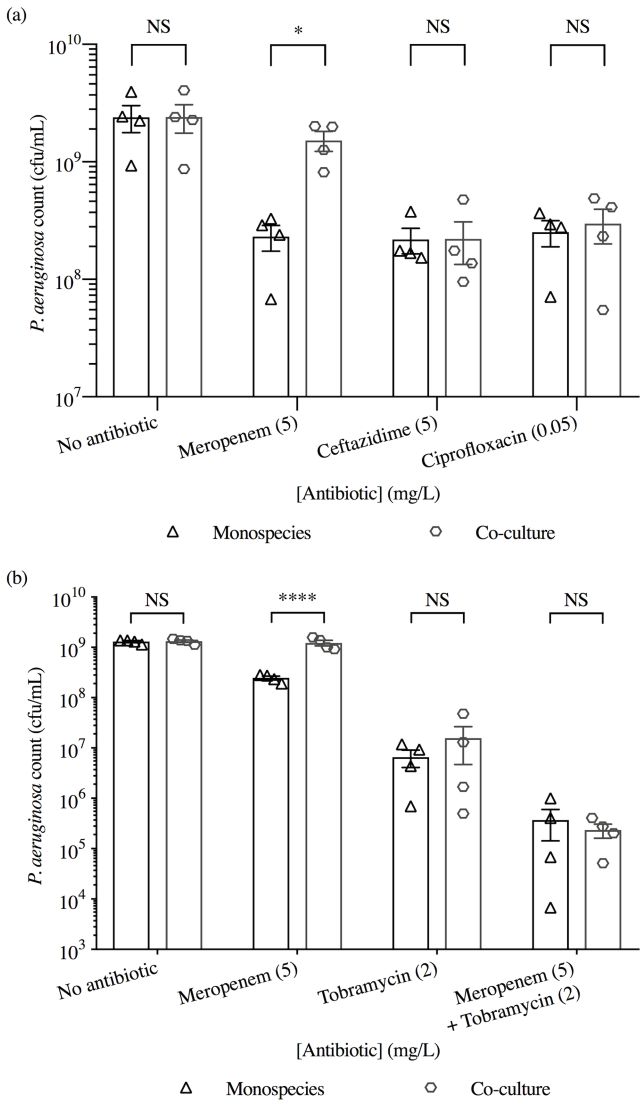


Figure S5. *C. albicans* does not enhance *P. aeruginosa* tolerance to other antibiotics. Preformed 24 h biofilms were incubated for 18 h in Mueller Hinton broth containing meropenem (5 mg/L), ceftazidime (5 mg/L), ciprofloxacin (0.05 mg/L), tobramycin (2 mg/L), or a combination of meropenem and tobramycin. These antibiotics were chosen due to their clinical relevance: meropenem is combined with the aminoglycoside, tobramycin, for the treatment of *P. aeruginosa* infections in the CF lung (Cystic Fibrosis Trust, 2009); the cephalosporin, ceftazidime, is a first-line therapy for the treatment of *P. aeruginosa* infections; and the fluoroquinolone, ciprofloxacin, is

used to treat chronic *P. aeruginosa* infections in the CF lung (Wagner *et al*, 2016). The concentrations tested represent those found in patients; the concentration of ceftazidime found in the epithelial lining fluid following a standard dose (20 mg per kg of body weight) is 6 mg/L (Cousson *et al*., 2015), the concentration of ciprofloxacin found in the epithelial lining fluid 24 h after a 500mg dose is negligible (Gotfried *et al*., 2001), and that of tobramycin 2 h after treatment is 1.67 mg/L (Caracas *et al*., 1999). **(a)** *C. albicans* does not enhance *p. aeruginosa* tolerance to ceftazidime or ciprofloxacin. **(b)** *C. albicans* does not enhance *p. aeruginosa* tolerance to tobramycin or combination meropenem–tobramycin treatment. Data are the mean ± the SEM from 4 biological replicates. Data were analysed using 2-way ANOVA and Holm-Sidak's multiple comparisons test (* $P < 0.05$; **** $P < 0.0001$).

References

Carcas AJ, García-Satué JL, Zapater P *et al.* Tobramycin penetration into epithelial lining fluid of patients with pneumonia. *Clin Pharmacol Ther* 1999; **65**: 245-50.

Cousson J, Floch T, Guillard T *et al.* Lung concentrations of ceftazidime administered by continuous versus intermittent infusion in patients with ventilator-associated pneumonia. *Antimicrob Agents* Chemother 2015; **59**: 1905-9.

Cystic Fibrosis Trust. Antibiotic treatment for cystic fibrosis: report of the UK Cystic Fibrosis Trust antibiotic working group. 3rd Ed. 2009; https://www.cysticfibrosis.org.uk/~/media/documents/life-with-cf/care-and-treatment/cd_antibiotic_treatment_for_cf_may_09.ashx?la=en.

Gotfried MH, Danziger LH, Rodvold KA. Steady-state plasma and intrapulmonary concentrations of levofloxacin and ciprofloxacin in healthy adult subjects. *Chest* 2001; **119**: 1114-22.

Wagner S, Sommer R, Hinsberger S *et al.* Novel strategies for the treatment of *Pseudomonas aeruginosa* infections. *J Med Chem* 2016; **59**: 5929-69.

SPOTLIGHT

Candida albicans

A shape-shifting fungus

The fungus *Candida albicans* has co-evolved with humans and our ancestors for millions of years. Microbiologist Farhana Alam examines how this fungus switches from being harmless to causing disease in its human hosts

Around 80% of humans host *Candida albicans*, a fungus, in their gut or mouth, without it causing any apparent symptoms. This classes it as a commensal organism. However, stresses such as the use of immunosuppressant drugs or antibiotics, or undergoing invasive surgery, can remove microbial competition. This enables *C. albicans* to grow more freely in the body. This can typically result in oral thrush, termed oral candidiasis, which affects 40–70% of otherwise healthy individuals at least once in their lifetime. Similarly, changes in *C. albicans* behaviour will cause vaginal candidiasis (vaginal thrush). Around 75% of females will be affected at some point during their lives.

If *C. albicans* gets into the bloodstream, it results in fungal-induced **sepsis**. This can spread throughout the body and to organs including the kidneys and liver, causing organ failure and leading to death in over 40% of cases. Around 250 000 people worldwide each year suffer such extreme infections. This makes *C. albicans* the fourth most common bloodstream infection in intensive care units, and is most common in older people.

It is estimated that there are up to 5 million species of fungi, but only around 100 000 have been identified to date, using genome sequencing methods. Many of these play vital roles in the functioning of ecosystems, in processes including

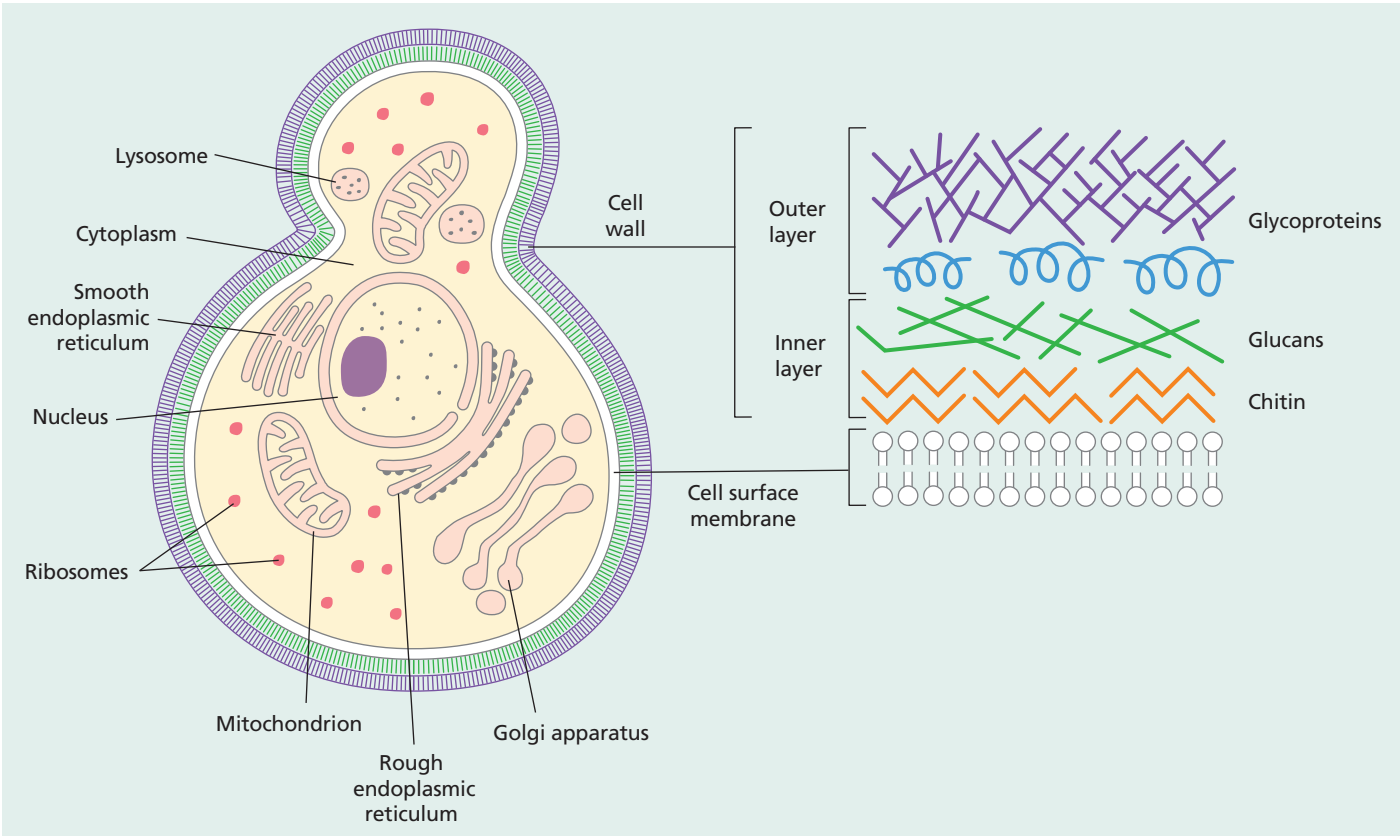


Figure 1 Structure of a *C. albicans* yeast cell

decomposition and nutrient cycling. Around 300 species impact human health, including *C. albicans*. The name comes from the Latin 'candidus' meaning white, and 'albicō' meaning 'becoming white'.

Structure of *C. albicans*

Fungi are eukaryotic organisms and fungal cells have the same organelles as animal cells. The feature of fungi that distinguishes them from other eukaryotes is their unique cell walls (see Figure 1), which differ from plant cell walls in both structure and composition. The cell wall of *C. albicans* is made of a thin inner layer of polysaccharides, including chitin and **glucans**, and a thick outer layer of **glycoproteins**. The inner layer provides structural support, maintaining cell shape and rigidity, while the outer layer is essential for cell–cell interactions and virulence in disease.

Immune response against fungal infection

Upon *C. albicans* infection, the human immune system mounts a response in an attempt to kill the invading cells. Macrophages, a type of white blood cell, migrate through the bloodstream to the infection site. These immune cells have specific receptors on their cell surfaces that can recognise the unique components of the fungal cell wall. This means that the fungal cell wall structures now act as **antigens**. For example, the macrophage receptor Dectin-1 recognises glucans, and Dectin-2 recognises the polysaccharides in the glycoprotein layer of the fungal cell wall (see Figure 2). The macrophage then engulfs *C. albicans* cells by **phagocytosis**. The fungus is killed and degraded by enzymes inside the macrophage.

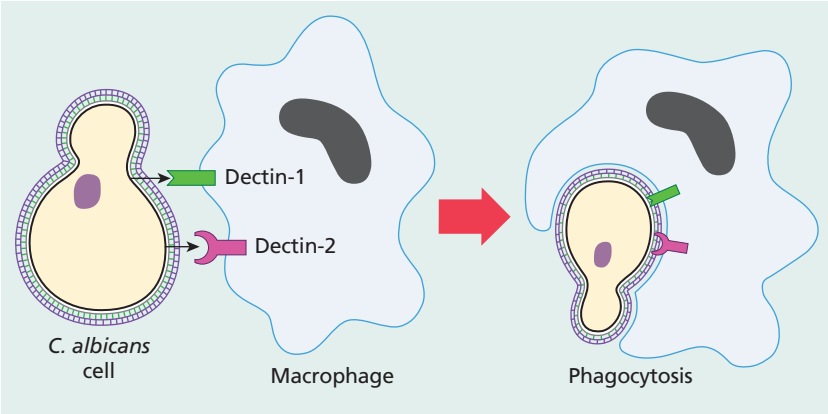


Figure 2 Recognition and phagocytosis of a *C. albicans* cell by a human macrophage cell

Fungi fight back

Unluckily for macrophages, *C. albicans* is a shape-shifter. In the presence of stressors, such as nutrient starvation, the cells can switch from being yeast-shaped (round or oval) to a filamentous form, by growing **hyphae** (see Figure 3). This makes the fungus more difficult for the macrophages to engulf. Yeast-shaped cells can even start producing hyphae after being phagocytosed by a



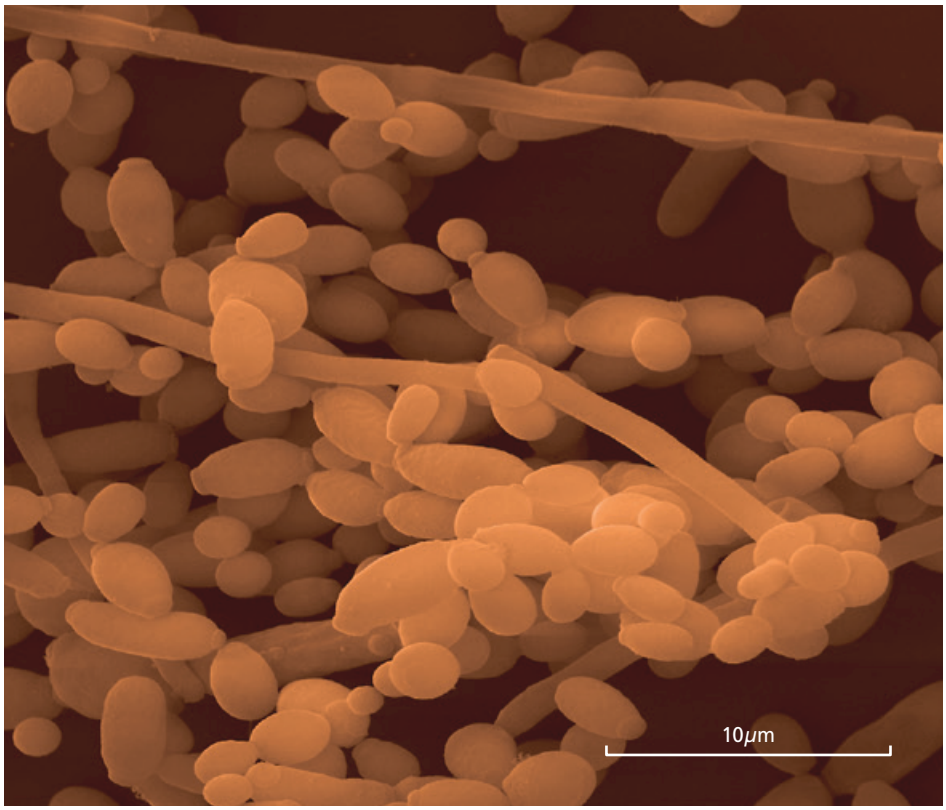


Figure 3 Scanning electron micrograph of *C. albicans* cells, showing both yeast and hyphal forms

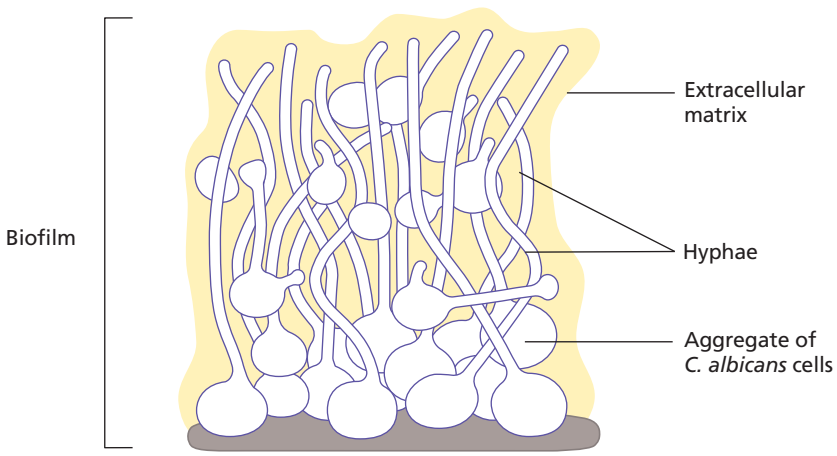


Figure 4 Structure of a *C. albicans* biofilm


Colonies of *C. albicans* growing on an agar plate

macrophage. The hyphae elongate and puncture the macrophage cell surface membrane, causing it to burst, and enabling the *C. albicans* cells to escape and evade the host immune system. The ability to form hyphae also helps *C. albicans* cells invade host tissues and penetrate deeper into an infection site, thus enhancing the virulence of the fungus.

Another way in which *C. albicans* cells grow is in biofilms. A biofilm is a thin (20–30 µm) multi-layered aggregate of cells, encased within a gel-like matrix made up of substances released from the cells (see Figure 4). Biofilms usually form on surfaces. *C. albicans* biofilms can form on implanted medical devices, such as catheters or prosthetics, on infected burn wounds, and on the cells lining the airways of cystic fibrosis (CF) patients. CF is a genetic disorder in which patients produce thick mucus that is difficult to clear, creating a perfect environment for microbial biofilm formation.

Antifungal drugs

Fungal infections are harder to treat than bacterial infections. This is because most antibiotics have been isolated or produced as a result of their antibacterial activities, so they only work against bacteria, which are prokaryotes. Fungi are eukaryotic, like the cells of their human host. This presents a challenge: an antifungal drug must kill fungal cells without also affecting host cells.

There are currently only three main classes of antifungal drugs – far fewer than the number of antibiotics – and some antifungal drugs have toxic side effects in human cells. One example is amphotericin B (AmB). This antifungal causes fungal cells to burst by forming pores in their cell surface membrane. The drug does this by binding to its drug target – ergosterol – which is the fungal version of cholesterol, present in the cell surface membrane. However, the structure of ergosterol is similar to that of human cholesterol, meaning that AmB treatment results in the side effect of killing some host cells.

Like bacteria and antibacterial drugs, fungi can develop resistance to antifungal drugs. If a varied population of fungal cells is treated with an antifungal agent, any cells with a genetic mutation making them resistant to the drug will have a selective advantage. These cells survive the antifungal treatment, multiply, and produce a population of antifungal-resistant fungi. There are several ways in which fungal cells may become resistant to antifungals.

1 **Over-production of the drug target**. A genetic mutation in the fungus results in more of the drug target being produced. Overproduction of the drug target enables the fungus to outcompete the drug, making the drug treatment less effective.

2 **Changing the structure of the drug target**. A genetic mutation in the fungus changes the structure of the drug target, so the drug no longer binds, becoming ineffective.

3 **Increased numbers of efflux pumps**. Efflux pumps are proteins in the cell surface membrane that pump antifungal drugs out of the fungal cell, reducing the drug concentration inside the cell. This is a bit like removing water from a sinking boat. The genes encoding these pumps get switched on at a higher level in response to drug treatment.

4 **Reduced cell permeability**. Some fungi respond to drug treatment by altering the composition of the cell wall, making the cells less permeable to the antifungal drug. For example, increasing the level of chitin can result in increased antifungal drug resistance, as it strengthens the wall.

5 **Forming biofilms**. Cells within biofilms are much more resistant to antifungal drugs than free-living cells. This is because the cells are shielded by extracellular material. Furthermore, cells deep within a biofilm have reduced metabolism, meaning that some drug targets are not produced by these cells. As a result, the drug has nothing to bind to, so it has no effect.

TERMS EXPLAINED

Antigen Any substance that induces an immune response.

Glucan Any polysaccharide that is a polymer of β-glucose.

Glycoprotein A protein with polysaccharides attached to it.

Hyphae Branching, filamentous structures formed by some species of fungus.

Phagocytosis The process by which a white blood cell engulfs invading cells.

Sepsis A whole body immune response to blood infection, leading to multiple organ failure.

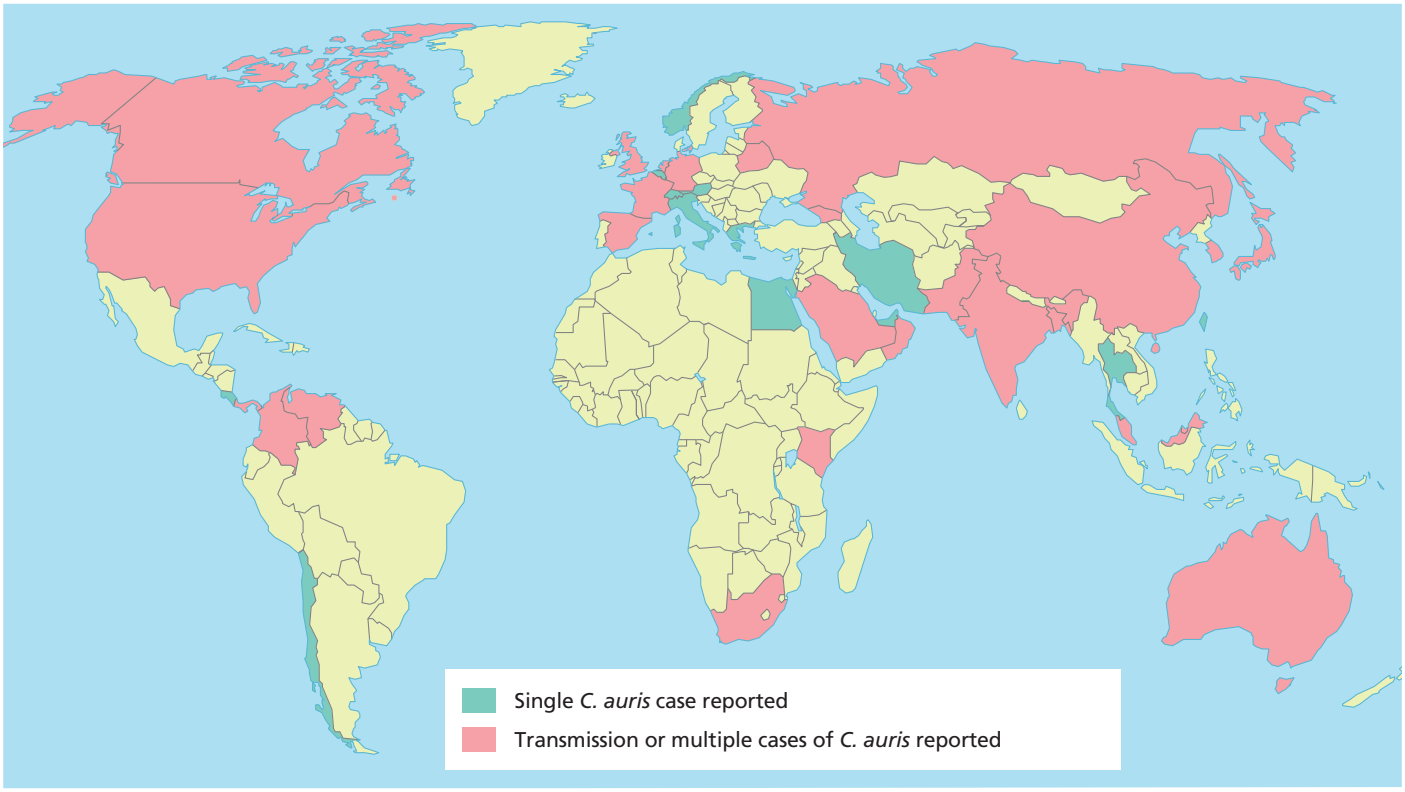


Figure 5 The worldwide distribution of *Candida auris* infections, as of 31 December 2019

Rise of a fungal superbug

In 2009, a new species of *Candida* was isolated from the ear canal of an elderly patient in a Japanese hospital. As a consequence, it was named *Candida auris*, after the Latin for 'ear', though it also causes bloodstream and wound infections. This species has recently gained media attention as the first fungal 'superbug', owing to its resistance to multiple drugs. Since its discovery, it has been identified in over 30 countries worldwide (see Figure 5).

The vast majority of *C. auris* infections are hospital-acquired, mostly affecting vulnerable patients, such as older people and immunocompromised individuals. The fungus survives for over 14 days on the surfaces of medical equipment, enabling transmission from one person to another if surface sterilisation is sub-optimal.

Scientists from Johns Hopkins University in Maryland, USA, have suggested that the emergence of this fungal 'superbug' is linked to the climate crisis. The laboratory of Professor Arturo Casadevall tested the temperature sensitivity of *C. auris* and compared it with that of its closest fungal relatives. They hypothesise that environmental fungi (e.g. fungi that live in soil) have adapted to higher global temperatures and evolved the ability to infect and survive in humans, despite the relatively high internal body temperature of 37°C. Although many other factors may have contributed to the emergence of *C. auris*, this is a worrying thought.

The future of fungal research

In the field of microbiology, there has been a shift towards studying how microorganisms work together. This is because the majority of infections are not caused by just one organism, but by several. This is why microbiologists are carrying out research into the interactions between fungi, bacteria, viruses and their hosts. Clinicians are also increasingly screening patients for fungal infections and not just bacterial infections. Over 1 billion people suffer from severe fungal diseases worldwide, with over 1.6 million deaths per year. Coupled with increasing levels of antifungal drug resistance, increasing our understanding of fungal infections is crucial.

Topics for discussion

- Some fungal species cause infections in animals, with knock-on effects on ecosystems. Find out what two types of fungi are causing large numbers of bat deaths in North America, and deaths of amphibians all around the world.
- In what ways could the climate crisis affect the distribution of infectious diseases around the world?

RESOURCES

A comprehensive introduction to fungi: **https://tinyurl.com/yby65w7h**

Facts about *Candida albicans*: **https://tinyurl.com/wrb8a42**

Up-to-date information about the 'superbug', *Candida auris*: **www.cdc.gov/fungal/candida-auris/index.html**

Farhana Alam is a researcher at the University of Birmingham's Institute of Microbiology and Infection. Her research focuses on understanding how bacteria and fungi interact to affect antimicrobial resistance in biofilms.

APPENDIX II: DUAL-SPECIES RNA-SEQ SUPPLEMENTARY DATA

I. SEQUENCE QUALITY & MAPPING STATISTICS

Per sample sequence quality

Table S1. Sample sequence statistics.

Sample ID	Number of reads	Yield (Mbases)	Mean quality score	% bases with mean quality score ≥ 30
CA-0M-4	95,015,262	29,685	36.02	88.74
CA-0M-6	103,393,241	31,018	35.92	88.15
CA-0M-7	98,083,011	30,893	35.77	87.70
CA-0M-8	94,340,529	29,571	35.78	88.13
CA-5M-4	103,085,837	32,249	36.31	88.95
CA-5M-6	99,012,438	31,197	35.85	87.92
CA-5M-7	97,741,253	30,594	36.10	88.54
CA-5M-8	99,184,509	30,798	36.16	89.31
PA-0M-4	204,624,152	32,146	36.19	88.73
PA-0M-6	211,418,756	33,251	36.12	88.67
PA-0M-7	215,030,556	33,901	36.14	88.50
PA-0M-8	202,626,966	31,842	36.22	88.88
PA-5M-4	198,545,132	31,119	36.10	88.86
PA-5M-6	383,991,496	39,343	35.95	93.97
PA-5M-7	218,100,198	34,136	36.52	89.14
PA-5M-8	195,881,280	30,559	36.06	89.31
PACA-0M-4	314,696,184	32,951	36.28	88.82
PACA-0M-6	299,246,550	31,495	35.88	88.06
PACA-0M-7	301,709,562	31,617	36.00	88.53
PACA-0M-8	327,015,240	34,243	36.36	88.86
PACA-5M-4	533,424,060	35,035	35.92	93.89
PACA-5M-6	288,183,114	30,417	35.53	87.78
PACA-5M-7	677,278,428	50,894	35.95	93.99
PACA-5M-8	338,600,229	35,070	36.68	89.89
Overall	5,700,227,983	794,024	36.08	89.31

Mapping statistics

Table S2. *P. aeruginosa* mapping statistics.

Sample ID	Total reads	Reads mapped to reference	Percent reads mapped to reference
PA-0M-4	204,624,152	181,662,871	88.78
PA-0M-6	211,418,756	189,032,498	89.41
PA-0M-7	215,030,556	192,423,776	89.49
PA-0M-8	202,626,966	177,503,206	87.60
PA-5M-4	198,545,132	183,640,716	92.49
PA-5M-6	383,991,496	354,998,011	92.45
PA-5M-7	218,100,198	198,483,628	91.01
PA-5M-8	195,881,280	177,746,365	90.74
PACA-0M-4	209,797,456	191,164,393	91.12
PACA-0M-6	199,497,700	181,692,226	91.07
PACA-0M-7	201,139,708	184,224,976	91.59
PACA-0M-8	218,010,160	197,117,734	90.42
PACA-5M-4	355,616,040	332,921,680	93.62
PACA-5M-6	192,122,076	178,719,617	93.02
PACA-5M-7	451,518,952	424,656,514	94.05
PACA-5M-8	225,733,486	211,794,503	93.83

Table S3. *C. albicans* mapping statistics.

Sample ID	Total reads	Total mapped reads	% Total mapped reads	Unique mapped reads	% Unique mapped reads
CA-0M-4	95,015,262	93,521,800	98.43	90,606,494	95.36
CA-0M-7	98,083,011	96,462,609	98.35	93,606,789	95.44
CA-0M-8	94,340,529	92,813,044	98.38	89,911,963	95.31
CA-5M-4	103,085,837	100,928,554	97.91	97,704,816	94.78
CA-5M-6	99,012,438	88,928,790	89.82	85,678,624	86.53
CA-5M-7	97,741,253	95,853,432	98.07	92,978,312	95.13
CA-5M-8	99,184,509	97,102,028	97.90	94,179,786	94.95
PACA-0M-4	104,898,728	95,267,617	90.82	92,341,645	88.03
PACA-0M-6	99,748,850	90,745,489	90.97	83,593,750	83.80
PACA-0M-7	100,569,854	91,820,885	91.30	88,788,300	88.29
PACA-0M-8	109,005,080	98,158,378	90.05	95,274,566	87.40
PACA-5M-4	177,808,020	165,982,223	93.35	128,500,024	72.27
PACA-5M-6	96,061,038	89,269,758	92.93	84,603,602	88.07
PACA-5M-7	225,759,476	211,934,786	93.88	164,131,918	72.70
PACA-5M-8	112,866,743	105,437,045	93.42	74,553,254	66.05

II. *P. AERUGINOSA* SIGNIFICANT DEGS: COMPARISON BETWEEN SINGLE- AND DUAL-SPECIES RESPONSES TO MEROPENEM

Table S4. *P. aeruginosa* genes significantly upregulated in response to meropenem.

	Gene list
173 genes uniquely upregulated in single-species	*arnF, cbrB, ccoO2, ccoP2, ccoQ2, cheY, chpA, clpA, cynS, fimV, gcd, gdhB, glmM, himA, hisF2, hisH2, icmP, kynA, lolA, lysC, metK, mucD, murF, nth, oprF, oprH, oprL, oprM, phuT, pilN, pilO, pilP, pilQ, pilR, pqqD, prrF1, prrF2, pslA, pslC, pslM, pta, rimK, rmlC, rplB, rplE, rplJ, rplN, rplP, rplV, rplW, rplX, rpmC, rpsC, rpsQ, rpsS, sdaA, sdhB, sucA, sucC, sucD, surA, tatA, tatB, tolA, tolB, tolQ, tolR, tufA, tufB, ubiB, ubiG, wapR, wbpD, wbpE, wbpG, wbpH, wbpI, wbpJ, wbpK, wbpL, wzx, wzy, PA0045, PA0097, PA0098, PA0134, PA0401, PA0433, PA0483, PA0880, PA0881, PA0919, PA0935, PA0943, PA1061, PA1065, PA1209, PA1210, PA1333, PA1402, PA1509, PA1527, PA1592, PA1600, PA1643, PA1810, PA1907, PA1945, PA2035, PA2145, PA2198, PA2228, PA2289, PA2362, PA2363, PA2441, PA2460, PA2560, PA2618, PA2631, PA2667, PA2696, PA2827, PA2984, PA2990, PA3024, PA3074, PA3075, PA3076, PA3077, PA3087, PA3157, PA3172, PA3187, PA3188, PA3205, PA3272, PA3291, PA3368, PA3400, PA3493, PA3494, PA3559, PA3758, PA3759, PA3835, PA3986, PA3995, PA4272.1, PA4282, PA4368, PA4384, PA4394, PA4401, PA4406.1, PA4420, PA4453, PA4492, PA4571, PA4689, PA4706, PA4735, PA4830, PA4832, PA4834, PA5001, PA5061, PA5087, PA5089, PA5104, PA5257, PA5285, PA5487*
181 genes commonly upregulated in both single- and dual-species	*ampC, ansA, clpV1, creD, cynR, ddlB, estA, fiuA, foxI, fptA, ftsA, ftsQ, ftsW, ftsZ, gcvT2, groEL, hcp1, icmF1, lasR, mliC, mraY, mscL, murC, murD, murE, murG, oprI, pchA, pchB, pchC, pchE, pchF, pchG, phaF, phzS, ppkA, pppA, pslB, pslD, pslE, pslF, ptxR, relA, vgrG1, vqsM, PA0041, PA0042, PA0046, PA0050, PA0070, PA0071, PA0072, PA0073, PA0076, PA0078, PA0079, PA0080, PA0082, PA0083, PA0084, PA0086, PA0087, PA0088, PA0089, PA0095, PA0096, PA0124, PA0126, PA0262, PA0277, PA0329, PA0360, PA0466, PA0467, PA0468, PA0469, PA0537, PA0563, PA0668.4, PA0735, PA0736, PA0853, PA0968, PA1068, PA1069, PA1451, PA1508, PA1510, PA1511, PA1573, PA1579, PA1612, PA1828, PA1844, PA1845, PA2116, PA2117, PA2137, PA2205, PA2222, PA2223, PA2224, PA2225, PA2226, PA2251, PA2323, PA2464, PA2525, PA2526, PA2527, PA2530, PA2535, PA2536, PA2537, PA2538, PA2539, PA2540, PA2541, PA2559a, PA2581, PA2684, PA2685, PA2702, PA2703, PA2725, PA2726, PA2729, PA2746a, PA3021, PA3078, PA3190, PA3212, PA3213, PA3284, PA3290, PA3292, PA3293, PA3317, PA3318, PA3484, PA3485, PA3716, PA3727, PA3728, PA3729, PA3796, PA3819, PA3850, PA3940, PA4111, PA4218, PA4219, PA4220, PA4222, PA4223, PA4280.2, PA4308, PA4322, PA4375, PA4377, PA4399, PA4400, PA4487, PA4488, PA4489, PA4490, PA4491, PA4513, PA4514, PA4517, PA4518, PA4690.2, PA4691, PA4736, PA4737, PA5033, PA5113, PA5114, PA5178, PA5182, PA5369.2*
123 genes uniquely upregulated in dual-species	*aguA, algR, arnD, arnE, bkdR, capB, chpC, cobP, cobU, dapB, ddlA, dnaJ, fpvR, galU, himD, hupB, mdcC, mdcD, mexC, minE, moeA2, ospR, pagL, pqqF, pslH, pslI, recD, rpsN, rsmY, selB, ssrA, PA0047, PA0064, PA0093, PA0209, PA0332, PA0333, PA0398, PA0435, PA0479, PA0490, PA0507, PA0536, PA0545, PA0547, PA0668.1, PA0749, PA0840, PA1048, PA1171, PA1200, PA1274, PA1280, PA1450, PA1648, PA1746, PA1749, PA1751, PA1753, PA1772, PA1804.1, PA1809, PA1833, PA1872, PA1885, PA1890, PA1969, PA1995, PA1997, PA2024, PA2229, PA2267, PA2271, PA2298, PA2410, PA2455, PA2469, PA2490, PA2491, PA2503, PA2550, PA2710, PA2737, PA2747, PA2756, PA2760, PA2774, PA2826, PA2844, PA3022, PA3056, PA3214, PA3256, PA3277, PA3314, PA3426, PA3730, PA3852, PA3908, PA4280.5, PA4319, PA4320, PA4332, PA4357, PA4373, PA4452, PA4486, PA4521, PA4575, PA4690.5, PA4714, PA4716, PA4717, PA4782, PA4833, PA4936, PA5079, PA5211, PA5258, PA5303, PA5369.5, PA5441, PA5481*

Table S5. *P. aeruginosa* genes significantly downregulated in response to meropenem.

	Gene list
227 genes uniquely downregulated in single-species	*adhC, aph, apt, argC, argS, aroC, betT1, ccmB, coaC, comL, crfX, cupC3, cyaB, cyoB, desT, dinB, dsbB, fabF2, ffh, fliC, fliD, folA, folK, gabP, glnD, glpF, glyQ, greB, hemE, iscR, kdpF, ksgA, ladS, lepA, lysP, mgtE, moaB1, modB, mreB, mreD, msuE, mucR, nadA, nalC, norB, nosR, nosY, ohr, opdE, panB, pcnB, pdxB, phnW, plsB, poxA, prfC, prs, psrA, purB, purM, pyrD, pyrF, recN, recQ, rhlI, ribA, rimM, rluD, rnpA, rpe, spdH, thiD, thiG, thiI, thiL, thyA, xerD, xseA, xseB, PA0172, PA0307, PA0311, PA0322, PA0335, PA0356, PA0380, PA0506, PA0602, PA0658, PA0664, PA0711, PA0734, PA0751, PA0752, PA0753, PA0757, PA0806, PA0823, PA0859, PA0906, PA0910, PA0911, PA0922, PA0926, PA0947, PA0957, PA1006, PA1031, PA1112a, PA1132, PA1142, PA1166, PA1170, PA1192, PA1241, PA1297, PA1298, PA1305, PA1363, PA1364, PA1365, PA1374, PA1397, PA1420, PA1428, PA1473, PA1504, PA1506, PA1567, PA1653, PA1678, PA1679, PA1750, PA1764, PA1796.2, PA1866a, PA1964, PA1966, PA1993, PA2376, PA2744.1, PA2762, PA2788, PA2795, PA2819.2, PA2819.3, PA2840, PA2867, PA2902, PA3019, PA3027, PA3079, PA3219, PA3242, PA3263, PA3341, PA3350, PA3352, PA3354, PA3355, PA3360, PA3367, PA3388, PA3389, PA3435, PA3472, PA3474, PA3510, PA3538, PA3580, PA3588, PA3606, PA3664, PA3665, PA3675, PA3678, PA3680, PA3685, PA3690, PA3717, PA3722, PA3726, PA3780, PA3781, PA3817, PA3828, PA3847, PA3866, PA3921, PA3955, PA3958, PA3960, PA4025, PA4046, PA4142, PA4292, PA4325, PA4404, PA4438, PA4507, PA4574, PA4627, PA4631, PA4636, PA4637, PA4724, PA4724.1, PA4746, PA4780, PA4789, PA4804, PA4852, PA4863, PA4928, PA4940, PA4986, PA4993, PA4998, PA5130, PA5244, PA5298, PA5324, PA5335, PA5357, PA5438, PA5442, PA5462*
282 genes commonly downregulated in both single- and dual-species	*accA, amiL, argF, armR, aspA, ccmA, cyoA, dapE, dnaE, exaB, fadH1, ffs, fleR, fleS, fliE, fliF, folD, gbuA, gbuR, gcp, gfnR, gidA, glpM, guaB, kdsA, lecA, lpxB, modA, mreC, mutS, ndvB, pcm, pcpS, pctA, pctB, plpD, plsX, potA, potB, potC, potD, prtN, prtR, ptrB, pyrG, pys2, queA, rep, rho, rimI, rnhB, rtcA, speD, surE, thrH, trkH, trpE, trpG, tyrS, vreI, ygbP, PA0013, PA0142, PA0313, PA0352, PA0358, PA0385, PA0508, PA0532, PA0573, PA0574, PA0574.1, PA0578, PA0585, PA0605, PA0606, PA0608, PA0613, PA0614, PA0615, PA0616, PA0617, PA0618, PA0619, PA0620, PA0621, PA0622, PA0623, PA0624, PA0625, PA0626, PA0627, PA0628, PA0629, PA0630, PA0631, PA0633, PA0634, PA0635, PA0636, PA0637, PA0638, PA0639, PA0640, PA0641, PA0643, PA0644, PA0645, PA0646, PA0647, PA0648, PA0663, PA0666, PA0669, PA0670, PA0671, PA0712, PA0714, PA0775, PA0776, PA0824, PA0825, PA0908, PA0909, PA0914, PA0915, PA0916, PA0924, PA0951a, PA0975, PA1007, PA1016, PA1026, PA1037, PA1045, PA1116, PA1117, PA1134, PA1168, PA1169, PA1263, PA1299, PA1361, PA1367, PA1416, PA1417, PA1418, PA1419, PA1425, PA1435, PA1468, PA1474, PA1531, PA1535, PA1536, PA1537, PA1538, PA1539, PA1563, PA1569, PA1608, PA1763, PA1790, PA1824, PA1835, PA1839, PA2282, PA2283, PA2284, PA2285, PA2351, PA2558, PA2563, PA2580, PA2652, PA2653, PA2654, PA2763, PA2766, PA2767, PA2768, PA2769, PA2770, PA2817, PA2860, PA2868, PA2900, PA2901, PA2916, PA2917, PA2954, PA2955, PA2956, PA2957, PA3080, PA3093, PA3094, PA3109, PA3140, PA3179, PA3180, PA3258, PA3262.1, PA3264, PA3265, PA3308, PA3340, PA3343, PA3359, PA3368.1, PA3413, PA3414, PA3415, PA3416, PA3473, PA3526, PA3532, PA3616, PA3626, PA3628, PA3631, PA3632, PA3634, PA3638, PA3641, PA3667, PA3669, PA3670, PA3671, PA3672, PA3681, PA3682, PA3683, PA3714, PA3718, PA3720, PA3741, PA3749, PA3818, PA3824.1, PA3825, PA3826, PA3920, PA3979, PA3980, PA4045, PA4118, PA4126, PA4139, PA4140, PA4326, PA4436, PA4437, PA4503, PA4504, PA4505, PA4506, PA4520, PA4582, PA4583, PA4584, PA4586, PA4629, PA4633, PA4634, PA4677, PA4816, PA4994, PA4995, PA5072, PA5139, PA5181.1, PA5238, PA5328, PA5458, PA5460, PA5466, PA5468, PA5469, PA5470, PA5471, PA5503*
34 genes uniquely downregulated in dual-species	*exaA, mexE, mexF, trpD, PA0572, PA0603, PA0604, PA0657, PA0709, PA0860, PA0876, PA0952, PA1051, PA1300, PA1542, PA1762, PA2286, PA2353, PA2669, PA2761, PA2782, PA2870, PA3959, PA4038, PA4141, PA4279, PA4354, PA4467, PA4817, PA4962, PA5137, PA5348, PA5430, PA5477*

III. *C. ALBICANS* SIGNIFICANT DEGS: RESPONSE TO *P. AERUGINOSA* IN UNTREATED BIOFILMS

Biological Process

Table S6. Assignment of the 431 significantly upregulated *C. albicans* genes to 40 GO Slim terms under the Biological Process category.

GO ID	GO term	Frequency	Gene list
42710	biofilm formation	9 out of 431 genes, 2.1%	*STE2 QDR3 CSA2 GCN4 UGA33 SUC1 HGC1 PGA7 SAP6*
8150	biological_process	164 out of 431 genes, 38.1%	*GTT13 C1_01220C_A C1_11320C_A CR_08420W_A RSN1 C2_08440W_A C6_02450W_A C4_05900C_A C4_03950C_A C1_05890W_A C3_07370W_A C3_02900W_A C6_02620C_A C3_05290C_A C2_01140C_A GBU1 C6_00730W_A C4_01970W_A C3_00050C_A C1_01840C_A C2_05990C_A C1_00020C_A MOH1 C4_02930W_A C5_03870C_A C3_05750C_A C3_03700C_A C1_02270C_A OP4 CR_09350C_A C1_03120W_A C1_11570W_A CR_06260W_A C7_03280C_A CR_02480W_A C1_09310C_A C2_08510W_A MED3 C6_01490C_A C3_04720C_A PEX22 C4_00080C_A C4_04400C_A CR_04220C_A C4_06670W_A C7_00260C_A C7_02920W_A CSO99 C2_08330W_A C3_04650W_A C6_03150C_A C1_01140C_A BLP1 C6_01620W_A C1_00580W_A BUL1 CR_07740W_A CR_08830W_A C4_02690W_A CR_09610C_A C1_13430C_A C1_01630W_A C7_03310W_A PGA17 C1_14180W_A C5_03890C_A C4_05120C_A ATO1 CR_10310W_A BIO32 C4_04380C_A POX18 C2_08260W_A C3_02990C_A C5_03340W_A C5_00390C_A C1_00030C_A C7_00770W_A CIRT4B C7_02140W_A C1_05440C_A C3_07070C_A C3_01420C_A C6_02020C_A C1_12880C_A PEX17 ATO9 BMT9 GST1 C6_00080C_A C1_05690C_A C3_02090C_A C3_03370C_A GTT1 C1_13090W_A C3_07720C_A C2_10870W_A CR_04860C_A C4_01350W_A C2_04400W_A C2_06060C_A C3_05060W_A C3_02660W_A TES1 C5_04980W_A C1_13100W_A CR_05770W_A CR_06020W_A C2_08890W_A C2_08690C_A C6_03280W_A C4_03960W_A C1_09770W_A C7_03820C_A C1_13180W_A IFK2 C2_02390W_A SMI1B C3_01060W_A C2_09800C_A C1_09340C_A CR_02060W_A CR_04850C_A PSO2 C3_04840C_A CR_01440C_A C4_00640W_A C4_07020C_A UBC15 C1_06870C_A C1_09300C_A C3_06040W_A C4_06940C_A C1_12070C_A C4_01340W_A C2_06630C_A C1_11260C_A CR_05540C_A C5_05180W_A C6_03530C_A C5_03710C_A C1_12060C_A C1_14020W_A C1_00190C_A C6_03670C_A AGA1 C6_01940W_A CR_07700W_A CR_06270W_A C4_03710C_A C1_01610C_A PGA46 C3_01270W_A C1_10060C_A C2_04830W_A TES15 C3_04330C_A C3_02630C_A PGA25 CR_10320W_A MRV2 CR_06770C_A C7_03580C_A C3_04190W_A*
5975	carbohydrate metabolic process	10 out of 431 genes, 2.3%	*HXK1 C1_14190C_A MDH1-3 SCW4 SUC1 FOX2 MNN41 C5_05360C_A INO1 PYC2*
7155	cell adhesion	2 out of 431 genes, 0.5%	*STE2 HIS4*
7114	cell budding	1 out of 431 genes, 0.2%	*C3_00400C_A*
7049	cell cycle	15 out of 431 genes, 3.5%	*FAR1 C4_00030C_A C1_14190C_A C7_01830W_A RAD6 UGT51C1 QDR3 MSO1 PPH3 CAP1 SET1 HGC1 RAD52 CR_04820W_A PSF1*
48468	cell development	6 out of 431 genes, 1.4%	*UGT51C1 QDR3 CAG1 MSO1 SET1 CR_04820W_A*
71555	cell wall organization	2 out of 431 genes, 0.5%	*RBR2 QDR3*
19725	cellular homeostasis	15 out of 431 genes, 3.5%	*HGT4 HXK1 C1_14190C_A C3_03760W_A OPT3 CRD2 CSA2 C2_00600C_A AMO1 CCC1 FRP1 HMX1 GPR1 C4_00500W_A C2_00350W_A*
6464	cellular protein modification process	20 out of 431 genes, 4.6%	*NPR1 C1_03270W_A C1_05370C_A RAD6 C1_00860W_A C1_12120W_A SAS3 PPH3 MNN41 SET1 CR_03220C_A C1_03330C_A APG7 C2_06780C_A ATG1 CEK2 C4_02570C_A C4_00500W_A C2_00350W_A PRR2*

45333	cellular respiration	4 out of 431 genes, 0.9%	*AOX2 MDH1-3 CTN1 C1_09440W_A*
746	conjugation	4 out of 431 genes, 0.9%	*STE2 CAG1 C7_03860W_A CEK2*
910	cytokinesis	0 out of 431 genes, 0%	*none*
7010	cytoskeleton organization	1 out of 431 genes, 0.2%	*C2_06780C_A*
6259	DNA metabolic process	12 out of 431 genes, 2.8%	*TERT C4_00030C_A RAD6 C2_08950W_A PPH3 SET1 RAD52 C2_08420W_A PSF1 CCE1 C2_00350W_A ELC1*
30447	filamentous growth	33 out of 431 genes, 7.7%	*HGT4 C6_03240W_A HXK1 WOR2 C1_14190C_A RAD6 YHB1 CR_03260W_A CAT8 GCN4 GLT1 STB5 CHA1 DAC1 BUD20 SSU1 FGR15 ECI1 GDH3 SET1 FGR12 HGC1 FGR28 CCC1 ZCF2 RAD52 C1_03870C_A MEP2 C5_05510C_A CEK2 GPR1 CTN3 SSY1*
6091	generation of precursor metabolites and energy	9 out of 431 genes, 2.1%	*HGT4 AOX2 HXK1 C1_14190C_A MDH1-3 CTN1 HPD1 C1_09440W_A C3_02850C_A*
70783	growth of unicellular organism as a thread of attached cells	6 out of 431 genes, 1.4%	*WOR2 CAT8 GLT1 GDH3 MEP2 GPR1*
30448	hyphal growth	1 out of 431 genes, 0.2%	*HXK1*
44419	interspecies interaction between organisms	18 out of 431 genes, 4.2%	*APS3 DUR1,2 HGT4 HXK1 YHB1 HIS4 GAT1 DAC1 FOX2 CAP1 SET1 HGC1 RAD52 PGA7 SAP6 PLB1 GPR1 SAP4*
6629	lipid metabolic process	23 out of 431 genes, 5.3%	*C6_03240W_A C2_01920C_A PXP2 C3_03760W_A UGT51C1 POT1 POX1-3 LCB4 POX1 C3_00400C_A MDH1-3 INO4 FOX2 PEX5 ECI1 CR_02570C_A ANT1 PEX6 C5_05360C_A INO1 FAA21 PLB1 C3_02850C_A*
6997	nucleus organization	1 out of 431 genes, 0.2%	*CAG1*
6996	organelle organization	29 out of 431 genes, 6.7%	*TERT C4_00030C_A C7_01830W_A C4_07210W_A RAD6 CAG1 OPT3 CR_02910W_A C1_00860W_A SAS3 PEX5 SET1 ANT1 CR_03220C_A C1_12150C_A C7_03860W_A C1_03330C_A PEX6 HSP78 YPT53 ATG9 RAD52 APG7 SFT1 C2_06780C_A ATG1 CCE1 C4_02570C_A AUT7*
other	other	59 out of 431 genes, 13.7%	*C6_03600C_A EHD3 MET2 CR_07250C_A ATO5 ARG3 C2_00390C_A BAT21 ARO3 ARG4 CR_07170W_A STF2 LYS4 HIS7 CR_03690W_A TRP4 C3_05360C_A ATF1 CDG1 FAA2-3 SOD6 C2_07250C_A HIS3 CPA1 C1_02970W_A UGA1 HOM3 C7_02010C_A FRP2 C1_01620C_A C4_03340C_A C1_05160C_A C4_02230C_A FOX3 UGA11 C3_02060W_A C3_04350C_A C4_02170C_A C2_09070C_A CYB2 CR_04230W_A CPA2 ALD6 MET13 CR_00380W_A LYS22 CR_04870C_A IFR1 C5_00230C_A ARO8 GOR1 C4_00290C_A LEU42 ARG1 DLD2 ECM42 IFG3 CR_06980W_A ARG8*
9405	pathogenesis	14 out of 431 genes, 3.2%	*APS3 DUR1,2 HGT4 HXK1 YHB1 GAT1 DAC1 FOX2 SET1 RAD52 PGA7 SAP6 PLB1 SAP4*
30163	protein catabolic process	8 out of 431 genes, 1.9%	*RAD6 PRB1 UBC8 C7_03860W_A SAP6 C4_00500W_A SAP4 ELC1*
6457	protein folding	3 out of 431 genes, 0.7%	*HSP78 OSM2 C1_02380C_A*
7124	pseudohyphal growth	2 out of 431 genes, 0.5%	*MEP2 GPR1*
50789	regulation of biological process	62 out of 431 genes, 14.4%	*NPR1 WOR4 HGT4 C3_02920W_A DRE2 HXK1 FAR1 WOR2 C4_00030C_A C1_14190C_A C4_07210W_A RAD6 STE18 C6_03290W_A STE2 CAG1 CAT8 OPT3 HAP2 LYS142 LCB4 GCN4 C2_08950W_A UBC8 UGA33 CR_02910W_A STB5 GAT1 ARF1 SUC1 INO4 ECM21 FGR15 SAS3 PPH3 CAP1 SNO1 C1_10140C_A SET1 MET28 ZCF32 YPT53 HGC1 SEF2 ZCF25 ZCF2 ZCF20 RAD52 ARG5,6 SAP6 MEP2 C2_09870W_A ZCF4 SUA72 C6_03320W_A GPR1 C4_02570C_A AUT7 INO2 C1_02380C_A SAP4 SSY1*
42221	response to chemical	49 out of 431 genes, 11.4%	*HGT4 C2_05060C_A C2_01920C_A FAR1 C3_03470W_A C1_14190C_A RAD6 YHB1 STE18 C1_01750W_A STE2 QDR3 CAG1 CAT8 CIP1 C6_01520W_A HAP2 GCN4 C2_07070W_A ROA1 ALT1 STB5 GAT1 ARF1 DAC1 HIS5 TPO4 PPH3 CAP1 AMO2 C1_03330C_A HGC1 SEF2 ZCF2 ZCF20 RAD52 C1_00830W_A CDR11 C6_01870C_A C2_06780C_A HMX1 C6_03320W_A GPR1 AUT7 C4_00500W_A PRR2 C3_02850C_A SSY1 C7_01170C_A*

42493	response to drug	11 out of 431 genes, 2.6%	*C1_14190C_A CAG1 ROA1 ALT1 PPH3 CAP1 AMO2 RAD52 C1_00830W_A PRR2 C7_01170C_A*
6950	response to stress	48 out of 431 genes, 11.1%	*HGT4 C2_05060C_A RBR2 C1_06860W_A C1_03270W_A C3_03470W_A C4_00030C_A RAD6 YHB1 GPX2 C1_12840W_A CIP1 GCN4 C2_08950W_A C2_07070W_A STB5 GAT1 ARF1 DAC1 BUD20 SSU1 MEP1 FGR15 PPH3 CAP1 SET1 FGR12 C7_03860W_A C1_03330C_A HSP78 FGR28 ZCF20 RAD52 C1_03870C_A C2_08420W_A MEP2 C2_09870W_A PSF1 FRP1 C5_05510C_A CEK2 HMX1 C6_03320W_A GPR1 AUT7 C4_00500W_A C2_00350W_A ELC1*
42254	ribosome biogenesis	0 out of 431 genes, 0%	*none*
16070	RNA metabolic process	11 out of 431 genes, 2.6%	*C6_02790C_A RAD6 C1_08140W_A CAT8 C2_02300W_A STB5 SUC1 C3_02750W_A ZCF25 NBP35 SUA72*
7165	signal transduction	15 out of 431 genes, 3.5%	*HGT4 FAR1 STE18 STE2 CAG1 LCB4 ARF1 PPH3 C1_10140C_A YPT53 MEP2 C6_03320W_A GPR1 AUT7 C1_02380C_A*
6412	translation	0 out of 431 genes, 0%	*none*
6810	transport	77 out of 431 genes, 17.9%	*NPR1 APS3 HGT4 SFT2 FTH1 TNA1 HXK1 ITR1 C3_03690W_A C6_03540W_A DUR3 YHB5 CR_06790C_A YHB1 C7_01510W_A C1_01750W_A QDR3 CAG1 C2_07580W_A OPT3 C6_01520W_A CSA2 MSO1 GNP3 GPT1 CR_02910W_A ROA1 C1_00860W_A OPT4 UGA4 ARF1 AAP1 OPT8 C4_00680W_A SSU1 MEP1 ECM21 TPO4 GAP2 PEX5 C3_07430W_A GIT2 ARR3 C5_03080C_A PTR2 ANT1 CR_03220C_A C4_06910W_A C1_03330C_A PEX6 YPT53 C3_05900W_A CCC1 C4_04250W_A ATG9 FRP3 PXA1 C1_00830W_A CDR11 C6_01870C_A YHB4 C1_03870C_A CAN3 APG7 SFT1 MEP2 FRP1 ATM1 FCY23 ATG1 C1_06980C_A C2_02230C_A PXA2 AUT7 FTR2 C1_02380C_A SSY1*
32196	transposition	0 out of 431 genes, 0%	*none*
16192	vesicle-mediated transport	7 out of 431 genes, 1.6%	*APS3 SFT2 FTH1 MSO1 ECM21 SFT1 AUT7*
6766	vitamin metabolic process	4 out of 431 genes, 0.9%	*C4_02040W_A SNO1 ISA2 SNZ1*

Table S7. Assignment of the 739 significantly downregulated *C. albicans* genes to 40 GO Slim terms under the Biological Process category.

GO ID	GO term	Frequency	Gene list
42710	biofilm formation	28 out of 739 genes, 3.8%	*C1_00160C_A C7_00490C_A CR_01410C_A HWP1 TEC1 AQY1 HWP2 WH11 YWP1 MFA1 NRG1 PGA26 BGL2 C2_07290W_A ADH1 NDT80 PBR1 ALS2 HYR1 SUR7 ALS3 PMT2 RHR2 PMT1 ZCF31 PMT4 IFD6 CSH1*
8150	biological_process	128 out of 739 genes, 17.3%	*C3_04210W_A C1_06620C_A C4_05730W_A C3_00360W_A RPS25B C1_02730W_A CR_05210W_A PGA53 YBN5 C3_00230C_A C1_12000C_A C2_04370W_A C1_10500W_A C5_01110W_A C6_01600W_A C3_01970C_A C5_03040W_A LDG3 RPS42 C2_07010W_A C1_07790C_A C2_05300C_A CR_06500C_A C7_01940C_A C2_05960C_A C4_06320C_A C1_11720W_A C3_06830C_A CR_10200W_A C6_00680C_A RPS4A MRV3 C7_02280W_A ECM331 C4_01800W_A SRP40 C1_07990C_A C2_01740C_A ASR3 PGA58 C5_04480C_A C6_03110C_A C2_00130W_A C2_04080W_A CR_09510C_A C7_02260W_A C4_01030W_A C1_10850W_A PGA12 PGA30 C6_00450C_A C7_01950W_A C1_09810W_A C4_01180W_A C1_13820C_A RHD2 PGA34 C5_00510W_A C3_07690C_A C3_07900C_A C4_07160W_A RPL24A C1_10170W_A C1_04270C_A C7_01010W_A CR_09330C_A C1_11930W_A C5_01090C_A PGA54 CR_06570C_A C2_10130W_A C1_09500W_A CR_10750C_A C7_03270W_A C3_01540W_A RPL82 ASR2 C1_03580W_A CR_09940W_A C6_02370C_A C6_02490C_A PRN4 C5_01550C_A PGA18 CR_09060W_A C2_01960C_A CR_09070C_A C5_03440W_A C1_01510W_A C1_09330W_A C1_03510C_A C1_12180C_A C1_08520C_A SLP2 C7_01380W_A RPL18 CR_00530W_A C2_04000C_A C3_01640C_A ASR1 PGA6 C3_06880W_A ROD1 C1_11050W_A USO6 CR_01640C_A C2_03020C_A C3_05450C_A C5_03630C_A C2_00890W_A C5_03410C_A C1_11990W_A C5_03000C_A FRP5 C1_11200W_A PGA11 C2_10010C_A C6_02080W_A C2_00670C_A C7_02210W_A C1_13150W_A PGA38 CR_02340W_A C3_00990C_A C1_12300W_A C3_07980C_A C1_10050W_A C5_00600C_A*

5975	carbohydrate metabolic process	43 out of 739 genes, 5.8%	*TPI1 GND1 CRH11 PFK1 CDA2 KRE5 GPD2 PGK1 GSL2 DAK2 EXG2 C4_02620C_A PGI1 BGL2 CHT3 FBA1 PHR2 TDH3 GUT2 PFK2 SOU1 TAL1 C1_00810W_A KAR2 GPM1 GCY1 C3_01570W_A C4_01220C_A ENO1 HXK2 BMT4 PMI1 C5_04940W_A HAL21 CHT2 RHR2 GRE3 KRE1 CDC19 LEU2 SCH9 C6_02420W_A SCW11*
7155	cell adhesion	19 out of 739 genes, 2.6%	*C5_02110W_A HWP1 TEC1 INT1 ALS4 NRG1 SFL2 TDH3 PBR1 ALS2 AAH1 ALS3 MSB1 RHR2 PMT1 ASC1 CSH1 C4_02260C_A C6_02420W_A*
7114	cell budding	4 out of 739 genes, 0.5%	*INT1 VRP1 CLN3 C4_07150W_A*
7049	cell cycle	48 out of 739 genes, 6.5%	*C6_02280W_A C7_03850W_A BFR1 CR_09140C_A GLC7 ARC40 CDA2 C1_03470C_A AQY1 SPO22 PFY1 INT1 SPR28 CYP1 POL30 REC8 TUB2 C1_11860W_A C4_02820W_A CR_02770C_A SAM2 VRP1 C4_05230C_A YOX1 TUB1 CHT3 AMN1 HHF22 NDT80 MIH1 SEC14 SUR7 COF1 MSS4 CLN3 MCD1 KAR4 ZPR1 C1_03790C_A GCN1 C1_06760C_A HHT2 CDC5 EXO1 C2_05270W_A C4_07150W_A ACT1 DLH1*
48468	cell development	13 out of 739 genes, 1.8%	*GLC7 CDA2 C1_03470C_A AQY1 CYP1 NRG1 PGI1 SEC14 SUR7 MSS4 C1_10620W_A SCH9 ACT1*
71555	cell wall organization	24 out of 739 genes, 3.2%	*MSB2 CRH11 HWP1 ENG1 WSC2 CDA2 KRE5 C1_03470C_A TSA1B SOD1 SSR1 PGA26 PGA13 BGL2 PHR2 SUR7 PGA59 PMT2 PMI1 PGA31 PGA62 PMT1 PMT4 ACT1*
19725	cellular homeostasis	13 out of 739 genes, 1.8%	*CFL2 GLC7 PFK1 C2_09590C_A TSA1B SOD1 PFK2 FET34 PMA1 ALS3 HXK2 POR1 C4_07150W_A*
6464	cellular protein modification process	49 out of 739 genes, 6.6%	*PNG2 DPM2 C4_00940W_A C1_09040C_A RMS1 SMP3 C7_00490C_A BFR1 C1_02440C_A GLC7 VRG4 KRE5 C1_03470C_A C4_05250W_A CYP1 CWH8 MNN12 C5_03640W_A PTP1 ANB1 C2_03830W_A NOP1 CR_02770C_A UBI3 DPM1 HHF22 C2_07290W_A MIH1 PTP2 HAT1 PDI1 C5_02400W_A C1_00810W_A PMT2 SRB1 PMI1 STT3 NAT4 C5_05020C_A CDC5 PTP3 HMT1 PMT1 PMT4 GDA1 C1_14160W_A SCH9 ACT1 OST1*
45333	cellular respiration	11 out of 739 genes, 1.5%	*GDS1 C6_03200W_A LSC2 C5_03530C_A FUM11 IDH2 MRF1 IDH1 MRPS9 PET9 MAM33*
746	conjugation	6 out of 739 genes, 0.8%	*ENG1 PFY1 MFA1 KAR4 KAR2 ASC1*
910	cytokinesis	10 out of 739 genes, 1.4%	*GLC7 ARC40 PFY1 INT1 VRP1 CHT3 COF1 CDC5 C4_07150W_A ACT1*
7010	cytoskeleton organization	22 out of 739 genes, 3%	*PCL1 C4_02720C_A TEF2 TEF1 CR_02690W_A GLC7 ARC40 PFY1 INT1 TUB2 SDA1 VRP1 TUB1 CHC1 C2_07290W_A SEC14 SUR7 COF1 MSS4 NCE102 CDC5 ACT1*
6259	DNA metabolic process	23 out of 739 genes, 3.1%	*C7_03850W_A HTA2 CR_09140C_A C6_03380W_A GLC7 CR_04120C_A RPC40 C4_01660W_A PRI2 C3_04810C_A POL30 REC8 C4_02820W_A C4_03230C_A DDR48 HAT1 HTB1 MCD1 HHT2 CDC5 EXO1 ACT1 DLH1*
30447	filamentous growth	74 out of 739 genes, 10.0%	*PCL1 MSB2 RPL16A TPI1 SSB1 ERG5 C1_10880W_A HGT12 GAP1 ERG13 TEC1 VRG4 DRG1 RBR1 ERG1 ARC40 KRE5 MTS1 HWP2 TSA1B INT1 CSI2 RFG1 ALS4 PES1 GZF3 SOD1 CHO1 ERG24 NRG1 FCY2 PTP1 DIP2 NOP5 PGA26 ENP1 YTM1 PGA13 RPL6 PGI1 VRP1 SFL2 PHR2 RNR1 DDR48 C2_07290W_A SSN6 NDT80 ALS2 SUR7 FET34 ALS3 PGA59 MSS4 CLN3 PMT2 FGR2 FGR41 ENO1 PMI1 ERG3 CHT2 CDC5 PMT1 ZCF3 NOC2 CDC19 IMH3 ASC1 PMT4 GDA1 C1_11120C_A SCH9 ACT1*
6091	generation of precursor metabolites and energy	27 out of 739 genes, 3.7%	*TPI1 TKL1 GND1 GDS1 C6_03200W_A LSC2 PFK1 ATP2 C5_03530C_A PGK1 PDC11 PGI1 FBA1 TDH3 FUM11 PFK2 TAL1 GPM1 IDH2 ENO1 HXK2 MRF1 IDH1 CDC19 MRPS9 PET9 MAM33*
70783	growth of unicellular organism as a thread of attached cells	6 out of 739 genes, 0.8%	*TEC1 PTP1 SFL2 MSS4 ZCF3 ASC1*
30448	hyphal growth	10 out of 739 genes, 1.4%	*VRG4 ALS4 PGI1 NDT80 ALS2 CLN3 PMT2 PMI1 PMT4 ACT1*
44419	interspecies interaction between organisms	52 out of 739 genes, 7.0%	*YCP4 TPI1 MET6 SSB1 TEF1 HWP1 TEC1 MTS1 HWP2 INT1 RFG1 WH11 ALS4 PES1 PGK1 YWP1 SOD1 ERG24 NRG1 PGA26 SOD5 BGL2 PST2 SFL2 FBA1 PHR2 TDH3 ADH1 SSN6 NDT80 ALS2 HYR1 RBE1 FET34 ALS3 GPM1 MSB1 ENO1 PST3 MSI3 NCE102 ERG3 RHR2 PMT1 CDC19 IMH3 ASC1 PMT4 LEU2 CSH1 SCH9 PHM7*
6629	lipid metabolic process	37 out of 739 genes, 5.0%	*ERG28 DPM2 FEN12 ERG6 SMP3 ERG12 ERG5 ERG25 ERG10 ERG13 ERG1 MTS1 HMG1 CWH8 ERG9 FAS1 ERG11 URA7 LKH1 CHO1 ERG24 MVD ERG4 DPM1 C1_02240W_A SEC14 C1_01050C_A*

			C1_00810W_A MSS4 LIP6 HAL21 ERG3 SAH1 ERG251 ERG2 MCR1 C6_02420W_A
6997	nucleus organization	9 out of 739 genes, 1.2%	*C4_04800W_A PGA63 C4_01660W_A GLE2 C1_02240W_A KAR4 KAR2 GSP1 C2_08160C_A*
6996	organelle organization	108 out of 739 genes, 14.6%	*C5_01540W_A PCL1 C4_05330C_A RPF2 TIF5 C1_09040C_A RPL25 RPP0 C4_02720C_A C1_09060C_A TEF2 HTA2 BFR1 C4_04800W_A TEF1 CR_09140C_A PGA63 CR_02690W_A C6_02380W_A C6_03380W_A GLC7 CR_04120C_A ARC40 C4_01660W_A RPS27 C7_01360C_A PFY1 INT1 MDN1 CSI2 CYP1 C1_04180W_A C1_02290C_A C3_04810C_A C2_02540W_A RPS17B C3_06050C_A YST1 POL30 RRS1 GLE2 REC8 TUB2 RPL3 C1_11860W_A C4_02820W_A SDA1 YTM1 NOP1 CR_02770C_A UBI3 RPL11 RPL6 VRP1 C4_05230C_A C1_02240W_A TIM50 RPS26A TUB1 CHC1 PHR2 HHF22 C2_04570W_A C2_07290W_A SSN6 SEC14 HAT1 HTB1 SUR7 RPL12 COF1 MSS4 CLN3 MCD1 KAR4 KAR2 C1_03790C_A C5_03550W_A C1_06760C_A C3_02020W_A GSP1 HHT2 EMP24 RPL5 SAM50 NCE102 NAT4 TOM20 C6_02690C_A DRS1 CDC5 EXO1 C4_05010W_A SEC24 RPS28B C2_05270W_A POR1 C7_01600W_A HHT21 C3_00730W_A C2_08160C_A NIP7 RPS14B ACT1 MAK21 ILV5 SSF1 DLH1*
other	other	38 out of 739 genes, 5.1%	*C2_06350C_A C7_04210C_A C6_02480W_A HPT1 UAP1 C2_07420W_A LSC1 C5_04300C_A GLO1 HEM13 C2_08530C_A MET15 C1_13790C_A MAE1 LAT1 RNR21 OSM1 DUT1 GUA1 AAT22 IPP1 MET3 MET18 C1_11790W_A PSA2 C4_01830C_A C7_02100W_A SOU2 C4_06710W_A URA1 URA5 XYL2 GUK1 DCG1 APT1 MET14 C6_01420C_A C6_03880W_A*
9405	pathogenesis	35 out of 739 genes, 4.7%	*YCP4 TEC1 MTS1 HWP2 INT1 RFG1 WH11 PES1 SOD1 ERG24 NRG1 PGA26 SOD5 BGL2 PST2 SFL2 PHR2 SSN6 NDT80 ALS2 RBE1 FET34 ALS3 PST3 MSI3 NCE102 ERG3 RHR2 PMT1 ASC1 PMT4 LEU2 CSH1 SCH9 PHM7*
30163	protein catabolic process	9 out of 739 genes, 1.2%	*CIC1 LKH1 AMN1 PDI1 PMT2 KAR2 MSI3 PMT1 SEC61*
6457	protein folding	13 out of 739 genes, 1.8%	*SSB1 SSZ1 CR_02690W_A C7_01360C_A CYP1 HGH1 CNS1 ERO1 PDI1 KAR2 C1_03790C_A ZUO1 MSI3*
7124	pseudohyphal growth	3 out of 739 genes, 0.4%	*TEC1 PTP1 SFL2*
50789	regulation of biological process	167 out of 739 genes, 22.6%	*C6_02280W_A UTP5 PCL1 YCP4 MSB2 C4_05330C_A TPI1 C4_00940W_A MET6 AGP2 SSB1 C5_02110W_A TIF5 C1_12570C_A C1_09040C_A RMS1 HSP12 C4_02720C_A EFT2 MED1 NOG2 TIF ELF1 HTA2 BFR1 TMA19 PIL1 SUT1 C1_02440C_A C6_03380W_A GLC7 RPL30 TEC1 WSC2 DRG1 ERG1 ARC40 C4_01660W_A C1_03470C_A NRM1 SPO22 TSA1B PFY1 CAM1 MDN1 RFG1 CYP1 PES1 GZF3 PGK1 C3_04810C_A C3_06050C_A SEC12 CAR1 ERG11 SOD1 POL30 CYS4 KTI12 C2_05860C_A EFB1 GLE2 NPL3 CHO1 C5_03640W_A MFA1 REC8 TUB2 PDC11 NRG1 PTP1 CYS3 ANB1 C1_11860W_A C2_07620W_A SDA1 C2_03830W_A PGA26 RPP2B PGA13 CR_02770C_A RPS9B RPP1A RHA1 PST2 VRP1 C4_05230C_A SFL2 C1_02240W_A OFI1 YOX1 TUB1 RPS23A AMN1 FBA1 PHR2 HHF22 TDH3 GCD6 ADH1 SSN6 NDT80 MIH1 SEC14 PTP2 HAT1 HTB1 MRT4 AAH1 PMA1 COF1 MSS4 CLN3 GCD7 PMT2 KAR4 RPP1 C1_14080W_A ZPR1 KAR2 C1_03790C_A GCN1 C5_03550W_A MSB1 C1_06760C_A C3_02040C_A GSP1 HHT2 ENO1 HXK2 C1_05630C_A PST3 NCE102 C3_05320W_A NAT4 C6_02690C_A C2_05160C_A NAN1 CDC5 EXO1 C7_00830C_A PTP3 HMT1 DBP2 PMT1 ZCF3 ZCF31 RPS28B CDC19 TFS1 IMH3 RPS21 ASC1 POR1 PMT4 UTP4 C4_07150W_A GDA1 HHT21 UTP15 CR_04300W_A C3_00730W_A MAM33 URA2 SCH9 TOS4 DLH1*
42221	response to chemical	114 out of 739 genes, 15.4%	*UTP5 GAR1 PCL1 YCP4 MSB2 ENP2 SOD2 RPL17B RPF2 C5_02110W_A ERG6 CAR2 C7_03850W_A UTP20 EFT2 GND1 PGA23 HGT7 LTV1 TMA19 SUT1 HGT12 C4_06210C_A GLC7 ERG13 NOP4 TEC1 ERG1 KRE5 AQY1 NRM1 TSA1B HMG1 C7_01360C_A RLP24 RFG1 PES1 GZF3 FAS1 GAD1 ERG11 NOP14 UTP22 SOD1 DAK2 RRS1 C2_05860C_A CHO1 ERG24 MFA1 TUB2 NRG1 FCY2 C1_11860W_A SSR1 DIP2 C2_03830W_A PGA26 CNS1 SOD5 RPO26 PST2 C4_05230C_A TUB1 RPS23A DDR48 SSN6 NDT80 SEN2 HAT1 MRT4 CNT PRT1 SUR7 PDI1 FET34 CR_01220W_A CLN3 RRP9 PMT2 KAR4 KAR2 GCY1 NIP1 C1_06760C_A FLU1 PST3 MSI3 NOC4 C3_05320W_A ERG3 PGA31 PGA62 DRS1 CDC5 C4_05010W_A RHR2 GRE3 PMT1 ZCF3 NOC2 ZCF31 ERG2 IMH3 PMT4 ERB1 UTP15 KRE30 CR_04300W_A MCR1 SCH9 SEC61 ACT1 MAK21*
42493	response to drug	68 out of 739 genes, 9.2%	*UTP5 GAR1 PCL1 ENP2 RPL17B RPF2 ERG6 CAR2 C7_03850W_A UTP20 EFT2 PGA23 HGT7 C4_06210C_A ERG13 NOP4 ERG1 KRE5*

			HMG1 RLP24 PES1 GZF3 FAS1 ERG11 NOP14 UTP22 RRS1 ERG24 TUB2 NRG1 SSR1 DIP2 C2_03830W_A CNS1 RPO26 C4_05230C_A TUB1 SSN6 NDT80 SEN2 MRT4 CNT PRT1 CR_01220W_A CLN3 RRP9 PMT2 GCY1 NIP1 C1_06760C_A MSI3 NOC4 ERG3 PGA31 PGA62 DRS1 C4_05010W_A PMT1 ZCF3 NOC2 ZCF31 ERG2 IMH3 PMT4 ERB1 UTP15 KRE30 MAK21
6950	response to stress	96 out of 739 genes, 13%	*PCL1 YCP4 MSB2 RPL16A TPI1 SOD2 MET6 SSB1 C5_02110W_A RMS1 HSP12 ERG5 C1_10880W_A GND1 HTA2 LTV1 C4_04800W_A TMA19 PIL1 HGT12 GLC7 ERG13 TEC1 WSC2 CR_04120C_A ERG1 ARC40 KRE5 C4_01660W_A YNK1 AQY1 TSA1B C7_01360C_A CSI2 RFG1 WH11 PES1 PRI2 GZF3 C3_04810C_A GAD1 SOD1 POL30 C2_05860C_A CHO1 NRG1 FCY2 DIP2 PGA26 ENP1 SOD5 YTM1 RPL6 PST2 VRP1 RPS23A RNR1 DDR48 NDT80 HAT1 HTB1 SUR7 PDI1 FET34 PMT2 MCD1 ZPR1 KAR2 GCY1 GCN1 FGR2 C5_03550W_A FGR41 HHT2 PST3 HAL21 C3_05320W_A CHT2 CDC5 EXO1 RHR2 GRE3 PMT1 NOC2 CDC19 IMH3 ASC1 HHT21 C1_11120C_A CR_04300W_A C2_08160C_A MCR1 SCH9 SEC61 ACT1 TOS4*
42254	ribosome biogenesis	150 out of 739 genes, 20.3%	*UTP5 GAR1 C5_01540W_A RPL7 C1_07660W_A C4_05330C_A ENP2 RPL17B RPF2 CR_10410C_A SSB1 TIF5 C1_09040C_A RPS15 RPL25 CR_10470C_A NOP15 RPP0 SSZ1 C7_03850W_A CIC1 UTP20 C1_10880W_A NOG2 RCL1 ELF1 LTV1 C7_01030C_A RPL37B JIP5 NSA1 RPL10A UTP18 C6_02380W_A CR_01780W_A C4_06210C_A RPS18 RPL30 DBP8 RPS10 NOP4 HAS1 C4_01660W_A PUS7 RPS27 CR_09740W_A RPS3 RLP24 MDN1 RPS6A CSI2 UTP13 PES1 PWP2 C3_05160C_A C3_04380C_A C2_02540W_A RPS17B YST1 C3_01560W_A RPS19A UTP21 CR_04170W_A KRR1 NOP14 RPS8A UTP22 RRS1 RPL3 SDA1 DIP2 NOP5 ENP1 YTM1 NOP1 UBI3 C3_06760W_A RPS9B RPL11 RPL6 C4_05230C_A SPB1 RPS26A RPS23A RPL8B C2_04570W_A CR_08500W_A RPS21B TSR1 TSR2 C2_04120C_A RRP42 MRT4 IMP4 NMD3 RPL12 CR_04110W_A SIK1 RRP9 ARX1 RPP1 C1_14080W_A C6_01890C_A RPS1 DIM1 C6_01040C_A C1_06760C_A C3_02040C_A C3_02020W_A RPS24 NOP8 GSP1 DBP7 RPL5 C1_10970W_A ZUO1 NOC4 RPS13 C2_05160C_A C1_04040C_A DRS1 NAN1 RPS7A RPS5 C4_05010W_A HCA4 DBP2 NOC2 RPS28B PWP1 RPS21 RPS20 RPS16A C1_10620W_A UTP4 ERB1 CR_02030C_A C2_09660W_A C1_05720W_A UTP15 C1_12680W_A KRE30 RPL35 CR_04240C_A C3_06370C_A NIP7 DBP3 RPS14B MAK21 SSF1*
16070	RNA metabolic process	161 out of 739 genes, 21.8%	*UTP5 GAR1 C5_01540W_A RRN3 RPL7 C1_07660W_A C4_05330C_A ENP2 C4_00940W_A THS1 RPL17B RPF2 CR_10410C_A SSB1 TIF5 C1_12570C_A RPC19 GUS1 CR_10470C_A NOP15 SSZ1 C7_03850W_A CIC1 UTP20 C1_10880W_A RCL1 MSS116 C7_01030C_A RPL37B C6_02880W_A C2_01070W_A C2_09180W_A UTP18 C6_02380W_A CR_01780W_A C4_06210C_A RPS18 RPL30 DBP8 NOP4 C1_01150C_A RPC40 HAS1 PUS7 RPS27 CR_09740W_A C4_03830W_A LHP1 MDN1 RPS6A CSI2 UTP13 PES1 PWP2 C3_05160C_A C3_04380C_A PRI2 C2_07630C_A ERF1 C2_02540W_A C1_01530C_A YST1 C3_01560W_A ARC1 UTP21 CR_04170W_A KRR1 NOP14 RPS8A UTP22 KTI12 RRS1 TRM1 NPL3 RPL3 CR_04160C_A SES1 C6_02350C_A KRS1 DIP2 NOP5 ENP1 RPA34 NOP1 RPO26 UBI3 C3_06760W_A RPS9B C4_05230C_A SPB1 C7_03660C_A RPS23A RPL8B HHF22 C2_04570W_A GCD6 RPS21B C2_09500W_A TSR1 TSR2 SEN2 C2_04120C_A RRP42 MRT4 IMP4 CR_04110W_A SIK1 RPA135 RRP9 RPP1 C1_14080W_A C7_02660C_A C6_01890C_A RPS1 DIM1 C3_07400W_A C6_01040C_A C1_06760C_A C3_02040C_A C3_02020W_A RPS24 NOP8 GSP1 HHT2 DBP7 RPA190 C1_10970W_A ZUO1 NOC4 RPS13 C4_04810C_A DPS1-1 C6_02690C_A C1_04040C_A DRS1 NAN1 ABP140 HCA4 C7_00830C_A DBP2 C3_00100W_A RPS28B PWP1 RPS20 RPS16A C1_10620W_A UTP4 ERB1 CR_02030C_A C7_02340C_A C1_05720W_A UTP15 RPL35 CR_04240C_A C3_06370C_A CR_04300W_A C3_00730W_A NIP7 DBP3 RPS14B SSF1*
7165	signal transduction	13 out of 739 genes, 1.8%	*MSB2 C4_02720C_A WSC2 C3_04810C_A C1_11860W_A MSS4 KAR2 GCN1 GSP1 C3_05320W_A CDC5 ASC1 SCH9*
6412	translation	115 out of 739 genes, 15.6%	*C2_02930C_A C5_01540W_A CAM1-1 RPL16A THS1 RPL17B SSB1 TIF5 GUS1 RPS15 RPL19A RPL25 C4_04390W_A C7_00490C_A RPP0 SSZ1 RPL20B CIC1 TEF2 EFT2 RPL29 RPL23A TIF TEF1 RPL37B TMA19 RPL10A C5_00030W_A RPL14 RPS18 RPL30 RPP2A DRG1 RPL2 RPS27 C2_07190C_A C5_02660C_A RPS3 C1_06470W_A CAM1 RPS6A RPL32 RPP1B RPL9B ERF1 C3_04810C_A RPS12 RPS17B C1_01530C_A YST1 ARC1 RPS19A RPS8A RPS30 EFB1 RPS22A NPL3 RPL3 CR_04160C_A ANB1 SES1 KRS1 C1_02330C_A RPP2B UBI3*

			C2_05410W_A RPS9B RPL11 RPL6 RPP1A RPL42 RPL38 C7_03660C_A RPS26A RPS23A GCD6 RPS21B RPL15A RPL4B C1_06890C_A C6_03730C_A RPL13 C2_05710C_A PRT1 RPL12 RPL43A GCD7 C6_01980C_A RPL40B NIP1 RPS1 C3_07400W_A RPL27A RPS24 RPL5 ZUO1 CEF3 RPS13 C1_03620C_A DPS1-1 CR_08480C_A RPS7A RPS5 RPL28 RPL21A RPS28B RPS21 RPS20 MRPS9 RPS16A C1_05720W_A RPL35 RPL39 RPS14B TIF3
6810	transport	127 out of 739 genes, 17.2%	*FRE10 FEN12 AGP2 CR_01630C_A SSB1 APE2 RPS15 OPT5 MUP1 TEF2 NOG2 ELF1 HGT7 LTV1 TEF1 CR_04610C_A RPL10A PGA63 HGT10 PIL1 HGT6 HGT12 C6_03390W_A GAP1 C4_06210C_A RPS18 ATP1 RPS10 VRG4 C4_01660W_A ATP2 ATP3 AQY1 C2_09590C_A C7_01360C_A PFY1 RPS3 MIR1 C2_05290C_A PTR22 C3_06050C_A YST1 RPS19A HXT5 UTP22 RRS1 CR_07220C_A LKH1 GLE2 NPL3 TUB2 FCY2 SDA1 ERV25 HGT19 ENP1 EGD1 SSH1 VRP1 C1_02240W_A TIM50 RPS26A TUB1 RPS23A CHC1 FBA1 HUT1 TDH3 HSP31 HSP30 CR_08500W_A HGT13 SEC14 MRT4 C3_01680C_A CNT SUR7 NMD3 RBE1 FET34 PMA1 ALS3 CR_01220W_A COF1 PMT2 ARX1 KAR2 ATP8 EGD2 FGR2 C5_03550W_A TVP18 C3_02040C_A GSP1 FLU1 EMP24 HXK2 GAP4 ZUO1 C1_05630C_A SAM50 NCE102 CR_03580C_A TOM20 ALP1 C1_04040C_A RPS5 HMT1 SEC24 PMT1 RPS28B RPS21 NTF2 C2_05270W_A C1_10620W_A C7_00630C_A POR1 C7_01600W_A PET9 KRE30 C2_02410W_A HGT8 C2_08160C_A YMC1 SEC61 C1_11920W_A ACT1*
32196	transposition	1 out of 739 genes, 0.1%	*RPC40*
16192	vesicle-mediated transport	17 out of 739 genes, 2.3%	*FEN12 PGA63 PIL1 ERV25 VRP1 CHC1 SEC14 SUR7 ALS3 COF1 TVP18 EMP24 SEC24 C1_10620W_A C2_08160C_A C1_11920W_A ACT1*
6766	vitamin metabolic process	4 out of 739 genes, 0.5%	*SPE3 RIB4 HMT1 SPE2*

Molecular Function

Table S8. Assignment of the 431 significantly upregulated *C. albicans* genes to 25 GO Slim terms under the Molecular Function category.

GO ID	GO term	Frequency	Gene list
3677	DNA binding	27 out of 431 genes, 6.3%	*WOR4 C2_05060C_A TERT C1_03270W_A C4_00030C_A RAD6 CAT8 HAP2 GCN4 C2_08950W_A STB5 GAT1 CIRT4B SUC1 INO4 C1_12880C_A CAP1 C2_08890W_A MET28 ZCF25 ZCF20 RAD52 PYC2 C2_08420W_A C4_02570C_A C2_00350W_A INO2*
30234	enzyme regulator activity	7 out of 431 genes, 1.6%	*C1_01840C_A FAR1 C1_14190C_A CR_02910W_A MNN41 HGC1 C1_14020W_A*
4386	helicase activity	2 out of 431 genes, 0.5%	*RAD6 C2_00350W_A*
16787	hydrolase activity	49 out of 431 genes, 11.4%	*DUR1,2 EHD3 C2_01920C_A GBU1 RBR2 RAD6 C1_08140W_A HIS7 CR_03690W_A C3_05360C_A C7_02920W_A CAG1 PRB1 C3_00400C_A HIS4 C1_05160C_A ROA1 SCW4 ARF1 DAC1 C3_02060W_A C3_02750W_A C4_02170C_A PPH3 C3_07430W_A SNO1 C1_09440W_A CR_02570C_A CR_03220C_A C4_06910W_A C7_03860W_A PEX6 PSO2 HSP78 YPT53 C5_05360C_A C5_00230C_A PXA1 CDR11 NBP35 C2_08420W_A SAP6 PLB1 ATM1 PXA2 CCE1 C2_00350W_A SNZ1 SAP4*
16853	isomerase activity	2 out of 431 genes, 0.5%	*ECI1 INO1*
16874	ligase activity	11 out of 431 genes, 2.6%	*DUR1,2 RAD6 C7_02920W_A CPA1 UBC8 CPA2 UBC15 PYC2 FAA21 APG7 ARG1*
8289	lipid binding	4 out of 431 genes, 0.9%	*POX18 C3_01420C_A C1_03330C_A AUT7*
16829	lyase activity	8 out of 431 genes, 1.9%	*C2_00390C_A ARG4 LYS4 HIS3 C1_02970W_A CHA1 FOX2 SNZ1*
3674	molecular_function	168 out of 431 genes, 39%	*APS3 C1_01220C_A C1_11320C_A SFT2 RSN1 C2_08440W_A C6_02450W_A C4_05900C_A C4_03950C_A C3_02920W_A C1_05890W_A C3_07370W_A C3_02900W_A C6_02620C_A C2_01140C_A C6_00730W_A C4_01970W_A C3_00050C_A C2_05990C_A C1_00020C_A C1_06860W_A ATO5 MOH1 C4_02930W_A C5_03870C_A C3_05750C_A C7_01830W_A C3_03700C_A C1_02270C_A C6_02790C_A OP4 CR_09350C_A C1_03120W_A C1_11570W_A CR_06260W_A C7_03280C_A STF2*

			CR_02480W_A C1_09310C_A C2_08510W_A MED3 C6_01490C_A C3_04720C_A PEX22 C4_00080C_A CR_03260W_A C1_12840W_A C4_04400C_A CR_04220C_A C4_06670W_A C7_00260C_A CSO99 C2_08330W_A C3_04650W_A CIP1 C6_03150C_A C1_01140C_A BLP1 MSO1 C1_00580W_A BUL1 CR_07740W_A CR_08830W_A CR_09610C_A C1_13430C_A C1_01630W_A C7_03310W_A PGA17 GNP3 C1_14180W_A C5_03890C_A C4_05120C_A ATO1 CR_10310W_A C4_04380C_A C2_08260W_A C2_02300W_A C3_02990C_A C5_03340W_A AAP1 C5_00390C_A C1_00030C_A C7_00770W_A C7_02140W_A C1_05440C_A C3_07070C_A C6_02020C_A PEX17 BUD20 ATO9 GST1 C6_00080C_A C1_05690C_A C3_02090C_A C3_03370C_A GTT1 C1_13090W_A C3_07720C_A C2_10870W_A CR_04860C_A C4_01350W_A C2_04400W_A C2_06060C_A C3_05060W_A C3_02660W_A TES1 C5_04980W_A C1_13100W_A CR_05770W_A CR_06020W_A C1_10140C_A C2_08690C_A C6_03280W_A C4_03960W_A C1_09770W_A C7_03820C_A C1_13180W_A IFK2 C2_02390W_A FGR12 SMI1B C3_01060W_A C2_09800C_A C1_12150C_A C1_09340C_A CR_02060W_A CR_04850C_A C3_04840C_A CR_01440C_A C4_00640W_A C4_07020C_A FGR28 C1_06870C_A ATG9 C4_06940C_A C1_12070C_A C4_01340W_A C2_06630C_A C1_11260C_A C5_05180W_A C6_03530C_A C5_03710C_A C1_12060C_A CR_04820W_A CAN3 C1_00190C_A C6_03670C_A C2_09870W_A PSF1 AGA1 C5_05510C_A C6_01940W_A CR_07700W_A CR_06270W_A C4_03710C_A C1_01610C_A PGA46 C3_01270W_A C1_10060C_A C2_04830W_A TES15 C3_04330C_A C3_02630C_A PGA25 CR_10320W_A MRV2 C7_03580C_A C3_04190W_A
3774	motor activity	0 out of 431 genes, 0%	*none*
16779	nucleotidyltransferase activity	1 out of 431 genes, 0.2%	*TERT*
other	other	28 out of 431 genes, 6.5%	*WOR2 STE2 FAA2-3 CRD2 C6_01620W_A LYS142 CSA2 C2_00600C_A C4_02690W_A UGA33 FGR15 PEX5 ZCF32 C1_09300C_A C3_06040W_A SEF2 ZCF2 CR_05540C_A PGA7 C1_03870C_A SFT1 ZCF4 C2_02230C_A C6_03320W_A CR_06980W_A GPR1 C1_02380C_A SSY1*
16491	oxidoreductase activity	51 out of 431 genes, 11.8%	*GTT13 C6_03240W_A C2_05060C_A C6_03600C_A DRE2 PXP2 CR_07250C_A AOX2 C3_03470W_A YHB5 CR_07170W_A YHB1 GPX2 CDG1 POX1-3 SOD6 C2_07250C_A C7_02010C_A FRP2 POX1 C1_01620C_A C2_07070W_A MDH1-3 C4_03340C_A HIS4 GLT1 C4_02230C_A C4_02040W_A C3_04350C_A AMO1 FOX2 CYB2 HPD1 GDH3 ALD6 AMO2 MET13 CR_00380W_A CR_04870C_A IFR1 ARG5,6 GOR1 YHB4 C4_00290C_A OSM2 FRP1 DLD2 HMX1 IFG3 C4_02570C_A C7_01170C_A*
8233	peptidase activity	6 out of 431 genes, 1.4%	*C3_05360C_A PRB1 CR_03220C_A C7_03860W_A SAP6 SAP4*
16791	phosphatase activity	2 out of 431 genes, 0.5%	*PPH3 C3_07430W_A*
5515	protein binding	13 out of 431 genes, 3.0%	*CR_08420W_A STE18 C6_03290W_A CAG1 PRB1 GCN4 INO4 ECM21 MET28 C7_03860W_A PEX6 HSP78 SUA72*
4672	protein kinase activity	6 out of 431 genes, 1.4%	*NPR1 C1_05370C_A C1_12120W_A ATG1 CEK2 PRR2*
3723	RNA binding	7 out of 431 genes, 1.6%	*C3_05290C_A TERT POT1 C2_07070W_A MDH1-3 C3_02750W_A SET1*
4871	signal transducer activity	0 out of 431 genes, 0%	*none*
5198	structural molecule activity	3 out of 431 genes, 0.7%	*EHD3 RBR2 ISA2*
988	transcription factor activity, protein binding	0 out of 431 genes, 0%	*none*
16740	transferase activity	54 out of 431 genes, 12.5%	*NPR1 GTT13 TERT MET2 HXK1 ARG3 BAT21 C4_07210W_A C1_05370C_A ARO3 RAD6 C3_03760W_A HIS7 TRP4 UGT51C1 ATF1 POT1 UGA1 HOM3 LCB4 C3_00400C_A C2_08950W_A UBC8 C2_07070W_A BIO32 ALT1 C1_00860W_A C1_12120W_A CTN1 FOX3 HIS5 UGA11 BMT9 C2_09070C_A SAS3 CR_04230W_A SET1 LYS22 IFR1 ARO8 ARG5,6 LEU42 C2_06780C_A ATG1 CEK2 ECM42 C4_00500W_A C2_00350W_A PRR2 CTN3 ARG8 CR_06770C_A C3_02850C_A ELC1*

45182	translation regulator activity	0 out of 431 genes, 0%	*none*
5215	transporter activity	44 out of 431 genes, 10.2%	*HGT4 FTH1 TNA1 ITR1 C3_03690W_A C6_03540W_A DUR3 CR_06790C_A C7_01510W_A C1_01750W_A QDR3 C2_07580W_A OPT3 C6_01520W_A GPT1 ROA1 OPT4 UGA4 OPT8 C4_00680W_A SSU1 MEP1 TPO4 GAP2 GIT2 ARR3 C5_03080C_A PTR2 ANT1 C4_06910W_A C3_05900W_A CCC1 C4_04250W_A FRP3 PXA1 C1_00830W_A CDR11 C6_01870C_A MEP2 ATM1 FCY23 C1_06980C_A PXA2 FTR2*
30533	triplet codon-amino acid adaptor activity	0 out of 431 genes, 0%	*none*

Table S9. Assignment of the 739 significantly downregulated *C. albicans* genes to 25 GO Slim terms under the Molecular Function category.

GO ID	GO term	Frequency	Gene list
3677	DNA binding	33 out of 739 genes, 4.5%	*RRN3 C1_00160C_A HTA2 C2_01070W_A TEC1 CR_04120C_A RFG1 PRI2 C1_13820C_A GZF3 C1_04180W_A C3_04810C_A C3_07690C_A POL30 C2_05860C_A NRG1 C4_02820W_A RPO26 SFL2 YOX1 HHF22 NDT80 HTB1 IMP4 C7_02100W_A RPA135 HHT2 RPA190 CDC5 EXO1 HHT21 ILV5 DLH1*
30234	enzyme regulator activity	21 out of 739 genes, 2.8%	*DPM2 PCL1 C4_05330C_A TIF5 RCL1 RLP24 ERF1 SEC12 CAR1 ARC1 POL30 RPP2B RPP1A CLN3 GCD7 GCN1 MSI3 TFS1 ASC1 C1_11920W_A DLH1*
4386	helicase activity	17 out of 739 genes, 2.3%	*TIF MSS116 C3_06830C_A C6_02380W_A DBP8 HAS1 CR_09740W_A C3_05160C_A C3_01560W_A C6_01890C_A C6_01040C_A DBP7 DRS1 HCA4 DBP2 DBP3 DLH1*
16787	hydrolase activity	84 out of 739 genes, 11.4%	*PNG2 C4_00940W_A YBN5 C2_07420W_A SSB1 APE2 C1_12570C_A C5_04300C_A TEF2 EFT2 RCL1 TIF ELF1 MSS116 TEF1 CRH11 C6_02880W_A C3_06830C_A C2_09180W_A C1_02440C_A ENG1 C6_02380W_A C4_06210C_A GLC7 DBP8 ATP1 CR_04120C_A HAS1 CDA2 ATP2 C4_01800W_A ATP3 CR_09740W_A C5_02660C_A MDN1 C3_05160C_A CWH8 C7_01950W_A DUT1 CAR1 C3_01560W_A IPP1 EXG2 LKH1 TUB2 PTP1 BGL2 C7_03660C_A TUB1 C4_01830C_A CHT3 PHR2 DDR48 MIH1 SEN2 PTP2 AAH1 PMA1 C5_02400W_A RPP1 KAR2 C6_01890C_A C4_01220C_A C6_01040C_A GSP1 DBP7 LIP6 CEF3 C5_04940W_A MSI3 HAL21 CHT2 SAH1 DRS1 EXO1 HCA4 RHR2 PTP3 DBP2 GDA1 KRE30 DBP3 C6_02420W_A DLH1*
16853	isomerase activity	14 out of 739 genes, 1.9%	*GAR1 TPI1 PUS7 CYP1 C6_02350C_A PGI1 ERO1 PDI1 GPM1 C1_03790C_A PMI1 DCG1 ERG2 C1_10620W_A*
16874	ligase activity	19 out of 739 genes, 2.6%	*THS1 LSC1 GUS1 C2_08530C_A LSC2 ATP1 ATP2 ATP3 GUA1 C1_01530C_A URA7 SES1 KRS1 C2_03830W_A CR_02770C_A C7_03660C_A ATP8 DPS1-1 URA2*
8289	lipid binding	9 out of 739 genes, 1.2%	*C5_02110W_A PIL1 PFY1 CAM1 ARC1 RBE1 MSS4 EGD2 TFS1*
16829	lyase activity	11 out of 739 genes, 1.5%	*GLO1 FAS1 GAD1 CYS4 PDC11 MVD CYS3 FBA1 FUM11 ENO1 SPE2*
3674	molecular_function	191 out of 739 genes, 25.8%	*C3_04210W_A C1_06620C_A C4_05730W_A C3_00360W_A UTP5 C2_02930C_A C1_02730W_A CAM1-1 C1_07660W_A ENP2 CR_05210W_A PGA53 C3_00230C_A AGP2 C1_12000C_A C2_04370W_A C1_10500W_A C5_01110W_A C6_01600W_A C3_01970C_A C5_03040W_A LDG3 HSP12 CR_10470C_A C4_02720C_A C2_07010W_A C1_07790C_A C1_09060C_A UTP20 PGA23 GDS1 CR_06500C_A LTV1 C4_04800W_A C7_01940C_A C7_01030C_A C2_05960C_A CR_04610C_A C4_06320C_A C1_11720W_A TMA19 CR_01410C_A CR_09140C_A JIP5 C6_03200W_A NSA1 C1_13790C_A CR_10200W_A UTP18 C6_00680C_A RPS10 MRV3 RBR1 C7_02280W_A ECM331 SRP40 C1_07990C_A ASR3 NRM1 HWP2 SPO22 PGA58 C6_03110C_A C2_00130W_A C2_04080W_A CR_09510C_A C7_02260W_A C4_01030W_A C1_10850W_A WH11 ALS4 C2_05290C_A PGA12 PWP2 PGA30 C6_00450C_A C2_07630C_A C4_01180W_A RHD2 PGA34 C5_00510W_A C3_07900C_A C4_07160W_A UTP21 C1_10170W_A UTP22 YWP1 MET18 C1_04270C_A GLE2 C7_01010W_A C1_11930W_A C5_01090C_A PGA54 CR_06570C_A C4_03230C_A SDA1 ERV25 NOP5 PGA26 C2_10130W_A YTM1 C1_09500W_A PGA13 CR_10750C_A C3_06760W_A C7_03270W_A C3_01540W_A RPL82 ASR2*

			C1_03580W_A RPL8B C2_04570W_A CR_09940W_A PBR1 C6_02490C_A TSR2 ALS2 PRN4 C5_01550C_A PGA18 CR_09060W_A C2_01960C_A RRP42 MRT4 C3_01680C_A CR_09070C_A C5_03440W_A C1_01510W_A SUR7 C1_09330W_A C1_03510C_A C1_12180C_A PGA59 SLP2 SIK1 C7_01380W_A RPL18 CR_00530W_A ARX1 C2_04000C_A C3_01640C_A ASR1 PGA6 C7_02660C_A C3_06880W_A MSB1 TVP18 ROD1 FGR41 EMP24 USO6 C2_03020C_A C3_05450C_A NOC4 NCE102 C5_03630C_A C2_00890W_A PGA31 PGA62 C1_11990W_A C4_05010W_A C5_03000C_A FRP5 NOC2 KRE1 C1_11200W_A PWP1 PGA11 C2_10010C_A C6_02080W_A C2_00670C_A C7_00630C_A C7_02210W_A UTP4 C2_09660W_A C1_11120C_A C2_02410W_A C3_06370C_A C4_02260C_A C1_13150W_A C2_08160C_A PGA38 CR_02340W_A C3_00990C_A PHM7 C1_12300W_A MAK21 C3_07980C_A C1_10050W_A C5_00600C_A
3774	motor activity	0 out of 739 genes, 0%	*none*
16779	nucleotidyltransferase activity	13 out of 739 genes, 1.8%	*UAP1 RPC19 C2_01070W_A RPC40 PRI2 MET3 RPA34 RPO26 PSA2 GCD6 RPA135 SRB1 RPA190*
other	other	33 out of 739 genes, 4.5%	*ERG28 MSB2 C7_03850W_A MED1 WSC2 DRG1 C5_04480C_A SPR28 C5_03530C_A C1_09810W_A C3_06050C_A KTI12 CR_09330C_A REC8 SSH1 RHA1 C4_05230C_A OFI1 TSR1 C1_06760C_A C1_11050W_A NOP8 CR_01640C_A ZUO1 SEC24 ZCF3 ZCF31 C3_00100W_A C2_05270W_A C7_01600W_A C4_07150W_A TOS4 SCW11*
16491	oxidoreductase activity	57 out of 739 genes, 7.7%	*C2_06350C_A FRE10 YCP4 C6_02480W_A SOD2 HEM13 ERG5 GND1 CFL2 ERG25 MAE1 ERG1 LAT1 TSA1B HMG1 GPD2 RNR21 OSM1 FAS1 ERG11 SOD1 ERG24 SOD5 ERG4 PST2 RNR1 TDH3 ERO1 C2_07290W_A ADH1 C2_09500W_A GUT2 SOU1 PDI1 FET34 SOU2 C1_01050C_A C4_06710W_A URA1 GCY1 IDH2 XYL2 MRF1 PST3 IDH1 ERG3 C5_05020C_A ERG251 GRE3 IMH3 LEU2 IFD6 CSH1 C6_01420C_A MCR1 ILV5 C6_03880W_A*
8233	peptidase activity	6 out of 739 genes, 0.8%	*APE2 C5_04300C_A C1_02440C_A C5_02660C_A C7_01950W_A LKH1*
16791	phosphatase activity	8 out of 739 genes, 1.1%	*C2_07420W_A GLC7 PTP1 MIH1 PTP2 HAL21 RHR2 PTP3*
5515	protein binding	70 out of 739 genes, 9.5%	*C6_02280W_A RRN3 CR_10410C_A SSB1 TIF5 SSZ1 TEF2 EFT2 HTA2 TEF1 HWP1 CR_02690W_A SUT1 RPC40 ARC40 TSA1B C7_01360C_A PFY1 INT1 RPS3 CAM1 GPD2 PGK1 C1_04180W_A C1_02290C_A SEC12 HGH1 CR_07220C_A EFB1 NPL3 MFA1 C1_11860W_A C2_07620W_A CNS1 EGD1 VRP1 C1_02240W_A AMN1 FBA1 HHF22 TDH3 GCD6 CR_08500W_A ADH1 SSN6 HAT1 HYR1 HTB1 PDI1 ALS3 COF1 GCD7 MCD1 ZPR1 KAR2 GPM1 NIP1 EGD2 C5_03550W_A GSP1 HHT2 ENO1 C3_05320W_A CDC5 ABP140 C7_00830C_A ASC1 NTF2 HHT21 C1_12680W_A*
4672	protein kinase activity	3 out of 739 genes, 0.4%	*C1_03470C_A CDC5 SCH9*
3723	RNA binding	107 out of 739 genes, 14.5%	*GAR1 RPL7 RPL16A C4_00940W_A RPF2 CR_10410C_A C1_00160C_A TIF5 C1_12570C_A RPL25 NOP15 RPS42 RPP0 CIC1 TEF2 EFT2 C1_10880W_A NOG2 TIF ELF1 BFR1 MSS116 TEF1 RPL10A C5_00030W_A C6_02380W_A C6_03380W_A RPL14 C4_06210C_A RPS18 RPL30 RPS4A NOP4 HAS1 C4_03830W_A LHP1 RPS3 CAM1 CSI2 UTP13 PES1 C3_05160C_A C3_04380C_A RPL9B ERF1 C2_02540W_A ARC1 CR_04170W_A KRR1 NOP14 RPL24A RRS1 TRM1 EFB1 NPL3 CR_04160C_A ANB1 C1_11860W_A C6_02350C_A DIP2 ENP1 C1_02330C_A NOP1 RPS9B RPL6 TDH3 GCD6 RPL15A C2_04120C_A PFK2 PRT1 IMP4 NMD3 CR_04110W_A RRP9 GCD7 RPP1 C1_14080W_A GCY1 NIP1 C3_02040C_A C3_02020W_A RPL5 C1_10970W_A CEF3 RPS13 DPS1-1 C6_02690C_A C2_05160C_A C1_04040C_A NAN1 HCA4 GRE3 RPL28 DBP2 RPS21 C1_10620W_A ERB1 UTP15 CR_04240C_A RPL39 CR_04300W_A C3_00730W_A NIP7 RPS14B SSF1 TIF3*
4871	signal transducer activity	0 out of 739 genes, 0%	*none*
5198	structural molecule activity	94 out of 739 genes, 12.7%	*RPS25B C5_01540W_A RPL16A RPL17B RPS15 RPL19A RPL25 C4_04390W_A RPS42 RPP0 RPL20B CIC1 RPL29 RPL23A C2_05300C_A RPL37B RPL10A PGA63 C5_00030W_A RPL14 RPS18 RPL30 RPP2A RPL2 C4_01660W_A C2_01740C_A RPS27 C2_07190C_A RPS3 C1_06470W_A RPS6A RPL32 RPP1B RPL9B RPS12 RPS17B YST1 RPS19A RPS8A RPS30 RPS22A TUB2 RPL3*

			SSR1 C1_02330C_A RPP2B UBI3 C2_05410W_A RPS9B RPL11 RPL6 RPP1A RPL42 RPL38 RPS26A TUB1 RPS23A CHC1 RPS21B RPL15A C6_02370C_A RPL4B C1_06890C_A C6_03730C_A RPL13 C2_05710C_A RPL12 C1_08520C_A RPL43A C6_01980C_A RPL40B RPS1 C5_03550W_A RPL27A RPS24 RPL5 RPS13 C1_03620C_A C5_03410C_A CR_08480C_A RPS7A RPS5 RPL28 RPL21A RPS28B RPS21 RPS20 MRPS9 RPS16A C1_05720W_A RPL35 RPL39 RPS14B ACT1
988	transcription factor activity, protein binding	0 out of 739 genes, 0%	*none*
16740	transferase activity	104 out of 739 genes, 14.1%	*C7_04210C_A DPM2 C6_02480W_A HPT1 UAP1 FEN12 MET6 ERG6 RPC19 C1_09040C_A RMS1 SMP3 C7_00490C_A TKL1 ERG12 CAR2 CRH11 MET15 ERG10 C2_01070W_A CR_01780W_A PFK1 ERG13 C1_01150C_A RPC40 KRE5 C1_03470C_A YNK1 LAT1 MTS1 C4_03830W_A C4_05250W_A SPE3 PRI2 PGK1 ERG9 FAS1 MNN12 AAT22 RIB4 CR_04170W_A GSL2 DAK2 MET3 TRM1 CHO1 C5_03640W_A C1_11790W_A CR_04160C_A RPA34 NOP1 RPO26 C4_02620C_A BGL2 SAM2 DPM1 SPB1 PSA2 PHR2 RNR1 GCD6 ADH1 HAT1 PFK2 TAL1 C4_06710W_A C1_00810W_A MSS4 RPA135 PMT2 KAR4 DIM1 C3_07400W_A C3_01570W_A URA5 SRB1 ENO1 RPA190 HXK2 BMT4 XYL2 MRF1 GUK1 STT3 C4_04810C_A NAT4 C5_05020C_A CDC5 ABP140 HMT1 PMT1 CDC19 APT1 MET14 PMT4 C1_14160W_A CR_02030C_A C7_02340C_A CR_04240C_A CR_04300W_A URA2 SCH9 ACT1 OST1*
45182	translation regulator activity	18 out of 739 genes, 2.4%	*TIF5 TEF2 EFT2 TIF ELF1 TEF1 CAM1 ERF1 EFB1 CR_04160C_A ANB1 GCD6 PRT1 GCD7 NIP1 CEF3 C2_05160C_A MAM33*
5215	transporter activity	45 out of 739 genes, 6.1%	*CR_01630C_A OPT5 MUP1 HGT7 HGT10 HGT6 HGT12 C6_03390W_A GAP1 ATP1 VRG4 ATP2 ATP3 AQY1 C2_09590C_A MIR1 PTR22 HXT5 FCY2 HGT19 C1_02240W_A TIM50 HUT1 HSP31 HSP30 HGT13 SEC14 CNT FET34 PMA1 CR_01220W_A ATP8 FGR2 FLU1 GAP4 C1_05630C_A SAM50 CR_03580C_A TOM20 ALP1 POR1 PET9 HGT8 YMC1 SEC61*
30533	triplet codon-amino acid adaptor activity	0 out of 739 genes, 0%	*none*

Cellular Component

Table S10. Assignment of the 431 significantly upregulated *C. albicans* genes to 27 GO Slim terms under the Cellular Component category.

GO ID	GO term	Frequency	Gene list
5938	cell cortex	1 out of 431 genes, 0.2%	*LCB4*
5618	cell wall	3 out of 431 genes, 0.7%	*RBR2 CRD2 INO1*
5933	cellular bud	1 out of 431 genes, 0.2%	*MSO1*
5575	cellular component	225 out of 431 genes, 52.2%	*C1_01220C_A DUR1,2 C1_11320C_A CR_08420W_A RSN1 C2_08440W_A C6_02450W_A C4_05900C_A C4_03950C_A C3_02920W_A C2_05060C_A C1_05890W_A C6_03600C_A C3_07370W_A C3_02900W_A C6_02620C_A C2_01140C_A GBU1 C6_00730W_A C4_01970W_A C3_00050C_A C2_05990C_A C1_00020C_A CR_07250C_A MOH1 C1_03270W_A C4_02930W_A C3_03470W_A C3_05750C_A C3_03700C_A C1_02270C_A C6_02790C_A C1_03120W_A C1_05370C_A C1_11570W_A ARO3 CR_06260W_A YHB5 CR_07170W_A C7_03280C_A STF2 CR_02480W_A C1_09310C_A C2_08510W_A GPX2 MED3 CR_03690W_A TRP4 C6_01490C_A PEX22 UGT51C1 C3_05360C_A ATF1 C4_04400C_A CR_04220C_A C4_06670W_A C7_00260C_A CDG1 C7_02920W_A CSO99 FAA2-3 C2_08330W_A C3_04650W_A C2_07250C_A HIS3 C1_01140C_A BLP1 C6_01620W_A C1_02970W_A HOM3 C7_02010C_A C1_00580W_A FRP2 BUL1 CR_07740W_A C1_01620C_A CR_08830W_A C4_02690W_A CR_09610C_A C2_08950W_A C1_13430C_A C1_01630W_A C7_03310W_A C2_07070W_A C1_14180W_A C5_03890C_A C4_03340C_A C4_05120C_A CR_10310W_A HIS4 C1_05160C_A BIO32 C4_04380C_A POX18 GLT1 C2_08260W_A SCW4 C3_02990C_A C5_03340W_A CHA1 C4_02230C_A C5_00390C_A C1_12120W_A C1_00030C_A C7_00770W_A*

			C4_02040W_A CIRT4B C7_02140W_A OPT8 C1_05440C_A C3_07070C_A C3_01420C_A FOX3 C6_02020C_A C1_12880C_A DAC1 PEX17 BUD20 HIS5 UGA11 BMT9 GST1 C3_04350C_A C6_00080C_A C1_05690C_A C3_02750W_A ECM21 C3_02090C_A C2_09070C_A C3_03370C_A FGR15 GTT1 C1_13090W_A C3_07720C_A CR_04860C_A C4_01350W_A C2_04400W_A C2_06060C_A C3_02660W_A TES1 CR_04230W_A C3_07430W_A C5_04980W_A MNN41 C1_13100W_A CR_05770W_A CR_06020W_A C2_08890W_A C1_10140C_A C2_08690C_A C6_03280W_A C4_03960W_A C1_09770W_A C7_03820C_A C1_13180W_A IFK2 C2_02390W_A ALD6 CR_03220C_A FGR12 SMI1B C3_01060W_A C2_09800C_A AMO2 MET13 C1_09340C_A CR_00380W_A CR_02060W_A CR_04850C_A PSO2 C3_04840C_A CR_01440C_A C4_00640W_A C4_07020C_A FGR28 UBC15 C1_06870C_A C1_09300C_A C3_06040W_A LYS22 C4_06940C_A C1_12070C_A C4_01340W_A C2_06630C_A CR_04870C_A IFR1 C1_11260C_A CR_05540C_A C5_05180W_A C6_03530C_A C5_03710C_A ARO8 C1_12060C_A YHB4 C4_00290C_A C1_03870C_A C1_00190C_A C6_03670C_A LEU42 FRP1 AGA1 C5_05510C_A C6_01940W_A CEK2 C2_02230C_A SUA72 CR_07700W_A IFG3 CR_06270W_A C1_01610C_A C3_01270W_A C1_10060C_A C2_04830W_A C4_02570C_A TES15 C3_04330C_A C3_02630C_A PRR2 CR_10320W_A INO2 MRV2 CR_06770C_A C7_01170C_A C7_03580C_A C3_04190W_A
5694	chromosome	12 out of 431 genes, 2.8%	*C4_00030C_A C7_01830W_A C4_07210W_A RAD6 C6_03290W_A PPH3 CAP1 C5_00230C_A RAD52 PSF1 C6_03320W_A C2_00350W_A*
5737	cytoplasm	106 out of 431 genes, 24.6%	*NPR1 GTT13 APS3 SFT2 C6_03240W_A EHD3 DRE2 C3_05290C_A PXP2 C1_01840C_A FTH1 MET2 AOX2 HXK1 FAR1 ARG3 C3_03690W_A C5_03870C_A C2_00390C_A BAT21 CR_09350C_A ARG4 RAD6 LYS4 YHB1 STE18 HIS7 C1_01750W_A POT1 CAG1 POX1-3 OPT3 CPA1 UGA1 PRB1 MSO1 C2_00600C_A LCB4 POX1 UBC8 MDH1-3 CR_02910W_A ROA1 ALT1 C1_00860W_A GAT1 UGA4 ARF1 CTN1 C4_00680W_A AMO1 FOX2 TPO4 C2_10870W_A GAP2 CYB2 HPD1 PEX5 ECI1 CAP1 SNO1 C1_09440W_A GDH3 CR_02570C_A C5_03080C_A ANT1 CPA2 C1_12150C_A C7_03860W_A C1_03330C_A PEX6 HSP78 YPT53 C3_05900W_A HGC1 CCC1 C4_04250W_A ATG9 C5_05360C_A ZCF20 PXA1 PYC2 ARG5,6 FAA21 C1_14020W_A NBP35 C2_08420W_A APG7 SFT1 ISA2 OSM2 C2_06780C_A ARG1 ATM1 ATG1 DLD2 ECM42 HMX1 PXA2 CR_06980W_A GPR1 CCE1 AUT7 CTN3 ARG8 SNZ1*
16023	cytoplasmic, membrane-bounded vesicle	0 out of 431 genes, 0%	*none*
5856	cytoskeleton	1 out of 431 genes, 0.2%	*C7_01830W_A*
12505	endomembrane system	14 out of 431 genes, 3.2%	*NPR1 SFT2 CAG1 OPT3 LCB4 ARF1 GAP2 C1_03330C_A YPT53 CCC1 SFT1 OSM2 HMX1 C3_02850C_A*
5783	endoplasmic reticulum	3 out of 431 genes, 0.7%	*LCB4 OSM2 HMX1*
5576	extracellular region	12 out of 431 genes, 2.8%	*OP4 CIP1 SOD6 C6_03150C_A UGA1 CSA2 C3_02060W_A GDH3 GOR1 SAP6 PLB1 SAP4*
5794	Golgi apparatus	7 out of 431 genes, 1.6%	*NPR1 SFT2 OPT3 LCB4 ARF1 CCC1 SFT1*
1411	hyphal tip	0 out of 431 genes, 0%	*none*
16020	membrane	82 out of 431 genes, 19.0%	*NPR1 APS3 HGT4 SFT2 FTH1 TNA1 C1_06860W_A ATO5 AOX2 ITR1 C3_03690W_A C6_03540W_A DUR3 CR_06790C_A C3_03760W_A STE18 C7_01510W_A C1_01750W_A C3_04720C_A STE2 QDR3 CAG1 C2_07580W_A CIP1 OPT3 C6_01520W_A MSO1 LCB4 GNP3 GPT1 ATO1 CR_02910W_A ROA1 OPT4 UGA4 AAP1 CTN1 C4_00680W_A SSU1 ATO9 MEP1 TPO4 C2_10870W_A GAP2 PEX5 GIT2 ARR3 C5_03080C_A PTR2 ANT1 C4_06910W_A C1_03330C_A YPT53 C3_05900W_A CCC1 C4_04250W_A ATG9 FRP3 PXA1 C1_00830W_A CDR11 C6_01870C_A CR_04820W_A CAN3 APG7 SFT1 MEP2 C2_09870W_A ATM1 FCY23 ATG1 C1_06980C_A DLD2 HMX1 PXA2 GPR1 C4_03710C_A CCE1 AUT7 FTR2 C3_02850C_A SSY1*
5624	membrane fraction	0 out of 431 genes, 0%	*none*
5815	microtubule organizing center	0 out of 431 genes, 0%	*none*
5740	mitochondrial envelope	8 out of 431 genes, 1.9%	*DRE2 POT1 CTN1 CYB2 ISA2 ATM1 DLD2 CCE1*

5739	mitochondrion	29 out of 431 genes, 6.7%	*EHD3 DRE2 AOX2 HXK1 ARG3 BAT21 LYS4 YHB1 POT1 CPA1 C2_00600C_A ALT1 CTN1 CYB2 HPD1 C1_09440W_A C5_03080C_A HSP78 C4_04250W_A ATG9 ZCF20 ARG5,6 ISA2 OSM2 ATM1 DLD2 ECM42 CCE1 ARG8*
5730	nucleolus	1 out of 431 genes, 0.2%	*TERT*
5634	nucleus	45 out of 431 genes, 10.4%	*WOR4 C6_03240W_A TERT HXK1 FAR1 WOR2 C4_00030C_A C1_14190C_A C7_01830W_A C4_07210W_A RAD6 C6_03290W_A C1_12840W_A CAT8 LYS142 GCN4 UGA33 C2_02300W_A STB5 GAT1 SUC1 INO4 SAS3 C3_05060W_A PPH3 CAP1 GDH3 SET1 ZCF32 HGC1 SEF2 ZCF25 ZCF2 ZCF20 C5_00230C_A RAD52 NBP35 C2_08420W_A C2_06780C_A PSF1 ZCF4 HMX1 CR_06980W_A C2_00350W_A ELC1*
other	other	14 out of 431 genes, 3.2%	*C2_01920C_A C1_08140W_A C4_00080C_A CR_03260W_A HAP2 C3_00400C_A PGA17 C4_02170C_A MET28 PGA7 PGA46 C4_00500W_A PGA25 C1_02380C_A*
5777	peroxisome	17 out of 431 genes, 3.9%	*PXP2 C2_00390C_A POT1 POX1-3 OPT3 POX1 MDH1-3 FOX2 PEX5 ECI1 CR_02570C_A ANT1 PEX6 PXA1 FAA21 PXA2 CTN3*
5886	plasma membrane	32 out of 431 genes, 7.4%	*NPR1 HGT4 FTH1 TNA1 AOX2 ITR1 DUR3 STE18 C1_01750W_A STE2 QDR3 CAG1 OPT3 C6_01520W_A MSO1 LCB4 ROA1 OPT4 SSU1 MEP1 TPO4 GAP2 ARR3 CCC1 FRP3 MEP2 FCY23 HMX1 GPR1 FTR2 C3_02850C_A SSY1*
5840	ribosome	1 out of 431 genes, 0.2%	*EHD3*
30427	site of polarized growth	2 out of 431 genes, 0.5%	*FAR1 MSO1*
70732	spindle envelope	0 out of 431 genes, 0%	*none*
5773	vacuole	17 out of 431 genes, 3.9%	*FTH1 C3_03690W_A C1_01750W_A PRB1 ROA1 UGA4 C4_00680W_A TPO4 C2_10870W_A GAP2 C7_03860W_A C1_03330C_A C3_05900W_A CCC1 ATG9 ATG1 AUT7*

Table S11. Assignment of the 739 significantly downregulated *C. albicans* genes to 27 GO Slim terms under the Cellular Component category.

GO ID	GO term	Frequency	Gene list
5938	cell cortex	11 out of 739 genes, 1.5%	*C4_04800W_A GLC7 PFY1 INT1 VRP1 CHC1 SUR7 COF1 KAR2 C2_08160C_A ACT1*
5618	cell wall	73 out of 739 genes, 9.9%	*TPI1 MET6 SSB1 C5_02110W_A APE2 HSP12 HEM13 TKL1 TEF2 EFT2 RPL23A TEF1 CRH11 MET15 HWP1 ENG1 GAP1 RPL14 ATP1 ECM331 HWP2 TSA1B INT1 RPS3 RPS6A WH11 ALS4 CYP1 PGA30 PGK1 IPP1 YWP1 EXG2 PDC11 SSR1 C1_02330C_A SOD5 PGA13 BGL2 PST2 SAM2 RPL38 CHT3 FBA1 PHR2 DDR48 TDH3 ADH1 ALS2 HYR1 PRT1 RBE1 TAL1 ALS3 PGA59 GPM1 PGA6 RPS1 SRB1 ENO1 XYL2 CEF3 RPS13 CHT2 PGA31 PGA62 CR_08480C_A KRE1 CDC19 RPS20 CSH1 RPS14B SCW11*
5933	cellular bud	11 out of 739 genes, 1.5%	*GLC7 WSC2 INT1 VRP1 CHT3 AMN1 FLU1 NCE102 CDC5 C2_05270W_A ACT1*
5575	cellular component	169 out of 739 genes, 22.9%	*C2_06350C_A C3_04210W_A C1_06620C_A C4_05730W_A C7_04210C_A C3_00360W_A C1_02730W_A CAM1-1 C6_02480W_A CR_05210W_A C2_07420W_A C3_00230C_A C1_12000C_A C2_04370W_A C1_10500W_A C1_09040C_A C5_01110W_A C6_01600W_A C3_01970C_A C5_03040W_A LDG3 GLO1 C2_07010W_A C1_07790C_A GDS1 CFL2 CR_06500C_A C7_01940C_A C2_08530C_A C2_05960C_A C4_06320C_A C1_11720W_A JIP5 C3_06830C_A CR_10200W_A C1_02440C_A C6_00680C_A ERG13 RPS4A NOP4 MRV3 C1_01150C_A C7_02280W_A CDA2 KRE5 C1_07990C_A ASR3 CR_09740W_A C4_03830W_A C5_04480C_A C6_03110C_A C2_00130W_A C2_04080W_A CR_09510C_A C7_02260W_A C4_01030W_A C1_10850W_A RFG1 SPR28 C6_00450C_A OSM1 C1_09810W_A C4_01180W_A DUT1 C1_13820C_A GUA1 RHD2 C5_00510W_A C3_07690C_A AAT22 C3_07900C_A C4_07160W_A GAD1 HGH1 C1_10170W_A DAK2 MET3 C1_04270C_A C5_03640W_A C7_01010W_A MFA1 CR_09330C_A C1_11930W_A C5_01090C_A MVD PTP1 CYS3 CR_06570C_A C4_03230C_A C2_03830W_A C2_10130W_A C1_09500W_A CR_10750C_A C4_02620C_A C7_03270W_A PSA2 RPL82 ASR2 OFI1 C1_03580W_A C4_01830C_A HUT1 CR_08500W_A C2_09500W_A CR_09940W_A PBR1 C6_02490C_A TSR2 PRN4 C5_01550C_A CR_09060W_A C2_01960C_A CR_09070C_A C5_03440W_A C1_01510W_A SOU1 AAH1 C1_09330W_A C1_12180C_A*

			C5_02400W_A SOU2 C4_06710W_A C7_01380W_A CR_00530W_A C2_04000C_A KAR4 C3_01640C_A ASR1 C3_01570W_A C4_01220C_A C3_06880W_A MSB1 ROD1 C1_11050W_A USO6 CR_01640C_A BMT4 PMI1 C2_03020C_A C3_05450C_A HAL21 C3_05320W_A NAT4 C5_03630C_A C2_00890W_A C1_11990W_A EXO1 C5_03000C_A FRP5 DCG1 C1_11200W_A PWP1 SPE2 MET14 C6_02080W_A C2_00670C_A C7_02210W_A IFD6 C1_11120C_A C4_02260C_A C3_00730W_A C1_13150W_A CR_02340W_A C3_00990C_A C1_12300W_A C3_07980C_A C1_10050W_A C6_03880W_A C5_00600C_A
5694	chromosome	35 out of 739 genes, 4.7%	*C6_02280W_A UTP5 HTA2 C6_02880W_A C6_03380W_A GLC7 TEC1 SPO22 CYP1 PRI2 C1_04180W_A POL30 REC8 C4_02820W_A NOP1 C4_05230C_A SFL2 YOX1 HHF22 NDT80 HAT1 HTB1 MCD1 C1_14080W_A C1_06760C_A HHT2 PST3 NAN1 CDC5 HHT21 UTP15 SCH9 ACT1 TOS4 DLH1*
5737	cytoplasm	304 out of 739 genes, 41.1%	*RPS25B C5_01540W_A YCP4 RPL16A TPI1 SOD2 FEN12 YBN5 THS1 RPL17B AGP2 SSB1 C5_02110W_A ERG6 APE2 LSC1 TIF5 GUS1 RPL19A RPL25 C4_04390W_A C5_04300C_A HSP12 HEM13 C7_00490C_A RPS42 RPP0 ERG12 CAR2 SSZ1 ERG5 RPL20B C1_09060C_A TEF2 UTP20 RPL29 RPL23A GND1 C2_05300C_A TIF ELF1 HGT7 BFR1 MSS116 LTV1 C4_04800W_A TEF1 RPL37B CR_04610C_A TMA19 CR_01410C_A CR_09140C_A C6_03200W_A LSC2 ERG25 RPL10A C1_13790C_A PGA63 C5_00030W_A CR_02690W_A ERG10 HGT6 C6_03390W_A C6_02380W_A C6_03380W_A CR_01780W_A RPL14 GLC7 RPL30 PFK1 ATP1 MAE1 CR_04120C_A VRG4 RPP2A DRG1 RPL2 ERG1 ARC40 C1_03470C_A YNK1 LAT1 ATP2 ATP3 PUS7 C2_01740C_A RPS27 NRM1 C2_07190C_A C2_09590C_A TSA1B C7_01360C_A C5_02660C_A PFY1 INT1 RPS3 MIR1 C1_06470W_A CAM1 GPD2 RPS6A RPL32 WH11 RNR21 CYP1 C5_03530C_A PWP2 RPP1B RPL9B PGK1 ERF1 C1_02290C_A C3_04810C_A ERG9 RPS12 FAS1 C3_06050C_A C1_01530C_A MNN12 CAR1 YST1 ARC1 RPS19A RIB4 IPP1 ERG11 RPS8A RPL24A SOD1 CYS4 KTI12 CR_07220C_A MET18 TRM1 EFB1 LKH1 RPS22A GLE2 NPL3 CHO1 TUB2 C1_11790W_A RPL3 PDC11 ANB1 SES1 C1_11860W_A KRS1 ERV25 ENP1 C1_02330C_A CNS1 RPP2B EGD1 SSH1 CR_02770C_A ERG4 UBI3 C2_05410W_A RPS9B RPL11 RPL6 PGI1 RPP1A RPL42 SAM2 VRP1 DPM1 RPL38 C4_05230C_A C7_03660C_A C1_02240W_A TIM50 TUB1 RPS23A AMN1 CHC1 FBA1 RPL8B PHR2 RNR1 TDH3 GCD6 ERO1 C2_07290W_A RPS21B ADH1 RPL15A TSR1 C6_02370C_A RPL4B SEC14 GUT2 SEN2 HAT1 C1_06890C_A FUM11 C6_03730C_A RRP42 C3_01680C_A PFK2 RPL13 C2_05710C_A PRT1 SUR7 NMD3 RPL12 PDI1 C1_08520C_A TAL1 C1_01050C_A C1_00810W_A COF1 URA1 RPL43A RPL18 GCD7 PMT2 ARX1 MCD1 RPP1 C6_01980C_A ZPR1 KAR2 GPM1 NIP1 ATP8 C7_02660C_A GCN1 EGD2 RPS1 C3_07400W_A TVP18 IDH2 RPL27A GSP1 SRB1 ENO1 FLU1 EMP24 HXK2 RPL5 ZUO1 MRF1 C1_05630C_A STT3 CEF3 NOC4 IDH1 RPS13 SAM50 DPS1-1 TOM20 ERG3 C5_05020C_A C5_03410C_A C6_02690C_A CR_08480C_A RPS5 C7_00830C_A RHR2 PTP3 RPL28 SEC24 PMT1 RPL21A ERG2 RPS28B CDC19 TFS1 IMH3 RPS21 RPS20 MRPS9 APT1 ASC1 C2_05270W_A POR1 C7_01600W_A PMT4 LEU2 PET9 GDA1 C1_14160W_A C7_02340C_A C1_05720W_A RPL35 CSH1 C2_02410W_A RPL39 C2_08160C_A MAM33 MCR1 NIP7 YMC1 URA2 SCH9 SEC61 C1_11920W_A ACT1 OST1 C6_02420W_A ILV5 TIF3*
16023	cytoplasmic, membrane-bounded vesicle	0 out of 739 genes, 0%	*none*
5856	cytoskeleton	15 out of 739 genes, 2.0%	*ENG1 GLC7 ARC40 INT1 CR_07220C_A TUB2 VRP1 C1_02240W_A TUB1 CHC1 COF1 CDC5 ABP140 C2_05270W_A ACT1*
12505	endomembrane system	60 out of 739 genes, 8.1%	*ERG28 DPM2 FEN12 AGP2 C5_02110W_A C1_00160C_A ERG6 APE2 SMP3 ERG5 BFR1 LTV1 C4_04800W_A ERG25 PGA63 VRG4 HAS1 ERG1 C4_01660W_A HMG1 CWH8 PRI2 ERG9 MNN12 SEC12 ERG11 TRM1 LKH1 GLE2 CHO1 C1_11860W_A SSH1 ERG4 DPM1 C1_02240W_A CHC1 ERO1 SEC14 PDI1 C1_01050C_A C1_00810W_A PMT2 KAR2 C5_03550W_A TVP18 EMP24 STT3 ERG3 C5_05020C_A SEC24 PMT1 ERG2 NTF2 PMT4 GDA1 C2_02410W_A C2_08160C_A SEC61 C1_11920W_A OST1*
5783	endoplasmic reticulum	30 out of 739 genes, 4.1%	*FEN12 ERG6 ERG5 BFR1 C4_04800W_A ERG25 ERG1 ERG9 ERG11 C1_11860W_A SSH1 ERG4 DPM1 ERO1 PDI1 C1_00810W_A PMT2 KAR2 EMP24 STT3 ERG3 C5_05020C_A SEC24 PMT1 ERG2 PMT4 C2_02410W_A C2_08160C_A SEC61 OST1*
5576	extracellular region	84 out of 739 genes, 11.4%	*MSB2 TPI1 HPT1 RPL17B MET6 APE2 C5_04300C_A HEM13 RPS42 TKL1 GND1 HGT7 C4_04800W_A TEF1 TMA19 CRH11 HGT6 ENG1 RPS18 YNK1 C4_01800W_A MTS1 PFY1 RPS3 MIR1 CAM1 SPE3 GPD2 ALS4*

			CYP1 C2_07630C_A PGK1 CAR1 IPP1 YWP1 SOD1 PDC11 SSR1 SOD5 UBI3 PGI1 BGL2 CHT3 PHR2 TDH3 ERO1 ADH1 ALS2 HYR1 SUR7 C1_03510C_A PDI1 RBE1 TAL1 FET34 PMA1 ALS3 KAR2 GPM1 GCY1 GCN1 RPS1 URA5 FGR41 GSP1 ENO1 LIP6 GAP4 GUK1 PST3 NCE102 CHT2 SAH1 RPS5 GRE3 APT1 ASC1 POR1 LEU2 PET9 C2_08160C_A SEC61 PHM7 SCW11
5794	Golgi apparatus	7 out of 739 genes, 0.9%	*C4_04800W_A VRG4 MNN12 CHC1 SEC14 TVP18 GDA1*
1411	hyphal tip	1 out of 739 genes, 0.1%	*ACT1*
16020	membrane	154 out of 739 genes, 20.8%	*PNG2 ERG28 DPM2 FRE10 YCP4 MSB2 C4_05330C_A RPL16A PGA53 FEN12 AGP2 CR_01630C_A SSB1 C5_02110W_A ERG6 OPT5 SMP3 TKL1 C4_02720C_A ERG5 MUP1 C1_09060C_A TEF2 EFT2 ELF1 HGT7 BFR1 LTV1 C4_04800W_A TEF1 CR_04610C_A CRH11 ERG25 PGA63 HGT10 HGT6 HGT12 C6_03390W_A GAP1 ATP1 VRG4 ERG1 C1_03470C_A ATP2 ECM331 ATP3 MTS1 AQY1 HMG1 PFY1 MIR1 C2_05290C_A C5_03530C_A CWH8 C7_01950W_A PGK1 ERG9 PTR22 C3_06050C_A SEC12 YST1 HXT5 ERG11 GSL2 EXG2 TRM1 CHO1 ERG24 PDC11 FCY2 C1_11860W_A SSR1 ERV25 HGT19 SSH1 ERG4 RPL6 PST2 SAM2 DPM1 C3_01540W_A TIM50 CHC1 FBA1 PHR2 TDH3 HSP31 HSP30 ERO1 ADH1 HGT13 RPL4B SEC14 GUT2 SEN2 HYR1 C3_01680C_A CNT SUR7 C1_03510C_A FET34 PMA1 C1_01050C_A SLP2 C1_00810W_A CR_01220W_A URA1 MSS4 PMT2 KAR2 ATP8 FGR2 TVP18 GSP1 SRB1 ENO1 FLU1 EMP24 HXK2 GAP4 STT3 CEF3 PST3 SAM50 NCE102 CR_03580C_A TOM20 ERG3 C5_05020C_A ALP1 ERG251 RPS5 SEC24 PMT1 CDC19 TFS1 C2_10010C_A C7_00630C_A POR1 C7_01600W_A PMT4 PET9 GDA1 C2_02410W_A HGT8 C2_08160C_A MCR1 URA2 SCH9 SEC61 C1_11920W_A ACT1 PHM7 OST1*
5624	membrane fraction	0 out of 739 genes, 0%	*none*
5815	microtubule organizing center	3 out of 739 genes, 0.4%	*GLC7 TUB2 CDC5*
5740	mitochondrial envelope	28 out of 739 genes, 3.8%	*C1_09060C_A HGT6 C6_03390W_A ATP1 YNK1 ATP2 ATP3 MIR1 CYP1 C5_03530C_A C3_06050C_A RIB4 SOD1 CHO1 TIM50 GUT2 SEN2 C3_01680C_A URA1 GPM1 ATP8 HXK2 SAM50 TOM20 POR1 C7_01600W_A PET9 MCR1*
5739	mitochondrion	75 out of 739 genes, 10.1%	*TPI1 SOD2 LSC1 GUS1 C1_09060C_A TEF2 C2_05300C_A MSS116 TEF1 TMA19 CR_09140C_A C6_03200W_A LSC2 C1_13790C_A C5_00030W_A HGT6 C6_03390W_A C6_02380W_A PFK1 ATP1 MAE1 CR_04120C_A YNK1 LAT1 ATP2 ATP3 C2_01740C_A C2_07190C_A C2_09590C_A C7_01360C_A MIR1 CYP1 C5_03530C_A PGK1 C1_02290C_A C3_06050C_A RIB4 SOD1 TRM1 CHO1 PGI1 TIM50 FBA1 TDH3 ADH1 C6_02370C_A GUT2 SEN2 FUM11 C6_03730C_A C3_01680C_A PFK2 C1_08520C_A URA1 MCD1 C6_01980C_A GPM1 ATP8 IDH2 ENO1 HXK2 MRF1 IDH1 SAM50 TOM20 C5_03410C_A MRPS9 POR1 C7_01600W_A PET9 MAM33 MCR1 YMC1 C6_02420W_A ILV5*
5730	nucleolus	87 out of 739 genes, 11.8%	*UTP5 GAR1 RRN3 RPL7 C1_07660W_A C4_05330C_A ENP2 RPF2 CR_10410C_A RPC19 CR_10470C_A NOP15 C7_03850W_A CIC1 UTP20 C1_10880W_A NOG2 RCL1 NSA1 C2_01070W_A UTP18 C4_06210C_A GLC7 DBP8 RPC40 HAS1 SRP40 LHP1 RLP24 CSI2 UTP13 PES1 PWP2 C3_05160C_A C3_04380C_A C2_02540W_A UTP21 CR_04170W_A KRR1 NOP14 UTP22 RRS1 DIP2 NOP5 ENP1 YTM1 RPA34 NOP1 RPO26 SPB1 C2_04570W_A TSR1 C2_04120C_A MRT4 IMP4 SIK1 RPA135 RRP9 ARX1 RPP1 C1_14080W_A C1_03790C_A C6_01890C_A C6_01040C_A C3_02040C_A C3_02020W_A NOP8 DBP7 RPA190 ZUO1 NOC4 C1_04040C_A NAN1 C4_05010W_A NOC2 RPS28B C1_10620W_A UTP4 ERB1 CR_02030C_A C2_09660W_A UTP15 C1_12680W_A C3_06370C_A DBP3 MAK21 SSF1*
5634	nucleus	197 out of 739 genes, 26.7%	*C6_02280W_A UTP5 GAR1 C2_02930C_A RRN3 RPL7 PCL1 C1_07660W_A C4_05330C_A ENP2 MET6 RPF2 CR_10410C_A C5_02110W_A C1_00160C_A RPC19 RMS1 HSP12 CR_10470C_A NOP15 C7_03850W_A CIC1 UTP20 MED1 RPL23A C1_10880W_A NOG2 RCL1 HTA2 LTV1 C7_01030C_A CR_01410C_A NSA1 C6_02880W_A C2_01070W_A C2_09180W_A SUT1 UTP18 C6_03380W_A C4_06210C_A GLC7 DBP8 TEC1 RPC40 HAS1 C4_01660W_A C1_03470C_A PUS7 SRP40 NRM1 SPO22 TSA1B HMG1 LHP1 CAM1 RLP24 MDN1 CSI2 UTP13 RNR21 CYP1 PES1 PWP2 C3_05160C_A C7_01950W_A C3_04380C_A PRI2 GZF3 C1_04180W_A C2_02540W_A C3_01560W_A UTP21 CR_04170W_A KRR1 NOP14 UTP22 SOD1 POL30 KTI12 RRS1 CR_07220C_A C2_05860C_A TRM1 GLE2 NPL3 REC8 C1_11790W_A CR_04160C_A PDC11 NRG1 C6_02350C_A C4_02820W_A SDA1 DIP2*

			NOP5 ENP1 YTM1 RPA34 NOP1 RPO26 CR_02770C_A RHA1 C4_05230C_A SPB1 SFL2 C1_02240W_A YOX1 TUB1 RPS23A AMN1 PHR2 HHF22 C2_04570W_A SSN6 TSR1 NDT80 SEC14 SEN2 PTP2 HAT1 C2_04120C_A RRP42 HTB1 MRT4 IMP4 CR_04110W_A TAL1 C7_02100W_A SIK1 MSS4 RPA135 CLN3 RRP9 ARX1 MCD1 RPP1 C1_14080W_A ZPR1 KAR2 C1_03790C_A C6_01890C_A C5_03550W_A C6_01040C_A C1_06760C_A C3_02040C_A C3_02020W_A NOP8 GSP1 HHT2 DBP7 ENO1 RPA190 HXK2 C1_10970W_A ZUO1 C1_05630C_A NOC4 DPS1-1 C6_02690C_A C1_04040C_A NAN1 CDC5 C4_05010W_A PTP3 RPL28 HMT1 DBP2 ZCF3 NOC2 ZCF31 C3_00100W_A RPS28B NTF2 C2_05270W_A C1_10620W_A UTP4 C4_07150W_A ERB1 C1_14160W_A HHT21 CR_02030C_A C7_02340C_A C2_09660W_A UTP15 C1_12680W_A KRE30 C3_06370C_A CR_04300W_A C2_08160C_A NIP7 DBP3 SCH9 ACT1 MAK21 SSF1 TOS4 DLH1
other	other	28 out of 739 genes, 3.8%	*C4_00940W_A UAP1 C1_12570C_A PGA23 PIL1 RPS10 RBR1 C4_05250W_A PGA58 PGA12 PGA34 URA7 PGA54 C2_07620W_A PGA26 C3_06760W_A MIH1 PGA18 DIM1 C5_04940W_A MSI3 C4_04810C_A DRS1 HCA4 PGA11 CR_04240C_A C6_01420C_A PGA38*
5777	peroxisome	1 out of 739 genes, 0.1%	*GND1*
5886	plasma membrane	90 out of 739 genes, 12.2%	*PNG2 FRE10 YCP4 MSB2 PGA53 AGP2 SSB1 C5_02110W_A ERG6 OPT5 TKL1 C4_02720C_A ERG5 MUP1 EFT2 ELF1 HGT7 CRH11 ERG25 HGT10 HGT6 HGT12 C6_03390W_A GAP1 ATP1 ERG1 ATP2 ECM331 ATP3 MTS1 AQY1 HMG1 PFY1 MIR1 PGK1 ERG9 PTR22 ERG11 GSL2 EXG2 PDC11 SSR1 ERV25 HGT19 SSH1 PST2 SAM2 DPM1 C3_01540W_A TIM50 CHC1 FBA1 PHR2 TDH3 HSP30 ADH1 HGT13 GUT2 HYR1 CNT SUR7 FET34 PMA1 MSS4 PMT2 SRB1 ENO1 FLU1 EMP24 GAP4 STT3 CEF3 PST3 SAM50 NCE102 TOM20 ERG3 ALP1 ERG251 PMT1 CDC19 C2_10010C_A POR1 PMT4 PET9 C2_02410W_A HGT8 SEC61 PHM7 OST1*
5840	ribosome	98 out of 739 genes, 13.3%	*RPS25B C5_01540W_A RPL16A RPL17B RPS15 RPL19A RPL25 C4_04390W_A RPS42 RPP0 RPL20B CIC1 EFT2 RPL29 RPL23A C2_05300C_A RPL37B RPL10A C5_00030W_A RPL14 RPS18 RPL30 RPP2A RPL2 C2_01740C_A RPS27 C2_07190C_A RPS3 C1_06470W_A RPS6A RPL32 RPP1B RPL9B RPS12 RPS17B YST1 RPS19A RPS8A RPL24A RPS30 EFB1 RPS22A RPL3 C1_02330C_A RPP2B EGD1 UBI3 C2_05410W_A RPS9B RPL11 RPL6 RPP1A RPL42 RPL38 RPS26A RPS23A RPL8B RPS21B RPL15A C6_02370C_A RPL4B C1_06890C_A C6_03730C_A RPL13 C2_05710C_A RPL12 C1_08520C_A RPL43A RPL18 C6_01980C_A RPL40B GCN1 EGD2 RPS1 RPL27A RPS24 RPL5 ZUO1 CEF3 RPS13 C1_03620C_A C5_03410C_A C2_05160C_A CR_08480C_A RPS7A RPS5 RPL28 RPL21A RPS28B RPS21 RPS20 MRPS9 ASC1 RPS16A C1_05720W_A RPL35 RPL39 RPS14B*
30427	site of polarized growth	14 out of 739 genes, 1.9%	*MSB2 ENG1 GLC7 WSC2 PFY1 INT1 VRP1 CHT3 PHR2 MSS4 NCE102 CDC5 C2_05270W_A ACT1*
70732	spindle envelope	0 out of 739 genes, 0%	*none*
5773	vacuole	14 out of 739 genes, 1.9%	*AGP2 APE2 TEF2 HGT7 LTV1 TEF1 CR_04610C_A LKH1 ENO1 FLU1 TFS1 YMC1 SCH9 SEC61*

Table S12. Assignment of the 431 significantly upregulated *C. albicans* genes to the top 20 most highly enriched KEGG pathways.

KEGG pathway	Gene list	No. of genes in input list	No. of genes in pathway	Enrichment ratio	Corrected P-value
alpha-Linolenic acid metabolism	*POX1-3, POX1, POT1, FOX3, PXP2*	5	7	0.714	1.07×10^{-04}
Arginine biosynthesis	*ARG8, GDH3, ARG1, ARG3, ARG4, ARG5, DUR1, ECM42, ALT1*	9	16	0.563	5.34×10^{-07}
beta-Alanine metabolism	*HPD1, EHD3, ALD6, UGA11, PXP2, POX1-3, UGA1, AMO2, POX1, FOX2, AMO1*	11	21	0.524	6.95×10^{-08}
Propanoate metabolism	*HPD1, EHD3, ALD6, UGA11, PXP2, POX1-3, UGA1, POX1, FOX2*	9	19	0.474	1.38×10^{-06}
Valine, leucine and isoleucine degradation	*HPD1, EHD3, BAT21, ALD6, UGA11, POT1, UGA1, FOX3*	8	18	0.444	6.65×10^{-06}
Biosynthesis of unsaturated fatty acids	*POX1-3, POX1, POT1, FOX3, PXP2*	5	14	0.357	1.07×10^{-03}
Alanine, aspartate and glutamate metabolism	*GDH3, GLT1, ARG1, UGA11, CPA1, ARG4, UGA1, CPA2, ALT1*	9	27	0.333	8.20×10^{-06}
Lysine biosynthesis	*ARO8, LYS4, LYS22, HOM3*	4	12	0.333	4.72×10^{-03}
ABC transporters	*PXA2, ATM1, PXA1, CDR11*	4	12	0.333	4.72×10^{-03}
Fatty acid degradation	*PXP2, POX1-3, ECI1, POT1, FOX3, FAA21, FAA2-3, POX1*	8	25	0.320	3.79×10^{-05}
2-Oxocarboxylic acid metabolism	*ARG8, BAT21, ARO8, LYS22, ARG5, LEU42, ECM42, HOM3, LYS4, ALT1*	10	32	0.313	4.72×10^{-06}
Histidine metabolism	*HIS4, HIS5, HIS7, HIS3*	4	13	0.308	5.72×10^{-03}
Peroxisome	*POT1, PEX5, PEX6, CTN3, PXP2, PXA2, POX1-3, ECI1, CTN1, FOX3, FAA21, FAA2-3, POX1, PXA1*	14	48	0.292	1.37×10^{-07}
Phenylalanine metabolism	*ARO8, AMO2, AMO1, HIS5*	4	16	0.250	9.81×10^{-03}
Nitrogen metabolism	*GLT1, GDH3*	2	8	0.250	8.58×10^{-02}
Valine, leucine and isoleucine biosynthesis	*CHA1, LEU42, BAT21*	3	13	0.231	3.31×10^{-02}
Fatty acid metabolism	*POX1, PXP2, POX1-3, POT1, FOX3, FAA2-3, FAA21*	7	31	0.226	7.54×10^{-04}
Vitamin B6 metabolism	*SNZ1, SNO1*	2	9	0.222	9.60×10^{-02}
Tyrosine metabolism	*ARO8, AMO2, AMO1, HIS5*	4	19	0.211	1.52×10^{-02}
Phenylalanine, tyrosine and tryptophan biosynthesis	*ARO8, HIS5, ARO3, TRP4*	4	19	0.211	1.52×10^{-02}

Table S13. Assignment of the 739 significantly downregulated *C. albicans* genes to the top 20 most highly enriched KEGG pathways.

KEGG pathway	Gene list	No. of genes in input list	No. of genes in pathway	Enrichment ratio	Corrected P-value
Ribosome	*RPS13, RPS12, RPL16A, RPS10, RPL5, RPS30, RPS15, RPS17B, RPL6, RPL7, RPL40B, RPS18, RPL2, RPL3, RPL9B, RPS5, RPS3, RPL8B, RPS1, RPL42, RPS24, RPS25B, RPL29, RPL23A, RPL25, RPS21, RPS19A, RPS23A, RPL82, RPS42, RPS9B, RPP2A, RPP2B, RPL20B, RPL27A, RPS4A, RPS14B, RPL24A, RPS22A, RPL17B, RPS16A, RPS26A, RPL43A, UBI3, RPS27, RPL19A, RPL14, RPP0, RPL11, RPL12, RPL13, RPL37B, RPL18, RPL32, RPL28, YST1, RPS21B, RPS6A, RPS20, RPS28B, RPL38, RPL39, RLP24, RPL35, MRPS9, RPL4B, RPL30, RPP1A, RPL10A, RPP1B, RPS7A, RPL21A, RPL15A, RPS8A*	74	119	0.622	3.06×10^{-34}
Steroid biosynthesis	*ERG4, ERG5, ERG6, ERG1, ERG2, ERG3, ERG11, ERG9, ERG251, ERG25, ERG24*	11	18	0.611	3.80×10^{-05}
Mannose type O-glycan biosynthesis	*PMT4, PMT1, PMT2*	3	5	0.600	7.52×10^{-02}
Fructose and mannose metabolism	*FBA1, TPI1, PFK1, PFK2, SOU1, DAK2, SOU2, PSA2, HXK2, PMI1, SRB1*	11	21	0.524	8.70×10^{-05}
Glycolysis / Gluconeogenesis	*ADH1, CDC19, LAT1, FBA1, PGI1, HXK2, PFK2, PFK1, PDC11, ENO1, TPI1, GPM1, TDH3, PGK1*	14	40	0.350	1.87×10^{-04}
Pentose phosphate pathway	*TAL1, FBA1, GND1, PFK2, TKL1, PGI1, PFK1*	7	21	0.333	2.02×10^{-02}
Selenocompound metabolism	*MET3, MET6, CYS3*	3	9	0.333	1.71×10^{-01}
Other types of O-glycan biosynthesis	*PMT4, PMT1, PMT2*	3	9	0.333	1.71×10^{-01}
Methane metabolism	*FBA1, PFK2, PFK1, ENO1, DAK2, GPM1*	6	20	0.300	4.89×10^{-02}
Amino sugar and nucleotide sugar metabolism	*CDA2, UAP1, PSA2, MCR1, PGI1, CHT3, CHT2, HXK2, PMI1, SRB1*	10	35	0.286	8.85×10^{-03}
Ribosome biogenesis in eukaryotes	*MDN1, UTP5, UTP4, SIK1, IMP4, NOP1, RCL1, DIP2, NOP5, NOP4, PWP2, UTP13, GSP1, UTP22, NOG2, UTP21, NAN1, NMD3, RPP1, UTP18, GAR1*	21	76	0.276	5.07×10^{-05}
Pyrimidine metabolism	*RNR21, URA7, URA5, URA2, URA1, DUT1, YNK1, RNR1*	8	30	0.267	3.05×10^{-02}
Sulfur metabolism	*MET3, MET14, MET15, HAL21*	4	15	0.267	1.62×10^{-01}
Terpenoid backbone biosynthesis	*MVD, ERG12, ERG13, ERG10, HMG1*	5	19	0.263	1.11×10^{-01}
Carbon metabolism	*LAT1, HXK2, TKL1, MAE1, TPI1, TDH3, LSC2, FUM11, FBA1, CDC19, PGI1, DAK2, AAT22, GND1, PGK1, TAL1, MET15, LSC1, IDH2, IDH1, PFK2, PFK1, ENO1, GPM1, ERG10*	25	98	0.255	2.99×10^{-05}
Ubiquinone and other terpenoid-quinone biosynthesis	*YCP4, PST3, PST2*	3	12	0.250	2.70×10^{-01}

Biosynthesis of antibiotics	*ERG4, ERG5, ERG6, CDC19, LAT1, ERG1, ERG2, ERG3, HXK2, ERG9, TKL1, PMI1, TPI1, TAL1, TDH3, CYS4, HMG1, CYS3, FUM11, FBA1, CAR2, CAR1, PGI1, ERG25, ERG24, YNK1, AAT22, GND1, PGK1, LSC2, MET15, LSC1, ILV5, IDH2, IDH1, UAP1, PFK2, PFK1, ENO1, MVD, MET3, ADH1, ERG251, PDC11, GPM1, ERG12, ERG13, ERG10, ERG11*	49	206	0.238	$5.48x10^{-09}$
Purine metabolism	*RNR21, MET3, MET14, IMH3, CDC19, HPT1, APT1, GUK1, GUA1, YNK1, RNR1, AAH1*	12	52	0.231	$1.31x10^{-02}$
Butanoate metabolism	*GAD1, ERG10, ERG13*	3	13	0.231	$2.94x10^{-01}$
Citrate cycle (TCA cycle)	*LSC2, LSC1, IDH2, IDH1, LAT1, FUM11*	6	27	0.222	$1.17x10^{-01}$

IV. *C. ALBICANS* SIGNIFICANT DEGS: RESPONSE TO *P. AERUGINOSA* IN MEROPENEM-TREATED BIOFILMS

Biological Process

Table S14. Assignment of the 380 significantly upregulated *C. albicans* genes to 40 GO Slim terms under the Biological Process category.

GO ID	GO term	Frequency	Gene list
42710	biofilm formation	7 out of 380 genes, 1.8%	*STE2 GCN4 UGA33 SUC1 ZFU2 PGA7 SAP6*
44419	biological process involved in interspecies interaction between organisms	14 out of 380 genes, 3.7%	*APS3 DUR1,2 HGT4 HXK1 YHB1 GAT1 FOX2 CAP1 HSP21 SET1 PGA7 SAP6 SAP4 ICL1*
8150	biological_process	150 out of 380 genes, 39.5%	*C1_00010W_A GTT13 C1_01220C_A C1_11320C_A C2_08440W_A C6_02450W_A C4_03950C_A C6_03600C_A C3_02900W_A C6_02620C_A C3_05290C_A C4_04620C_A C6_00730W_A C3_00050C_A C4_01970W_A C1_01840C_A C1_12900W_A C7_03470W_A C1_00020C_A C5_03970W_A MOH1 C4_02930W_A C5_03870C_A C3_05750C_A C5_00750C_A C3_03700C_A C1_02270C_A OP4 C1_11570W_A C7_03280C_A CR_02480W_A C1_09310C_A C2_08510W_A C3_04720C_A PEX22 C4_00080C_A CR_04220C_A C4_06670W_A C7_00260C_A C7_02920W_A CSO99 C2_08330W_A C3_04650W_A C6_03150C_A BLP1 C1_01140C_A C6_01620W_A C1_00580W_A FRP2 BUL1 CR_07740W_A CR_08830W_A CR_09610C_A C1_13430C_A C1_01630W_A PGA17 C3_04630W_A C1_14180W_A C1_12870C_A CR_10310W_A BIO32 C4_04380C_A POX18 C2_08260W_A C3_02990C_A C7_00770W_A C1_00030C_A CIRT4B C7_02140W_A C1_09700W_A C1_05440C_A C3_01420C_A C1_00050C_A CR_05040W_A PEX17 CR_06310W_A ATO9 BMT9 GST1 C3_04450C_A C1_05690C_A C3_02090C_A C3_03370C_A GTT1 C3_07720C_A CR_04860C_A C1_13090W_A C2_10870W_A C4_01350W_A C2_04400W_A C3_05060W_A C3_02660W_A TES1 C5_04980W_A C1_13100W_A CR_06020W_A CR_04990C_A C2_08690C_A C6_03280W_A C4_03960W_A C1_09770W_A C7_03820C_A C1_13180W_A HRQ2 IFK2 C2_02390W_A SMI1B C2_09800C_A C3_01060W_A C1_09340C_A CR_04850C_A CR_02060W_A PSO2 C3_04840C_A C4_07020C_A C4_00640W_A C1_06870C_A C1_09300C_A C3_06040W_A C4_06940C_A C2_06630C_A IFR1 C1_11260C_A C4_05800C_A C6_03530C_A CR_05750W_A C1_14020W_A C7_03740C_A C1_00190C_A C6_03670C_A AGA1 C1_03970W_A C6_01940W_A CR_07700W_A C4_03710C_A CR_06270W_A C1_01610C_A CR_08850W_A PGA46 C3_01270W_A C1_10060C_A C2_04830W_A TES15 ASG7 C3_04330C_A C3_02630C_A PGA25 MRV2 CR_06770C_A C3_04190W_A*
5975	carbohydrate metabolic process	14 out of 380 genes, 3.7%	*HXK1 C1_14190C_A MDH1-3 SCW4 C2_10150W_A SUC1 FOX2 MNN41 HSP21 MLS1 INO1 PYC2 ARA1 ICL1*
7155	cell adhesion	1 out of 380 genes, 0.3%	*STE2*
7114	cell budding	1 out of 380 genes, 0.3%	*C3_00400C_A*
7049	cell cycle	11 out of 380 genes, 2.9%	*FAR1 C4_00030C_A C1_14190C_A RAD6 MSO1 KIN3 PPH3 CAP1 SET1 CR_04820W_A PSF1*
48468	cell development	3 out of 380 genes, 0.8%	*MSO1 SET1 CR_04820W_A*
71555	cell wall organization	1 out of 380 genes, 0.3%	*RBR2*
19725	cellular homeostasis	10 out of 380 genes, 2.6%	*HGT4 HXK1 C1_14190C_A C3_03760W_A CRD2 C2_00600C_A AMO1 CCC1 FRP1 HMX1*

6464	cellular protein modification process	17 out of 380 genes, 4.5%	*NPR1 C1_03270W_A RAD6 PDK2 RER2 C1_00860W_A KIN3 PPH3 MNN41 SET1 C1_03330C_A C6_02160W_A APG7 C2_06780C_A ATG1 CEK2 PRR2*
45333	cellular respiration	5 out of 380 genes, 1.3%	*AOX2 CM_00250W MDH1-3 CTN1 C1_09440W_A*
746	conjugation	3 out of 380 genes, 0.8%	*STE2 C7_03860W_A CEK2*
910	cytokinesis	0 out of 380 genes, 0%	*none*
7010	cytoskeleton organization	2 out of 380 genes, 0.5%	*KIN3 C2_06780C_A*
6259	DNA metabolic process	10 out of 380 genes, 2.6%	*C4_00030C_A RAD6 CM_00250W RAD16 C4_04180C_A PPH3 SET1 C2_08420W_A PSF1 CCE1*
30447	filamentous growth	28 out of 380 genes, 7.4%	*HGT4 C6_03240W_A HXK1 WOR2 C1_14190C_A RAD6 YHB1 CR_03260W_A CAT8 GCN4 GLT1 STB5 CHA1 BUD20 SSU1 FGR15 ECI1 HSP21 GDH3 SET1 CCC1 ZFU2 C1_03870C_A MEP2 C5_05510C_A CEK2 CTN3 SSY1*
6091	generation of precursor metabolites and energy	10 out of 380 genes, 2.6%	*HGT4 AOX2 HXK1 C1_14190C_A CM_00250W MDH1-3 CTN1 HPD1 C1_09440W_A C3_02850C_A*
70783	growth of unicellular organism as a thread of attached cells	5 out of 380 genes, 1.3%	*WOR2 CAT8 GLT1 GDH3 MEP2*
30448	hyphal growth	1 out of 380 genes, 0.3%	*HXK1*
6629	lipid metabolic process	24 out of 380 genes, 6.3%	*C6_03240W_A PXP2 C2_01920C_A C3_03760W_A POT1 POX1-3 LCB4 POX1 C3_00400C_A RER2 MDH1-3 SFC1 FOX2 C4_04180C_A PEX5 ECI1 CR_02570C_A ANT1 PEX6 MLS1 INO1 FAA21 C3_02850C_A ICL1*
6997	nucleus organization	0 out of 380 genes, 0%	*none*
6996	organelle organization	20 out of 380 genes, 5.3%	*C4_00030C_A RAD6 RAD16 C1_00860W_A KIN3 PEX5 SET1 ANT1 C7_03860W_A C1_12150C_A C1_03330C_A PEX6 HSP78 YPT53 ATG9 APG7 C2_06780C_A ATG1 CCE1 AUT7*
other	other	49 out of 380 genes, 12.9%	*EHD3 GBU1 ATO5 ARG3 C2_00390C_A BAT21 ARO3 ARG4 C1_04460C_A LYS4 HIS7 CR_03690W_A C3_05360C_A ATF1 FAA2-3 SOD6 HIS3 CPA1 C1_02970W_A UGA1 HOM3 C7_02010C_A C1_01620C_A GCV1 C1_05160C_A C4_02230C_A FOX3 UGA11 C3_04350C_A C4_02170C_A C2_09070C_A CYB2 CR_04230W_A CPA2 ALD6 MET13 LYS22 CR_04870C_A C5_00230C_A ARO8 GOR1 C4_00290C_A LEU42 ARG1 DLD2 ECM42 IFG3 CR_06980W_A ARG8*
9405	pathogenesis	0 out of 380 genes, 0%	*none*
30163	protein catabolic process	8 out of 380 genes, 2.1%	*C1_03990W_A RAD6 PRB1 UBC8 RAD16 C7_03860W_A SAP6 SAP4*
6457	protein folding	3 out of 380 genes, 0.8%	*HSP78 OSM2 C1_02380C_A*
7124	pseudohyphal growth	1 out of 380 genes, 0.3%	*MEP2*
50789	regulation of biological process	49 out of 380 genes, 12.9%	*NPR1 HGT4 DRE2 C4_02770C_A HXK1 FAR1 WOR2 C4_00030C_A C1_14190C_A RAD6 STE18 C6_03290W_A STE2 PDK2 CAT8 HAP2 LCB4 GCN4 UBC8 UGA33 STB5 KIN3 GAT1 ARF1 SUC1 C2_00640W_A FGR15 PPH3 CAP1 SNO1 SET1 MET28 ZCF32 YPT53 SEF2 ZFU2 ZCF25 ZCF20 ARG5,6 SAP6 MEP2 C2_09870W_A ZCF4 SUA72 C6_03320W_A AUT7 C1_02380C_A SAP4 SSY1*
42221	response to chemical	40 out of 380 genes, 10.5%	*HGT4 C2_05060C_A C2_01920C_A FAR1 C1_03990W_A C1_14190C_A RAD6 YHB1 STE18 STE2 PDK2 CAT8 CIP1 HAP2 GCN4 C2_07070W_A ROA1 ALT1 STB5 GAT1 ARF1 HIS5 TPO4 PPH3 CAP1 HSP21 AMO2 C1_03330C_A SEF2 ZCF20 C1_00830W_A CDR11 C6_01870C_A C2_06780C_A HMX1 C6_03320W_A AUT7 PRR2 C3_02850C_A SSY1*
42493	response to drug	9 out of 380 genes, 2.4%	*C1_14190C_A PDK2 ROA1 ALT1 PPH3 CAP1 AMO2 C1_00830W_A PRR2*
6950	response to stress	40 out of 380 genes, 10.5%	*HGT4 C2_05060C_A RBR2 C1_06860W_A C1_03270W_A C4_00030C_A RAD6 YHB1 GPX2 CIP1 GCN4 RAD16 C2_07070W_A STB5 GAT1 ARF1 BUD20 SSU1 MEP1 FGR15 C4_04180C_A PPH3 CAP1 HSP21 SET1 C7_03860W_A C1_03330C_A HSP78 ZCF20 C1_03870C_A C2_08420W_A MEP2 C2_09870W_A PSF1 FRP1 C5_05510C_A CEK2 HMX1 C6_03320W_A AUT7*

42254	ribosome biogenesis	0 out of 380 genes, 0%	*none*
16070	RNA metabolic process	11 out of 380 genes, 2.9%	*C6_02790C_A RAD6 CAT8 C2_02300W_A STB5 SUC1 C3_02750W_A ZCF25 C1_08660C_A NBP35 SUA72*
7165	signal transduction	13 out of 380 genes, 3.4%	*HGT4 FAR1 STE18 STE2 LCB4 KIN3 ARF1 PPH3 YPT53 MEP2 C6_03320W_A AUT7 C1_02380C_A*
6412	translation	0 out of 380 genes, 0%	*none*
6810	transport	66 out of 380 genes, 17.4%	*NPR1 APS3 HGT4 FTH1 HXK1 ITR1 C3_03690W_A C6_03540W_A DUR3 YHB5 YHB1 C7_01510W_A C2_07580W_A MSO1 RER2 GNP3 GPT1 XUT1 ROA1 C1_00860W_A OPT4 UGA4 ARF1 AAP1 OPT8 C4_00680W_A SFC1 SSU1 MEP1 TPO4 GAP2 PEX5 C3_07430W_A GIT2 ARR3 C5_03080C_A PTR2 ANT1 C4_06910W_A C1_03330C_A PEX6 YPT53 CCC1 C4_04250W_A ATG9 FRP3 PXA1 C1_00830W_A CDR11 C6_01870C_A YHB4 C1_03870C_A CAN3 APG7 MEP2 FRP1 ATM1 FCY23 ATG1 C1_06980C_A C2_02230C_A PXA2 AUT7 FTR2 C1_02380C_A SSY1*
32196	transposition	0 out of 380 genes, 0%	*none*
16192	vesicle-mediated transport	5 out of 380 genes, 1.3%	*APS3 FTH1 MSO1 RER2 AUT7*
6766	vitamin metabolic process	4 out of 380 genes, 1.1%	*C4_02040W_A SNO1 ISA2 SNZ1*

Table S15. Assignment of the 615 significantly downregulated *C. albicans* genes to 40 GO Slim terms under the Biological Process category.

GO ID	GO term	Frequency	Gene list
42710	biofilm formation	26 out of 615 genes, 4.2%	*CZF1 CRZ2 C1_00160C_A C7_00490C_A CR_01410C_A HWP1 TEC1 AQY1 WH11 YWP1 MFA1 NRG1 PGA26 C2_07290W_A NDT80 PBR1 ALS2 ALS3 PMT2 RHR2 PMT1 C3_06700C_A PMT4 IFD6 ALS9 CSH1*
44419	biological process involved in interspecies interaction between organisms	54 out of 615 genes, 8.8%	*YCP4 TPI1 MET6 SSB1 TEF1 TCC1 RIM101 HWP1 TEC1 MTS1 TSA1 INT1 RFG1 ALS4 WH11 PES1 ZCF21 PGK1 NAG3 SOD1 YWP1 ERG24 NRG1 MIG2 WAL1 PGA26 SOD5 PST2 SFL2 FBA1 PHR2 TDH3 SSN6 NDT80 ALS2 RBE1 FET34 ALS3 GPM1 MSB1 ENO1 PST3 NCE102 ERG3 RHR2 PMT1 CDC19 ASC1 PMT4 LEU2 RBT1 ALS9 CSH1 SCH9*
8150	biological_process	106 out of 615 genes, 17.2%	*C3_00360W_A RPS25B C1_02730W_A CR_05210W_A PGA53 C3_00230C_A C1_12000C_A CR_05150W_A C5_01110W_A LDG3 C4_06700W_A C2_09910C_A C1_07790C_A C2_05300C_A CR_06500C_A C7_01940C_A C2_05960C_A C4_06320C_A C1_11720W_A CR_10200W_A C2_03880C_A C6_00680C_A AHP2 RPS4A MRV3 C7_02280W_A ECM331 C1_07990C_A ASR3 PGA58 C2_00130W_A MRV5 C7_02260W_A C1_10850W_A PGA12 C7_01950W_A OSM1 C1_09810W_A C1_13820C_A PGA34 C5_00510W_A CR_03000C_A C3_07900C_A C1_05520W_A RPL24A C1_10170W_A C3_05990C_A C1_04270C_A C7_01010W_A CR_09330C_A C1_11930W_A C3_01180C_A C5_01090C_A PGA54 CR_06570C_A C4_03300C_A C2_10130W_A CR_09460C_A C7_03270W_A C3_01540W_A ASR2 C6_02490C_A PRN4 C4_06750C_A PGA18 C5_01550C_A C2_01960C_A CR_09070C_A C5_03440W_A C3_07880C_A C1_01510W_A C1_09330W_A C1_03240W_A C1_03510C_A C1_12180C_A C4_06710W_A SLP2 C7_01380W_A RPL18 ASR1 PGA6 C3_06880W_A ROD1 C1_11050W_A USO6 XYL2 C2_03020C_A C3_05450C_A C1_11990W_A C5_03000C_A FRP5 C3_02790W_A C4_00730C_A C1_11200W_A C1_13460W_A PGA11 C2_10010C_A C2_00670C_A C7_02210W_A C1_07010W_A C2_08030W_A C3_02160C_A C6_01420C_A C1_13150W_A PGA38 C6_04140C_A*
5975	carbohydrate metabolic process	42 out of 615 genes, 6.8%	*GLK4 TPI1 GND1 CRH11 GLK1 PFK1 KRE5 GPD2 PGK1 GSL2 DAK2 EXG2 C4_02620C_A PGI1 CHT3 FBA1 PHR2 TDH3 GUT2 PFK2 SOU1 TAL1 KAR2 GPM1 GCY1 C3_01570W_A C4_01220C_A ENO1 HXK2 BMT4 PMI1 HAL21 CHT2 RHR2 GRE3 KRE1 CDC19 LEU2 C3_06860C_A C3_01820W_A SCH9 SCW11*
7155	cell adhesion	19 out of 615 genes, 3.1%	*C5_02110W_A HWP1 TEC1 INT1 ALS4 NRG1 SFL2 TDH3 PBR1 ALS2 AAH1 ALS3 MSB1 RHR2 PMT1 ASC1 ALS9 CSH1 C4_02260C_A*
7114	cell budding	4 out of 615 genes, 0.7%	*INT1 VRP1 CLN3 C4_07150W_A*

7049	cell cycle	45 out of 615 genes, 7.3%	*C6_02280W_A C7_03850W_A BFR1 CR_09140C_A RIM101 GLC7 ARC40 AQY1 MSC7 PFY1 INT1 CYP1 C1_10350C_A POL30 C1_11860W_A C4_02820W_A CR_02770C_A CCN1 C4_05230C_A VRP1 SAM2 YOX1 TUB1 CHT3 AMN1 HHF22 NDT80 ESC4 MIH1 SEC14 COF1 MSS4 CLN3 MCD1 ZPR1 C1_03790C_A GCN1 C1_06760C_A HHT2 MSH6 CDC5 EXO1 C4_07150W_A HTA3 C1_00090W_A*
48468	cell development	10 out of 615 genes, 1.6%	*RIM101 GLC7 AQY1 CYP1 NRG1 PGI1 SEC14 MSS4 C1_00090W_A SCH9*
71555	cell wall organization	22 out of 615 genes, 3.6%	*MSB2 CRH11 HWP1 ENG1 WSC2 KRE5 TSA1B TSA1 SOD1 SSR1 PGA26 PGA13 PHR2 PGA59 PMT2 PMI1 PGA31 PGA62 PMT1 PMT4 RBT1 C1_00090W_A*
19725	cellular homeostasis	16 out of 615 genes, 2.6%	*GLK4 RIM101 GLK1 GLC7 PFK1 C2_09590C_A TSA1B TSA1 SOD1 PFK2 FET34 PMA1 ALS3 HXK2 POR1 C4_07150W_A*
6464	cellular protein modification process	43 out of 615 genes, 7%	*PNG2 DPM2 C4_00940W_A C1_09040C_A RMS1 SMP3 C7_00490C_A BFR1 GLC7 VRG4 C1_07640C_A KRE5 C4_05250W_A CYP1 CWH8 MNN12 PTP1 ANB1 NOP1 CR_02770C_A UBI3 DPM1 HHF22 C2_07290W_A MIH1 PTP2 HAT1 PDI1 C5_02400W_A PMT2 SRB1 PMI1 STT3 NAT4 CDC5 PTP3 HMT1 PMT1 PMT4 GDA1 C1_14160W_A SCH9 OST1*
45333	cellular respiration	8 out of 615 genes, 1.3%	*LSC2 FUM11 IDH2 MRF1 IDH1 C3_06700C_A MRPS9 MAM33*
746	conjugation	5 out of 615 genes, 0.8%	*ENG1 PFY1 MFA1 KAR2 ASC1*
910	cytokinesis	8 out of 615 genes, 1.3%	*GLC7 ARC40 PFY1 INT1 VRP1 CHT3 COF1 C4_07150W_A*
7010	cytoskeleton organization	18 out of 615 genes, 2.9%	*TEF2 TEF1 CR_02690W_A GLC7 ARC40 PFY1 INT1 WAL1 VRP1 TUB1 CHC1 C2_07290W_A SEC14 COF1 MSS4 NCE102 CDC5 C2_06770W_A*
6259	DNA metabolic process	22 out of 615 genes, 3.6%	*C7_03850W_A HTA2 CR_09140C_A C6_03380W_A GLC7 ADAEC MSC7 TSA1 C3_04810C_A C7_02420C_A POL30 C4_02820W_A C4_03230C_A DDR48 ESC4 HAT1 HTB1 MCD1 HHT2 MSH6 CDC5 EXO1*
30447	filamentous growth	74 out of 615 genes, 12.0%	*CZF1 MSB2 RPL16A TPI1 SSB1 C2_05640W_A ERG5 C1_10880W_A TCC1 RIM101 GRF10 HGT12 ERG13 TEC1 VRG4 DRG1 ARC40 KRE5 MTS1 TSA1B TSA1 INT1 CSI2 RFG1 ALS4 PES1 GZF3 SOD1 CHO1 ERG24 NRG1 FCY2 PTP1 WAL1 DIP2 NOP5 PGA26 YTM1 PGA13 CCN1 RPL6 PGI1 VRP1 SFL2 PHR2 DDR48 RNR1 C2_07290W_A SSN6 NDT80 ESC4 ALS2 FET34 ALS3 PGA59 MSS4 CLN3 PMT2 FGR41 ENO1 PMI1 ERG3 CHT2 CDC5 PMT1 ZCF3 NOC2 CDC19 C3_06700C_A ASC1 PMT4 GDA1 C1_11120C_A SCH9*
6091	generation of precursor metabolites and energy	25 out of 615 genes, 4.1%	*TPI1 TKL1 GND1 LSC2 GLK1 PFK1 ATP2 PGK1 PDC11 PGI1 FBA1 TDH3 FUM11 PFK2 TAL1 GPM1 IDH2 ENO1 HXK2 MRF1 IDH1 CDC19 C3_06700C_A MRPS9 MAM33*
70783	growth of unicellular organism as a thread of attached cells	6 out of 615 genes, 1%	*TEC1 PTP1 SFL2 MSS4 ZCF3 ASC1*
30448	hyphal growth	10 out of 615 genes, 1.6%	*VRG4 ALS4 CCN1 PGI1 NDT80 ALS2 CLN3 PMT2 PMI1 PMT4*
6629	lipid metabolic process	33 out of 615 genes, 5.4%	*ERG28 DPM2 LIP3 FEN12 ERG6 SMP3 ERG5 ERG10 ERG13 MTS1 HMG1 CWH8 PLB4.5 ERG9 FAS1 URA7 LKH1 CHO1 ERG24 MVD ERG4 DPM1 C1_02240W_A SEC14 C1_01050C_A MSS4 LIP6 HAL21 ERG3 SAH1 ERG251 ERG2 MCR1*
6997	nucleus organization	5 out of 615 genes, 0.8%	*C4_04800W_A PGA63 C1_02240W_A KAR2 GSP1*
6996	organelle organization	112 out of 615 genes, 18.2%	*C5_01540W_A C4_05330C_A RPF2 C1_09040C_A RPL25 RPP0 C1_09060C_A TEF2 CIC1 HTA2 BFR1 LTV1 C4_04800W_A TEF1 CR_09140C_A CR_01410C_A JIP5 PGA63 GRF10 CR_02690W_A UTP18 C6_02380W_A C6_03380W_A GLC7 NOP4 ARC40 RPS27 MSC7 C7_01360C_A PFY1 INT1 CSI2 CYP1 PWP2 C1_04180W_A C3_04810C_A C2_02540W_A RPS17B YST1 C3_01560W_A UTP22 POL30 RRS1 GLE2 RPL3 C1_11860W_A WAL1 C4_02820W_A IST2 YTM1 NOP1 CR_02770C_A UBI3 RPL6 C4_05230C_A VRP1 C1_02240W_A RPS26A TUB1 CHC1 PHR2 HHF22 C2_04570W_A C2_07290W_A SSN6 TSR1 SEC14 HAT1 HTB1 RPL12 PMA1 COF1 MSS4 CLN3 MCD1 KAR2 C1_03790C_A NHP6A C5_03550W_A C1_06760C_A C3_02040C_A HHT2 GSP1 RPA190 FLU1 DHH1 EMP24 RPL5 C5_02780W_A SAM50 NCE102 NAT4 C6_02690C_A C2_05160C_A MSH6 DRS1 CDC5 EXO1 C4_05010W_A SEC24 NOC2 RPS28B POR1 C7_01600W_A ERB1 HTA3 HHT21 C2_06770W_A NIP7 RPS14B ILV5 SSF1*

other	other	28 out of 615 genes, 4.6%	*C7_04210C_A C6_02480W_A C2_07420W_A LSC1 C5_04300C_A GLO1 HEM13 MET15 C1_13790C_A ARO4 MAE1 LAT1 RNR21 DUT1 GUA1 AAT22 IPP1 MET3 C1_11790W_A PSA2 C4_01830C_A C7_02100W_A URA1 GUK1 DCG1 APT1 MET14 C6_03880W_A*
9405	pathogenesis	0 out of 615 genes, 0%	*none*
30163	protein catabolic process	8 out of 615 genes, 1.3%	*CIC1 LKH1 AMN1 PDI1 PMT2 KAR2 PMT1 SEC61*
6457	protein folding	13 out of 615 genes, 2.1%	*SSB1 SSZ1 CR_02690W_A C7_01360C_A TSA1 CYP1 HGH1 GLX3 PDI1 KAR2 C1_03790C_A ZUO1 C1_10820C_A*
7124	pseudohyphal growth	3 out of 615 genes, 0.5%	*TEC1 PTP1 SFL2*
50789	regulation of biological process	153 out of 615 genes, 24.9%	*CZF1 C6_02280W_A UTP5 YCP4 MSB2 C4_05330C_A TPI1 C4_00940W_A MET6 CRZ2 SSB1 C5_02110W_A C1_12570C_A C1_09040C_A RMS1 HSP12 EFT2 TIF HTA2 BFR1 TMA19 TCC1 RIM101 GRF10 PIL1 C6_03380W_A GLC7 RPL30 ADAEC TEC1 C2_02530W_A WSC2 DRG1 ARC40 NRM1 TSA1B PFY1 TSA1 CAM1 RFG1 CYP1 PES1 ZCF21 GZF3 PGK1 C3_04810C_A SEC12 CAR1 C1_10350C_A RGS2 SOD1 POL30 CYS4 KTI12 EFB1 GLE2 CHO1 MFA1 NRG1 PDC11 PTP1 MIG2 CYS3 ANB1 C1_11860W_A WAL1 C2_07620W_A PGA26 IST2 CR_02770C_A PGA13 CCN1 RPS9B RHA1 PST2 C4_05230C_A VRP1 SFL2 C1_02240W_A OFI1 YOX1 TUB1 AMN1 FBA1 PHR2 HHF22 TDH3 GCD6 SSN6 NDT80 ESC4 MIH1 SEC14 PTP2 HAT1 HTB1 MRT4 AAH1 PMA1 COF1 MSS4 CLN3 PMT2 RPP1 ZPR1 KAR2 C1_03790C_A GCN1 C5_03550W_A MSB1 C1_06760C_A C3_02040C_A HHT2 GSP1 ENO1 DHH1 HXK2 C1_05630C_A PST3 C5_02780W_A NCE102 C3_05320W_A NAT4 C6_02690C_A C2_05160C_A MSH6 NAN1 CDC5 EXO1 C7_00830C_A PTP3 HMT1 DBP2 PMT1 ZCF3 RPS28B CDC19 TFS1 RPS21 ASC1 POR1 PMT4 UTP4 C4_07150W_A GDA1 HTA3 HHT21 C2_06770W_A C3_00730W_A MAM33 URA2 SCH9 TOS4*
42221	response to chemical	103 out of 615 genes, 16.7%	*UTP5 GAR1 YCP4 MSB2 SOD2 RPL17B RPF2 CRZ2 OPT1 C5_02110W_A ERG6 CAR2 C7_03850W_A EFT2 GND1 PGA23 HGT7 LTV1 TMA19 RIM101 HGT12 GLC7 ERG13 NOP4 TEC1 KRE5 NRM1 AQY1 TSA1B HMG1 C7_01360C_A TSA1 RLP24 RFG1 PES1 GZF3 FAS1 GAD1 NAG3 NOP14 UTP22 SOD1 DAK2 RRS1 CHO1 ERG24 MFA1 NRG1 FCY2 MIG2 C1_11860W_A SSR1 DIP2 PGA26 SOD5 RPO26 CCN1 PST2 C4_05230C_A TUB1 GLX3 C7_01430C_A DDR48 SSN6 NDT80 SEN2 HAT1 MRT4 CNT PRT1 PDI1 FET34 CR_01220W_A CLN3 RRP9 PMT2 KAR2 GCY1 C1_06760C_A FLU1 PST3 C3_05320W_A ERG3 PGA31 PGA62 DRS1 CDC5 C1_10820C_A C4_05010W_A RHR2 GRE3 PMT1 ZCF3 NOC2 ERG2 PMT4 ERB1 C3_06860C_A ALS9 KRE30 MCR1 SCH9 SEC61*
42493	response to drug	59 out of 615 genes, 9.6%	*UTP5 GAR1 RPL17B RPF2 OPT1 ERG6 CAR2 C7_03850W_A EFT2 PGA23 HGT7 RIM101 ERG13 NOP4 KRE5 HMG1 RLP24 PES1 GZF3 FAS1 NAG3 NOP14 UTP22 RRS1 ERG24 NRG1 MIG2 SSR1 DIP2 RPO26 CCN1 C4_05230C_A TUB1 C7_01430C_A SSN6 NDT80 SEN2 MRT4 CNT PRT1 CR_01220W_A CLN3 RRP9 PMT2 GCY1 C1_06760C_A ERG3 PGA31 PGA62 DRS1 C1_10820C_A C4_05010W_A PMT1 ZCF3 NOC2 ERG2 PMT4 ERB1 KRE30*
6950	response to stress	93 out of 615 genes, 15.1%	*CZF1 YCP4 MSB2 RPL16A TPI1 MET6 CRZ2 SSB1 C5_02110W_A RMS1 HSP12 ERG5 C1_10880W_A GND1 HTA2 LTV1 C4_04800W_A TMA19 RIM101 PIL1 HGT12 GLC7 ERG13 ADAEC TEC1 WSC2 ARC40 KRE5 YNK1 AQY1 TSA1B C7_01360C_A TSA1 CSI2 RFG1 WH11 PES1 GZF3 C3_04810C_A GAD1 SOD1 POL30 CHO1 NRG1 FCY2 WAL1 DIP2 PGA26 SOD5 YTM1 RPL6 PST2 VRP1 GLX3 DDR48 RNR1 NDT80 ESC4 HAT1 HTB1 PDI1 FET34 PMT2 MCD1 ZPR1 KAR2 GCY1 GCN1 C5_03550W_A HHT2 FGR41 PST3 HAL21 C3_05320W_A CHT2 MSH6 CDC5 EXO1 RHR2 GRE3 PMT1 NOC2 CDC19 ASC1 HHT21 C3_06860C_A ALS9 C1_11120C_A WSC4 MCR1 SCH9 SEC61 TOS4*
42254	ribosome biogenesis	109 out of 615 genes, 17.7%	*UTP5 GAR1 C5_01540W_A C1_07660W_A C4_05330C_A RPL17B RPF2 CR_10410C_A SSB1 C1_09040C_A RPS15 RPL25 RPP0 SSZ1 C7_03850W_A CIC1 C1_10880W_A LTV1 C7_01030C_A RPL37B CR_01410C_A JIP5 RPL10A NSA1 UTP18 C6_02380W_A RPS18 RPL30 RPS10 NOP4 PUS7 RPS27 CR_09740W_A RLP24 RPS6A CSI2 PES1 PWP2 C2_02540W_A RPS17B YST1 C3_01560W_A RPS19A UTP21 NOP14 RPS8A UTP22 RRS1 RPL3 NUP159 WAL1 DIP2 NOP5 YTM1 NOP1 UBI3 C3_06760W_A RPS9B RPL6 C4_05230C_A RPS26A RPL8B C2_04570W_A CR_08500W_A RPS21B TSR1 TSR2 MRT4 NMD3 RPL12 CR_04110W_A SIK1 RRP9 ARX1 RPP1 RPS1 DIM1 C1_06760C_A C3_02040C_A RPS24 GSP1 RPA190 FLU1 RPL5 ZUO1 RPS13 C2_05160C_A DRS1 NAN1 RPS7A C4_05010W_A RPS5 DBP2 NOC2*

			RPS28B PWP1 RPS21 RPS20 RPS16A UTP4 ERB1 C1_05720W_A KRE30 RPL35 CR_04240C_A NIP7 DBP3 RPS14B SSF1
16070	RNA metabolic process	109 out of 615 genes, 17.7%	*UTP5 GAR1 C5_01540W_A RRN3 C1_07660W_A C4_05330C_A C4_00940W_A THS1 RPL17B RPF2 CR_10410C_A SSB1 C1_12570C_A RPC19 GUS1 SSZ1 C7_03850W_A CIC1 C1_10880W_A C7_01030C_A RPL37B UTP18 C6_02380W_A RPS18 RPL30 NOP4 C1_01150C_A PUS7 RPS27 CR_09740W_A LHP1 RPS6A CSI2 PES1 PWP2 C2_07630C_A C2_02540W_A C1_01530C_A YST1 ARC1 C3_01560W_A UTP21 NOP14 RPS8A UTP22 KTI12 RRS1 TRM1 RPL3 C6_02350C_A KRS1 DIP2 NOP5 NOP1 RPO26 UBI3 C3_06760W_A RPS9B C4_05230C_A RPL8B HHF22 C2_04570W_A GCD6 RPS21B C2_09500W_A TSR1 TSR2 SEN2 MRT4 CR_04110W_A SIK1 RRP9 RPP1 C7_02660C_A RPS1 NHP6A DIM1 C1_06760C_A C3_02040C_A RPS24 HHT2 GSP1 RPA190 DHH1 ZUO1 RPS13 DPS1-1 C6_02690C_A DRS1 NAN1 C7_00830C_A DBP2 RPS28B C3_00100W_A PWP1 RPS20 RPS16A UTP4 ERB1 HTA3 C7_02340C_A C1_05720W_A RPL35 CR_04240C_A C3_00730W_A NIP7 DBP3 RPS14B SSF1*
7165	signal transduction	14 out of 615 genes, 2.3%	*MSB2 RIM101 WSC2 C3_04810C_A RGS2 C1_11860W_A MSS4 KAR2 GCN1 GSP1 C3_05320W_A CDC5 ASC1 SCH9*
6412	translation	90 out of 615 genes, 14.6%	*C2_02930C_A C5_01540W_A CAM1-1 RPL16A THS1 RPL17B SSB1 GUS1 RPS15 RPL19A RPL25 C7_00490C_A RPP0 SSZ1 RPL20B TEF2 CIC1 EFT2 RPL29 RPL23A TIF RPL37B TEF1 TMA19 RPL10A C5_00030W_A RPL14 RPS18 RPL30 RPP2A DRG1 RPL2 RPS27 C2_07190C_A C5_02660C_A CAM1 RPS6A RPL32 RPP1B C3_04810C_A RPS12 RPS17B C1_01530C_A YST1 ARC1 RPS19A RPS8A EFB1 RPS22A RPL3 ANB1 KRS1 UBI3 RPS9B C2_05410W_A RPL6 RPL42 RPL38 RPS26A GCD6 RPS21B RPL15A RPL4B C1_06890C_A RPL13 PRT1 RPL12 RPL43A C6_01980C_A RPL40B RPS1 RPL27A RPS24 RPL5 ZUO1 CEF3 RPS13 DPS1-1 RPS7A RPS5 RPL28 RPL21A RPS28B RPS21 RPS20 MRPS9 RPS16A C1_05720W_A RPL35 RPS14B*
6810	transport	106 out of 615 genes, 17.2%	*FRE10 ATP19 FEN12 OPT1 CR_01630C_A SSB1 APE2 RPS15 TEF2 HGT7 LTV1 NUP TEF1 CR_04610C_A RPL10A PGA63 PIL1 HGT10 BUD7 HGT6 HGT12 GLK1 RPS18 ATP1 RPS10 VRG4 ATP2 AQY1 C2_09590C_A C7_01360C_A PFY1 C2_05290C_A PTR22 YST1 RPS19A NAG3 HXT5 UTP22 RRS1 CR_07220C_A C4_06680C_A LKH1 GLE2 NUP159 FCY2 WAL1 HGT19 ERP5 C7_02000C_A EGD1 VRP1 C1_02240W_A RPS26A TUB1 CHC1 FBA1 TDH3 HSP31 HSP30 CR_08500W_A HGT13 SEC14 MRT4 C3_01680C_A ATP5 CNT NMD3 RBE1 FET34 PMA1 ALS3 COF1 CR_01220W_A PMT2 ARX1 KAR2 EGD2 C5_03550W_A C3_02040C_A GSP1 FLU1 EMP24 HXK2 GAP4 ZUO1 C1_05630C_A SAM50 NCE102 CR_03580C_A ALP1 RPS5 HMT1 SEC24 PMT1 RPS28B RPS21 C7_00630C_A POR1 C7_01600W_A KRE30 C2_02410W_A WSC4 HGT8 YMC1 SEC61 C1_11920W_A*
32196	transposition	0 out of 615 genes, 0%	*none*
16192	vesicle-mediated transport	14 out of 615 genes, 2.3%	*FEN12 PGA63 PIL1 BUD7 C4_06680C_A WAL1 VRP1 CHC1 SEC14 ALS3 COF1 EMP24 SEC24 C1_11920W_A*
6766	vitamin metabolic process	4 out of 615 genes, 0.7%	*SPE3 RIB4 HMT1 SPE2*

Molecular Function

Table S16. Assignment of the 380 significantly upregulated *C. albicans* genes to 25 GO Slim terms under the Molecular Function category.

GO ID	GO term	Frequency	Gene list
3677	DNA binding	20 out of 380 genes, 5.3%	*C2_05060C_A C4_04620C_A C1_03270W_A C4_00030C_A RAD6 CM_00250W CAT8 HAP2 GCN4 RAD16 STB5 GAT1 CIRT4B SUC1 CAP1 MET28 ZCF25 ZCF20 PYC2 C2_08420W_A*
30234	enzyme regulator activity	5 out of 380 genes, 1.3%	*C1_01840C_A FAR1 C1_14190C_A MNN41 C1_14020W_A*
4386	helicase activity	2 out of 380 genes, 0.5%	*RAD6 RAD16*
16787	hydrolase activity	44 out of 380 genes, 11.6%	*DUR1,2 EHD3 C2_01920C_A GBU1 RBR2 C5_00750C_A RAD6 CM_00250W HIS7 CR_03690W_A C3_05360C_A C7_02920W_A PRB1 C3_00400C_A RAD16 C1_05160C_A ROA1 SCW4 ARF1 C3_02750W_A C4_02170C_A PPH3 C3_07430W_A SNO1*

			C1_09440W_A CR_02570C_A C4_06910W_A C7_03860W_A PEX6 PSO2 HSP78 YPT53 C5_00230C_A PXA1 CDR11 FAA21 NBP35 C2_08420W_A SAP6 ATM1 PXA2 CCE1 SNZ1 SAP4
16853	isomerase activity	2 out of 380 genes, 0.5%	*ECI1 INO1*
16874	ligase activity	10 out of 380 genes, 2.6%	*DUR1,2 RAD6 C7_02920W_A CPA1 UBC8 CPA2 PYC2 FAA21 APG7 ARG1*
8289	lipid binding	4 out of 380 genes, 1.1%	*POX18 C3_01420C_A C1_03330C_A AUT7*
16829	lyase activity	9 out of 380 genes, 2.4%	*C2_00390C_A ARG4 LYS4 HIS3 C1_02970W_A CHA1 FOX2 SNZ1 ICL1*
3674	molecular_function	149 out of 380 genes, 39.2%	*C1_00010W_A APS3 C1_01220C_A C1_11320C_A C2_08440W_A C6_02450W_A C4_03950C_A C3_02900W_A C6_02620C_A C6_00730W_A C3_00050C_A C4_01970W_A C1_12900W_A C7_03470W_A C1_00020C_A C1_06860W_A ATO5 C5_03970W_A MOH1 C4_02930W_A C5_03870C_A C3_05750C_A C3_03700C_A C6_02790C_A C1_02270C_A OP4 C1_11570W_A C7_03280C_A CR_02480W_A C1_09310C_A C2_08510W_A C3_04720C_A PEX22 C4_00080C_A CR_03260W_A CR_04220C_A C4_06670W_A C7_00260C_A CSO99 C2_08330W_A C3_04650W_A CIP1 C6_03150C_A BLP1 C1_01140C_A MSO1 C1_00580W_A BUL1 CR_07740W_A CR_08830W_A CR_09610C_A C1_13430C_A C1_01630W_A PGA17 C3_04630W_A GNP3 C1_14180W_A C1_12870C_A CR_10310W_A C4_04380C_A C2_08260W_A C2_02300W_A C3_02990C_A AAP1 C7_00770W_A C1_00030C_A C7_02140W_A C1_09700W_A C1_05440C_A C1_00050C_A CR_05040W_A PEX17 BUD20 ATO9 GST1 C3_04450C_A C1_05690C_A C3_02090C_A C3_03370C_A GTT1 C3_07720C_A CR_04860C_A C1_13090W_A C2_10870W_A C4_04180C_A C4_01350W_A C2_04400W_A C3_05060W_A C3_02660W_A TES1 C5_04980W_A C1_13100W_A CR_06020W_A CR_04990C_A HSP21 C2_08690C_A C6_03280W_A C4_03960W_A C1_09770W_A C7_03820C_A C1_13180W_A HRQ2 IFK2 C2_02390W_A SMI1B C2_09800C_A C3_01060W_A C1_12150C_A C1_09340C_A CR_04850C_A CR_02060W_A C3_04840C_A C4_07020C_A C4_00640W_A C1_06870C_A ATG9 C4_06940C_A C2_06630C_A C1_11260C_A C4_05800C_A C6_03530C_A CR_05750W_A CR_04820W_A C7_03740C_A CAN3 C1_00190C_A C6_03670C_A C2_09870W_A AGA1 PSF1 C5_05510C_A C1_03970W_A C6_01940W_A CR_07700W_A C4_03710C_A CR_06270W_A C1_01610C_A CR_08850W_A PGA46 C3_01270W_A C1_10060C_A C2_04830W_A TES15 ASG7 C3_04330C_A C3_02630C_A PGA25 MRV2 C3_04190W_A*
3774	motor activity	0 out of 380 genes, 0%	*none*
16779	nucleotidyltransferase activity	0 out of 380 genes, 0%	*none*
other	other	26 out of 380 genes, 6.8%	*C4_02770C_A WOR2 C1_03990W_A STE2 FAA2-3 CRD2 C6_01620W_A C2_00600C_A UGA33 C2_10150W_A C2_00640W_A FGR15 PEX5 ZCF32 C1_09300C_A C3_06040W_A SEF2 ZFU2 PGA7 C1_03870C_A ZCF4 C2_02230C_A C6_03320W_A CR_06980W_A C1_02380C_A SSY1*
16491	oxidoreductase activity	45 out of 380 genes, 11.8%	*GTT13 C6_03240W_A C2_05060C_A C6_03600C_A DRE2 PXP2 AOX2 YHB5 C1_04460C_A CM_00250W YHB1 GPX2 POX1-3 SOD6 C7_02010C_A FRP2 POX1 C1_01620C_A C2_07070W_A MDH1-3 GCV1 GLT1 C4_02230C_A C4_02040W_A C3_04350C_A AMO1 FOX2 CYB2 HPD1 GDH3 ALD6 AMO2 MET13 CR_04870C_A IFR1 ARG5,6 GOR1 YHB4 C4_00290C_A OSM2 FRP1 DLD2 HMX1 IFG3 ARA1*
8233	peptidase activity	5 out of 380 genes, 1.3%	*C3_05360C_A PRB1 C7_03860W_A SAP6 SAP4*
16791	phosphatase activity	3 out of 380 genes, 0.8%	*C5_00750C_A PPH3 C3_07430W_A*
5515	protein binding	9 out of 380 genes, 2.4%	*STE18 C6_03290W_A PRB1 GCN4 MET28 C7_03860W_A PEX6 HSP78 SUA72*
4672	protein kinase activity	7 out of 380 genes, 1.8%	*NPR1 PDK2 KIN3 C6_02160W_A ATG1 CEK2 PRR2*
3723	RNA binding	7 out of 380 genes, 1.8%	*C3_05290C_A POT1 C2_07070W_A MDH1-3 C3_02750W_A SET1 C1_08660C_A*
4871	signal transducer activity	0 out of 380 genes, 0%	*none*

5198	structural molecule activity	3 out of 380 genes, 0.8%	*EHD3 RBR2 ISA2*
988	transcription factor activity, protein binding	0 out of 380 genes, 0%	*none*
16740	transferase activity	50 out of 380 genes, 13.2%	*NPR1 GTT13 HXK1 ARG3 BAT21 ARO3 RAD6 C3_03760W_A HIS7 ATF1 POT1 PDK2 UGA1 HOM3 LCB4 C3_00400C_A UBC8 RAD16 RER2 C2_07070W_A GCV1 BIO32 ALT1 C1_00860W_A KIN3 CTN1 FOX3 CR_06310W_A HIS5 UGA11 BMT9 C2_09070C_A CR_04230W_A SET1 LYS22 C6_02160W_A IFR1 MLS1 ARO8 ARG5,6 LEU42 C2_06780C_A ATG1 CEK2 ECM42 CTN3 PRR2 ARG8 CR_06770C_A C3_02850C_A*
45182	translation regulator activity	0 out of 380 genes, 0%	*none*
5215	transporter activity	40 out of 380 genes, 10.5%	*HGT4 FTH1 ITR1 C3_03690W_A C6_03540W_A DUR3 CM_00250W C7_01510W_A C2_07580W_A GPT1 XUT1 ROA1 OPT4 UGA4 OPT8 C4_00680W_A SFC1 SSU1 MEP1 TPO4 GAP2 GIT2 ARR3 C5_03080C_A PTR2 ANT1 C4_06910W_A CCC1 C4_04250W_A FRP3 PXA1 C1_00830W_A CDR11 C6_01870C_A MEP2 ATM1 FCY23 C1_06980C_A PXA2 FTR2*
30533	triplet codon-amino acid adaptor activity	0 out of 380 genes, 0%	*none*

Table S17. Assignment of the 615 significantly downregulated *C. albicans* genes to 25 GO Slim terms under the Molecular Function category.

GO ID	GO term	Frequency	Gene list
3677	DNA binding	36 out of 615 genes, 5.9%	*CZF1 RRN3 C1_00160C_A C2_05640W_A HTA2 RIM101 GRF10 ADAEC TEC1 C2_02530W_A RFG1 ZCF21 C1_13820C_A GZF3 C1_04180W_A C3_04810C_A POL30 NRG1 C4_02820W_A RPO26 SFL2 YOX1 HHF22 NDT80 HTB1 C7_02100W_A NHP6A HHT2 RPA190 C5_02780W_A MSH6 CDC5 EXO1 HTA3 HHT21 ILV5*
30234	enzyme regulator activity	21 out of 615 genes, 3.4%	*DPM2 C4_05330C_A PFY1 TSA1 CAM1 RLP24 SEC12 CAR1 ARC1 RGS2 POL30 EFB1 NUP159 C2_07620W_A CCN1 GCD6 CLN3 GCN1 TFS1 ASC1 C1_11920W_A*
4386	helicase activity	8 out of 615 genes, 1.3%	*TIF C6_02380W_A CR_09740W_A C3_01560W_A DHH1 DRS1 DBP2 DBP3*
16787	hydrolase activity	63 out of 615 genes, 10.2%	*PNG2 LIP3 C4_00940W_A C2_07420W_A SSB1 APE2 C1_12570C_A C5_04300C_A SSZ1 TEF2 EFT2 TIF TEF1 CRH11 ENG1 C6_02380W_A GLC7 ATP1 ATP2 CR_09740W_A C5_02660C_A CWH8 C7_01950W_A DUT1 PLB4.5 CAR1 C3_01560W_A IPP1 EXG2 LKH1 PTP1 TUB1 C4_01830C_A CHT3 PHR2 DDR48 MIH1 SEN2 PTP2 AAH1 PMA1 C5_02400W_A RPP1 KAR2 C4_01220C_A GSP1 LIP6 DHH1 CEF3 HAL21 CHT2 SAH1 MSH6 DRS1 C1_10820C_A EXO1 RHR2 PTP3 DBP2 GDA1 KRE30 C3_01820W_A DBP3*
16853	isomerase activity	12 out of 615 genes, 2%	*GAR1 TPI1 PUS7 CYP1 C6_02350C_A PGI1 PDI1 GPM1 C1_03790C_A PMI1 DCG1 ERG2*
16874	ligase activity	14 out of 615 genes, 2.3%	*THS1 LSC1 GUS1 LSC2 ATP1 ATP2 GUA1 C1_01530C_A URA7 KRS1 CR_02770C_A ATP5 DPS1-1 URA2*
8289	lipid binding	10 out of 615 genes, 1.6%	*C5_02110W_A PIL1 PFY1 CAM1 ARC1 IST2 RBE1 MSS4 EGD2 TFS1*
16829	lyase activity	12 out of 615 genes, 2%	*GLO1 FAS1 GAD1 CYS4 PDC11 MVD CYS3 GLX3 FBA1 FUM11 ENO1 SPE2*
3674	molecular_function	160 out of 615 genes, 26.0%	*C3_00360W_A UTP5 C2_02930C_A C1_02730W_A C1_07660W_A CAM1-1 ATP19 CR_05210W_A PGA53 C3_00230C_A C1_12000C_A C5_01110W_A LDG3 HSP12 C4_06700W_A C2_09910C_A C1_07790C_A C1_09060C_A PGA23 CR_06500C_A LTV1 C4_04800W_A C7_01030C_A C7_01940C_A CR_04610C_A C2_05960C_A C4_06320C_A C1_11720W_A TMA19 CR_09140C_A TCC1 CR_01410C_A JIP5 NSA1 C1_13790C_A CR_10200W_A UTP18 C2_03880C_A C6_00680C_A RPS10 MRV3 C7_02280W_A ECM331 C1_07990C_A ASR3 NRM1 PGA58 C2_00130W_A MRV5 C7_02260W_A C1_10850W_A ALS4 WH11 C2_05290C_A PGA12 PWP2 C2_07630C_A PGA34 C5_00510W_A CR_03000C_A C3_07900C_A C1_10350C_A C1_05520W_A UTP21 C1_10170W_A UTP22 YWP1 C4_06680C_A C1_04270C_A GLE2 C7_01010W_A C1_11930W_A C3_01180C_A C5_01090C_A PGA54 CR_06570C_A C4_03230C_A NOP5 C4_03300C_A ERP5*

			PGA26 C2_10130W_A YTM1 PGA13 C3_06760W_A CR_09460C_A C7_03270W_A C3_01540W_A ASR2 RPL8B C7_01430C_A C2_04570W_A ESC4 C6_02490C_A PBR1 TSR2 ALS2 PRN4 C4_06750C_A PGA18 C5_01550C_A C2_01960C_A MRT4 C3_01680C_A CR_09070C_A C5_03440W_A C3_07880C_A C1_01510W_A C1_09330W_A C1_03240W_A C1_03510C_A C1_12180C_A PGA59 SLP2 SIK1 C7_01380W_A RPL18 ARX1 ASR1 PGA6 C7_02660C_A C3_06880W_A MSB1 ROD1 FGR41 EMP24 USO6 C2_03020C_A C3_05450C_A NCE102 PGA31 PGA62 C1_11990W_A C4_05010W_A C5_03000C_A FRP5 C3_02790W_A C4_00730C_A KRE1 NOC2 C1_11200W_A C1_13460W_A PWP1 PGA11 C3_06700C_A C2_10010C_A C2_00670C_A C7_00630C_A C7_02210W_A UTP4 C1_07010W_A RBT1 C2_08030W_A C1_11120C_A C2_02410W_A C4_02260C_A C1_00090W_A C1_13150W_A PGA38 C6_04140C_A
3774	motor activity	0 out of 615 genes, 0%	*none*
16779	nucleotidyltransferase activity	8 out of 615 genes, 1.3%	*RPC19 C7_02420C_A MET3 RPO26 PSA2 GCD6 SRB1 RPA190*
other	other	29 out of 615 genes, 4.7%	*ERG28 MSB2 CRZ2 C7_03850W_A WSC2 DRG1 C1_09810W_A KTI12 C3_05990C_A CR_09330C_A MIG2 RHA1 C4_05230C_A OFI1 TSR1 C1_06760C_A C1_11050W_A ZUO1 C1_05630C_A C3_05320W_A SEC24 ZCF3 C3_00100W_A C7_01600W_A C4_07150W_A ALS9 C3_02160C_A TOS4 SCW11*
16491	oxidoreductase activity	51 out of 615 genes, 8.3%	*FRE10 YCP4 C6_02480W_A SOD2 HEM13 ERG5 GND1 AHP2 MAE1 LAT1 MSC7 TSA1B HMG1 TSA1 GPD2 RNR21 OSM1 FAS1 SOD1 ERG24 SOD5 ERG4 PST2 RNR1 TDH3 C2_07290W_A C2_09500W_A GUT2 SOU1 PDI1 FET34 C1_01050C_A C4_06710W_A URA1 GCY1 IDH2 XYL2 MRF1 PST3 IDH1 ERG3 ERG251 GRE3 LEU2 IFD6 C3_06860C_A CSH1 C6_01420C_A MCR1 ILV5 C6_03880W_A*
8233	peptidase activity	6 out of 615 genes, 1%	*APE2 C5_04300C_A C5_02660C_A C7_01950W_A LKH1 C1_10820C_A*
16791	phosphatase activity	8 out of 615 genes, 1.3%	*C2_07420W_A GLC7 PTP1 MIH1 PTP2 HAL21 RHR2 PTP3*
5515	protein binding	53 out of 615 genes, 8.6%	*C6_02280W_A RRN3 CR_10410C_A SSB1 SSZ1 TEF2 EFT2 HTA2 TEF1 HWP1 CR_02690W_A BUD7 ARC40 TSA1B C7_01360C_A PFY1 TSA1 INT1 GPD2 PGK1 C1_04180W_A HGH1 CR_07220C_A MFA1 C1_11860W_A WAL1 EGD1 VRP1 C1_02240W_A AMN1 FBA1 HHF22 TDH3 CR_08500W_A SSN6 HAT1 HTB1 PDI1 ALS3 COF1 MCD1 ZPR1 KAR2 GPM1 EGD2 HHT2 ENO1 CDC5 C7_00830C_A ASC1 HTA3 HHT21 C2_06770W_A*
4672	protein kinase activity	3 out of 615 genes, 0.5%	*C1_07640C_A CDC5 SCH9*
3723	RNA binding	73 out of 615 genes, 11.9%	*GAR1 RPL16A C4_00940W_A RPF2 CR_10410C_A C1_00160C_A C1_12570C_A RPL25 RPP0 TEF2 CIC1 EFT2 C1_10880W_A TIF BFR1 TEF1 RPL10A C5_00030W_A C6_02380W_A C6_03380W_A RPL14 RPS18 RPL30 RPS4A NOP4 LHP1 CAM1 CSI2 PES1 C2_02540W_A C7_02420C_A ARC1 NOP14 RPL24A RRS1 TRM1 EFB1 ANB1 C1_11860W_A C6_02350C_A DIP2 NOP1 RPS9B RPL6 TDH3 GCD6 RPL15A PFK2 PRT1 NMD3 CR_04110W_A RRP9 RPP1 GCY1 C3_02040C_A DHH1 RPL5 CEF3 RPS13 DPS1-1 C6_02690C_A C2_05160C_A NAN1 GRE3 RPL28 DBP2 RPS21 ERB1 CR_04240C_A C3_00730W_A NIP7 RPS14B SSF1*
4871	signal transducer activity	0 out of 615 genes, 0%	*none*
5198	structural molecule activity	73 out of 615 genes, 11.9%	*RPS25B C5_01540W_A RPL16A RPL17B RPS15 CR_05150W_A RPL19A RPL25 RPP0 RPL20B CIC1 RPL29 RPL23A C2_05300C_A RPL37B RPL10A PGA63 C5_00030W_A RPL14 RPS18 RPL30 RPP2A RPL2 RPS27 C2_07190C_A RPS6A RPL32 RPP1B RPS12 RPS17B YST1 RPS19A RPS8A RPS22A RPL3 NUP159 SSR1 UBI3 RPS9B C2_05410W_A RPL6 RPL42 RPL38 RPS26A TUB1 CHC1 RPS21B RPL15A RPL4B C1_06890C_A RPL13 RPL12 RPL43A C6_01980C_A RPL40B RPS1 C5_03550W_A RPL27A RPS24 RPL5 RPS13 RPS7A RPS5 RPL28 RPL21A RPS28B RPS21 RPS20 MRPS9 RPS16A C1_05720W_A RPL35 RPS14B*
988	transcription factor activity, protein binding	0 out of 615 genes, 0%	*none*
16740	transferase activity	83 out of 615 genes, 13.5%	*GLK4 C7_04210C_A DPM2 C6_02480W_A FEN12 MET6 ERG6 RPC19 C1_09040C_A RMS1 SMP3 C7_00490C_A TKL1 CAR2 CRH11 MET15 ERG10 GLK1 ARO4 PFK1 ERG13 ADAEC*

			C1_01150C_A C1_07640C_A KRE5 LAT1 YNK1 MTS1 C4_05250W_A SPE3 PGK1 ERG9 FAS1 MNN12 C7_02420C_A AAT22 RIB4 GSL2 DAK2 MET3 TRM1 CHO1 C1_11790W_A NOP1 RPO26 C4_02620C_A DPM1 SAM2 PSA2 PHR2 RNR1 GCD6 HAT1 PFK2 TAL1 C4_06710W_A MSS4 PMT2 DIM1 C3_01570W_A SRB1 ENO1 RPA190 HXK2 BMT4 XYL2 MRF1 GUK1 STT3 NAT4 CDC5 HMT1 PMT1 CDC19 APT1 MET14 PMT4 C1_14160W_A C7_02340C_A CR_04240C_A URA2 SCH9 OST1
45182	translation regulator activity	12 out of 615 genes, 2%	*TEF2 EFT2 TIF TEF1 CAM1 EFB1 ANB1 GCD6 PRT1 CEF3 C2_05160C_A MAM33*
5215	transporter activity	37 out of 615 genes, 6.0%	*OPT1 CR_01630C_A HGT7 NUP HGT10 HGT6 HGT12 ATP1 VRG4 ATP2 AQY1 C2_09590C_A PTR22 NAG3 HXT5 FCY2 HGT19 C7_02000C_A HSP31 HSP30 HGT13 SEC14 ATP5 CNT FET34 PMA1 CR_01220W_A FLU1 GAP4 SAM50 CR_03580C_A ALP1 POR1 WSC4 HGT8 YMC1 SEC61*
30533	triplet codon-amino acid adaptor activity	0 out of 615 genes, 0%	*none*

Cellular Component

Table S18. Assignment of the 380 significantly upregulated *C. albicans* genes to 27 GO Slim terms under the Cellular Component category.

GO ID	GO term	Frequency	Gene list
5938	cell cortex	1 out of 380 genes, 0.3%	*LCB4*
5618	cell wall	3 out of 380 genes, 0.8%	*RBR2 CRD2 INO1*
5933	cellular bud	1 out of 380 genes, 0.3%	*MSO1*
5575	cellular_component	192 out of 380 genes, 50.5%	*C1_00010W_A C1_01220C_A DUR1,2 C1_11320C_A C2_08440W_A C6_02450W_A C4_03950C_A C2_05060C_A C6_03600C_A C3_02900W_A C6_02620C_A C4_04620C_A GBU1 C6_00730W_A C3_00050C_A C4_01970W_A C1_12900W_A C7_03470W_A C1_00020C_A C4_02770C_A MOH1 C1_03270W_A C4_02930W_A C1_03990W_A C3_05750C_A C5_00750C_A C3_03700C_A C6_02790C_A C1_02270C_A C1_11570W_A ARO3 YHB5 C7_03280C_A CR_02480W_A C1_04460C_A C1_09310C_A C2_08510W_A GPX2 CR_03690W_A PEX22 C3_05360C_A ATF1 CR_04220C_A C4_06670W_A C7_00260C_A C7_02920W_A CSO99 FAA2-3 C2_08330W_A C3_04650W_A HIS3 BLP1 C1_01140C_A C6_01620W_A C1_02970W_A HOM3 C7_02010C_A C1_00580W_A FRP2 BUL1 CR_07740W_A C1_01620C_A CR_08830W_A CR_09610C_A C1_13430C_A C1_01630W_A C3_04630W_A C2_07070W_A C1_14180W_A C1_12870C_A CR_10310W_A C1_05160C_A BIO32 C4_04380C_A POX18 GLT1 C2_08260W_A SCW4 C3_02990C_A CHA1 C4_02230C_A C7_00770W_A C1_00030C_A C4_02040W_A CIRT4B C7_02140W_A C1_09700W_A OPT8 C1_05440C_A C2_10150W_A C3_01420C_A FOX3 C1_00050C_A CR_05040W_A PEX17 CR_06310W_A BUD20 HIS5 UGA11 BMT9 GST1 C3_04450C_A C3_04350C_A C1_05690C_A C3_02750W_A C2_00640W_A C3_02090C_A C2_09070C_A C3_03370C_A GTT1 FGR15 C3_07720C_A CR_04860C_A C1_13090W_A C4_01350W_A C2_04400W_A C3_02660W_A CR_04230W_A TES1 C3_07430W_A C5_04980W_A MNN41 C1_13100W_A CR_06020W_A CR_04990C_A C2_08690C_A C6_03280W_A C4_03960W_A C1_09770W_A C7_03820C_A C1_13180W_A HRQ2 IFK2 C2_02390W_A ALD6 SMI1B C2_09800C_A C3_01060W_A AMO2 MET13 C1_09340C_A CR_04850C_A CR_02060W_A PSO2 C3_04840C_A C4_07020C_A C4_00640W_A C1_06870C_A C1_09300C_A C3_06040W_A LYS22 C4_06940C_A C6_02160W_A CR_04870C_A C2_06630C_A IFR1 C1_11260C_A C4_05800C_A C6_03530C_A ARO8 CR_05750W_A C7_03740C_A YHB4 C4_00290C_A C1_03870C_A C1_00190C_A C6_03670C_A LEU42 AGA1 FRP1 C5_05510C_A C1_03970W_A C6_01940W_A C2_02230C_A CEK2 SUA72 CR_07700W_A IFG3 CR_06270W_A C1_01610C_A CR_08850W_A C3_01270W_A C1_10060C_A C2_04830W_A TES15 ASG7 C3_04330C_A C3_02630C_A PRR2 MRV2 CR_06770C_A C3_04190W_A*

5694	chromosome	7 out of 380 genes, 1.8%	*C4_00030C_A RAD6 C6_03290W_A PPH3 C5_00230C_A PSF1 C6_03320W_A*
5737	cytoplasm	104 out of 380 genes, 27.4%	*NPR1 GTT13 APS3 C6_03240W_A EHD3 DRE2 C3_05290C_A PXP2 C1_01840C_A FTH1 AOX2 HXK1 FAR1 ARG3 C3_03690W_A C5_03870C_A C2_00390C_A BAT21 ARG4 RAD6 LYS4 YHB1 STE18 HIS7 POT1 PDK2 POX1-3 CPA1 UGA1 PRB1 MSO1 C2_00600C_A LCB4 POX1 UBC8 RER2 MDH1-3 GCV1 XUT1 ROA1 ALT1 C1_00860W_A GAT1 UGA4 ARF1 CTN1 C4_00680W_A SFC1 AMO1 FOX2 TPO4 GAP2 C2_10870W_A C4_04180C_A CYB2 HPD1 PEX5 ECI1 CAP1 SNO1 C1_09440W_A GDH3 CR_02570C_A C5_03080C_A ANT1 CPA2 C7_03860W_A C1_12150C_A C1_03330C_A PEX6 HSP78 YPT53 CCC1 C4_04250W_A ATG9 MLS1 ZCF20 PXA1 PYC2 FAA21 ARG5,6 C1_14020W_A NBP35 APG7 C2_08420W_A ISA2 OSM2 C2_06780C_A ARG1 ATM1 ATG1 DLD2 ECM42 HMX1 PXA2 CR_06980W_A CCE1 AUT7 CTN3 ARG8 SNZ1 C3_02850C_A ARA1 ICL1*
16023	cytoplasmic, membrane-bounded vesicle	0 out of 380 genes, 0%	*none*
5856	cytoskeleton	1 out of 380 genes, 0.3%	*KIN3*
12505	endomembrane system	12 out of 380 genes, 3.2%	*NPR1 LCB4 RER2 ARF1 GAP2 C4_04180C_A C1_03330C_A YPT53 CCC1 OSM2 HMX1 C3_02850C_A*
5783	endoplasmic reticulum	6 out of 380 genes, 1.6%	*LCB4 RER2 C4_04180C_A OSM2 HMX1 C3_02850C_A*
5576	extracellular region	7 out of 380 genes, 1.8%	*OP4 SOD6 C6_03150C_A GDH3 GOR1 SAP6 SAP4*
5794	Golgi apparatus	4 out of 380 genes, 1.1%	*NPR1 LCB4 ARF1 CCC1*
1411	hyphal tip	0 out of 380 genes, 0%	*none*
16020	membrane	75 out of 380 genes, 19.7%	*NPR1 APS3 HGT4 FTH1 C1_06860W_A ATO5 AOX2 C5_03970W_A ITR1 C3_03690W_A C6_03540W_A DUR3 C3_03760W_A CM_00250W STE18 C7_01510W_A C3_04720C_A STE2 C2_07580W_A CIP1 MSO1 LCB4 RER2 GNP3 GPT1 XUT1 ROA1 OPT4 UGA4 AAP1 CTN1 C4_00680W_A SFC1 SSU1 ATO9 MEP1 TPO4 GAP2 C2_10870W_A C4_04180C_A PEX5 GIT2 ARR3 C5_03080C_A PTR2 ANT1 C4_06910W_A C1_03330C_A YPT53 CCC1 C4_04250W_A ATG9 FRP3 PXA1 C1_00830W_A CDR11 C6_01870C_A CR_04820W_A CAN3 APG7 MEP2 C2_09870W_A ATM1 FCY23 ATG1 C1_06980C_A DLD2 HMX1 PXA2 C4_03710C_A CCE1 AUT7 FTR2 C3_02850C_A SSY1*
5624	membrane fraction	0 out of 380 genes, 0%	*none*
5815	microtubule organizing center	1 out of 380 genes, 0.3%	*KIN3*
5740	mitochondrial envelope	8 out of 380 genes, 2.1%	*DRE2 POT1 CTN1 CYB2 ISA2 ATM1 DLD2 CCE1*
5739	mitochondrion	31 out of 380 genes, 8.2%	*EHD3 DRE2 AOX2 HXK1 ARG3 BAT21 LYS4 YHB1 POT1 PDK2 CPA1 C2_00600C_A ALT1 CTN1 SFC1 CYB2 HPD1 C1_09440W_A C5_03080C_A HSP78 C4_04250W_A ATG9 ZCF20 ARG5,6 ISA2 OSM2 ATM1 DLD2 ECM42 CCE1 ARG8*
5730	nucleolus	0 out of 380 genes, 0%	*none*
5634	nucleus	37 out of 380 genes, 9.7%	*C6_03240W_A HXK1 FAR1 WOR2 C4_00030C_A C1_14190C_A RAD6 C6_03290W_A CAT8 HAP2 GCN4 RAD16 UGA33 C2_02300W_A STB5 KIN3 GAT1 SUC1 C3_05060W_A PPH3 CAP1 GDH3 SET1 ZCF32 SEF2 ZFU2 ZCF25 ZCF20 C5_00230C_A C1_08660C_A NBP35 C2_08420W_A C2_06780C_A PSF1 ZCF4 HMX1 CR_06980W_A*
other	other	12 out of 380 genes, 3.2%	*C2_01920C_A C4_00080C_A CR_03260W_A C3_00400C_A PGA17 C4_02170C_A HSP21 MET28 PGA7 PGA46 PGA25 C1_02380C_A*
5777	peroxisome	18 out of 380 genes, 4.7%	*PXP2 C2_00390C_A POT1 POX1-3 POX1 MDH1-3 FOX2 PEX5 ECI1 CR_02570C_A ANT1 PEX6 MLS1 PXA1 FAA21 PXA2 CTN3 ICL1*
5886	plasma membrane	28 out of 380 genes, 7.4%	*NPR1 HGT4 FTH1 AOX2 C5_03970W_A ITR1 DUR3 STE18 STE2 MSO1 LCB4 XUT1 ROA1 OPT4 SFC1 SSU1 MEP1 TPO4 GAP2 ARR3 CCC1 FRP3 MEP2 FCY23 HMX1 FTR2 C3_02850C_A SSY1*
5840	ribosome	1 out of 380 genes, 0.3%	*EHD3*
30427	site of polarized growth	2 out of 380 genes, 0.5%	*FAR1 MSO1*
70732	spindle envelope	0 out of 380 genes, 0%	*none*

5773	vacuole	16 out of 380 genes, 4.2%	*FTH1 C3_03690W_A PRB1 XUT1 ROA1 UGA4 C4_00680W_A TPO4 GAP2 C2_10870W_A C7_03860W_A C1_03330C_A CCC1 ATG9 ATG1 AUT7*

Table S19. Assignment of the 615 significantly downregulated *C. albicans* genes to 27 GO Slim terms under the Cellular Component category.

GO ID	GO term	Frequency	Gene list
5938	cell cortex	10 out of 615 genes, 1.6%	*C4_04800W_A GLC7 PFY1 INT1 WAL1 IST2 VRP1 CHC1 COF1 KAR2*
5618	cell wall	68 out of 615 genes, 11.1%	*TPI1 MET6 SSB1 C5_02110W_A APE2 HSP12 HEM13 TKL1 TEF2 EFT2 RPL23A TEF1 CRH11 MET15 HWP1 ENG1 RPL14 ATP1 ECM331 TSA1B TSA1 INT1 RPS6A ALS4 WH11 CYP1 PGK1 IPP1 YWP1 EXG2 PDC11 SSR1 SOD5 PGA13 PST2 RPL38 SAM2 CHT3 GLX3 FBA1 PHR2 DDR48 TDH3 ALS2 PRT1 RBE1 TAL1 ALS3 PGA59 GPM1 PGA6 RPS1 SRB1 ENO1 XYL2 CEF3 RPS13 CHT2 PGA31 PGA62 KRE1 CDC19 RPS20 RBT1 ALS9 CSH1 RPS14B SCW11*
5933	cellular bud	11 out of 615 genes, 1.8%	*GLC7 WSC2 INT1 WAL1 IST2 VRP1 CHT3 AMN1 FLU1 NCE102 CDC5*
5575	cellular_component	153 out of 615 genes, 24.9%	*GLK4 C7_04210C_A C3_00360W_A C1_02730W_A CAM1-1 C6_02480W_A CR_05210W_A C2_07420W_A C3_00230C_A CRZ2 C1_12000C_A C2_05640W_A C1_09040C_A C5_01110W_A LDG3 GLO1 C4_06700W_A C2_09910C_A C1_07790C_A CR_06500C_A C7_01940C_A C2_05960C_A C4_06320C_A C1_11720W_A JIP5 CR_10200W_A GLK1 C6_00680C_A ARO4 ERG13 ADAEC AHP2 RPS4A NOP4 C2_02530W_A MRV3 C1_01150C_A C1_07640C_A C7_02280W_A KRE5 C1_07990C_A ASR3 CR_09740W_A MSC7 C2_00130W_A MRV5 C7_02260W_A C1_10850W_A RFG1 OSM1 C1_09810W_A DUT1 C1_13820C_A GUA1 C5_00510W_A CR_03000C_A C7_02420C_A C3_07900C_A AAT22 C1_10350C_A GAD1 C1_05520W_A HGH1 C1_10170W_A RGS2 DAK2 MET3 C3_05990C_A C1_04270C_A C7_01010W_A MFA1 CR_09330C_A C1_11930W_A C3_01180C_A C5_01090C_A MVD PTP1 MIG2 CYS3 CR_06570C_A C4_03230C_A C4_03300C_A C2_10130W_A C4_02620C_A CR_09460C_A C7_03270W_A PSA2 ASR2 OFI1 C4_01830C_A C7_01430C_A CR_08500W_A C2_09500W_A C6_02490C_A PBR1 TSR2 PRN4 C4_06750C_A C5_01550C_A C2_01960C_A CR_09070C_A C5_03440W_A C3_07880C_A SOU1 C1_01510W_A AAH1 C1_09330W_A C1_03240W_A C1_12180C_A C5_02400W_A C4_06710W_A C7_01380W_A ASR1 C3_01570W_A C4_01220C_A C3_06880W_A MSB1 ROD1 C1_11050W_A USO6 BMT4 PMI1 C2_03020C_A C3_05450C_A HAL21 C5_02780W_A C3_05320W_A NAT4 C1_11990W_A EXO1 C5_03000C_A FRP5 C3_02790W_A C4_00730C_A DCG1 C1_11200W_A C1_13460W_A PWP1 SPE2 MET14 C2_00670C_A C7_02210W_A IFD6 C1_07010W_A C3_06860C_A C2_08030W_A C1_11120C_A C4_02260C_A C3_00730W_A C1_13150W_A C3_01820W_A C6_04140C_A C6_03880W_A*
5694	chromosome	23 out of 615 genes, 3.7%	*C6_02280W_A UTP5 HTA2 GLC7 TEC1 CYP1 C1_04180W_A POL30 C4_02820W_A NOP1 SFL2 HHF22 NDT80 ESC4 HTB1 MCD1 HHT2 PST3 NAN1 CDC5 HTA3 HHT21 SCH9*
5737	cytoplasm	258 out of 615 genes, 42%	*ERG28 DPM2 RPS25B C5_01540W_A YCP4 ATP19 RPL16A TPI1 SOD2 FEN12 THS1 RPL17B OPT1 SSB1 C5_02110W_A ERG6 APE2 LSC1 GUS1 CR_05150W_A RPL19A RPL25 C5_04300C_A HSP12 SMP3 HEM13 C7_00490C_A RPP0 CAR2 SSZ1 ERG5 RPL20B C1_09060C_A TEF2 RPL29 RPL23A GND1 C2_05300C_A TIF HGT7 BFR1 LTV1 C4_04800W_A RPL37B TEF1 CR_04610C_A TMA19 CR_09140C_A CR_01410C_A LSC2 RPL10A C1_13790C_A PGA63 GRF10 C5_00030W_A CR_02690W_A ERG10 BUD7 HGT6 C6_02380W_A C6_03380W_A RPL14 GLC7 RPL30 PFK1 ATP1 MAE1 VRG4 RPP2A DRG1 ARC40 RPL2 LAT1 YNK1 ATP2 PUS7 RPS27 NRM1 C2_07190C_A C2_09590C_A TSA1B HMG1 C7_01360C_A PFY1 C5_02660C_A TSA1 INT1 CAM1 GPD2 RPS6A RPL32 WH11 RNR21 CYP1 PWP2 CWH8 RPP1B PGK1 C3_04810C_A ERG9 RPS12 FAS1 C1_01530C_A MNN12 SEC12 YST1 CAR1 ARC1 RPS19A RIB4 IPP1 RPS8A RPL24A SOD1 CYS4 KTI12 CR_07220C_A C4_06680C_A TRM1 EFB1 LKH1 RPS22A GLE2 CHO1 C1_11790W_A RPL3 PDC11 ANB1 C1_11860W_A WAL1 KRS1 IST2 EGD1 CR_02770C_A ERG4 UBI3 RPS9B C2_05410W_A RPL6 PGI1 RPL42 C4_05230C_A RPL38 VRP1 DPM1 SAM2 C1_02240W_A TUB1 AMN1 GLX3 CHC1 FBA1 RPL8B*

			PHR2 RNR1 TDH3 GCD6 C2_07290W_A RPS21B RPL15A TSR1 RPL4B SEC14 GUT2 SEN2 HAT1 C1_06890C_A FUM11 C3_01680C_A ATP5 PFK2 RPL13 PRT1 NMD3 RPL12 PDI1 TAL1 C1_01050C_A COF1 URA1 RPL43A RPL18 PMT2 ARX1 MCD1 RPP1 C6_01980C_A ZPR1 KAR2 GPM1 C7_02660C_A GCN1 RPS1 EGD2 IDH2 RPL27A GSP1 SRB1 ENO1 FLU1 DHH1 EMP24 HXK2 RPL5 ZUO1 MRF1 C1_05630C_A STT3 CEF3 IDH1 RPS13 SAM50 DPS1-1 ERG3 C6_02690C_A C1_10820C_A RPS5 C7_00830C_A RHR2 PTP3 RPL28 SEC24 PMT1 RPL21A RPS28B ERG2 CDC19 TFS1 C3_06700C_A RPS21 RPS20 APT1 MRPS9 ASC1 POR1 C7_01600W_A PMT4 LEU2 GDA1 C1_14160W_A C7_02340C_A C1_05720W_A RPL35 C3_02160C_A C2_02410W_A CSH1 WSC4 C1_00090W_A MAM33 MCR1 NIP7 URA2 YMC1 SCH9 SEC61 C1_11920W_A OST1 ILV5
16023	cytoplasmic, membrane-bounded vesicle	0 out of 615 genes, 0%	*none*
5856	cytoskeleton	13 out of 615 genes, 2.1%	*ENG1 GLC7 ARC40 INT1 CR_07220C_A WAL1 VRP1 C1_02240W_A TUB1 CHC1 COF1 CDC5 C2_06770W_A*
12505	endomembrane system	54 out of 615 genes, 8.8%	*ERG28 DPM2 FEN12 OPT1 C1_00160C_A C5_02110W_A ERG6 APE2 SMP3 ERG5 BFR1 LTV1 C4_04800W_A PGA63 BUD7 ATP1 VRG4 ATP2 HMG1 CWH8 ERG9 MNN12 SEC12 C4_06680C_A TRM1 LKH1 GLE2 CHO1 NUP159 C1_11860W_A IST2 ERG4 DPM1 C1_02240W_A CHC1 SEC14 PDI1 C1_01050C_A PMT2 KAR2 C5_03550W_A EMP24 STT3 ERG3 SEC24 PMT1 ERG2 PMT4 GDA1 C2_02410W_A WSC4 SEC61 C1_11920W_A OST1*
5783	endoplasmic reticulum	35 out of 615 genes, 5.7%	*ERG28 DPM2 FEN12 ERG6 SMP3 ERG5 BFR1 C4_04800W_A ATP1 ATP2 HMG1 CWH8 ERG9 SEC12 C4_06680C_A CHO1 C1_11860W_A IST2 ERG4 DPM1 PDI1 C1_01050C_A PMT2 KAR2 EMP24 STT3 ERG3 SEC24 PMT1 ERG2 PMT4 C2_02410W_A WSC4 SEC61 OST1*
5576	extracellular region	56 out of 615 genes, 9.1%	*MSB2 LIP3 RPL17B MET6 APE2 HEM13 HGT7 C4_04800W_A TEF1 CRH11 HGT6 ENG1 RPS18 YNK1 MTS1 CAM1 SPE3 GPD2 ALS4 CYP1 PLB4.5 IPP1 SOD1 YWP1 SSR1 SOD5 UBI3 CHT3 PHR2 TDH3 ALS2 PDI1 RBE1 TAL1 FET34 PMA1 ALS3 KAR2 GCN1 RPS1 FGR41 GSP1 ENO1 LIP6 GAP4 PST3 NCE102 CHT2 C1_10820C_A RPS5 GRE3 ASC1 POR1 RBT1 SEC61 SCW11*
5794	Golgi apparatus	8 out of 615 genes, 1.3%	*OPT1 C4_04800W_A BUD7 VRG4 MNN12 CHC1 SEC14 GDA1*
1411	hyphal tip	1 out of 615 genes, 0.2%	*WAL1*
16020	membrane	135 out of 615 genes, 22%	*PNG2 ERG28 DPM2 FRE10 YCP4 MSB2 ATP19 C4_05330C_A RPL16A PGA53 FEN12 OPT1 CR_01630C_A SSB1 C5_02110W_A ERG6 SMP3 TKL1 ERG5 C1_09060C_A TEF2 EFT2 HGT7 BFR1 LTV1 C4_04800W_A NUP TEF1 CR_04610C_A CRH11 PGA63 HGT10 HGT6 HGT12 ATP1 VRG4 ATP2 ECM331 MTS1 AQY1 HMG1 PFY1 C2_05290C_A CWH8 C7_01950W_A PGK1 ERG9 PTR22 SEC12 YST1 NAG3 HXT5 GSL2 EXG2 C4_06680C_A TRM1 CHO1 ERG24 PDC11 FCY2 C1_11860W_A SSR1 HGT19 ERP5 IST2 C7_02000C_A ERG4 RPL6 PST2 DPM1 SAM2 C3_01540W_A CHC1 FBA1 PHR2 TDH3 HSP31 HSP30 HGT13 RPL4B SEC14 GUT2 SEN2 C3_01680C_A ATP5 CNT C1_03510C_A FET34 PMA1 C1_01050C_A SLP2 CR_01220W_A URA1 MSS4 PMT2 KAR2 GSP1 SRB1 ENO1 FLU1 DHH1 EMP24 HXK2 GAP4 STT3 CEF3 PST3 SAM50 NCE102 CR_03580C_A ERG3 ALP1 ERG251 RPS5 SEC24 PMT1 CDC19 TFS1 C3_06700C_A C2_10010C_A C7_00630C_A POR1 C7_01600W_A PMT4 GDA1 C2_02410W_A WSC4 HGT8 C1_00090W_A MCR1 URA2 SCH9 SEC61 C1_11920W_A OST1*
5624	membrane fraction	0 out of 615 genes, 0%	*none*
5815	microtubule organizing center	2 out of 615 genes, 0.3%	*GLC7 CDC5*
5740	mitochondrial envelope	22 out of 615 genes, 3.6%	*ATP19 C1_09060C_A HGT6 ATP1 YNK1 ATP2 CYP1 RIB4 SOD1 CHO1 GUT2 SEN2 C3_01680C_A ATP5 URA1 GPM1 HXK2 SAM50 C3_06700C_A POR1 C7_01600W_A MCR1*
5739	mitochondrion	59 out of 615 genes, 9.6%	*ATP19 TPI1 SOD2 LSC1 GUS1 CR_05150W_A C1_09060C_A TEF2 C2_05300C_A TEF1 TMA19 CR_09140C_A LSC2 C1_13790C_A C5_00030W_A HGT6 C6_02380W_A PFK1 ATP1 MAE1 LAT1 YNK1 ATP2 C2_07190C_A C2_09590C_A C7_01360C_A CYP1 PGK1 RIB4 SOD1 TRM1 CHO1 PGI1 FBA1 TDH3 GUT2 SEN2 FUM11 C3_01680C_A ATP5 PFK2 URA1 MCD1 C6_01980C_A GPM1 IDH2 ENO1 HXK2 MRF1 IDH1 SAM50 C3_06700C_A MRPS9 POR1 C7_01600W_A MAM33 MCR1 YMC1 ILV5*
5730	nucleolus	49 out of 615 genes, 8%	*UTP5 GAR1 RRN3 C1_07660W_A C4_05330C_A RPF2 CR_10410C_A RPC19 C7_03850W_A CIC1 C1_10880W_A NSA1 UTP18 GLC7 LHP1*

			RLP24 CSI2 PES1 PWP2 C2_02540W_A UTP21 NOP14 UTP22 RRS1 DIP2 NOP5 YTM1 NOP1 RPO26 C2_04570W_A TSR1 ESC4 MRT4 SIK1 RRP9 ARX1 RPP1 C1_03790C_A C3_02040C_A RPA190 ZUO1 NAN1 C4_05010W_A NOC2 RPS28B UTP4 ERB1 DBP3 SSF1
5634	nucleus	144 out of 615 genes, 23.4%	*CZF1 C6_02280W_A UTP5 GAR1 C2_02930C_A RRN3 C1_07660W_A C4_05330C_A MET6 RPF2 CR_10410C_A C1_00160C_A C5_02110W_A RPC19 RMS1 HSP12 C7_03850W_A CIC1 RPL23A C1_10880W_A HTA2 LTV1 C7_01030C_A TCC1 CR_01410C_A RIM101 NSA1 GRF10 UTP18 C2_03880C_A GLC7 TEC1 PUS7 NRM1 TSA1B HMG1 LHP1 TSA1 CAM1 RLP24 CSI2 RNR21 CYP1 PES1 PWP2 C7_01950W_A ZCF21 GZF3 C1_04180W_A C2_02540W_A C3_01560W_A UTP21 NOP14 UTP22 SOD1 POL30 KTI12 RRS1 CR_07220C_A TRM1 GLE2 C1_11790W_A NRG1 NUP159 PDC11 C6_02350C_A C4_02820W_A DIP2 NOP5 YTM1 NOP1 RPO26 CR_02770C_A CCN1 RHA1 C4_05230C_A SFL2 C1_02240W_A YOX1 TUB1 AMN1 PHR2 HHF22 C2_04570W_A SSN6 NDT80 TSR1 ESC4 SEC14 SEN2 PTP2 HAT1 HTB1 MRT4 TAL1 CR_04110W_A C7_02100W_A SIK1 MSS4 CLN3 RRP9 ARX1 MCD1 RPP1 ZPR1 KAR2 C1_03790C_A NHP6A C5_03550W_A C1_06760C_A C3_02040C_A HHT2 GSP1 ENO1 RPA190 HXK2 ZUO1 C1_05630C_A DPS1-1 C6_02690C_A MSH6 NAN1 CDC5 C4_05010W_A PTP3 RPL28 HMT1 DBP2 ZCF3 NOC2 RPS28B C3_00100W_A UTP4 C4_07150W_A ERB1 C1_14160W_A HTA3 C7_02340C_A KRE30 NIP7 DBP3 SCH9 SSF1 TOS4*
other	other	26 out of 615 genes, 4.2%	*C4_00940W_A C1_12570C_A PGA23 PIL1 RPS10 C4_05250W_A PGA58 PGA12 C2_07630C_A PGA34 URA7 PGA54 C2_07620W_A PGA26 C3_06760W_A MIH1 PGA18 GCY1 DIM1 GUK1 SAH1 DRS1 PGA11 CR_04240C_A C6_01420C_A PGA38*
5777	peroxisome	1 out of 615 genes, 0.2%	*GND1*
5886	plasma membrane	72 out of 615 genes, 11.7%	*PNG2 FRE10 YCP4 MSB2 ATP19 PGA53 OPT1 SSB1 C5_02110W_A ERG6 TKL1 ERG5 EFT2 HGT7 CRH11 HGT10 HGT6 HGT12 ATP1 ATP2 ECM331 MTS1 AQY1 HMG1 PFY1 PGK1 ERG9 PTR22 GSL2 EXG2 PDC11 SSR1 HGT19 IST2 PST2 DPM1 SAM2 C3_01540W_A CHC1 FBA1 PHR2 TDH3 HSP30 HGT13 GUT2 CNT FET34 PMA1 MSS4 PMT2 SRB1 ENO1 FLU1 EMP24 GAP4 STT3 CEF3 PST3 SAM50 NCE102 ERG3 ALP1 ERG251 PMT1 CDC19 C2_10010C_A POR1 PMT4 C2_02410W_A HGT8 SEC61 OST1*
5840	ribosome	79 out of 615 genes, 12.8%	*RPS25B C5_01540W_A RPL16A RPL17B RPS15 CR_05150W_A RPL19A RPL25 RPP0 RPL20B CIC1 EFT2 RPL29 RPL23A C2_05300C_A RPL37B RPL10A C5_00030W_A RPL14 RPS18 RPL30 RPP2A RPL2 RPS27 C2_07190C_A RPS6A RPL32 RPP1B RPS12 RPS17B YST1 RPS19A RPS8A RPL24A EFB1 RPS22A RPL3 EGD1 UBI3 RPS9B C2_05410W_A RPL6 RPL42 RPL38 RPS26A RPL8B RPS21B RPL15A RPL4B C1_06890C_A RPL13 RPL12 RPL43A RPL18 C6_01980C_A RPL40B GCN1 RPS1 EGD2 RPL27A RPS24 RPL5 ZUO1 CEF3 RPS13 C2_05160C_A RPS7A RPS5 RPL28 RPL21A RPS28B RPS21 RPS20 MRPS9 ASC1 RPS16A C1_05720W_A RPL35 RPS14B*
30427	site of polarized growth	13 out of 615 genes, 2.1%	*MSB2 ENG1 GLC7 WSC2 PFY1 INT1 WAL1 VRP1 CHT3 PHR2 MSS4 NCE102 CDC5*
70732	spindle envelope	0 out of 615 genes, 0%	*none*
5773	vacuole	14 out of 615 genes, 2.3%	*APE2 TEF2 HGT7 LTV1 TEF1 CR_04610C_A LKH1 ENO1 FLU1 C1_10820C_A TFS1 YMC1 SCH9 SEC61*

Table S20. Assignment of the 370 significantly upregulated *C. albicans* genes to the top 20 most highly enriched KEGG pathways.

KEGG pathway	Gene list	No. of genes in input list	No. of genes in pathway	Enrichment ratio	Corrected P-value
alpha-Linolenic acid metabolism	*POX1-3, POX1, POT1, FOX3, PXP2*	5	7	0.714	5.67×10^{-05}
Arginine biosynthesis	*ARG8, GDH3, ARG1, ARG3, ARG4, ARG5, DUR1, ECM42, ALT1*	9	16	0.563	1.72×10^{-07}
beta-Alanine metabolism	*HPD1, EHD3, ALD6, UGA11, PXP2, POX1-3, UGA1, AMO2, POX1, FOX2, AMO1*	11	21	0.524	2.22×10^{-08}
Propanoate metabolism	*HPD1, EHD3, ALD6, UGA11, PXP2, POX1-3, UGA1, POX1, FOX2*	9	19	0.474	4.63×10^{-07}
Valine, leucine and isoleucine degradation	*HPD1, EHD3, BAT21, ALD6, UGA11, UGA1, POT1, FOX3*	8	18	0.444	2.69×10^{-06}
Biosynthesis of unsaturated fatty acids	*POX1-3, POX1, POT1, FOX3, PXP2*	5	14	0.357	6.16×10^{-04}
Alanine, aspartate and glutamate metabolism	*GDH3, GLT1, ARG1, UGA11, CPA1, ARG4, UGA1, CPA2, ALT1*	9	27	0.333	3.28×10^{-06}
Lysine biosynthesis	*ARO8, LYS4, LYS22, HOM3*	4	12	0.333	3.00×10^{-03}
ABC transporters	*PXA2, ATM1, PXA1, CDR11*	4	12	0.333	3.00×10^{-03}
Fatty acid degradation	*POX1, PXP2, POX1-3, ECI1, POT1, FOX3, FAA2-3, FAA21*	8	25	0.320	1.54×10^{-05}
2-Oxocarboxylic acid metabolism	*ARG8, ARG5, BAT21, ARO8, LYS22, HOM3, LEU42, ECM42, LYS4, ALT1*	10	32	0.313	1.53×10^{-06}
Peroxisome	*POT1, PEX5, PEX6, CTN3, ECI1, PXP2, PXA2, POX1-3, FOX3, CTN1, FAA21, FAA2-3, POX1, PXA1*	14	48	0.292	2.85×10^{-08}
Phenylalanine metabolism	*ARO8, AMO2, AMO1, HIS5*	4	16	0.250	6.60×10^{-03}
Nitrogen metabolism	*GLT1, GDH3*	2	8	0.250	6.16×10^{-02}
Histidine metabolism	*HIS5, HIS7, HIS3*	3	13	0.231	2.27×10^{-02}
Valine, leucine and isoleucine biosynthesis	*CHA1, LEU42, BAT21*	3	13	0.231	2.27×10^{-02}
Fatty acid metabolism	*POX1, PXP2, POX1-3, POT1, FOX3, FAA2-3, FAA21*	7	31	0.226	3.73×10^{-04}
Vitamin B6 metabolism	*SNZ1, SNO1*	2	9	0.222	7.15×10^{-02}
Tyrosine metabolism	*ARO8, AMO2, AMO1, HIS5*	4	19	0.211	1.03×10^{-02}
Glyoxylate and dicarboxylate metabolism	*GOR1, MLS1, MDH1-3, ICL1, GCV1*	5	26	0.192	5.42×10^{-03}

Table S21. Assignment of the 615 significantly downregulated *C. albicans* genes to the top 20 most highly enriched KEGG pathways.

KEGG pathway	Gene list	No. of genes in input list	No. of genes in pathway	Enrichment ratio	Corrected P-value
Mannose type O-glycan biosynthesis	*PMT4, PMT1, PMT2*	3	5	0.600	5.36×10^{-02}
Fructose and mannose metabolism	*SOU1, FBA1, TPI1, PFK1, PFK2, GLK4, DAK2, PSA2, HXK2, PMI1, SRB1, GLK1*	12	21	0.571	5.93×10^{-06}
Ribosome	*RPS13, RPS12, RPS21B, RPS10, RPL5, RPS25B, RPS15, RPS17B, RPL6, RPS9B, RPL40B, RPS18, RPL2, RPL3, RPP1B, RPL16A, RPS5, RPL8B, RPS1, RPL42, RPL29, RPL23A, RPL25, RPS19A, RPS21, RPS24, RPP2A, RPS6A, RPL20B, RPL27A, RPS4A, RPS14B, RPL24A, RPS22A, RPL17B, RPS16A, RPS26A, RPL43A, UBI3, RPS27, RPL19A, RPL14, RPP0, RPS8A, RPL12, RPL13, RPL37B, RPL18, RPL32, RPL28, YST1, RPL15A, RPS20, RPS28B, RPL38, RLP24, RPL35, MRPS9, RPL4B, RPL30, RPL10A, RPS7A, RPL21A*	63	119	0.529	4.29×10^{-29}
Steroid biosynthesis	*ERG4, ERG5, ERG6, ERG2, ERG3, ERG9, ERG251, ERG24*	8	18	0.444	1.39×10^{-03}
Glycolysis / Gluconeogenesis	*PDC11, LAT1, FBA1, PGI1, CDC19, PFK2, PFK1, GLK4, ENO1, TPI1, GPM1, GLK1, HXK2, TDH3, PGK1*	15	40	0.375	1.31×10^{-05}
Pentose phosphate pathway	*TAL1, FBA1, GND1, PFK2, TKL1, PGI1, PFK1*	7	21	0.333	1.08×10^{-02}
Selenocompound metabolism	*MET3, MET6, CYS3*	3	9	0.333	1.36×10^{-01}
Other types of O-glycan biosynthesis	*PMT4, PMT1, PMT2*	3	9	0.333	1.36×10^{-01}
Galactose metabolism	*GLK4, PFK2, GLK1, PFK1, HXK2*	5	16	0.313	4.51×10^{-02}
Methane metabolism	*FBA1, PFK2, PFK1, ENO1, DAK2, GPM1*	6	20	0.300	3.07×10^{-02}
Amino sugar and nucleotide sugar metabolism	*PSA2, MCR1, GLK4, PGI1, CHT3, CHT2, GLK1, HXK2, PMI1, SRB1*	10	35	0.286	3.35×10^{-03}
Carbon metabolism	*LAT1, TDH3, TKL1, MAE1, TPI1, HXK2, LSC2, FUM11, FBA1, CDC19, GLK4, PGI1, DAK2, GLK1, AAT22, GND1, PGK1, TAL1, MET15, LSC1, IDH2, IDH1, PFK2, PFK1, ENO1, GPM1, ERG10*	27	98	0.276	2.35×10^{-07}
Sulfur metabolism	*MET3, MET14, MET15, HAL21*	4	15	0.267	1.19×10^{-01}
Ubiquinone and other terpenoid-quinone biosynthesis	*YCP4, PST3, PST2*	3	12	0.250	1.94×10^{-01}
Pentose and glucuronate interconversions	*XYL2, GRE3*	2	8	0.250	3.24×10^{-01}
Pyrimidine metabolism	*RNR21, URA7, URA2, URA1, DUT1, YNK1, RNR1*	7	30	0.233	4.26×10^{-02}
Butanoate metabolism	*GAD1, ERG10, ERG13*	3	13	0.231	2.20×10^{-01}
Biosynthesis of antibiotics	*ERG4, ERG5, ERG6, CDC19, LAT1, ERG2, ERG3, TDH3, ERG9, TKL1, PMI1, TPI1, TAL1, HXK2, CYS4, HMG1, CYS3, FUM11, ARO4, FBA1,*	46	206	0.223	1.86×10^{-09}

	CAR2, CAR1, GLK4, PGI1, GLK1, ERG24, YNK1, AAT22, GND1, PGK1, LSC2, MET15, LSC1, ILV5, IDH2, IDH1, PFK2, PFK1, ENO1, MVD, MET3, ERG251, PDC11, GPM1, ERG13, ERG10				
Citrate cycle (TCA cycle)	*LSC2, LSC1, IDH2, IDH1, LAT1, FUM11*	6	27	0.222	7.46×10^{-02}
Cysteine and methionine metabolism	*MET6, MET15, SPE2, SPE3, SAH1, SAM2, CYS4, AAT22, CYS3*	9	41	0.220	2.57×10^{-02}